

frontiers RESEARCH TOPICS

ENVIRONMENTAL BIOINORGANIC CHEMISTRY OF AQUATIC MICROBIAL ORGANISMS

Topic Editors

Christel Hassler, Martha Gledhill,
and Veronique Schoemann



frontiers in
MICROBIOLOGY



frontiers

FRONTIERS COPYRIGHT STATEMENT

© Copyright 2007-2013
Frontiers Media SA.
All rights reserved.

All content included on this site, such as text, graphics, logos, button icons, images, video/audio clips, downloads, data compilations and software, is the property of or is licensed to Frontiers Media SA ("Frontiers") or its licensees and/or subcontractors. The copyright in the text of individual articles is the property of their respective authors, subject to a license granted to Frontiers.

The compilation of articles constituting this e-book, as well as all content on this site is the exclusive property of Frontiers. Images and graphics not forming part of user-contributed materials may not be downloaded or copied without permission.

Articles and other user-contributed materials may be downloaded and reproduced subject to any copyright or other notices. No financial payment or reward may be given for any such reproduction except to the author(s) of the article concerned.

As author or other contributor you grant permission to others to reproduce your articles, including any graphics and third-party materials supplied by you, in accordance with the Conditions for Website Use and subject to any copyright notices which you include in connection with your articles and materials.

All copyright, and all rights therein, are protected by national and international copyright laws.

The above represents a summary only. For the full conditions see the Conditions for Authors and the Conditions for Website Use.

Cover image provided by Ibbl sarl, Lausanne CH

ISSN 1664-8714

ISBN 978-2-88919-130-7

DOI 10.3389/978-2-88919-130-7

ABOUT FRONTIERS

Frontiers is more than just an open-access publisher of scholarly articles: it is a pioneering approach to the world of academia, radically improving the way scholarly research is managed. The grand vision of Frontiers is a world where all people have an equal opportunity to seek, share and generate knowledge. Frontiers provides immediate and permanent online open access to all its publications, but this alone is not enough to realize our grand goals.

FRONTIERS JOURNAL SERIES

The Frontiers Journal Series is a multi-tier and interdisciplinary set of open-access, online journals, promising a paradigm shift from the current review, selection and dissemination processes in academic publishing.

All Frontiers journals are driven by researchers for researchers; therefore, they constitute a service to the scholarly community. At the same time, the Frontiers Journal Series operates on a revolutionary invention, the tiered publishing system, initially addressing specific communities of scholars, and gradually climbing up to broader public understanding, thus serving the interests of the lay society, too.

DEDICATION TO QUALITY

Each Frontiers article is a landmark of the highest quality, thanks to genuinely collaborative interactions between authors and review editors, who include some of the world's best academicians. Research must be certified by peers before entering a stream of knowledge that may eventually reach the public - and shape society; therefore, Frontiers only applies the most rigorous and unbiased reviews.

Frontiers revolutionizes research publishing by freely delivering the most outstanding research, evaluated with no bias from both the academic and social point of view.

By applying the most advanced information technologies, Frontiers is catapulting scholarly publishing into a new generation.

WHAT ARE FRONTIERS RESEARCH TOPICS?

Frontiers Research Topics are very popular trademarks of the Frontiers Journals Series: they are collections of at least ten articles, all centered on a particular subject. With their unique mix of varied contributions from Original Research to Review Articles, Frontiers Research Topics unify the most influential researchers, the latest key findings and historical advances in a hot research area!

Find out more on how to host your own Frontiers Research Topic or contribute to one as an author by contacting the Frontiers Editorial Office: researchtopics@frontiersin.org

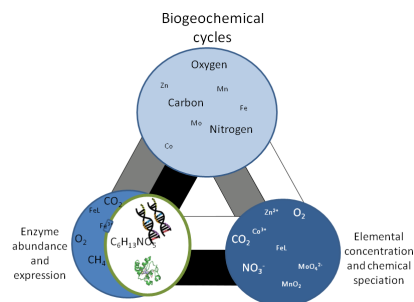
ENVIRONMENTAL BIOINORGANIC CHEMISTRY OF AQUATIC MICROBIAL ORGANISMS

Topic Editors:

Christel Hassler, University of Technology Sydney, Australia

Martha Gledhill, University of Southampton, United Kingdom

Veronique Schoemann, Royal Netherlands Institute for Sea Research, Netherlands



The infinite triangle linking biogeochemical cycles, elemental concentrations, chemical speciation, enzyme expression and enzyme abundance. Figure by Martha Gledhill.

The Environmental Bioinorganic Chemistry of Aquatic Microbial Organisms describes the interactions between metals and aquatic prokaryotic and eukaryotic microorganisms in their environment. Metals influence microbial growth in the aquatic environment as they can be either toxic to aquatic microbes, if present at too high concentrations in the environment, or limiting, if bio-essential and present at very low concentrations. In turn, microorganisms influence the biogeochemical cycling of metals as they affect trace metal concentrations, distributions between particulate and dissolved phase, and chemical speciation.

At the sub cellular level, metalloproteins are the catalysts driving many steps in the biogeochemical cycles of major elements such as carbon, nitrogen and sulfur. Metals thus provide a link between the abundance and activity of enzymes, the growth of microorganisms, and the biogeochemical cycles of major climate influencing elements. Furthermore, the evolution of the chemistry of aquatic environments and atmosphere has left its mark on the microbial proteome as a direct result of changes in the solubility of metals. The aquatic microbial metallome thus has the potential to reveal information about key biogeochemical processes, their spatial and seasonal occurrence, and also to reveal how the geochemical environment is shaping the microbial population itself.

The aim of this Research Topic is to highlight recent advances in our understanding of how metals influence the activity of aquatic microbes, and how microbes influence the biogeochemical cycling of metals. Applications of techniques in proteomics, spectroscopy,

mass spectrometry and genomics are all leading to a greater understanding of the interactions between the microbial metallome and the “aquatic metallome” and thus the influence of metals on the biogeochemical cycles of climatically important elements such as carbon, nitrogen and sulfur. Both reviews and original research on the occurrence and abundance of microbial metal proteins and peptides, the utilisation of metals by aquatic microbes, the influence of microbially produced exudates on metal speciation and the biogeochemical cycling, and the toxicity of metals to microbial organisms are welcome.

Table of Contents

- 05 *The Environmental Bioinorganic Chemistry of Aquatic Microbial Organisms***
Martha Gledhill, Christel S. Hassler and Veronique Schoemann
- 06 *Feedback Interactions Between Trace Metal Nutrients and Phytoplankton in the Ocean***
William G. Sunda
- 28 *Disassembling Iron Availability to Phytoplankton***
Yeala Shaked and Hagar Lis
- 54 *Exploring the Link between Micronutrients and Phytoplankton in the Southern Ocean during the 2007 Austral Summer***
Christel S. Hassler, Marie Sinoir, Lesley A. Clementson and Edward C. V. Butler
- 80 *Impacts of Microbial Activity on the Optical and Copper-Binding Properties of Leaf-Litter Leachate***
Chad W. Cuss and Celine Guéguen
- 90 *Iron Utilization in Marine Cyanobacteria and Eukaryotic Algae***
Joe Morrissey and Chris Bowler
- 103 *Factors Influencing the Diversity of Iron Uptake Systems in Aquatic Microorganisms***
Dhwani K. Desai, Falguni D. Desai and Julie LaRoche
- 123 *Mining Genomes of Marine Cyanobacteria for Elements of Zinc Homeostasis***
James P. Barnett, Andrew Millard, Amira Z. Ksibe, David J. Scanlan, Ralf Schmid and Claudia Andrea Blindauer
- 144 *Trace Metal Requirements for Microbial Enzymes Involved in the Production and Consumption of Methane and Nitrous Oxide***
Jennifer B. Glass and Victoria J. Orphan
- 164 *The Unique Biogeochemical Signature of the Marine Diazotroph Trichodesmium***
Jochen Nuester, Stefan Vogt, Matthew Newville, Adam B. Kustka and Benjamin S. Twining
- 179 *Characterization of Lead-Phytochelatin Complexes by Nano-Electrospray Ionization Mass Spectrometry***
Christian Scheidegger, Marc J.-F. Suter, Renata Behra and Laura Sigg
- 186 *Modeling the Habitat Range of Phototrophs in Yellowstone National Park: Toward the Development of a Comprehensive Fitness Landscape***
Eric S. Boyd, Kristopher M. Fecteau, Jeff R. Havig, Everett L. Shock and John W. Peters
- 197 *Effect of Metals on the Lytic Cycle of the Coccolithovirus, EhV86***
Martha Gledhill, Aurélie Devez, Andrea Highfield, Chloe Singleton, Eric P. Achterberg and Declan Schroeder



The environmental bioinorganic chemistry of aquatic microbial organisms

Martha Gledhill^{1*}, Christel S. Hassler² and Veronique Schoemann³

¹ National Oceanography Centre, School of Ocean and Earth Science, University of Southampton, Southampton, UK

² Plant Functional Biology and Climate Change Cluster, University of Technology Sydney, Broadway, NSW, Australia

³ Department of Biological Oceanography, Royal Netherlands Institute for Sea Research, AB Den Burg, Texel, Netherlands

*Correspondence: martha@soton.ac.uk

Edited by:

Bradley M. Tebo, Oregon Health & Science University, USA

Reviewed by:

Bradley M. Tebo, Oregon Health & Science University, USA

A few key inorganic elements, many of them metals, are essential for life. Approximately 40% of all proteins are metalloproteins which are at the center of the fundamental biological processes that drive biogeochemical cycles. Metalloproteins split water, acquire carbon, reduce carbon, and reoxidize carbon. They are also integral to the nitrogen and oxygen cycles.

In aquatic systems, metals are present at an extraordinarily wide range of concentrations from metal rich hydrothermal systems to the extremely metal poor Southern Ocean. Moreover, the relative abundance of metals to each other is not universal. Such differences are primarily a result of the metal source, input rate, and the major ion (S, O, Cl) composition of their environment. Transition metals, in particular, exhibit diverse environmental behaviors and biological availability, with changes in oxidation state and affinity for non-metals combining to create a rich chemistry and diversity of uses.

It is thus not surprising that this diversity results in a plethora of metal geomes and metal biomes, with organisms exploiting and altering their metallo-environments. A research topic exploring current research themes in environmental aquatic bioinorganic chemistry should thus incorporate articles on a diverse range of subjects. We have been honored to include both reviews and original research articles that taken together, reflect the interdisciplinary nature of the subject area and the diversity of geomes and biomes in which inorganic elements, particularly metals, play a fundamental role.

We have thus been able to include articles on metals, their speciation, and interactions with phytoplankton (Cuss and Gueguen, 2012; Hassler et al., 2012; Shaked and Lis, 2012; Sunda, 2012), on metal acquisition and use by microbes (Barnett et al., 2012; Desai et al., 2012; Glass and Orphan, 2012; Morrissey and Bowler, 2012; Nuester et al., 2012; Scheidegger et al., 2012) and on the effect of inorganic ions in the environment on organism interactions and community structure (Boyd et al., 2012; Gledhill et al., 2012).

REFERENCES

- Barnett, J. P., Millard, A., Ksibe, A., Scanlan, D. J., Schmid, R., and Blindauer, C. A. (2012). Mining genomes of cyanobacteria for elements of zinc homeostasis. *Front. Microbiol.* 3:142. doi: 10.3389/fmicb.2012.00142
- Boyd, E., Fecteau, K., Havig, J., Shock, E., and Peters, J. W. (2012). Modeling the habitat range of phototrophic microorganisms in Yellowstone National Park: toward the development of a comprehensive fitness landscape. *Front. Microbiol.* 3:221. doi: 10.3389/fmicb.2012.00221
- Cuss, C., and Gueguen, C. (2012). Impacts of microbial activity on the optical and copper-binding properties of leaf-litter leachate. *Front. Microbiol.* 3:166. doi: 10.3389/fmicb.2012.00166
- Desai, D. K., Desai, F., and Laroche, J. (2012). Factors influencing the diversity of iron uptake systems in aquatic microorganisms. *Front. Microbiol.* 3:362. doi: 10.3389/fmicb.2012.00362
- Glass, J., and Orphan, V. J. (2012). Trace metal requirements for microbial enzymes involved in the production and consumption of methane and nitrous oxide. *Front. Microbiol.* 3:61. doi: 10.3389/fmicb.2012.00061
- Gledhill, M., Devez, A., Highfield, A., Singleton, C., Achterberg, E. P., and Schroeder, D. (2012). Effect of metals on the lytic cycle of the coccolithovirus, EhV86. *Front. Microbiol.* 3:155. doi: 10.3389/fmicb.2012.00155
- Hassler, C., Sinoir, M., Clementson, L., and Butler, E. C. V. (2012). Exploring the link between micronutrients and phytoplankton in the Southern Ocean during the 2007 austral summer. *Front. Microbiol.* 3:202. doi: 10.3389/fmicb.2012.00202
- Morrissey, J., and Bowler, C. (2012). Iron utilization in marine cyanobacteria and eukaryotic algae. *Front. Microbiol.* 3:43. doi: 10.3389/fmicb.2012.00043
- Nuester, J., Vogt, S., Newville, M., Kustka, A. B., and Twining, B. S. (2012). The unique biogeochemical signature of the marine diazotroph *Trichodesmium*. *Front. Microbiol.* 3:150. doi: 10.3389/fmicb.2012.00150
- Scheidegger, C., Suter, M. J.-F., Behra, R., and Sigg, L. (2012). Characterization of lead-phytochelatin complexes by nano-electrospray ionization mass spectrometry. *Front. Microbiol.* 3:41. doi: 10.3389/fmicb.2012.00041
- Shaked, Y., and Lis, H. (2012). Disassembling iron availability to phytoplankton. *Front. Microbiol.* 3:123. doi: 10.3389/fmicb.2012.00123
- Sunda, W. (2012). Feedback interactions between trace metal nutrients and phytoplankton in the ocean. *Front. Microbiol.* 3:204. doi: 10.3389/fmicb.2012.00204

Received: 28 March 2013; accepted: 08 April 2013; published online: 25 April 2013.

Citation: Gledhill M, Hassler CS and Schoemann V (2013) The environmental bioinorganic chemistry of aquatic microbial organisms. *Front. Microbiol.* 4:100. doi: 10.3389/fmicb.2013.00100

This article was submitted to *Frontiers in Microbiological Chemistry*, a specialty of *Frontiers in Microbiology*.

Copyright © 2013 Gledhill, Hassler and Schoemann. This is an open-access article distributed under the terms of the Creative Commons Attribution License, which permits use, distribution and reproduction in other forums, provided the original authors and source are credited and subject to any copyright notices concerning any third-party graphics etc.



Feedback interactions between trace metal nutrients and phytoplankton in the ocean

William G. Sunda*

National Ocean Service, National Oceanic and Atmospheric Administration, Beaufort, NC, USA

Edited by:

Martha Gledhill, University of Southampton, UK

Reviewed by:

Christel Hassler, University of Technology Sydney, Australia

Kenneth Bruland, University of California at Santa Cruz, USA

***Correspondence:**

William G. Sunda, National Ocean Service, National Oceanic and Atmospheric Administration, 101 Pivers Island Road, Beaufort, NC 28512, USA.
e-mail: bill.sunda@noaa.gov

In addition to control by major nutrient elements (nitrogen, phosphorus, and silicon) the productivity and species composition of marine phytoplankton communities are also regulated by a number of trace metal nutrients (iron, zinc, cobalt, manganese, copper, and cadmium). Of these, iron is most limiting to phytoplankton growth and has the greatest effect on algal species diversity. It also plays an important role in limiting di-nitrogen (N_2) fixation rates, and thus is important in controlling ocean inventories of fixed nitrogen. Because of these effects, iron is thought to play a key role in regulating biological cycles of carbon and nitrogen in the ocean, including the biological transfer of carbon to the deep sea, the so-called biological CO_2 pump, which helps regulate atmospheric CO_2 and CO_2 -linked global warming. Other trace metal nutrients (zinc, cobalt, copper, and manganese) have lesser effects on productivity; but may exert an important influence on the species composition of algal communities because of large differences in metal requirements among species. The interactions between trace metals and ocean plankton are reciprocal: not only do the metals control the plankton, but the plankton regulate the distributions, chemical speciation, and cycling of these metals through cellular uptake and recycling processes, downward flux of biogenic particles, biological release of organic chelators, and mediation of redox reactions. This two way interaction has influenced not only the biology and chemistry of the modern ocean, but has had a profound influence on biogeochemistry of the ocean and earth system as a whole, and on the evolution of marine and terrestrial biology over geologic history.

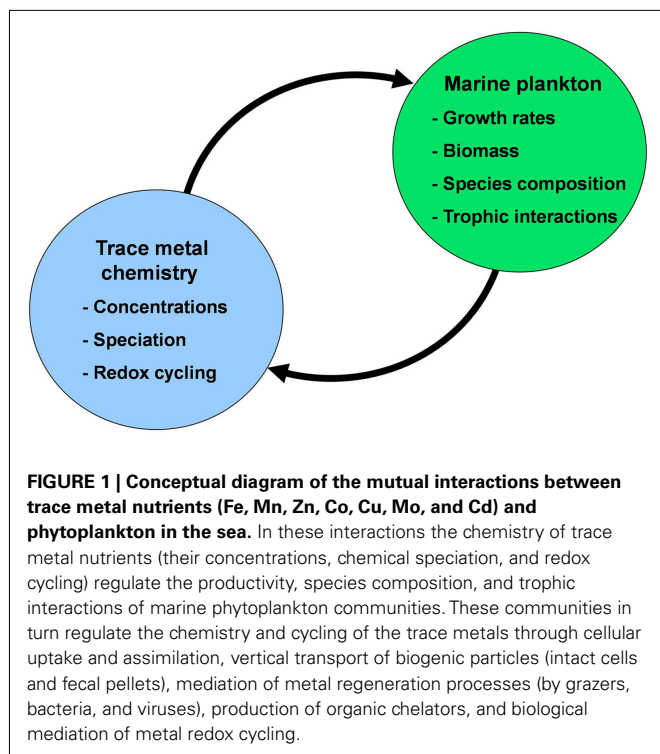
Keywords: Phytoplankton, trace metal nutrients, iron, zinc, cobalt, manganese, cadmium, trace metal chemistry

INTRODUCTION

Life in the ocean is dependent on fixation of carbon (C) and nitrogen (N) by planktonic microalgae, ranging in diameter from <1 to $>100\ \mu\text{m}$. These “phytoplankton” consist of eukaryotic algae, which photosynthetically fix carbon dioxide (CO_2) into organic matter, and cyanobacteria that fix CO_2 and also fix di-nitrogen (N_2) to form ammonium. They make up less than 1% of the plant biomass on earth, but account for almost 50% of global primary production (Field et al., 1998) and are a major source of trace gases such as dimethylsulfide that influence climate (Charlson et al., 1987; Andreae and Crutzen, 1997). Up until the ground breaking experiments of John Martin (Martin and Fitzwater, 1988; Martin et al., 1991), the growth of marine phytoplankton was thought to be primarily limited by the availability of the major nutrient nitrogen and to a lesser extent phosphorus. However, numerous iron-addition experiments in bottles and in mesoscale patches of surface seawater in the ensuing decades have demonstrated that the trace metal nutrient iron limits the growth of phytoplankton and regulates their species composition in 30–40% of the world ocean, especially in high nitrate-low chlorophyll (HNLC) regions: the Southern Ocean, the equatorial and subarctic Pacific, and some coastal upwelling systems (Hutchins et al., 2002; Moore et al., 2002, 2004; Coale et al., 2004; Boyd et al., 2007). In addition, there is substantial evidence that iron limits the fixation of N_2 by

cyanobacteria in the ocean, and thus, controls oceanic inventories of biologically available fixed nitrogen (Rueter, 1983; Falkowski, 1997; Wu et al., 2000; Sohm et al., 2011). Several other trace metal nutrients (zinc, cobalt, manganese, and copper) have also been shown to stimulate phytoplankton growth in bottle incubation experiments with natural ocean water, but their effects are usually less substantial than those for iron (Coale, 1991; Crawford et al., 2003; Franck et al., 2003; Saito et al., 2005). However, these metals may play important roles in regulating the species composition of phytoplankton communities because of large differences in cellular trace metal concentrations and growth requirements among species (Brand et al., 1983; Sunda and Huntsman, 1995a,b; Crawford et al., 2003; Ho et al., 2003).

In this review, I will discuss interactions between trace metal nutrients [iron (Fe), zinc (Zn), cobalt (Co), manganese (Mn), copper (Cu), nickel (Ni), cadmium (Cd), and molybdenum (Mo)] and phytoplankton in the ocean. These interactions involve not only the effect of the metals on the growth and species composition of phytoplankton communities, but also the profound effect of marine plankton on the distribution, speciation chemistry, and biological availability of these nutrient metals (Figure 1). There are many aspects to consider in these interactions, including (1) the distribution of metal nutrients in the ocean on various temporal and spatial scales; (2) the sources, sinks, and cycling of metals; (3)



metal speciation and redox cycling, (4) the influence of these metals on phytoplankton metabolism and growth at different levels of biological organization (molecular, cellular, population, community, ecosystem, ocean/earth system), and (5) the influence of phytoplankton and the planktonic community as a whole on the chemistry and cycling of metal nutrients in the ocean.

METAL DISTRIBUTIONS IN THE OCEAN

The distribution patterns of trace metal nutrients in the ocean have a profound influence on phytoplankton communities. Concentrations of filterable Fe and Zn (that which passes through a 0.2 or 0.4 μm -pore filter) are often extremely low (0.02–0.1 nM) in surface open ocean waters (Bruland, 1980; Martin et al., 1989; Johnson et al., 1997). Filterable concentrations of Cd, a nutrient analog for Zn, can reach values as low as 0.002–0.004 nM in surface waters of the North Pacific and Atlantic Oceans (Bruland, 1980; Bruland and Franks, 1983; Table 1). Filterable levels of these and other trace metal nutrients can increase by orders of magnitude in surface transects from the open ocean to coastal and estuarine waters owing to metal inputs from continental sources: rivers, ground water, aeolian dust, and coastal sediments (Bruland and Franks, 1983; Sunda, 1988/89). Filterable Fe can reach micromolar levels in estuaries and 10–20 μM in high humic rivers, 1000 to 10,000-fold higher than concentrations in surface ocean waters. Filterable iron in rivers occurs largely as colloidal particles (0.02–0.4 μm diameter), which are rapidly lost from estuarine and coastal waters via salt-induced coagulation and particulate settling (Boyle et al., 1977). Because of this efficient removal, much of the iron in rivers is deposited in estuarine and coastal sediments, and little directly reaches the open sea. However, reducing conditions in organic-rich shelf and margin sediments can re-mobilize some of

the river-derived particulate Fe via reduction to soluble Fe(II), and thereby provide an important Fe source to the ocean (Moore and Braucher, 2008). Another equally if not more important source of iron to the ocean is aeolian deposition of iron-containing mineral dust transported by the wind from arid regions (Duce and Tindale, 1991; Jickells et al., 2005). These aeolian inputs change seasonally with variations in rainfall and prevailing winds and are highest in waters downwind of deserts (Measures and Vink, 1999; Jickells and Spokes, 2001). Regions far removed from aeolian and sedimentary continental sources, such as the South Pacific and Southern Ocean receive low external iron inputs and are among the most iron-limited areas of the oceans (Martin et al., 1990; Behrenfeld and Kolber, 1999; Coale et al., 2004). Other external sources such as glaciers/iceberg melt, seasonal sea ice melting, island wakes, volcanism, and hydrothermal activity can provide important local inputs of iron and other metals (Boyd and Ellwood, 2010).

Because of the much lower trace metal concentrations in the open ocean relative to those in coastal waters, oceanic algal species have evolved the ability to grow at much lower external and intracellular concentrations of Fe, Zn, and Mn (Brand et al., 1983; Brand, 1991; Sunda and Huntsman, 1986, 1992, 1995a,b). In doing so they have been forced to rearrange their metabolic architecture (e.g., by decreasing the abundance of iron-rich protein complexes [photosystem I and the cytochrome b_6/f complex] in photosynthesis; Strzepek and Harrison, 2004), by switching from iron-containing enzymes to less carbon-efficient metal free enzymes (the replacement of ferredoxin by flavodoxin in photosynthetic electron transport (La Roche et al., 1996) and N_2 -fixation (Saito et al., 2011), or by switching from scarce metals to more-abundant ones in some critical metalloenzymes [e.g., the replacement of cytochrome c_6 which contains iron with the copper protein plastocyanin in photosynthetic electron transport (Peers and Price, 2006)]).

Residence times of trace metal nutrients in the ocean vary over a wide range – from 20 to 40 years for Mn (Landing and Bruland, 1987; Bruland et al., 1994) to ~800,000 years for Mo (Emerson and Husted, 1991; Morford and Emerson, 1999). Concentrations of Zn, Cd, Ni, and Cu, which have intermediate to long residence times (3000–100,000 years; Bruland and Lohan, 2003) relative to the average ventilation time of ocean water (~1000 years for deep ocean water), increase with depth, similar to increases observed for major nutrients (nitrate, phosphate, and silicic acid; Figures 2 and 3). In the northeast Pacific, filterable concentrations of Zn and Cd increase by 80-fold and 400-fold, respectively, between the surface and 1000 m (Bruland, 1980). The similarity between vertical profiles of trace metal nutrients and those of major nutrients suggest that both sets of nutrients undergo similar biological uptake and regeneration processes in which each is taken up by phytoplankton in sunlit surface waters and are thereby efficiently removed from solution. Much of these assimilated metals and major nutrients are recycled within the euphotic zone by the coupled processes of zooplankton grazing and excretion, viral lysis of cells, and bacterial degradation of organic materials (Hutchins et al., 1993; Hutchins and Bruland, 1994; Poorvin et al., 2004; Strzepek et al., 2005; Boyd and Ellwood, 2010). However, a portion of the assimilated metals and major nutrients is continuously lost from the euphotic zone by vertical settling of biogenic particulate matter, including intact

Table 1 | Organic complexation of Fe, Cu, Zn, and Cd in filtered (0.4 μ m) surface and deep waters of the Northeast Pacific Ocean (n.d. – not detected, n.c. – not computed).

Metal	Depth (m) (Obs.)	Total M (nM)	L1 (nM) L2 (nM)	Log $K_{L1,M'}$ Log $K_{L2,M'}$	–log [M']	Percent total metal			Reference
						(M')	ML ₁	ML ₂	
Fe	20–300 (6)	0.22 \pm 0.07	0.48 \pm 0.07 1.47 \pm 0.07	13.04 \pm 0.16 11.49 \pm 0.10	13.2 \pm 0.2	0.03 \pm 0.01	86.5 \pm 2.7	13.5 \pm 2.7	Rue and Bruland (1995)
	500–2000 (3)	0.72 \pm 0.05	n.d. 2.57 \pm 0.21	n.d. 11.58 \pm 0.16	12.0 \pm 0.2	0.15 \pm 0.06	n.d.	99.8 \pm 0.1	Rue and Bruland (1995)
Cu	25–120* (18)	0.53 \pm 0.07	1.77 \pm 0.56 5.7 \pm 2.8	11.58 \pm 0.30 8.72 \pm 0.46	11.9 \pm 0.2	0.31 \pm 0.24	98.8 \pm 0.9	0.9 \pm 0.7	Coale and Bruland (1990)
Zn	22–200 (9)	0.23 \pm 0.07	1.15 \pm 0.19	10.66 \pm 0.13	11.3 \pm 0.3	2.6 \pm 1.0	97.4 \pm 1.0	n.d.	Bruland (1989)
	600 (1)	4.77	n.c.	n.c.	8.5	73.4	26.6	n.d.	Bruland (1989)
Cd	22–100 (8)	0.003 \pm 0.001	0.08 \pm 0.03	10.40 \pm 0.22	12.0 \pm 0.2	36.6 \pm 12.5	63.4 \pm 12.5	n.d.	Bruland (1992)
	600 (2)	0.78	n.d.	n.d.	9.0 \pm 0.0	100	n.d.	n.d.	Bruland (1992)

*Near-surface values only are given because of a potential problem with the differential pulse anodic stripping titration data in the deep water samples (Moffett and Dupont, 2007).

algal cells, zooplankton fecal pellets, and organic detritus. The macro- and micro-nutrients contained in these settling biogenic particles are then returned to solution in non-lit deeper waters by bacterial degradation processes, with the rate of this regeneration decreasing exponentially with water depth. Over time the uptake, settling, and regeneration processes deplete trace metal and major nutrients in sunlit surface waters to low levels and increase concentrations at depth at elemental ratios equal to average values in phytoplankton. This set of processes also transfers CO₂ to the deep sea and is important in regulating atmospheric CO₂ concentrations (Sigman and Boyle, 2000). The cycle is completed when the nutrient and CO₂ reservoirs in deeper waters are returned to the surface via vertical mixing and advection (upwelling) processes.

Based on the above dynamics, the plots of trace metal nutrients with longer residence times (Cu, Zn, Ni, and Cd) vs those of major nutrients (e.g., phosphate) should have slopes equal the average ratios of trace metals to major nutrients in marine plankton. Such behavior was previously demonstrated for depth dependent plots of nitrate vs phosphate concentrations in which the slope of these relationships (16 mol mol^{–1}) equaled the average N:P measured in ocean plankton (Redfield et al., 1963). Similar behavior has been observed for plots of Zn, Cd, Ni, and Cu vs phosphate, but with several caveats (Martin et al., 1976; Sunda and Huntsman, 1992, 1995c, 2000; Croot et al., 2011; Figure 4). In depth profiles for the northeastern Pacific (Figure 2), the concentrations of three of the metals (Ni, Cu, Cd) within the nutricline are linearly related to those of phosphate, and for Cu and Cd, the metal:P slopes (or equivalent metal:C ratios) agree well with values measured in net plankton samples or in algae cultured at the concentration of unchelated metal [M'] (or other controlling metals in the case of Cd) observed in the sunlit surface layer (Figures 4B,C; Table 2). However, unlike N vs P plots, these relationships have positive

γ -intercepts for Cu and Ni, indicating that these metals are not completely “used up” biologically in N- and P-depleted surface waters. By contrast, the Zn:P relationship exhibits increasing slopes with increasing Zn concentrations and a negative γ -intercept for a linear regression of Zn vs P (Figure 4A; Table 2). Here the Zn:P slope (and associated Zn:C molar ratio) in the productive surface layer (0–185 m) agrees with Zn:P and Zn:C values for marine algae grown at the measured [Zn'] range within the surface layer (Tables 1 and 2; Figure 5) and the Zn:C ratio (3.7 μ mol mol^{–1}) in phytoplankton growing in near-surface seawater in the northeast Pacific (Lohan et al., 2005). However at greater depths (185–800 m), the Zn:P slope and associated Zn:C ratio (22 μ mol mol^{–1}) is similar to average values for phytoplankton growing at the much higher [Zn'] range observed at depth (Sunda and Huntsman, 1992; Table 2; Figure 5).

The non-linearity of the Zn vs P plots likely reflects the very large variation in [Zn'] in ocean waters and the associated variation in Zn:P and Zn:C ratios in phytoplankton growing in these waters (Sunda and Huntsman, 1992). Although waters with high [Zn'] are usually found below the photic zone, and thus, cannot influence the removal of metals by algal growth and uptake, thermohaline and wind-driven upwelling can bring these high-nutrient, high-zinc waters to the surface, especially in polar regions. As a consequence of these processes, filterable Zn in surface waters of the Atlantic sector of the Southern Ocean increased from 0.5 nM at a latitude of 46°S to 4.5 nM at 66°S along with increases in phosphate and nitrate (Croot et al., 2011). The [Zn'] in surface waters increased to as high 1.8 nM, as the zinc concentration exceeded that of strong Zn binding ligands (Baars and Croot, 2011), a value \sim 400-fold higher than mean surface [Zn'] in the North Pacific (Table 1). Subsequently, the lateral changes in nutrient and metal concentrations in these near-surface waters caused by algal uptake,

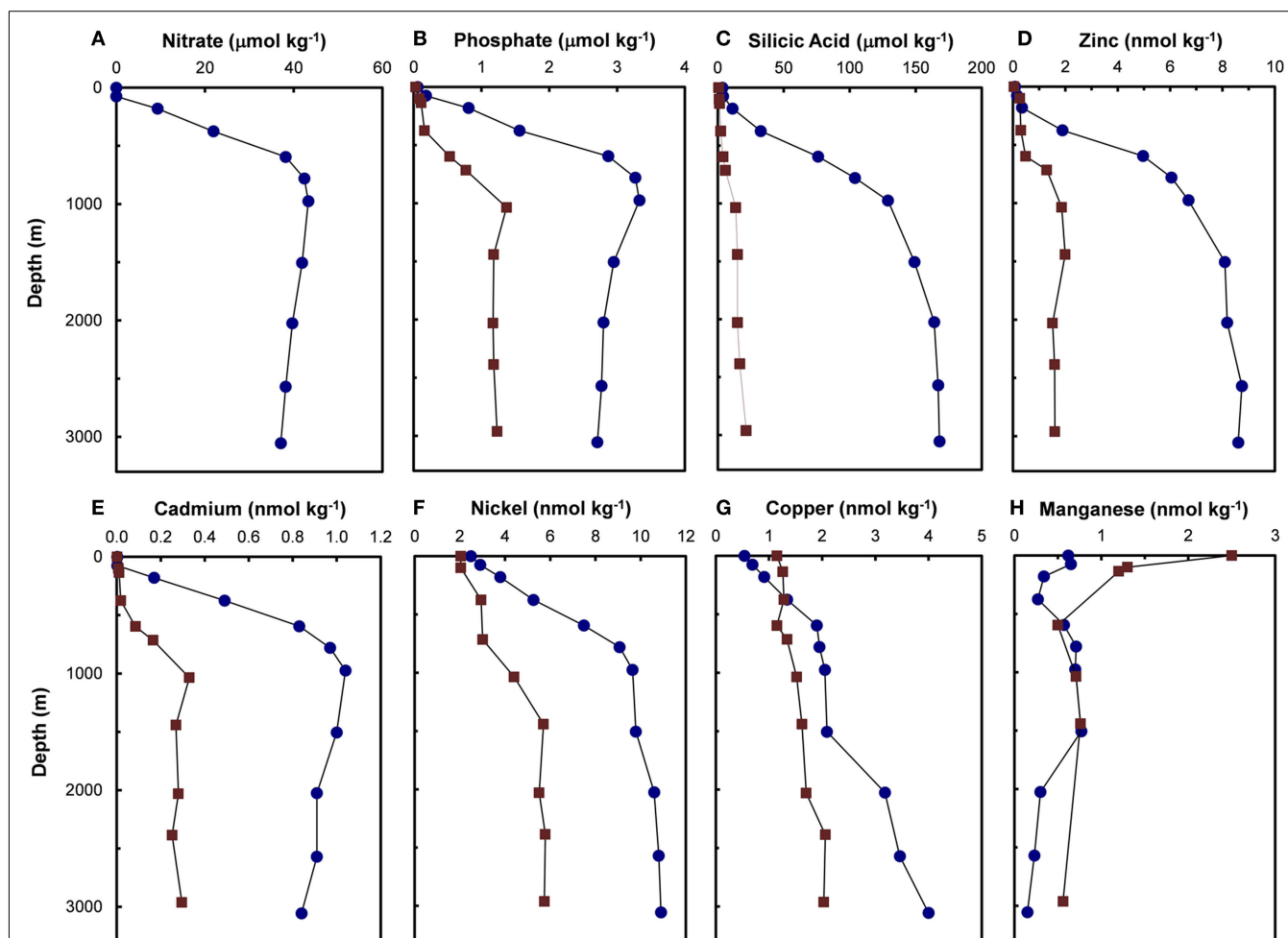


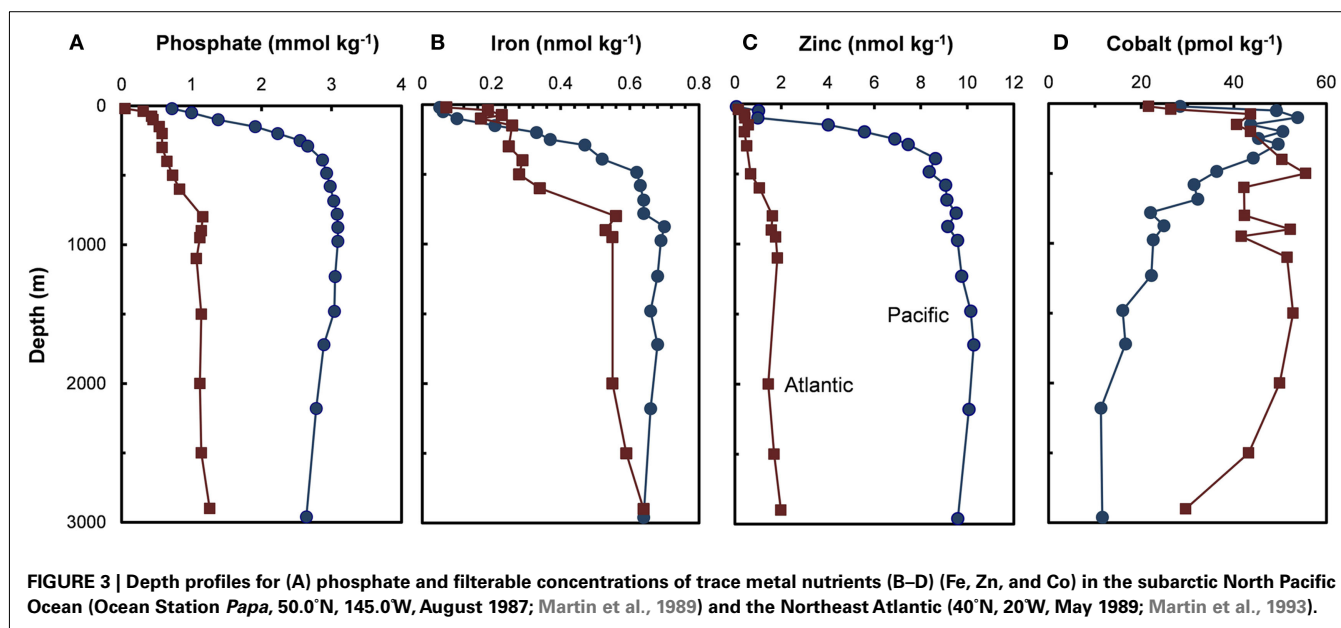
FIGURE 2 | Depth profiles for major nutrients (A–C) [nitrate (Pacific only), phosphate, and silicic acid] and filterable concentrations (that passing a 0.4- μm filter) of trace metal nutrients (D–H) (Zn, Cd, Ni, Cu, and Mn) in the central North Pacific (●, 32.7°N, 145.0°W, September 1977) and North Atlantic (■, 34.1°N, 66.1°W, July 1979; Bruland and Franks, 1983). Manganese concentrations in the Pacific were analyzed in acidified, unfiltered seawater samples.

biogenic particulate settling, and net regeneration in deeper waters are transposed to deeper depths and more northern latitudes with downwelling and lateral advection, which is most intense during winter (Redfield et al., 1963). In this way near-surface processes of algal uptake, settling, and shallow water regeneration can influence the composition and vertical structure of major and trace metal nutrients in deep ocean waters worldwide. Indeed, at depths at and just above the phosphate maximum in the Atlantic Ocean (600–800 m; see **Figures 2B** and **3A**), about half of the phosphate occurs as “preformed phosphate,” which was present when the water originally subducted from the surface to form the Antarctic Intermediate water layer, while the remainder occurs as regenerated phosphate (Redfield et al., 1963). Likewise, only a portion of the trace metal nutrients at depth are likely derived from regeneration of settling biogenic particles, while the remainder must occur as “preformed metal nutrients.”

The deep water concentrations of both major nutrient elements (N, P, and Si) and many longer-lived metal micro-nutrients (Zn, Cd, Ni, and Cu) are two- to fivefold higher in deep waters of the

North Pacific than the North Atlantic (**Figures 2** and **3**) because of large scale differences in the thermohaline circulation patterns between the Atlantic and Pacific oceans. In the Pacific the major water inflow occurs at depth where concentrations of nutrients and longer-lived nutrient metals are high (Broecker, 1991). Consequently, the Pacific acts as a nutrient trap and concentrates high levels of nutrients and longer-lived nutrient metals in its deeper waters (Broecker, 1991). The Atlantic, by contrast, has the opposite circulation pattern, with its major inflow at the surface where nutrients and metals are depleted, and its major outflow at depth, the North Atlantic Deep water. As might be expected, this circulation pattern tends to lower deep water concentrations of major nutrients and longer-lived nutrient metals.

Two trace metal nutrients with short ocean residence times (Mn and Co), show the opposite pattern to Cu, Zn, Cd, and Ni, and have highest concentrations at or near the surface and lower deep water concentrations in North Pacific than in the North Atlantic (**Figures 2H** and **3D**; Landing and Bruland, 1987; Jickells and Burton, 1988; Martin et al., 1989). The short residence times and



low concentrations in the older deep waters of the North Pacific are due to bacterially catalyzed oxidation of soluble Mn(II) and Co(II) to insoluble Mn(III and IV) and Co(III) oxides, and subsequent removal via particulate aggregation and settling as the water advects along its flow path. Likewise, iron is scavenged from deep ocean waters by oxide formation and adsorption onto particles, but it is also avidly taken up by phytoplankton in surface waters. It has moderately short residence times (~70–200 years) and shows similar deepwater concentrations in the North Atlantic and Pacific (Johnson et al., 1997; **Figure 3B**). It exhibits surface depletion and increasing concentrations with depth in iron-limited regions such as the subarctic Pacific and northeast Atlantic during spring (**Figure 3B**), but can show pronounced surface maxima in stratified ocean waters receiving high aeolian inputs (Bruland et al., 1994; Measures and Vink, 1999).

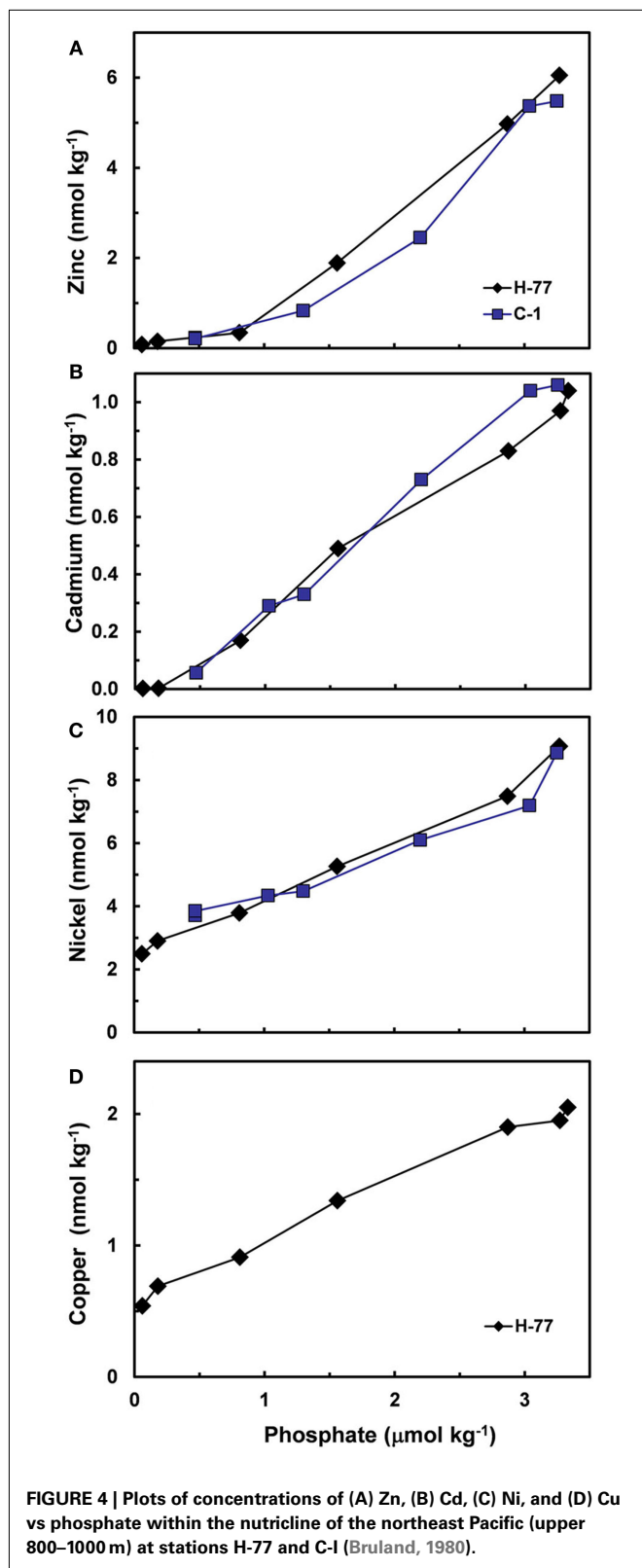
In contrast to the other nutrient metals, Mo occurs at essentially the same concentration (100–110 nM) independent of depth or ocean basin (Collier, 1985). Its concentration is roughly proportional to salinity and its lack of depletion in surface waters indicates minimal removal of Mo by marine plankton relative to its seawater concentration, which is orders of magnitude higher than surface levels of other trace metal nutrients (**Figures 1 and 2**).

COMPLEXATION AND REDOX CHEMISTRY

Trace metal nutrients in the ocean exist as a variety of different chemical species and forms, which strongly influences their biological uptake and biogeochemical cycling. All but Mo occur as cationic metal ions that are complexed to varying degrees by inorganic and organic ligands or are adsorbed onto or bound within various abiotic and biotic particles. Many of these metals (Fe, Cu, Mn, and Co) occur in different oxidation states, which have different solubilities, binding strengths with organic ligands, ligand exchange kinetics, and biological availabilities. Consequently, the redox chemistry of these metals has a major influence on their chemical behavior, biological uptake, and biogeochemical cycling.

Ni, Zn, and Cd exist in oxygenated seawater as soluble divalent cations that are complexed to varying degrees by inorganic ligands (Cl^- , OH^- , and CO_3^{2-} ; Byrne et al., 1988) and organic chelators. Only a small percentage of Ni is complexed by organic ligands (0–30%; Saito et al., 2004), while ~97% of the filterable zinc (Bruland, 1989) and ~63% of filterable cadmium (Bruland, 1992) is chelated in North Pacific surface waters by unidentified strong organic ligands present at low concentrations (**Table 1**). Similar strong chelation of Zn has been observed in the North Atlantic and in subantarctic waters (Ellwood and van den Berg, 2000; Ellwood, 2004). Based on Zn concentrations in filtered surface waters from the North Pacific (0.06–0.9 nM; Bruland, 1980) and organic complexation data (Bruland, 1989), the concentration of biologically available dissolved inorganic zinc species (Zn') can be as low as 1–2 pM in surface ocean water, low enough to limit the growth of at least some algal species (Sunda and Huntsman, 1992, 1995a). However, in deep ocean waters (Bruland, 1989), and upwelled surface waters in the Southern Ocean (Baars and Croot, 2011), Zn concentrations exceed the concentration of strong Zn binding ligands, resulting in up to 1000-fold increases in Zn' levels (**Table 1**).

Manganese exists in seawater in three oxidation states: Mn(II), Mn(III), and Mn(IV). Insoluble Mn(III) and Mn(IV) oxides are the stable redox forms of this metal in oxygenated seawater, although Mn(III) also occurs as soluble chelates with organic ligands in some environments (e.g., hypoxic waters; Trouwborst et al., 2006). These oxides can be reduced chemically and photochemically to dissolved Mn(II), which is highly soluble and is not bound appreciably by organic ligands (Sunda and Huntsman, 1994). Although Mn(II) is unstable with respect to oxidation by molecular oxygen (O_2), the chemical kinetics of this reaction are exceedingly slow in seawater (with a half life of 500 years at pH 8.1), allowing Mn(II) to persist despite its thermodynamic instability (Morgan, 1967). Enzymes present within the outer polysaccharide sheath of certain bacteria, catalyze Mn(II) oxidation to Mn(IV)



oxides (Tebo et al., 2004; Anderson et al., 2009), a reaction which appears to account for virtually all Mn(II) oxidation in marine waters (Emerson et al., 1982; Sunda and Huntsman, 1988). The

bacterial formation of Mn oxides, and their subsequent removal via particle settling results in short residence times and low-Mn concentrations in deep ocean waters as noted earlier (Figure 2H). In the ocean's surface mixed layer, oxidation is greatly diminished owing to photo-inhibition of the Mn-oxidizing bacteria while Mn oxides are dissolved by photo-reduction to Mn(II; Sunda and Huntsman, 1988, 1994; Moffett, 1990). In the southwestern Sargasso Sea, Mn oxidation rates increased from undetectable levels ($<0.2\%$ day $^{-1}$) in the surface mixed layer to 3.3% day $^{-1}$ at 160 m just below the chlorophyll maximum (Sunda and Huntsman, 1988). By contrast, estimated rates of Mn oxide reductive dissolution decreased from $\sim 70\%$ to 8.5% day $^{-1}$ over this same depth interval. The combination of decreased Mn(II) oxidation rates and increased rates of Mn oxide reductive dissolution caused a large decrease in Mn oxide concentration between 160 m and the surface and a concomitant four- to fivefold increase in dissolved Mn(II). Similar high concentrations of dissolved Mn(II) in surface seawater are widespread in the ocean (Figure 2H), enhancing the supply of Mn needed to support algal photosynthesis (Sunda and Huntsman, 1988).

The chemical behavior of iron, biologically the most important trace metal nutrient, is arguably the most complex. In oxygenated seawater its stable oxidation state Fe(III) forms sparingly soluble iron hydroxide and oxide precipitates, whose solubility, lability, and biological availability decreases with oxide aging (Wells et al., 1991; Kuma et al., 1996; Lui and Millero, 2002; Yoshida et al., 2006). This oxide formation and the tendency of ferric ions to adsorb onto particle surfaces results in low deep ocean concentrations (0.4–0.8 nM; Johnson et al., 1997; Boyd and Ellwood, 2010) despite iron's high crustal abundance (it is the fourth most abundant element by weight). Most ($>99.9\%$) of the filterable Fe(III) in seawater is strongly bound to complex mixtures of organic ligands (Gledhill and van den Berg, 1994; Rue and Bruland, 1995; Buck and Bruland, 2007; Gledhill and Buck, 2012). This organic complexation minimizes iron adsorption and precipitation, and thus reduces iron removal from seawater by particulate scavenging processes (Johnson et al., 1997). Titrations utilizing ligand competition/cathodic stripping voltammetry reveal two classes of iron chelating ligands in near-surface seawater, a high-affinity class (L_1) and lower affinity class (L_2), with most of the filterable iron bound to the L_1 class (Rue and Bruland, 1995; Cullen et al., 2006; Table 1). However in deeper water (≥ 500 m) only L_1 class ligands are detected (Table 1), suggesting that they are produced by biological processes in the productive surface layers of the ocean. The two ligand classes and their iron chelates exist in both soluble (i.e., dissolved) and colloidal (0.02–0.4 μ m size range) phases, with most of the ligands present in the soluble phase and some of the colloidal iron being inert to ligand exchange (Wu et al., 2001; Cullen et al., 2006).

The identity of the two ligand classes is yet to be determined (Vraspir and Butler, 2009; Gledhill and Buck, 2012). Many of the high-affinity ligands may be bacterial siderophores, strong ferric chelators produced by bacteria to solubilize iron and facilitate its intracellular uptake (Macrellis et al., 2001). Individual siderophores, largely in the hydroxamate class, have been identified in ocean waters, but their concentrations account for only a few percent of the strong iron-binding ligands (Mawji et al., 2008,

Table 2 | Comparison of slopes of nutrient metal to phosphate plots for station H-77 (Bruland, 1980) in the northeast Pacific with metal:P ratios in net plankton (Martin et al., 1976) and metal:C ratios in cultured marine algae.

Metal	Depth range (m)	P range (μM)	M vs P slope (mmol mol^{-1})	Intercept (nM)	R^2 (n)	M:P of net plankton (mmol mol^{-1})	M:C from slopes* ($\mu\text{mol mol}^{-1}$)	M:C in cultured algae
Zn	185–780	0.81–3.27	2.32 ± 0.06	-1.62 ± 0.14	0.998 (4)	1.9 ± 1.6	22.2 ± 0.6	
	0–185	0.06–0.81	0.33 ± 0.04	0.07 ± 0.02	0.987 (3)		3.1 ± 0.4	$3.7(2.2\text{--}5.5)^{\dagger}$
Cd	75–975	0.18–3.33	0.32 ± 0.01	-0.06 ± 0.03	0.994 (6)	0.43 ± 0.14	3.0 ± 0.1	$2.5\text{--}4.1^{\dagger}$
Ni	0–780	0.06–3.27	1.93 ± 0.10	2.36 ± 0.20	0.989 (6)	0.47 ± 0.26	18.2 ± 1.0	
Cu	0–975	0.06–3.33	0.44 ± 0.02	0.57 ± 0.04	0.992 (7)	0.41 ± 0.13	4.2 ± 0.2	$4.4 \pm 0.6^{\S}$

*Based on a C:P for marine plankton of 106 (Redfield et al., 1963).

[†]Mean and range based on mean and range of $[\text{Zn}']$ computed from the Zn chelation data of Bruland (1989; see Table 1) and the Zn:C vs $[\text{Zn}']$ relationship for the oceanic diatom *Thalassiosira oceanica* (Figure 5).

[§]Based on the mean Cu:C in the diatoms *T. oceanica* and *T. pseudonana*, and the coccolithophore *Emiliana huxleyi* at the mean $\log [\text{Cu}']$ in northeast Pacific ocean water (-11.8 , see Table 1; Sunda and Huntsman, 1995c).

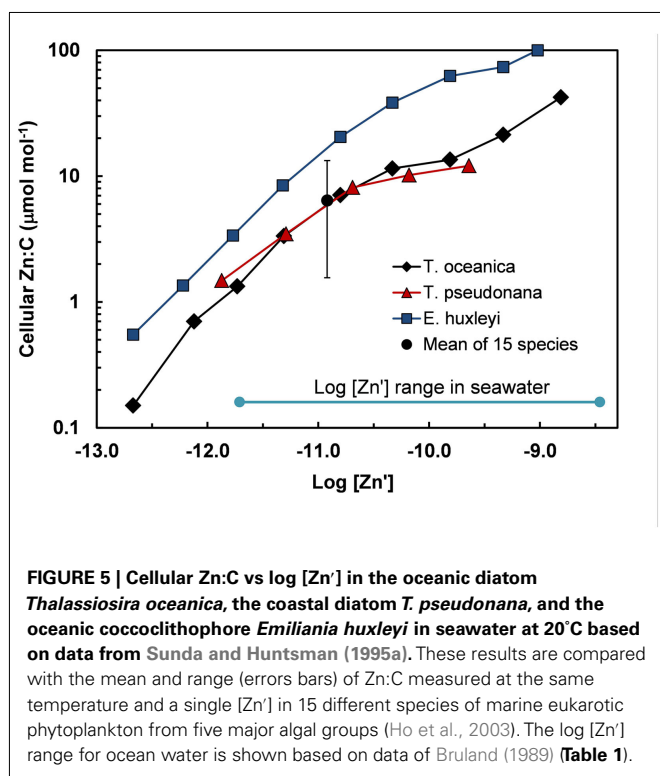
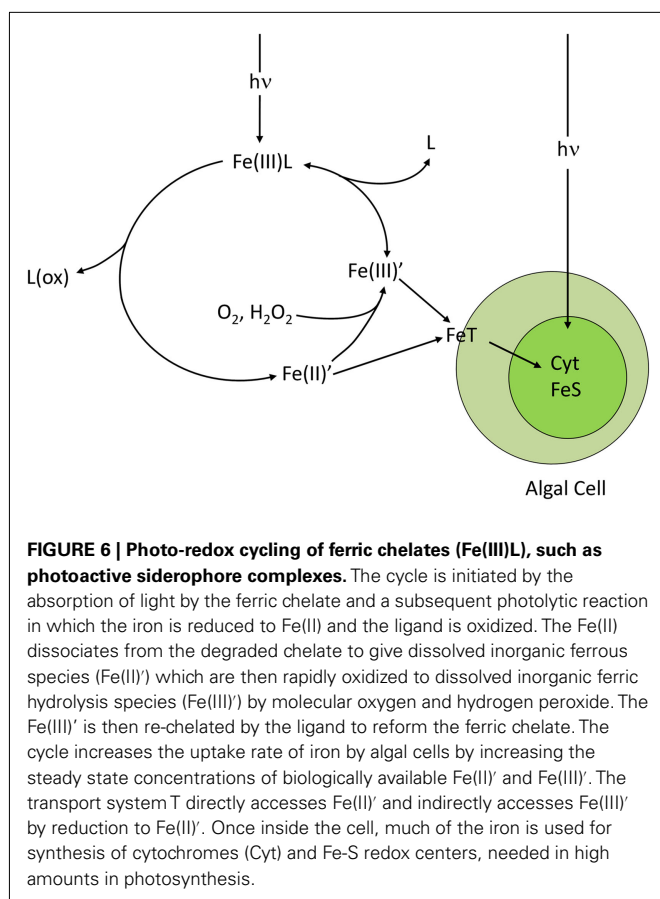


FIGURE 5 | Cellular Zn:C vs $\log [\text{Zn}']$ in the oceanic diatom *Thalassiosira oceanica*, the coastal diatom *T. pseudonana*, and the oceanic coccolithophore *Emiliana huxleyi* in seawater at 20°C based on data from Sunda and Huntsman (1995a). These results are compared with the mean and range (errors bars) of Zn:C measured at the same temperature and a single $[\text{Zn}']$ in 15 different species of marine eukaryotic phytoplankton from five major algal groups (Ho et al., 2003). The $\log [\text{Zn}']$ range for ocean water is shown based on data of Bruland (1989) (Table 1).

2011; Velasquez et al., 2011). The low measured abundance of identifiable siderophores, however, may largely reflect our inability to quantitatively isolate other more-abundant classes of marine siderophores (e.g., catecholates and carboxylates) or reflect the presence of a large number of yet to be identified siderophores released by marine bacteria (Velasquez et al., 2011; Gledhill and Buck, 2012). There is also evidence that humic substances comprise at least some of the iron-binding ligands in coastal and deep ocean water and that many of these ligands may be derived from rivers and sedimentary sources (Laglera and van den Berg, 2009; Laglera et al., 2011). Other iron ligands with weak to moderate binding strengths are released from biological sources (e.g., grazing, viral lysis, and algal or bacterial secretion) and include

porphyrins (Hunter and Boyd, 2007; Vong et al., 2007), acidic polysaccharides (Hassler et al., 2011a,b), and secreted chelating compounds such as domoic acid (Rue and Bruland, 2001).

Ferric iron can be reduced in seawater to highly soluble Fe(II) (ferrous iron) by several processes, including, biological reduction at cell surfaces (Maldonado and Price, 2001; Shaked et al., 2005), direct photolysis of ferric chelates (Kuma et al., 1992; Barbeau et al., 2001; Barbeau, 2006), reduction by photochemically or biologically produced superoxide radicals (O_2^- ; Voelker and Sedlak, 1995; Rose et al., 2005; Kustka et al., 2005), or reduction within O_2 depleted zones in organic particles or aggregates (Balzano et al., 2009). As a result up to 64% of the filterable iron in near-surface seawater occurs as Fe(II), with the highest percentage observed during daytime near the surface, suggesting a largely photochemical or algal source (Waite et al., 1995; Croot et al., 2008; Roy et al., 2008; Shaked, 2008; Sarthou et al., 2011). Because Fe(II) binds much more weakly to organic ligands than Fe(III) and because direct photolysis of ferric chelates involves oxidation and degradation of the ligand, the photo-reduction or biological reduction of chelated-Fe(III) often results in dissociation of Fe(II) from the chelate (Barbeau, 2006; Figure 6). The resulting soluble Fe(II) is unstable in the presence of O_2 , and is re-oxidized to dissolved Fe(III) hydrolysis species $[\text{Fe}(\text{III})']$, which are then re-chelated by organic ligands (Sunda, 2001). Because $\text{Fe}(\text{II})'$ and $\text{Fe}(\text{III})'$ are continuously produced during redox cycling, elevated steady state concentrations of each are often established (Sunda and Huntsman, 2003), with Fe(II) residence times that increase with decreasing temperature, pH, and concentrations of oxidants (primarily O_2 ; Santana-Casiano et al., 2005). In air-equilibrated seawater at pH 8.0, computed residence times for $\text{Fe}(\text{II})'$ range from 3.2 h at 0°C to 2.2 min at 30°C (Santana-Casiano et al., 2005). There is evidence for Fe(II) chelation by unidentified organic ligands, which retards oxidation rates in some regions (Croot et al., 2008; Roy et al., 2008) and increases them in others (Roy and Wells, 2011), apparently linked to differences in the chemical nature of the complexing ligands. The nature and degree of organic complexation of Fe(II) needs to be quantified as it not only affects redox cycling of iron, but may also influence iron uptake by phytoplankton (Shaked and Lis, 2012).



Thus, iron undergoes a dynamic redox cycling in surface seawater, which can greatly enhance its biological availability to phytoplankton by increasing concentrations of highly available dissolved inorganic Fe(II)' and Fe(III)' species (Anderson and Morel, 1982; Sunda, 2001; Maldonado et al., 2005; Fan, 2008; **Figure 6**). The photochemical enhancement of iron uptake by phytoplankton increases with decreasing temperature because the photolysis of Fe(III) chelates should be largely insensitive to temperature while the oxidation rates of photochemically produced Fe(II) to dissolved Fe(III)' slows as does the re-chelation of Fe(III)' by organic ligands (Sunda and Huntsman, 2011; **Figure 6**). These slower reoxidation and re-chelation rates at lower temperatures increases the steady state concentrations of the highly biologically available Fe(II)' and Fe(III)' species in the presence of sunlight, as shown for ferric complexes with the synthetic chelator EDTA (Sunda and Huntsman, 2003, 2011). This enhanced photochemical effect should increase the availability of iron to phytoplankton in iron-limited polar regions such as the Southern Ocean, and without this effect, these regions might experience even more severe iron limitation.

Other micronutrient metals such as Cu and Co also exist in different oxidation states and are heavily chelated by organic ligands. Copper can exist in seawater as thermodynamically stable Cu(II), or as unstable Cu(I) (Moffett and Zika, 1988). Most (>99%) of the Cu in near-surface seawater is heavily chelated by strong organic ligands ($\log K_{\text{Cu}^{\text{II}}, \text{L1}} = 12\text{--}15$) present at low

concentrations (2–6 nM in open ocean waters), which decreases Cu(II)' concentrations to very low levels (0.001–10 pM; Coale and Bruland, 1990; Moffett, 1995; Moffett and Dupont, 2007; Buck et al., 2010; **Table 1**). Different electrochemical methods show consistent strong chelation of Cu in surface waters; however, in the deeper waters of the North Pacific (>200 m) the results diverge, with differential pulse anodic stripping voltammetry showing a complete loss of the strong L₁ ligand class at depths below 200 m, while ligand competition/cathodic stripping voltammetry shows continued strong complexation of copper by this ligand class down to at least 2500 m (Coale and Bruland, 1988, 1990; Moffett and Dupont, 2007). The reasons for these analytical differences are not known, but may be related to a change in the nature of the ligands and possibly the oxidation state of the bound copper between the surface and deeper waters (Moffett and Dupont, 2007).

Cu(II) can be reduced to Cu(I) by photochemical processes (Moffett and Zika, 1988), reduction at cell surfaces (Jones et al., 1987) or by reaction with chemical reducing agents, such as sulfur containing organic ligands (Leal and van den Berg, 1998). In surface waters, the resulting Cu(I) is re-oxidized by reaction with O₂ on time scales of minutes and steady state Cu(I) concentrations can comprise 5–10% of the filterable copper (Moffett and Zika, 1988; Sharma and Millero, 1988). However, the effect of this redox cycling on the biological availability of copper is not known.

The chemistry of cobalt is also highly complex. Cobalt exists in seawater as soluble Co(II) or as Co(III), which forms insoluble oxides at the pH of seawater. The formation of these oxides appears to be microbially mediated and may be largely responsible for the removal of this metal from deep ocean waters (Tebo et al., 1984; Moffett and Ho, 1996; **Figure 3D**). Much of the filterable Co in seawater (up to 100%) is strongly bound to organic ligands (Ellwood and van den Berg, 2001; Saito and Moffett, 2001; Saito et al., 2005). The conditional stability constant(s) for the Co complexes is extremely high ($10^{15.6}$ to $\geq 10^{16.8} \text{ M}^{-1}$), consistent with Co binding as kinetically inert Co(III) chelates (Saito et al., 2005).

CELLULAR UPTAKE PROCESSES

Trace metal nutrients, like major nutrients, are taken up intracellularly by specialized transport proteins on the cytoplasmic membrane of algal cells. Consequently, uptake rates generally follow Michaelis-Menten enzyme kinetics

$$\text{Uptake rate} = \frac{V_{\text{max}}[M]}{(K_s + [M])} \quad (1)$$

as observed for Mn, Fe, Zn, and Cu (Sunda and Huntsman, 1986, 1998a; Hudson and Morel, 1990; Lane et al., 2008; Guo et al., 2010). In Eq. 1 V_{max} is the maximum uptake rate, [M] is the concentration of chemical species that react with receptor sites on the transport protein (and thus are bioavailable by definition), and K_s is the [M] at which half of the transport sites are bound to the nutrient metal and the uptake rate is half of V_{max} . Virtually all of these proteins act as pumps and require energy for intracellular transport. With some exceptions, the binding of metals to the receptor sites on these proteins is determined by the concentration of free aquated metal ions or in many cases, the concentration of kinetically labile dissolved inorganic species, M' (aquated metal

ions and inorganic complexes with Cl^- , OH^- , and CO_3^{2-} ; Hudson and Morel, 1993; Sunda and Huntsman, 1998b). Thus, chelation by organic ligands generally decreases metal uptake and chemical speciation is extremely important in regulating the cellular uptake of metals (Hudson, 1998).

Although Eq. 1 is relatively simple, its application is not entirely straight forward. One complicating factor is that the relevant substrate concentration, $[\text{M}]$, is that at the surface of the cell membrane, which can be much less than that in bulk seawater in cases where the uptake rate approaches the maximum rate of diffusive flux of available metal species to the cell surface (Hudson and Morel, 1993). This indeed occurs for uptake of Zn and Co(II) by small diatoms and coccolithophores (3.5–6 μm diameter) at low Zn' and Co' concentrations (Sunda and Huntsman, 1995a; Figure 7). Since diffusive flux per unit of cell biovolume varies with the inverse square the cell diameter, diffusion limitation of uptake intensifies substantially as the cell size increases, and can be a major impediment for the uptake of some nutrient metals (Zn, Co, Fe) in larger cells (Hudson and Morel, 1993; Sunda and Huntsman, 1995a; Sunda, 2001). Another complicating factor is

that the V_{max} of metal uptake systems is often under negative feedback regulation by the cell and can decrease substantially with increases in $[\text{M}']$ and intracellular metal pools (Sunda and Huntsman, 1992, 1998b). This behavior can be particularly problematic in fitting Eq. 1 to the results of short-term metal uptake experiments as the V_{max} of the transport system investigated can vary during the course of the experiment (Sunda and Huntsman, 1985, 1986, 1992). A final complicating factor is that the values of K_s can increase and V_{max} decrease with increasing concentrations of competing metals that bind with and are taken up intracellularly by the transport system, as occurs for Cu, Cd, and Zn inhibition of Mn uptake and Cu inhibition of Zn uptake (Sunda and Huntsman, 1996, 1998c). All of these complicating factors must be taken into account for the proper application of the Michaelis-Menten equation to laboratory and field metal uptake data.

Uptake systems are highly variable and range from simple to highly complex depending on the chemical speciation of the metal, its biological demand (requirement) relative to its seawater availability, and the range of concentrations of available metal species. Uptake systems appear to be simplest for dissolved Mn(II), which is taken up in phytoplankton by a single high-affinity transport system ($K_s = 15\text{--}140 \text{ nM Mn}'$) that is under negative feedback regulation (Sunda and Huntsman, 1985, 1986). In this negative feedback, as the concentration of $\text{Mn(II)}'$ decreases, the V_{max} of the transport system is increased to maintain relatively constant Mn uptake rates and intracellular Mn concentration. This constant regulated cellular Mn level is two to four times higher than that needed to support the maximum growth rate, providing a buffer against decreasing Mn' concentrations ($[\text{Mn}']$) or increases in cellular demand, as occurs with decreasing light intensity (see below). At sufficiently low $[\text{Mn}']$ the V_{max} values reach a maximum constant value and the cellular Mn uptake rate and intracellular Mn concentration decreases with further decreases in $[\text{Mn}']$ causing Mn-limitation of growth rate.

Uptake systems for Zn, Cd, Co, and Cu are more complex. Like that of Mn(II), algal uptake of these metals is believed to be related to the concentration of dissolved inorganic metal species ($\text{M}' = \text{Zn}', \text{Cd}', \text{Co}', \text{and Cu}'$) and metal chelates are generally not directly available for metal uptake, with the exception of some Cu chelates at low Cu' levels (Hudson, 1998; Sunda and Huntsman, 1998b; Guo et al., 2010). The phytoplankton species examined to date have at least two separate Zn transport systems, a low-affinity system whose V_{max} is relatively constant, and an inducible high-affinity system, whose affinity ($1/K_s$) and V_{max} increase with decreasing Zn' concentration ($[\text{Zn}']$) and decreasing intracellular Zn (Sunda and Huntsman, 1992). The low-affinity system has higher V_{max} and K_s values and transports Zn at high $[\text{Zn}']$. The inducible high-affinity system is responsible for Zn uptake at low $[\text{Zn}']$. At very low $[\text{Zn}']$ ($<10 \text{ pM}$), Zn uptake approaches limiting rates for the diffusion of Zn' species to the cell surface, and consequently the Zn uptake rate is proportional to $[\text{Zn}']$ in the medium (Sunda and Huntsman, 1992, 1995a; Figure 7). Similar biphasic high and low-affinity uptake systems, whose high-affinity uptake system is under negative feedback regulation, are observed for Cu in an oceanic diatom (Guo et al., 2010). The existence of high and low-affinity transport systems results in sigmoidal relationships between uptake rates for Zn and Cu (and cellular Zn:C and Cu:C

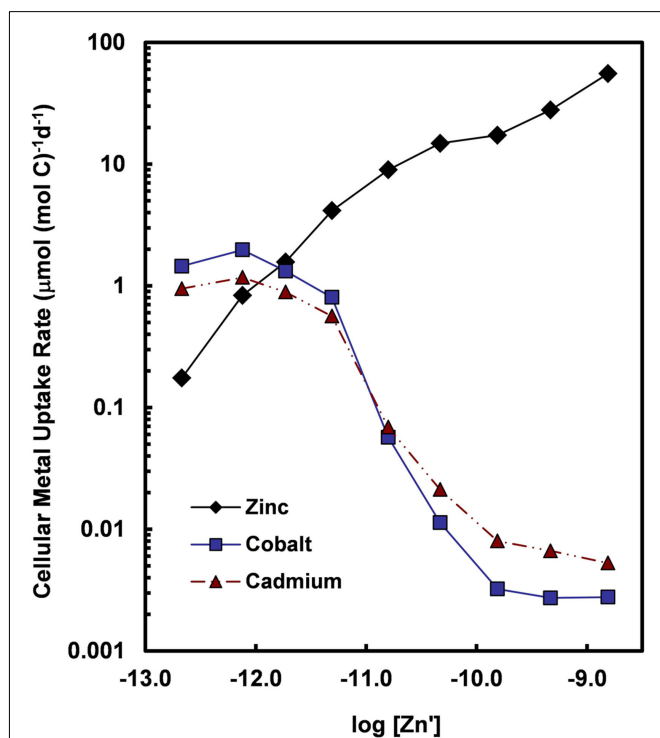


FIGURE 7 | Cellular uptake rates for Zn, Co, and Cd (normalized per mol of cell carbon) for the oceanic diatom *Thalassiosira oceanica* plotted as a function of the \log_{10} of the molar concentration of dissolved inorganic zinc species (Zn'). Concentrations of Cd' and Co' were held constant at 2.7 and 1.5 pM, respectively, within the range of values for near-surface ocean water (Bruland, 1992; Saito et al., 2004). Uptake rates for Cd and Co increase by at least two orders of magnitude when Zn' concentrations decrease below 10^{-10} M . The large increase in uptake rates reflect the induction of a high-affinity cellular transport system (or systems) for Cd and Co in response to declining intracellular Zn levels or transport of the two metals into the cell by an inducible high-affinity Zn transport system. Data are from Sunda and Huntsman (2000).

ratios) and Zn' and Cu' concentrations (Figures 4 and 7; Sunda and Huntsman, 1992, 1995a,c).

Co and sometimes Cd can metabolically substitute for Zn in many Zn enzymes such as carbonic anhydrase (Price and Morel, 1990; Lane and Morel, 2000; Xu et al., 2008). To facilitate this substitution, the uptake of these divalent metals is increased by over 100-fold in diatoms and coccolithophores with decreasing $[Zn']$ in the external medium and decreasing cellular Zn (Figure 7; Sunda and Huntsman, 1995a, 2000). Uptake of Cd and Co by this inducible transport system (or systems) is down-regulated at high $[Zn']$ and intracellular Zn levels (Figure 7). Under these conditions, Cd is taken up into the cell by the cellular Mn(II) transport system (Sunda and Huntsman, 1996, 2000) or a putative Fe(II) transport system (Lane et al., 2008), and consequently, is inversely related to concentrations of Mn(II)' and Fe(II)'. Thus, cellular uptake of Cd in the ocean is regulated by complex interactions among dissolved concentrations of Cd' , Zn' , Mn(II)', and Fe(II)' (Sunda and Huntsman, 2000; Cullen and Sherrell, 2005; Lane et al., 2009). Likewise, since Co uptake is repressed at high $[Zn']$, biological removal of Co often does not occur until after Zn is depleted, as observed in the subarctic Pacific (Figure 8; Sunda and Huntsman, 1995a).

Iron is the most limiting trace metal nutrient, and its chemistry is arguably the most complex. As noted earlier, iron is highly bound in seawater as ferric chelates and ferric ions associated with various particulate phases such as Fe(III) oxyhydroxides. Early evidence suggested that cyanobacteria and eukaryotic marine algae utilized fundamentally different uptake systems to access this bound iron (Wilhelm and Trick, 1994; Hutchins et al., 1999). Both cyanobacteria and heterotrophic bacteria were thought to utilize primarily siderophore uptake systems, in which high-affinity Fe(III)-binding ligands (siderophores) were released extracellularly, followed by intracellular uptake of the resulting ferric-siderophore chelates (Martinez et al., 2000; Sandy and Butler, 2009). Siderophore uptake systems are widespread in terrestrial and enteric bacteria, and may also be common in sedimentary and particle-associated marine bacteria (Sandy and Butler, 2009). However, recent genomic data from cultures and natural communities shows little evidence for proteins involved in siderophore biosynthesis or for cellular uptake of ferric-siderophore chelates in the picocyanobacteria (*Synechococcus* and *Prochlorococcus*) that often dominate open ocean phytoplankton communities, or by major oceanic N_2 -fixing cyanobacteria such as *Trichodesmium* or *Crocospaera* (Hopkinson and Morel, 2009; Hopkinson and Barbeau, 2012). Instead these species possessed a high abundance of Fe^{3+} ATP binding cassette (ABC) transporters, which can acquire iron from ligand exchange reactions with dissolved labile Fe(III) species such as $Fe(III)'$ (Hopkinson and Barbeau, 2012). A reductive step, however, may be required to free the iron from ferric chelates, prior to its uptake (Rose et al., 2005; Kranzler et al., 2011; Shaked and Lis, 2012), and many marine cyanobacteria also possess non-specific metal transporters that transport Fe(II) and other divalent metals (Hopkinson and Barbeau, 2012). A coastal *Synechococcus* isolate produced a suite of siderophores (synechobactins), which like many other marine siderophores, are both photoreactive and amphiphilic (Ito and Butler, 2005). But how widespread

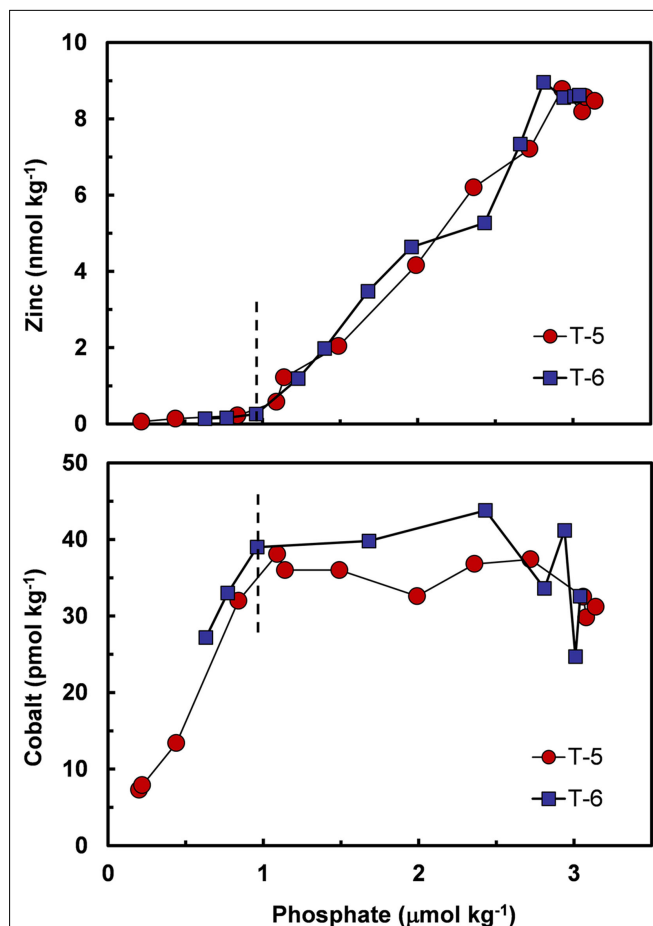


FIGURE 8 | Plots of filterable Zn and Co vs phosphate concentrations at two stations in the subarctic Pacific (Station T-5, 39.6°N, 140.8°W and Station T-6, 45.0°N, 142.9°W, August 1987). The decrease in zinc with decreasing phosphate is caused by the simultaneous removal of both metals via cellular uptake and assimilation by phytoplankton. Cobalt decreases with decreasing phosphate only after zinc concentrations drop to very low levels ($<0.2 \text{ nmol kg}^{-1}$). This pattern is consistent with metabolic replacement of Co for Zn, as observed in phytoplankton cultures (see Figure 5). Data plots after Sunda and Huntsman (1995a).

such siderophore production is in coastal cyanobacterial species is currently unknown (Hopkinson and Morel, 2009).

Eukaryotic phytoplankton do not appear to produce siderophores and there is little evidence for the direct cellular uptake of ferric-siderophore chelates (Sunda, 2001). Instead there is mounting evidence for the utilization of a high-affinity transport system that accesses a variety of Fe(III) coordination species (including $Fe(III)'$ and ferric chelates) via reduction to Fe(II; Maldonado and Price, 2001; Kustka et al., 2007; Amin et al., 2009; Strzepek et al., 2011). The released Fe(II)' binds to Fe(II) receptors on specific transmembrane proteins, which transport the iron into the cell. This intracellular transport involves the reoxidation of bound Fe(II) to Fe(III) by a copper protein (a multi-Cu oxidase; Maldonado et al., 2006). The ability of this transport system to access iron is dependent on the ease of reduction of

ferric complex species, which is inversely related to the stability of the Fe(III) coordination complex (Maldonado and Price, 2001). Weakly complexed ferric hydrolysis species Fe(III)' are reduced at orders of magnitude higher rates than strongly bound Fe-siderophore chelates, and are thus much more accessible for cellular uptake (Shaked et al., 2005; Morel et al., 2008). Likewise Fe(III) colloids are less available because of their slow diffusion kinetics within the cell's diffusive boundary layer and because interior ferric ions within the colloid are not readily accessible for reduction and subsequent release as dissolved Fe(II). As a consequence, iron uptake by this system is highly dependent on the chemical speciation of iron in seawater, and increases in dissolved Fe(II)' or Fe(III)' concentrations can considerably increase the biological availability of iron (Hudson and Morel, 1990; Morel et al., 2008). Photo-reductive dissociation of ferric chelates increases iron uptake by diatoms and other eukaryotic algae by increasing steady state Fe(II)' and Fe(III)' concentrations, as shown in culture experiments with photolabile ferric complexes with synthetic chelators (e.g., ethylenediaminetetraacetic acid, EDTA; Anderson and Morel, 1982; Sunda and Huntsman, 2011), marine siderophores (Barbeau et al., 2001; Amin et al., 2009), and sugar acids (Ozturk et al., 2004; **Figure 6**). Similarly, in an incubation experiment in the Southern Ocean, natural planktonic assemblages exhibited higher iron uptake rates from an added photoactive siderophore (^{57}Fe -aerobactin) in the presence of sunlight than from a non-photoactive one (^{57}Fe -desferrioximine b; Buck et al., 2010).

In other recent iron uptake experiments in Southern Ocean waters, the pre-equilibration of ^{55}Fe -labeled iron with the monosaccharide glucuronic acid increased the uptake of the radiolabeled iron by ~ 2 -fold compared to the uptake observed when iron was added by itself (Hassler et al., 2011b). Similar enhanced uptake was observed with the addition of polysaccharides. These effects may be attributed to the formation of more biologically available weak organic chelates (Hassler et al., 2011b; Benner, 2011). However as noted above, dissolved ferric chelates and coordination complexes of adsorbed sugar acids and polysaccharides on the surfaces of iron oxyhydroxides can undergo photolysis and subsequent iron redox cycling, which should increase Fe(II)' and Fe(III)' concentrations (Kuma et al., 1992; Ozturk et al., 2004; Steigenberger et al., 2010), thereby providing a plausible alternative explanation for the observed results. The influence of mono and polysaccharides on iron chemistry, photochemical redox cycling, and bioavailability needs further investigation given the high abundance of these compounds in dissolved and colloidal marine organic matter and the widespread production of extracellular polysaccharides by marine phytoplankton and bacteria (Steigenberger et al., 2010; Benner, 2011; Hassler et al., 2011a,b).

CELLULAR TRACE METAL QUOTAS AND METAL:CARBON RATIOS

The trace metal concentration in algal cells normalized to cell volume or to cell carbon is not only dependent on the rates of intracellular metal uptake by transport systems (as discussed above) or adsorption on cell surfaces (Tovar-Sanchez et al., 2003), but also by the rate of biodilution by new biomass or cell carbon (Sunda and Huntsman, 1998b). The rate of change in cellular metal per

mole of cell carbon (dQ/dt) equals the cellular uptake rate V_M (normalized to cell carbon) minus the rate of biodilution, which equals the net specific rate of C-fixation (μ_c) times the cellular metal:C ratio (Q):

$$\frac{dQ}{dt} = V_M - \mu_c Q \quad (2)$$

At steady state $dQ/dt = 0$ and the equation collapses to:

$$Q = \frac{V_M}{\mu_c} \quad (3)$$

Based on these equations, any factor that decreases growth rate but has no or a lesser effect on the metal uptake rate will increase the cellular metal:C ratio. This is seen in the response of cell Fe:C, Mn:C, and Zn:C ratios in diatoms and dinoflagellates to light limitation of growth rate, where a 60–70% decrease in specific growth rate with a decrease in light intensity from 500 to 50 $\mu\text{mol quanta m}^{-2} \text{ s}^{-1}$ increased the cell metal:C ratios by two- to threefold for a given $[M']$ (Sunda and Huntsman, 1997, 1998c, 2005). For Mn and Fe, the higher Mn:C and Fe:C values helped the cells to photoacclimate to the low light conditions (see Fe and Mn sections below and **Figure 9**), and for Zn, the higher Zn:C ratio lowered the $[Zn']$ needed to achieve maximum growth rate. However, as discussed previously, decreasing light can also decrease Fe and Mn uptake rates by decreasing $[Fe']$ and $[Mn(II)']$ levels, so the overall effect of lower light may still be to lower cell Fe:C and Mn:C ratios (Sunda and Huntsman, 2011). Temperature, another major growth-controlling factor, could potentially also affect cellular M:C ratios, but in the one case examined to date, a temperature decrease from 20 to 10°C caused similar decreases in V_M and specific growth rate (at constant $[Fe']$) so there was no effect on cellular Fe:C ratios (Sunda and Huntsman, 2011).

Equations 2 and 3 also have important implications for diel changes in cellular M:C ratios. Carbon is photosynthetically fixed only during the day (and a portion is respired at night), but metal uptake can continue during both the light and dark period (Sunda and Huntsman, 2004). Consequently, cellular M:C ratios should decrease during the light period and increase at night. In agreement with this prediction, the cell Fe:C ratio in an iron-limited diatom (*Thalassiosira pseudonana*) growing at a specific rate of 1.6 day^{-1} decreased by 60% (from 63 to 25 $\mu\text{mol Fe mol C}^{-1}$) from the beginning to the end of the 14 h light period (Sunda and Huntsman, 2004). This result was for a metal chelate system (Fe-nitrilotriacetic acid) with no photochemical enhancement of $[Fe']$ during the day, and the diel effect can be less or even reversed in marine systems with substantial photochemical redox cycling of iron (Sunda and Huntsman, 2004). For Zn, Co, Cd, and Ni, where photochemical cycling does not occur, the cellular M:C ratios should also decrease during the light period. This effect was observed in the diatom *T. pseudonana* where cell Zn:C decreased by twofold over the course of the light period (Sunda and Huntsman, 2004).

Metal uptake rates invariably increase with the concentration of available metal as observed for Zn uptake in the oceanic diatom *Thalassiosira oceanica* (**Figure 7**). For this diatom and the coccolithophore *Emiliania huxleyi* the specific growth rate is unaffected

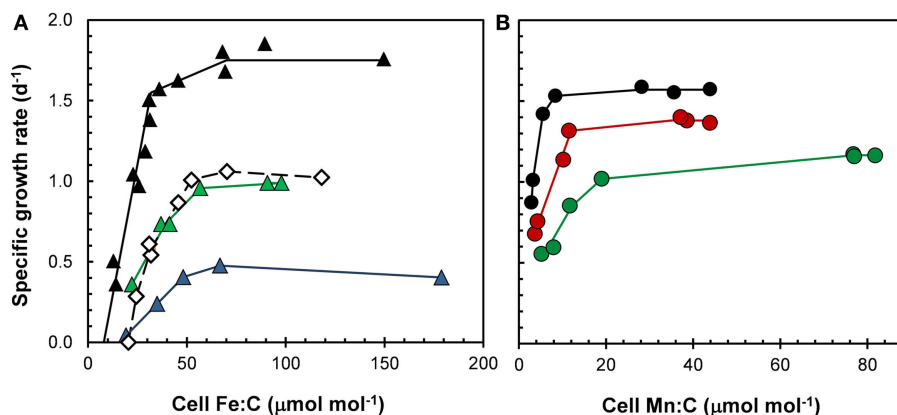


FIGURE 9 | Effect of light on cellular growth requirements for (A) iron and (B) manganese in the coastal diatom *Thalassiosira pseudonana* at 20°C. (A) Relationships between specific growth rate and Fe:C molar ratio for cells growing under a 14:10 h light:dark cycle at light intensities of 500 (black triangles), 85 (green triangles), and 50 (blue triangles) $\mu\text{mol photons m}^{-2} \text{s}^{-1}$. Open diamonds give data for cells growing at the highest light intensity (500 $\mu\text{mol photons m}^{-2} \text{s}^{-1}$) but a 50% shorter daily photoperiod (7 h). (B) Relationships between specific growth rate and cellular Mn:C molar ratio for cell growing under a 14:10 h light:dark cycle at light intensities of 500 (black circles), 160 (red circles), and 90 (green circles) $\mu\text{mol photons m}^{-2} \text{s}^{-1}$.

over most the oceanic $[\text{Zn}']$ range ($\log [\text{Zn}'] = -11.8$ to -8.7). Consequently, the cellular Zn:C is proportional to the cellular Zn uptake rate, and increases with increasing $[\text{Zn}']$ (see **Figures 5** and **7**).

Cellular metal:C ratios can vary substantially among species. The cell Zn:C was two- to fivefold higher in the coccolithophore *E. huxleyi* than the diatoms *T. oceanica* and *T. pseudonana*, depending on the $[\text{Zn}']$ in the culture medium (Sunda and Huntsman, 1995a; **Figure 5**). Data of Ho et al. (2003) are consistent with those of Sunda and Huntsman (1995a) and show a 10-fold variation in Zn:C ratios in 15 different marine algal species representing five major algal groups (**Figure 5**). Even larger variations of 13-, 71-, and 50-fold, respectively, were observed for Cu:C, Co:C, Cd:C ratios in these same algal species grown at a constant set of $[\text{M}']$ values (Ho et al., 2003).

Recent advances in synchrotron X-ray fluorescence microscopy has allowed measurement of metal:P and metal:S ratios in single cells for a wide array of trace metals. As in the above culture data, large intriguing variations were observed in different algal cells and cell types present in the same water samples (Twining et al., 2004, 2010, 2011). In a recent study in the equatorial Pacific, diatoms had sevenfold higher Ni:P ratios and fourfold higher Fe:P and Zn:P ratios than autotrophic flagellates (e.g., coccolithophores and dinoflagellates), but had 2.5-fold lower Co:P ratios (Twining et al., 2011).

Cells have the capacity to take up iron and other nutrient metals in far excess of that needed to support growth and metabolism, which helps them to take advantage of pulsed inputs, such as episodic increases in aeolian iron deposition associated with large desert dust storms (Sunda and Huntsman, 1995b; Marchetti et al., 2006). This “luxury” uptake also protects cells from future declines in metal availability as blooms develop or to increases in metabolic demand for iron and other metals linked to decreases in light or increases in temperature (Sunda and Huntsman, 2011). In addition, because of a certain degree of non-specificity of transport systems, many reactive trace metals

(including metal nutrients, e.g., Cu and Cd), can leak into cells via the transport systems for other metal nutrients such as Mn and Zn (Sunda and Huntsman, 1996, 1998c). Within the cell unchelated redox active metals such as iron and copper can mediate the formation of toxic reactive oxygen species (e.g., hydroxyl radicals via Fenton chemistry) and reactive metals such as Cu, Cd, and Zn can adventiciously bind with coordination sites of proteins or displace nutrient metals from their active sites in metalloproteins (Hartwig, 2001; Valko et al., 2005). Consequently, it is essential that “excess” concentrations of these metals be sequestered within algal cells to prevent metal toxicity or inhibition of metabolism (Finney and O’Halloran, 2003). Excess iron not occurring in metabolic proteins is bound within the iron storage protein ferritin in the pennate diatom *Pseudo-nitzschia* (Marchetti et al., 2009), and in Dps protein (another member of the ferritin protein family) in the N_2 -fixing cyanobacterium *Trichodesmium* (Castruita et al., 2006). Both of these algae have unusually high storage capacities for excess iron (Kustka et al., 2003a; Marchetti et al., 2006). Many marine picocyanobacteria (e.g., *Synechococcus*) possess genes for Dps or bacterioferritin iron storage proteins although the actual presence of these proteins has not yet been verified (Scanlan et al., 2009). Other marine eukaryotic phytoplankton such as centric diatoms also have substantial capacities to store excess intracellular iron (Sunda and Huntsman, 1995b), but the means by which they do so remains unclear.

High intracellular levels of Cd or Cu in a variety of eukaryotic phytoplankton are bound by phytochelatins, a set of sulfhydryl containing chelating ligands found in terrestrial plants, microalgae, and fungi. These ligands consist of small polymers of glutathione with the structure $(\gamma\text{-glutamate-cysteine})_n\text{-glycine}$, where $n = 2\text{--}11$ (Ahner et al., 1995; Ahner and Morel, 1995; Ahner et al., 1997). Although low basal levels of these cellular chelators exist in cells, the cellular synthesis of phytochelatins is up-regulated by exposure to high concentrations of toxic nutrient or non-nutrient metals (e.g., Cd, Cu, or Hg) or low levels of competing

metal nutrients such as Zn or Mn, which promote increased cellular Cd or Cu uptake (Ahner et al., 1998; see **Figure 7**).

METABOLIC METAL REQUIREMENTS AND THEIR RELATION TO OTHER LIMITING RESOURCES

Trace metal nutrients are essential for the metabolism, growth, and reproduction of all marine phytoplankton. They play essential roles in photosynthetic C-fixation, respiration, N₂-fixation, and the uptake and metabolic assimilation of major nutrient elements (N, P, and C). Thus the growth requirements of specific metals are influenced by the availability of light and the concentration and chemical forms of inorganic carbon, phosphorus and nitrogen species. Of the trace metal nutrients, iron is needed in the greatest amount for algal growth and most frequently limits the growth of marine phytoplankton. It serves essential metabolic functions in photosynthetic electron transport, respiration, nitrate and nitrite reduction, sulfate reduction, N₂-fixation, and detoxification of reactive oxygen species such as superoxide radicals and hydrogen peroxide (Raven, 1988; da Silva and Williams, 1991; Raven et al., 1999).

The major requirement for iron in phytoplankton and likely all phototrophs is in the primary photochemical reactions of photosynthesis and associated photosynthetic electron transport (Raven, 1990; Strzepek and Harrison, 2004). To acclimate to low, sub-saturating light conditions, phytoplankton increase the cellular concentration of photosynthetic pigments, reaction centers, and electron transport proteins and protein complexes, and to do this they need an increased amount of cellular iron (Raven, 1990). These iron-containing photosynthetic components include photosystem II (2–3 Fe), the cyt *b*₆ complex (5 Fe), photosystem I (12 Fe), cytochrome *c*₆ (1 Fe), and ferredoxin (2 Fe; Raven et al., 1999). This increased growth requirement for iron under low light conditions has been confirmed in culture experiments (Sunda and Huntsman, 1997, 2011; Strzepek and Harrison, 2004; **Figure 9A**). Such interactions between light and iron limitation can lead to iron-light co-limitation of algal growth in low light environments such as occur with deep vertical mixing during winter at higher latitudes (e.g., the subarctic Pacific and Southern Ocean; Maldonado et al., 1999) and in the deep chlorophyll maximum near the bottom of the photic zone in thermally stratified mid-ocean gyres (Sunda and Huntsman, 1997; Hopkinson and Barbeau, 2008). Algal cells acclimate similarly to a decrease in the photoperiod by increasing their photosynthetic pigments and cellular iron requirement for daily C-fixation and growth (Sunda and Huntsman, 2004, 2011; **Figure 9A**). Such day length effects could contribute to a higher level of iron limitation of phytoplankton growth during the shorter days of the fall than during the spring at high latitudes.

Iron is also needed for the assimilation of important chemical forms of nitrogen, which next to carbon is the second most abundant nutrient element in the cell. Nitrogen limits the growth and biomass of phytoplankton in roughly 60% of the ocean (Moore et al., 2002, 2004) and the overwhelming majority of biologically available fixed nitrogen in deep ocean reservoirs occurs as nitrate (**Figure 2A**). Nitrate is supplied to sunlit surface waters by upwelling and vertical mixing of deep ocean waters, but to utilize this substrate algal cells must first reduce it to ammonium, a process catalyzed by two iron-containing enzymes: nitrate

reductase and nitrite reductase. In addition, both enzymatic reactions require the input of cellular energy (adenosine triphosphate, ATP) and reductant molecules (NADPH), and large amounts of cellular iron are needed for their photosynthetic production. Based on model calculations (Raven, 1988) and empirical measurements (Maldonado and Price, 1996), algal cells growing on nitrate require ~50% more iron to support a given growth rate than do cells growing on ammonium. Consequently, iron can be especially limiting in oceanic upwelling systems (such as the equatorial and subarctic Pacific) where waters containing high nitrate concentrations, but low-iron, are advected to the surface (Martin and Fitzwater, 1988; Coale et al., 1996; Boyd et al., 2007). The low-iron concentrations favor the growth of small phytoplankton, which are rapidly grazed by microzooplankton, preventing blooms from developing, whose formation ultimately must be supported by inputs of upwelled nitrate (Price et al., 1991, 1994). The rapid grazing also supplies recycled ammonium which is more efficiently assimilated by the iron-limited cells. Thus the net population growth of such systems can be viewed as being co-limited by iron and nitrate due to the high iron requirement for nitrate utilization (Price et al., 1994).

A more important iron-nitrogen linkage is provided by the large metabolic requirement for iron in N₂-fixation. All eukaryotic algae and most cyanobacteria are incapable of assimilating N₂ which is present at a high concentration in the atmosphere (a mole fraction of 0.81) and in all ocean waters. Certain marine cyanobacteria, such as members of the genera *Trichodesmium* and *Chroocospha*, are able to enzymatically reduce N₂ to ammonium (referred to as N₂-fixation; Zehr, 2011). N₂-fixation requires very high amounts of cellular iron, and consequently, *Trichodesmium* growing on N₂ as a nitrogen source require up to five times more cellular iron for growth than cells growing on ammonium (Kustka et al., 2003a). This much higher iron requirement is partly caused by the large amount of iron in the N₂-fixation enzyme nitrogenase, and the low catalytic rate of this enzyme (Kustka et al., 2003b). However, it is also caused by the large amount of energy in the form of ATP needed to break the N₂ triple bond (16 ATP per N₂ molecule), which must be supplied either directly or indirectly from photosynthesis. As a result of the high metabolic iron cost and the low-iron concentrations in seawater, iron appears to limit N₂-fixation in large regions of the ocean, and along with denitrification (respiratory reduction of NO₃⁻ to N₂), controls oceanic inventories of fixed nitrogen (Rueter et al., 1992; Falkowski, 1997; Kustka et al., 2003a; Sohm et al., 2011). Consequently, nitrogen is the primary limiting major nutrient in most ocean waters (Moore et al., 2004), while in lakes, where iron concentrations are much higher, phosphate is typically the primary limiting nutrient (Schindler, 1977). Because the low level of fixed nitrogen in the ocean is largely caused by iron limitation of N₂-fixation, the ocean can be viewed as being co-limited by iron and nitrogen.

Ocean N₂-fixation is largely restricted to warm tropical and subtropical waters (Moore et al., 2004; Zehr, 2011). N₂-fixation varies regionally in these waters and is greatest in areas receiving high iron inputs from deposition of desert dust (or other continental sources), such as the subtropical North Atlantic, Arabian Sea, and the western margin of the Pacific (Sohm et al., 2011). And N₂-fixation is lowest in the South Atlantic and South Pacific where continental inputs of iron are low. N₂-fixation in regions with high

atmospheric iron inputs tend to be dominated by *Trichodesmium*, which typically forms colonies 1–3 mm in diameter (Sohm et al., 2011). The colonies are able to intercept iron-containing dust particles and physically transport them to the colony's interior where the iron is solubilized and assimilated by unidentified reductive processes (Rueter et al., 1992; Rubin et al., 2011). The colonies can vertically migrate at velocities exceeding 3 m h^{-1} , as enabled by the large colony size and variations in specific gravity (Walsby, 1992). This vertical movement increases the colony's encounter frequency with iron-containing dust particles, which further facilitates iron uptake (Sunda, 2001).

In the mid-ocean waters of the subtropical and tropical Pacific, continental inputs of iron are low as are iron concentrations, and here N_2 -fixation is dominated by much smaller unicellular cyanobacteria, such as *Crocosphaera watsonii* (Montoya et al., 2004; Sohм et al., 2011). The much smaller cell size (2–6 μm diameter), and attendant higher surface to volume ratios and higher diffusive flux of soluble iron to cell surfaces (per unit of biomass) help increase cellular iron uptake by these cyanobacteria in these low-iron waters (Sunda, 2001). In addition, recent proteomic data indicate that these cells undergo a large scale diel cellular cycle in which a portion of the iron-containing proteins involved in photosynthesis are degraded near the end of the light period and the iron released is then used to synthesize the iron-containing nitrogenase needed for nighttime fixation of N_2 , which is fueled by the ATP produced from respiratory consumption of stored carbohydrates (Saito et al., 2011). The nitrogenase proteins are then degraded near the end of the dark period and the liberated iron is reused to synthesize iron-containing photosynthetic proteins needed for C-fixation. This cellular strategy is energetically expensive, but solves two critical problems in iron-limited oceanic waters: it temporally separates N_2 -fixation and photosynthesis, and thereby avoids poisoning of nitrogenase enzyme complex by photosynthetically produced O_2 (Zehr et al., 2001); and equally important, it reduces the cellular iron requirement for diazotrophic growth by ~40% (Saito et al., 2011). The combination of higher iron uptake rates related to small cell size and the lower cellular iron requirement for diazotrophic growth provide a competitive advantage to *Crocosphaera* in low-iron oceanic waters, such as those in vast regions of the tropical and subtropical Pacific.

Due to iron limitation of C-fixation and N_2 -fixation in major regions of the ocean, iron plays a significant role in regulating carbon and nitrogen cycles in the ocean. It thus helps regulate the biological CO_2 pump discussed earlier, which along with the physical CO_2 pump, controls the ocean/atmosphere CO_2 balance and CO_2 -linked greenhouse warming (Martin, 1990; Sigman and Boyle, 2000). There is evidence that climatically driven variations in the input of iron-rich continental dust to the ocean has played an important role in regulating glacial-interglacial climate cycles by influencing the intensity of the biological CO_2 pump (Martin, 1990; Falkowski, 1997; Martínez-García et al., 2011).

Manganese may influence the growth and species composition in certain low-Mn environments such as the subarctic Pacific and Southern Ocean, where Mn additions have been observed to stimulate algal growth in bottle incubation experiments (Buma et al., 1991; Coale, 1991). Mn occurs in the water oxidizing complex of photosystem II (which contains four Mn atoms), and thus is

essential for oxygenic photosynthesis. Consequently, like iron, it is needed in higher amounts for algal growth at low light intensities (Raven, 1990; Sunda and Huntsman, 1998d; **Figure 9B**), such as the bottom of the photic zone where Mn concentrations are often lower than at the surface (**Figure 2H**). Mn also occurs in superoxide dismutase, an antioxidant enzyme that removes toxic superoxide radicals, produced as byproducts of photosynthesis (Peers and Price, 2004; Wolfe-Simon et al., 2006). Because it has fewer metabolic functions, its cellular growth requirement is less than that for iron (**Figure 9A, B**).

Quantitative requirements for Zn in marine phytoplankton are similar to those for Mn (Sunda and Huntsman, 1995a, 1998d). Zn is needed in a variety of essential proteins needed for cell growth and replication (da Silva and Williams, 1991). It occurs in carbonic anhydrase (CA), an enzyme that catalyzes the reversible reaction:



Thus CA is critical to intracellular CO_2 transport and fixation and is needed to support the cell's CO_2 concentrating mechanism(s) (Badger and Price, 1994). Higher amounts of this enzyme are needed at low CO_2 concentrations, leading to potential co-limitation by Zn and CO_2 in the ocean (Morel et al., 1994; Sunda and Huntsman, 2005). However, the ~40% increase in CO_2 in the atmosphere and surface ocean waters from the burning of fossil fuels makes Zn- CO_2 co-limitation less likely in the modern ocean than in pre-industrial times. Zinc occurs in zinc finger proteins and RNA polymerase, involved in DNA regulation and transcription, and in tRNA synthetase, involved in tRNA translation into proteins (da Silva and Williams, 1991). It is also found in alkaline phosphatase, needed to acquire orthophosphate via hydrolysis of organic phosphate esters, which dominate phosphate pools in surface ocean waters with low P concentrations (Lomas et al., 2010). Consequently, Zn and P may co-limit algal growth in ocean regions where both nutrients occur at low levels such as the Sargasso Sea (Wu et al., 2000; Shaked et al., 2006; Jakuba et al., 2008). Zn additions have been found to stimulate algal growth in bottle incubation experiments in the subarctic Pacific and in some coastal upwelling regimes along the eastern margin of the Pacific, but the effects were modest relative to those for added Fe (Coale, 1991; Crawford et al., 2003; Franck et al., 2003). However, Zn addition had a large effect on algal species composition, and preferentially stimulated the growth of the coccolithophore *E. huxleyi* (Crawford et al., 2003), which has an unusually large cellular uptake and growth requirement for Zn/Co (Sunda and Huntsman, 1995a; see **Figure 5**). *E. huxleyi* and other coccolithophores are largely responsible for calcium carbonate formation and regulation of ocean water alkalinity, which in turn influences the air-sea exchange of CO_2 (Dymond and Lyle, 1985). Thus, by affecting the growth of coccolithophores, Zn (and possibly Co, see below) could indirectly affect atmospheric CO_2 and global climate.

Co and sometimes Cd can substitute for Zn in CA, alkaline phosphatase and other Zn enzymes, leading to complex interactions among the three metals in marine phytoplankton (Price and Morel, 1990; Sunda and Huntsman, 1995a; Xu et al., 2007; Jakuba et al., 2008; Saito and Goepfert, 2008; **Figure 7**). The presence of Cd in CA appears to explain its nutrient-like distribution in

ocean waters (**Figure 2E**), and the identification of a unique Cd-CA enzyme in zinc-limited marine diatoms means that it functions as a micronutrient in these microalgae (Park et al., 2007; Xu et al., 2008). However, the substitution of Zn for Cd in this protein yields a more catalytically active enzyme (Xu et al., 2008), suggesting that Zn may have been evolutionarily the original metal center for this enzyme.

Co also occurs in vitamin B₁₂, an essential vitamin required for growth of many eukaryotic algal species (Croft et al., 2005). This vitamin is synthesized by bacteria but not by eukaryotic phytoplankton, resulting in potential interactions among Co availability, B₁₂-production by bacteria and B₁₂-utilization by eukaryotic algae in the ocean (Croft et al., 2005; Bertrand et al., 2007; Panzeca et al., 2008). A specific requirement for Co not involving B₁₂ or a metabolic replacement for Zn is seen in marine cyanobacteria, including members of the genera *Synechococcus* and *Prochlorococcus*, but the biochemical basis for this is not known (Sunda and Huntsman, 1995a; Saito et al., 2002). A similar Co-requirement for optimal growth is observed in the bloom-forming prymnesiophytes *E. huxleyi* (Sunda and Huntsman, 1995a; Jakuba et al., 2008) and *Chrysochromulina polylepis* (Granéli and Risinger, 1994). Because of its unique requirement by cyanobacteria, Co may influence their growth in the ocean, as demonstrated by growth stimulation of *Synechococcus* by added Co in the Costa Rico upwelling dome (Saito et al., 2005).

Copper is also an essential micronutrient. It occurs along with iron in cytochrome oxidase, the terminal protein in respiratory electron transport that reduces O₂ to H₂O (da Silva and Williams, 1991). And it occurs in plastocyanin, which substitutes for the iron protein cytochrome *c*₆ in photosynthetic electron transport in oceanic diatoms (Peers and Price, 2006), some cyanobacteria (Scanlan et al., 2009), and the prymnesiophyte *E. huxleyi* (Guo et al., 2012). It is also an essential component of the high-affinity iron transport system of at least some eukaryotic algae (Maldonado et al., 2006; Kustka et al., 2007) and possibly some oceanic cyanobacteria (Guo et al., 2012). Because Cu is needed for Fe uptake and can metabolically substitute for Fe, co-limitations can occur for Cu and Fe, as observed in diatom cultures (Peers et al., 2005; Annett et al., 2008), and also in deck-board incubation experiments in iron-limited ocean water (Coale, 1991). These co-limitations are most prevalent for oceanic algal species, where substitutions of Cu proteins (plastocyanonin and Cu/Zn-SOD) for iron enzymes (cytochrome *c*₆ and Fe-SOD) may help decrease the Fe growth requirements of oceanic species (Annett et al., 2008; Guo et al., 2012).

Nickel has only a minimal known usage in marine phytoplankton. It serves as the active metal center in urease, which hydrolyzes urea to ammonium. Consequently, it is essential for utilization of urea, an important nitrogen source in N-limited oceanic waters (Price and Morel, 1991). Recently a Ni-superoxide dismutase (Ni-SOD) was found to occur in marine cyanobacteria, a dominant group of picophytoplankton in open ocean waters (Dupont et al., 2008a,b). This finding may explain the unusually high Ni:P ratios in picoplankton (which were presumed to be cyanobacteria) in the equatorial Pacific (Twining et al., 2011). The Ni-SOD findings may be of significance evolutionarily as other forms of this critical antioxidant enzyme, which contain other metals in their catalytic

centers (i.e., Fe-SOD, Mn-SOD, and Cu/Zn-SOD), are the main SODs in eukaryotic algae and virtually all land plants and animals. Thus, the occurrence of Ni-SOD in oceanic cyanobacteria may help to reduce the biochemical demand for other micronutrient metals (Fe, Zn, Cu, and Mn) which generally occur at lower concentrations than Ni in surface ocean waters (see **Figures 2 and 3**).

Mo occurs with Fe in several key N-assimilation enzymes, including nitrogenase and nitrate reductase (da Silva and Williams, 1991). Thus, it is important in the ocean's nitrogen cycle; however, it is unlikely to limit algal growth due to the high concentration of molybdate ions in ocean water (105 nM; Collier, 1985). In addition to the Fe-Mo enzyme, some N₂-fixing bacteria also contain other isoforms of nitrogenase, one that contains a homologous Fe-S cluster without Mo in its active center and another that contains Fe and vanadium (Boyd et al., 2011). Thus Mo is not absolutely essential for N₂-fixation. However, the Fe-Mo enzyme is at least 50% more catalytically active than either of the other two isoforms which helps to minimize Fe-limitation of N₂-fixation in the ocean (Anbar and Knoll, 2002).

BIOLOGICAL FEEDBACK ON SEAWATER CHEMISTRY

The interactions between trace metal nutrients and marine phytoplankton are reciprocal. While trace metals clearly influence the productivity and species composition of planktonic algae and bacteria, these microorganisms in turn have a profound effect on the chemistry and cycling of these metals in the ocean on a variety of time and spatial scales (**Figure 1**). One example of this interaction is the effect of algal uptake, particulate settling, and regeneration cycles on the vertical distribution and inter-ocean transfer of nutrient metals, as described earlier (**Figures 2 and 3**). In addition marine biota influence the chemical speciation of metals through a variety of processes: (1) the release of metal chelates and metal chelating ligands through zooplankton grazing, digestion, and defecation, and through viral lysis of cells and microbial degradation processes (Poore et al., 2004; Strzepek et al., 2005); (2) the active release of chelating compounds such as siderophores (Butler and Theisen, 2010) and polysaccharides (Hassler et al., 2011a), and (3) the reduction and oxidation of redox active metals (Fe, Mn, Co, and Cu) by various biological processes. These processes include the reduction of iron and copper by cell surface reductases (Strzepek et al., 2011) or by biologically produced reducing agents (Rose et al., 2005), reduction of metals within particulate reducing microzones generated by microbial respiration, and oxidation of Mn(II), Co(II), and Fe(II) to their respective oxides by specific groups of bacteria (Moffett and Ho, 1996).

One of the most important effects of microorganisms on trace metal chemistry is in mediating the production of organic ligands that chelate Fe, Cu, Zn, and Co, especially in oceanic environments where the supply of terrestrial humic materials and other land-derived chelators is minimal. This chelation minimizes the loss of these essential metals by abiotic (and biotic) particulate scavenging and thereby minimizes their loss from ocean waters. The organic carbon needed for the *in situ* formation of these ligands is ultimately derived from algal photosynthesis, and thus the production of these ligands is at least indirectly dependent on marine algal productivity. However, many of these ligands

appear to directly result from biological processes, and at least some directly facilitate biological uptake of metals. The release of siderophores clearly facilitates biological uptake of iron, as the releasing bacteria have specific transport systems for active uptake of iron-siderophore chelates (Butler and Theisen, 2010). However, most iron-siderophore chelates are orders of magnitude less available for algal uptake than is unchelated Fe' (Shaked et al., 2005), and thus, in facilitating their own iron uptake, the bacteria could inadvertently lessen the uptake of iron by phytoplankton. Such an effect in turn could lessen photosynthetic production of organic carbon on which the bacteria depend for growth and survival. To avoid this conundrum, nature may have devised a clever mechanism to allow the bacteria to sequester iron for their own use, and at the same time make it more available to support photosynthetic fixation of carbon in sunlit surface ocean waters. Unlike the siderophores produced by soil and enteric bacteria, whose iron-siderophore chelates are unaffected by exposure to sunlight, the iron chelates of most siderophores produced by near-surface marine bacteria undergo photolysis owing to the presence of alpha hydroxy-carboxylate functional groups (Barbeau et al., 2003; Vraspir and Butler, 2009; Butler and Theisen, 2010). By contrast, these photoactive functional groups are relatively rare in terrestrial siderophores (Barbeau et al., 2003). The photolysis of the siderophore chelates can substantially increase the steady state concentrations of biologically available Fe(II)'^+ and Fe(III)'^+ species, and thereby increases the uptake of iron by phytoplankton, as directly shown in culture experiments with marine diatoms and dinoflagellates (Barbeau et al., 2001; Amin et al., 2009). In this way the bacteria are not only able to increase the availability of iron to themselves, but to phytoplankton in sunlit surface waters, thereby promoting the photosynthetic production of organic carbon needed for bacterial growth and reproduction, and ultimately for the production of siderophores. It is noteworthy that the marine bacteria found in close mutualistic association with marine dinoflagellates and cocolithophores produce a weaker iron-siderophore (vibrioferin; $\log K_{\text{Fe}'} = 10.9$), which contains two alpha hydroxy ligand groups, and is 10- to 20-times more photoreactive than the siderophores produced by free living marine bacteria (Amin et al., 2009). The *in situ* photolysis of this siderophore in the presence of attenuated sunlight increased the iron uptake rate in the dinoflagellate *Scrippsiella trochoidea* by 20-fold but also increased the iron uptake rate by the producing bacterium (*Marinobacter* sp.) by 70% (Amin et al., 2009). Here the photolysis reaction not only promoted iron uptake by the mutualistic algal partner, but also by the siderophore-producing bacterium.

There is also evidence that the strong ligands that tightly chelate Cu in seawater are produced by phytoplankton, especially cyanobacteria. In stratified waters of the North Pacific and Atlantic such strong Cu-binding ligands often occur at highest levels near the deep chlorophyll maximum where cyanobacteria are abundant (Coale and Bruland, 1988, 1990; Moffett, 1995). The chelators appear to perform an important function of detoxifying copper. In the presence of the Cu-chelators the average Cu' in surface Northeast Pacific waters occurred at a non-toxic concentration (1.2 pM; Table 1) while in their absence Cu' levels would have been 500 pM, a level toxic to many marine phytoplankton (Brand

et al., 1986; Coale and Bruland, 1988). Ligands having similar Cu-binding strength ($\log K_{\text{Cu}'} = 11.8$) as many of the strong chelators in surface seawater are produced by *Synechococcus*, an abundant group of oceanic cyanobacteria, that are particularly sensitive to copper toxicity (Brand et al., 1986; Moffett, 1995; Moffett and Brand, 1996). In experiments with *Synechococcus*, the production of the ligand was greatly enhanced in response to additions of toxic levels of Cu, indicating that the cyanobacteria can actively modulate the availability and toxicity of Cu in their external environment via production of Cu-chelators. Similar enhanced ligand production in response to added Cu was observed in cultures of eukaryotic phytoplankton, but the stability constants for Cu-binding by these ligands ($\log K_{\text{Cu}'} = 9.2\text{--}10.8$) were lower than those for the chelators released by *Synechococcus* (Croot et al., 2000).

There is also evidence from laboratory and field experiments that the strong ligands that chelate Co in seawater are also produced by cyanobacteria, and that these ligands, like siderophores, facilitate the uptake of the chelated metal (Co) by these organisms (Saito et al., 2002, 2005).

Thus, trace metal nutrients and planktonic communities comprise an interactive system in the ocean in which each exerts a controlling influence on the other (Figure 1). On longer geological time scales, the feedback interactions between microorganisms and the chemistry and availability trace metals have been profound, and have substantially influenced the overall chemistry and cycling of major biological elements (C, O, H, N, and S) in the ocean and the earth as a whole, and have had a major impact on the evolution of life on this planet (da Silva and Williams, 1991). Currently, the air we breathe and virtually the entire ocean contain high concentrations of dioxygen molecules (O_2), generated over billions of years from the release of O_2 as a byproduct of oxygenic photosynthesis. Because of the presence of O_2 , the modern ocean is oxidizing, which as noted previously, limits the solubility of critical trace metal nutrients (Fe, Co, and Mn) whose stable oxidation states under oxic conditions are sparingly soluble Fe(III) oxyhydroxides and insoluble Co(III) and Mn(IV) oxides. However, prior to the advent of oxygenic photosynthesis ca 3 billion years ago (Blankenship et al., 2007) and the appearance of O_2 in the atmosphere 2.4–2.3 billion years ago (Bekker et al., 2004), the chemistry of the atmosphere and the ocean were far different from what exists today. There was no free O_2 and the entire ocean, and earth's surface and atmosphere were chemically much more reducing (da Silva and Williams, 1991). Under these conditions the stable redox states of Fe, Mn, and Co were soluble Fe(II) , Mn(II) , and Co(II) , and that of copper was Cu(I) . Furthermore, the stable redox form of sulfur was sulfide ($\text{S}[-\text{II}]$), rather than sulfate ($\text{S}[\text{VI}]$), which occurs in present day seawater at a high concentration (28 mM). The presence of moderate to high levels of sulfide greatly restricted the availability of Zn, Cu, Mo, and Cd, which form insoluble sulfide precipitates and biologically less available metal sulfide complexes; but it had a much a lesser impact on other metals [Mn(II) , Fe(II) , Co(II) , and Ni(II)] which form much more soluble metal sulfides (da Silva and Williams, 1991; Saito et al., 2003). Thus, early life in the ocean likely evolved in an environment of high availability of Fe, Mn, Co, and Ni and much lower availabilities of Zn, Mo, Cu, and Cd, contrasting the situation in the modern ocean.

Given the utility of Fe as a versatile redox catalyst and its abundance in the earth's crust and early ocean, it is perhaps not surprising that this metal was utilized in the evolution of many of the central redox catalysts of life (Mauzerall, 2007). It occurs in high amounts in the redox centers of nitrogenase responsible for N₂ reduction to NH₃ and in the various cytochromes and Fe-S redox centers involved in anoxygenic and oxygenic photosynthesis (da Silva and Williams, 1991; Raven et al., 1999). In addition, the abundant soluble Mn(II) in the ancient ocean was utilized in the evolution of the water oxidizing centers of photosystem II, which allowed cyanobacteria to utilize abundant water molecules as a photosynthetic electron donor, thereby freeing photosynthetic primary producers from the need to utilize much less abundant substrates such as sulfide or ferrous ions (Mauzerall, 2007). The resultant oxidation of H₂O to O₂ and burial of photosynthetically produced organic carbon in marine sediments and sedimentary rocks, slowly (over 1–2 billion years) oxidized Fe(II) to Fe(III) oxides and sulfide minerals to soluble sulfate, ultimately resulting in the buildup of free O₂ first in the atmosphere and surface ocean beginning ca. 2.3 billion years ago, and gradually in the ocean as a whole by ~500–600 million years before present (Anbar and Knoll, 2002; Katz et al., 2007). The precipitation of ferric oxides

from the sea has resulted in the chronic Fe-limitation of C-fixation and N₂-fixation that we currently observe in the ocean. However, this negative effect is more than offset by the large amount of biological energy produced by O₂-dependent respiration utilized by all present day plants and animals and most aerobic microbes. Indeed the large amount of energy obtained from the respiratory reaction of O₂ with organic molecules likely was essential for the development of multicellular forms of life, paving the way for the evolution of mammals, including man (Mauzerall, 2007). Furthermore, the release of Zn, Cu, Mo, and Cd from insoluble sulfides and biologically unavailable sulfide complexes allowed for the proliferation of numerous enzymes utilizing these metals (including many Zn and Cu enzymes), many of which appear to have evolved following the appearance of free O₂ (da Silva and Williams, 1991). Thus, evolution has involved a continuous feedback between biological systems and the surrounding chemical environment, with biological trace metal catalysts playing a central mediating role in this process.

ACKNOWLEDGMENTS

I thank Mark Vandersea for help in formatting the figures and Yeala Shaked, Christel Hassler, and Ken Bruland for useful comments.

REFERENCES

- Ahner, B. A., Kong, S., and Morel, F. M. M. (1995). Phytochelatin production in marine algae. 1. An interspecies comparison. *Limnol. Oceanogr.* 40, 649–657.
- Ahner, B. A., Lee, J. G., Price, N. M., and Morel, F. M. M. (1998). Phytochelatin concentrations in the equatorial Pacific. *Deep Sea Res.* 45, 1779–1796.
- Ahner, B. A., and Morel, F. M. M. (1995). Phytochelatin production in marine algae. 2. Induction by various metals. *Limnol. Oceanogr.* 40, 658–665.
- Ahner, B. A., Morel, F. M. M., and Moffet, J. W. (1997). Trace metal control of phytochelatin production in coastal waters. *Limnol. Oceanogr.* 42, 601–608.
- Amin, S. A., Green, D. H., Hart, M. C., Küpper, F. C., Sunda, W. G., and Carrano, C. J. (2009). Photolysis of iron-siderophore chelates promotes bacterial-algal mutualism. *Proc. Natl. Acad. Sci. U.S.A.* 106, 17071–17076.
- Anbar, A. D., and Knoll, A. H. (2002). Proterozoic ocean chemistry and evolution: a bioinorganic bridge? *Science* 297, 1137–1142.
- Anderson, C. R., Johnson, H. A., Caputo, N., Davis, R. E., Torpey, J. W., and Tebo, B. M. (2009). Mn(II) oxidation is catalyzed by heme peroxidases in “*Aurantimonas manganoxydans*” strain SI85-9A1 and *Erythrobacter* sp strain SD-21. *Appl. Environ. Microbiol.* 75, 4130–4138.
- Anderson, M. A., and Morel, F. M. M. (1982). The influence of aqueous iron chemistry on the uptake of iron by the coastal diatom *Thalassiosira weissflogii*. *Limnol. Oceanogr.* 27, 789–813.
- Andreae, M. O., and Crutzen, P. J. (1997). Atmospheric aerosols: biogeochemical sources and role in atmospheric chemistry. *Science* 276, 1052–1058.
- Annett, A. L., Lapi, S., Ruth, T. J., and Maldonado, M. T. (2008). The effects of Cu and Fe availability on the growth and Cu:C ratios of marine diatoms. *Limnol. Oceanogr.* 53, 2451–2461.
- Baars, O., and Croot, P. L. (2011). Speciation of dissolved zinc in the Atlantic sector of the southern ocean. *Deep Sea Res II* 58, 2720–2732.
- Badger, M. R., and Price, G. D. (1994). The role of carbonic anhydrase in photosynthesis. *Annu. Rev. Plant Physiol. Plant Mol. Biol.* 45, 369–392.
- Balzano, S., Statham, P. J., Pancost, R. D., and Lloyd, J. R. (2009). Role of microbial populations in the release of reduced iron to the water column from marine aggregates. *Aquat. Microb. Ecol.* 54, 291–303.
- Barbeau, K. (2006). Photochemistry of organic iron(III) complexing ligands in oceanic systems. *Photochem. Photobiol.* 82, 1505–1516.
- Barbeau, K., Rue, E. L., Bruland, K. W., and Butler, A. (2001). Photochemical cycling of iron in the surface ocean mediated by microbial iron(III)-binding ligands. *Nature* 413, 409–413.
- Barbeau, K., Rue, E. L., Trick, C. G., and Bruland, K. W., and Butler, A. (2003). Photochemical reactivity of siderophores produced by marine heterotrophic bacteria and cyanobacteria based on characteristic Fe(III) binding groups. *Limnol. Oceanogr.* 48, 1069–1078.
- Behrenfeld, M. J., and Kolber, Z. S. (1999). Widespread iron limitation of phytoplankton in the South Pacific Ocean. *Science* 283, 840–843.
- Bekker, A., Holland, H. D., Wang, P. L., Rumble, D., Stein, H. J., Hannah, J. L., Coetsee, L. L., and Beukes, N. J. (2004). Dating the rise of atmospheric oxygen. *Nature* 427, 117–120.
- Benner, R. (2011). Loose ligands and available iron in the ocean. *Proc. Natl. Acad. Sci. U.S.A.* 108, 893–894.
- Bertrand, E. M., Saito, M. A., Rose, J. M., Riesselman, C. R., Lohan, M. C., Noble, A. E., Lee, P. A., and DiTullio, G. R. (2007). Vitamin B-12 and iron colimitation of phytoplankton growth in the Ross Sea. *Limnol. Oceanogr.* 52, 1079–1093.
- Blankenship, R. E., Sadekar, S., and Raymond, J. (2007). “The evolutionary transition from anoxygenic to oxygenic photosynthesis,” in *Evolution of primary production in the sea*, eds P. G. Falkowski and A. H. Knoll (Amsterdam: Elsevier), 21–35.
- Boyd, E. S., Hamilton, T. L., and Peters, J. W. (2011). An alternative path for the evolution of biological nitrogen fixation. *Front. Microbiol.* 2:205. doi:10.3389/fmicb.2011.00205
- Boyd, P. W., and Ellwood, M. J. (2010). The biogeochemical cycle of iron in the ocean. *Nat. Geosci.* 3, 675–682.
- Boyd, P. W., Jickells, T., Law, C. S., Blain, S., Boyle, E. A., Buesseler, K. O., Coale, K. H., Cullen, J. J., de Baar, H. J. W., Follows, M., Harvey, M., Lancelot, C., Levasseur, M., Owens, N. P. J., Pollard, R., Rivkin, R. B., Sarmiento, J., Choe-mann, V., Smetacek, V., Takeda, S., Tsuda, A., Turner, S., and Watson, A. J. (2007). Mesoscale iron enrichment experiments 1993–2005: synthesis and future directions. *Science* 315, 612–617.
- Boyle, E., Edmond, J. M., and Sholkovitz, E. R. (1977). The mechanism of iron removal in estuaries. *Geochim. Cosmochim. Acta* 41, 1313–1324.
- Brand, L. E. (1991). Minimum iron requirements of marine phytoplankton and the implications for the biogeochemical control of new production. *Limnol. Oceanogr.* 36, 1756–1771.
- Brand, L. E., Sunda, W. G., and Guillard, R. L. L. (1983). Limitation of marine phytoplankton reproductive rates by zinc, manganese and iron. *Limnol. Oceanogr.* 28, 1182–1198.

- Brand, L. E., Sunda, W. G., and Guilford, R. R. L. (1986). Reduction of marine phytoplankton reproduction rates by copper and cadmium. *J. Exp. Mar. Biol. Ecol.* 96, 225–250.
- Broecker, W. S. (1991). The great ocean conveyor. *Oceanography* 4, 79–89.
- Bruland, K. W. (1980). Oceanographic distributions of cadmium, zinc, nickel and copper in the North Pacific. *Earth Planet. Sci. Lett.* 47, 176–198.
- Bruland, K. W. (1989). Complexation of zinc by natural organic ligands in the central North Pacific. *Limnol. Oceanogr.* 34, 267–285.
- Bruland, K. W. (1992). Complexation of cadmium by natural organic ligands in the central North Pacific. *Limnol. Oceanogr.* 37, 1008–1017.
- Bruland, K. W., and Franks, R. P. (1983). “Mn, Ni, Cu, Zn and Cd in the Western North Atlantic,” in *Trace Metals in Sea Water*, eds C. S. Wong, E. Boyle, K. W. Bruland, J. D. Burton, and E. D. Goldberg (New York: Plenum Press), 395–414.
- Bruland, K. W., and Lohan, M. C. (2003). “Controls of trace metals in seawater,” in *Treatise on Geochemistry*, eds D. H. Heinrich and K. T. Karl (Oxford: Pergamon), 23–47.
- Bruland, K. W., Orjans, K. J., and Cowen, J. P. (1994). Reactive trace metals in the stratified central North Pacific. *Geochim. Cosmochim. Acta* 58, 3171–3182.
- Buck, K. N., and Bruland, K. W. (2007). The physicochemical speciation of dissolved iron in the Bering Sea, Alaska. *Limnol. Oceanogr.* 52, 1800–1808.
- Buck, K. N., Selph, K. E., and Barbeau, K. A. (2010). Iron-binding ligand production and copper speciation in an incubation experiment of Antarctic Peninsula shelf waters from the Bransfield Strait, Southern Ocean. *Mar. Chem.* 122, 148–159.
- Buma, A. G. J., de Baar, H. J. W., Nolting, R. F., and van Bennekom, A. J. (1991). Metal enrichment experiments in the Weddell-Scotia Seas: effects of iron and manganese on various plankton communities. *Limnol. Oceanogr.* 36, 1865–1878.
- Butler, A., and Theisen, R. M. (2010). Iron(III)-siderophore coordination chemistry: reactivity of marine siderophores. *Coord. Chem. Rev.* 254, 288–296.
- Byrne, R. H., Kump, L. R., and Cantrell, K. J. (1988). The influence of temperature and pH on trace metal speciation in seawater. *Mar. Chem.* 25, 163–181.
- Castruita, M., Saito, M., Schottel, P. C., Elmgreen, L. A., Myneni, S., Stiefel, E. I., and Morel, F. M. M. (2006). Overexpression and characterization of an iron storage and DNA-binding Dps protein from *Trichodesmium erythraeum*. *Appl. Environ. Microbiol.* 72, 2918–2924.
- Charlson, R. J., Lovelock, J. E., Andreae, M. O., and Warren, S. G. (1987). Oceanic phytoplankton, atmospheric sulfur, cloud albedo and climate. *Nature* 326, 655–661.
- Coale, K. H. (1991). Effects of iron, manganese, copper, and zinc enrichments on productivity and biomass in the subarctic Pacific. *Limnol. Oceanogr.* 36, 1851–1864.
- Coale, K. H., and Bruland, K. W. (1988). Copper complexation in the northeast Pacific. *Limnol. Oceanogr.* 33, 1084–1101.
- Coale, K. H., and Bruland, K. W. (1990). Spatial and temporal variation of copper complexation in the North Pacific. *Deep Sea Res.* 47, 317–336.
- Coale, K. H., Fitzwater, S. E., Gordon, R. M., Johnson, K. S., and Barber, R. T. (1996). Control of community growth and export production by upwelled iron in the equatorial Pacific Ocean. *Nature* 379, 621–624.
- Coale, K. H., Johnson, K. S., Chavez, F. P., Buesseler, K. O., Barber, R. T., Brzezinski, M. A., Cochlan, W. P., Millero, F. J., Falkowski, P. G., Bauer, J. E., Wanninkhof, R. H., Kudela, R. M., Altabet, M. A., Hales, B. E., Takahashi, T., Landry, M. R., Bidigare, R. R., Wang, X., Chase, Z., Strutton, P. G., Friederich, G. E., Gorbunov, M. Y., Lance, V. P., Hiltling, A. K., Hiscock, M. R., Demarest, M., Hiscock, W. T., Sullivan, K. F., Tanner, S. J., Gordon, R. M., Hunter, C. N., Elrod, V. A., Fitzwater, S. E., Jones, J. L., Tozzi, S., Kobalick, M., Roberts, A. E., and Herndon, J. (2004). Southern ocean iron enrichment experiment: carbon cycling in high- and low-Si waters. *Science* 304, 408–414.
- Collier, R. W. (1985). Molybdenum in the northeast Pacific Ocean. *Limnol. Oceanogr.* 30, 1351–1354.
- Crawford, D. W., Lipsen, M. S., Purdie, D. A., Lohan, M. C., Statham, P. J., Whitney, F. A., Putland, J. N., Johnson, W. K., Sutherland, N., Peterson, T. D., Harrison, P. J., and Wong, C. S. (2003). Influence of zinc and iron enrichments on phytoplankton growth in the northeastern subarctic Pacific. *Limnol. Oceanogr.* 48, 1583–1600.
- Croft, M. T., Lawrence, A. D., Raux-Deery, E., Warren, M. J., and Smith, A. G. (2005). Algae acquire vitamin B₁₂ through a symbiotic relationship with bacteria. *Nature* 438, 90–93.
- Croft, P. L., Baars, O., and Streu, P. (2011). The distribution of dissolved zinc in the Atlantic sector of the Southern Ocean. *Deep Sea Res. II* 58, 2707–2719.
- Croft, P. L., Bluhm, K., Schlosser, C., Streu, P., Breitbarth, E., Frew, R., and Van Ardelan, M. (2008). Regeneration of Fe(II) during EIfEX and SOFeX. *Geophys. Res. Lett.* 35, L19606.
- Croft, P. L., Moffett, J. W., and Brand, L. E. (2000). Production of extracellular ligands by eucaryotic phytoplankton in response to Cu stress. *Limnol. Oceanogr.* 45, 619–627.
- Cullen, J. T., Bergquist, B. A., and Moffett, J. W. (2006). Thermodynamic characterization of the partitioning of iron between soluble and colloidal species in the Atlantic Ocean. *Mar. Chem.* 98, 295–303.
- Cullen, J. T., and Sherrell, R. M. (2005). Effects of dissolved carbon dioxide, zinc, and manganese on the cadmium to phosphorus ratio in natural phytoplankton assemblages. *Limnol. Oceanogr.* 50, 1193–1204.
- da Silva, J. J. R. F., and Williams, R. J. P. (1991). *The Biological Chemistry of the Elements*. Oxford: Clarendon Press.
- Duce, R. A., and Tindale, N. W. (1991). Atmospheric transport of iron and its deposition in the ocean. *Limnol. Oceanogr.* 36, 1715–1726.
- Dupont, C. L., Barbeau, K., and Palenik, B. (2008a). Ni uptake and limitation in marine *Synechococcus* strains. *Appl. Environ. Microbiol.* 74, 23–31.
- Dupont, C. L., Neupane, K., Shearer, J., and Palenik, B. (2008b). Diversity, function and evolution of genes coding for putative Ni-containing superoxide dismutases. *Environ. Microbiol.* 10, 1831–1843.
- Dymond, J., and Lyle, M. (1985). Flux comparisons between sediments and sediment traps in the eastern tropical Pacific: implications for atmospheric CO₂ variations during the Pleistocene. *Limnol. Oceanogr.* 30, 699–712.
- Ellwood, M. J. (2004). Zinc and cadmium speciation in subantarctic waters east of New Zealand. *Mar. Chem.* 87, 37–58.
- Ellwood, M. J., and van den Berg, C. M. G. (2000). Zinc speciation in the Northeastern Atlantic Ocean. *Mar. Chem.* 68, 295–306.
- Ellwood, M. J., and van den Berg, C. M. G. (2001). Determination of organic complexation of cobalt in seawater by cathodic stripping voltammetry. *Mar. Chem.* 75, 33–47.
- Emerson, S., Kalhorn, S., Jacobs, L., Tebo, B. M., Neelson, K. H., and Rosson, R. A. (1982). Environmental oxidation rate of manganese(II): bacterial catalysis. *Geochim. Cosmochim. Acta* 46, 1073–1079.
- Emerson, S. R., and Husted, S. S. (1991). Ocean anoxia and the concentration of molybdenum and vanadium in seawater. *Mar. Chem.* 34, 177–196.
- Falkowski, P. G. (1997). Evolution of the nitrogen cycle and its influence on the biological sequestration of CO₂ in the ocean. *Nature* 387, 272–275.
- Fan, S.-M. (2008). Photochemical and biochemical controls on reactive oxygen and iron speciation in the pelagic surface ocean. *Mar. Chem.* 109, 152–164.
- Field, C. B., Behrenfeld, M. J., Randerson, J. T., and Falkowski, P. (1998). Primary production of the biosphere: integrating terrestrial and oceanic components. *Science* 281, 237–240.
- Finney, L. A., and O'Halloran, T. V. (2003). Transition metal speciation in the cell: insights from the chemistry of metal ion receptors. *Science* 300, 931–936.
- Franck, V. M., Bruland, K. W., Hutchins, D. A., and Brzezinski, M. A. (2003). Iron and zinc effects on silicic acid and nitrate uptake kinetics in three high-nutrient, low-chlorophyll (HNLC) regions. *Mar. Ecol. Prog. Ser.* 252, 15–33.
- Gledhill, M., and Buck, K. N. (2012). The organic complexation of iron in the marine environment: a review. *Front. Microbiol.* 3:69. doi:10.3389/fmicb.2012.00069
- Gledhill, M., and van den Berg, C. M. G. (1994). Determination of complexation of iron(III) with natural organic complexing ligands in seawater using cathodic stripping voltammetry. *Mar. Chem.* 47, 41–54.
- Granéli, E., and Risinger, L. (1994). Effects of cobalt and vitamin B12 on the growth of *Cryochromulina polyplepis* (Prymnesiophyceae). *Mar. Ecol. Prog. Ser.* 113, 177–183.
- Guo, J., Annett, A. L., Taylor, R. L., Lapi, S., Ruth, T. J., and Maldonado, M. T. (2010). Copper-uptake kinetics of coastal and oceanic diatoms. *J. Phycol.* 46, 1218–1228.
- Guo, J., Lapi, S., Ruth, T. J., and Maldonado, M. T. (2012). The effects of iron and copper availability on the copper stoichiometry of marine phytoplankton. *J. Phycol.* 48, 312–325.
- Hartwig, A. (2001). Zinc finger proteins as potential targets for toxic metal ions: differential effects on structure and function. *Antioxid. Redox Signal.* 3, 625–634.

- Hassler, C. S., Alasonati, E., Mancuso Nichols, C. A., and Slaveykova, V. I. (2011a). Exopolysaccharides produced by bacteria isolated from the pelagic Southern Ocean – role in Fe binding, chemical reactivity, and bioavailability. *Mar. Chem.* 123, 88–98.
- Hassler, C. S., Schoemann, V., Nichols, C. M., Butler, E. C. V., and Boyd, P. W. (2011b). Saccharides enhance iron bioavailability to southern ocean phytoplankton. *Proc. Natl. Acad. Sci. U.S.A.* 108, 1076–1081.
- Ho, T. -Y., Quigg, A., Finkel, Z. V., Milligan, A. J., Wyman, K., Falkowski, P. G., and Morel, F. M. M. (2003). The elemental composition of some marine phytoplankton. *J. Phycol.* 39, 1145–1159.
- Hopkinson, B. M., and Barbeau, K. A. (2008). Interactive influences of iron and light limitation on phytoplankton at subsurface chlorophyll maxima in the eastern North Pacific. *Limnol. Oceanogr.* 53, 1303–1318.
- Hopkinson, B. M., and Barbeau, K. A. (2012). Iron transporters in marine prokaryotic genomes. *Environ. Microbiol.* 14, 114–128.
- Hopkinson, B. M., and Morel, F. M. M. (2009). The role of siderophores in iron acquisition by photosynthetic marine microorganisms. *Biometals* 22, 659–669.
- Hudson, R. J. M., and Morel, F. M. M. (1990). Iron transport in marine phytoplankton: kinetics of cellular and medium coordination reactions. *Limnol. Oceanogr.* 35, 1002–1020.
- Hudson, R. J. M. (1998). Which aqueous species control the rates of trace metal uptake by aquatic biota? Observations and predictions of non-equilibrium effects. *Sci. Total Environ.* 219, 95–115.
- Hudson, R. J. M., and Morel, F. M. M. (1993). Trace metal transport by marine microorganisms: implications of metal coordination kinetics. *Deep Sea Res.* 40, 129–150.
- Hunter, K. A., and Boyd, P. W. (2007). Iron-binding ligands and their role in the ocean biogeochemistry of iron. *Environ. Chem.* 4, 221–232.
- Hutchins, D. A., and Bruland, K. W. (1994). Grazer-mediated regeneration and assimilation of Fe, Zn, and Mn from planktonic prey. *Mar. Ecol. Prog. Ser.* 110, 259–269.
- Hutchins, D. A., DiTullio, G. R., and Bruland, K. W. (1993). Iron and regenerated production: evidence for biological iron recycling in two marine environments. *Limnol. Oceanogr.* 38, 1242–1255.
- Hutchins, D. A., Hare, C. E., Weaver, R. S., Zhang, Y., Fier, G. F., DiTullio, G. R., Alm, M. B., Riseman, S. F., Maucher, J. M., Geesey, M. E., Trick, C. G., Smith, G. J., Rue, E. L., Conn, J., and Bruland, K. W. (2002). Phytoplankton iron limitation in the Humboldt current and Peru upwelling. *Limnol. Oceanogr.* 47, 997–1011.
- Hutchins, D. A., Witter, A. E., Butler, A., and Luther, G. W. (1999). Competition among marine phytoplankton for different chelated iron speciation. *Nature* 400, 858–861.
- Ito, Y., and Butler, A. (2005). Structure of synechobactins, new siderophores of the marine cyanobacterium *Synechococcus* sp. PCC 7002. *Limnol. Oceanogr.* 50, 1918–1923.
- Jakuba, R. W., Moffett, J. W., and Dyhrman S. T. (2008). Evidence for the linked biogeochemical cycling of zinc, cobalt, and phosphorus in the western North Atlantic Ocean. *Global Biogeochem. Cycles* 22, GB4012.
- Jickells, T. D., An, Z. S., Andersen, K. K., Baker, A. R., Bergametti, G., Brooks, N., Cao, J. J., Boyd, P. W., Duce, R. A., Hunter, K. A., Kawahata, H., Kubilay, N., LaRoche, J., Liss, P. S., Mahowald, N., Prospero, J. M., Ridgwell, A. J., Tegen, I., and Torres, R. (2005). Global iron connections between desert dust, ocean biogeochemistry and climate. *Science* 308, 67–71.
- Jickells, T. D., and Burton, J. D. (1988). Cobalt, copper, manganese and nickel in the Sargasso Sea. *Mar. Chem.* 23, 131–144.
- Jickells, T. D., and Spokes, L. J. (2001). “Atmospheric iron input to the oceans,” in *The Biogeochemistry of Iron in Seawater*, eds D. R. Turner and K. A. Hunter (New York: Wiley), 85–121.
- Johnson, K. S., Gordon, R. M., and Coale, K. H. (1997). What controls dissolved iron concentrations in the world ocean? *Mar. Chem.* 57, 137–161.
- Jones, G. J., Palenik, B. P., and Morel, F. M. M. (1987). Trace metal reduction by phytoplankton: the role of plasmalemma redox enzymes. *J. Phycol.* 23, 237–244.
- Katz, M. E., Fennel, K., and Falkowski, P. G. (2007). “Geochemical and biological consequences of phytoplankton evolution,” in *Evolution of Primary Production in the Sea*, eds P. G. Falkowski and A. H. Knoll (Amsterdam: Elsevier), 405–430.
- Kranzler, C., Lis, H., Shaked, Y., and Keren, N. (2011). The role of reduction in iron uptake processes in a unicellular, planktonic cyanobacterium. *Environ. Microbiol.* 13, 2990–2999.
- Kuma, K., Nakabayashi, S., Suzuki, Y., Kudo, I., and Matsunaga, K. (1992). Photoreduction of Fe(III) by dissolved organic substances and existence of Fe(II) in seawater during spring blooms. *Mar. Chem.* 37, 15–27.
- Kuma, K., Nishioka, J., and Matsunaga, K. (1996). Controls on iron(III) hydroxide solubility in seawater: the influence of pH and natural organic chelators. *Limnol. Oceanogr.* 41, 396–407.
- Kustka, A. B., Allen, A. E., and Morel, F. M. M. (2007). Sequence analysis and transcriptional regulation of iron acquisition genes in two marine diatoms. *J. Phycol.* 43, 715–729.
- Kustka, A. B., Sañudo-Wilhelmy, S., Carpenter, E. J., Capone, D., Burns, J., and Sunda, W. G. (2003a). Iron requirements for dinitrogen and ammonium supported growth in cultures of *Trichodesmium* (IMS 101): comparison with nitrogen fixation rates and iron:carbon ratios of field populations. *Limnol. Oceanogr.* 48, 1869–1884.
- Kustka, A. B., Sañudo-Wilhelmy, S., Carpenter, E. J., Capone, D. G., and Raven, J. A. (2003b). A revised estimate of the iron use efficiency of nitrogen fixation, with special reference to the marine cyanobacterium *trichodesmium* spp. (Cyanophyta). *J. Phycol.* 39, 12–25.
- Kustka, A. B., Shaked, Y., Milligan, A. J., King, D. W., and Morel, F. M. M. (2005). Extracellular production of superoxide by marine diatoms: contrasting effects on iron redox chemistry and bioavailability. *Limnol. Oceanogr.* 50, 1172–1180.
- La Roche, J., Boyd, P. W., McKay, M. L., and Geider, R. J. (1996). Flavodoxin as an in situ marker for iron stress in phytoplankton. *Nature* 382, 802–805.
- Laglera, L. M., and van den Berg, C. M. G. (2009). Evidence for geochemical control of iron by humic substances in seawater. *Limnol. Oceanogr.* 54, 610–619.
- Laglera, L. M., Battaglia, G., and van den Berg, C. M. G. (2011). Effect of humic substances on the iron speciation in natural waters by CLE/CSV. *Mar. Chem.* 127, 134–143.
- Landing, W. M., and Bruland, K. W. (1987). The contrasting biogeochemistry of iron and manganese in the Pacific Ocean. *Geochim. Cosmochim. Acta* 51, 29–43.
- Lane, E. S., Jang, K., Cullen, J. T., and Maldonado, M. T. (2008). The interaction between inorganic iron and cadmium uptake in the marine diatom *Thalassiosira oceanica*. *Limnol. Oceanogr.* 53, 1784–1789.
- Lane, E. S., Semeniuk, D. M., Strzepek, R. F., Cullen, J. T., and Maldonado, M. T. (2009). Effects of iron limitation on intracellular cadmium of cultured phytoplankton: implications for surface dissolved cadmium to phosphate ratios. *Mar. Chem.* 115, 155–162.
- Lane, T. W., and Morel, F. M. M. (2000). Regulation of carbonic anhydrase expression by zinc, cobalt, and carbon dioxide in the marine diatom *Thalassiosira weissflogii*. *Plant Physiol.* 123, 345–352.
- Leal, M. F. C., and van den Berg, C. M. G. (1998). Evidence for strong copper(I) complexation by organic matter in seawater. *Aquat. Geochem.* 4, 49–75.
- Lohan, M. C., Crawford, D. W., Purdie, D. A., and Statham, P. J. (2005). Iron and zinc enrichments in the northeastern subarctic Pacific: ligand production and zinc availability in response to phytoplankton growth. *Limnol. Oceanogr.* 50, 1427–1437.
- Lomas, M. W., Burke, A. L., Lomas, D. A., Bell, D. W., Shen, C., Dyhrman, S. T., and Ammerman, J. W. (2010). Sargasso Sea phosphorus biogeochemistry: an important role for dissolved organic phosphorus (DOP). *Biogeochemistry* 7, 695–710.
- Lui, X., and Millero, F. J. (2002). The solubility of iron in seawater. *Mar. Chem.* 77, 43–54.
- Macrellis, H. M., Trick, C. G., Rue, E. L., Smith, G., and Bruland, K. W. (2001). Collection and detection of natural iron-binding ligands from seawater. *Mar. Chem.* 76, 175–187.
- Maldonado, M. T., Allen, A. E., Chong, J. S., Lin, K., Leus, D., Karpenko, N., and Harris, S. L. (2006). Copper-dependent iron transport in coastal and oceanic diatoms. *Limnol. Oceanogr.* 51, 1729–1743.
- Maldonado, M. T., Boyd, P. W., Harrison, P. J., and Price, N. M. (1999). Co-limitation of phytoplankton growth by light and Fe during winter in the NE subarctic Pacific Ocean. *Deep Sea Res.* 46, 2475–2485.
- Maldonado, M. T., and Price, N. M. (1996). Influence of N substrate on Fe requirements of marine centric diatoms. *Mar. Ecol. Prog. Ser.* 141, 161–172.
- Maldonado, M. T., and Price, N. M. (2001). Reduction and transport of organically bound iron by

- Thalassiosira oceanica*. *J. Phycol.* 37, 298–310.
- Maldonado, M. T., Strzepek, R. F., Sander, S., and Boyd, P. W. (2005). Acquisition of iron bound to strong organic complexes, with different Fe binding groups and photochemical reactivities, by plankton communities in Fe-limited subantarctic waters. *Global Biogeochem. Cycles* 19, GB4S23.
- Marchetti, A., Maldonado, M. T., Lane, E. S., and Harrison, P. J. (2006). Iron requirements of the pennate diatom *Pseudo-nitzschia*: comparison of oceanic (high-nitrate, low-chlorophyll waters) and coastal species. *Limnol. Oceanogr.* 51, 2092–2101.
- Marchetti, A., Parker, M. S., Moccia, L. P., Lin, E. O., Arrieta, A. L., Ribalet, F., Murphy, M. E. P., Maldonado, M. T., and Armbrust, E. V. (2009). Ferritin is used for iron storage in bloom-forming marine pennate diatoms. *Nature* 457, 467–470.
- Martin, J. H. (1990). Glacial-interglacial CO₂ change: the iron hypothesis. *Paleoceanography* 5, 1–13.
- Martin, J. H., Bruland, K. W., and Broenkow, W. W. (1976). "Cadmium transport in the California current," in *Marine Pollutant Transfer*, eds H. L. Windom and R. A. Duce (Toronto: D. C. Heath and Co.), 159–184.
- Martin, J. H., and Fitzwater, S. E. (1988). Iron deficiency limits phytoplankton growth in the north-east Pacific subarctic. *Nature* 331, 341–343.
- Martin, J. H., Fitzwater, S. E., Gordon, R. M., Hunter, C. N., and Tanner, S. J. (1993). Iron, primary production and carbon-nitrogen flux studies during the JGOFS North Atlantic Bloom Experiment. *Deep Sea Res.* 40, 115–134.
- Martin, J. H., Gordon, R. M., Fitzwater, S., and Broenkow, W. W. (1989). VERTEX: phytoplankton/iron studies in the Gulf of Alaska. *Deep Sea Res.* 36, 649–680.
- Martin, J. H., Gordon, R. M., and Fitzwater, S. E. (1990). Iron in Antarctic waters. *Nature* 345, 156–158.
- Martin, J. H., Gordon, R. M., and Fitzwater, S. E. (1991). The case for iron. *Limnol. Oceanogr.* 36, 1793–1802.
- Martinez, J. S., Zhang, G. P., Holt, P. D., Jung, H. -T., Carrano, C. J., Haygood, M. G., and Butler, A. (2000). Self-assembling amphiphilic siderophores from marine bacteria. *Science* 287, 1245–1247.
- Martinez-Garcia, A., Rosell-Mele, A., Jaccard, S. L., Geibert, W., Sigman, D. M., and Haug, G. H. (2011). Southern Ocean dust-climate coupling over the past four million years. *Nature* 476, 312–315.
- Mauzerall, D. (2007). "Oceanic photochemistry and evolution of elements and cofactors in the early stages of the evolution of life," in *Evolution of Primary Production in the Sea*, eds P. G. Falkowski and A. H. Knoll (Amsterdam: Elsevier), 7–19.
- Mawji, E., Gledhill, M., Milton, J. A., Tarran, G. A., Ussher, S., Thompson, A., Wolff, G. A., Worsfold, P. J., and Achterberg, E. P. (2008). Hydroxamate siderophores: occurrence and importance in the Atlantic Ocean. *Environ. Sci. Technol.* 42, 8675–8680.
- Mawji, E., Gledhill, M., Milton, J. A., Zubkov, M. V., Thompson, A., Wolff, G. A., and Achterberg, E. P. (2011). Production of siderophore type chelates in Atlantic Ocean waters enriched with different carbon and nitrogen sources. *Mar. Chem.* 124, 90–99.
- Measures, C. I., and Vink, S. (1999). Seasonal variations in the distribution of Fe and Al in the surface waters of the Arabian Sea. *Deep Sea Res.* 46, 1597–1622.
- Moffett, J. W. (1990). Microbially mediated cerium oxidation in sea water. *Nature* 345, 421–423.
- Moffett, J. W. (1995). Temporal and spatial variability of strong copper complexing ligands in the Sargasso Sea. *Deep Sea Res.* 42, 1273–1295.
- Moffett, J. W., and Brand, L. E. (1996). Production of strong, extracellular Cu chelators by marine cyanobacteria in response to Cu stress. *Limnol. Oceanogr.* 41, 388–395.
- Moffett, J. W., and Dupont, C. (2007). Cu complexation by organic ligands in the sub-arctic NW Pacific and Bering Sea. *Deep Sea Res.* 54, 586–595.
- Moffett, J. W., and Ho, J. (1996). Oxidation of cobalt and manganese in seawater via a common microbially catalyzed pathway. *Geochim. Cosmochim. Acta* 60, 3415–3424.
- Moffett, J. W., and Zika, R. G. (1988). Measurement of copper(II) in surface waters of the subtropical Atlantic and Gulf of Mexico. *Geochim. Cosmochim. Acta* 52, 1849–1857.
- Montoya, J. P., Holl, C. M., Zehr, J. P., Hansen, A., Villareal, T. A., and Capone, D. G. (2004). High rates of N₂ fixation by unicellular diazotrophs in the oligotrophic Pacific Ocean. *Nature* 430, 1027–1031.
- Moore, J., Doney, S., and Lindsay, K. (2004). Upper ocean ecosystem dynamics and iron cycling in a global three-dimensional model. *Global Biogeochem. Cycles* 18, ARTN GB4028, doi: 10.1029/2004GB002220
- Moore, J. K., and Braucher, O. (2008). Sedimentary and mineral dust sources of dissolved iron to the world ocean. *Biogeosciences* 5, 631–656.
- Moore, J. K., Doney, S. C., Glover, D. M., and Fung, I. Y. (2002). Iron cycling and nutrient-limitation patterns in surface waters of the World Ocean. *Deep Sea Res.* 49, 463–507.
- Morel, F. M. M., Kustka, A. B., and Shaked, Y. (2008). The role of unchelated Fe in the iron nutrition of phytoplankton. *Limnol. Oceanogr.* 53, 400–404.
- Morel, F. M. M., Reinfelder, J. R., Roberts, S. B., Chamberlain, C. P., Lee, J. G., and Yee, D. (1994). Zinc and carbon co-limitation of marine phytoplankton. *Nature* 369, 740–742.
- Morford, J., and Emerson, S. (1999). Geochemistry of redox sensitive trace metals in sediments. *Geochim. Cosmochim. Acta* 63, 1735–1750.
- Morgan, J. J. (1967). "Chemical equilibria and kinetic properties of manganese in natural waters" in *Principles and Applications of Water Chemistry*, eds S. D. Faust and J. V. Hunter (New York: Wiley), 561–620.
- Ozturk, M., Croot, P. L., Bertilsson, S., Abrahamsson, K., Karlson, B., David, R., Franssog, A., and Sakshaug, E. (2004). Iron enrichment and photoreduction of iron under UV and PAR in the presence of hydroxycarboxylic acid: implications for phytoplankton growth in the Southern Ocean. *Deep Sea Res.* 51, 2841–2856.
- Panzeca, C., Beck, A. J., Leblanc, K., Taylor, G. T., Hutchins, D. A., and Sañudo-Wilhelmy, S. A. (2008). Potential cobalt limitation of vitamin B12 synthesis in the North Atlantic Ocean. *Global Biogeochem. Cycles* 22, GB2029.
- Park, H., Song, B., and Morel, F. M. M. (2007). Diversity of the cadmium-containing carbonic anhydrase in marine diatoms and natural waters. *Environ. Microbiol.* 9, 403–413.
- Peers, G., and Price, N. M. (2004). A role for manganese in superoxide dismutases and growth of iron-deficient diatoms. *Limnol. Oceanogr.* 49, 1774–1783.
- Peers, G., and Price, N. M. (2006). Copper-containing plastocyanin used for electron transport by an oceanic diatom. *Nature* 441, 341–344.
- Peers, G., Quesnel, S. A., and Price, N. M. (2005). Copper requirements for iron acquisition and growth of coastal and oceanic diatoms. *Limnol. Oceanogr.* 50, 1149–1158.
- Poorvin, L., Rinta-Kanto, J. M., Hutchins, D. A., and Wilhelm, S. W. (2004). Viral release of iron and its bioavailability to marine plankton. *Limnol. Oceanogr.* 49, 1734–1741.
- Price, N. M., Ahner, B. A., and Morel, F. M. M. (1994). The equatorial Pacific Ocean: grazer-controlled phytoplankton population in an iron-limited ecosystem. *Limnol. Oceanogr.* 39, 520–534.
- Price, N. M., Andersen, L. F., and Morel, F. M. M. (1991). Iron and nitrogen nutrition of equatorial Pacific plankton. *Deep Sea Res.* 38, 1361–1378.
- Price, N. M., and Morel, F. M. M. (1990). Cadmium and cobalt substitution for zinc in a marine diatom. *Nature* 344, 658–660.
- Price, N. M., and Morel, F. M. M. (1991). Colimitation of phytoplankton growth by nickel and nitrogen. *Limnol. Oceanogr.* 36, 1071–1077.
- Raven, J. A. (1988). The iron and molybdenum use efficiencies of plant growth with different energy, carbon and nitrogen sources. *New Phytol.* 109, 279–287.
- Raven, J. A. (1990). Predictions of Mn and Fe use efficiencies of phototrophic growth as a function of light availability for growth and C assimilation pathway. *New Phytol.* 116, 1–18.
- Raven, J. A., Evans, M. C. W., and Korb, R. E. (1999). The role of trace metals in photosynthetic electron transport in O₂-evolving organisms. *Photosyn. Res.* 60, 111–149.
- Redfield, A. C., Ketchum, B. H., and Richards, F. A. (1963). "The influence of organisms on the composition of sea-water," in *The Sea*, ed. M. N. Hill (New York: Interscience Publication), 26–77.
- Rose, A. L., Salmon, T. P., Lukondeh, T., Neilan, B. A., and Waite, T. D. (2005). Use of superoxide as an electron shuttle for iron acquisition by the marine cyanobacterium *Lyngbya majuscula*. *Environ. Sci. Technol.* 39, 3708–3715.
- Roy, E. G., and Wells, M. L. (2011). Evidence for regulation of Fe(II) oxidation by organic complexing ligands in the Eastern Subarctic Pacific. *Mar. Chem.* 127, 115–122.
- Roy, E. G., Wells, M. L., and King, D. W. (2008). Persistence of iron(II) in surface waters of the western subarctic Pacific. *Limnol. Oceanogr.* 53, 89–98.
- Rubin, M., Berman-Frank, I., and Shaked, Y. (2011). Dust- and mineral-iron utilization by the

- marine dinitrogen-fixer *Trichodesmium*. *Nat. Geosci.* 4, 529–534.
- Rue, E., and Bruland, K. (2001). Domoic acid binds iron and copper: a possible role for the toxin produced by the marine diatom *Pseudo-nitzschia*. *Mar. Chem.* 76, 127–134.
- Rue, E. L., and Bruland, K. W. (1995). Complexation of iron(III) by natural organic-ligands in the central north pacific as determined by a new competitive ligand equilibration adsorptive cathodic stripping voltammetric method. *Mar. Chem.* 50, 117–138.
- Rueter, J. G. (1983). Theoretical iron limitation of microbial N₂ fixation in the oceans. *Eos (Washington DC)* 63, 445.
- Rueter, J. G., Hutchins, D. A., Smith, R. W., and Unsworth, N. L. (1992). "Iron nutrition of *Trichodesmium*," in *Marine pelagic cyanobacteria: Trichodesmium and other Diazotrophs*, eds E. J. Carpenter, D. G. Capone, and J. G. Rueter (Dordrecht: Kluwer), 289–306.
- Saito, M. A., Bertrand, E. M., Bulyn, V., Moran, D., Dutkiewicz, S., Monteiro, F. M., Follows, M. J., Valois, F. W., and Waterbury, J. B. (2011). Iron conservation by reduction of metalloenzyme inventories in the marine diazotroph *Crocospaera watsonii*. *Proc. Natl. Acad. Sci. U.S.A.* 108, 2184–2189.
- Saito, M. A., and Goepfert, T. J. (2008). Zinc-cobalt colimitation of *Phaeocystis antarctica*. *Limnol. Oceanogr.* 53, 266–275.
- Saito, M. A., and Moffett, J. W. (2001). Complexation of cobalt by natural organic ligands in the Sargasso Sea as determined by a new high-sensitivity electrochemical cobalt speciation method suitable for open ocean work. *Mar. Chem.* 75, 49–68.
- Saito, M. A., Moffett, J. W., Chisholm, S. W., and Waterbury J. B. (2002). Cobalt limitation and uptake in *Prochlorococcus*. *Limnol. Oceanogr.* 47, 1629–1636.
- Saito, M. A., Moffett, J. W., and DiTullio, G. R. (2004). Cobalt and nickel in the Peru upwelling region: a major flux of labile cobalt utilized as a micronutrient. *Global Biogeochem. Cycles* 18, GB4030, doi: 10.1029/2003GB002216
- Saito, M. A., Rocap, G., and Moffett, J. W. (2005). Production of cobalt binding ligands in a *Synechococcus* feature at the Costa Rica upwelling dome. *Limnol. Oceanogr.* 50, 279–290.
- Saito, M. A., Sigman, D. M., and Morel, F. M. M. (2003). The bioinorganic chemistry of the ancient ocean: the co-evolution of cyanobacterial metal requirements and biogeochemical cycles at the Archean-Proterozoic boundary? *Inorgan. Chem. Acta* 356, 308–318.
- Sandy, M., and Butler, A. (2009). Microbial iron acquisition: marine and terrestrial siderophores. *Chem. Rev.* 109, 4580–4595.
- Santana-Casiano, J. M., Gonzalez-Davila, M., and Millero, F. J. (2005). Oxidation of nanomolar levels of Fe(II) with oxygen in natural waters. *Environ. Sci. Technol.* 39, 2073–2079.
- Sarthou, G., Bucciarelli, E., Chever, F., Hansard, S. P., Gonzalez-Davila, M., Santana-Casiano, J. M., Planchon, F., and Speich, S. (2011). Labile Fe(II) concentrations in the Atlantic sector of the Southern Ocean along a transect from the subtropical domain to the Weddell Sea Gyre. *Biogeochemistry* 8, 2461–2479.
- Scanlan, D. J., Ostrowski, M., Mazard, S., Dufresne, A., Garczarek, L., Hess, W. R., Post, A. F., Hagemann, M., Paulsen, I., and Partensky, F. (2009). Ecological genomics of marine picocyanobacteria. *Microb. Mol. Biol. Rev.* 73, 249–299.
- Schindler, D. W. (1977). Evolution of phosphorus limitation in lakes. *Science* 195, 260–262.
- Shaked, Y. (2008). Iron redox dynamics in the surface waters of the Gulf of Aqaba, Red Sea. *Geochim. Cosmochim. Acta* 72, 1540–1554.
- Shaked, Y., Kustka, A. B., and Morel, F. M. M. (2005). A general kinetic model for iron acquisition by eucaryotic phytoplankton. *Limnol. Oceanogr.* 50, 872–882.
- Shaked, Y., and Lis, H. (2012). Disassembling iron availability to phytoplankton. *Front. Microbiol. Chem.* 3:123. doi:10.3389/fmicb.2012.00123
- Shaked, Y., Xu, Y., Leblanc, K., and Morel, F. M. M. (2006). Zinc availability and alkaline phosphatase activity in *Emiliania huxleyi*: implications for Zn-P co-limitation in the ocean. *Limnol. Oceanogr.* 51, 299–309.
- Sharma, V. K., and Millero, F. J. (1988). Oxidation of copper(I) in seawater. *Environ. Sci. Technol.* 22, 768–771.
- Sigman, D. M., and Boyle, E. A. (2000). Glacial/interglacial variations in atmospheric carbon dioxide. *Nature* 407, 859–869.
- Sohm, J. A., Webb, E. A., and Capone, D. G. (2011). Emerging patterns of marine nitrogen fixation. *Nat. Rev. Microbiol.* 9, 499–508.
- Steigenberger, S., Statham, P. J., Voelker, C., and Passow, U. (2010). The role of polysaccharides and diatom exudates in the redox cycling of Fe and the photoproduction of hydrogen peroxide in coastal seawaters. *Biogeochemistry* 7, 109–119.
- Strzepek, R. F., and Harrison, P. J. (2004). Photosynthetic architecture differs in coastal and oceanic diatoms. *Nature* 431, 689–692.
- Strzepek, R. F., Maldonado, M. T., Higgins, J. L., Hall, J., Safi, K., Wilhelm, S. W., and Boyd, P. W. (2005). Spinning the "Ferrous Wheel": the importance of the microbial community in an iron budget during the FeCycle experiment. *Global Biogeochem. Cycles* 19, GB4S26.
- Strzepek, R. F., Maldonado, M. T., Hunter, K. A., Frew, R. D., and Boyd, P. W. (2011). Adaptive strategies by Southern Ocean phytoplankton to lessen iron limitation: uptake of organically complexed iron and reduced cellular iron requirements. *Limnol. Oceanogr.* 56, 1983–2002.
- Sunda, W., and Huntsman, S. (2003). Effect of pH, light, and temperature on Fe-EDTA chelation and Fe hydrolysis in seawater. *Mar. Chem.* 84, 35–47.
- Sunda, W. G. (2001). "Bioavailability and bioaccumulation of iron in the sea," in *The Biogeochemistry of Iron in Seawater*, eds D. R. Turner and K. A. Hunter (New York: Wiley), 41–84.
- Sunda, W. G., and Huntsman, S. A. (1985). Regulation of cellular manganese and manganese transport rates in the unicellular alga *Chlamydomonas*. *Limnol. Oceanogr.* 30, 71–80.
- Sunda, W. G., and Huntsman, S. A. (1986). Relationships among growth rate, cellular manganese concentrations and manganese transport kinetics in estuarine and oceanic species of the diatom *Thalassiosira*. *J. Phycol.* 22, 259–270.
- Sunda, W. G., and Huntsman, S. A. (1988). Effect of sunlight on redox cycles of manganese in the southwestern Sargasso Sea. *Deep Sea Res.* 35, 1297–1317.
- Sunda, W. G., and Huntsman, S. A. (1992). Feedback interactions between zinc and phytoplankton in seawater. *Limnol. Oceanogr.* 37, 25–40.
- Sunda, W. G., and Huntsman, S. A. (1994). Photoreduction of manganese oxides in seawater. *Mar. Chem.* 46, 133–152.
- Sunda, W. G., and Huntsman, S. A. (1995a). Cobalt and zinc interrelationship in marine phytoplankton: biological and geochemical implications. *Limnol. Oceanogr.* 40, 1404–1417.
- Sunda, W. G., and Huntsman, S. A. (1995b). Iron uptake and growth limitation in oceanic and coastal phytoplankton. *Mar. Chem.* 50, 189–206.
- Sunda, W. G., and Huntsman, S. A. (1995c). Regulation of copper concentration in the oceanic nutrient cycle by phytoplankton uptake and regeneration cycles. *Limnol. Oceanogr.* 40, 132–137.
- Sunda, W. G., and Huntsman, S. A. (1996). Antagonisms between cadmium and zinc toxicity and manganese limitation in a coastal diatom. *Limnol. Oceanogr.* 41, 373–387.
- Sunda, W. G., and Huntsman, S. A. (1997). Interrelated influence of iron, light and cell size on marine phytoplankton growth. *Nature* 390, 389–392.
- Sunda, W. G., and Huntsman, S. A. (1998a). Control of Cd concentrations in a coastal diatom by interactions among free ionic Cd, Zn, and Mn in seawater. *Environ. Sci. Technol.* 32, 2961–2968.
- Sunda, W. G., and Huntsman, S. A. (1998b). Processes regulating cellular metal accumulation and physiological effects: phytoplankton as model systems. *Sci. Total Environ.* 219, 165–181.
- Sunda, W. G., and Huntsman, S. A. (1998c). Interactions among Cu²⁺, Zn²⁺, and Mn²⁺ in controlling cellular Mn, Zn, and growth rate in the coastal alga *Chlamydomonas*. *Limnol. Oceanogr.* 43, 1055–1064.
- Sunda, W. G., and Huntsman, S. A. (1998d). Interactive effects of external manganese, the toxic metals copper and zinc, and light in controlling cellular manganese and growth in a coastal diatom. *Limnol. Oceanogr.* 43, 1467–1475.
- Sunda, W. G., and Huntsman, S. A. (2000). Effect of Zn, Mn, and Fe on Cd accumulation in phytoplankton: implications for oceanic Cd cycling. *Limnol. Oceanogr.* 45, 1501–1516.
- Sunda, W. G., and Huntsman, S. A. (2004). Relationships among photoperiod, carbon fixation, growth, chlorophyll a and cellular iron and zinc in a coastal diatom. *Limnol. Oceanogr.* 49, 1742–1753.
- Sunda, W. G., and Huntsman, S. A. (2005). Effect of CO₂ supply and demand on zinc uptake and growth limitation in a coastal diatom. *Limnol. Oceanogr.* 50, 1181–1192.
- Sunda, W. G., and Huntsman, S. A. (2011). Interactive effects of light and temperature on iron limitation in a marine diatom: implications for marine productivity and carbon cycling. *Limnol. Oceanogr.* 56, 1475–1488.

- Sunda, W. G. (1988/1989). Trace metal interactions with marine phytoplankton. *Biol. Oceanogr.* 6, 411–442.
- Tebo, B., Nealson, K., Emerson, S., and Jacobs, L. (1984). Microbial mediation of Mn(II) and Co(II) precipitation at the O₂/H₂ interfaces in two anoxic fjords. *Limnol. Oceanogr.* 29, 1247–1258.
- Tebo, B. M., Bargar, J. R., Clement, B. G., Dick, G. J., Murray, K. J., Parker, D., Verity, R., and Webb, S. M. (2004). Biogenic manganese oxides: properties and mechanisms of formation. *Annu. Rev. Earth Planet. Sci.* 32, 287–328.
- Tovar-Sanchez, A., Sanudo-Wilhelmy, S. A., Garcia-Vargas, M., Weaver, R. S., Popels, L. C., and Hutchins, D. A. (2003). A trace metal clean reagent to remove surface bound iron from marine phytoplankton. *Mar. Chem.* 82, 91–99.
- Trouwborst, R. E., Clement, B. G., Tebo, B. M., Glazer, B. T., and Luther, G. W. (2006). Soluble Mn(III) in suboxic zones. *Science* 313, 1955–1957.
- Twining, B. S., Baines, S. B., Bozard, J. B., Vogt, S., Walker, E. A., and Nelson, D. M. (2011). Metal quotas of plankton in the equatorial Pacific Ocean. *Deep Sea Res. II Top. Stud. Oceanogr.* 58, 325–341.
- Twining, B. S., Baines, S. B., and Fisher, N. S. (2004). Element stoichiometries of individual plankton cells collected during the southern ocean iron experiment (SOFEX). *Limnol. Oceanogr.* 49, 2115–2128.
- Twining, B. S., Nunez-Milland, D., Vogt, S., Johnson, R. S., and Sedwick, P. N. (2010). Variations in *Synechococcus* cell quotas of phosphorus, sulfur, manganese, iron, nickel, and zinc within mesoscale eddies in the Sargasso Sea. *Limnol. Oceanogr.* 55, 492–506.
- Valko, M., Morris, H., and Cronin, M. T. D. (2005). Metals, toxicity and oxidative stress. *Curr. Med. Chem.* 12, 1161–1208.
- Velasquez, I., Nunn, B. L., Ibanm, E., Goodlet, D. R., Hunter, K. A., and Sander, S. G. (2011). Detection of hydroxamate siderophores in coastal and sub-antarctic waters off the southeastern coast of New Zealand. *Mar. Chem.* 126, 97–107.
- Voelker, B. M., and Sedlak, D. L. (1995). Iron reduction by photoproducted superoxide in seawater. *Mar. Chem.* 50, 93–102.
- Vong, L., Laes, A., and Blain, S. (2007). Determination of iron-porphyrin-like complexes at nanomolar levels in seawater. *Anal. Chim. Acta* 588, 237–244.
- Vraspir, J. M., and Butler, A. (2009). Chemistry of marine ligands and siderophores. *Annu. Rev. Mar. Sci.* 1, 43–63.
- Waite, T. D., Szymczak, R., Espey, Q. I., and Furnas, M. J. (1995). Diel variations in iron speciation in northern Australian shelf waters. *Mar. Chem.* 50, 79–92.
- Walsby, A. E. (1992). “The gas vesicles and buoyancy of *Trichodesmium*,” in *Marine Pelagic Cyanobacteria: Trichodesmium and Other Diazotrophs*, eds E. J. Carpenter, D. G. Capone, and J. G. Rueter (Dordrecht: Kluwer), 141–161.
- Wells, M. L., Mayer, L. M., and Guillard, R. R. L. (1991). A chemical method for estimating the availability of iron to phytoplankton in seawater. *Mar. Chem.* 33, 23–40.
- Wilhelm, S. W., and Trick, C. G. (1994). Iron-limited growth of cyanobacteria: multiple siderophore production is a common response. *Limnol. Oceanogr.* 39, 1979–1984.
- Wolfe-Simon, F., Starovoytov, V., Reinfelder, J. R., Schofield, O., and Falkowski, P. J. (2006). Localization and role of manganese superoxide dismutase in a marine diatom. *Plant Physiol.* 142, 1701–1709.
- Wu, J., Boyle, E., Sunda, W., and Wen, L. (2001). Soluble and colloidal iron in the oligotrophic North Atlantic and North Pacific. *Science* 293, 847–849.
- Wu, J., Sunda, W. G., Boyle, E. A., and Karl, D. M. (2000). Phosphate depletion in the western North Atlantic Ocean. *Science* 289, 759–762.
- Xu, Y., Feng, L., Jeffrey, P. D., Shi, Y., and Morel, F. M. M. (2008). Structure and metal exchange in the cadmium carbonic anhydrase of marine diatoms. *Nature* 452, 56–61.
- Xu, Y., Tang, D., Shaked, Y., and Morel, F. M. M. (2007). Zinc, cadmium, and cobalt interreplacement and relative use efficiencies in the coccolithophore *Emiliania huxleyi*. *Limnol. Oceanogr.* 52, 2294–2305.
- Yoshida, M., Kuma, K., Iwade, S., Isoda, Y., Takata, H., and Yamada, M. (2006). Effect of aging time on the availability of freshly precipitated ferric hydroxide to coastal marine diatoms. *Mar. Biol.* 149, 379–392.
- Zehr, J. P. (2011). Nitrogen fixation by marine cyanobacteria. *Trends Microbiol.* 19, 162–173.
- Zehr, J. P., Waterbury, J. B., Turner, P. J., Montoya, J. P., Omoregie, E., Steward, G. F., Hansen, A., and Karl, D. M. (2001). Unicellular cyanobacteria fix N₂ in the subtropical North Pacific Ocean. *Nature* 412, 635–638.

Conflict of Interest Statement: The author declares that the research was conducted in the absence of any commercial or financial relationships that could be construed as a potential conflict of interest.

Received: 28 December 2011; accepted: 17 May 2012; published online: 07 June 2012.

Citation: Sunda WG (2012) Feed-back interactions between trace metal nutrients and phytoplankton in the ocean. *Front. Microbio.* 3:204. doi: 10.3389/fmicb.2012.00204

This article was submitted to *Frontiers in Microbiological Chemistry*, a specialty of *Frontiers in Microbiology*.

Copyright © 2012 Sunda. This is an open-access article distributed under the terms of the Creative Commons Attribution Non Commercial License, which permits non-commercial use, distribution, and reproduction in other forums, provided the original authors and source are credited.



Disassembling iron availability to phytoplankton

Yeala Shaked^{1,2*} and Hagar Lis^{1,2}

¹ Interuniversity Institute for Marine Sciences in Eilat, Eilat, Israel

² Institute of Earth Sciences, Hebrew University of Jerusalem, Jerusalem, Israel

Edited by:

Martha Gledhill, University of Southampton, UK

Reviewed by:

Andrew Rose, Southern Cross University, Australia

Mark Wells, University of Maine, USA

Micha Rijkenberg, Royal Netherlands Institute for Sea Research, Netherlands

*Correspondence:

Yeala Shaked, Interuniversity Institute for Marine Sciences in Eilat, P.O. Box 469, Eilat 88103, Israel.
e-mail: yshaked@vms.huji.ac.il

The bioavailability of iron to microorganisms and its underlying mechanisms have far reaching repercussions to many natural systems and diverse fields of research, including ocean biogeochemistry, carbon cycling and climate, harmful algal blooms, soil and plant research, bioremediation, pathogenesis, and medicine. Within the framework of ocean sciences, short supply and restricted bioavailability of Fe to phytoplankton is thought to limit primary production and curtail atmospheric CO₂ drawdown in vast ocean regions. Yet a clear-cut definition of bioavailability remains elusive, with elements of iron speciation and kinetics, phytoplankton physiology, light, temperature, and microbial interactions, to name a few, all intricately intertwined into this concept. Here, in a synthesis of published and new data, we attempt to disassemble the complex concept of iron bioavailability to phytoplankton by individually exploring some of its facets. We distinguish between the fundamentals of bioavailability – the acquisition of Fe-substrate by phytoplankton – and added levels of complexity involving interactions among organisms, iron, and ecosystem processes. We first examine how phytoplankton acquire free and organically bound iron, drawing attention to the pervasiveness of the reductive uptake pathway in both prokaryotic and eukaryotic autotrophs. Turning to acquisition rates, we propose to view the availability of various Fe-substrates to phytoplankton as a spectrum rather than an absolute “all or nothing.” We then demonstrate the use of uptake rate constants to make comparisons across different studies, organisms, Fe-compounds, and environments, and for gaging the contribution of various Fe-substrates to phytoplankton growth *in situ*. Last, we describe the influence of aquatic microorganisms on iron chemistry and fate by way of organic complexation and bio-mediated redox transformations and examine the bioavailability of these bio-modified Fe species.

Keywords: iron, bioavailability, uptake, phytoplankton, speciation, redox reactions, biogeochemistry, organic complexation

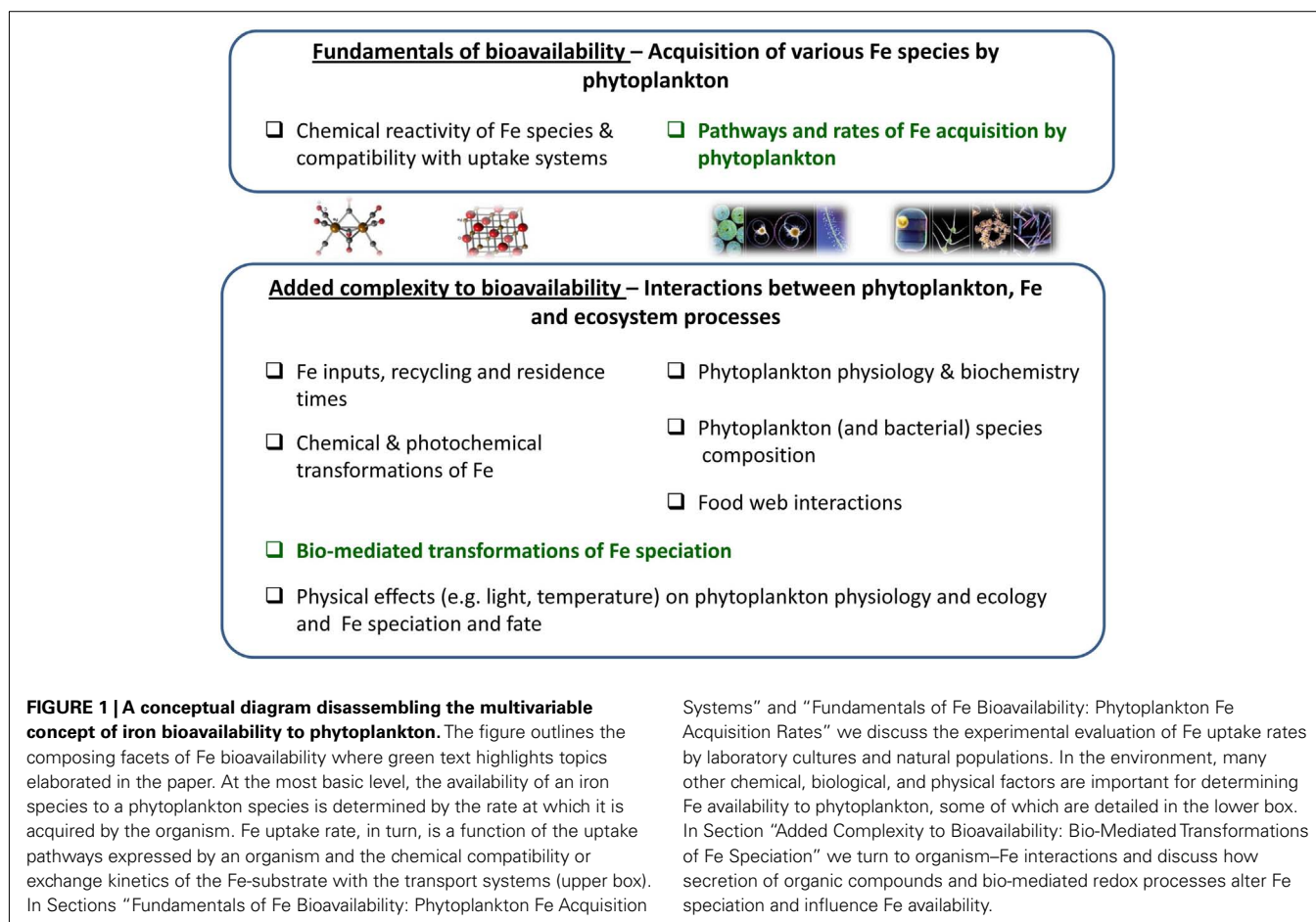
INTRODUCTION

By virtue of its flexible redox chemistry, iron (Fe) plays an integral role in many biological processes such as photosynthesis, respiration, processing of reactive oxygen species, and nutrient acquisition. In view of these functions, it is not surprising that iron inputs and bioavailability in aquatic environments have far reaching repercussions for many natural systems and diverse areas of study as briefly outlined in **Box 1**. At the basis of these lies the role of iron in controlling phytoplankton growth. Photosynthetic life on Earth originated in reduced, low oxygen aquatic environments where the soluble ferrous iron – Fe(II) – was abundant and freely available. The rise of oxygenic photosynthesis favored the oxidized ferric form – Fe(III) – which rapidly precipitates out of oxic solutions as iron oxides or hydroxides. Modern day oceans and lakes thus cater poorly to the Fe requirements of phytoplankton with surface waters bearing picomolar to nanomolar concentrations of dissolved unchelated inorganic iron, Fe' (Johnson et al., 1997), the most readily available form of Fe to phytoplankton, be it in ferrous Fe(II)' or ferric form Fe(III)' (Morel et al., 2008).

Extensive research on iron bioavailability to phytoplankton has been conducted over recent decades, yet a clear-cut definition of this term remains elusive. Bioavailability may be defined as the

degree to which a certain compound can be accessed and utilized by an organism. However this definition may be oversimplistic as elements of iron speciation and kinetics, phytoplankton physiology, light, temperature, and microbial interactions, to name a few, are all intricately intertwined into what we term “bioavailability” (Wells et al., 1995; Worms et al., 2006). Given the complex and interdisciplinary nature of Fe bioavailability, progress in understanding this concept depends on addressing its sub-aspects by means of well-defined questions and multiple analytical techniques. In this contribution, rather than seeking a definition capable of encompassing the multiple aspects and scales of Fe bioavailability to phytoplankton, we attempt to disassemble this concept into its composing facets and explore them further.

At a fundamental level, cellular Fe acquisition or uptake rates are indicative of the availability of any single Fe-substrate to a specific phytoplankton species (**Figure 1**). Fe uptake rate, in turn, is a function of the uptake pathways expressed by an organism and the chemical compatibility or exchange kinetics of the Fe-substrate with the transport systems (**Figure 1**). Rates of Fe acquisition can be determined experimentally using model or naturally occurring phytoplankton and Fe-substrates. In the next two sections we discuss the experimental evaluation of Fe uptake



pathways and rates and suggest the use of uptake rate constants as a means of comparing between organisms, Fe species, and environments, and gaging the relative contribution of specific Fe-compounds to phytoplankton in a natural setting. Needless to say, the availability of Fe to natural phytoplankton assemblages in oceans and lakes is influenced by many chemical, biological, and physical factors outside the experimental beaker (see **Figure 1** for an outline of some of these factors). For example, both Fe speciation and phytoplankton physiology are dynamic in time and space and to complicate matters even further, these two factors are interconnected. Moreover, interactions among the various organisms in the ecosystem, in addition to a host of environmental variables, can strongly impact the ability of phytoplankton to meet their Fe requirements. While a complete description of this added complexity to bioavailability is beyond the scope of this contribution, in the last section we describe how aquatic microorganisms influence iron chemistry and fate by way of organic complexation and bio-mediated redox transformations, emphasizing the resulting effects on Fe bioavailability to phytoplankton.

FUNDAMENTALS OF Fe BIOAVAILABILITY: PHYTOPLANKTON Fe ACQUISITION SYSTEMS

In order to determine the effects of Fe inputs on phytoplankton productivity it is essential to identify the relationship between

the concentration of various Fe species and their uptake by phytoplankton. As such, phytoplankton iron transport systems, uptake strategies, and rates are important for our understanding of Fe availability. In the next two sections we tackle the question of bioavailability at the organism level and look at mechanistic studies of iron acquisition pathways and rates under controlled conditions – an approach which has provided much insight into Fe bioavailability in natural systems (Hudson and Morel, 1993; Sunda and Huntsman, 1995; Hutchins et al., 1999; Maldonado and Price, 1999; Maldonado et al., 1999; Shaked et al., 2005; Morel et al., 2008). In Section “Uptake Pathways of Aquatic Phytoplankton” we explore two well-studied iron uptake pathways in aquatic phytoplankton – siderophore mediated and reductive Fe uptake – looking at the environmental relevance of each strategy. Since our focus is phytoplankton, we will not cover Fe uptake pathways of heterotrophic bacteria. More on this subject can be found in a recent report by Hopkinson and Barbeau (2012). In Section “Behavioral Patterns of Iron Mining” we briefly mention some behavioral patterns amongst phytoplankton which may be relevant to Fe acquisition from seawater.

UPTAKE PATHWAYS OF AQUATIC PHYTOPLANKTON

Several uptake pathways for free inorganic iron (Fe^{II}) and organically bound iron (FeL) have been described amongst aquatic phytoplankton. While Fe^{II} is clearly an important iron source,

Box 1 | Scope of iron influence on natural systems and research fields.

Aquatic iron biogeochemistry has been in the limelight over the past three decades with numerous studies linking Fe to carbon cycling and global climate (Martin et al., 1990; Watson et al., 2000; Blain et al., 2007; Martinez-Garcia et al., 2011). A particular emphasis has been placed on Fe availability to phytoplankton since over 45% of global photosynthesis occurs in aquatic environments (Falkowski et al., 1998) and photosynthetic systems are heavily dependent on iron (e.g., Raven, 1990; Greene et al., 1991). It is now well established that limited iron availability lowers phytoplankton pigment content and light harvesting capabilities, hinders photosynthesis and growth rates, and subsequently diminishes the production of organic matter and biogenic minerals (CaCO_3 and opal) and curtails CO_2 drawdown in vast ocean regions (Figure 2; Boyd et al., 2007). Many biogenic gases other than CO_2 are important determinants of atmospheric chemistry and climate, but far less is known about the controls iron exerts on the sea-atmosphere fluxes of such gases (Figure 2; Liss, 2007; Buesseler et al., 2008). What is known however, is that phytoplankton growth, death, and decomposition, all of which may be controlled by Fe availability, result in emissions of dimethylsulfide (DMS) and isoprene (cloud formation promoters), N_2O and CH_4 (potent greenhouse gases), and CO and OH (reactive species influencing the atmosphere oxidation potential; Law and Ling, 2001; Meskhidze and Nenes, 2006). The combined effects of these emissions on atmospheric radiative forcing remain largely unknown (Lampitt et al., 2008).

By controlling phytoplankton standing stocks, Fe availability may also influence the surface ocean light field, and subsequently

play a role in the surface ocean heat budget (Figure 2; Manizza et al., 2005). In addition to constraining primary productivity, iron deficiency impedes biogenic element cycling since phytoplankton cannot synthesize the enzymes required for utilizing major nutrients such as nitrate and N_2 (Figure 2; Milligan and Harrison, 2000; Kustka et al., 2002; Sohm et al., 2011). Low iron availability may also alter ecosystem structure and function: under Fe limitation smaller phytoplankton are favored, resulting in rapid carbon regeneration and lowered carbon export flux to the deep ocean (Figure 2; Price et al., 1994; Finkel et al., 2010). As limited Fe availability alters nutrient assimilation ratios and phytoplankton species composition, it bares implications for the reconstruction of ocean paleo-productivity and paleo-nutrient distributions. Examples include the intensively studied sedimentary records of diatoms, whose abundance, morphology, and composition is strongly regulated by Fe (Figure 2; Strzepek and Harrison, 2004; Marchetti et al., 2006; Marchetti and Cassar, 2009). An additional, less explored example, is the recently reported effect of Fe limitation on cadmium (Cd) drawdown from seawater by phytoplankton (Lane et al., 2009). Subsequently, Fe limitation may alter seawater Cd:P ratios (Cullen et al., 1999) and thus bias past reconstruction of PO_4^{3-} distributions which is based on seawater Cd:P ratios (Figure 2; Boyle, 1988; Elderfield and Rickaby, 2000). Recent attention has also been drawn to the effect of iron inputs and availability on toxic algal species occurrence and toxin production in oceans and lakes (Figure 2; e.g., Trick et al., 2010; Alexova et al., 2011).

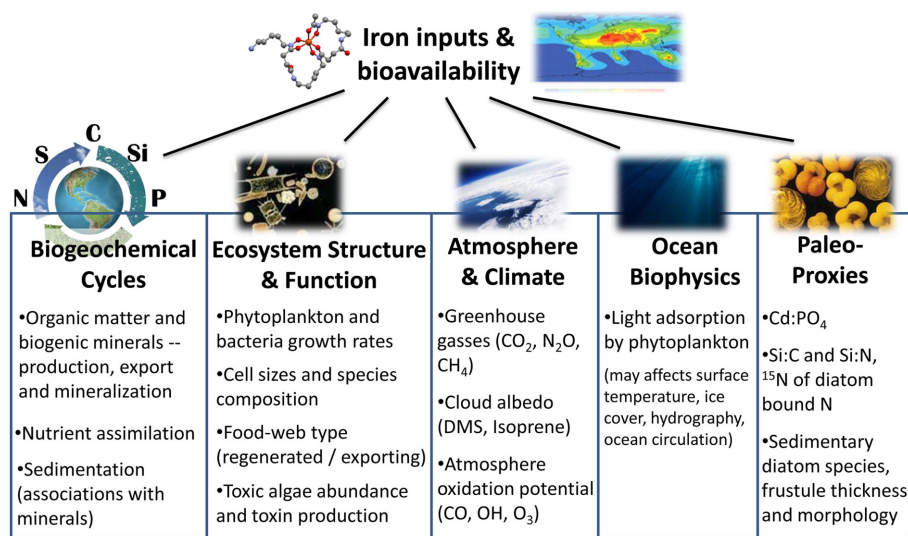


FIGURE 2 | Summary of processes, systems, and research fields which are influenced by iron inputs and bioavailability (see text for details).

we focus on FeL, where the transport machinery an organism employs will dictate the accessibility of a specific compound (Morel et al., 2008). To date, two major FeL uptake pathways have been described for phytoplankton: siderophore mediated Fe acquisition (e.g., Goldman et al., 1983; Soria-Dengg et al., 2001) and the reductive iron uptake pathway (Allnut and Bonner, 1987; Eckhardt and Buckhout, 1998; Maldonado and Price, 2001; Shaked et al., 2005). According to a prevalent paradigm shared by many oceanographers, prokaryotic phytoplankton

adopt siderophore-based Fe uptake systems while eukaryotes utilize a reductive strategy (e.g., Hutchins et al., 1999). However, genetic evidence (Webb et al., 2001; Hopkinson and Morel, 2009) as well as results of short term iron uptake experiments (Rose et al., 2005; Lis and Shaked, 2009; Fujii et al., 2010; Kranzler et al., 2011), contradict this paradigm. We propose that the occurrence of siderophore vs. reductive iron uptake can be put down to environmental rather than taxonomic considerations and that reductive iron uptake is a prevalent Fe

acquisition strategy amongst phytoplankton (Figure 3; Table A1 in Appendix).

Siderophore mediated Fe uptake involves the synthesis and secretion of ferric iron chelators which are capable of solubilizing, capturing, and delivering Fe(III) to the cell (Kraemer, 2004). The efficiency of this uptake pathway depends on: (a) the probability of the siderophore finding an Fe-substrate and (b) the probability of the ferrisiderophore complex finding its way back to the secreting cell. The build-up and maintenance of an Fe-siderophore diffusion gradient bringing iron back to the host cell is an essential feature of this strategy (Hutchins et al., 1991; Völker and Wolf-Gladrow, 1999). Therefore, siderophore production works best at high cell densities and in quiet waters or contained environments where turbulent disruption is unlikely (e.g., within biogenic aggregates or dense algal colonies). Consequently, siderophore production would be impractical in open waters, with high turbulence, and low cell densities (Hutchins et al., 1991). Indeed, a conspicuous lack of siderophore synthesis or uptake genes amongst open ocean cyanobacteria and eukaryotic phytoplankton (Hopkinson and Morel, 2009) suggests that this strategy may be ill suited to free-living aquatic phototrophs. Given the limitations of siderophore mediated iron uptake in dilute media, particularly open ocean waters, we turn our attention to an alternative strategy better suited to these conditions – Fe acquisition by means of reduction.

Reductive iron uptake offers a practical alternative to siderophore production as demonstrated in the numerical model constructed by Völker and Wolf-Gladrow (1999) comparing the

efficiency of these two strategies in the marine environment. Several studies, as well as our own data, support the prevalence of reductive iron uptake amongst a variety of representative phytoplankton from both eukaryotic and prokaryotic taxa as well as in natural phytoplankton communities in high Fe and low Fe environments (Figure 3; Table A1 in Appendix). Reduction operates on both Fe' and FeL where it involves the dissociation of Fe from its chelating ligand followed by transport of free iron into the cell (Atkinson and Guerinot, 2011). A key feature of this uptake pathway is the formation of an Fe(II) intermediate and thus experimental assays for reductive Fe uptake employ a ferrous iron binding ligand such as ferrozine or bathophenanthrolinedisulfonic acid (BPDS) which competes with the cell for Fe(II) and inhibits Fe uptake (see Figures A1 and A2 in Appendix; Shaked et al., 2004, 2005). On a genetic level, cell surface ferric reductases, similar to those in the yeast *Saccharomyces cerevisiae*, have been found in green algae (Allen et al., 2007) and ocean dwelling diatoms (Kustka et al., 2007; Bowler et al., 2010). These reductases may operate in conjunction with permease-oxidase complexes which reoxidize the Fe(II) as it is transported into the cell (Maldonado et al., 2006; Chen et al., 2008; Terzulli and Kosman, 2010). Not much is known about the reductive processes only recently shown to exist in aquatic cyanobacteria (Rose et al., 2005; Lis and Shaked, 2009; Kranzler et al., 2011).

The greatest advantage of the reductive strategy is its potential to operate not only on Fe' but also across a range of organically bound iron complexes, even Fe bound to strong siderophores

Laboratory cultures	
Eukaryotes	Prokaryotes
Green Algae <i>Chlamydomonas reinhardtii</i> ^{a-b} <i>Dunaliella bardawil</i> ^c <i>Chlorella</i> spp. ^{d-e} <i>Tetraselmis suecica</i> ⁺ <i>Chlorococcum littorale</i> ^f Dinoflagellates <i>Peridinium gatunense</i> ^g	Diatoms <i>Thalassiosira</i> spp. ^{h-j} <i>Cylindrotheca fusiformis</i> ⁺ <i>Phaeodactylum tricornutum</i> ^k Haptophytes <i>Emiliania huxleyi</i> ⁺
	Cyanophytes <i>Synechocystis</i> PCC6803 ^l <i>Trichodesmium erythraeum</i> ⁺ <i>Synechococcus</i> WH8102 ⁺ <i>Synechococcus</i> WH7803 ⁺ <i>Microcystis aeruginosa</i> ^m <i>Lyngbya majuscula</i> ⁿ
Natural environments	
Low Fe waters (HNLC)	High Fe waters
Southern Ocean ^o Subarctic Pacific (> 3μm) ^p Bering Sea (> 5μm) ^q	Gulf of Aqaba (> 0.2μm) ^r Loch Scridain (> 20μm) ⁺ Lake Kinneret ^g

FIGURE 3 | Prevalence of the reductive iron uptake pathway amongst phytoplankton. Listed are laboratory cultures and natural environments for which inhibition of uptake by Fe(II) binding ligands (Ferrozine/BPDS) was observed experimentally and taken to indicate the formation of an Fe(II) intermediate during iron transport. For some species, genomic and proteomic research identified various components of the reductive iron uptake pathway including ferrireductases and multicopper oxidases. See Appendix for supporting data and methodology (Tables A1 and A2 and Figures A1 and A2 in Appendix). Note on locations: The Gulf of Aqaba is located at the northern

tip of the Red Sea, Loch Scridain is a sea loch located on the Atlantic coastline of the island of Mull, Scotland, and Lake Kinneret (Sea of Galilee) is a fresh water lake in the north of Israel. References: ^aEckhardt and Buckhout (1998), ^bWeger (1999), ^cKeshtacher et al. (1999), ^dAllnutt and Bonner (1987), ^eMiddlemiss et al. (2001), ^fSasaki et al. (1998), ^gShaked et al. (2002), ^hShaked et al. (2005), ⁱJones and Morel (1988), ^jMaldonado and Price (2001), ^kSoria-Dengg and Horstmann (1995), ^lKranzler et al. (2011), ^mFujii et al. (2010), ⁿRose et al. (2005), ^oMaldonado et al. (2005), ^pMaldonado and Price (1999), ^qShaked et al. (2004), ^rLis and Shaked (2009), ⁺Lis and Shaked, in preparation.

such as ferrioxamine B (FeDFB; Maldonado et al., 2005; Shaked et al., 2005; Lis and Shaked, 2009; Shi et al., 2010; Kranzler et al., 2011). Phytoplankton equipped with this strategy would be able to integrate iron from a variety of sources, giving them an obvious competitive advantage in Fe acquisition. While we advance the idea of reduction as a prevalent Fe uptake strategy in aquatic systems, we by no means claim it to be exclusive. A single organism may possess both direct FeL uptake pathways (e.g., ferrisiderophore transporters) as well as iron reductases, a classic example being baker's yeast (Kosman, 2003). Moreover, siderophore mediated and reductive iron uptake do not discount the existence of other Fe uptake pathways, be they under investigation (e.g., Stintzi et al., 2000; Pick et al., 2008; Sutak et al., 2010; Wirtz et al., 2010) or undiscovered.

BEHAVIORAL PATTERNS OF IRON MINING

The data covered thus far clearly demonstrates that phytoplankton are not passive in their quest for iron. A major energetic investment is clearly required in order to accumulate intracellular Fe concentrations that are four to six orders of magnitude greater than those in their surrounding environment (Morel and Price, 2003). Some phytoplankton take this a step further and exhibit behavioral patterns which aid in the active mining of iron from the environment. The most striking example is the collection and processing of iron-rich dust particles by colonies of the globally important N_2 fixing cyanobacterium *Trichodesmium* spp. (Rueter et al., 1992; Rubin et al., 2011). The positively buoyant *Trichodesmium* forms massive blooms at the sea surface where it is likely to encounter dust deposits. Recently, we reaffirmed previous observations on efficient capturing and retention of dust by natural *Trichodesmium* colonies and documented a specialized ability to actively shuffle dust and iron oxides from the colony periphery to its core (Rubin et al., 2011). Packaging of dust in the colony interior can minimize its detachment and loss and also facilitate its chemical processing within a semi-enclosed microenvironment (Rubin et al., 2011). We found that *Trichodesmium* colonies were able to mediate dust dissolution, most likely via reduction (Rubin et al., 2011; Shaked, unpublished). Our mechanistic study complements several field observations documenting the ability of *Trichodesmium* to utilize iron from dust (Moore et al., 2009; Chen et al., 2011). Additionally, large diatoms (such as *Rhizosolenia* spp. and *Ethmodiscus* spp.) and dinoflagellates (such as *Alexandrium* spp. and *Gymnodinium* spp.) are known to migrate vertically to the nutricline to stock up on nutrients (Villareal et al., 1999; Ralston et al., 2007). While vertical migration was repeatedly proven efficient in nitrogen accumulation (Singer and Villareal, 2005), no clear evidence for iron mining at depth is present (McKay et al., 2000).

FUNDAMENTALS OF Fe BIOAVAILABILITY: PHYTOPLANKTON Fe ACQUISITION RATES

The discussion so far has centered on the mechanisms phytoplankton employ for acquiring Fe, knowledge which is crucial for analyzing and predicting their ability to access iron from various Fe pools in the environment (Shaked et al., 2005; Morel et al., 2008). We now focus on a more common approach to determining Fe availability: rate of transport. In this line of research the bioavailability of an Fe-substrate is ascertained by means of

growth or short term iron uptake experiments. Although this approach is very promising, it faces significant challenges in terms of quantitative extrapolation to systems outside the experimental framework (be it a beaker or a grow-out incubation). In Section "Experimental Probing of Availability" we discuss the importance of experimental design, stressing the use of well-defined experimental media and organisms in the pursuit of unambiguous data regarding the accessibility of different Fe species to various phytoplankton. However, even when high quality data are obtained, it is very difficult to reach a consensus regarding the availability of any one Fe-compound. The same Fe-substrate, for example, may be available to one organism but not to another, making bioavailability not only a question of "what?" but also of "to whom?". Moreover, the same organism may employ additional transport pathways upon Fe limitation, further extending the question to "when?" and "where?" in natural environments. In Section "Computing Availability Using Uptake Constants," we describe the use of uptake rate constants for comparing between studies, organisms, compounds, and environments as well as for gauging the contribution of specific Fe species to phytoplankton growth *in situ*. We propose that the availability of Fe species to phytoplankton can be viewed as a spectrum rather than an absolute "all or nothing" and establish a relative scale of bioavailability for a range of Fe species and various phytoplankton cultures and natural populations.

EXPERIMENTAL PROBING OF AVAILABILITY

Two common experimental approaches for probing the bioavailability of a given Fe-compound are: (1) long term or steady state iron uptake experiments which follow growth rates and/or intracellular Fe quotas of cells grown on a certain Fe-substrate, and (2) short term uptake experiments where the change in intracellular iron is followed over several hours. In order to enable inter- and intra-study comparisons, common grounds in methodology must be established by means of a robust experimental design in which medium and/or organism are well-defined.

Due to the fast hydrolysis and precipitation of Fe(III), an artificial or natural Fe complexing agent is required to keep dissolved iron in solution during experiments. For the study of free inorganic iron (Fe'), EDTA (ethylenediaminetetraacetic acid), and other carboxylic acid compounds are typically used (e.g., Anderson and Morel, 1982). The FeEDTA complex itself is membrane impermeable and not bioavailable (Shaked et al., 2005) and EDTA buffers an easily calculated pool of unchelated iron or Fe' in the medium (Sunda et al., 2005). There has been some criticism of the applicability of EDTA based studies to natural systems (Gerringa et al., 2000) but the alternative of using uncomplexed $FeCl_3$ when trying to measure free inorganic iron uptake rates has serious pitfalls. When spiking experimental media with $FeCl_3$, the iron is found in two pools – dissolved Fe and freshly precipitated colloids – whose relative proportions and bioavailability fluctuate over time (Wells et al., 1983; Kuma et al., 1996). When examining the bioavailability of organically bound iron (FeL, where L is an organic ligand) many chemical factors such as ligand strength, metal to ligand ratios, FeL equilibration time, and photolability should be taken into consideration. Sufficiently high FeL complex stability and/or a sufficient excess of the ligand compared to Fe are important in order to prevent iron precipitation. On the other hand, high

concentrations of free ligand (L) were shown to slow Fe uptake rates down due to competition with the cells for unchelated Fe which is formed during reductive uptake (Maldonado and Price, 2001; Shaked et al., 2005; Lis and Shaked, 2009). Experiments probing the bioavailability of partially complexed, particulate, or colloidal iron require careful support measurements and/or use of chemical speciation modeling software which establish Fe speciation in the experimental medium (e.g., Nodwell and Price, 2001; Rijkenberg et al., 2006, 2008; Hassler et al., 2011a). The concentration of Fe used in short term uptake experiments is often a compromise between environmentally relevant low concentrations and those required for adequate signal. However, it must be noted that in order to compare between experiments Fe concentrations must be sub-saturating (see Computing Availability Using Uptake Constants).

Characterization of the experimental organism is no less important than defining Fe speciation, as physiological status and growth phase can greatly affect experimental outcomes. Iron limitation, for example, is known to cause the upregulation of high affinity Fe acquisition systems (Maldonado and Price, 1999, 2001; Maldonado et al., 2006; Kustka et al., 2007; Allen et al., 2008), allowing access to previously unavailable Fe pools. This high affinity acquisition system allows iron limited diatoms to acquire iron bound to the xenosiderophore ferrioxamine B (FeDFB), whereas this complex is non-accessible to iron replete diatoms (see Figure 5A; Maldonado and Price, 2001). Growth phase may also affect Fe uptake since various transport pathways may be inactivated during different growth phases (Lis and Shaked, unpublished). In addition, the presence of bacteria in uptake assays using non-axenic cultures or natural assemblages may influence the availability of specific compounds to the studied algae or bias the uptake signal through bacterial acquisition of compounds unavailable to the studied organism (Soria-Dengg et al., 2001; Roe et al., 2011). Experimental choices regarding cell density, illumination, temperature, use of pH buffers, and experiment duration, to name a few, may alter uptake rates by influencing both algal physiology and Fe chemistry, and should be carefully evaluated in preliminary experiments. As a rule of thumb, cell density should be kept as low as possible to minimize bio-mediated changes in Fe chemistry (e.g., through the secretion of Fe-binding compounds into the medium), and experimental length should be kept short to avoid changes in the transport systems (Sunda et al., 2005). Short experiments (4–12 h) are preferably conducted in the dark or under red light (which prevents Fe photochemistry while supplying photo-synthetically active irradiation (Kranzler et al., 2011). Many organic pH buffers bind Fe and their effect on uptake rates should be carefully examined (Shi et al., 2009). Whenever possible, data points should be collected several times throughout the experiment rather than at its beginning and end. This ensures the measurement of meaningful rates that can be extrapolated further.

Once answers to fundamental questions of bioavailability have been established using model phytoplankton species and Fe-substrates, the next level of complexity may be added by conducting experiments with either natural aquatic communities or natural ligands (e.g., Maldonado et al., 2005; Shi et al., 2010). This combination of basic laboratory based research and field work has proven to be a powerful tool in unraveling the complexities of

natural systems. Experiments of this kind are analytically challenging and involve considerable planning and careful determination of the desired goals. Examples include studying the effect of photochemistry on the availability of model and natural Fe complexes to size fractionated natural phytoplankton communities (Maldonado et al., 2005) and the use of well-studied model organisms to report on changes in the availability of natural Fe-compounds due to variations in pH (Shi et al., 2010).

COMPUTING AVAILABILITY USING UPTAKE CONSTANTS

As stated above, uptake data are experiment-specific and thus often hard to extrapolate to other organisms or environments. Here we propose a relatively straight forward approach using the uptake rate constant – k_{up} – for comparing between experiments conducted with strongly bound organically complexed Fe (FeL) or unchelated Fe (Fe'). When an Fe-substrate is applied at sub-saturating concentrations, its rate of cellular uptake (ρ) is proportional to its concentration (Eq. 1, Figure 4):

$$\rho = k_{up} \times [\text{Fe}] \quad (1)$$

where ρ is cellular Fe uptake rate ($\text{mol Fe cell}^{-1} \text{ day}^{-1}$) and $[\text{Fe}]$ is Fe-substrate concentration (mol L^{-1}). Under these conditions (linear range in Figure 4), the dependency of cellular uptake rate on Fe concentration is described by the uptake constant – k_{up} with units of $\text{L cell}^{-1} \text{ day}^{-1}$ (different units may be used in accordance with the units of uptake rate). Unlike cellular uptake rate (ρ), which varies with Fe concentration, k_{up} is a more faithful representation of the ability of an organism to internalize the iron. In order to convert uptake rates to uptake constants, an action which can also be regarded as normalization, we need to define the concentration of Fe that serves as a substrate for uptake. In experiments probing the uptake of strongly complexed FeL, where Fe' concentrations are negligible, the substrate for uptake equals the total Fe added to the experiment as precomplexed FeL (Figure 4). In contrast, when probing Fe' uptake in the presence of the metal buffer EDTA, the total Fe is present predominantly as FeEDTA which is biologically unavailable, while Fe' – the substrate for uptake is found at minute concentrations (Shaked et al., 2005). The k_{up} calculation cannot be performed for weak FeL complexes as the experimental media contains both Fe' and FeL. Experiments using FeCl_3 are also hard to analyze due to Fe precipitation, unless Fe is added at concentrations lower than its solubility limits in seawater (0.2–0.5 nM; Liu and Millero, 2002). Despite its limitations, the uptake rate constant, k_{up} , is highly useful in comparing the “relative bioavailability” of different Fe-substrates to various phytoplankton, both in the laboratory or in natural environments. Moreover, we can use k_{up} to predict if a specific Fe-compound can support phytoplankton Fe demands *in situ*. These two applications are described below and in Figures 4 and 5 and Table 1.

Relative bioavailability scale as a means of comparing organisms, Fe species, and environments

We first demonstrate the use of k_{up} in comparing the bioavailability of Fe' and FeDFB (where DFB is the strong siderophore ferrioxamine B) to Fe-limited cultures of the open ocean coccolithophore *Emiliania huxleyi* (Figure 4). In these experiments we determined

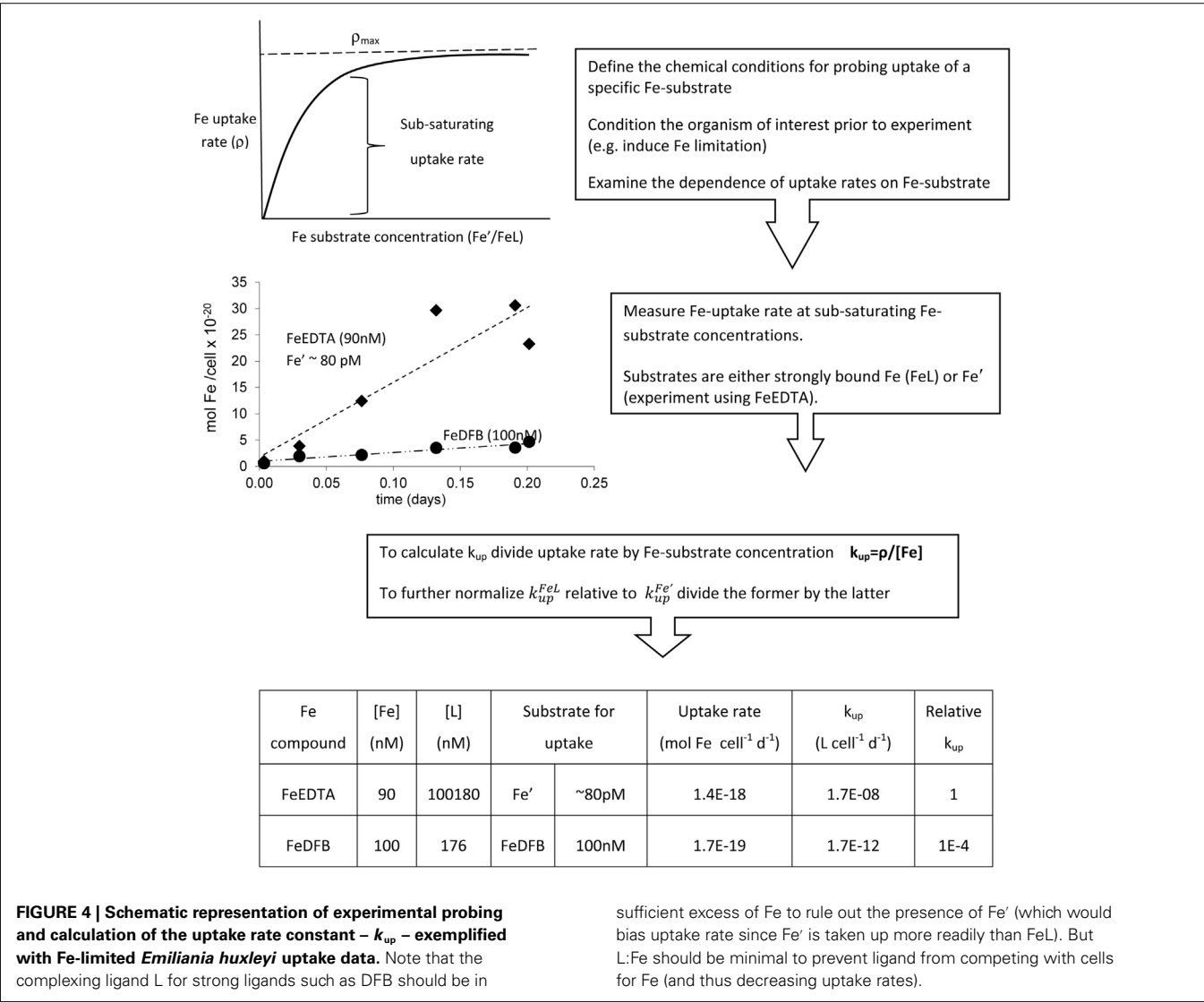


Table 1 | A comparison between the minimal daily Fe requirements and the daily FeDFB uptake capacity of *Synechococcus* spp.

Daily FeDFB uptake capacity: $k_{up} \times [Fe]$			Minimal daily Fe requirement: $Q \times \mu$	
k_{up} (DFB)–	[Fe]–	Q –	μ –	
Uptake rate constant for FeDFB ^a	Fe-substrate concentration ^b	intracellular Fe quota for <i>Synechococcus</i> spp. ^c	Fe-limited growth rate ^d	
$\sim 3 \times 10^{-13}$ L cell ⁻¹ day ⁻¹	$\sim 4 \times 10^{-9}$ mol L ⁻¹	$\sim 10^{-18}$ mol cell ⁻¹	~ 0.4 day ⁻¹	
$\sim 1.2 \times 10^{-21}$ mol Fe cell ⁻¹ day ⁻¹			$\sim 4 \times 10^{-18}$ mol Fe cell ⁻¹ day ⁻¹	

Minimal daily Fe requirements are calculated by multiplying intracellular Fe quota (Q) by Fe-limited growth rates (μ). Uptake capacity is calculated by multiplying k_{up} by the concentration of Fe-substrate $[Fe]$ in the environment. Calculating for FeDFB, we take a generous estimate of dissolved iron concentrations in open ocean waters and assume this pool it is made up entirely of FeDFB-like compounds.

^a See Figure A1; in Appendix, $\rho = 2.6 \times 10^{-20} \pm 8.2 \times 10^{-22}$ mol Fe cell⁻¹ day⁻¹; FeDFB = 90 nM.
^b Hypothetical dissolved iron value in open ocean waters. We assume all dissolved iron is FeDFB.
^c Henley and Yin (1998).
^d Based on Kudo and Harrison (1997) and Brand (1991).

Fe uptake rates of *E. huxleyi* from 100 nM radiolabeled FeDFB (Fe:DFB ratio 1:1.1) to 90 nM radiolabeled FeEDTA (Fe:EDTA ratio 1:1111; Fe' ~80 pM). While uptake rate of Fe' (in the presence of EDTA) is only about twice as fast as for FeDFB, the uptake constants span four orders of magnitude with $k_{up}^{Fe'} = 1.7 \times 10^{-8}$ mol Fe cell⁻¹ day⁻¹ and $k_{up}^{FeDFB} = 1.7 \times 10^{-12}$ mol Fe cell⁻¹ day⁻¹ (Figure 4). This marked difference in k_{up} stems from the much lower substrate concentration of Fe' as compared to FeDFB. While

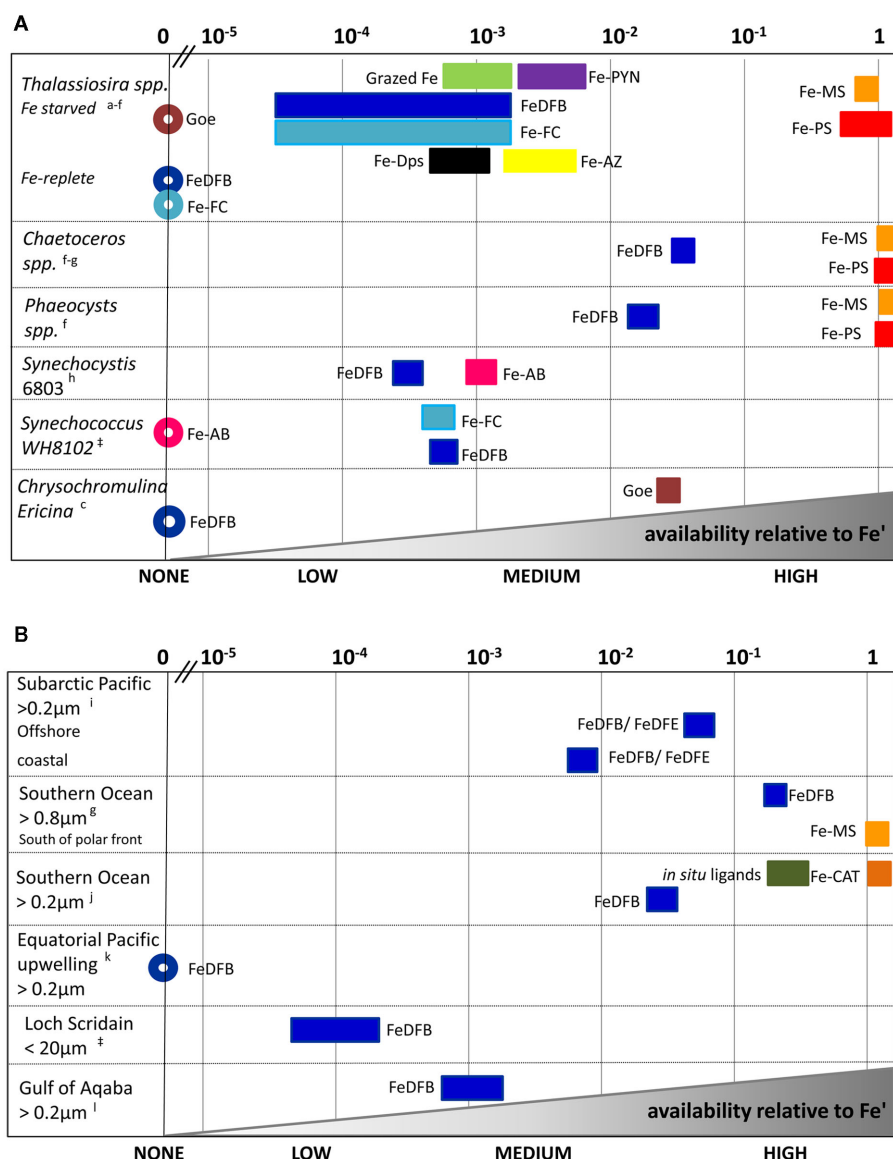


FIGURE 5 | Relative scale of Fe availability established from phytoplankton uptake rates obtained for cultures (A) and natural assemblages (B). By converting experimental data to uptake-rate constants, and normalizing it further relative to Fe', comparisons across organisms, Fe-substrates and environments are made possible (see text and **Figure 4** for details). Different Fe-complexes are presented as different colors, while bar length represents variations among experiments, and circles denote no uptake. Abbreviations: Goe, goethite; DfB, desferrioxamine B; AB, Aerobactin; FC, ferrichrome; PYN, Porphyrin;

MS, Monosaccharides; PS, Polysaccharides; AZ, Azotochelin; DPS, DNA binding protein from starved cells (iron storage proteins); CAT, Galliccatechin; DfE, desferrioxamine E. See Appendix for supporting data and **Figure 3** for location descriptions. References: ^aShaked et al. (2005), ^bChen and Wang (2008), ^cNodwell and Price (2001), ^dKustka et al. (2005), ^eMaldonado and Price (2001), ^fHassler and Schoemann (2009), ^gHassler et al. (2011b), ^hKranzler et al. (2011), ⁱMaldonado and Price (1999), ^jMaldonado et al. (2005), ^kWells et al. (1994); ^lLis and Shaked (2009), [‡]Lis and Shaked, unpublished.

browsing through published uptake data it becomes apparent that k_{up} values for any specific Fe-compound varies among organisms in accordance with their sizes and degree of Fe limitation (Sunda and Huntsman, 1995; Shaked et al., 2005). Seeking a way to present data on many Fe-compounds and many phytoplankton species simultaneously, we chose to establish a relative bioavailability scale which is illustrated in **Figure 5**. Here, we divide the uptake constants of various Fe complexes by the uptake constant of Fe' where both constants are obtained from a single study. The resulting ratio

represents the availability of model Fe-compounds relative to Fe', shown on a logarithmic scale for a variety of cultured phytoplankton in **Figure 5A**. A similar calculation was conducted for natural phytoplankton populations as shown in **Figure 5B**.

The data presented in **Figure 5** clearly show that both in the laboratory and natural environment Fe' is highly bioavailable as compared to most organically bound iron forms and colloids, as previously suggested by Morel et al. (2008). A notable exception to this is the recently reported high availability of Fe bound to

saccharides, tested using model mono- and polysaccharides with several cultured species, and natural phytoplankton (Figures 5A,B and references therein). Iron bound to siderophores such as ferriochrome (FC), ferrioxamine B (DFB), aerobactin (AB), and azotochelin (AZ) is accessible to several cultured phytoplankton at a low to intermediate degree as compared to Fe'. However, when grown under Fe-replete conditions, diatoms from the genus *Thalassiosira* (and we estimate that this is probably true for other diatoms) are unable to access siderophore bound Fe (Figure 5A). Similarly, ferrioxamine complexes are more accessible to natural phytoplankton assemblages in low Fe than high Fe waters (e.g., Southern Ocean vs. Loch Scridain or offshore vs. coastal stations in the subarctic Pacific, Figure 5B). While centric *Thalassiosira* spp. diatoms acquire Fe from a wide range of organic substrates, they are unable to internalize stable Fe oxides (Rich and Morel, 1990). On the other hand, mixotrophic dinoflagellates capable of consuming particles (e.g., *Chrysochromulina ericina*) are able to utilize goethite but not FeDFB (Maranger et al., 1998; Nodwell and Price, 2001). It is important to keep in mind that the source of variation between phytoplankton species and Fe-compounds in Figure 5 may also be attributed to experimental conditions. For example, the relative bioavailability FeDFB may change depending on the amount of excess free DFB present in the experimental medium, where a higher excess makes FeDFB seem less bioavailable. Nonetheless, we find this method of comparison illuminating when considering the bioavailability of different Fe-substrates to aquatic phytoplankton. In this respect, the use of EDTA to buffer known Fe' concentrations is indispensable since Fe' is easily calculated despite differences in experimental set-ups.

Gauging the contribution of Fe-substrates to meeting phytoplankton Fe demand in situ

Experimentally obtained uptake rate constants can help examine the availability of various Fe species in natural settings. This is done by multiplying k_{up} by measured or predicted concentrations of a specific Fe-compound. For example, multiplying typical HNLC Fe concentrations of 70 pM chelated Fe (FeL) and 0.07 pM unchelated Fe (Fe', Rue and Bruland, 1995) by representative uptake constants- $k_{up}^{FeL} \sim 2 \times 10^{-9} \text{ L cell}^{-1} \text{ day}^{-1}$ and $k_{up}^{Fe'} \sim 1 \times 10^{-6} \text{ L cell}^{-1} \text{ day}^{-1}$ (Shaked et al., 2005), results in FeL uptake rate of $\sim 1.4 \times 10^{-19} \text{ mol Fe cell}^{-1} \text{ day}^{-1}$ and Fe' uptake rate of $\sim 7 \times 10^{-20} \text{ mol Fe cell}^{-1} \text{ day}^{-1}$. The overall uptake rate of $2 \times 10^{-19} \text{ mol Fe cell}^{-1} \text{ day}^{-1}$, contributed 2/3 by FeL and 1/3 by Fe', is well within the estimated steady state uptake of natural phytoplankton of 2×10^{-20} – $4 \times 10^{-18} \text{ mol Fe cell}^{-1} \text{ day}^{-1}$ (e.g., Strzepek et al., 2005). Since the k_{up} of most FeL complexes is much lower than that of Fe' (Figure 5A), 1 pM Fe' in the ocean can be equated to 100–10000 pM of organically bound Fe, making Fe' a potentially important Fe source, despite its low concentrations. Therefore, Fe' formed by processes such as photoreductive dissolution of Fe oxides (Waite and Morel, 1984; Wells et al., 1991; Barbeau and Moffett, 2000) or the degradation of photolabile Fe complexes (Barbeau et al., 2001; Rijkenberg et al., 2006; Amin et al., 2009; Steigenberger et al., 2010) may contribute to a transient yet significant Fe pool which caters, at least partially, to phytoplankton iron requirements in surface waters (Morel et al., 2008).

Such calculations can also be used to examine if a specific compound is likely to support *in situ* growth of certain phytoplankton species by comparison to the minimal daily Fe requirements. As an example we examine the ability of FeDFB to support *Synechococcus* spp. growth. Table 1 details the calculation and shows that the minimal theoretical daily Fe requirement of *Synechococcus* is three orders of magnitude greater than its FeDFB uptake capacity, even given an overshoot in the estimated concentration of FeDFB-like Fe complexes in natural waters. Therefore while *Synechococcus* is capable of transporting DFB bound iron (i.e., FeDFB can be termed bioavailable should uptake be the single criterion for bioavailability), FeDFB or similar compounds alone are insufficient in meeting the Fe demands of this organism.

Needless to say, care should be taken in the use of k_{up} as a tool of comparison: factors such as experimental conditions and environmental constraints should be taken into account. When synthesizing laboratory and field data it is important to bear in mind that the degree to which a specific organic Fe complex (FeL) supports phytoplankton growth *in situ* is influenced by factors other than its direct uptake rate. The residence time of FeL in surface water and its tendency to undergo chemical and physical transformations all influence its final availability, an issue we further explore in the next section.

ADDED COMPLEXITY TO BIOAVAILABILITY: BIO-MEDIATED TRANSFORMATIONS OF Fe SPECIATION

Having discussed the fundamentals of bioavailability in the form of uptake pathways and rates – we now turn our attention to the added complexity of Fe–organism interactions (Figure 1). While iron inputs and availability are widely recognized as factors shaping the biology of marine and fresh water environments, biological activities, in turn, exert strong control on iron speciation and cycling in aquatic ecosystems, and may even influence its inputs (Figure 6). Here we explore how Fe–organism interactions can affect iron bioavailability in complex and sometimes unexpected ways due to the many players and intricacies involved in natural systems. We endeavor to address some of these complexities in the present section.

Basic life processes significantly impact the inputs, speciation and fate of iron in aquatic ecosystems (Figure 6). Secretion of exopolymers and siderophores, bacterial Fe-oxide respiration, and food web interactions involving bacteria, phytoplankton, grazers, and viruses may all alter iron chemistry and resulting bioavailability (Figure 6; e.g., Poorvin et al., 2004; Boye et al., 2005; Sarthou et al., 2008; Schlosser and Croot, 2009). Thus, far from being slaves to Fe, microorganisms are able to manipulate iron speciation in their surroundings to some extent. Having said this, it should be noted that very few microbial processes influencing iron chemistry are clearly intended to serve iron acquisition purposes and more importantly, not all biological modifications of iron speciation influence its bioavailability favorably. In this section we classify a number of major pathways by which microbial communities alter iron speciation in aquatic environments. Microorganisms are able to mediate Fe redox transformations in their immediate surroundings while biological production and release of Fe-binding ligands are imperative to keeping iron in solution. No less important is the role microbial food web interactions play in the rapid



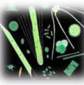
 External iron inputs	 Iron speciation	 Iron cycling
<ul style="list-style-type: none"> <input type="checkbox"/> Organic complexation of dFe & pFe from hydrothermal vents – facilitating Fe dispersion in the ocean ^{a,b} <input type="checkbox"/> Dissimilatory reduction of Fe minerals in shelf sediments – remobilization & dispersion ^{c,d} <input type="checkbox"/> Binding of riverine Fe by humics – increased fluvial Fe input ^e <input type="checkbox"/> Retention and processing of dust Fe – increased solubility ^{f,g} 	<ul style="list-style-type: none"> <input type="checkbox"/> pFe ingestion & dissolution by zooplankton & mixotrophs ^{h,i} <input type="checkbox"/> Release of Fe binding molecules influencing both dFe & pFe ^{j,k} <input type="checkbox"/> Reductive dissolution of Fe minerals in aggregates ^l <input type="checkbox"/> Bio-mediated reductive dissociation of organically bound Fe ^{m,n} 	<ul style="list-style-type: none"> <input type="checkbox"/> Release of cellular Fe content through viral lysis, grazing and cell death/mortality ^{o,p,q} <input type="checkbox"/> Bacterial remineralization of organic Fe ^r <input type="checkbox"/> Fe packaging in zooplankton faecal pellets – accelerated export ^s <input type="checkbox"/> Fe solubility and residence times enhanced due to organic complexation ^t

FIGURE 6 | Selected examples of biological interactions with external iron inputs (e.g., aeolian dust deposition, sediment resuspension, fluvial, and hydrothermal Fe) and organism mediated influences on iron speciation and recycling in aquatic environments.

While the microbial web in its entirety (from grazers to primary producers, viruses and heterotrophic bacteria) influences iron dynamics and availability to all community members, we focus on resultant Fe bioavailability to photosynthetic microorganisms. Abbreviations: dFe,

dissolved iron; cFe, colloidal iron; pFe, particulate Fe. References:

^aSander and Koschinsky (2011), ^bWu et al. (2011), ^cLohan and Bruland (2008), ^dSevermann et al. (2010), ^eBatchelli et al. (2010), ^fBoyd et al. (2010b), ^gRubin et al. (2011), ^hBarbeau et al. (1996), ⁱTang et al. (2011), ^jSato et al. (2007), ^kBuck et al. (2010), ^lBalzano et al. (2009), ^mMaldonado and Price (1999), ⁿShaked et al. (2002), ^oHiggins et al. (2009), ^pStrzepek et al. (2005), ^qTsuda et al. (2007), ^rBoyd et al. (2010a), ^sBoyd and Ellwood (2010), ^tKuma et al. (1996).

recycling of iron in surface waters. Iron regeneration has received some recent attention (Strzepek et al., 2005; Boyd et al., 2010a) and will not be discussed in detail here. Rather, we will focus on the two former processes and their impact on the Fe pool available to phytoplankton.

BIOLOGICAL CONTROL ON Fe REDOX TRANSFORMATIONS

Iron has two oxidation states of importance to its aquatic chemistry – Fe(II) and Fe(III). Processes of Fe oxidation and reduction, known as redox reactions, take place throughout the water column, across chemical gradients, in sediments, and microenvironments. Redox reactions are central in determining the physical and chemical form of iron and its subsequent chemical and biological reactivity (Figure 7; Table 2). While both abiotic and biotic processes regulate iron redox transformations, we focus on the role biology plays in mediating iron redox cycling and the resulting effects on Fe availability to phytoplankton. We also attempt to distinguish between redox reactions of dissolved inorganic, dissolved organic and colloidal/particulate iron, as the governing factors and the ensuing changes in Fe bioavailability are likely to vary between the different iron species (Figure 7; Table 2).

Speciation and reactions

In oxygenated, neutral pH surface waters iron persists predominantly in its oxidized form – Fe(III), as fluxes of the thermodynamically unstable Fe(II) will undergo prompt oxidation by oxygen and hydrogen peroxide (Figure 7; Table 2; Gonzalez-Davila et al., 2005; Santana-Casiano et al., 2005). Fe(II) oxidation rates are not only regulated by the abiotic factors of temperature, pH, and salinity (Santana-Casiano et al., 2006), but also by biology. Bio-generated redox reactive species, oxygen consumption and release via respiration, as well as photosynthesis are able to influence oxidizing agent type and concentration as well as local pH conditions. In environments characterized by high biomass, low turbulence,

poor ventilation, or low alkalinity (e.g., marine aggregates, coastal waters, oxygen minimum zones, and lakes) significant biological modifications of the reactants and/or conditions involved in Fe(II) oxidation have been reported (Emmenegger et al., 2001; Shaked et al., 2002; Moffett et al., 2007; Lohan and Bruland, 2008). In pelagic, low biomass surface ocean waters, biology is thought to exert minor controls on Fe(II) oxidation rates (e.g., Miller et al., 1995; Shaked, 2008). However, this view may require reassessment given the biological production of superoxide and hydrogen peroxide recently observed in several new open ocean studies (Rose et al., 2008; Hansard et al., 2010; Vermilyea et al., 2010).

In order for Fe(II) to persist at measurable concentrations in oxygen rich water, continuous Fe(II) production and/or Fe(II) supply must take place (Figure 7; Table 2). Multiple Fe reduction pathways were studied and suggested to operate at varying degrees in surface waters, including direct photochemical reduction, reduction by superoxide of photochemical or biological origin, thermal reduction, reduction by phytoplankton cell surface enzymes, and microbial reduction in isolated suboxic and anoxic microenvironments such as settling fecal pellets and aggregates (Table 2; Alldredge and Cohen, 1987; Kuma et al., 1992; Johnson et al., 1994; Voelker and Sedlak, 1995; Maldonado and Price, 2001; Shaked et al., 2002; Kustka et al., 2005; Rose et al., 2005; Barbeau, 2006; Rijkenberg et al., 2006; Balzano et al., 2009; Roy and Wells, 2011). Fe(II) may be supplied from external sources such as sediments, anoxic or suboxic water, hydrothermal vents, rain and aerosols, or originate from the *in situ* recycling of cellular iron through grazing and viral lysis (Kieber et al., 2001; Croot et al., 2005; Statham et al., 2005; Buck et al., 2006; Breitbarth et al., 2009). In addition, retardation of Fe(II) oxidation by low temperature, low pH, or complexation by Fe(II) stabilizing organic ligands are thought to contribute to the maintenance of measurable Fe(II) concentrations (Croot et al., 2001, 2008; Roy et al., 2008).

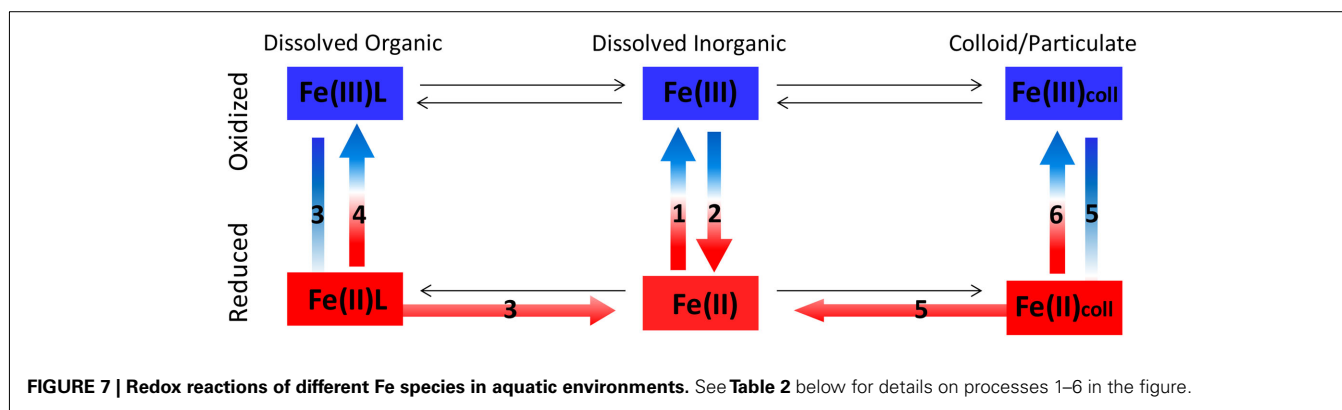


Table 2 | Redox reactions of different Fe species in aquatic environments, their governing factors, and potential influence on Fe speciation and bioavailability (this table accompanies Figure 7).

Mediators and governing factors	Effects on speciation and bioavailability	References
1. Fe(III)' OXIDATION		
<ul style="list-style-type: none"> • O_2, O_2^-, H_2O_2 • Regulated by pH, temp, salinity 	<ul style="list-style-type: none"> • Fe(III) formation and subsequent hydrolysis and precipitation, decreases bioavailability 	a–c
2. Fe(III)' REDUCTION		
<ul style="list-style-type: none"> • Enzymatic– phytoplankton (assimilatory) & bacteria (dissimilatory – low oxygen) • Direct photolysis or reduction by photo-produced reactive transients • O_2^- (photochemical/biological origin) • Humic and fulvic acids 	<ul style="list-style-type: none"> • Elevated [Fe(II)s.s] and maintenance of active redox cycle, both of which slow down Fe(III) hydrolysis and precipitation • Availability is enhanced when [Fe'] increases (as Fe(III) and Fe(II) are equally bioavailable) 	d–g
3. Fe(III)L REDUCTION AND DISSOCIATION		
<ul style="list-style-type: none"> • Enzymatic (as above) • Photochemical (as above) • Superoxide (as above) 	<ul style="list-style-type: none"> • Weaker ligand binding to Fe(II) (compared to Fe(III)L) may favor dissociation of free Fe(II) and increase in [Fe'] and bioavailability • If Fe(II) remains complexed – its oxidation may be stalled/accelerated compared to Fe(II). Bioavailability of Fe(II)L – unknown 	h–i
4. Fe(II)L OXIDATION		
<ul style="list-style-type: none"> • O_2, O_2^-, H_2O_2 • Ligands (L)– some stabilize the complex as Fe(II)L, some accelerate its oxidation 	<ul style="list-style-type: none"> • Rates are slower/faster than Fe(II) oxidation resulting in elevated/lowered [Fe(II)Ls.s] • Bioavailability of Fe(II)L – unknown 	j–k
5. REDUCTIVE DISSOLUTION OF SOLID PHASE IRON		
<ul style="list-style-type: none"> • Bacterial dissimilatory reduction in aggregates • Ingested colloids (zooplankton) • Direct photolysis and light enhanced siderophore mediated dissolution 	<ul style="list-style-type: none"> • Elevated [Fe'] due to increased Fe(II) flux • Elevated FeL (when ligands are at play) • Dissolution enhances bioavailability as solid phase iron is largely inaccessible 	l–m
6. OXIDATION OF SURFACE ADSORBED Fe(II)		
<ul style="list-style-type: none"> • O_2 and mineral surfaces (O_2 oxidizes surface bound Fe(II) much faster than dissolved Fe(II)) 	<ul style="list-style-type: none"> • If oxidation precedes detachment of Fe(II): decreased flux of Fe(II) • Following oxidation, the newly precipitated Fe is more reactive than the original mineral 	n

[Fe(II)s.s] , steady state Fe(II) concentrations.

References: a. Santana-Casiano et al. (2005), b. Gonzalez-Davila et al. (2005), c. King et al. (1995), d. Shaked et al. (2002), e. Kustka et al. (2005), f. Voelker and Sedlak (1995), g. Miller et al. (1995), h. Barbeau et al. (2001), i. Rijkenberg et al. (2006), j. Rose and Waite (2002), k. Rose and Waite (2003), l. Balzano et al. (2009), m. Barbeau et al. (1996), n. Stumm and Sulzberger (1992).

Thanks to the development of rapid and sensitive flow injection based chemiluminescence techniques (FI-CL), Fe(II) datasets in the oxygenated upper waters of oceans and lakes have recently begun to accumulate (Emmenegger et al., 2001; Shaked et al., 2002; Ussher et al., 2007; Shaked, 2008; Hansard et al., 2009; Sarthou et al., 2011). Some of these measurements point to a strong biological control on Fe(II) formation as attested to by the co-variance of chlorophyll and Fe(II) concentrations as well as measurable nighttime Fe(II) levels. Commonly, the presence of non-photochemical Fe(II) in the photic zone is suggested to reflect Fe reduction by assimilatory cell surface enzymes of phytoplankton or by biologically produced superoxide (e.g., Sarthou et al., 2011). Assimilatory Fe reduction by cell surface enzymes is not likely to generate high fluxes of Fe(II), as the Fe(II) is probably generated within an enclosed protein complex and subsequently internalized by an adjacent transport protein (Kustka et al., 2005; Shaked et al., 2005). Rather, superoxide, a diffusible reducing agent which has recently been shown to be generated non-photochemically throughout the photic zone (Rose et al., 2008, 2010; Hansard et al., 2010), may be a central player in Fe(II) formation. Similarly, experimental observations of phytoplankton mediated Fe reduction in flow through systems [where Fe(II) is detected downstream of membrane-mounted cells], may be caused by superoxide released from the cells (Milne et al., 2009; Saragosti et al., 2010) in addition to or rather than cell surface enzymes. Despite emerging evidence for non-photochemical Fe(II) formation, photochemistry should not be underestimated as a strong mediator of Fe redox reactions. Currently, it is analytically challenging to detect photochemically produced Fe(II) as it oxidizes completely by the time the water is retrieved and analyzed. Minimizing collection time with high throughput pumps, Shaked (2008) observed a highly active photo-induced redox cycle in the surface waters of the Gulf of Aqaba.

Bioavailability

As Fe(II) is far more soluble than Fe(III), reductive processes generating Fe(II) and/or the occurrence of the thermodynamically unstable Fe(II) in surface waters are commonly linked to enhanced iron bioavailability (e.g., Sunda, 2001). This often justified notion merits careful consideration as some Fe(II) species may not be available and since not all reductive processes increase Fe availability. Aided with Table 2 and Figure 7, we outline the effects of several reductive processes on Fe bioavailability below.

While Fe(II) is potentially the more bioavailable redox state of Fe, several factors will determine whether iron availability is indeed increased by reductive processes. These include the characteristics of the Fe species undergoing reduction, the reductive pathway, the presence of other ligands and oxidants in the immediate surroundings, and ultimately the uptake machinery of the phytoplankton utilizing this iron. As a rule of thumb, redox processes that increase the concentrations of dissolved inorganic Fe (be it Fe(II)' or Fe(III)'), will generally tend to boost the bioavailability of iron. With this in mind, we discuss the potential for Fe' release and/or changes to Fe lability occurring in different reductive processes.

Reductive dissolution of solid phase Fe. As solid phase Fe is considered unavailable to phytoplankton (Rich and Morel, 1990; Wells et al., 1991), reductive dissolution of mineral Fe or

surface adsorbed Fe generate Fe', and thus enhance Fe availability (Figure 7; Table 2). Even when the Fe' formed through reductive dissolution exceeds its solubility limit, it will hydrolyze and form fresh hydroxides which serve as a better iron source than their parent minerals (Stumm and Sulzberger, 1992; Yoshida et al., 2006). When reductive dissolution of mineral Fe is mediated, assisted, or occurs in the presence of organic ligands, it results in FeL (organically bound Fe) rather than Fe' (Kraemer, 2004; Borer et al., 2005). As stated previously, Fe' is acquired at faster rates than most studied dissolved organic Fe-complexes (see section "Phytoplankton Fe Acquisition Rates", Figure 5), and hence the presence of organics may slow uptake down. On the other hand, organic complexation may sustain dissolved Fe in surface waters for longer and at concentrations exceeding its solubility limit (see next section "Biological Production and Release of Iron Binding Ligands"), subsequently providing phytoplankton with Fe over a longer duration.

Reduction of organically bound Fe(III). As reasoned above, reductive release of Fe' from organic complexes is likely to enhance uptake, at least over short time scales (Figure 7; Table 2). When the ligand (L) undergoes photo-destruction, free, unchelated Fe(II) is liberated and Fe' increases, as has been extensively demonstrated for Fe(III)EDTA (Hudson and Morel, 1993; Sunda and Huntsman, 1997). In other cases, Fe(II) may remain complexed as Fe(II)L, undergo reoxidation to Fe(III)L or dissociate as unchelated Fe(II) due to reduced ligand affinity for Fe(II) (Harrington and Crumbliss, 2009). Hence, some of these redox transformations will ultimately not alter Fe speciation, but others may temporarily shift Fe(III) from strong complexes into weak complexes, possibly enhancing Fe bioavailability.

Reduction of Fe(III)'. Unlike the former reductive processes which enhance Fe' concentrations, the total unchelated iron pool remains unchanged when ferric Fe' transforms into ferrous Fe(II)' (Figure 7; Table 2). Nonetheless, this reaction mediated by enzymes on the cell surface, is central to the acquisition of Fe' through the reductive uptake pathway described in Section "Uptake Pathways of Aquatic Phytoplankton," at least for eukaryotes (Shaked et al., 2005). Fe(III)' may alternatively undergo reduction by superoxide in the bulk solution (Voelker and Sedlak, 1995), but the effect of this process on Fe availability is disputable. Kustka et al. (2005) found that Fe' uptake by diatoms remained unaffected by superoxide mediated reduction of Fe(III)' in the experimental medium, while Rose et al. (2005) reported that superoxide enhanced Fe' uptake by cyanobacteria. More work is required to evaluate the importance of bulk solution Fe' reduction in increasing Fe availability.

Thus far we examined the effect of reductive processes on Fe availability and now we turn to the chemical nature and bioavailability of Fe(II), where increasing reports suggest that some of the measured Fe(II) in the ocean is organically bound (Croot et al., 2008; Roy et al., 2008). The existence of Fe(II) binding ligands is deduced from deviations in Fe(II) oxidation kinetics in some natural samples as compared to seawater free of organic matter (Roy et al., 2008). Currently, neither the identity nor the bioavailability of these complexes is known and hence elevated Fe(II) levels are not necessarily indicative of enhanced bioavailability. Indeed,

phytoplankton iron stress was not alleviated in Fe fertilized areas where Fe(II) accounted for a significant fraction of the dissolved iron pool (Croot et al., 2008; Roy et al., 2008). Moreover, as the iron in Fe(II)L complexes is already reduced, phytoplankton cannot employ reductive pathways to liberate it from the complex prior to transport as they do for Fe(III)L (see Uptake Pathways of Aquatic Phytoplankton). Thus, if these Fe(II)L are slow to oxidize, we are faced with yet another challenge in determining the transport pathways of Fe(II)L.

BIOLOGICAL PRODUCTION AND RELEASE OF IRON BINDING LIGANDS

Over the course of their short life span, aquatic microbes release copious amounts of biomolecules into their immediate environments. These diverse secretions and exudates include waste products, secondary metabolites, sugars, and proteins as well as cellular contents released via grazing, viral attack or programmed cell death (Bidle and Falkowski, 2004; Poorvin et al., 2004; Strzepek et al., 2005; Dalbec and Twining, 2009; Boyd et al., 2010a). While the minority of microbial secretions are synthesized and released with the explicit purpose of binding iron, many do possess an Fe-binding capacity of some kind (Rijkenberg et al., 2008; Hassler et al., 2011a; Levy et al., 2011). It is now well established that the overwhelming majority of dissolved (and in some cases colloidal) iron in most aquatic environments is found as organic complexes (Hunter and Boyd, 2007; Vraspir and Butler, 2009). Research efforts to elucidate the nature and origin of these Fe-binding organic ligands have yielded ambiguous results, reflecting the fact that (a) organic ligands may be introduced into aquatic systems via multiple pathways within and outside the water column and (b) organically bound iron (FeL) may be subjected to further biological and chemical transformations (Figure 7; Table 3). Not all organic Fe complexes are available to all phytoplankton, and even those FeL which are utilized are most likely less available than dissolved inorganic iron (Fe'; Figure 5; Morel et al., 2008). Nonetheless, iron binding ligands are vital for the maintenance of dissolved iron concentrations well above the Fe solubility limit and for retarding Fe aggregation and loss from surface waters (Kuma et al., 1996). Here we provide an abridged overview of some of the organic Fe complexes thought to exist in seawater, highlighting the ways in which organic complexation affects Fe speciation and bioavailability.

Speciation

Organic ligands capable of binding iron (and other metals), were detected in pelagic and coastal ocean waters, estuaries, lakes, and rivers, often in excess of dissolved Fe concentrations (Boye et al., 2001; Nagai et al., 2007; Duckworth et al., 2009; Hassler et al., 2009; Laglera and van den Berg, 2009; Buck et al., 2010). Using competitive ligand exchange (CLE) techniques, researchers have classified two major organic Fe ligand groups based on their stability constants with regards to Fe³⁺ – the strong L1 and weaker L2 class (e.g., Gledhill and van den Berg, 1994; Ibisani et al., 2011). A common view is that the strong L1 ligand class consists of siderophore-like molecules, while the less strongly complexing L2 ligands consist of cellular degradation products. However, the picture is probably more complex and there are additional weaker natural Fe ligands, such as saccharides, overlooked by CLE

Table 3 | The influence of siderophore and saccharide release on iron chemistry and availability in aquatic environments.

Siderophores	Saccharides (EPS, TEP)
RESULTING IRON SPECIES	
Strongly bound organic dFe & cFe Fe(III)L	Organically bound/adsorbed dFe, cFe, & pFe
IRON SPECIES ACTED UPON	
dFe, cFe, & pFe	dFe & cFe
IMPACT	
<ul style="list-style-type: none"> • Maintain Fe in solution • Fe proximity to cell (amphiphilic) • Particulate Fe dissolution 	<ul style="list-style-type: none"> • Maintain Fe in solution or promote its aggregation and export from photic zone • Fe proximity to cell
SUBSEQUENT TRANSFORMATIONS	
Photochemical reduction	<ul style="list-style-type: none"> • Photochemical reduction • Ligand exchange • Adsorption/desorption of dFe
ORGANISMS AT PLAY	
Heterotrophic bacteria, fresh water phytoplankton	Phytoplankton, Bacteria, Viruses, Zooplankton
BIOAVAILABILITY	
Varies between complexes and organisms but probably lower compared to Fe'	As high as Fe' for all studied organisms
REFERENCE	
a–f	g–m

dFe, dissolved iron; cFe, colloidal iron; pFe, particulate Fe.

References: a. Sandy and Butler (2009), b. Vraspir and Butler (2009), c. Holmén and Casey (1996), d. Martinez et al. (2000), e. Kraemer et al. (2005), f. Barbeau et al. (2003), g. Hassler et al. (2011a), h. Hassler and Schoemann (2009), i. Steigenberger et al. (2010), j. Passow (2002), k. Strmecki et al. (2010), l. Berman-Frank et al. (2007), m. Decho (1990).

methods (Town and Filella, 2000; Hunter and Boyd, 2007; Boyd and Ellwood, 2010).

The most studied microbial Fe-binding exudates are siderophores, compounds which have been isolated from both freshwater and seawater (Table 3; Macrellis et al., 2001; Mawji et al., 2008; Velasquez et al., 2011). Typified by an exceptionally high Fe-binding capacity and low molecular weight, siderophores are produced under iron limitation by marine heterotrophic bacteria and some fresh water cyanobacteria (e.g., Haygood et al., 1993; Vraspir and Butler, 2009), while production by marine cyanobacteria remains controversial (Hopkinson and Morel, 2009). Less studied, but widely spread microbial exudates capable of binding iron are exopolymer substances (EPS) and their transparent exopolymer particles (TEP) derivatives (Table 3). These high molecular weight saccharide-rich exopolymers are secreted by most microorganisms, including phytoplankton, bacteria, and zooplankton (Decho, 1990; Passow, 2002; Wotton, 2004; Croot et al., 2007). EPS are thought to weakly bind iron compared to siderophores based on recent data from several model saccharides (Hassler et al., 2011a). TEP, on the other hand, have been shown to have a high affinity for Fe (Quigley et al., 2002). Many other compounds secreted or released due to grazing and lysis contribute to

the “Fe ligand soup” in aquatic environments (Boye et al., 2005; Tsuda et al., 2007; Strmecki et al., 2010; Poorvin et al., 2011). The release of iron binding ligands in cultures supplemented with Fe was reported for the marine haptophyte *E. huxleyi* and two diatom species, qualifying these as non-siderophore Fe-binding ligands (Boye and van den Berg, 2000; Rijkenberg et al., 2008). Some toxins, capable of binding Fe (but not as strongly as siderophores) are known to be synthesized by harmful bloom forming phytoplankton upon Fe limitation (Rue and Bruland, 2001). Secretion of both the neurotoxin domoic acid (a water soluble amino acid produced by *Pseudo-nitzschia* spp.) and the hepatotoxin microcystin (a peptide produced by *Microcystis aeruginosa*) were shown to improve growth under low Fe conditions (Maldonado et al., 2002; Wells et al., 2005; Alexova et al., 2011). Interestingly, these toxins do not directly provide the cell with Fe, but rather increase copper supply for *Pseudo-nitzschia* spp. enabling the synthesis of copper containing high affinity iron uptake proteins (Maldonado et al., 2002; Wells et al., 2005), and probably aid *M. aeruginosa* in oxidative damage protection (Alexova et al., 2011). In addition, terrestrial humics have recently been suggested to be important iron binding ligands in open ocean waters (van den Berg, 1995; Laglera and van den Berg, 2009; Laglera et al., 2011).

Bioavailability

At the cellular level, acquisition of a specific compound depends to a large degree on the uptake machinery possessed by an organism (see Phytoplankton Fe Acquisition Systems). In the natural environment, additional parameters such as the compound residence time in surface waters and its tendency to undergo biological and chemical transformation influence its ability to support growth (Figure 1). In this section we briefly examine the effect of environmental and chemical factors on phytoplankton Fe acquisition from EPS and siderophore bound iron.

At the organism level, recent studies have found that iron bound to model saccharides is highly available to diatoms and natural phytoplankton assemblages (Figure 5; Table 3; Hassler and Schoemann, 2009; Hassler et al., 2011a,b). This was accounted for by the ability of saccharides to stabilize iron in the dissolved and colloidal form and increase the labile Fe pool (Hassler et al., 2011b). In the natural environment, the effect of saccharides on Fe solubility and residence time in the surface water is less clear. EPS and TEP were shown to promote aggregate formation and particle export (Decho, 1990; Passow, 2002), thus possibly shortening the residence time of saccharide bound Fe in surface waters (Berman-Frank et al., 2007). Additionally, iron bound to saccharides may be subjected to chemical and photochemical transformations, further altering its fate and accessibility to phytoplankton. Iron is weakly bound to saccharides and may be exchanged with stronger ligands such as siderophores (Hunter and Boyd, 2007). Photochemical Fe(II) production from saccharide bound iron was recently reported (Steigenberger et al., 2010), but its environmental repercussions are unexplored as yet. Lastly, EPS often create protective microenvironments around microbial consortia, single cells, and cell aggregates (Decho, 1990; Passow, 2002). The formation of such microhabitats impacts all concentration dependent processes and, as such, EPS surrounded cells may be diffusion limited when it comes to acquiring dissolved Fe from the surrounding

waters. However, EPS confers two significant advantages on cells: firstly, EPS are highly adsorbent allowing for the storage and easier processing of iron and secondly the confined microenvironment provides protection from diffusive losses of Fe associated with the EPS (Sunda, 2001; Hassler et al., 2011a).

The role of siderophores in supporting phytoplankton growth *in situ* has received more attention than any other Fe chelator, but in turn raised many new questions (Table 3; Maldonado et al., 2005; Pickell et al., 2009). As the acquisition of siderophores was detailed in Section “Phytoplankton Fe Acquisition Systems,” we briefly discuss two chemical features of siderophores with potential repercussions for iron fate and bioavailability. Firstly, many of the Fe-siderophore complexes isolated from marine bacteria are photolabile (Barbeau et al., 2001, 2003; Vraspir and Butler, 2009). However, due to the fast oxidation of Fe(II) within the complex and since the photoproduct still binds Fe with high affinity, this photo-reactivity does not seem to confer any clear biological advantage (Vraspir and Butler, 2009). This is not always the case however: recently, photo-reduction of iron bound to a newly identified siderophore, vibrioferrin, and the subsequent release of Fe⁺ was reported to enhance iron uptake by dinoflagellates (Amin et al., 2009). Vibrioferrin undergoes photo-degradation and does not retain significant Fe-binding capacity, thus releasing Fe⁺. Secondly, many marine siderophore isolates also tend to be amphiphilic and closely associate with bacterial membranes, possibly preventing their loss by diffusion in the marine environment (Vraspir and Butler, 2009). Although the study of amphiphilic siderophore partitioning to membranes is at a very early stage, it may bear interesting implications for the function of siderophores in iron acquisition in the ocean.

SUMMATION

The topic of iron bioavailability has garnered wide spread interest from the scientific community, yet due to its intrinsic complexity a well-rounded understanding of this concept is lacking. In this contribution we have attempted to disassemble bioavailability and address some of its more biologically orientated facets. Of the many topics covered in this synthesis, we conclude with a summary of the principal arguments and perhaps unorthodox perspectives which we hope lend some insights into Fe bioavailability in the aquatic environment.

- Iron acquisition by means of reduction is a widespread Fe uptake strategy in the ocean, common to both eukaryotic and prokaryotic phytoplankton. Both experimental and genomic data challenge the prevalent paradigm of siderophore-based Fe uptake as an exclusive iron acquisition pathway amongst marine cyanobacteria. We propose that the occurrence of siderophore vs. reductive iron uptake can be put down to environmental rather than taxonomic considerations. Organisms residing in densely populated, low turbulence environments (e.g., fecal pellets, marine snow, or colony-consortiums) will favor siderophore-based Fe acquisition, while pelagic phytoplankton will favor the non-specific reductive strategy enabling them to access the dilute, heterogeneous Fe pool.
- The availability of various Fe-substrates to phytoplankton can be viewed as a spectrum rather than an absolute “all or nothing.”

A bioavailability scale can be established by comparing substrate normalized uptake rates (by means of the uptake rate constant – k_{up}). We suggest that a further normalization of FeL uptake constants relative to the Fe' uptake constant is highly useful in the comparison of different studies, organisms and environments. Hence, in order to establish a baseline for the determination of relative bioavailability, we urge for the use of EDTA in order to better regulate Fe' instead of or in addition to ligand-free FeCl₃. Looking beyond short term uptake, k_{up} can be used to gage if a specific compound is likely to be a significant contributor to the Fe requirements of phytoplankton in the environment. This same approach can be extended to natural systems where k_{up} values of natural ligands by known organisms may be compared to model ligands while the k_{up} values of known Fe-substrates by natural communities may be contrasted with those of model organisms.

- For a fuller understanding of iron bioavailability we look beyond phytoplankton iron uptake pathways and rates. Microorganisms are not only influenced by their environment but are themselves agents of change when it comes to Fe bioavailability. Bio-mediated redox transformations, microbial exudates and secretions as well as food web interactions impact iron speciation, residence time in surface waters and ultimate accessibility to phytoplankton be it in a positive or negative manner.

REFERENCES

- Alexova, R., Fujii, M., Birch, D., Cheng, J., Waite, T. D., Ferrari, B. C., and Neilan, B. A. (2011). Iron uptake and toxin synthesis in the bloom-forming *Microcystis aeruginosa* under iron limitation. *Environ. Microbiol.* 13, 1064–1077.
- Allredge, A. L., and Cohen, Y. (1987). Can microscale chemical patches persist in the sea – microelectrode study of marine snow, fecal pellets. *Science* 235, 689–691.
- Allen, A. E., Laroche, J., Maheswari, U., Lommer, M., Schauer, N., Lopez, P. J., Finazzi, G., Fernie, A. R., and Bowler, C. (2008). Whole-cell response of the pennate diatom *Phaeodactylum tricornutum* to iron starvation. *Proc. Natl. Acad. Sci. U.S.A.* 105, 10438–10443.
- Allen, M. D., Del Campo, J. A., Kropat, J., and Merchant, S. S. (2007). FEA1, FEA2, and FRE1, encoding two homologous secreted proteins and a candidate ferrireductase, are expressed coordinately with FOX1 and FTR1 in iron-deficient *Chlamydomonas reinhardtii*. *Eukaryotic Cell* 6, 1841–1852.
- Allnutt, F. C. T., and Bonner, W. D. J. (1987). Evaluation of reductive release as a mechanism for iron uptake from ferrioxamine B by *Chlorella vulgaris*. *Plant Physiol.* 85, 751–756.
- Amin, S. A., Green, D. H., Kuepper, F. C., and Carrano, C. J. (2009). Vibrioferrin, an unusual marine siderophore: iron binding, photochemistry, and biological implications. *Inorg. Chem.* 48, 11451–11458.
- Anderson, M. A., and Morel, F. M. M. (1982). The influence of aqueous iron chemistry on the uptake of iron by the coastal diatom *Thalassiosira weissflogii*. *Limnol. Oceanogr.* 27, 789–813.
- Atkinson, A., and Guerinot, M. (2011). “Metal transport,” in *The Plant Plasma Membrane*, eds A. S. Murphy, B. Schulz, and W. Peer (Berlin: Springer), 303–330.
- Balzano, S., Statham, P. J., Pancost, R. D., and Lloyd, J. R. (2009). Role of microbial populations in the release of reduced iron to the water column from marine aggregates. *Aquat. Microb. Ecol.* 54, 291–303.
- Barbeau, K. (2006). Photochemistry of organic iron(III) complexing ligands in oceanic systems. *Photochem. Photobiol.* 82, 1505–1516.
- Barbeau, K., and Moffett, J. W. (2000). Laboratory and field studies of colloidal iron oxide dissolution as mediated by phagotrophy and photolysis. *Limnol. Oceanogr.* 45, 827–835.
- Barbeau, K., Moffett, J. W., Caron, D. A., Croot, P. L., and Erdner, D. L. (1996). Role of protozoan grazing in relieving iron limitation of phytoplankton. *Nature* 380, 61–64.
- Barbeau, K., Rue, E. L., Bruland, K. W., and Butler, A. (2001). Photochemical cycling of iron in the surface ocean mediated by microbial iron (III) -binding ligands. *Nature* 413, 409–413.
- Barbeau, K., Rue, E. L., Trick, C. G., Bruland, K. T., and Butler, A. (2003). Photochemical reactivity of siderophores produced by marine heterotrophic bacteria and cyanobacteria based on characteristic Fe(III) binding groups. *Limnol. Oceanogr.* 48, 1069–1078.
- Batchelli, S., Muller, F. L. L., Chang, K.-C., and Lee, C.-L. (2010). Evidence for strong but dynamic iron-humic colloidal associations in humic-rich coastal waters. *Environ. Sci. Technol.* 44, 8485–8490.
- Berman-Frank, I., Rosenberg, G., Levitan, O., Haramaty, L., and Mari, X. (2007). Coupling between autocatalytic cell death and transparent exopolymeric particle production in the marine cyanobacterium *Trichodesmium*. *Environ. Microbiol.* 9, 1415–1422.
- Bidle, K. D., and Falkowski, P. G. (2004). Cell death in planktonic, photosynthetic microorganisms. *Nat. Rev. Microbiol.* 2, 643–655.
- Blain, S., Queguiner, B., Armand, L., Belviso, S., Bombled, B., Bopp, L., Bowie, A., Brunet, C., Brussaard, C., Carlotti, F., Christaki, U., Corbiere, A., Durand, I., Ebersbach, F., Fuda, J.-L., Garcia, N., Gerringa, L., Griffiths, B., Guigue, C., Guillermin, C., Jacquet, S., Jeandel, C., Laan, P., Lefevre, D., Lo Monaco, C., Malits, A., Mosseri, J., Obernosterer, I., Park, Y.-H., Picheral, M., Pondaven, P., Remenyi, T., Sandroni, V., Sarthou, G., Savoye, N., Scouarnec, L., Souhaut, M., Thuiller, D., Timmermans, K., Trull, T., Uitz, J., Van Beek, P., Veldhuis, M., Vincent, D., Viollier, E., Vong, L., and Wagener, T. (2007). Effect of natural iron fertilization on carbon sequestration in the Southern Ocean. *Nature* 446, U1070–U1071.
- Borer, P. M., Sulzberger, B., Reichard, P., and Kraemer, S. M. (2005). Effect of siderophores on the light-induced dissolution of colloidal iron(III) (hydr)oxides. *Mar. Chem.* 93, 179–193.
- Bowler, C., Vardi, A., and Allen, A. E. (2010). Oceanographic and biogeochemical insights from diatom genomes. *Ann. Rev. Mar. Sci.* 2, 333–365.
- Boyd, P. W., and Ellwood, M. J. (2010). The biogeochemical cycle of iron in the ocean. *Nat. Geosci.* 3, 675–682.
- Boyd, P. W., Ibsanmi, E., Sander, S. G., Hunter, K. A., and Jackson, G. A. (2010a). Remineralization of upper ocean particles: implications for iron biogeochemistry. *Limnol. Oceanogr.* 55, 1271–1288.
- Boyd, P. W., Mackie, D. S., and Hunter, K. A. (2010b). Aerosol iron deposition to the surface ocean – modes of

ACKNOWLEDGMENTS

We wish to thank M. Maldonado, B. Sunda, B. Hopkinson, F. Morel, P. Croot, and C. Kranzler for their insights prior and during the preparation of this manuscript as well as the reviewers and editor for their valuable comments. This work was supported in part by the Israel Science Foundation grant 933/07, the Israel USA Binational Science Foundation grant 2008097 and the Assemble FP7 research grant awarded to H. Lis. This work is in partial fulfillment of the requirements for a Ph. D thesis to H. Lis from the Hebrew University.

- iron supply and biological responses. *Mar. Chem.* 120, 128–143.
- Boyd, P. W., Jickells, T., Law, C. S., Blain, S., Boyle, E. A., Buesseler, K. O., Coale, K. H., Cullen, J. J., De Baar, H. J. W., Follows, M., Harvey, M., Lancelot, C., Levasseur, M., Owens, N. P. J., Pollard, R., Rivkin, R. B., Sarmiento, J., Schoemann, V., Smetacek, V., Takeda, S., Tsuda, A., Turner, S., and Watson, A. J. (2007). Mesoscale iron enrichment experiments 1993–2005: synthesis and future directions. *Science* 315, 612–617.
- Boye, M., Nishioka, J., Croot, P. L., Laan, P., Timmermans, K. R., and De Baar, H. J. W. (2005). Major deviations of iron complexation during 22 days of a mesoscale iron enrichment in the open Southern Ocean. *Mar. Chem.* 96, 257–271.
- Boye, M., and van den Berg, C. M. G. (2000). Iron availability and the release of iron-complexing ligands by *Emiliania huxleyi*. *Mar. Chem.* 70, 277–287.
- Boye, M., Van Den Berg, C. M. G., De Jong, J. T. M., Leach, H., Croot, P., and De Baar, H. J. W. (2001). Organic complexation of iron in the Southern Ocean. *Deep Sea Res. Part I Oceanogr. Res. Pap.* 48, 1477–1497.
- Boyle, E. A. (1988). Cadmium: chemical tracer of deepwater paleoceanography. *Paleoceanography* 3, 471–489.
- Brand, L. E. (1991). Minimum iron requirements of marine phytoplankton and the implications for biogeochemical control of new production. *Limnol. Oceanogr.* 36, 1756–1772.
- Breitbarth, E., Gelting, J., Walve, J., Hoffmann, L. J., Turner, D. R., Hasselov, M., and Ingri, J. (2009). Dissolved iron (II) in the Baltic Sea surface water and implications for cyanobacterial bloom development. *Biogeosciences* 6, 2397–2420.
- Buck, C. S., Landing, W. M., Resing, J. A., and Lebon, G. T. (2006). Aerosol iron and aluminum solubility in the northwest Pacific Ocean: results from the 2002 IOC cruise. *Geochim. Geophys. Geosyst.* 7, Q04M07.
- Buck, K. N., Selph, K. E., and Barbeau, K. A. (2010). Iron-binding ligand production and copper speciation in an incubation experiment of Antarctic Peninsula shelf waters from the Bransfield Strait, Southern Ocean. *Mar. Chem.* 122, 148–159.
- Buesseler, K. O., Doney, S. C., Karl, D. M., Boyd, P. W., Caldeira, K., Chai, F., Coale, K. H., De Baar, H. J. W., Falkowski, P. G., Johnson, K. S., Lampitt, R. S., Michaels, A. F., Naqvi, S. W. A., Smetacek, V., Takeda, S., and Watson, A. J. (2008). Environment – ocean iron fertilization – moving forward in a sea of uncertainty. *Science* 319, 162.
- Chen, J.-C., Hsieh, S. I., Kropat, J., and Merchant, S. S. (2008). A ferroxidase encoded by FOX1 contributes to iron assimilation under conditions of poor iron nutrition in *Chlamydomonas*. *Eukaryotic Cell* 7, 541–545.
- Chen, M., and Wang, W. (2008). Accelerated uptake by phytoplankton of iron bound to humic acids. *Aquat. Biol.* 3, 155–166.
- Chen, Y., Tovar-Sanchez, A., Siefert, R. L., Sanudo-Wilhelmy, S. A., and Zhuang, G. (2011). Luxury uptake of aerosol iron by *Trichodesmium* in the western tropical North Atlantic. *Geophys. Res. Lett.* 38, L18602.
- Croot, P. L., Bluhm, K., Schlosser, C., Streu, P., Breitbarth, E., Frew, R., and Van Ardelan, M. (2008). Regeneration of Fe(II) during EIFeX and SOFeX. *Geophys. Res. Lett.* 35, L19606.
- Croot, P. L., Bowie, A. R., Frew, R. D., Maldonado, M. T., Hall, J. A., Safi, K. A., La Roche, J., Boyd, P. W., and Law, C. S. (2001). Retention of dissolved iron and Fe-II in an iron induced Southern Ocean phytoplankton bloom. *Geophys. Res. Lett.* 28, 3425–3428.
- Croot, P. L., Laan, P., Nishioka, J., Strass, V., Cisevski, B., Boye, M., Timmermans, K. R., Bellerby, R. G., Goldson, L., Nightingale, P., and De Baar, H. J. W. (2005). Spatial and temporal distribution of Fe(II) and H₂O₂ during EisenEx, an open ocean mesoscale iron enrichment. *Mar. Chem.* 95, 65–88.
- Croot, P. L., Passow, U., Assmy, P., Jansen, S., and Strass, V. H. (2007). Surface active substances in the upper water column during a Southern Ocean Iron Fertilization Experiment (EIFEX). *Geophys. Res. Lett.* 34, C06015.
- Cullen, J. T., Lane, T. W., Morel, F. M. M., and Sherrell, R. M. (1999). Modulation of cadmium uptake in phytoplankton by seawater CO₂ concentration. *Nature* 402, 165–167.
- Dalbec, A., and Twining, B. (2009). Remineralization of bioavailable iron by a heterotrophic dinoflagellate. *Aquat. Microb. Ecol.* 54, 279–290.
- Decho, A. (1990). Microbial exopolymer secretions in ocean environments: their role(s) in food webs and marine processes. *Oceanogr. Mar. Biol. Ann. Rev.* 28, 73–153.
- Duckworth, O. W., Holmstrom, S. J. M., Pena, J., and Sposito, G. (2009). Biogeochemistry of iron oxidation in a circumneutral freshwater habitat. *Chem. Geol.* 260, 149–158.
- Eckhardt, U., and Buckhout, T. J. (1998). Iron assimilation in *Chlamydomonas reinhardtii* involves ferric reduction and is similar to strategy I higher plants. *J. Exp. Bot.* 49, 1219–1226.
- Elderfield, H., and Rickaby, R. E. M. (2000). Oceanic Cd/P ratio and nutrient utilization in the glacial Southern Ocean. *Nature* 405, 305–310.
- Emmenegger, L., Schonenberger, R. R., Sigg, L., and Sulzberger, B. (2001). Light-induced redox cycling of iron in circumneutral lakes. *Limnol. Oceanogr.* 46, 49–61.
- Falkowski, P. G., Barber, R. T., and Smetacek, V. (1998). Biogeochemical controls and feedbacks on ocean primary production. *Science* 281, 200–206.
- Finkel, Z. V., Beardall, J., Flynn, K. J., Quigg, A., Rees, T. A. V., and Raven, J. A. (2010). Phytoplankton in a changing world: cell size and elemental stoichiometry. *J. Plankton Res.* 32, 119–137.
- Fujii, M., Rose, A. L., Omura, T., and Waite, T. D. (2010). Effect of Fe(II) and Fe(III) transformation kinetics on iron acquisition by a toxic strain of *Microcystis aeruginosa*. *Environ. Sci. Technol.* 44, 1980–1986.
- Gerringa, L. J. A., De Baar, H. J. W., and Timmermans, K. R. (2000). A comparison of iron limitation of phytoplankton in natural oceanic waters and laboratory media conditioned with EDTA. *Mar. Chem.* 68, 335–346.
- Gledhill, M., and van den Berg, C. M. G. (1994). Determination of complexation of iron(III) with natural organic complexing ligands in seawater using cathodic stripping voltammetry. *Mar. Chem.* 47, 41–54.
- Goldman, S. J., Lammers, P. J., Berman, M. S., and Sanders-Loehr, J. (1983). Siderophore-mediated iron uptake in different strains of *Anabaena* sp. *J. Bacteriol.* 156, 1144–1150.
- Gonzalez-Davila, M., Santana-Casiano, J. M., and Millero, F. J. (2005). Oxidation of Iron(II) nanomolar with H₂O₂ in seawater. *Geochim. Cosmochim. Acta* 69, 83–93.
- Greene, R. M., Geider, R. J., and Falkowski, P. G. (1991). Effect of iron limitation on photosynthesis in a marine diatom. *Limnol. Oceanogr.* 36, 1772–1782.
- Hansard, S. P., Landing, W. M., Measures, C. I., and Voelker, B. M. (2009). Dissolved iron(II) in the Pacific Ocean: measurements from the PO2 and P16N CLIVAR/CO₂ repeat hydrography expeditions. *Deep Sea Res. Part I Oceanogr. Res. Pap.* 56, 1117–1129.
- Hansard, S. P., Vermilyea, A. W., and Voelker, B. M. (2010). Measurements of superoxide radical concentration and decay kinetics in the Gulf of Alaska. *Deep Sea Res. Part I Oceanogr. Res. Pap.* 57, 1111–1119.
- Harrington, J., and Crumbliss, A. (2009). The redox hypothesis in siderophore-mediated iron uptake. *Biometals* 22, 679–689.
- Hassler, C. S., Alasonati, E., Nichols, C. A. M., and Slaveykova, V. I. (2011a). Exopolysaccharides produced by bacteria isolated from the pelagic Southern Ocean – role in Fe binding, chemical reactivity, and bioavailability. *Mar. Chem.* 123, 88–98.
- Hassler, C. S., Schoemann, V., Nichols, C. M., Butler, E. C. V., and Boyd, P. W. (2011b). Saccharides enhance iron bioavailability to Southern Ocean phytoplankton. *Proc. Natl. Acad. Sci. U.S.A.* 108, 1076–1081.
- Hassler, C. S., Havens, S. M., Bullerjahn, G. S., McKay, R. M. L., and Twiss, M. R. (2009). An evaluation of iron bioavailability and speciation in western Lake Superior with the use of combined physical, chemical, and biological assessment. *Limnol. Oceanogr.* 54, 987–1001.
- Hassler, C. S., and Schoemann, V. (2009). Bioavailability of organically bound Fe to model phytoplankton of the Southern Ocean. *Biogeosciences* 6, 2281–2296.
- Haygood, M. G., Holt, P. D., and Butler, A. (1993). Aerobactin production by a planktonic marine *Vibrio* Sp. *Limnol. Oceanogr.* 38, 1091–1097.
- Henley, W. J., and Yin, Y. (1998). Growth and photosynthesis of marine *Synechococcus* (Cyanophyceae) under iron stress. *J. Phycol.* 34, 94–103.
- Higgins, J. L., Kudo, I., Nishioka, J., Tsuda, A., and Wilhelm, S. W. (2009). The response of the virus community to the SEEDS II mesoscale iron fertilization. *Deep Sea Res. Part II Top. Stud. Oceanogr.* 56, 2788–2795.
- Holmén, B. A., and Casey, W. H. (1996). Hydroxamate ligands, surface chemistry, and the mechanism of ligand-promoted dissolution of goethite [α-FeOOH(s)]. *Geochim. Cosmochim. Acta* 60, 4403–4416.
- Hopkinson, B. M., and Barbeau, K. A. (2012). Iron transporters in marine prokaryotic genomes and metagenomes. *Environ. Microbiol.* 14, 114–128.
- Hopkinson, B. M., and Morel, F. M. M. (2009). The role of siderophores in iron acquisition by photosynthetic

- marine microorganisms. *Biometals* 22, 659–669.
- Hudson, R. J. M., and Morel, F. M. M. (1993). Trace metal transport by marine microorganisms: implications of metal coordination kinetics. *Deep Sea Res. A* 40, 129–150.
- Hunter, K. A., and Boyd, P. W. (2007). Iron-binding ligands and their role in the ocean biogeochemistry of iron. *Environ. Chem.* 4, 221–232.
- Hutchins, D. A., Rueter, J. G., and Fish, W. (1991). Siderophore production and nitrogen fixation are mutually exclusive strategies in *Anabaena* 7120. *Limnol. Oceanogr.* 36, 1–12.
- Hutchins, D. A., Witter, A. E., Butler, A., and Luther, G. W. (1999). Competition among marine phytoplankton for different chelated iron speciation. *Nature* 400, 858–861.
- Ibisanmi, E., Sander, S. G., Boyd, P. W., Bowie, A. R., and Hunter, K. A. (2011). Vertical distributions of iron-(III) complexing ligands in the Southern Ocean. *Deep Sea Res. Part II Top. Stud. Oceanogr.* 58, 2113–2125.
- Johnson, K. S., Coale, K. H., Elrod, V. A., and Tindale, N. W. (1994). Iron photochemistry in seawater from the equatorial Pacific. *Mar. Chem.* 46, 319–334.
- Johnson, K. S., Gordon, R. M., and Coale, K. H. (1997). What controls dissolved iron concentrations in the world ocean? *Mar. Chem.* 57, 137–161.
- Jones, G. J., and Morel, F. M. M. (1988). Plasmalemma redox activity in the diatom *Thalassiosira*. *Plant Physiol.* 87, 143–147.
- Keshtacher, L. E., Hadar, Y., and Chen, Y. (1999). Fe nutrition demand and utilization by the green alga *Dunaliella bardawil*. *Plant Soil* 215, 175–182.
- Kieber, R. J., Williams, K., Willey, J. D., Skrabal, S., and Avery, G. B. Jr. (2001). Iron speciation in coastal rainwater: concentration and deposition to seawater. *Mar. Chem.* 73, 83–95.
- King, D. W., Lounsbury, H. A., and Millero, F. J. (1995). Rates and mechanism of Fe(II) oxidation at nanomolar total iron concentrations. *Environ. Sci. Technol.* 29, 818–824.
- Kosman, D. J. (2003). Molecular mechanisms of iron uptake in fungi. *Mol. Microbiol.* 47, 1185–1197.
- Kraemer, S. M. (2004). Iron oxide dissolution and solubility in the presence of siderophores. *Aquat. Sci.* 66, 3–18.
- Kraemer, S. M., Butler, A., Borer, P., and Cervini-Silva, J. (2005). “Siderophores and the dissolution of iron-bearing minerals in marine systems,” in *Molecular Geomicrobiology*, eds J. E. Banfield, J. Cervini-Silva, and K. H. Nealson (Mineralogical Society of America, Geochemical Society), 53–84.
- Kranzler, C., Lis, H., Shaked, Y., and Keren, N. (2011). The role of reduction in iron uptake processes in a unicellular, planktonic cyanobacterium. *Environ. Microbiol.* 13, 2990–2999.
- Kudo, I., and Harrison, P. J. (1997). Effect of iron nutrition on the marine cyanobacterium *Synechococcus* grown on different N sources and irradiances. *J. Phycol.* 33, 232–240.
- Kuma, K., Nakabayashi, S., Suzuki, Y., Kudo, I., and Matsunaga, K. (1992). Photo-reduction of iron(III) by dissolved organic substances and existence of iron(II) in seawater during spring blooms. *Mar. Chem.* 37, 15–27.
- Kuma, K., Nishioka, J., and Matsunaga, K. (1996). Controls on iron(III) hydroxide solubility in seawater: the influence of pH and natural organic chelators. *Limnol. Oceanogr.* 41, 396–407.
- Kustka, A., Carpenter, E. J., and Sanudo-Wilhelmy, S. A. (2002). Iron and marine nitrogen fixation: progress and future directions. *Res. Microbiol.* 153, 255–262.
- Kustka, A. B., Allen, A. E., and Morel, F. M. M. (2007). Sequence analysis and transcriptional regulation of iron acquisition genes in two marine diatoms. *J. Phycol.* 43, 715–729.
- Kustka, A. B., Shaked, Y., Milligan, A. J., King, D. W., and Morel, F. M. M. (2005). Extracellular production of superoxide by marine diatoms: contrasting effects on iron redox chemistry and bioavailability. *Limnol. Oceanogr.* 50, 1172–1180.
- Laglera, L. M., Battaglia, G., and Van Den Berg, C. M. G. (2011). Effect of humic substances on the iron speciation in natural waters by CLE/CSV. *Mar. Chem.* 127, 134–143.
- Laglera, L. M., and van den Berg, C. M. G. (2009). Evidence for geochemical control of iron by humic substances in seawater. *Limnol. Oceanogr.* 54, 610–619.
- Lampitt, R. S., Achterberg, E. P., Anderson, T. R., Hughes, J. A., Iglesias-Rodriguez, M. D., Kelly-Gerreyn, B. A., Lucas, M., Popova, E. E., Sanders, R., Shepherd, J. G., Smythe-Wright, D., and Yool, A. (2008). Ocean fertilization: a potential means of geoengineering? *Philos. Transact. R. Soc. A Math. Phys. Eng. Sci.* 366, 3919–3945.
- Lane, E. S., Semeniuk, D. M., Strzepek, R. F., Cullen, J. T., and Maldonado, M. T. (2009). Effects of iron limitation on intracellular cadmium of cultured phytoplankton: implications for surface dissolved cadmium to phosphate ratios. *Mar. Chem.* 115, 155–162.
- Law, C. S., and Ling, R. D. (2001). Nitrous oxide flux and response to increased iron availability in the Antarctic Circumpolar Current. *Deep Sea Res. Part II Top. Stud. Oceanogr.* 48, 2509–2527.
- Levy, J., Zhang, H., Davison, W., and Groben, R. (2011). Using diffusive gradients in thin films to probe the kinetics of metal interaction with algal exudates. *Environ. Chem.* 8, 517–524.
- Lis, H., and Shaked, Y. (2009). Probing the bioavailability of organically bound iron: a case study in the *Synechococcus*-rich waters of the Gulf of Aqaba. *Aquat. Microb. Ecol.* 56, 241–253.
- Liss, P. S. (2007). Trace gas emissions from the marine biosphere. *Philos. Transact. R. Soc. A Math. Phys. Eng. Sci.* 365, 1697–1704.
- Liu, X. W., and Millero, F. J. (2002). The solubility of iron in seawater. *Mar. Chem.* 77, 43–54.
- Lohan, M. C., and Bruland, K. W. (2008). Elevated Fe(II) and dissolved Fe in hypoxic shelf waters off Oregon and Washington: an enhanced source of iron to coastal upwelling regimes. *Environ. Sci. Technol.* 42, 6462–6468.
- Macrellis, H. M., Trick, C. G., Rue, E. L., Smith, G., and Bruland, K. W. (2001). Collection and detection of natural iron-binding ligands from seawater. *Mar. Chem.* 76, 175–187.
- Maldonado, M. T., Allen, A. E., Chong, J. S., Dan Leus, K. L., Karpenko, N., and Harris, S. L. (2006). Copper-dependent iron transport in coastal and oceanic diatoms. *Limnol. Oceanogr.* 51, 1729–1743.
- Maldonado, M. T., Boyd, P. W., Harrison, P. J., and Price, N. M. (1999). Co-limitation of phytoplankton growth by light and Fe during winter in the NE subarctic Pacific Ocean. *Deep Sea Res. Part II Top. Stud. Oceanogr.* 46, 2475–2485.
- Maldonado, M. T., Hughes, M. P., Rue, E. L., and Wells, M. L. (2002). The effect of Fe and Cu on growth and domoic acid production by *Pseudo-nitzschia* multiseres and *Pseudo-nitzschia australis*. *Limnol. Oceanogr.* 47, 515–526.
- Maldonado, M. T., and Price, N. M. (1999). Utilization of iron bound to strong organic ligands by plankton communities in the subarctic Pacific Ocean. *Deep Sea Res. Part II Top. Stud. Oceanogr.* 46, 2447–2473.
- Maldonado, M. T., and Price, N. M. (2001). Reduction and transport of organically bound iron by *Thalassiosira oceanica* (Bacillariophyceae). *J. Phycol.* 37, 298–309.
- Maldonado, M. T., Strzepek, R. F., Sander, S., and Boyd, P. W. (2005). Acquisition of iron bound to strong organic complexes, with different Fe binding groups and photochemical reactivities, by plankton communities in Fe-limited subantarctic waters. *Global Biogeochem. Cycles* 19, GB4S23.
- Manizza, M., Le Quere, C., Watson, A. J., and Buitenhuis, E. T. (2005). Bio-optical feedbacks among phytoplankton, upper ocean physics and sea-ice in a global model. *Geophys. Res. Lett.* 32, L05603.
- Maranger, R., Bird, D. F., and Price, N. M. (1998). Iron acquisition by photosynthetic marine phytoplankton from ingested bacteria. *Nature* 396, 248–251.
- Marchetti, A., and Cassar, N. (2009). Diatom elemental and morphological changes in response to iron limitation: a brief review with potential paleoceanographic applications. *Geobiology* 7, 419–431.
- Marchetti, A., Maldonado, M. T., Lane, E. S., and Harrison, P. J. (2006). Iron requirements of the pennate diatom *Pseudo-nitzschia*: comparison of oceanic (high-nitrate, low-chlorophyll waters) and coastal species. *Limnol. Oceanogr.* 51, 2092–2101.
- Martin, J. H., Fitzwater, S. E., and Gordon, R. M. (1990). Iron deficiency limits phytoplankton growth in Antarctic waters. *Global Biogeochem. Cycles* 4, 5–12.
- Martinez, J. S., Zhang, G. P., Holt, P. D., Jung, H. T., Carrano, C. J., Haygood, M. G., and Butler, A. (2000). Self-assembling amphiphilic siderophores from marine bacteria. *Science* 287, 1245–1247.
- Martinez-Garcia, A., Rosell-Mele, A., Jaccard, S. L., Geibert, W., Sigman, D. M., and Haug, G. H. (2011). Southern Ocean dust-climate coupling over the past four million years. *Nature* 476, 312–315.
- Mawji, E., Gledhill, M., Milton, J. A., Tarran, G. A., Ussher, S., Thompson, A., Wolff, G. A., Worsfold, P. J., and Achterberg, E. P. (2008). Hydroxamate Siderophores: occurrence and Importance in the Atlantic Ocean. *Environ. Sci. Technol.* 42, 8675–8680.

- McKay, R. M. L., Villareal, T. A., and La Roche, J. (2000). Vertical migration by *Rhizosolenia* spp. (Bacillariophyceae): implications for Fe acquisition. *J. Phycol.* 36, 669–674.
- Meskhidze, N., and Nenes, A. (2006). Phytoplankton and cloudiness in the Southern Ocean. *Science* 314, 1419–1423.
- Middlemiss, J. K., Anderson, A. M., Stratilo, C. W., and Weger, H. G. (2001). Oxygen consumption associated with ferric reductase activity and iron uptake by iron-limited cells of *Chlorella kessleri* (Chlorophyceae). *J. Phycol.* 37, 393–399.
- Miller, W. L., King, D. W., Lin, J., and Kester, D. R. (1995). Photochemical redox cycling of iron in coastal seawater. *Mar. Chem.* 50, 63–77.
- Milligan, A. J., and Harrison, P. J. (2000). Effects of non-steady-state iron limitation on nitrogen assimilatory enzymes in the marine diatom *Thalassiosira weissflogii* (Bacillariophyceae). *J. Phycol.* 36, 78–86.
- Milne, A., Davey, M. S., Worsfold, P. J., Achterberg, E. P., and Taylor, A. R. (2009). Real-time detection of reactive oxygen species generation by marine phytoplankton using flow-injection chemiluminescence. *Limnol. Oceanogr. Methods* 7, 705–716.
- Moffett, J. W., Goeffert, T. J., and Naqvi, S. W. A. (2007). Reduced iron associated with secondary nitrite maxima in the Arabian Sea. *Deep Sea Res. Part I Oceanogr. Res. Pap.* 54, 1341–1349.
- Moore, C. M., Mills, M. M., Achterberg, E. P., Geider, R. J., Laroche, J., Lucas, M. I., McDonagh, E. L., Pan, X., Poulton, A. J., Rijkenberg, M. J. A., Suggett, D. J., Ussher, S. J., and Woodward, E. M. S. (2009). Large-scale distribution of Atlantic nitrogen fixation controlled by iron availability. *Nat. Geosci.* 2, 867–871.
- Morel, F. M. M., Kustka, A. B., and Shaked, Y. (2008). The role of unchelated Fe in the iron nutrition of phytoplankton. *Limnol. Oceanogr.* 53, 400–404.
- Morel, F. M. M., and Price, N. M. (2003). The biogeochemical cycles of trace metals in the oceans. *Science* 300, 944–947.
- Nagai, T., Imai, A., Matsushige, K., Yokoi, K., and Fukushima, T. (2007). Dissolved iron and its speciation in a shallow eutrophic lake and its inflowing rivers. *Water Res.* 41, 775–784.
- Nodwell, L., and Price, N. (2001). Direct use of inorganic colloidal iron by marine mixotrophic phytoplankton. *Limnol. Oceanogr.* 46, 755–777.
- Passow, U. (2002). Transparent exopolymer particles (TEP) in aquatic environments. *Prog. Oceanogr.* 55, 287–333.
- Pick, U., Paz, Y., Weiss, M., and Katz, A. (2008). A unique mechanism for Fe³⁺ and Fe²⁺ acquisition in a halo-tolerant alga. *Plant Biol. (Rockville)* 2008, 142.
- Pickell, L. D., Wells, M. L., Trick, C. G., and Cochlan, W. P. (2009). A sea-going continuous culture system for investigating phytoplankton community response to macro- and micro-nutrient manipulations. *Limnol. Oceanogr. Methods* 7, 21–32.
- Poorvin, L., Rinta-Kanto, J. M., Hutchins, D. A., and Wilhelm, S. W. (2004). Viral release of iron and its bioavailability to marine plankton. *Limnol. Oceanogr.* 49, 1734–1741.
- Poorvin, L., Sander, S. G., Velasquez, I., Ibsanmi, E., Leclerc, G. R., and Wilhelm, S. W. (2011). A comparison of Fe bioavailability and binding of a catechol siderophore with virus-mediated lysates from the marine bacterium *Vibrio alginolyticus* PWH3a. *J. Exp. Mar. Biol. Ecol.* 399, 43–47.
- Price, N. M., Ahner, B. A., and Morel, F. M. M. (1994). The equatorial Pacific Ocean: grazer-controlled phytoplankton populations in an iron-limited system. *Limnol. Oceanogr.* 39, 520–534.
- Quigley, M. S., Santschi, P. H., and Hung, C. C. (2002). Importance of acid polysaccharides for 234Th complexation to marine organic matter. *Limnol. Oceanogr.* 47, 367–377.
- Ralston, D. K., McGillicuddy, D. J. Jr., and Townsend, D. W. (2007). Asynchronous vertical migration and bimodal distribution of motile phytoplankton. *J. Plankton Res.* 29, 803–821.
- Raven, J. A. (1990). Predictions of Mn and Fe use efficiencies of phototrophic growth as a function of light availability for growth and of C assimilation pathway. *New Phytol.* 116, 1–18.
- Rich, H. W., and Morel, F. M. M. (1990). Availability of well-defined iron colloids to the marine diatom *Thalassiosira weissflogii*. *Limnol. Oceanogr.* 35, 652–662.
- Rijkenberg, M. J. A., Gerringa, L. J. A., Carolus, V. E., Velzeboer, I., and De Baar, H. J. W. (2006). Enhancement and inhibition of iron photoreduction by individual ligands in open ocean seawater. *Geochim. Cosmochim. Acta* 70, 2790–2805.
- Rijkenberg, M. J. A., Gerringa, L. J. A., Timmermans, K. R., Fischer, A. C., Kroon, K. J., Buma, A. G. J., Wolterbeek, B. T., and De Baar, H. J. W. (2008). Enhancement of the reactive iron pool by marine diatoms. *Mar. Chem.* 109, 29–44.
- Roe, K. L., Barbeau, K., Mann, E. L., and Haygood, M. G. (2011). Acquisition of iron by *Trichodesmium* and associated bacteria in culture. *Environ. Microbiol.* doi: 10.1111/j.1462-2920.2011.02653.x
- Rose, A. L., Godrant, A., Furnas, M., and Waite, T. D. (2010). Dynamics of nonphotochemical superoxide production and decay in the Great Barrier Reef lagoon. *Limnol. Oceanogr.* 55, 1521–1536.
- Rose, A. L., Salmon, T. P., Lukondeh, T., Neilan, B. A., and Waite, T. D. (2005). Use of superoxide as an electron shuttle for iron acquisition by the marine cyanobacterium *Lyngbya majuscula*. *Environ. Sci. Technol.* 39, 3708–3715.
- Rose, A. L., and Waite, T. D. (2002). Kinetic model for Fe(II) oxidation in seawater in the absence and presence of natural organic matter. *Environ. Sci. Technol.* 36, 433–444.
- Rose, A. L., and Waite, T. D. (2003). Effect of dissolved natural organic matter on the kinetics of ferrous iron oxygenation in seawater. *Environ. Sci. Technol.* 37, 4877–4886.
- Rose, A. L., Webb, E. A., Waite, T. D., and Moffett, J. W. (2008). Measurement and implications of nonphotochemically generated superoxide in the equatorial Pacific Ocean. *Environ. Sci. Technol.* 42, 2387–2393.
- Roy, E. G., and Wells, M. L. (2011). Evidence for regulation of Fe(II) oxidation by organic complexing ligands in the Eastern Subarctic Pacific. *Mar. Chem.* 127, 115–122.
- Roy, E. G., Wells, M. L., and King, D. W. (2008). Persistence of iron(II) in surface waters of the western subarctic Pacific. *Limnol. Oceanogr.* 53, 89–98.
- Rubin, M., Berman-Frank, I., and Shaked, Y. (2011). Dust- and mineral-iron utilization by the marine dinitrogen-fixer *Trichodesmium*. *Nat. Geosci.* 4, 529–534.
- Rue, E., and Bruland, K. (2001). Domoic acid binds iron and copper: a possible role for the toxin produced by the marine diatom *Pseudo-nitzschia*. *Mar. Chem.* 76, 127–134.
- Rue, E. L., and Bruland, K. W. (1995). Complexation of iron(III) by natural organic ligands in the central North Pacific as determined by a new competitive ligand equilibration/adsorptive cathodic stripping voltammetric method. *Mar. Chem.* 50, 117–138.
- Rueter, J. G., Hutchins, D. A., Smith, R. W., and Unsworth, N. L. (1992). “Iron nutrition in *Trichodesmium*,” in *Marine Pelagic Cyanobacteria: Trichodesmium and Other Diazotrophs*, eds E. J. Carpenter, D. G. Capone, and J. G. Rueter (Dordrecht: Kluwer Academic), 289–306.
- Sander, S. G., and Koschinsky, A. (2011). Metal flux from hydrothermal vents increased by organic complexation. *Nat. Geosci.* 4, 145–150.
- Sandy, M., and Butler, A. (2009). Microbial iron acquisition: marine and terrestrial siderophores. *Chem. Rev.* 109, 4580–4595.
- Santana-Casiano, J. M., Gonzales-Davila, M., and Millero, F. J. (2005). Oxidation of nanomolar levels of Fe(II) with oxygen in natural waters. *Environ. Sci. Technol.* 39, 2073–2079.
- Santana-Casiano, J. M., Gonzalez-Davila, A., and Millero, F. J. (2006). The role of Fe(II) species on the oxidation of Fe(II) in natural waters in the presence of O₂ and H₂O₂. *Mar. Chem.* 99, 70–82.
- Saragosti, E., Tchervov, D., Katsir, A., and Shaked, Y. (2010). Extracellular production and degradation of superoxide in the coral *Stylophora pistillata* and cultured *Symbiodinium*. *PLoS ONE* 5, e12508. doi:10.1371/journal.pone.0012508
- Sarthou, G., Bucciarelli, E., Chever, F., Hansard, S. P., Gonzalez-Davila, M., Santana-Casiano, J. M., Planchon, F., and Speich, S. (2011). Labile Fe(II) concentrations in the Atlantic sector of the Southern Ocean along a transect from the subtropical domain to the Weddell Sea Gyre. *Biogeosciences* 8, 2461–2479.
- Sarthou, G., Vincent, D., Christaki, U., Obernosterer, I., Timmermans, K. R., and Brussaard, C. P. D. (2008). The fate of biogenic iron during a phytoplankton bloom induced by natural fertilisation: impact of copepod grazing. *Deep Sea Res. Part II Top. Stud. Oceanogr.* 55, 734–751.
- Sasaki, T., Kurano, N., and Miyachi, S. (1998). Induction of ferric reductase activity and of iron uptake activity in *Chloccocum littorale* cells under extremely high-CO₂ and iron-deficient conditions. *Plant Cell Physiol.* 39, 405–410.
- Sato, M., Takeda, S., and Furuya, K. (2007). Iron regeneration and organic iron(III)-binding ligand production during in situ zooplankton grazing experiment. *Mar. Chem.* 106, 471–488.

- Schlosser, C., and Croot, P. L. (2009). Controls on seawater Fe(III) solubility in the Mauritanian upwelling zone. *Geophys. Res. Lett.* 36, L18606.
- Severmann, S., Mcmanus, J., Berelson, W. M., and Hammond, D. E. (2010). The continental shelf benthic iron flux and its isotope composition. *Geochim. Cosmochim. Acta* 74, 3984–4004.
- Shaked, Y. (2008). Iron redox dynamics in the surface waters of the Gulf of Aqaba, Red Sea. *Geochim. Cosmochim. Acta* 72, 1540–1554.
- Shaked, Y., Erel, Y., and Sukenik, A. (2002). Phytoplankton-mediated redox cycle of iron in the epilimnion of Lake Kinneret. *Environ. Sci. Technol.* 36, 460–467.
- Shaked, Y., Kustka, A. B., and Morel, F. M. M. (2005). A general kinetic model for iron acquisition by eukaryotic phytoplankton. *Limnol. Oceanogr.* 50, 872–882.
- Shaked, Y., Kustka, A. B., Morel, F. M. M., and Erel, Y. (2004). Simultaneous determination of iron reduction and uptake by phytoplankton. *Limnol. Oceanogr. Methods* 2, 137–145.
- Shi, D., Xu, Y., Hopkinson, B. M., and Morel, F. M. M. (2010). Effect of ocean acidification on iron availability to marine phytoplankton. *Science* 327, 676–679.
- Shi, D., Xu, Y., and Morel, F. M. M. (2009). Effects of the pH/pCO₂ control method on medium chemistry and phytoplankton growth. *Biogeosciences* 6, 1199–1207.
- Singler, H. R., and Villareal, T. A. (2005). Nitrogen inputs into the euphotic zone by vertically migrating Rhizosolenia mats. *J. Plankton Res.* 27, 545–556.
- Sohm, J. A., Webb, E. A., and Capone, D. G. (2011). Emerging patterns of marine nitrogen fixation. *Nat. Rev. Microbiol.* 9, 499–508.
- Soria-Dengg, S., and Horstmann, U. (1995). Ferrioxamines B and E as iron sources for the marine diatom *Phaeodactylum tricornutum*. *Mar. Ecol. Prog. Ser.* 127, 269–277.
- Soria-Dengg, S., Reissbrodt, R., and Horstmann, U. (2001). Siderophores in marine, coastal waters and their relevance for iron uptake by phytoplankton: experiments with the diatom *Phaeodactylum tricornutum*. *Mar. Ecol. Prog. Ser.* 220, 73–82.
- Statham, P. J., German, C. R., and Connelly, D. P. (2005). Iron (II) distribution and oxidation kinetics in hydrothermal plumes at the Kairei and Edmond vent sites, Indian Ocean. *Earth Planet. Sci. Lett.* 236, 588–596.
- Steigenberger, S., Statham, P. J., Voelker, C., and Passow, U. (2010). The role of polysaccharides and diatom exudates in the redox cycling of Fe and the photoproduction of hydrogen peroxide in coastal seawaters. *Biogeosciences* 7, 109–119.
- Stintzi, A., Barnes, C., Xu, L., and Raymond, K. N. (2000). Microbial iron transport via a siderophore shuttle: a membrane ion transport paradigm. *Proc. Natl. Acad. Sci. U.S.A.* 97, 10691–10696.
- Strmecki, S., Plavsic, M., Steigenberger, S., and Passow, U. (2010). Characterization of phytoplankton exudates and carbohydrates in relation to their complexation of copper, cadmium and iron. *Mar. Ecol. Prog. Ser.* 408, 33–46.
- Strzepek, R. F., and Harrison, P. J. (2004). Photosynthetic architecture differs in coastal and oceanic diatoms. *Nature* 431, 689–692.
- Strzepek, R. F., Maldonado, M. T., Higgins, J. L., Hall, J., Safi, K., Wilhelm, S. W., and Boyd, P. W. (2005). Spinning the “Ferrous Wheel”: the importance of the microbial community in an iron budget during the FeCycle experiment. *Global Biogeochem. Cycles* 19, GB4S26.1–GB4S26.14.
- Stumm, W., and Sulzberger, B. (1992). The cycling of iron in natural environments: considerations based on laboratory studies of heterogeneous redox processes. *Geochim. Cosmochim. Acta* 56, 3233–3257.
- Sunda, W., Price, N. M., and Morel, F. M. M. (2005). “Trace metal ion buffers and their use in culture studies,” in *Algal Culturing Techniques*, ed. R. Anderson (Burlington: Academic Press), 35–63.
- Sunda, W. G. (2001). “Bioavailability and bioaccumulation of iron in the sea,” in *Biogeochemistry of Fe in Seawater*, eds. K. Hunter and D. Turner (West Sussex: John Wiley & Sons), 41–84.
- Sunda, W. G., and Huntsman, S. A. (1995). Iron uptake and growth limitation in oceanic and coastal phytoplankton. *Mar. Chem.* 50, 189–206.
- Sunda, W. G., and Huntsman, S. A. (1997). Interrelated influence of iron, light and cell size on marine phytoplankton growth. *Nature* 390, 389–392.
- Sutak, R., Slapeta, J., San Roman, M., Camadro, J.-M., and Lesuisse, E. (2010). Nonreductive iron uptake mechanism in the marine alveolate *Chromera velia*. *Plant Physiol.* 154, 991–1000.
- Tang, K. W., Glud, R. N., Glud, A., Rysgaard, S., and Nielsen, T. G. (2011). Copepod guts as biogeochemical hotspots in the sea: evidence from microelectrode profiling of *Calanus* spp. *Limnol. Oceanogr.* 56, 666–672.
- Terzulli, A., and Kosman, D. J. (2010). Analysis of the high-affinity iron uptake system at the *Chlamydomonas reinhardtii* plasma membrane. *Eukaryotic Cell* 9, 815–826.
- Town, R. M., and Filella, M. (2000). Dispelling the myths: is the existence of L1 and L2 ligands necessary to explain metal ion speciation in natural waters? *Limnol. Oceanogr.* 45, 1341–1357.
- Trick, C. G., Bill, B. D., Cochlan, W. P., Wells, M. L., Trainer, V. L., and Pickell, L. D. (2010). Iron enrichment stimulates toxic diatom production in high-nitrate, low-chlorophyll areas. *Proc. Natl. Acad. Sci. U.S.A.* 107, 5887–5892.
- Tsuda, A., Takeda, S., Saito, H., Nishioka, J., Kudo, I., Nojiri, Y., Suzuki, K., Uematsu, M., Wells, M. L., Tsumune, D., Yoshimura, T., Aono, T., Aramaki, T., Cochlan, W. P., Hayakawa, M., Imai, K., Isada, T., Iwamoto, Y., Johnson, W. K., Kameyama, S., Kato, S., Kiyosawa, H., Kondo, Y., Lévassieur, M., Machida, R. J., Nagao, I., Nakagawa, F., Nakanishi, T., Nakatsuka, S., Narita, A., Noiri, Y., Obata, H., Ogawa, H., Oguma, K., Ono, T., Sakuragi, T., Sasakawa, M., Sato, M., Shimamoto, A., Takata, H., Trick, C. G., Watanabe, Y. W., Wong, C. S., and Yoshie, N. (2007). Evidence for the grazing hypothesis: grazing reduces phytoplankton responses of the HNLC ecosystem to iron enrichment in the western subarctic pacific (SEEDS II). *J. Oceanogr.* 63, 983–994.
- Ussher, S. J., Worsfold, P. J., Achterberg, E. P., Laes, A., Blain, S., Laan, P., and De Baar, H. J. W. (2007). Distribution and redox speciation of dissolved iron on the European continental margin. *Limnol. Oceanogr.* 52, 2530–2539.
- van den Berg, C. M. G. (1995). Evidence for organic complexation of iron in seawater. *Mar. Chem.* 50, 139–157.
- Velasquez, I., Nunn, B. L., Ibsanmi, E., Goodlett, D. R., Hunter, K. A., and Sander, S. G. (2011). Detection of hydroxamate siderophores in coastal and Sub-Antarctic waters off the South Eastern Coast of New Zealand. *Mar. Chem.* 126, 97–107.
- Vermilyea, A. W., Hansard, S. P., and Voelker, B. M. (2010). Dark production of hydrogen peroxide in the Gulf of Alaska. *Limnol. Oceanogr.* 55, 580–588.
- Villareal, T. A., Joseph, L., Brzezinski, M. A., Shipe, R. F., Lipschultz, F., and Altabet, M. A. (1999). Biological and chemical characteristics of the giant diatom *Ethmodiscus* (Bacillariophyceae) in the central North Pacific gyre. *J. Phycol.* 35, 896–902.
- Voelker, B. M., and Sedlak, D. L. (1995). Iron reduction by photoproduced superoxide in seawater. *Mar. Chem.* 50, 93–102.
- Völker, C., and Wolf-Gladrow, D. A. (1999). Physical limits on iron uptake mediated by siderophores or surface reductases. *Mar. Chem.* 65, 227–244.
- Vraspir, J. M., and Butler, A. (2009). Chemistry of marine ligands and siderophores. *Ann. Rev. Mar. Sci.* 1, 43–63.
- Waite, T. D., and Morel, F. M. M. (1984). Photoreductive dissolution of colloidal iron oxides in natural waters. *Environ. Sci. Technol.* 18, 860–868.
- Watson, A. J., Bakker, D. C. E., Ridgwell, A. J., Boyd, P. W., and Law, C. G. (2000). Effect of iron supply on southern ocean CO₂ uptake and implications for glacial atmospheric CO₂. *Nature* 407, 730–733.
- Webb, E. A., Moffett, J. W., and Waterbury, J. B. (2001). Iron stress in open-ocean cyanobacteria (*Synechococcus*, *Trichodesmium*, and *Crocospheera* spp.): identification of the IdiA protein. *Appl. Environ. Microbiol.* 67, 5444–5452.
- Weger, H. G. (1999). Ferric and cupric reductase activities in the green alga *Chlamydomonas reinhardtii*: experiments using iron-limited chemostats. *Planta* 207, 377–384.
- Wells, M. L., Mayer, L. M., Donard, O. F. X., De Souza Sierra, M. M., and Ackelson, S. G. (1991). The photolysis of colloidal iron in the oceans. *Nature* 353, 248–250.
- Wells, M. L., Price, N. M., and Bruland, K. W. (1994). Iron limitation and the cyanobacterium *Synechococcus* in equatorial Pacific waters. *Limnol. Oceanogr.* 39, 1481–1486.
- Wells, M. L., Price, N. M., and Bruland, K. W. (1995). Iron chemistry in seawater and its relationship to phytoplankton: a workshop report. *Mar. Chem.* 48, 157–182.
- Wells, M. L., Trick, C. G., Cochlan, W. P., Hughes, M. P., and Trainer, V. L. (2005). Domoic acid: the synergy of iron, copper, and the toxicity of diatoms. *Limnol. Oceanogr.* 50, 1908–1917.

- Wells, M. L., Zorkin, N. G., and Lewis, A. G. (1983). The role of colloid chemistry in providing a source of iron to phytoplankton. *J. Mar. Res.* 41, 731–746.
- Wirtz, N. L., Treble, R. G., and Weger, H. G. (2010). Siderophore-independent iron uptake by iron-limited cells of the cyanobacterium *Anabaena flos-aquae*. *J. Phycol.* 46, 947–957.
- Worms, I., Simon, D. F., Hassler, C. S., and Wilkinson, K. J. (2006). Bioavailability of trace metals to aquatic microorganisms: importance of chemical, biological and physical processes on bioavailability. *Biochimie* 88, 1721–1731.
- Wotton, R. S. (2004). The ubiquity and many roles of exopolymers (EPS) in aquatic systems. *Sci. Mar.* 68, 13–21.
- Wu, J., Wells, M. L., and Rember, R. (2011). Dissolved iron anomaly in the deep tropical-subtropical Pacific: evidence for long-range transport of hydrothermal iron. *Geochim. Cosmochim. Acta* 75, 460–468.
- Yoshida, M., Kuma, K., Iwade, S., Isoda, Y., Takata, H., and Yamada, M. (2006). Effect of aging time on the availability of freshly precipitated ferric hydroxide to coastal marine diatoms. *Mar. Biol.* 149, 379–392.
- Conflict of Interest Statement:** The authors declare that the research was conducted in the absence of any commercial or financial relationships that could be construed as a potential conflict of interest.
- Received: 30 November 2011; accepted: 14 March 2012; published online: 17 April 2012.
- Citation: Shaked Y and Lis H (2012) Disassembling iron availability to phytoplankton. *Front. Microbio.* 3:123. doi: 10.3389/fmicb.2012.00123
- This article was submitted to *Frontiers in Microbiological Chemistry*, a specialty of *Frontiers in Microbiology*.
- Copyright © 2012 Shaked and Lis. This is an open-access article distributed under the terms of the Creative Commons Attribution Non Commercial License, which permits non-commercial use, distribution, and reproduction in other forums, provided the original authors and source are credited.

APPENDIX

DATA IN SUPPORT OF THE PREVALENCE OF REDUCTIVE IRON UPTAKE AMONGST PHYTOPLANKTON (FIGURE 3)

The laboratory cultures (Table A1) and field populations (Table A2) included in Figure 3 were taken from various studies which demonstrate the presence of a reductive mechanism by one or more of the following techniques:

- Colorimetric detection of cell-mediated Fe reduction – measured as accumulation of Fe(II) over time in the presence of cells and a ferrous trapping ligand that binds Fe(II) prior to its oxidation by oxygen or transport. Commonly, cell-mediated Fe reduction is measured via colorimetric methods in the presence of Ferrozine (Fz) or Bathophenanthrolinedisulfonic acid (BPDS). This method requires relatively high micromolar iron concentrations due to its low sensitivity. Shaked et al. (2004) developed a sensitive assay for cell-mediated Fe' reduction using radiolabeled iron. This reduction assay is conducted simultaneously with Fe' uptake at physiologically relevant nanomolar iron concentrations, and it was applied for many of the data presented here.
- Genetic studies which find components of the reductive uptake system.
- EPR – Electron paramagnetic resonance showing Fe reduction.
- Inhibition of uptake by Fz/BPDS – Comparing uptake rates in the presence and absence of the membrane impermeable Fe(II) ligands, Ferrozine or BPDS. Here, Fe(II) formed by cell-mediated reduction is trapped and made unavailable for uptake by the cell, hence inhibiting iron uptake by cells employing this strategy. An explanatory illustration of this procedure is found in Figure A1 while Figure A2 provides an example of experimental data using this method.

DATA SUPPORTING THE RELATIVE BIOAVAILABILITY SCALE (FIGURE 5)

Tables A3 and A4, outline the data used for constructing Figure 5.

Uptake rates obtained from different sources were first normalized to Fe-substrate concentration (either Fe' for FeEDTA or to FeL for iron bound to ligand L, providing ligand L complexed iron strongly and/or was present in sufficient excess to rule out Fe precipitation) in order to calculate k_{up} according to Eq. 1:

$$k_{up} = \rho / [\text{Fe}]. \quad (\text{A1})$$

where ρ is Fe uptake rate [$\text{mol Fe cell}^{-1} \text{h}^{-1}$], $[\text{Fe}]$ is Fe-substrate concentration [mol L^{-1}]. The calculation applies only to *sub-saturating* uptake rates. The k_{up} obtained for the different Fe complexes – k_{up}^{FeL} were further normalized by dividing it by $k_{up}^{\text{Fe'}}$.

Note on Fe-substrates

Goe – goethite is an Fe-oxide mineral (FeOOH); DFB – desferrioxamine B is a trihydroxamate siderophore; AB – Aerobactin is hydroxamate photolabile siderophore; FC – ferrichrome is a trihydroxamate siderophore; PYN – Porphyrin; MS – Monosaccharides; PS – Polysaccharides; AZ – Azotochelin is a *bis*-catechol siderophore produced by nitrogen-fixing soil bacterium *Azotobacter vinelandii*; DPS – DNA binding protein from starved cells (iron storage proteins); CAT – Galocatechin is a polyhydroxybenzene catechol derivative found in green tea; DFE-desferrioxamine E is a trihydroxamate siderophore.

Note on the saccharides uptake data

In the saccharides uptake experiments no Fe' uptake data was reported. Since we view these as potentially important experiments we chose to normalize the saccharide uptake constant to that of FeCl_3 added at concentration of 1 nM. Given a solubility limit of 0.2–0.5 nM (Liu and Millero, 2002), it is possible that some of the Fe precipitated in the experiments. This was demonstrated in control measurements – roughly 30% of the FeCl_3 remained in the dissolved fraction, about 12% was in colloidal form and the remainder in the particulate fraction. To calculate $k_{up}^{\text{Fe'}}$ we related to the dissolved fraction as the Fe-substrate concentration.

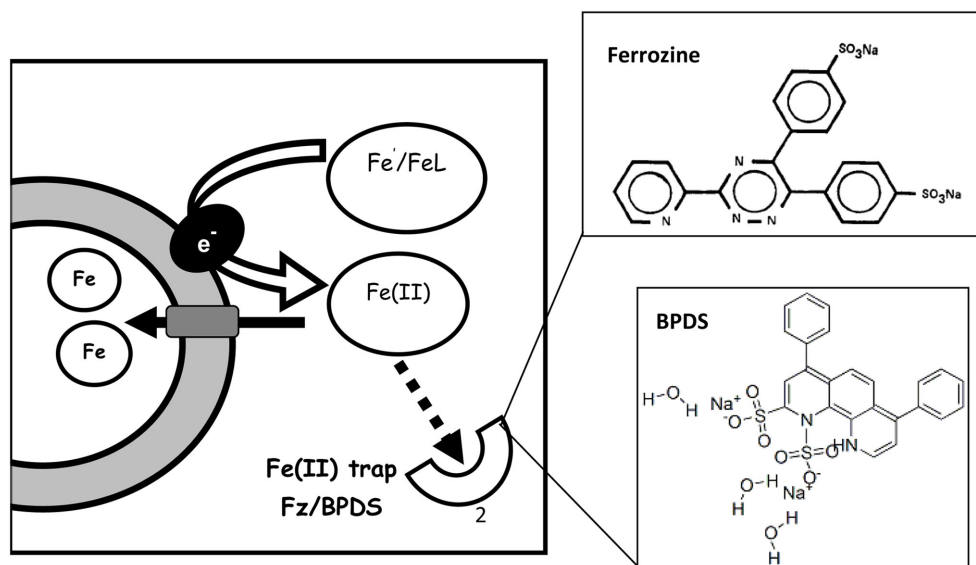


FIGURE A1 | Trapping of ferrous iron formed during Fe³⁺ reduction with ferrozine (Fz) or Bathophenanthrolinedisulfonic acid (BPDS). The Fe(II) trap competes with cells over ferrous iron formed during cell-mediated Fe reduction. The structures of two such traps – ferrozine and BPDS – are shown

on the right top and bottom respectively. Fe(II)Fz₃ and Fe(II)BPDS₃ are detected spectrophotometrically at 562 and 533 nm, respectively. Additionally Fe(II)Fz₃ and inhibition of Fe uptake by Fz/BPDS can be detected in radioactive experiments. Figure based on Lis and Shaked (2009).

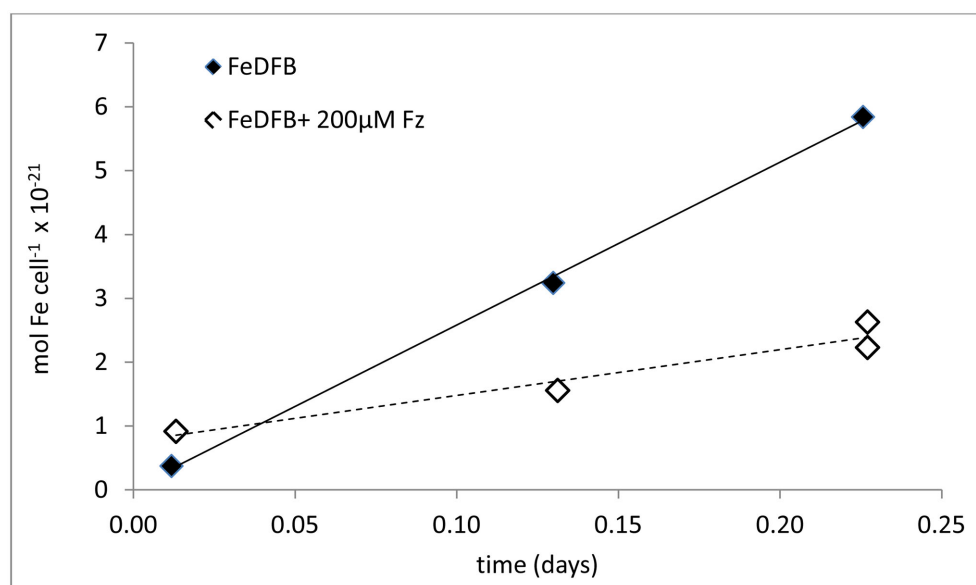


FIGURE A2 | Experimental data of iron uptake by *Synechococcus* WH8102 in the presence and absence of Ferrozine (Fz), on the basis of which the occurrence of the Fe reductive pathway is deduced. The uptake of iron

from 90 nM ⁵⁵FeDFB by iron limited *Synechococcus* WH8102 was inhibited in the presence of 200 μM Fz. The inhibitory effect stems from the trapping of Fe(II) formed through cell surface enzymatic reduction during Fe uptake.

Table A1 | Experimental evidence showing the existence of an iron reductive uptake pathway in laboratory cultures.

Organism	Type of evidence	Reference
<i>Thalassiosira pseudonana</i>	FZ/BPDS inhibits uptake, Fe reduction Genetic – Fe reductase, multi-Cu oxidase	Kustka et al. (2005), Shaked et al. (2005), Maldonado et al. (2006)
<i>Thalassiosira weissflogii</i>	FZ/BPDS inhibits uptake; Fe reduction	Jones et al. (1987), Shaked et al. (2005)
<i>Thalassiosira oceanica</i>	FZ/BPDS inhibits uptake; Fe reduction Cu induced Fe uptake inhibition multi-Cu oxidase	Maldonado and Price (2001), Maldonado et al. (2006)
<i>Cylindrotheca fusiformis</i>	FZ/BPDS inhibits uptake; Fe reduction	Lis and Shaked (in preparation)
<i>Phaeodactylum tricornutum</i>	FZ/BPDS inhibits uptake; Fe reduction	Soria-Dengg and Horstmann (1995)
<i>Peridinium gatunense</i>	FZ/BPDS inhibits uptake; Fe reduction	Shaked et al. (2002)
<i>Tetraselmis suecica</i>	FZ/BPDS inhibits uptake	Lis and Shaked (in preparation)
<i>Chlamydomonas reinhardtii</i>	Fe reduction; Genetic – Fe reductase, multi-Cu oxidase	Eckhardt and Buckhout (1998), Weger (1999), Allen et al. (2007), Chen et al. (2008)
<i>Dunaliella bardawil</i>	Fe reduction; Genetic – Fe reductase	Keshtacher et al. (1999), Paz et al. (2007)
<i>Chlorella vulgaris</i>	FZ/BPDS inhibits uptake; Fe reduction EPR	Allnutt and Bonner (1987)
<i>Chlorella kessleri</i>	Fe reduction	Middlemiss et al. (2001)
<i>Chlorococcum littorale</i>	Fe reduction	Sasaki et al. (1998)
<i>Emiliana huxleyi</i>	FZ/BPDS inhibits uptake; Fe reduction	Lis and Shaked (in preparation)
<i>Synechococcus</i> WH7803	FZ/BPDS inhibits uptake; Fe reduction	Lis and Shaked (in preparation)
<i>Synechococcus</i> WH8102	FZ/BPDS inhibits uptake; Fe reduction	Lis and Shaked (in preparation)
<i>Synechocystis</i> PCC6803	FZ/BPDS inhibits uptake; Fe reduction	Kranzler et al. (2011)
<i>Microcystis aeruginosa</i>	FZ/BPDS inhibits uptake; Fe reduction	Fujii et al. (2010)
<i>Lyngbya majuscula</i>	FZ/BPDS inhibits uptake; Fe reduction	Rose et al. (2005)
<i>Trichodesmium erythraeum</i>	FZ/BPDS inhibits uptake; Fe reduction	Shaked (unpublished)

Table A2 | Experimental evidence showing the existence of the reductive iron uptake pathway in field populations.

Field location	Type of evidence	Reference
Southern ocean	Calculation	Maldonado et al. (2005)
Subarctic Pacific (>3 μm)	Uptake	Maldonado and Price (1999)
Bering Sea (>5 μm)	Uptake	Shaked et al. (2004)
Gulf of Aqaba (>0.2 μm)	Uptake	Lis and Shaked (2009)
Loch Scridain (>20 μm)	Uptake	Lis and Shaked (in preparation)
Lake Kinneret	Uptake	Shaked et al. (2002)

Table A3 | Data used in the calculation of relative bioavailability of laboratory cultures (Figure 5A).

Organism	Fe Ligand	Avg k_{up}	Units	Rel. bioavail	Reference	Notes
THALASSIOSIRA PSEUDONANA						
Fe-limited	Fe'	4.6E-09	L ⁻¹ cell ⁻¹ h ⁻¹		Shaked et al. (2005)	Fe(diss) estimated at 0.1 nM
	Fe'	2.9E-07	L ⁻¹ μm ⁻² h ⁻¹		Chen and Wang (2008)	Based on growth rates
	Fe'	3.7E+07	L ⁻¹ mol ⁻¹ day ⁻¹		Nodwell and Price (2001)	
	DFB	6.0E-13	L ⁻¹ cell ⁻¹ h ⁻¹	1.3E-04	Shaked et al. (2005)	Fe:DFB (1:5)
	DFB	7.2E-10	L ⁻¹ μm ⁻² h ⁻¹	2.5E-03	Chen and Wang (2008)	Fe:DFB (1:1.1)
	Ferrichrome	1.2E-10	L ⁻¹ μm ⁻² h ⁻¹	4.1E-04	Chen and Wang (2008)	Fe:FC (1:200)
Fe-replete	Goethite	0		0	Nodwell and Price (2001)	Based on growth rates
	DFB	0		0	Chen and Wang (2008)	Fe:DFB (1:5)
	Ferrichrome	0		0	Chen and Wang (2008)	Fe:FC (1:200)
SYNECHOCYSTIS PCC6803						
	Fe'	12.9E-10	L ⁻¹ cell ⁻¹ h ⁻¹		Kranzler et al. (2011)	
	DFB	6.6E-14	L ⁻¹ cell ⁻¹ h ⁻¹	3.4E-04	Kranzler et al. (2011)	Fe:DFB (1:1.3)
	Aerobactin	2.3E-13	L ⁻¹ cell ⁻¹ h ⁻¹	1.2E-03	Kranzler et al. (2011)	Fe:AB (1:2.3)
PHAEOCYSTIS spp						
	Fe'	4.1E-09	L ⁻¹ cell ⁻¹ h ⁻¹		Hassler and Schoemann (2009)	~30% of FeCl ₃ in dissolved phase
	DFB	6.10E-11	L ⁻¹ cell ⁻¹ h ⁻¹	1.5E-02	Hassler and Schoemann (2009)	Fe:DFB (1:15)
	Monosaccharides	4.8E-09	L ⁻¹ cell ⁻¹ h ⁻¹	1.2	Hassler and Schoemann (2009)	Fe:MS (1:15)
	Polysaccharides	6.2E-09	L ⁻¹ cell ⁻¹ h ⁻¹	1.53	Hassler and Schoemann (2009)	Fe:PS (1:15)
SYNECHOCOCCUS spp						
	Fe'	4.2E-08	L ⁻¹ μm ⁻² h ⁻¹		Chen and Wang (2008)	Fe(diss) estimated at 0.1 nM
	Fe'	2.2E-11	L ⁻¹ cell ⁻¹ h ⁻¹		Lis and Shaked (in preparation)	
	DFB	2.8E-11	L ⁻¹ μm ⁻² h ⁻¹	6.7E-04	Chen and Wang (2008)	Fe:DFB (1:5)
	DFB	1.2E-14	L ⁻¹ cell ⁻¹ h ⁻¹	5.4E-04	Lis and Shaked (in preparation)	Fe:DFB (1:2)
	Ferrichrome	2.0E-11	L ⁻¹ μm ⁻² h ⁻¹	4.8E-04	Chen and Wang (2008)	Fe:FC (1:200)
THALASSIOSIRA WEISSFLOGII						
	Fe'	6.00E-08	L ⁻¹ cell ⁻¹ h ⁻¹		Shaked et al. (2005)	Fe' from Shaked et al. (2005) used for all T:w ratio calculations
	DFB	2.90E-11	L ⁻¹ cell ⁻¹ h ⁻¹	4.8E-04	Shaked et al. (2005)	Fe:DFB (1:1.1)
	DFB	2.56E-11	L ⁻¹ cell ⁻¹ h ⁻¹	4.3E-04	Shi et al. (2010)	Fe:DFB (1:2)
	Ferrichrome	1.6E-10	L ⁻¹ cell ⁻¹ h ⁻¹	2.7E-03	Shaked et al. (2005)	
	Deuteroporphyrin	1.9E-10	L ⁻¹ cell ⁻¹ h ⁻¹	3.2E-03	Kustka et al. (2005)	
	Grazed Fe	3.4E-11	L ⁻¹ cell ⁻¹ h ⁻¹	5.6E-04	Shi et al. (2010)	
	Fe-Azotochelin	1.6E-10	L ⁻¹ cell ⁻¹ h ⁻¹	2.7E-03	Shi et al. (2010)	
	Fresh ferrihydrite	3.3E-10	L ⁻¹ cell ⁻¹ h ⁻¹	5.6E-03	Shi et al. (2010)	
	Fe-dPS	4.5E-11	L ⁻¹ cell ⁻¹ h ⁻¹	7.5E-04	Shi et al. (2010)	
THALASSIOSIRA OCEANICA						
	Fe'	2.56E-08	L ⁻¹ cell ⁻¹ h ⁻¹		Maldonado and Price (1996)	
	DFB	4.0E-12	L ⁻¹ cell ⁻¹ h ⁻¹	1.6E-04	Maldonado and Price (2001)	Fe:DFB (1:10)
CHRYSOCHROMULINA ERICINA						
	Fe'	2.0E+07	L ⁻¹ mol ⁻¹ day ⁻¹		Nodwell and Price (2001)	Based on growth rates
	DFB	0	L ⁻¹ mol ⁻¹ day ⁻¹	0	Nodwell and Price (2001)	Based on growth rates
	Goethite	5.0E+05	L ⁻¹ mol ⁻¹ day ⁻¹	2.53E-02	Nodwell and Price (2001)	Based on growth rates

(Continued)

Table A3 | Continued

Organism	Fe Ligand	Avg k_{up}	Units	Rel. bioavail	Reference	Notes
CHAETOCEROS spp						
	Fe'	2.0E-09	L ⁻¹ cell ⁻¹ h ⁻¹		Hassler and Schoemann (2009)	~30% of FeCl ₃ in dissolved phase
	DFB	6.1E-11	L ⁻¹ cell ⁻¹ h ⁻¹	3.1E-02	Hassler and Schoemann (2009)	Fe:DFB (1:15)
	Monosaccharides	2.6E-09	L ⁻¹ cell ⁻¹ h ⁻¹	1.3E+00	Hassler and Schoemann (2009)	Fe:MS (1:15)
	Polysaccharides	3.5E-09	L ⁻¹ cell ⁻¹ h ⁻¹	1.8E+00	Hassler and Schoemann (2009)	Fe:PS (1:15)
THALASSIOSIRA ANTARCTICA						
	Fe'	3.67E-08	L ⁻¹ cell ⁻¹ h ⁻¹		Hassler and Schoemann (2009)	~30% of FeCl ₃ in dissolved phase
	DFB	6.1E-11	L ⁻¹ cell ⁻¹ h ⁻¹	1.7E-03	Hassler and Schoemann (2009)	Fe:DFB (1:15)
	Monosaccharides	2.9E-08	L ⁻¹ cell ⁻¹ h ⁻¹	7.9E-01	Hassler and Schoemann (2009)	Fe:MS (1:15)
	Polysaccharides	3.5E-08	L ⁻¹ cell ⁻¹ h ⁻¹	9.6E-01	Hassler and Schoemann (2009)	Fe:PS (1:15)

Table A4 | Data used in the calculation of relative bioavailability of natural assemblages (Figure 5B).

Field study location	Fe ligand	Avg k_{up}	Units	Rel. bioavail.	Reference	Notes
SUBARCTIC PACIFIC (>0.2 μm)						
Coastal (station P4)	Fe'	9.2E−01	L ^{−1} mol ^{−1} C h ^{−1}		Maldonado and Price (1999)	Data taken from 1996 study performed along line P which runs from coast (P4, high Fe) to offshore (P26, lower Fe) waters
	DFB	7.3E−03		8.0E−03		
	DFE	7.7E−03		8.3E−03		
Offshore (station P26)	Fe'	5.8E−02				FeL at ratio of 1:5 for DFB and DFE
	DFB	3.2E−03		5.4E−02		
	DFE	3.1E−03		5.2E−02		
SOUTHERN OCEAN >0.8 μm						
South of polar front	Fe'	2.5E−13	L ^{−1} h ^{−1}		Hassler et al. (2011)	Fe' assumed to be 1 nM Uptake rates from lowest concentration of ligand additions
	DFB	5.0E−14		2.0E−01		
	Monsaccharides	3.8E−13		1.5E+00		
SOUTHERN OCEAN >0.2 μm						
	Fe'	2.6E+02	L ^{−1} mol ^{−1} C h ^{−1}		Maldonado et al. (2005)	Uptake rates from dark experiments
	FeDFB	7.9E+00		3.0E−02		
	Gallocatechin	4.8E+02		1.8E+00		
	<i>in situ</i> ligands	1.1E+02		4.2E−01		FeL is 1:10 for organic ligands, DFB, and Gallocatechin
EQUATORIAL PACIFIC >0.2 μm						
Upwelling region	FeDFB	0		0	Wells et al. (1994)	Fe:DFB (1:5); population dominated by <i>Synechococcus</i> spp.
LOCH SCRIDIAN <20 μm						
	Fe'	7.9E−02	L ^{−1} mol ^{−1}	7.0E−05	Lis and Shaked (in preparation)	Fe:DFB (1:2); population dominated by <i>Pseudo-nitzschia</i> spp. diatoms
	DFB	5.6E−06				
GULF OF AQABA >0.2 μm						
	Fe'	1.6E−01			Lis and Shaked (in preparation)	Fe:DFB (1:2); population dominated by <i>Synechococcus</i> spp.
	FeDFB	2.5E−04		1.6E−03		

REFERENCES

- Allen, M. D., Del Campo, J. A., Kropat, J., and Merchant, S. S. (2007). FEA1, FEA2, and FRE1, encoding two homologous secreted proteins and a candidate ferrireductase, are expressed coordinately with FOX1 and FTR1 in iron-deficient *Chlamydomonas reinhardtii*. *Eukaryotic Cell* 6, 1841–1852.
- Allnutt, F. C. T., and Bonner, W. D. J. (1987). Evaluation of reductive release as a mechanism for iron uptake from ferrioxamine B by *Chlorella vulgaris*. *Plant Physiol.* 85, 751–756.
- Chen, J.-C., Hsieh, S. I., Kropat, J., and Merchant, S. S. (2008). A ferroxidase encoded by FOX1 contributes to iron assimilation under conditions of poor iron nutrition in *Chlamydomonas*. *Eukaryotic Cell* 7, 541–545.
- Chen, M., and Wang, W. (2008). Accelerated uptake by phytoplankton of iron bound to humic acids. *Aquat. Biol.* 3, 155–166.
- Eckhardt, U., and Buckhout, T. J. (1998). Iron assimilation in *Chlamydomonas reinhardtii* involves ferric reduction and is similar to strategy I higher plants. *J. Exp. Bot.* 49, 1219–1226.
- Fujii, M., Rose, A. L., Omura, T., and Waite, T. D. (2010). Effect of Fe(II) and Fe(III) transformation kinetics on iron acquisition by a toxic strain of *Microcystis aeruginosa*. *Environ. Sci. Technol.* 44, 1980–1986.
- Hassler, C. S., and Schoemann, V. (2009). Bioavailability of organically bound Fe to model phytoplankton of the Southern Ocean. *Biogeosciences* 6, 2281–2296.
- Hassler, C. S., Schoemann, V., Nichols, C. M., Butler, E. C. V., and Boyd, P. W. (2011). Saccharides enhance iron bioavailability to Southern Ocean phytoplankton. *Proc. Natl. Acad. Sci. U.S.A.* 108, 1076–1081.
- Jones, G. J., Palenik, B. P., and Morel, F. M. (1987). Trace metal reduction by phytoplankton: the role of plasmalemma redox enzymes. *J. Phycol.* 23, 237–244.
- Keshtacher, L. E., Hadar, Y., and Chen, Y. (1999). Fe nutrition demand and utilization by the green alga *Dunaliella bardawil*. *Plant Soil* 215, 175–182.
- Kranzler, C., Lis, H., Shaked, Y., and Keren, N. (2011). The role of reduction in iron uptake processes in a unicellular, planktonic cyanobacterium. *Environ. Microbiol.* 13, 2990–2999.
- Kustka, A. B., Shaked, Y., Milligan, A. J., King, D. W., and Morel, F. M. M. (2005). Extracellular production of superoxide by marine diatoms: contrasting effects on iron redox chemistry and bioavailability. *Limnol. Oceanogr.* 50, 1172–1180.
- Lis, H., and Shaked, Y. (2009). Probing the bioavailability of organically bound iron: a case study in the *Synechococcus*-rich waters of the Gulf of Aqaba. *Aquat. Microb. Ecol.* 56, 241–253.
- Liu, X. W., and Millero, F. J. (2002). The solubility of iron in seawater. *Mar. Chem.* 77, 43–54.
- Maldonado, M. T., Allen, A. E., Chong, J. S., Dan Leus, K. L., Karpenko, N., and Harris, S. L. (2006). Copper-dependent iron transport in coastal and oceanic diatoms. *Limnol. Oceanogr.* 51, 1729–1743.
- Maldonado, M. T., and Price, N. M. (1996). Influence of N substrate on Fe requirements of marine centric diatoms. *Mar. Ecol. Prog. Ser.* 141, 161–172.
- Maldonado, M. T., and Price, N. M. (1999). Utilization of iron bound to strong organic ligands by plankton communities in the subarctic Pacific Ocean. *Deep Sea Res. Part II Top. Stud. Oceanogr.* 46, 2447–2473.
- Maldonado, M. T., and Price, N. M. (2001). Reduction and transport of organically bound iron by *Thalassiosira oceanica* (Bacillariophyceae). *J. Phycol.* 37, 298–309.
- Maldonado, M. T., Strzepek, R. F., Sander, S., and Boyd, P. W. (2005). Acquisition of iron bound to strong organic complexes, with different Fe binding groups and photochemical reactivities, by plankton communities in Fe-limited subantarctic waters. *Global Biogeochem. Cycles* 19, GB4S23.
- Middlemiss, J. K., Anderson, A. M., Stratilo, C. W., and Weger, H. G. (2001). Oxygen consumption associated with ferric reductase activity and iron uptake by iron-limited cells of *Chlorella kessleri* (Chlorophyceae). *J. Phycol.* 37, 393–399.
- Nodwell, L., and Price, N. (2001). Direct use of inorganic colloidal iron by marine mixotrophic phytoplankton. *Limnol. Oceanogr.* 46, 755–777.
- Paz, Y., Katz, A., and Pick, U. (2007). Multicopper ferroxidase involved in iron binding to transferins in *Dunaliella salina* plasma membranes. *J. Biol. Chem.* 282, 8658–8666.
- Rose, A. L., Salmon, T. P., Lukondeh, T., Neilan, B. A., and Waite, T. D. (2005). Use of superoxide as an electron shuttle for iron acquisition by the marine cyanobacterium *Lyngbya majuscula*. *Environ. Sci. Technol.* 39, 3708–3715.
- Sasaki, T., Kurano, N., and Miyachi, S. (1998). Induction of ferric reductase activity and of iron uptake activity in *Chloccum littorale* cells under extremely high-CO₂ and iron-deficient conditions. *Plant Cell Physiol.* 39, 405–410.
- Shaked, Y., Erel, Y., and Sukenik, A. (2002). Phytoplankton-mediated redox cycle of iron in the epilimnion of Lake Kinneret. *Environ. Sci. Technol.* 36, 460–467.
- Shaked, Y., Kustka, A. B., and Morel, F. M. M. (2005). A general kinetic model for iron acquisition by eukaryotic phytoplankton. *Limnol. Oceanogr.* 50, 872–882.
- Shaked, Y., Kustka, A. B., Morel, F. M. M., and Erel, Y. (2004). Simultaneous determination of iron reduction and uptake by phytoplankton. *Limnol. Oceanogr. Methods* 2, 137–145.
- Shi, D., Xu, Y., Hopkinson, B. M., and Morel, F. M. M. (2010). Effect of ocean acidification on iron availability to marine phytoplankton. *Science* 327, 676–679.
- Soria-Dengg, S., and Horstmann, U. (1995). Ferrioxamines B and E as iron sources for the marine diatom *Phaeodactylum tricornutum*. *Mar. Ecol. Prog. Ser.* 127, 269–277.
- Weger, H. G. (1999). Ferric and cupric reductase activities in the green alga *Chlamydomonas reinhardtii*: experiments using iron-limited chemostats. *Planta* 207, 377–384.
- Wells, M. L., Price, N. M., and Bruland, K. W. (1994). Iron limitation and the cyanobacterium *Synechococcus* in equatorial Pacific waters. *Limnol. Oceanogr.* 39, 1481–1486.



Exploring the link between micronutrients and phytoplankton in the Southern Ocean during the 2007 austral summer

Christel S. Hassler^{1,2*}, Marie Sinoir^{2,3}, Lesley A. Clementson² and Edward C. V. Butler^{2,4†}

¹ Plant Functional Biology and Climate Change Cluster, University of Technology Sydney, Broadway, NSW, Australia

² Marine and Atmospheric Research, Commonwealth Scientific and Industrial Research Organisation, Hobart, TAS, Australia

³ University of Tasmania, Sandy Bay, TAS, Australia

⁴ Ultramarine Concepts, Sandy Bay, TAS, Australia

Edited by:

Veronique Schoemann, Royal Netherlands Institute for Sea Research, Netherlands

Reviewed by:

Peter Croot, National University of Ireland – Galway, Ireland
Sylvia McDevitt, Skidmore College, USA

*Correspondence:

Christel S. Hassler, Plant Functional Biology and Climate Change Cluster, University of Technology Sydney, PO Box 123, Broadway 2007, NSW, Australia.

e-mail: christel.hassler@uts.edu.au

†Present address:

Edward C. V. Butler, Australian Institute of Marine Science, Arafura Timor Research Facility, Darwin, NT, Australia.

Bottle assays and large-scale fertilization experiments have demonstrated that, in the Southern Ocean, iron often controls the biomass and the biodiversity of primary producers. To grow, phytoplankton need numerous other trace metals (micronutrients) required for the activity of key enzymes and other intracellular functions. However, little is known of the potential these other trace elements have to limit the growth of phytoplankton in the Southern Ocean. This study, investigates whether micronutrients other than iron (Zn, Co, Cu, Cd, Ni) need to be considered as parameters for controlling the phytoplankton growth from the Australian Subantarctic to the Polar Frontal Zones during the austral summer 2007. Analysis of nutrient disappearance ratios, suggested differential zones in phytoplankton growth control in the study region with a most intense phytoplankton growth limitation between 49 and 50°S. Comparison of micronutrient disappearance ratios, metal distribution, and biomarker pigments used to identify dominating phytoplankton groups, demonstrated that a complex interaction between Fe, Zn, and Co might exist in the study region. Although iron remains the pivotal micronutrient for phytoplankton growth and community structure, Zn and Co are also important for the nutrition and the growth of most of the dominating phytoplankton groups in the Subantarctic Zone region. Understanding of the parameters controlling phytoplankton is paramount, as it affects the functioning of the Southern Ocean, its marine resources and ultimately the global carbon cycle.

Keywords: subantarctic zone, pigments, Zn, Co, SAZ-Sense, trace element, subantarctic, polar

INTRODUCTION

The circumpolar Subantarctic Zone (SAZ) is an important biome of the global ocean which separates the High Nutrient Low Chlorophyll (HNLC) Southern Ocean from the mostly Low Nutrient Low Chlorophyll (LNLC) subtropical water from the Indian, Pacific, and Atlantic Oceans (Bowie et al., 2011a). The SAZ region forms a “belt” of important carbon sequestration accompanied by a phytoplankton biomass characterized by a low seasonality (Banse, 1996; Metzl et al., 1999; McNeil et al., 2001). However it is still unclear what parameters mostly constrain phytoplankton growth and how the dynamics of the SAZ region will be affected in the future.

The recent SAZ-Sense project took advantage of the natural variability in the SAZ region around Tasmania to study the impact of predicted future changes that will affect its functioning. This project focused on parameters likely to control phytoplankton biomass and carbon fixation, such as macro- (N, P, and Si) and micronutrients (essential trace metals), grazing and cell lysis promoted by the microbial loop, and as well, carbon export. Project outputs would help resolve the extent of future SAZ contribution to atmospheric CO₂ fixation and climate regulation. The SAZ region west of Tasmania (W-SAZ) is characteristic of most of the SAZ region nowadays (Trull et al., 2001), whereas the region east of Tasmania (E-SAZ), with greater intrusion of macronutrient-poor,

northern subtropical waters, and enhanced micronutrient inputs (e.g., iron, Hill et al., 2008; Bowie et al., 2009) mimics future predicted changes in the SAZ region. The two contrasting regions were compared to the waters south of Tasmania in the Polar Frontal Zone (PFZ) as an example of typical HNLC waters that could fuel the SAZ more significantly in the future (Herraiz Borreguero and Rintoul, 2011). The scientific rationale behind this study is summarized in Bowie et al. (2011a) and most of the results have been published in a special issue in Deep-Sea Research II (Table A1 in Appendix).

The difference in phytoplankton communities observed in the E-SAZ and the W-SAZ cannot be solely explained by considering macronutrients, light, grazing rates, and temperature (Kidston et al., 2011; Mongin et al., 2011; Pearce et al., 2011). It is believed that iron and silicic acid are mostly limiting the growth of phytoplankton, and thus, their ability to fix carbon (Bowie et al., 2009, 2011a; Lannuzel et al., 2011). Results from the SAZ-Sense project, demonstrate that silicic acid was limiting diatoms (de Salas et al., 2011; Fripiat et al., 2011) and iron was potentially limiting the growth of entire phytoplankton communities both in the W-SAZ and the PFZ (Lannuzel et al., 2011). Maximum photosynthetic quantum yield and results from iron phytoplankton uptake rates suggest that the W-SAZ was the main iron-limited region at the

time (Schoemann et al., unpublished). In the E-SAZ, iron was not limiting (Lannuzel et al., 2011) and diatoms were practically absent. Analysis of the phytoplankton communities revealed marked differences among the W-SAZ, PFZ, and E-SAZ, with the E-SAZ being dominated by nanoplankton (2–20 μm) and dinoflagellates (de Salas et al., 2011; Pearce et al., 2011). In the E-SAZ, despite possible light limitation (euphotic depth of 47 m and shallow mixed layer depth (MLD) of 16 m, but main mixed layer down to 79 m; Mongin et al., 2011; Westwood et al., 2011; **Table A1** in Appendix), the parameters controlling phytoplankton growth remain largely unresolved. Interestingly, phytoplankton carbon fixation and export were comparable or greater in the W-SAZ and the E-SAZ, despite a 1.4-fold average greater integrated chlorophyll *a* in the E-SAZ (Ebersbach et al., 2011; Jacquet et al., 2011; Westwood et al., 2011; **Table A1** in Appendix), demonstrating that iron limitation and carbon fixation and export were not directly related during SAZ-Sense. If the E-SAZ represents the future of the SAZ region, then iron limitation is likely to be decreased and other micronutrients could play a role in capping phytoplankton growth, particularly if they are supplied by pathways differing from iron. It, thus, becomes urgent to explore the potential of other micronutrients to co-limit the growth of phytoplankton.

This study investigates the role of other micronutrients Zn, Co, Cu, which share several properties with iron in limiting the growth of phytoplankton, or at the least, in mediating community structure (Morel et al., 1994; Sunda and Huntsman, 1995a,b;

Buitenhuis et al., 2003; Saito and Goepfert, 2008; Saito et al., 2008). These micronutrients are co-factors of enzymes that catalyze essential reactions for the growth of phytoplankton, and key structural compounds (Morel and Price, 2003; Morel et al., 2003). Their possible limitation in marine systems are suggested by several laboratory studies (e.g., Morel et al., 1994; Saito et al., 2010) and phytoplankton have evolved high affinity uptake transport systems to survive under limited supply (Sunda and Huntsman, 1995b; Saito et al., 2002). These micronutrients are present at low concentrations in the open ocean (Lohan et al., 2002; Ellwood et al., 2005; Ellwood, 2008; Saito et al., 2010; Croot et al., 2011; Butler et al., in revision), they readily associate with organic compounds, and thus, are mostly complexed by organic ligands (Moffett and Brand, 1996; Saito and Moffett, 2001; Ellwood, 2004, 2008; Ellwood et al., 2005; Lohan et al., 2005), which decrease their bioavailability to sustain phytoplankton growth. This study also includes other potentially interesting micronutrients recently reported as essential in marine phytoplankton (Cd, Ni, e.g., Sunda and Huntsman, 2000; Lane et al., 2005; Dupont et al., 2008, 2010).

Because different phytoplankton species and functional groups have different biological requirements for growth (Buitenhuis et al., 2003; Sarthou et al., 2005; Sedwick et al., 2007; Saito and Goepfert, 2008) leading to differences in intracellular nutrient quota and drawdown (de Baar et al., 1997; Arrigo et al., 1999; Ho et al., 2003; Quigg et al., 2003, 2011; Twining et al., 2004a,b; Finkel et al., 2007, 2010), we investigate the relation between the

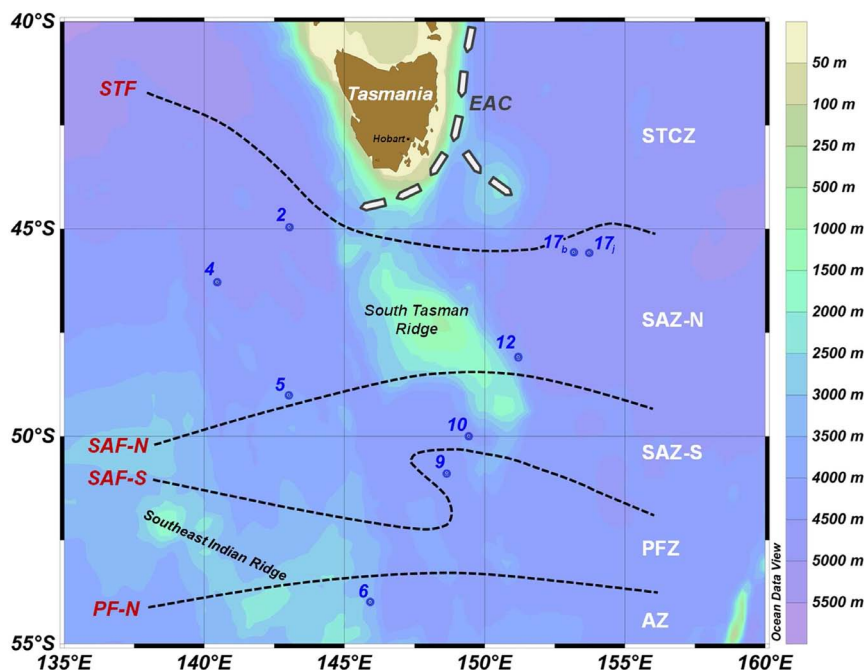


FIGURE 1 | Location of stations (number) as part of the SAZ – Sense voyage (January–February 2007) superimposed on bathymetry. The notations to the left of the dashed lines indicate the approximate location of fronts (following Sokolov and Rintoul, 2002) at the time of this voyage. The notations to the right define the zones between the fronts. The dashed arrows, tagged with EAC, indicate the East Australian Current extension characterized by mesoscale eddy features; the path around the south of

Tasmania is the Tasman Outflow (Ridgway, 2007). Fronts (red text on left): STF, Subtropical Front; SAF-N, Subantarctic Front–North; SAF-S, Subantarctic Front–South; PF-N, Polar Front–North. Zones between fronts (white text on right): STCZ, Subtropical Convergence Zone; SAZ-N, Subantarctic Zone–North; SAZ-S, Subantarctic Zone–South; PFZ, Polar Frontal Zone; AZ, Antarctic Zone. Station 17 was sampled twice (on cast b and j on the 11 February 2007 and 17 February 2007, respectively).

distributions of dissolved nutrients and phytoplankton biomarker pigments, which can be used to infer phytoplankton community composition by using CHEMTAX at 5 locations during the SAZ-Sense expedition (e.g., de Salas et al., 2011). In addition, biological requirement for micronutrients is related to the size-aspect ratio (Sarhou et al., 2005; Hassler and Schoemann, 2009; Finkel et al., 2010). Size fractionation of pigments also pointed to different dominating phytoplankton groups in the SAZ and the Tasman Sea (de Salas et al., 2011; Hassler et al., 2011; Pearce et al., 2011). For these reasons, the link between micronutrients with large and small phytoplankton biomarker pigments is studied to gain further insight into their potential control on phytoplankton biomass, biodiversity, and contribution to carbon export. As done in previous studies, the disappearance ratio of nutrients is discussed to gain an understanding of the underlying processes at play (e.g., de Baar et al., 1997; Arrigo et al., 1999; Saito et al., 2010; Croot et al., 2011).

MATERIALS AND METHODS

STUDY REGION

The SAZ-Sense voyage (*RV Aurora Australis*, 17 January–20 February 2007) visited contrasting water masses in the SAZ region around Tasmania (E-SAZ and W-SAZ) as well as further south in the PFZ, and crossed several fronts as summarized in **Figure 1**. The oceanography of the region is highly variable as a result of spatially heterogeneous inputs from subtropical waters from the north, and Subantarctic Mode Water and Antarctic Intermediate Water from the South (Bowie et al., 2011a; Herraiz Borreguero and Rintoul, 2011); nutrients from dust deposition and the continental margin (e.g., Bowie et al., 2009) provide a further overlay. The whole system creates naturally contrasting regions relevant to the study of controls on phytoplankton dynamics and their associated carbon fixation, recycling, and export. Oceanography of the region is summarized and put in a larger context elsewhere (Bowie et al., 2011b; Herraiz Borreguero and Rintoul, 2011). Critical properties of selected stations are summarized in **Table A1** in Appendix.

The SAZ-Sense project took advantage of the natural variability in the SAZ region around Tasmania to study the impact of predicted changes in major currents (e.g., Antarctic Circumpolar Current (ACC), East Australian Current (EAC, Hill et al., 2008; Toggweiler and Russell, 2008) that modulate important parameters for phytoplankton growth, such as the depth of the mixed layer, and micro- and macronutrient input (Bowie et al., 2009). The SAZ region west of Tasmania (W-SAZ) has low phytoplankton biomass characteristic of much of the SAZ region as it is nowadays (Trull et al., 2001), whereas the region East of Tasmania (E-SAZ) is characterized by high biomass persisting from the spring to summer, likely due to micronutrient (iron) input from eddy fields, arising from EAC activity and from Australian dust (Bowie et al., 2009, 2011a; Lannuzel et al., 2011; Mongin et al., 2011). In the future, the EAC is expected to strengthen (Hill et al., 2008) possibly bringing more eddies into the E-SAZ and Australian continent will become drier, with more terrigenous input from dust storms and bush-fires expected to deposit in the South Tasman Sea (Matear et al., submitted).

Table 1 | FI-SPE-ICP-MS conditions for determination of trace metals in seawater (O'Sullivan et al., in preparation).

Typical ICP-MS Conditions	
Nebuliser gas flow (mL/min)	1.02
Auxiliary gas flow (mL/min)	1.2
Plasma gas flow (mL/min)	15
ICP RF power (W)	1400
Skimmer/sample cones	Platinum
Sweep/readings	1
Readings/replicates	60
Number of replicates	1
Process signal profile	Sum
Dwell time (ms)	40
No of isotopes analyzed	21
Integration time (ms)	2400

Table 2 | Figures of Merit for FI-SPE-ICP-MS analyses.

	Detection limit ^a and precision ^b	SAFe S	SAFe D2	NASS 5
⁵⁹ Co	0.003 8%	0.006 ± 0.002 (0.005 ± 0.002)	0.032 ± 0.003 (0.045 ± 0.004)	0.188 ± 0.012 (0.187 ± 0.05)
⁶⁰ Ni	0.03 6%	2.47 ± 0.19 (2.31 ± 0.10)	8.84 ± 0.51 (8.58 ± 0.30)	4.52 ± 0.31 (4.31 ± 0.48)
⁶⁵ Cu	0.05 5%	0.56 ± 0.07 (0.51 ± 0.05)	2.26 ± 0.11 (2.25 ± 0.11)	4.82 ± 0.25 (4.67 ± 0.72)
⁶⁶ Zn	0.22 7%	<0.22 (0.064 ± 0.019)	7.09 ± 0.49 (7.20 ± 0.50)	1.42 ± 0.08 (1.56 ± 0.60)
¹¹¹ Cd	0.005 3%	<0.005 (0.001 ± 0.0002)	0.84 ± 0.02 (0.986 ± 0.027)	0.178 ± 0.015 (0.205 ± 0.030)

Average metal concentration (±1 standard deviation) are given for SAFe S 430 and 125 (n = 10), SAFe D2 414 (n = 8), and NASS 5 (n = 8) reference samples. Consensus and certified values for these samples are given in bracket (<http://www.es.ucsc.edu/~kbruland/GeotracesSaFe/kwbGeotracesSaFe.html>, Consensus values from November 2011). Concentrations are given in nmol/kg. Note that here no UV-irradiation is done prior to analysis.

^aDetection limit calculated on 3 × standard deviation of 0.1% HCl blank (n = 8).

^bCoefficient of variation of SAFe seawater D2 (n = 8).

WATER SAMPLING

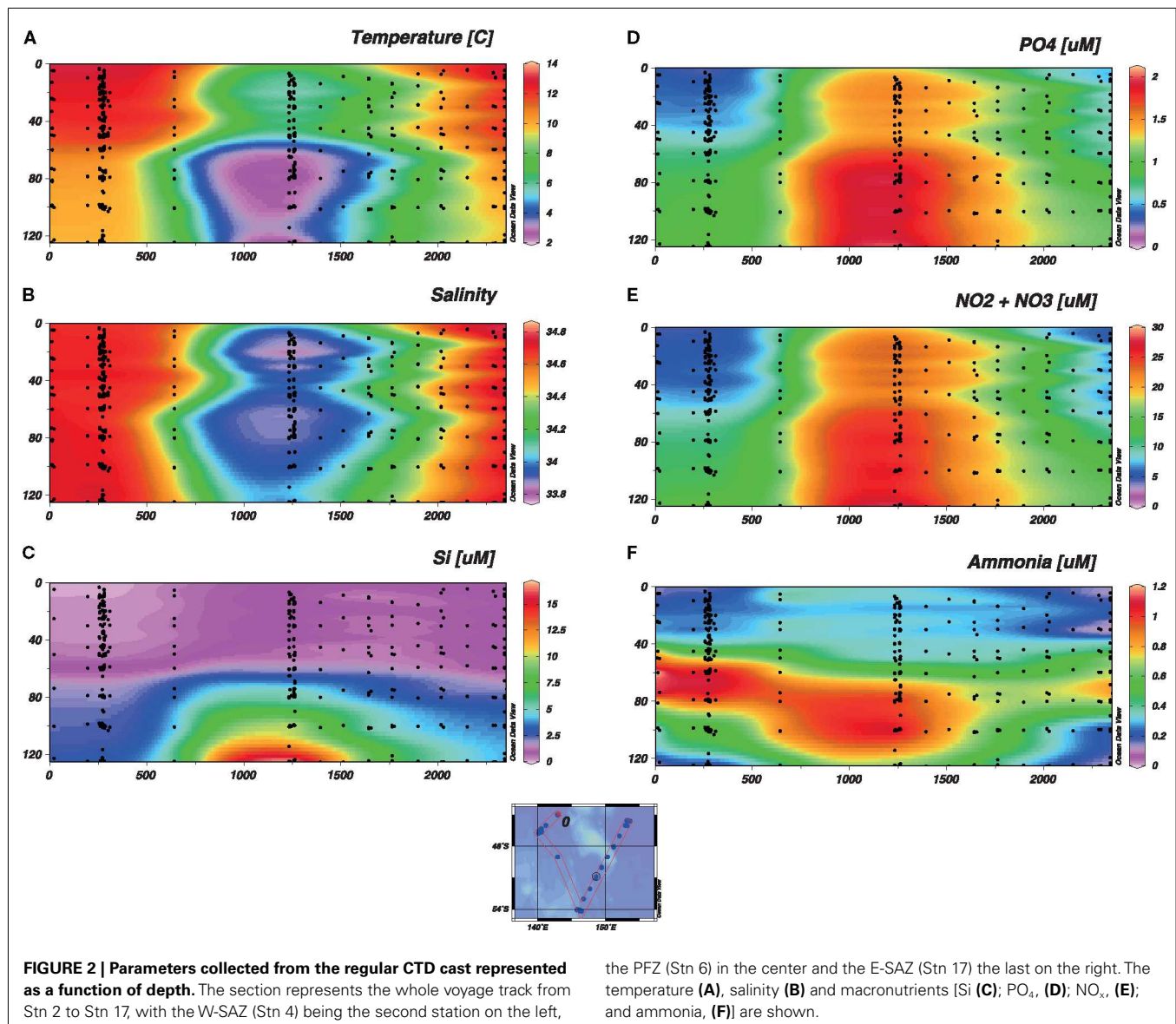
Samples for trace metal analyses and some pigment analyses (Stns 2, 6, 17, **Figure 1**) were taken using Teflon-coated Niskin X-1010 bottles (General Oceanics, USA) mounted on an autonomous rosette (Model 1018, General Oceanics, USA) and deployed using a Kevlar hydroline (Strongrope, AU). Water samples for micronutrient analysis were collected and filtered (Pall, Acropack 200) in a clean van under a HEPA filter (ISO Class 5 conditions). Sample acquisition and handling was as per GEOTRACES recommendations¹, using acid-washed non-contaminating material as detailed elsewhere (Bowie et al., 2009; Lannuzel et al., 2011). Samples were acidified using quartz-distilled HCl (1 mL L⁻¹, Seastar Baseline, Canada) and kept for 6 months doubly bagged in plastic boxes in clean storage, prior to analysis.

¹www.geotraces.org/libraries/documents/Intercalibration/Cookbook.pdf

Salinity, temperature, fluorescence, and oxygen were obtained from calibrated conductivity-temperature-depth (CTD, SeaBird SBE9plus) data using water collected from Niskin bottles (General Oceanics) per Rosenberg (2007). Macronutrients (reactive phosphorus, PO₄; silicic acid, Si; nitrate-plus-nitrite, NO_x; ammonium, NH₄) were obtained by the analysis of unfiltered water using automated flow-injection analyzer and colorimetric techniques (Watson et al., 2005; Rosenberg, 2007). Samples were also collected for pigment determination (Stns 4, 9, 12). CTD deployments were performed close (within 0.1° latitude and longitude and 3.2 h) to the autonomous rosette to ensure that profiles of trace elements and other parameters describe the same water column (Bowie et al., 2011a).

MICRONUTRIENTS

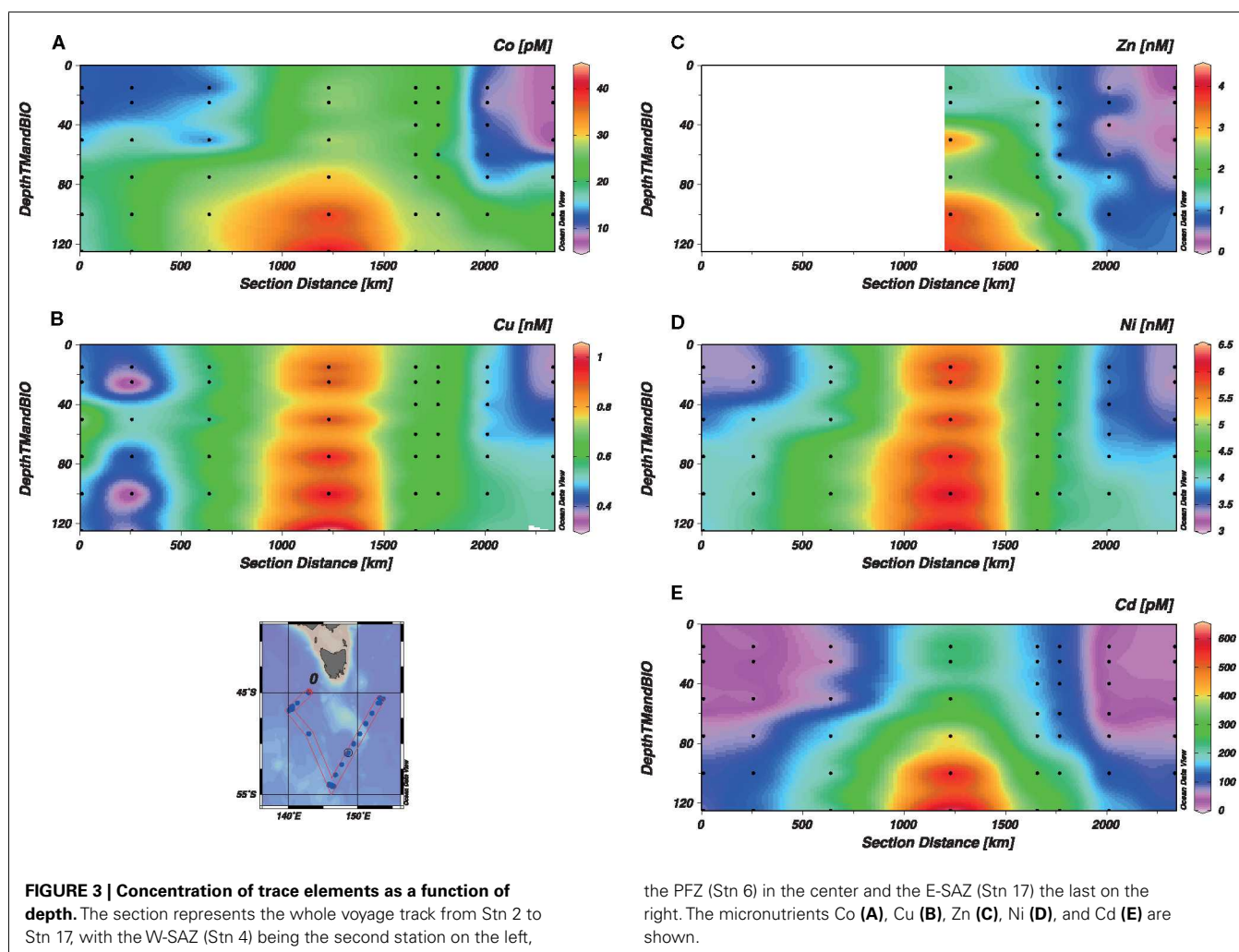
Micronutrients were determined in an ISO class 5 Clean laboratory using automated flow-injection, solid phase extraction coupled to



inductively coupled plasma-mass spectrometry (FI-SPE-ICP-MS; method and performance described in Butler et al., in revision, and full details in O'Sullivan et al. in preparation; **Table 1**). Briefly, 7.0-mL subsamples are decanted into acid-cleaned, 10-mL screw-cap polypropylene tubes, which are set in the tray of a CETAC ASX-520 auto sampler. Initiation of the ICP-MS control program sees the preconcentration/matrix-elimination step proceed on a PerkinElmer FIAS 400 system, with the sample stream merged with cleaned 1 M ammonium acetate buffer. The buffered sample ($\text{pH } 5.7 \pm 0.2$) is then passed through the iminodiacetate (IDA) chelating sorbent (Toyopearl AF chelate-650M resin, 40–90 μm , Tosoh Bioscience GmbH, Germany) packed in 1-cm Global FIA (USA) cartridge mounted in the switching valve position. After loading, the solid phase is rinsed with buffered Milli-Q (Millipore, USA) deionized water to flush. With the switching valve moved to "Inject," the eluent [0.8 M HNO_3 (Seastar, Canada) + internal standard 10 ppb Rh] carries the adsorbed trace metals directly into the nebuliser (concentric quartz Meinhard-type with cyclonic spray chamber) and then into the quadrupole ICP-MS (PerkinElmer Elan DRC II, USA). The instrumental conditions for ICP-MS operation are summarized in **Table 1**. With each analysis of two casts (24 samples), calibration standards (standard additions to

seawater sample for matrix matching), blanks and reference seawaters (NASS 5, SAFe S, and D2) were run. The instrument was controlled, and data collected and put through primary processing, using Elan v3.4 software, with subsequent data processing done with MS Excel. "Figures of Merit" for this analytical method are presented in **Table 2**. Based on accuracy, blank, and performance in the measurement of reference seawaters (NASS 5, SAFe S, and D2), this version of the technique can be used for the measurement of Zn, Co, Cd, Cu, Ni, and Pb in seawater.

Seawater samples were not UV irradiated before analysis. Very recent work indicates that not all dissolved species of Co, and possibly Cu, in seawater will be measured under such circumstances, because some strongly complexed forms of these two metals only become detectable after photo-oxidative destruction of the organic ligands (Shelley et al., 2010; Biller and Bruland, 2012). Our method detects dissolved *labile* concentrations of metals; those which can be displaced by the IDA chelating sorbent. For the other metals Cd, Ni, Zn, and Pb, dissolved labile concentrations are comparable to total dissolved concentrations in oceanic waters. For our purposes, dissolved labile concentrations determined directly by the FI-SPE-ICP-MS method are a useful representation of the bioavailable fraction.

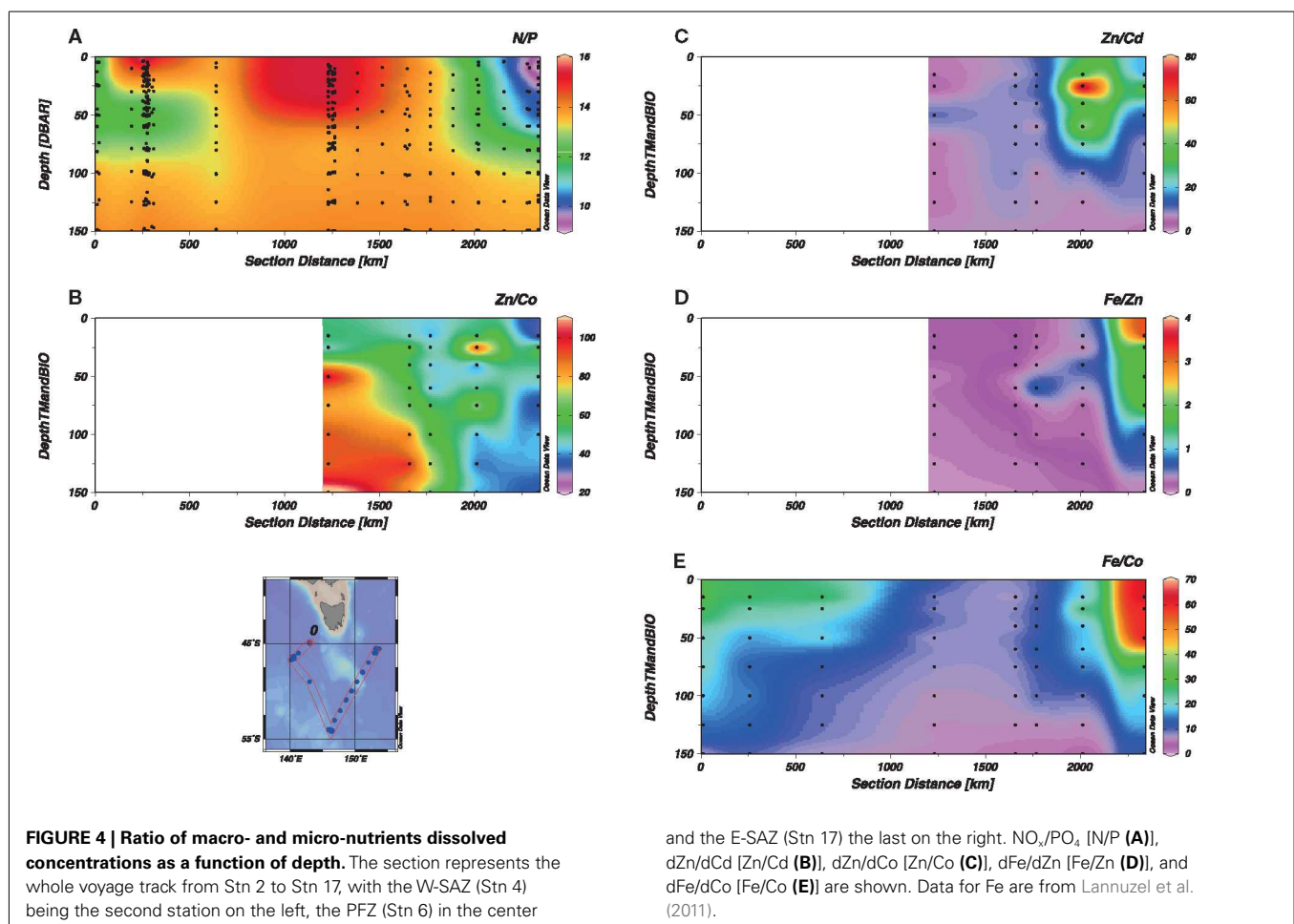


PIGMENT ANALYSIS

Pigment samples were collected in two size fractions, [$\geq 10 \mu\text{m}$ (L-phyto) and $0.8\text{--}10 \mu\text{m}$ (S-phyto)] using gentle sequential filtration ($<5 \text{ mmHg}$) of approximately 1 L of seawater through 10 and $0.8\text{-}\mu\text{m}$ polycarbonate filters (Millipore). Filters were then stored in cryo-vials in liquid nitrogen prior to being analyzed back on shore. To extract the pigments, the filters were cut into small pieces and covered with 100% methanol (3 mL) in a 10-mL centrifuge tube. The samples were vortexed for about 30 s and then sonicated in an ice-water bath for 15 min in the dark. The samples were then kept in the dark at 4°C for approximately 15 h. After this time, $200 \mu\text{L}$ water was added to the methanol such that the extract mixture was 90:10 methanol:water (vol:vol) and sonicated once more in an ice-water bath for 15 min. The extracts were quantitatively transferred to a clean a centrifuge tube and centrifuged to remove the filter paper. The final extract was filtered through a $0.2\text{-}\mu\text{m}$ membrane filter (Whatman, Anotop) prior to analysis by HPLC using a Waters – Alliance high performance liquid chromatography system, comprising a 2695XE separations module with column heater and refrigerated auto sampler and a 2996 photo-diode array detector. Immediately prior to injection the sample extract was mixed with a buffer solution (90:10 28 mM tetrabutyl ammonium acetate, pH 6.5: methanol) within the sample loop. After injection pigments were separated using a Zorbax

Eclipse XDB-C8 stainless steel $150 \text{ mm} \times 4.6 \text{ mm ID}$ column with $3.5 \mu\text{m}$ particle size (Agilent Technologies) and a binary gradient system with an elevated column temperature following a modified version of the van Heukelem and Thomas (2001) method. The separated pigments were detected at 436 nm and identified against standard spectra using Waters Empower software. Concentrations of chlorophyll *a* (Chl*a*), chlorophyll *b* (Chl*b*), and β,β -carotene in sample chromatograms were determined from standards (Sigma), while all other pigment concentrations were determined from standards (DHI, Denmark).

Pigments which relate specifically to an algal class are termed marker or diagnostic pigments (Jeffrey and Vesik, 1997; Jeffrey and Wright, 2006). Some of these diagnostic pigments are found exclusively in one algal class (e.g., alloxanthin in cryptophytes), while others are the principal pigments of one class, but are also found in other classes (e.g., fucoxanthin in diatoms and some haptophytes; 19'-butanoyloxyfucoxanthin in chrysophytes and some haptophytes). The presence or absence of these diagnostic pigments can provide a simple guide to the composition of a microalgal community, including identifying classes of small flagellates that cannot be determined by light microscopy techniques. Given that our dataset is limited, it was validated by comparison to the extensive total Chl*a* measurements made by de Salas et al. (2011) and relative fluorescence recorded from the CTD. To push the comparison



further, the CHEMTAX matrix used in de Salas et al. (2011) was applied to our data from stations 2, 6, and 17 to represent dominating large and small phytoplankton groups in the W-SAZ, PFZ, and E-SAZ, respectively.

DATA ANALYSES AND PLOTS

Sections of the voyage track (**Figure 1**) were plotted using Ocean Data View (version 4.5; Schlitzer, 2012). Since our goal is to compare micronutrients' distribution with phytoplankton biomass, size class, and functional groups, data above 125 m depth are presented. Full depth profiles and oceanography of trace elements have been discussed elsewhere (Lannuzel et al., 2011; Butler et al., in revision). The disappearance ratio between micronutrients with macronutrients (e.g., dCo/dPO₄, Arrigo et al., 1999, also referred to the dissolved ecological stoichiometric ratio, Saito et al., 2010) was

used as a proxy for phytoplankton uptake and growth rate (Arrigo et al., 1999; Cullen et al., 2003; Finkel et al., 2010; Croot et al., 2011). To identify the potential of each micronutrient to limit the growth of phytoplankton, the disappearance ratio is compared to phytoplankton cellular quotas, reflecting their biological requirement for growth, and dissolved macronutrient (e.g., NO_x/PO₄) and micronutrient (e.g., dZn/dCd) spot ratios, reflecting maximal micronutrient stock available for phytoplankton growth. It is to be noted that chemical speciation is not considered in this study. The labile dissolved metal considered likely overestimates the fraction that is bioavailable to support phytoplankton growth.

The statistical relations between micro- and macronutrient with temperature, salinity, chlorophyll *a*, and biomarker pigments were analyzed using the Excel package XLSTAT. Depths of the

Table 3 | Summary of dissolved disappearance ratios and biological requirement for phytoplankton growth for Cd, Zn, Co, Ni, and Cu.

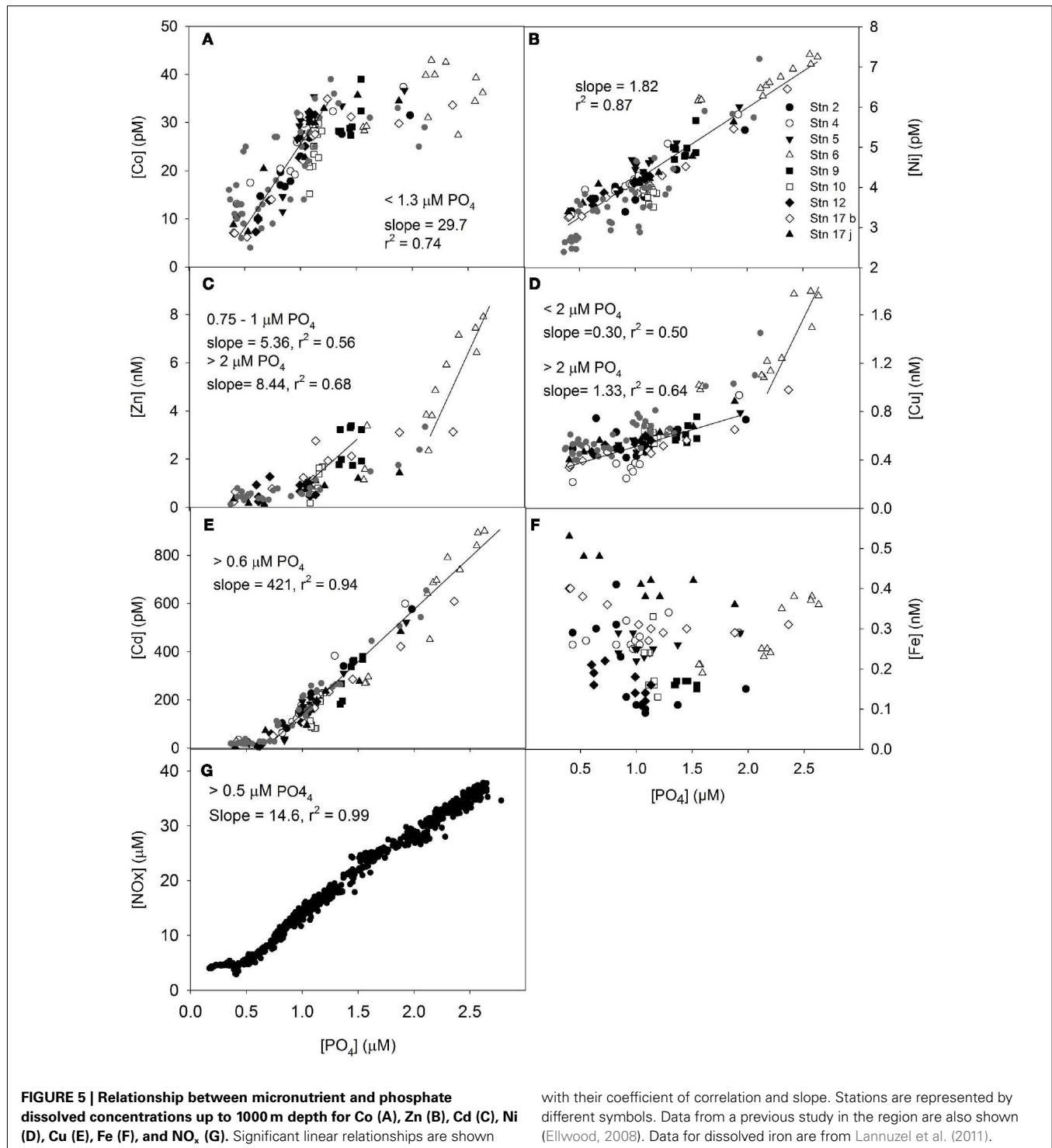
Micronutrient (M)	dM/PO ₄	r ²	Depth (m)	Location
DISSOLVED DISAPPEARANCE RATIO (dM/PO ₄ , μmol mol ⁻¹)				
Cd	323	0.88	15–100	Southern Ocean (SAZ and PFZ, >0.6 μ.M PO ₄) ^a
	461	0.94	30–100	Southern Ocean (SAZ and PFZ, >0.6 μ.M PO ₄) ^b
	608	0.89	0–125	Southern Ocean (Ross Sea) ^c
Zn	450	0.87	20–150	Subarctic Pacific (<1.2 μ.M PO ₄) ^{d,e}
	1637	0.61	15–100	Southern Ocean (SAZ and PFZ, >0.6 μ.M PO ₄) ^a
	NA	0.001	30–100	Southern Ocean (SAZ and PFZ) ^b
	484	0.79	0–125	Southern Ocean (Ross Sea) ^c
	4857	0.73	>500	Southern Ocean (Drake passage and Zero meridian) ^f
	~2000–7000		0–400	
	251–370	0.70–0.99	8–150	Subarctic Pacific (<1.2 μ.M PO ₄) ^{d,g}
Co	797	0.99	30–300	Southern Ocean (Drake Passage) ^{g,h}
	17	0.79	15–100	Southern Ocean (SAZ and PFZ) ^a
	25	0.62	30–100	Southern Ocean (SAZ and PFZ) ^b
	19	0.54	0–125	Southern Ocean (Ross Sea) ^c
	35–40	0.98–0.99	8–150	Subarctic Pacific ^{d,g}
	38	0.87	5–500	Southern Ocean (Ross Sea) ^h
Ni	1881	0.84	15–100	Southern Ocean (SAZ and PFZ) ^a
	1903	0.72	30–100	Southern Ocean (SAZ and PFZ) ^b
	1181	0.61	0–125	Southern Ocean (Ross Sea) ^c
Cu	441	0.73	15–100	Southern Ocean (SAZ and PFZ) ^a
	598	0.80	30–100	Southern Ocean (SAZ and PFZ) ^b
	846	0.72	0–125	Southern Ocean (Ross Sea) ^c
	430–450	0.96–0.99	0–985	North Pacific ^{d,j,k}
	680	0.92	30–300	Southern Ocean (Drake Passage) ^{h,k}
Strain	Zn/P**g	Co/P**g	Cu/P ^k	
BIOLOGICAL REQUIREMENT FOR PHYTOPLANKTON GROWTH (CELLULAR M/P, μmol mol ⁻¹)				
<i>E. huxleyi</i>	1272 (0.7 μ _{max})	264 (0.9 μ _{max})	35 (0.9 μ _{max} , low Cu) 758 (0.9 μ _{max} , high Cu)	
<i>T. oceanica</i>	63 (0.9 μ _{max})	1314 (0.7 μ _{max})	216 (0.9 μ _{max})	
<i>T. pseudonana</i>	232 (0.6 μ _{max})	1675 (0.5 μ _{max})	NA	
<i>Synechococcus</i> sp	ND	8.5 (0.6 μ _{max})	NA	

^aThis study; ^bEllwood (2008); ^cFitzwater et al. (2000); ^dMartin et al. (1989); ^eSunda and Huntsman (2000); ^fCroot et al. (2011); ^gSunda and Huntsman (1995a); ^hMartin et al. (1990); ⁱSaito et al. (2010); ^jBruland (1980); ^kSunda and Huntsman (1995b).

* No Co added, ** No Zn added. ND = not detected, NA = not applicable.

mixed layer and the euphotic zone (Westwood et al., 2011) were used to define the depths considered in statistical tests and comparison (0–100 m for stations 9, 0–75 m for other stations; **Table A1** in Appendix). This results in dataset of 32 observations for which measurements of physical parameters, micro- and macronutrients, as well as biological parameters, were considered. Correlation tests were done using Pearson's coefficient with a 95% interval of confidence to highlight the occurrence of significant positive or

negative linear relationship between two parameters. The most significant relationships are graphically presented. Canonical Correspondence Analysis (CCA) was done to extract the pattern and illustrate the relation existing between the different parameters and observations. CCA was applied to represent the correspondence between (i) biological and physical parameters with the chemistry of the sites, and (ii) small and large phytoplankton communities and micronutrients.



RESULTS

WATER MASSES

A snapshot of the hydrology along the relevant portion of the SAZ-Sense voyage track is shown in **Figure 2**. Temperature and salinity (**Figures 2A,B**, respectively) broadly characterize the regional water masses (see also Bowie et al., 2011b, with front definitions after Sokolov and Rintoul, 2002). The bulk was SAZ with salinity and temperature in the respective ranges, 34.2–34.8 and 2–12°C. The northernmost stations, west and east, were very close to the Subtropical Front (STF) with salinities at 34.9 (and temperature at 150 falling from 12 to 10°C across the STF, data not shown). The Polar Front is classically delineated by the subsurface $T_{\min} < 2^{\circ}\text{C}$, that occurs deeper than the section shown. A less precise indicator is surface salinity falling below 34 for the southernmost station (**Figure 2B**). The oceanography of the region during the SAZ-Sense expedition is fully described in Bowie et al. (2011b).

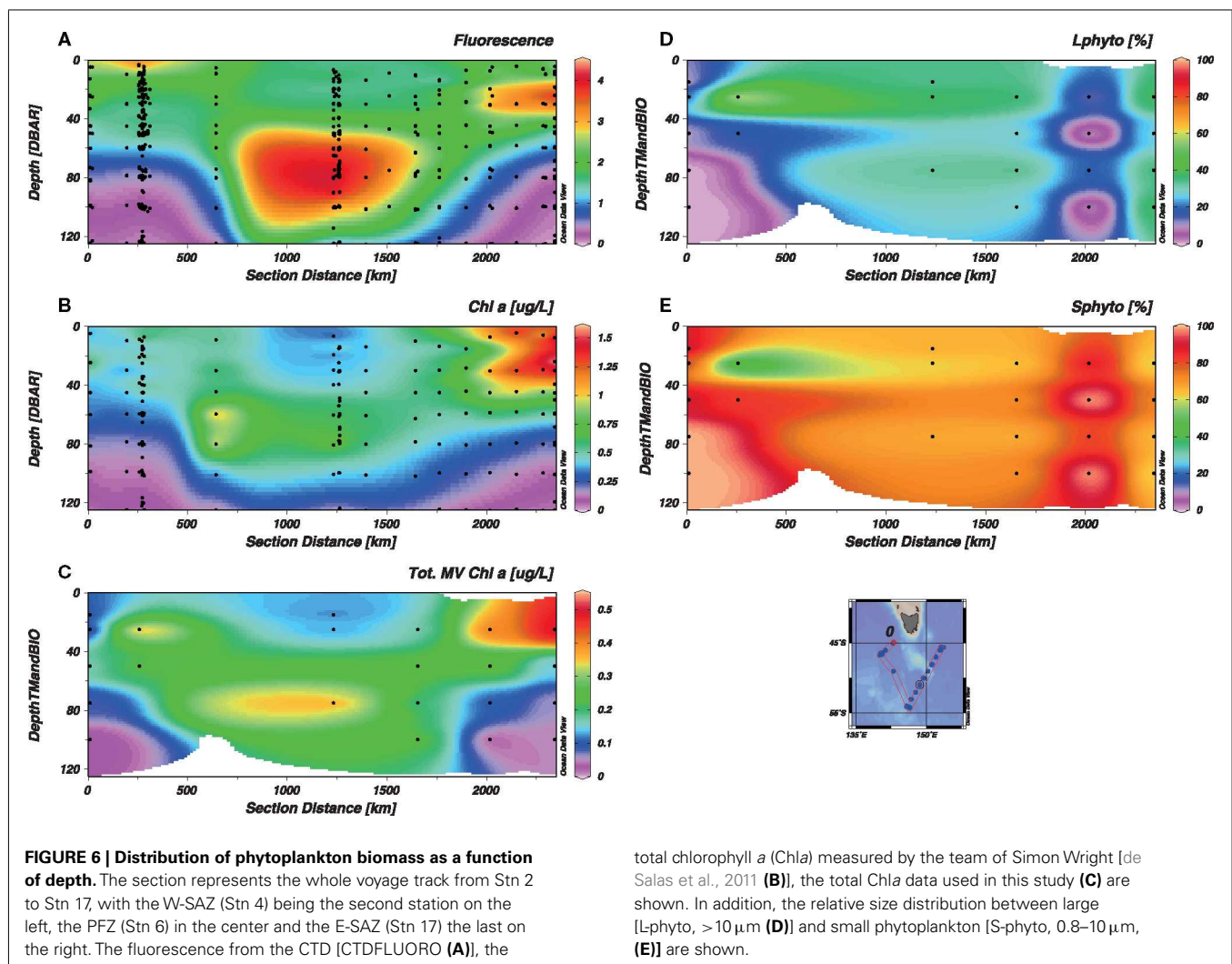
MACRONUTRIENTS

Sections of Si , PO_4 , NO_x , and NH_4 are depicted in **Figures 2C–F**, respectively. PO_4 and NO_x showed very similar progressions along the voyage track. In northern SAZ surface waters, PO_4 was drawn

down to $\leq 0.5 \mu\text{M}$ and NO_x to $\leq 5 \mu\text{M}$. Beyond the SAF-S front, concentrations began to ramp up, with surface waters $\sim 1.5 \mu\text{M}$ PO_4 and $\sim 20 \mu\text{M}$ NO_x . The nutricline typically varied between 60 and 80 m throughout the study region. Si was strongly depleted to a few micromolar concentrations in the upper 60 m for all stations (**Figure 2C**). Only beneath the nutricline, and poleward of SAF-S into PFZ waters, did Si begin to increase in concentration. NH_4 ranged from undetectable ($< 0.01 \mu\text{M}$) to $< 0.4 \mu\text{M}$ in surface waters (**Figure 2F**). It has distinct subsurface maxima at the nutricline and deeper (to 120 m) at all stations, but they are more pronounced ($> 1 \mu\text{M}$) on the western side of the voyage track than the east. Beyond 200 m (data not shown), NH_4 declined rapidly to background levels ($\leq 0.01 \mu\text{M}$). NH_4 is a useful indicator of remineralization of organic matter. Data demonstrated a significant remineralization just below the MLD in the W-SAZ and in the PFZ but not in the E-SAZ (**Figure 2**; **Table A1** in Appendix).

MICRONUTRIENTS

Dissolved labile concentrations of micronutrient metals along the voyage track are shown in **Figure 3**. Complete records have been plotted for Cd, Co, Cu, and Ni, but stations before Stn 6 were

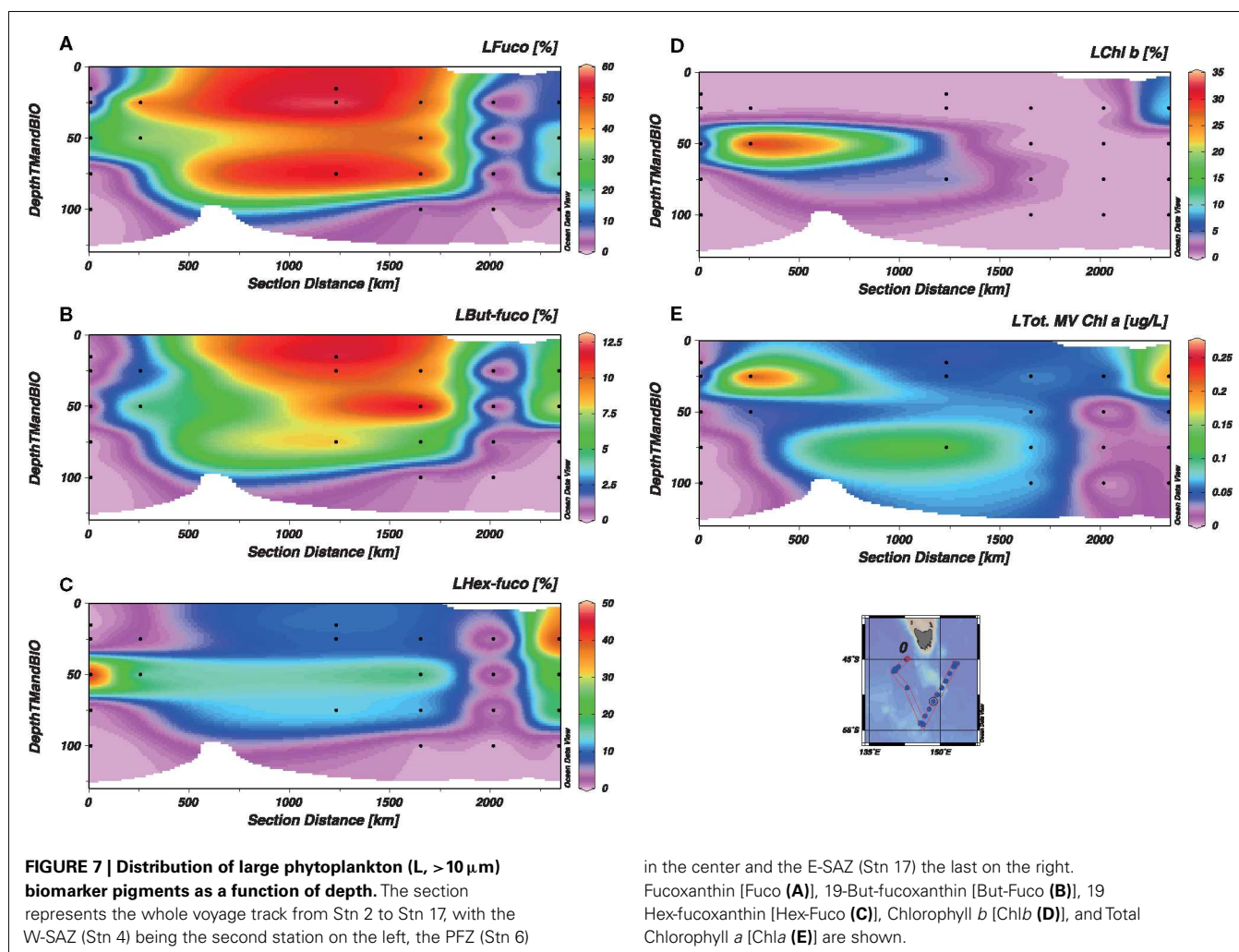


assessed as contaminated for Zn. The contaminated results were identified by irregularities in the depth profiles and recurrent outliers in property-property plots (i.e., metal vs. hydrological properties, metal vs. macronutrient (e.g., Si), and metal vs. metal). The distributions of these micronutrients in the SAZ-Sense study region is fully described in Butler et al., in revision. Cd, Cu, and Ni were closely related to PO_4 (Figure 2D and below), but the extent of their biological depletion was quite different. Relative to a reference depth of 150–200 m (see Bowie et al., 2011b), the depletion of Cd was 6 to >96%, that of Cu 11–35%, and Ni 7–20%. For each, the surface water depletion declined poleward. Co was also strongly depleted (31–70%). Zn was more comparable to the macronutrient Si in being depleted in most surface waters. Its depletion often extended well into the water column (≥ 200 m), so a reference depth of 150–200 m was not suitable for evaluating degree of depletion.

NUTRIENTS SPOT AND DISAPPEARANCE RATIO

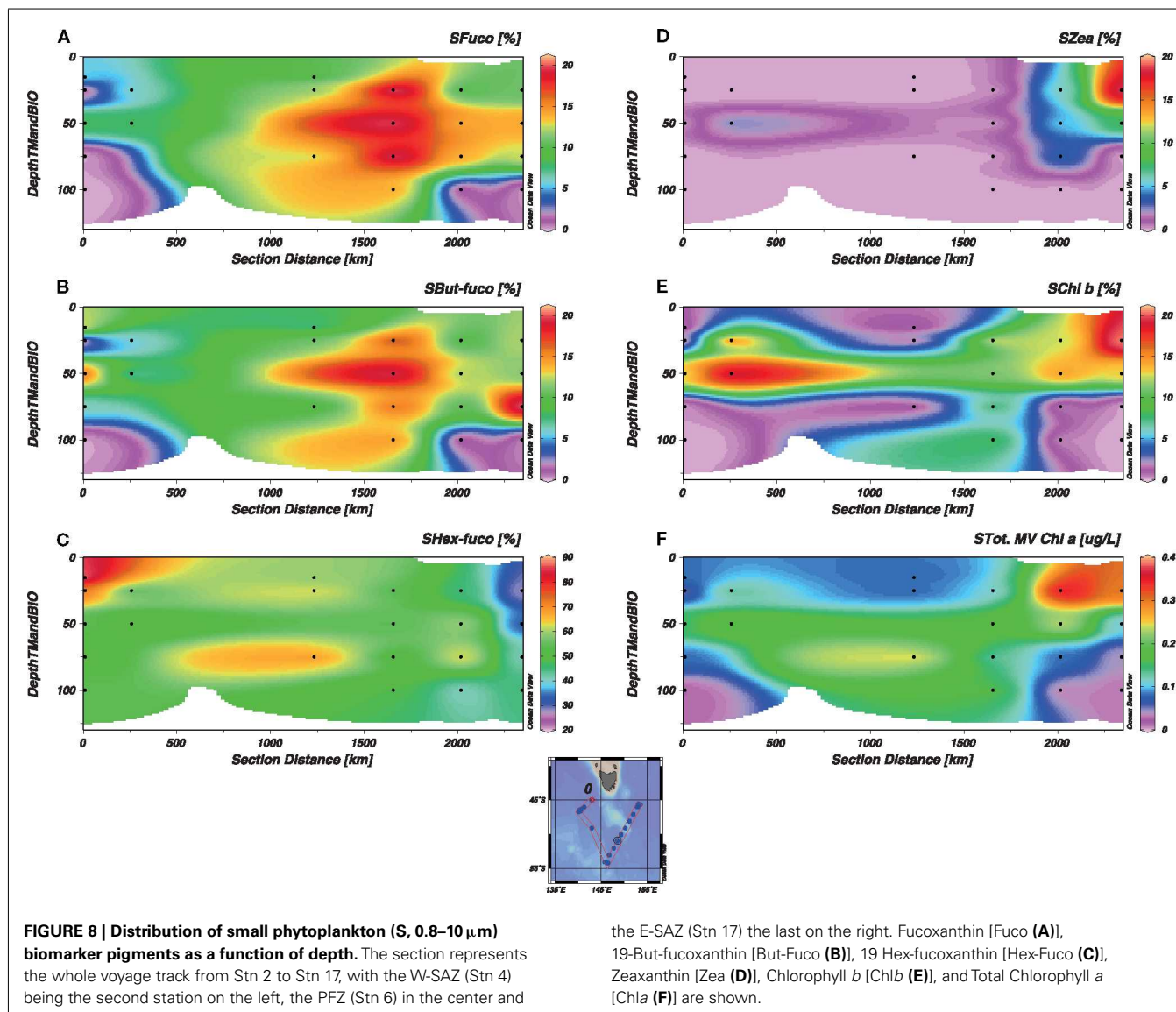
Considering data from all depths, the macronutrient ratios between NO_x and PO_4 for the study region were close to an optimal value of 16 [14.6 ± 0.07 (standard error), $r^2 = 0.98$, $n > 750$, Figure 5G; Redfield et al., 1963]. However, a kink was observed

for $[\text{PO}_4] < 0.5 \mu\text{M}$ (Figure 5G), suggesting that less NO_x was relatively consumed in surface water of the W-SAZ and E-SAZ. The dissolved NO_x/PO_4 spot ratios are suboptimal in the W-SAZ (at depth) and the E-SAZ regions (Figure 4A). Considering data from 0 to 100 m depth only (Figure A1G in Appendix), a close to optimal disappearance ratio was observed (slope 18.0 ± 0.18 , $r^2 = 0.98$) for phosphate concentrations between 0.5 and $1.6 \mu\text{M}$. For $[\text{PO}_4] > 1.6 \mu\text{M}$, representing waters from the PFZ (Stn6), a significantly lower N/P disappearance ratio was observed (slope 7.00 ± 0.40 , $r^2 = 0.85$). Because Fe, Zn, and Co could limit or co-limit the growth of oceanic phytoplankton (e.g., Martin et al., 1990; Morel et al., 1994; Coale et al., 2003), and Zn, Co, Cd are interchangeable enzymatic co-factors that can all support the growth of some marine phytoplankton (Price and Morel, 1990; Sunda and Huntsman, 1995b; Timmermans et al., 2001), the ratios between these micronutrients were investigated (Figures 4B–E; Table A2 in Appendix). Dissolved zinc was present in excess compared to Co ($\text{dZn/dCo} > 1$, Figure 4B) with greatest ratios in the PFZ (Stn 6) and lowest ratios in the surface of the E-SAZ (Stn 17). The ratio dZn/dCd was close to unity in the PFZ and greater at Stn 12 just south of the E-SAZ. The ratios dFe/dZn and dFe/dCo (Figures 4D,E) were lower at the PFZ and greater in the



surface waters of the E-SAZ. For all micronutrients, except Fe, a disappearance ratio could be calculated from the linear regression between dissolved micronutrient and PO_4 concentrations (Table 3; Figure 5; Figure A1 in Appendix). A kink was observed at low PO_4 concentrations ($<0.5\text{--}0.6\ \mu\text{M}\ \text{PO}_4$) for Cd and Zn and below $2\ \mu\text{M}\ \text{PO}_4$ for Cu. Ni is the only micronutrient for which no kink was observed. For Zn, data suggested two kinks separated by a plateau between 1.5 and $2\ \mu\text{M}\ \text{PO}_4$, however, the coefficient of correlation considering all data between 0 and $2\ \mu\text{M}\ \text{PO}_4$ was only slightly lower ($r^2 = 0.47$, slope $1764\ \mu\text{mol}\ \text{Zn}\ \text{mol}^{-1}\ \text{PO}_4$, Figure 5B). For Co, Zn, and Cu inter-station differences were observed (Figure 5). For Co, Stns 6, and 9 were on the plateau (Figure 5A) and the slope $d\text{Co}/d\text{PO}_4$ was the greatest for Stns 5 and 10 (slope of $66\text{--}77\ \mu\text{mol}\ \text{mol}^{-1}$) as compared to the other stations ($32\text{--}49$). For Zn, no correlation ($r^2 < 0.5$) was observed for Stns 12 and 17, and greater $d\text{Zn}/d\text{PO}_4$ slopes ($9\text{--}11\ \mu\text{mol}\ \text{mol}^{-1}$) were observed at Stns 9 and 10, suggesting greater Zn biological uptake at these stations. Correlations between Cu and PO_4

dissolved concentrations ($r^2 > 0.5$) were only observed at Stns 4 ($r^2 = 0.94$, slope $= 0.65$), 5 ($r^2 = 0.78$, slope $= 0.26\ \text{mmol}\ \text{mol}^{-1}$), 12 ($r^2 = 0.83$, slope $= 0.24\ \text{mmol}\ \text{mol}^{-1}$), and 17 ($r^2 = 0.94$ and 0.90 , slope $= 0.19$ and $0.28\ \text{mmol}\ \text{mol}^{-1}$). When considering only the data from the top $100\ \text{m}$ for all stations, the relation between micronutrients and PO_4 was slightly altered (Table 3; Figure A1, Table A2 in Appendix). In this case, the disappearance ratios followed the order $\text{Ni} \sim \text{Zn} > \text{Cu} \sim \text{Cd} > \text{Co}$. The disappearance ratio for Zn was 5.1 and 96 times greater than for Cd and Co, respectively, suggesting greater biological utilization of Zn as compared to Cd and Co. Similar ratios were obtained using NO_x , whereas the significance of the correlation was much lower using Si (see Figure A1 in Appendix). Considering the disappearance ratios calculated in surface water ($0\text{--}100\ \text{m}$) and at depth ($125\text{--}1000\ \text{m}$) for each station (Table A1 in Appendix), revealed interesting trends. For all metals, except Co, the surface disappearance ratio in surface waters was equal or lower than the ratio calculated at depth. In addition, a loss of significant correlation between



dissolved metal and phosphate was observed in the PFZ. Generally, a region between 49 and 50°S with greater disappearance ratios separated the surface waters between the SAZ and the PFZ (Table A1 in Appendix).

CHLOROPHYLL AND BIOMARKER PIGMENTS

Our dataset for total Chl *a* (Figure 6C) showed good correlation with the more extensive dataset from the fluorometer (CTD data, Figure 6A) and previous pigment analysis (de Salas et al., 2011, Figure 6B). The maximum Chl *a* concentration was observed in the surface of the E-SAZ (Stn 17) and the W-SAZ (Stn 4) and at depth in the PFZ (Stn 12). Total Chl *a* data from de Salas et al. (2011) were greater than our data, likely reflecting different extraction procedures and our sequential filtration step. Sequential filtration removes larger phytoplankton, decreasing clogging of the filter, and avoiding an overestimation of pigments' concentration.

In the study region, contrasting distribution of phytoplankton from different size classes was observed (Figures 6D,E). Small phytoplankton (0.8–10 μm , S-phyto) dominated at all stations, except in surface water of the W-SAZ (stn 4). In the northern W-SAZ waters (Stn 2) and south of the E-SAZ (Stn 12), S-phyto represented >80% of the total Chl *a*. Large phytoplankton ($\geq 10 \mu\text{m}$, L-phyto) represented a significant fraction (25–40%) of total Chl *a* only in the PFZ, Stn 9, and in the E-SAZ.

Using the distribution of the relative biomarker pigment concentrations (normalized against Chl *a*), dominating phytoplankton groups can be identified (Jeffrey and Wright, 2006). Maximum Chl *a* associated with larger phytoplankton correlated with total Chl *a* distribution (Figures 6 and 7). Large phytoplankton, present at the depth of Chl *a* maximum were mainly diatoms in the W-SAZ and PFZ (as indicated by a clear dominance of fucoxanthin) and were mainly haptophytes in the E-SAZ (dominance of 19-hexanoyloxyfucoxanthin, Figure 7). In the PFZ and E-SAZ, the Chl *a* associated with small phytoplankton correlated with total Chl *a* maximum (Figures 6 and 8). In the W-SAZ, most of the S-phyto were present at 50 m, below the total Chl *a* maximum (Figure 8). Haptophytes and diatoms were mainly present in the subantarctic water west of Tasmania (Stn 2). In the W-SAZ (Stn 4), haptophytes, and green algae (Chl *b*) dominated in surface water; some cyanobacteria (zeaxanthin and Chl *b*) and diatoms were also present at 50 m. At the depth of total Chl *a* maximum, small diatoms, and haptophytes dominated in the PFZ, whereas cyanobacteria and diatoms dominated in the E-SAZ. Peridinin was only significantly present in the E-SAZ (data not shown), representing 24 and 8% of large and small phytoplankton Chl *a*, respectively. Prasinoxanthin was only present at marginal levels (1% of Chl *a*) at Stns 12 and 17 (data not shown).

The use of CHEMTAX revealed that, except for prasinophytes, representing up to 35% of the large and small phytoplankton in the W-SAZ, the composition of the phytoplankton community calculated by CHEMTAX was similar in the W-SAZ and the PFZ (Figures 9A,B). In these two zones, large phytoplankton were dominated by diatoms, whereas small phytoplankton were dominated by haptophytes. Dinoflagellates were present in both phytoplankton size fractions, representing 10–30% of the phytoplankton community. In the E-SAZ, the composition of the phytoplankton community inferred by CHEMTAX was more complex

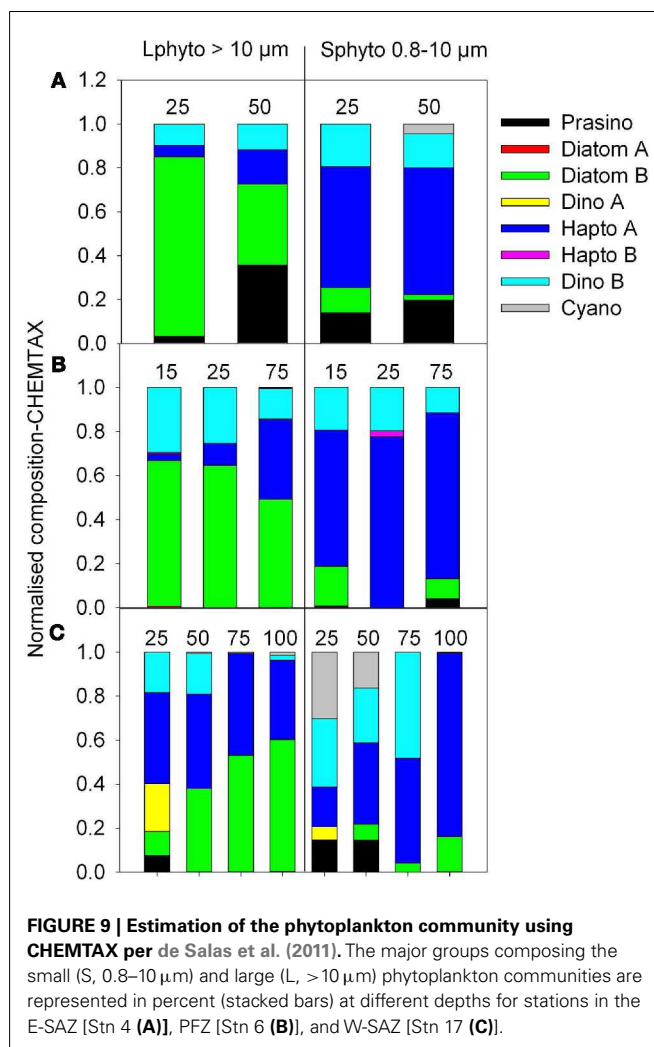
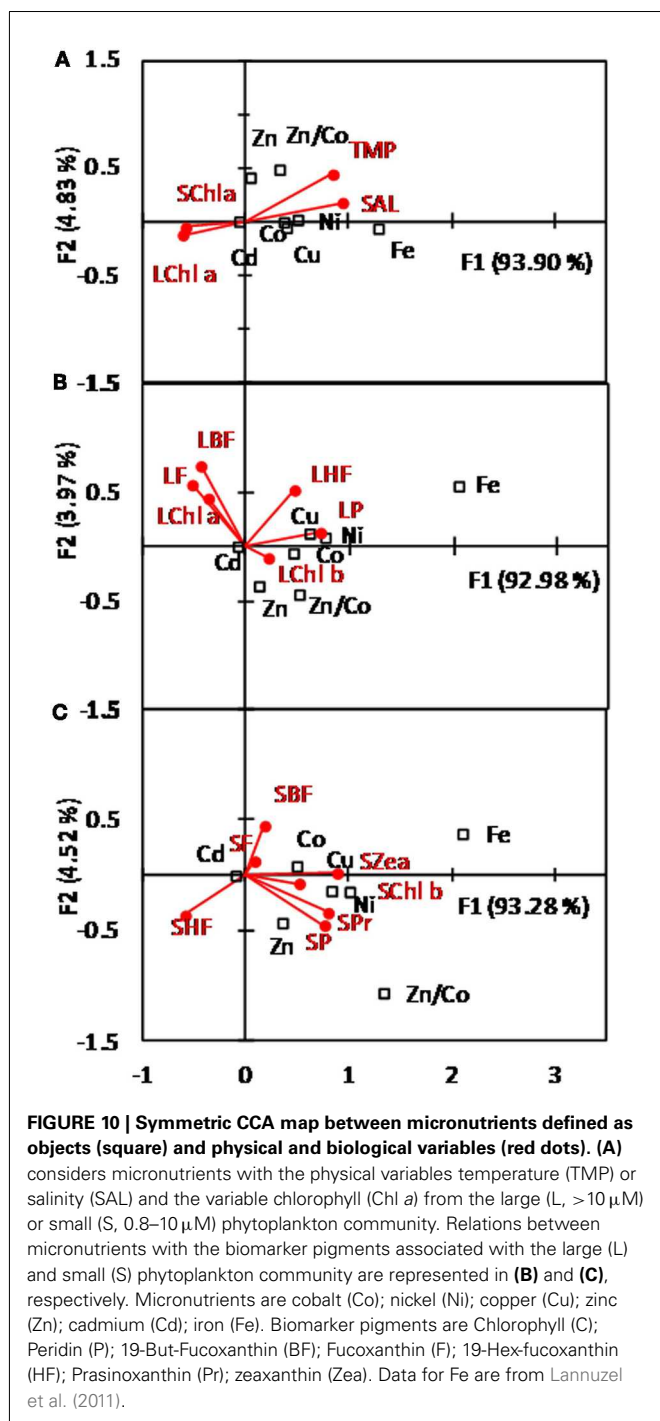


(Figure 9C). In the phytoplankton bloom (top 40 m, Figure 6), diatoms are only marginal (10%, Figure 9C), likely due to Si depletion. Large phytoplankton are mainly composed of dinoflagellates and haptophytes (40% each), whereas small phytoplankton mainly contained dinoflagellates (37%), and cyanobacteria (30%), with some haptophytes (18%) and prasinophytes (14%).

STATISTICAL CORRELATIONS OF NUTRIENTS WITH PHYSICAL AND BIOLOGICAL PARAMETERS

Canonical correspondence analysis representation of micronutrients according to temperature, salinity, small, and large phytoplankton Chl *a* (Figure 10A, 0–100 m), demonstrated four micronutrient “clusters”, with Fe being closer to physical parameters and Cd closer to Chl *a*. The other micronutrients were intermediately located with Cu, Co, and Ni closer to physical parameters and Zn closer to Chl *a*. These data were also supported by the Pearson's correlation tests (Table A1 in Appendix). Indeed, Fe was the only micronutrient to significantly positively correlate with temperature and salinity but not significantly with NO_x and PO_4 . No significant correlation between micronutrients and silicic acid were obtained. Co, Cu, Ni, Cd, and Zn were significantly



positively inter-correlated and all negatively correlated with Fe. Fe was also significantly negatively correlated to ratio dZn/dCo (Table A1 in Appendix).

No statistically significant Pearson's coefficient of correlation was observed between micronutrients and Chla throughout the study region (total, large, and small phytoplankton, Table A1 in Appendix). However, the degree of significance of positive correlation followed the order Cd > Zn > Ni, Cu, Co, with Ni and Cu more related to small phytoplankton Chla. Fe was only weakly

correlated (−0.1) to Chla. These correlations are represented for Cd, Zn, Co, and Fe in Figure 11. Data from the depths of Chla maximum (labeled as “*” in Figures 11A–F) significantly deviated from dCd/Chla and dZn/Chla relations. Exclusion of these points, resulted in a significant correlation between dissolved Cd and Zn with total, small, and large Chla concentrations. No correlation was observed between Co, Fe, and Chla (Figures 11G–L).

Canonical correspondence analysis representations of micronutrients with large (L- Figure 10B) and small (S- Figure 10C) phytoplankton biomarker pigments confirmed that Fe was poorly related to phytoplankton. Fe was closest to L-peridinin and S-zeaxanthin, the only two pigments for which a significant positive correlation was obtained (Table A1 in Appendix), suggesting that Fe could affect the dynamics of dinoflagellates and cyanobacteria in the E-SAZ. Cd was the micronutrient that was the most closely related to all biomarker pigments (Figures 10B,C), whereas Cu and Ni formed a cluster closely related to L-peridinin, L-hex-fucoxanthin, and S-zeaxanthin, S-prasinoxanthin, S-Chlb, and S-peridinin. Co and Zn were differentiated by Co being closer to L-peridinin and L-Chlb, S-fucoxanthin, S-but-fucoxanthin, S-Chlb and S-zeaxanthin, and Zn being closer to L-Chlb and S-peridinin, S-prasinoxanthin and S-Chlb. The ratio dZn/dCo was more associated with biomarker pigments from large rather than small phytoplankton. Co, Ni, Cu, and Cd were statistically positively correlated with L-but-fucoxanthin, L-fucoxanthin, and negatively correlated to S-Chlb. Co was also significantly negatively correlated to S-zeaxanthin. Zn is only significantly positively correlated with Shex-fucoxanthin and dZn/dCo to L-hex-fucoxanthin (Table A1 in Appendix). Pearson's correlation tests also showed significant positive correlations between NO_x and PO₄ with L-but-fucoxanthin and L-fucoxanthin, between Si and S-fucoxanthin, and between nitrite (NO₂) and S-hex-fucoxanthin (Table A1 in Appendix).

DISCUSSION

Previous studies from the SAZ-Sense project have demonstrated that the E-SAZ, despite greater Chla was less productive than the W-SAZ at the time of observation (Cavagna et al., 2011; Westwood et al., 2011; Table A1 in Appendix). Biomarker pigments and CHEMTAX analysis showed a contrasted phytoplankton community in the study region. Distribution of phytoplankton size classes and dominant groups accorded with microscopic observations, pigment size class, and CHEMTAX calculations done during the SAZ-Sense voyage (de Salas et al., 2011; Pearce et al., 2011). There is, therefore, a clear difference between these two SAZ regions.

Our distribution of micronutrients agreed with previous studies in the region (Ellwood, 2008; Lai et al., 2008). Similar hydrology for these studies, despite the difference in season and location (winter and eastwards of the SAZ-Sense study for Ellwood, 2008), allow a comparison of the distribution of micronutrients. Similar Cd, Cu, and Ni distribution in the SAZ, closely related to PO₄ (see Figure 5), suggested that this distribution of micronutrients, is the result of long term processes (seasonal and longer – see also Butler et al., in revision). Co, too, was closely related to PO₄ in the top 150–200 m and with a distribution that tracks with timescales of seasonal or longer. Deeper in the SAZ water column, Co is known to display scavenged characteristics, and is strongly

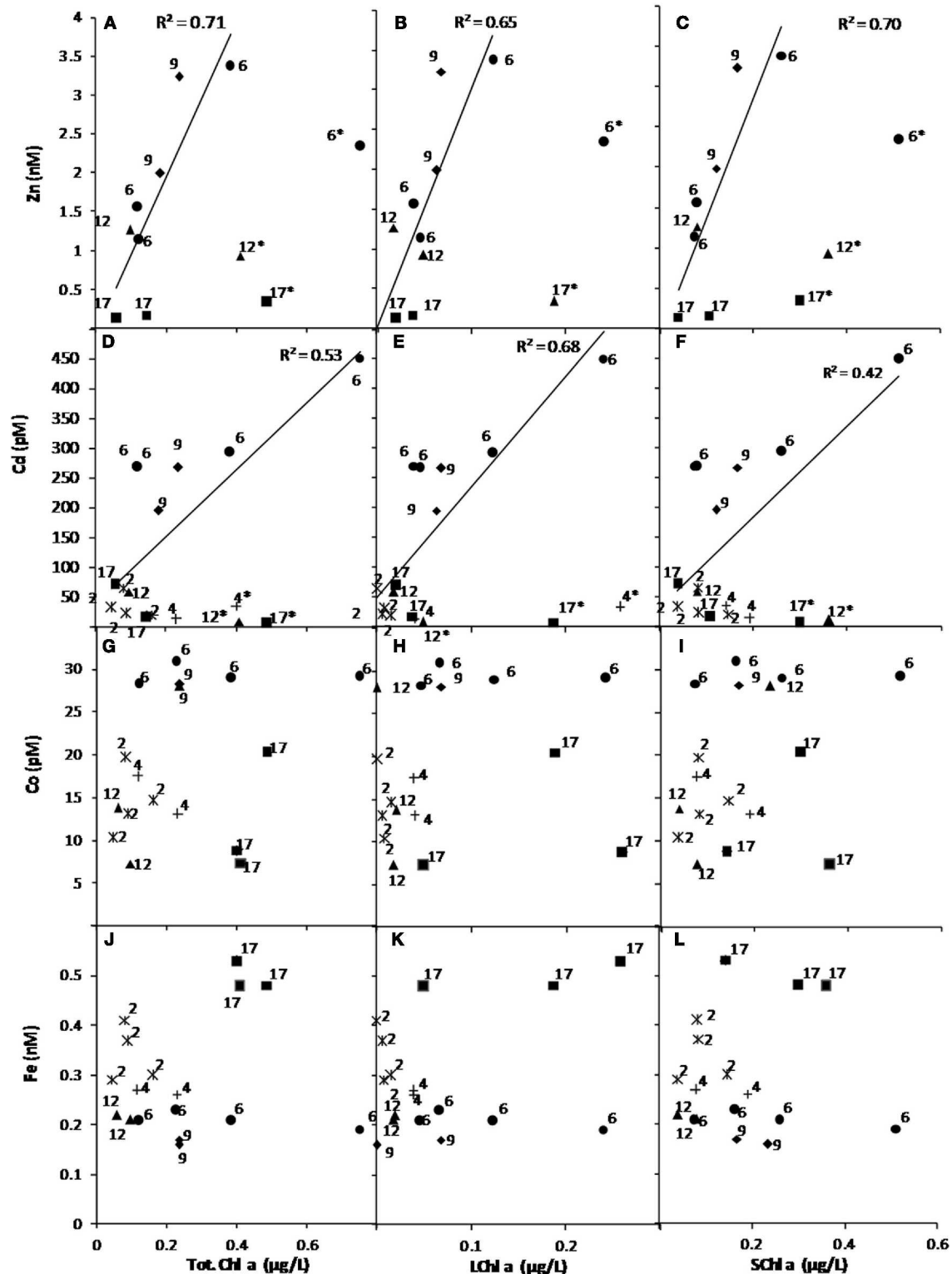


FIGURE 11 | Relation between dissolved micronutrients and chlorophyll *a* associated with the total [Chl*a*, (A), (D), (G), (J)], large [LChl*a*, >10 µm, (B), (E), (H), (K)], and small [SChl*a*, 0.8–10 µm, (C), (F), (I), (L)] phytoplankton communities. Relationships are shown for Zn (A–C), Cd (D–F), Co (G–I) and Fe (J–L) and coefficient of correlation are

given when significant relationships were found (Zn and Cd only). Each station has been represented using a different symbol and the station labeled with “*” correspond to depth with a maximum of Chl*a* and were removed to obtain a significant correlation for Cd and Zn. Fe data are from Lannuzel et al. (2011).

influenced by concentrating processes in the Antarctic Zone (seen to some degree here at Stns 6, 9, and 10) and intermediate water formation (Butler et al., submitted). By comparison, the dissolved iron distribution resulted from short term processes, involving a rapid recycling, episodic dust input, and intrusion of oligotrophic subtropical water into the SAZ region, generating a patchy distribution of dissolved iron (Bowie et al., 2009, 2011a,b; Lannuzel et al., 2011; Mongin et al., 2011). Butler et al. (in revision) have also proposed that distribution of Zn in SAZ-E waters was modulated by short term processes at the time of the SAZ-Sense voyage, although it was quite unlike that of Fe, which is supported by their lack of correlation reported here. The patchiness of Fe and Zn at SAZ-E results from region being dominated by the East Australian Current eddy field, the different supply mechanisms for the two pivotal metals, and the ensuing sub-mesoscale irregularities in phytoplankton productivity.

Determination of the control by the full suite of micronutrients (Fe, Zn, and other transition metals) on phytoplankton biomass and community structure is, thus, first step to elucidate how primary productivity and the balance between carbon export and recycling are controlled. However, the identification of the nutritive status (e.g., limited, co-limited, replete) of *in situ* phytoplankton communities is a major challenge. Statistical analyses of the relationship between micronutrients and phytoplankton, revealed complex heterogeneous relationships in which all micronutrients (Fe, Zn, Cd, Co, Cu, and Ni) are important for specific phytoplankton groups. All the micronutrients studied were depleted in surface waters and presented good correlations with dissolved PO_4 (except Fe), demonstrating their nutritive role in phytoplankton growth. The role of micro-nutrients in shaping the phytoplankton community can be further explored by comparing their disappearance ratios in reference to PO_4 with the dissolved metal spot ratios, with previously reported phytoplankton cellular quotas and biological requirements (e.g., Sunda and Huntsman, 1995a,b; Ho et al., 2003; Finkel et al., 2007; Saito et al., 2010; Croot et al., 2011).

In surface water, a greater disappearance ratio is often associated with a greater relative biological uptake but could also be related to differential recycling and remineralization. Several studies have reported a “kink” in the disappearance ratio for Cd which, despite a poor understanding of the mechanisms at play, can be related to a decreased phytoplankton growth rate or “biodilution effect” (Sunda and Huntsman, 2000; Cullen et al., 2003). It is, thus, not surprising that, in the CCA, Cd was the closest to total Chla and to most of the biomarker pigments. Cadmium was the most depleted micronutrient in surface waters (from comparison with concentrations at 150–200 m depth – see Bowie et al., 2011b) and it also showed significant correlation with several biomarker pigments. The disappearance ratio for Cd observed here was slightly lower than for the Ross Sea and the subarctic Pacific (Table 3).

In this study, kinks in disappearance ratios were observed for NO_x , Zn, and Cd. The kinks observed for NO_x and Cd correspond to the surface water (25–50 m) of the W- and E-SAZ (Stns 2,4, and 17) but the kink observed for Zn extends deeper at these stations and further south to Stns 5 and 12, suggesting a complex control on phytoplankton growth rate in the region. This is emphasized by the fact that inter-station disappearance ratio is variable and follows a general pattern, where disappearance ratios are increasing southwards with a loss of correlation in the PFZ. Such loss of correlation

could be due to nutrients supply from Upper Circumpolar Deep Water sufficient to swamp the imprint of biological uptake. On the other hand, the disappearance ratio for NO_x is lower in the PFZ. In the Southern Ocean, such a poleward increase in disappearance ratio was recently reported for Zn (Croot et al., 2011), whereas a lower dNO_x/PO_4 was reported in the PFZ and southwards (Levititus et al., 1993; de Baar et al., 1997). These observations were attributed to variation in phytoplankton growth rate and specific phytoplankton uptake ratio (de Baar et al., 1997; Arrigo et al., 1999; Croot et al., 2011). Parameters usually discussed as a control in phytoplankton growth rate with impact on disappearance ratios in the region are (i) iron limitation (e.g., Martin et al., 1990; de Baar et al., 1997; Cullen et al., 2003; Twining et al., 2004a,b; Croot et al., 2011), (ii) combined effect of micronutrients (Sunda and Huntsman, 2000; Twining et al., 2004b; Cullen and Sherrell, 2005), and (iii) community structure (e.g., Sunda and Huntsman, 1995b, 2000; de Baar et al., 1997; Arrigo et al., 1999; Ho et al., 2003; Quigg et al., 2003; Twining et al., 2004a,b; Finkel et al., 2010). It is to be noted that the dependency of disappearance ratios on growth rate and iron addition is not an invariant attribute; it can differ between phytoplankton groups and micronutrients (e.g., Twining et al., 2004b; Finkel et al., 2007). Finally, the effects of light and temperature have also to be considered (Finkel et al., 2007, 2010; Croot et al., 2011).

Comparison of the distribution of the Chla (Figure 6) with the depths of the euphotic zone and the mixed layer (Table A1 in Appendix) allows discussion of the impact of light limitation. In both the W-SAZ and PFZ, most of the Chla is found at the bottom of the euphotic layer, just below the MLD. This clearly illustrates a trade-off between light and nutrient limitation at these sites. In the E-SAZ, light might constrain the bloom in surface waters (Mongin et al., 2011; Westwood et al., 2011; Table A1 in Appendix), but phytoplankton found in the top 16 m are not light limited. Temperature is known to exert a control in the growth of cyanobacteria (Li, 1998) and can, thus, curtail their extension southwards. However, temperature cannot account for the absence of cyanobacteria in the W-SAZ. In addition, as previously noted, it is likely that phytoplankton present at these high latitudes are well adapted to low temperatures (e.g., Croot et al., 2002). Therefore, it is not expected that temperature acts as a fundamental control of phytoplankton growth here.

During SAZ-Sense, Fe, and Si limitation were postulated in the W-SAZ and the PFZ using microscopic observations (Pearce et al., 2011), diatom silification rate (Fripiat et al., 2011), Si^* , and Fe^* concentrations (Lannuzel et al., 2011), incubation and Fv/Fm (Schoemann et al., unpublished). Interestingly, except for prasinophytes, the composition of the phytoplankton community was similar at these two locations. The lower disappearance ratio for NO_x in the PFZ could be related to diatoms, such as *Fragilariopsis kerguelensis*, present at Stn 9 (de Salas et al., 2011), and iron limitation (de Baar et al., 1997). By comparison, in the E-SAZ, where a less productive but more complex and diverse phytoplankton community prevailed (this study, de Salas et al., 2011), no iron limitation was observed. In the surface waters of the E-SAZ, the decreased dZn/dCo and dZn/dCd likely reflected biological uptake, whereas the increased dFe/dCo and dFe/dZn likely reflected the iron aerosol input (Bowie et al., 2009; Mongin et al., 2011). The dissolved Fe/PO_4 ratio also indicated iron

enrichment in the surface waters of the W-SAZ and E-SAZ. Based on the iron biological requirement for phytoplankton growth (i.e., half saturation constant), the dissolved iron concentrations measured in surface water were indeed enough to sustain the growth of most diatoms (Coale et al., 2003; Sarthou et al., 2005), and the haptophyte genus, *Phaeocystis* (Coale et al., 2003; Sedwick et al., 2007). However, diatoms were a marginal phytoplankton group, and nanoflagellates and dinoflagellates were the most dominant groups in the E-SAZ at the time of study (this study; de Salas et al., 2011; Pearce et al., 2011). Dinoflagellates were previously reported as dominating the phytoplankton community in the SAZ region south of Australia during austral spring and summer (Kopczynska et al., 2001, 2007). Studies of elemental ratios in phytoplankton have demonstrated that optimal iron content, follows the order cyanobacteria > haptophytes ≥ dinoflagellates ≥ diatoms (Ho et al., 2003; Twining et al., 2004b; Finkel et al., 2010) and that iron enrichment favors the growth of diatoms, but also autotrophic and heterotrophic flagellates (e.g., Twining et al., 2004a). In this case, additional iron sources in the E-SAZ might have relieved iron limitation and favored the growth of flagellates and cyanobacteria. Indeed, dissolved iron concentrations were significantly related to L-Peridin (dinoflagellates – type 1) and S-zeaxanthin (cyanobacteria), both biomarkers present only in the E-SAZ. In this case, phytoplankton in the E-SAZ were not iron-limited at the time of sampling; however, iron had an important effect of the phytoplankton community structure in this region.

The extended Redfield ratio based on micronutrient cellular quota from phytoplankton cultures of $P_1Fe_{7.5}Zn_{0.80}Cu_{0.38}Co_{0.19}Cd_{0.21}$ (Ho et al., 2003), suggests that the biological requirement for growth is usually smaller for other micronutrients than for iron. However, a significantly different extended Redfield ratio of $P_1Zn_{5.4}Fe_{1.8}Ni_{0.61}$ was calculated from a field study during the Southern Ocean Iron Experiment (SOFEX, Twining et al., 2004b), suggesting that Zn biological requirement exceeds the requirement for iron. These differences could be related to different water chemistry, light and phytoplankton species as all of these parameters affect cellular quotas (Finkel et al., 2010). In the study region, the concentrations of micronutrients are lower than iron, especially in the SAZ regions, suggesting that they might play a role in controlling phytoplankton growth or community structure.

Cd and Co nutrition in phytoplankton is coupled to Zn nutrition, because Zn can interchange with Cd and Co to support key enzymes, such as the carbonic anhydrase in some (Price and Morel, 1990; Morel et al., 1994; Sunda and Huntsman, 1995a, 2000; Saito and Goepfert, 2008), but not all phytoplankton species (Timmermans et al., 2001). Laboratory studies suggested that Cd, Co, and Zn use the same biological transport system, which is regulated by cellular Zn concentrations for diatoms and coccolithophores (Sunda and Huntsman, 1995a, 2000). Cobalt is associated with vitamin B₁₂ which is essential to, but not synthesized by eukaryotic phytoplankton (Saito et al., 2002; Saito and Goepfert, 2008).

The kink observed for dZn/PO₄, could be related to the induction of high affinity transporters which are efficient in maintaining a nearly constant cellular Zn concentration despite decreasing free Zn concentrations (Sunda and Huntsman, 1995a). Zn was the only micronutrient for which significant differences in the relation with other macronutrients were observed (Figure 5; Table 3). In Ellwood (2008), dissolved Zn and PO₄ concentrations were not

significantly related in surface waters ($r^2 < 0.001$, 0–100 m, see Figure A1 in Appendix) but dissolved Zn and Si were strongly related ($r^2 = 91$). Our data suggest a greater role for Zn in phytoplankton nutrition. The lack of dZn/Si relationship observed here (Figure A2 in Appendix) could be related to diatoms not being the dominant phytoplankton group in the SAZ at the time set of our study (de Salas et al., 2011), likely related to Si depletion and limitation (Fripiat et al., 2011).

Here, the ratios dZn/PO₄:dCd/PO₄ of 5 and dZn/PO₄:dCo/PO₄ of 96 (Table 3) showed indeed that Zn had an important nutritive role in the study region. The Zn/PO₄ measured here is much higher than data previously reported (Table 3, except for Croot et al., 2011). The dZn/PO₄ ratio observed here (>0.5 μM PO₄) was close to the cellular ratio for which growth inhibition is observed in *Emiliania huxleyi* (Table 3, in absence of Co and Cd, Sunda and Huntsman, 1995a). For a similar Zn²⁺/Cd²⁺ than the dZn/dCd ratio observed here, the cellular Zn:P ratio in *E. huxleyi* (1494 μmol mol⁻¹; Sunda and Huntsman, 2000) was close to the dZn/PO₄ ratio observed. This suggests that Zn was present at concentrations which could limit or co-limit the growth of coccolithophores, even considering Zn-Cd biological substitution. However, in the E-SAZ, the ratios between Zn and Co dissolved concentrations were smaller than 96, suggesting that Co could be important to complement Zn nutrition. The disappearance ratio for Co was smaller than the cellular Co:P ratios under which growth inhibition was observed for diatoms and coccolithophores (Table 3), suggesting that phytoplankton in the E-SAZ could be limited or co-limited by Co.

Based on the Pearson's correlation coefficient, dissolved Zn concentrations were related to L-Chlb, S-Chlb, S-peridinin, and S-prasinoxanthin, biomarker pigments mostly present in the E-SAZ and at depth in the W-SAZ (50 m), suggesting that Zn nutrition is important in these regions. This observation is reinforced by the fact that higher dissolved ecological stoichiometry was observed at Stns 9 and 10 and that data from the depth of the Chl maximum had a Zn and Cd concentration much lower than those predicted from the dZn/Chla and dCd/Chla. Co was significantly related to L-peridinin, L-Chlb, S-Chlb, S-fucoxanthin, S-but-fucoxanthin, and S-zeaxanthin. Because these biomarker pigments are mainly present in the W-SAZ (Stn 4, 50 m) and in the E-SAZ (Stns 10–17), it suggests that Co could shape the structure of the phytoplankton community in the SAZ region. The effect of Co on S-Chlb and S-zeaxanthin is not surprising given that studies have demonstrated a strict Co requirement in cyanobacteria (Sunda and Huntsman, 1995a; Saito et al., 2002). Oceanic prasinophytes and dinoflagellates, the dominating phytoplankton in the SAZ region, have a greater requirement in Zn, Co, and Cd than diatoms (Ho et al., 2003). Laboratory work demonstrated that the haptophyte, *Phaeocystis*, and diatoms prefer Zn to satisfy their growth requirement, while the haptophyte, *E. huxleyi* prefers Co (Sunda and Huntsman, 2000; Saito and Goepfert, 2008). An elevated dZn/dCo ratio, could favor the growth of diatoms and *Phaeocystis* and be a disadvantage for the growth of *E. huxleyi* (Sunda and Huntsman, 1995a; Saito and Goepfert, 2008). In this study, dZn/dCo was more strongly related to hex-fucoxanthin a biomarker for haptophytes and dinoflagellates (type 2), but not significantly related to fucoxanthin. This might be because fucoxanthin is not only present in diatoms, but also in haptophytes, chrysophytes, and

some dinoflagellates (Jeffrey and Wright, 2006). It should be noted that, in the field, the preference for Zn or Co for natural phytoplankton communities remains largely unknown (e.g., Croot et al., 2002).

Iron is also known to affect the biological uptake of other micronutrients (e.g., Cullen et al., 2003; Ho et al., 2003; Twining et al., 2004b; Cullen and Sherrell, 2005). It, therefore, appears that complex interconnections exist between these metals and phytoplankton. In fact, a significant negative correlation for dFe with dZn/dCo and a high coefficient of correlation (although not statistically significant, 0.4) with hex-fucoxanthin, suggest an interaction between Fe, Zn, and Co in the control of the phytoplankton community in the SAZ region.

This study also focuses on other micronutrients for which data are yet limited. Both Cu and Ni had the same pattern of correlations with biomarker pigments; however, little is known of a coupled effect for Cu and Ni on phytoplankton growth. Both these micronutrients were significantly correlated to L-peridinin, S-peridinin, L-hex-fucoxanthin, S-zeaxanthin, S-prasinolanthin, S-Chl*b*, demonstrating an effect on most major phytoplankton groups, except diatoms. Cu is involved in nitrogen cycling, electron transfer associated with photosynthesis and Fe uptake (Morel et al., 2003; Maldonado et al., 2006), and Ni is involved in urea assimilation and protection against reactive oxygen species (Morel et al., 2003; Dupont et al., 2010). The disappearance ratios for Ni and Cu are close to previously reported values (Table 3). Comparison of the dCu/PO₄ with cellular Cu:P ratio for *Thalassiosira oceanica* and *E. huxleyi* (Table 3), as well as other oceanic species including dinoflagellates (Cu:P 60–110 μmol:μmol, Ho et al., 2003), suggests that Cu was present at an optimal level for the growth of these eukaryotic phytoplankton. For dCu, a relation with PO₄ ($r^2 > 0.75$) was only observed for stations within the W-SAZ and E-SAZ, suggesting a nutrition role in these regions. For Ni, the disappearance ratio measured here (Table 3) was also greater than cellular Ni:P ratios for diatoms and flagellates (160–1150 μmol:μmol, Twining et al., 2004b), suggesting optimal conditions for growth in the study region.

As a cautionary note, the disappearance ratios used here can be influenced by scavenging processes, surface input, organic complexation, recycling, and remineralization, biological uptake, and drawdown (e.g., Saito et al., 2010; Croot et al., 2011). Recent studies highlighted important differences in Zn organic speciation between the SAZ and the PFZ, with greater inorganic Zn concentration found in the PFZ (e.g., Ellwood, 2004; Baars and Croot, 2011). For micronutrients that are influenced by short time processes (such as Fe), it is expected that this relation (metal to PO₄) will be significantly blurred, and less meaningful. In addition, snapshot studies will invariably fail to represent the dynamic situation between micronutrients and phytoplankton. For example, grazing, recycling, supply, and phytoplankton succession are not considered. During SAZ-Sense, regenerated production exceeded new production (Cavagna et al., 2011) and grazing dilution experiments demonstrated the complexity of the processes at

play with on average 36–37% herbivory, 39–42% bacterivory, and 21–24% cyanobacterivory (Stns 4 and 17; Pearce et al., 2011). Grazing is paramount for nutrient recycling, which was very efficient for Fe in the E-SAZ (Bowie et al., 2009). Nonetheless, our study provides much needed information on the biological relevance of micronutrients, other than iron during the austral summer of 2007. It indicated that Zn, Co, and Cd inter-replacement was influential in the E-SAZ region and that interaction between these micronutrients and Fe needs to be considered. Our results also demonstrated that different phytoplankton size classes and functional groups are related differently to micronutrients, possibly attributed to variable biological requirements for growth. Generally, larger phytoplankton have greater micronutrient requirement for growth (Sarothou et al., 2005; Hassler and Schoemann, 2009; Finkel et al., 2010). Here, L-phyto were not more strongly related to micronutrients than S-phyto, illustrating the complexity at play in the field.

If the E-SAZ, represents the future of the SAZ region, further investigations on the relations among Fe, Cd, Zn, and Co and their ability to shape the structure of the phytoplankton community is required. In addition, effort should be made to increase our knowledge of the micronutrient requirement for dinoflagellates, a dominant group in the E-SAZ. To integrate the key processes at play, ship-board experiments would be required to study the effect of micronutrients on the natural phytoplankton community and measure their requirement for growth (e.g., Coale et al., 2003). Because macro- and micronutrients support biological processes that are interrelated or have synergistic or antagonistic relations, an experimental approach at sea should investigate these complex interactions, rather than focusing on a single element.

ACKNOWLEDGMENTS

This research was supported by the Australian Government Cooperative Research Centres Programme through the Antarctic Climate and Ecosystems CRC (ACE CRC), by Australian Antarctic Science grants AAS 2720 and AAS 2602, and it was formally part of the International Polar Year – GEOTRACES project. Hassler was supported by CSIRO and UTS Chancellor Fellowships, Sinoir was supported by the Quantitative Marine Science program from the University of Tasmania. We are grateful to Andrew Bowie, Brian Griffiths, and Tom Trull for giving us the opportunity to join the SAZ-Sense voyage, the captain and crew of RSV *Aurora Australis*, Philip Boyd, Delphine Lanuzel, Tomas Remenyi, Véronique Schoemann, Isabelle Dumont, Thibault Wagener, and Florence Masson for their assistance at sea, Jeanette O'Sullivan and Roslyn Watson for their carrying out the FI-SPE-ICP-MS analysis, Mark Rosenberg, Neale Johnston, Alicia Navidad, and Suellen Cook for the determination of macronutrients and other hydrological parameters at sea and calibration of the CTD sensors, Simon Wright for the total Chl*a* dataset associated with CTD operations, and Diana Davies for the maintenance of the SAZ-Sense website (www.cmar.csiro.au/datacentre/saz-sense).

REFERENCES

- Arrigo, K. R., Robinson, D. H., Worthen, D. L., Dunbar, R. B., DiTullio, G. R., Van Woert, M., and Lizotte, M. P. (1999). Phytoplankton community structure and the drawdown of nutrients and CO₂ in the Southern Ocean. *Science* 283, 365–367.
- Baars, O., and Croot, P. L. (2011). The speciation of dissolved zinc in the Atlantic sector of the Southern Ocean. *Deep Sea Res.* Part 2 Top. Stud. Oceanogr. 58, 2720–2732.
- Banase, K. (1996). Low seasonality of low concentrations of surface

- chlorophyll in the Subantarctic water ring: underwater irradiance, iron, or grazing? *Prog. Oceanogr.* 37, 241–291.
- Billar, D. V., and Bruland, K. W. (2012). Analysis of Mn, Fe, Co, Ni, Cu, Zn, Cd, and Pb in seawater using the Nobias-chelate PA1 resin and magnetic sector inductively coupled plasma mass spectrometry (ICP-MS). *Mar. Chem.* 130–131, 12–20.
- Bowie, A. R., Lannuzel, D., Remenyi, T. A., Wagener, T., Lam, P. J., Boyd, P. W., Guieu, C., Townsend, A. T., and Trull, T. W. (2009). Biogeochemical iron budgets of the Southern Ocean south of Australia: decoupling of iron and nutrient cycles in the subantarctic zone by the summertime supply. *Global Biogeochem. Cycles* 23, GB4034.
- Bowie, A. R., Trull, T. W., Griffiths, F. B., and Dehairs, F. (2011a). Estimating the sensitivity of the subantarctic zone to environmental change: the SAZ-Sense project. *Deep Sea Res. Part II Top. Stud. Oceanogr.* 58, 2051–2058.
- Bowie, A. R., Griffiths, F. B., Dehairs, F., and Trull, T. W. (2011b). Oceanography of the subantarctic and polar frontal zones south of Australia during summer: setting for the SAZ-Sense study. *Deep Sea Res. Part 2 Top. Stud. Oceanogr.* 58, 2059–2070.
- Bruland, K. W. (1980). Oceanographic distributions of cadmium, zinc, nickel and copper in the North Pacific. *Earth Planet. Sci. Lett.* 47, 176–198.
- Buitenhuis, E., Timmermans, K. R., and de Baar, H. J. W. (2003). Zinc-bicarbonate colimitation of *Emiliania huxleyi*. *Limnol. Oceanogr.* 48, 1575–1582.
- Cavagna, A. J., Elskens, M., Griffiths, F. B., Fripiat, F., Jacquet, S. H. M., Westwood, K. J., and Dehairs, F. (2011). Contrasting regimes of production and potential for carbon export in the Sub-Antarctic and Polar Frontal Zones south of Tasmania. *Deep Sea Res. Part 2 Top. Stud. Oceanogr.* 58, 2235–2247.
- Coale, K. H., Wang, X., Tanner, S. J., and Johnson, K. S. (2003). Phytoplankton growth and biological response to iron and zinc addition in the Ross Sea and Antarctic Circumpolar Current along 170°W. *Deep Sea Res. Part 2 Top. Stud. Oceanogr.* 50, 653–653.
- Croft, P. L., Baars, O., and Streu, P. (2011). The Distribution of zinc in the Atlantic sector of the Southern Ocean. *Deep Sea Res. Part 2 Top. Stud. Oceanogr.* 58, 2707–2719.
- Croft, P. L., Karlson, B., Wulff, A., Linares, F., and Andersson, K. (2002). Trace metal/phytoplankton interactions in the skagerrak. *J. Mar. Syst.* 35, 39–60.
- Cullen, J. T., Chase, Z., Coale, K. H., Fitzwater, S. E., and Sherrell, R. M. (2003). Effect of iron limitation on the cadmium to phosphorous ratio of natural phytoplankton assemblages from the Southern Ocean. *Limnol. Oceanogr.* 48, 1079–1087.
- Cullen, J. T., and Sherrell, R. M. (2005). Effects of dissolved carbon dioxide, zinc, and manganese on the cadmium to phosphorus ratio in natural phytoplankton assemblages. *Limnol. Oceanogr.* 50, 1193–1204.
- de Baar, H. J. W., van Leeuwe, M. A., Scharek, R., Goeyens, L., Bakker, K. M. J., and Fritsche, P. (1997). Nutrient anomalies in *Fragilariopsis kerguelensis* blooms, iron deficiency and the nitrate/phosphate ratio (A. C. Redfield) of the Antarctic Ocean. *Deep Sea Res. Part 2 Top. Stud. Oceanogr.* 44, 229–260.
- de Salas, M. F., Eriksen, R., Davidson, A. T., and Wright, S. W. (2011). Protistan communities in the Australian sector of the Sub-Antarctic zone during SAZ-Sense. *Deep Sea Res. Part 2 Top. Stud. Oceanogr.* 58, 2135–2149.
- Dupont, C. L., Barbeau, K., and Palenik, B. (2008). Ni limitation and uptake in marine *Synechococcus*. *Appl. Environ. Microbiol.* 74, 23–31.
- Dupont, C. L., Buck, K. N., Palenik, B., and Barbeau, K. (2010). Nickel utilization in phytoplankton assemblages from contrasting oceanic regimes. *Deep Sea Res. Part 2 Top. Stud. Oceanogr.* 57, 553–566.
- Ebersbach, F., Trull, T. W., Davies, D. M., and Bray, S. G. (2011). Controls on mesopelagic particle fluxes in the Sub-Antarctic and Polar Frontal Zones in the Southern Ocean south of Australia in summer – perspectives from free-drifting sediment traps. *Deep Sea Res. Part 2 Top. Stud. Oceanogr.* 58, 2260–2276.
- Ellwood, M. J. (2004). Zinc and cadmium speciation in subantarctic waters east of New Zealand. *Mar. Chem.* 87, 37–58.
- Ellwood, M. J. (2008). Wintertime trace metal (Zn, Cu, Ni, Cd, Pb and Co) and nutrient distributions in the subantarctic zone between 40–52°S; 155–160°E. *Marine Chem.* 112, 107–117.
- Ellwood, M. J., van den Berg, C. M. G., Boye, M., Veldhuis, M., Jong, J. T. M., de Baar, H. J. W., de Croot, P. L., and Kattner, G. (2005). Organic complexation of cobalt across the Antarctic Polar Front. *Mar. Freshw. Res.* 56, 1069–1075.
- Finkel, Z. V., Beardall, J., Flynn, K. J., Quigg, A., Rees, T. A. V., and Raven, J. A. (2010). Phytoplankton in a changing world: cell size and elemental stoichiometry. *J. Plankton Res.* 32, 119–137.
- Finkel, Z. V., Quigg, A. S., Chimpampi, R. K., Schofield, O. E., and Falkowski, P. G. (2007). Phylogenetic diversity in cadmium: phosphorus ratio regulation by marine phytoplankton. *Limnol. Oceanogr.* 52, 1131–1138.
- Fitzwater, S. E., Johnson, K. S., Gordon, R. M., Coale, K. H., and Smith, W. O. Jr. (2000). Trace metal concentrations in the Ross Sea and their relationship with nutrients and phytoplankton growth. *Deep Sea Res. Part 2 Top. Stud. Oceanogr.* 47, 3159–3179.
- Fripiat, F., Leblanc, K., Elskens, M., Cavagna, A. J., Armand, L., André, L., Dehairs, F., and Cardinal, D. (2011). Efficient silicon recycling in summer in both the Polar Frontal and Subantarctic Zones of the Southern Ocean. *Mar. Ecol. Prog. Ser.* 435, 33–45.
- Hassler, C. S., and Schoemann, V. (2009). Bioavailability of organically bound Fe to model phytoplankton of the Southern Ocean. *Biogeosciences* 6, 2281–2296.
- Hassler, C. S., Schoemann, V., Mancuso Nichols, C. A., Butler, E. C. V., and Boyd, P. W. (2011). Saccharides enhance iron bioavailability to southern ocean phytoplankton. *Proc. Natl. Acad. Sci. U.S.A.* 108, 1076–1081.
- Herraiz Borreguero, L., and Rintoul, S. R. (2011). Regional circulation and its impact on upper ocean variability south of Tasmania. *Deep Sea Res. Part 2 Top. Stud. Oceanogr.* 58, 2071–2081.
- Hill, K. S., Rintoul, S. R., Coleman, R., and Ridgway, K. R. (2008). Wind forced low frequency variability of the East Australia Current. *Geophys. Res. Lett.* 35, L08602.
- Ho, T. Y., Quigg, A., Finkel, Z. V., Milligan, A. J., Wyman, K., Falkowski, P. G., and Morel, F. M. M. (2003). The elemental composition of some marine phytoplankton. *J. Phycol.* 39, 1145–1159.
- Jacquet, S. H. M., Lam, P. J., Trull, T. W., and Dehairs, F. (2011). Carbon export production in the Sub-Antarctic zone and Polar Front Zone south of Tasmania. *Deep Sea Res. Part 2 Top. Stud. Oceanogr.* 58, 2277–2292.
- Jeffrey, S. W., and Vesik, M. (1997). “Introduction to marine phytoplankton and their pigment signatures”, in *Phytoplankton Pigments in Oceanography: Guidelines to Modern Methods*, eds S. W. Jeffrey, R. F. C. Mantoura, and S. W. Wright (Paris: UNESCO Publishing), 37–84.
- Jeffrey, S. W., and Wright, S. W. (2006). “Photosynthetic pigments in marine microalgae: insights from cultures and the sea”, in *Algal Cultures, Analogies of Blooms and Applications*, ed. D. V. Subba Rao (Enfield, NH: Science Publishers), 33–90.
- Kidston, M., Matear, R., and Baird, M. E. (2011). Parameter optimization of a marine ecosystem model at two contrasting stations in the sub-Antarctic zone. *Deep Sea Res. Part 2 Top. Stud. Oceanogr.* 58, 2301–2315.
- Kopczynska, E., Savoye, N., Dehairs, F., Cardinal, D., and Elskens, M. (2007). Spring phytoplankton assemblages in the Southern Ocean between Australia and Antarctica. *Polar Biol.* 31, 77–88.
- Kopczynska, E. E., Dehairs, F., Elskens, M., and Wright, S. (2001). Phytoplankton and microzooplankton variability between the Subtropical and Polar Fronts south of Australia: thriving under regenerative and new production in late summer. *J. Geophys. Res.* 106, 31597–31609.
- Lai, X., Norisuye, K., Mikata, M., Minami, T., Bowie, A. R., and Sohrin, Y. (2008). Spatial and temporal distribution of Fe, Ni, Cu and Pb along 140°E in the Southern Ocean during austral summer 2001/02. *Mar. Chem.* 111, 171–183.
- Lane, T. W., Saito, M. A., George, G. N., Pickering, I. J., Prince, R. C., and Morel, F. M. (2005). A cadmium enzyme from a marine diatom. *Nature* 435, 42.
- Lannuzel, D., Remenyi, T., Lam, P. J., Townsend, A., Ibanmami, E., Butler, E., Wagener, T., Schoemann, V., and Bowie, A. R. (2011). Distributions of dissolved and particulate iron in the Sub-Antarctic and Polar Frontal Southern Ocean (Australian sector). *Deep Sea Res. Part 2 Top. Stud. Oceanogr.* 58, 2094–2112.
- Levitov, S., Conkright, M. E., Reid, J. L., Najjar, R. G., and Mantyla, A. (1993). Distribution of nitrate, phosphate and silicate in the world oceans. *Prog. Oceanogr.* 31, 245–273.
- Li, W. K. W. (1998). Annual average abundance of heterotrophic bacteria and *Synechococcus* in surface ocean waters. *Limnol. Oceanogr.* 43, 1745–1753.

- Lohan, M. C., Crawford, D. W., Purdie, D. A., and Statham, P. J. (2005). Iron and zinc enrichment in the north eastern subarctic Pacific: ligand production and zinc bioavailability in response to phytoplankton growth. *Limnol. Oceanogr.* 50, 1427–1437.
- Lohan, M. C., Statham, P. J., and Crawford, D. W. (2002). Total dissolved Zinc in the upper water column of the subarctic North east Pacific. *Deep Sea Res. Part 2 Top. Stud. Oceanogr.* 24–25, 5793–5808.
- Maldonado, M. T., Allen, A. E., Chong, J. S., Lin, K., Leus, D., Karpenko, N., and Harris, S. L. (2006). Copper-dependent iron transport in coastal and oceanic diatoms. *Limnol. Oceanogr.* 51, 1729–1743.
- Martin, J. H., Gordon, R. M., and Fitzwater, S. E. (1990). Fe in Antarctic waters. *Nature* 345, 156–158.
- Martin, J. H., Gordon, R. M., Fitzwater, S. E., and Broenkow, W. W. (1989). VERTEX: phytoplankton/iron studies in the Gulf of Alaska. *Deep Sea Res. Part 2 Top. Stud. Oceanogr.* 36, 649–680.
- McNeil, B. I., Tillbrook, B., and Matear, R. J. (2001). Accumulation and uptake of anthropogenic CO₂ in the Southern Ocean, south of Australia between 1968 and 1996. *J. Geophys. Res.* 106, C12.
- Metzl, N., Tillbrook, B., and Poisson, A. (1999). The annual fCO₂ cycle and the air-sea CO₂ flux in the sub-Antarctic ocean. *Tellus B Chem. Phys. Meteorol.* 51B, 849–861.
- Moffett, J. W., and Brand, L. E. (1996). Production of strong extracellular Cu chelators by marine cyanobacteria in response to Cu stress. *Limnol. Oceanogr.* 41, 388–395.
- Mongin, M., Matear, R., and Chamberlain, M. (2011). Seasonal and spatial variability of remotely sensed chlorophyll and physical fields in the SAZ-Sense region. *Deep Sea Res. Part 2 Top. Stud. Oceanogr.* 58, 2082–2093.
- Morel, F. M. M., Milligan, A. J., and Saito, M. A. (2003). Marine bioinorganic chemistry: the role of trace of metals in the oceanic cycles of major nutrients. *Treatise Geochem.* 6, 113–143.
- Morel, F. M. M., and Price, N. M. (2003). The biogeochemical cycles of trace metals in the oceans. *Science* 300, 944–947.
- Morel, F. M. M., Reinfelder, J. R., Roberts, S. B., Chamberlain, C. P., Lee, J. G., and Yee, D. (1994). Zinc and carbon co-limitation of marine phytoplankton. *Nature* 369, 740–742.
- Pearce, I., Davidson, A. T., Thomson, P., Wright, S. W., and van den Enden, R. (2011). Marine microbial ecology in the Sub-Antarctic Zone: rates of bacterial and phytoplankton growth and grazing by heterotrophic protists. *Deep Sea Res. Part 2 Top. Stud. Oceanogr.* 58, 2248–2259.
- Price, N. M., and Morel, F. M. M. (1990). Cd and Co substitution for Zn in a marine diatom. *Nature* 344, 658–660.
- Quigg, A., Finkel, Z. V., Irwin, A. J., Rosenthal, Y., Ho, T. Y., Reinfelder, J. R., Schofield, O., Morel, F. M. M., and Falkowski, P. G. (2003). The evolutionary inheritance of elemental stoichiometry in marine phytoplankton. *Nature* 425, 291–294.
- Quigg, A., Irwin, A. J., and Finkel, Z. V. (2011). Evolutionary inheritance of elemental stoichiometry in phytoplankton. *Proc. R. Soc. B Biol. Sci.* 278, 526–534.
- Redfield, A. C., Ketchum, B. H., and Richards, F. A. (1963). “The influence of organisms on the composition of sea-water”, in *The Composition of Seawater. Comparative and Descriptive Oceanography. The Sea: Ideas and Observations on Progress in the Study of the Seas*, Vol. 2, ed. M. N. Hill (New York, NY: Interscience), 26–77.
- Ridgway, K. R. (2007). Seasonal circulation around Tasmania: an interface between eastern and western boundary dynamics. *J. Geophys. Res.* 112, C10016.
- Rintoul, S. R., and Trull, T. W. (2001). Seasonal evolution of the mixed layer in the Subantarctic Zone, south of Australia. *J. Geophys. Res.* 106, 31447–31462.
- Rosenberg, M. (2007). *Saz-Sense, Marine Science Cruise Au0703 – Oceanographic Field Measurements and Analysis*. unpublished report, Ace Cooperative Research Centre. Hobart, TAS, 23.
- Saito, M. A., and Goepfert, T. J. (2008). Zinc-cobalt colimitation in *Phaeocystis* Antarctica. *Limnol. Oceanogr.* 53, 266–275.
- Saito, M. A., Goepfert, T. J., Noble, A. E., Sedwick, P. N., and DiTullio, G. R. (2010). A seasonal study of dissolved cobalt in the Ross Sea of Antarctica: micronutrient control, absence of observed scavenging, and relationships with Zn, Cd, and P. *Biogeochemistry* 7, 4059–4082.
- Saito, M. A., Goepfert, T. J., and Ritt, J. T. (2008). Some thoughts on the concept of co-limitation: three definitions and the importance of bioavailability. *Limnol. Oceanogr.* 53, 276–290.
- Saito, M. A., and Moffett, J. W. (2001). Complexation of cobalt by natural organic ligands in the Sargasso Sea as determined by a new high-sensitivity electrochemical cobalt speciation method suitable for open ocean work. *Mar. Chem.* 75, 49–68.
- Saito, M. A., Moffett, J. W., Chisholm, S. W., and Waterbury, J. B. (2002). Cobalt uptake in *Prochlorococcus*. *Limnol. Oceanogr.* 47, 1629–1636.
- Sarthou, G., Timmermans, K., Blain, S., and Tréguer, P. (2005). Growth physiology and fate of diatoms in the ocean: a review. *J. Sea Res.* 53, 25–42.
- Schlitzer, R. (2012). *Ocean Data View (version 4.5)*. Available at: <http://odv.awi.de>
- Sedwick, P. N., Garcia, N. S., Riseman, S. F., Marsay, C. M., and DiTullio, G. R. (2007). Evidence for high iron requirements of colonial *Phaeocystis antarctica* at low irradiance. *Biogeochemistry* 83, 83–97.
- Shelley, R. U., Zachhuber, B., Sedwick, P. N., Worsfold, P. J., and Lohan, M. C. (2010). Determination of total dissolved cobalt in UV-irradiated seawater using flow injection with chemiluminescence detection. *Limnol. Oceanogr. Methods* 8, 352–362.
- Sokolov, S., and Rintoul, S. R. (2002). Structure of Southern Ocean fronts at 140°E. *J. Mar. Syst.* 37, 151–184.
- Sunda, W. G., and Huntsman, S. A. (1995a). Regulation of copper concentration in the oceanic nutricline by phytoplankton uptake and regeneration cycles. *Limnol. Oceanogr.* 40, 132–137.
- Sunda, W. G., and Huntsman, S. A. (1995b). Cobalt and zinc interreplacement in marine phytoplankton: biological and biogeochemical implications. *Limnol. Oceanogr.* 40, 1404–1407.
- Sunda, W. G., and Huntsman, S. A. (2000). Effect of Zn, Mn, and Fe on Cd accumulation in phytoplankton: implications for oceanic Cd cycling. *Limnol. Oceanogr.* 45, 1501–1516.
- Timmermans, K. R., Snoek, J., Gerringa, L. J. A., Zondervan, I., and de Baar, H. J. W. (2001). Not all eukaryotic algae can replace zinc with cobalt: *Chaetoceros* *Calcitrans* (Bacillariophyceae) versus *Emiliania huxleyi* (Prymnesiophyceae). *Limnol. Oceanogr.* 46, 699–703.
- Toggweiler, J. R., and Russell, J. (2008). Ocean circulation in a warming climate. *Nature* 451, 286–288.
- Trull, T. W., Rintoul, S. R., Hadfield, M., and Abraham, E. R. (2001). Circulation and seasonal evolution of Polar waters south of Australia: implications for iron fertilisation of the Southern Ocean. *Deep Sea Res. Part II Top. Stud. Oceanogr.* 48, 2439–2466.
- Twining, B. S., Baines, S. B., Fisher, N. S., and Landry, M. R. (2004a). Cellular iron contents of plankton during the Southern Ocean Iron Experiment (SOFEX). *Deep Sea Res. Part II Top. Stud. Oceanogr.* 51, 1827–1850.
- Twining, B. S., Baines, S. B., and Fisher, N. S. (2004b). Element stoichiometries of individual plankton cells collected during the Southern Ocean Iron Experiment (SOFEX). *Limnol. Oceanogr.* 49, 2115–2128.
- van Heukelem, L., and Thomas, C. (2001). Computer assisted high-performance liquid chromatography method development with applications to the isolation and analysis of phytoplankton pigments. *J. Chromatogr. A* 910, 31–49.
- Watson, R. J., Butler, E. C. V., Clementson, L. A., and Berry, K. M. (2005). Flow analysis with fluorescence detection for the determination of trace levels of ammonium in seawater. *J. Environ. Monit.* 7, 37–42.
- Westwood, K. J., Griffiths, F. B., Webb, J. P., and Wright, S. W. (2011). Primary production in the Sub-Antarctic and Polar Frontal zones south of Tasmania, Australia; SAZ-Sense survey, 2007. *Deep Sea Res. Part II Top. Stud. Oceanogr.* 58, 2162–2178.

Conflict of Interest Statement: The authors declare that the research was conducted in the absence of any commercial or financial relationships that could be construed as a potential conflict of interest.

Received: 09 December 2011; accepted: 16 May 2012; published online: 10 July 2012.
Citation: Hassler CS, Sinoir M, Clementson LA and Butler ECV (2012) Exploring the link between micronutrients and phytoplankton in the Southern Ocean during the 2007 austral summer. *Front. Microbio.* 3:202. doi: 10.3389/fmicb.2012.00202
This article was submitted to *Frontiers in Microbiological Chemistry*, a specialty of *Frontiers in Microbiology*.
Copyright © 2012 Hassler, Sinoir, Clementson and Butler. This is an open-access article distributed under the terms of the Creative Commons Attribution License, which permits use, distribution and reproduction in other forums, provided the original authors and source are credited and subject to any copyright notices concerning any third-party graphics etc.

APPENDIX

Table A1 | Summary of important properties from the W-SAZ (Stn 4), PFZ (Stn 6), and E-SAZ (Stn 9) during the SAZ-Sense study.

Properties	W-SAZ	PFZ	E-SAZ
Euphotic layer depth ¹ , m	61 ± 5	76 ± 14	47 ± 13
Mixed layer depth ² , m	41 ± 18	53 ± 6	79 ± 2 (16 ± 2)
Integrated Chl <i>a</i> ³	46.0 ± 11.5	58.8 ± 2.9	62.4 ± 20.0
Gross primary production ⁴	93 ± 49	37 ± 7	60 ± 29
Grazing rate ⁵	82 ± 38	47 ± 10	67 ± 12
Remineralization rate ⁶	2.1 ± 0.4	5.0 ± 1.6	3.7 ± 0.4
Nitrate seasonal depletion ⁷	8.9 ± 1.8	8.1 ± 0.4	11.0 ± 1.7
N:P seasonal depletion ratio ⁸	16 ± 6	12 ± 1	17 ± 3

¹From Westwood et al. (2011), ²Calculated after Rintoul and Trull (2001), a distinct shallow mixed layer depth is shown in bracket for the E-SAZ, see Mongin et al. (2011), ³0–150 m (mg m⁻²), from Westwood et al. (2011), ⁴mmol Cm⁻² d⁻¹, from Cavagna et al. (2011), ⁵% Total Primary Production removed, from Pearce et al. (2011), ⁶Mesopelagic C remineralization, 100–600 m (mmol Cm⁻² d⁻¹) from Jacquet et al. (2011), ⁷Mixed layer N depletion uses means from 150 to 200 m depth to represent winter surface values (mmol L⁻¹) from Bowie et al. (2011b), ⁸Mixed layer N:P ratio uses means from 150 to 200 m depth to represent winter surface values from Bowie et al. (2011b).

Table A2 | Metal disappearance ratio relative to dissolved phosphate for each station.

Stn #	Latitude (°S)	Longitude (°E)	Co	Zn	Cd	Ni	Cu
2	44.89	143.05	20.4	NA	147	1.52	ND
			(0.92)		(0.52)	(1.00)	0.28
			11.0		433	1.67	(0.85)
4	46.32	140.61	(0.54)	NA	(0.99)	(0.91)	
			13.6		159	1.12	ND
			(0.84)		(0.74)	(0.60)	0.63
5	48.99	143	12.5	NA	486	1.84	(0.95)
			(0.58)		(0.96)	(0.95)	
			106		871	5.50	0.27
6	54.00	145.88	(0.98)	NA	(1.00)	(0.96)	(0.76)
			7.02		379	1.70	0.31
			(0.53)		(0.99)	(0.98)	(0.87)
9	50.87	148.65	ND	4.73	489	0.73	0.72
			ND	(0.60)	(0.92)	(0.73)	(0.71)
				7.38	463	1.58	1.31
10	50.00	149.42	(0.86)	NA	(0.90)	(0.95)	(0.76)
			ND		ND	ND	–2.55
			79.4		258	4.73	(0.45)
12	48.06	151.20	(0.72)	NA	(0.67)	(0.40)	ND
			180		ND	ND	ND
			(0.42)		931	ND	ND
17b	45.55	153.18	ND	8.36	(0.84)		
				(0.50)			
				7.64			
17j	45.55	153.18	(0.41)	NA			
			46.8		456	1.70	0.62
			(0.90)		(0.97)	(0.57)	(0.78)
17b	45.55	153.18	59.2	5.77	451	1.32	0.29
			(0.70)	(0.48)	(0.76)	(0.64)	(0.34)
			20.6	ND			
17j	45.55	153.18	(0.80)	NA			
			5.00		84.9	1.46	0.35
			(0.32)		(0.86)	(0.91)	(0.98)
17j	45.55	153.18	24 (0.73)	1.29	346	1.92	0.35
			6.17	(0.59)	(0.98)	(1.00)	(0.91)
			(0.62)	(0.54)	(0.86)	(0.72)	(0.72)
17j	45.55	153.18		0.73	142	1.08	0.24
				(0.54)	(0.86)	(0.72)	(0.72)
				0.61	371	1.78	0.36
17j	45.55	153.18		(0.83)	(0.94)	(0.98)	(0.92)

Disappearance ratios are presented with their coefficient of correlation (r^2 , in bracket) for depths between 0 and 100 m (roman font, $n = 4$) and 125–1000 m (italic font, $n = 7$). Disappearance ratio is given in $\text{pM}/\mu\text{M}$ for Co, Cd, and Ni, and in $\text{nM}/\mu\text{M}$ for Cu and Zn. NA = not applicable due to lack of data, ND = not detected as $r^2 < 0.3$.

[illegible]

The significance of the correlation is based on the *p* value (*p* > 0.05) obtained for a 95% confidence interval (data not shown). Values in red are significantly negatively correlated in and values in yellow are significantly positively correlated. The correlation between physical properties (temperature, *T*, and salinity, *S*), macronutrients, micronutrients, and the chlorophyll *a* (Chl *a*) associated with the total, large (L_r > 10 μ m) and small (S , 0.8–10 μ m) phytoplankton communities were analyzed. Macronutrients are: silicic acid (Si); $\text{NO}_2 + \text{NO}_3$ (NOx); phosphate (Ph); ammonia (A); nitrite (Ni); copper (Cu); zinc (Zn); cadmium (Cd); iron (Fe). Fe data are from Lannuzel et al. (2011).

Table A4 | Pearson correlation table showing the coefficient of correlation between two parameters considering all stations and al depths (0–125 m).

Variables		SI														
NOx		0.19														
Ph		0.28	0.98													
A		−0.05	0.00	0.12												
N		−0.32	0.52	0.54	0.45											
LP		−0.22	−0.30	−0.27	0.27	−0.23										
LBF		0.21	0.79	0.76	−0.14	0.09	0.08									
LF		−0.10	0.77	0.76	0.05	0.24	−0.16	LBF	0.82							
LHF		0.22	0.002	0.03	0.47	−0.40	0.51	0.19	0.25	0.09	LHF					
LChl		−0.21	0.38	0.33	−0.02	0.21	0.21	0.08	0.09	0.16	LChl b					
SP		−0.23	−0.36	−0.34	0.22	−0.23	0.48	−0.15	−0.30	0.09	0.04	SP				
SBF		0.35	−0.158	−0.13	0.39	−0.16	0.04	0.05	0.05	0.41	−0.23	−0.04	SBF	0.71	−0.03	sf
SF		0.71	0.33	0.37	0.37	−0.005	0.003	0.39	0.32	0.21	−0.11	−0.03	0.98	−0.03	−0.03	SPr
SPr		−0.25	−0.39	−0.36	0.26	−0.26	0.65	−0.11	−0.30	0.20	0.09	0.40	−0.20	−0.28	−0.45	SHF
SHF		−0.09	0.09	0.11	−0.20	0.76	−0.46	−0.04	0.07	−0.43	−0.20	0.62	−0.01	0.10	0.73	SZea
SZea		0.03	−0.35	−0.33	0.21	−0.42	0.866	−0.02	−0.34	0.41	0.23	0.37	0.08	0.19	−0.58	−0.62
SChl b		−0.21	−0.33	−0.34	0.30	−0.43	0.42	−0.07	−0.08	0.38	0.47	0.41	0.41	0.41	0.57	

The significance of the correlation is based on the p value ($p > 0.05$) obtained for a 95% confidence interval (data not shown). Values in red are significantly negatively correlated in and values in yellow are significantly positively correlated. The correlation between macronutrients and the pigments representative of the different phytoplankton species found in the community were analyzed. Pigments associated with the large (> 10 μm) and the small (S, 0.8–10 μm) phytoplankton communities were distinguished. The parameters selected are silicic acid (SI), NO₂ + NO₃ (NOx); phosphates (Ph); ammonia (A); nitrite (N); Chlorophyll b (Chl b); Peridin (P); 19-But-Fucoxanthin (BF); Fucoxanthin (F); 19-Hex-fucoxanthin (HF); Prasinoxanthin (Pr); zeaxanthin (Zea).

Table A5 | Pearson correlation table showing the coefficient of correlation between two parameters considering all stations and al depths (0–125 m).

Variables		Co															
Ni	0.90																
Cu	0.77	0.91															
Zn	0.72	0.63	0.51														
Cd	0.90	0.93	0.82	0.75													
Fe	-0.55	-0.54	-0.40	-0.77	0.55												
Zn/Co	0.13	0.14	0.08	0.71	0.23	Fe	-0.74										
LP	-0.30	-0.23	-0.24	-0.34	-0.22	Zn/Co	0.52	-0.24									
LBF	0.54	0.77	0.66	0.62	0.64	LP	0.19	0.08	LBF	0.82							
LF	0.65	0.73	0.58	0.62	0.64	LBF	-0.16	0.25	0.51	0.08	LF	0.20					
LHF	-0.15	-0.09	0.08	-0.50	-0.17	LF	-0.67	0.47	-0.40	0.21	LHF	0.16	LChl b				
LChl b	-0.08	-0.11	-0.15	-0.05	-0.22	LHF	0.06	0.06	0.11	0.30	0.09	0.41	0.23	0.04	SP		
SP	-0.47	-0.27	-0.28	-0.33	-0.30	LChl b	0.18	0.18	-0.37	0.05	0.32	0.21	-0.11	-0.03	SBF	SF	SPi
SBF	0.18	0.02	0.04	-0.20	0.07	SP	-0.24	-0.02	0.21	-0.30	0.20	0.09	-0.20	-0.28	-0.45	SHF	SZea
SF	0.34	0.33	0.13	0.16	0.34	SBF	0.32	0.22	0.42	0.43	0.07	0.34	0.41	0.23	0.37	0.08	0.41
SPi	-0.47	-0.28	-0.30	-0.37	-0.32	SF	0.27	0.27	0.55	-0.20	-0.03	0.21	-0.07	0.42	0.42	0.42	0.57
SHF	0.26	0.25	0.35	0.64	0.27	SPi	-0.40	-0.40	-0.49	-0.36	-0.58	-0.62	-0.58	-0.62	-0.58	-0.62	-0.57
SZea	-0.55	-0.37	-0.38	-0.54	-0.40	SHF	-0.49	-0.49	-0.58	-0.58	-0.62	-0.58	-0.62	-0.58	-0.62	-0.58	-0.57
SChl b	-0.48	-0.49	-0.58	-0.58	-0.49	SZea	-0.48	-0.48	-0.58	-0.58	-0.62	-0.58	-0.62	-0.58	-0.62	-0.58	-0.57

The significance of the correlation is based on the p value ($p > 0.05$) obtained for a 95% confidence interval (data not shown). Values in red are significantly negatively correlated in and values in yellow are significantly positively correlated. The correlation between micronutrients and the pigments representative of the different phytoplankton species found in the community were analyzed. Pigments associated with the large (> 10 μm) and the small (5, 0.8–10 μm) phytoplankton communities were distinguished. The parameters selected are cobalt (Co); nickel (Ni); copper (Cu); zinc (Zn); cadmium (Cd); iron (Fe); sum of Chlorophyll c (Chl c sum); Chlorophyll b (Chl b); Peridin (P); 19- But-Fucoxanthin (BF); Fucoxanthin (F); 19-Hex-fucoxanthin (HF); Prasinoxanthin (Pr); zeaxanthin (Zea). Fe data are from Lannuzel et al. (2011).

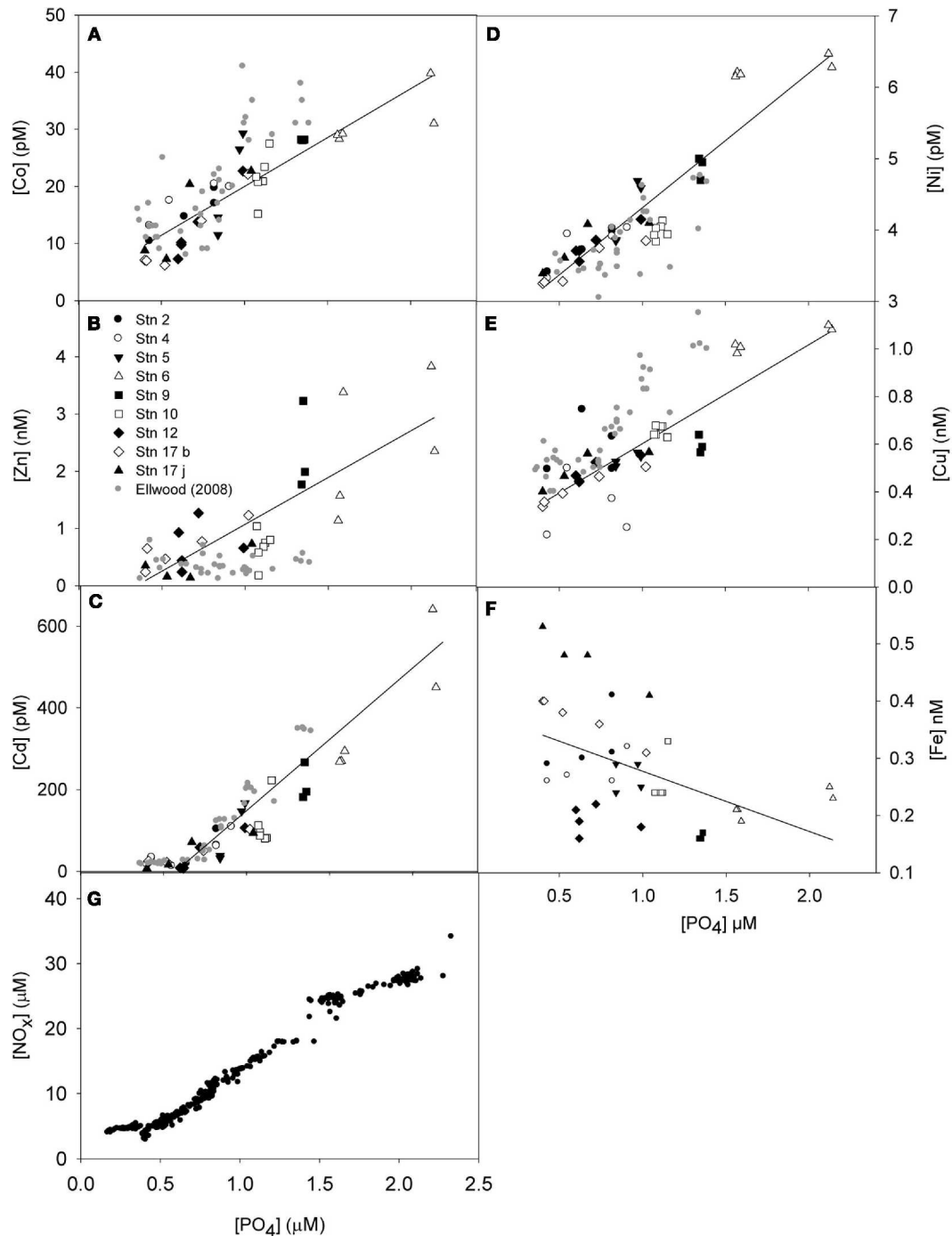


FIGURE A1 | Disappearance ratio of dissolved micronutrients Co (A), Zn (B), Cd (C), Ni (D), Cu (E), Fe (F) and macronutrient NO_3^- (G) with dissolved phosphate (PO_4) for the top 100 m for the Subantarctic and Polar Frontal Zone (Australian sector). Depths and stations are distinguished by different symbol. The slope and the

coefficient of correlation for linear regression are shown. Data from a previous study in the region is also shown (Ellwood, 2008). It is to be noted that Ellwood (2008) did not cross the North Polar Front into Antarctic Zone, which could explain some discrepancy. Data for Fe are from Lannuzel et al. (2011).

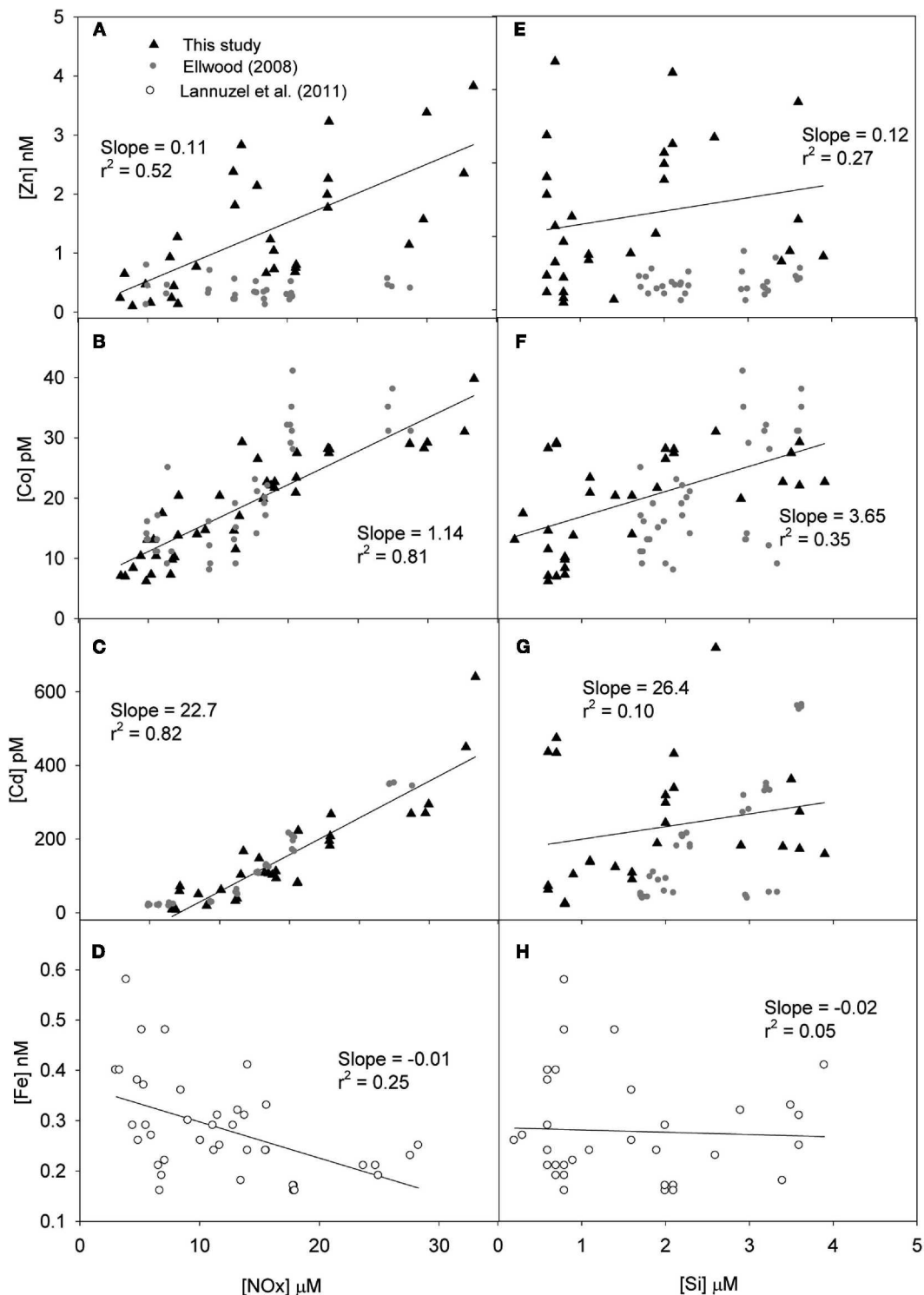


FIGURE A2 | Disappearance ratio of dissolved micronutrients (Zn, Co, Cd, Fe) with dissolved NO_x ($\text{NO}_2 + \text{NO}_3$, panels A, B, C, D, respectively) and silicic acid (Si, panels E, F, G, H, respectively) for the top 100 m for the Subantarctic and Polar Frontal Zone (Australian sector). Depths and stations are not differentiated. The

slope and the coefficient of correlation for linear regression are shown. Data from a previous study in the region is also shown (Ellwood, 2008). It is to be noted that Ellwood (2008) did not cross the North Polar Front into Antarctic Zone, which could explain some discrepancy. Data for Fe are from Lannuzel et al. (2011).



Impacts of microbial activity on the optical and copper-binding properties of leaf-litter leachate

Chad W. Cuss¹ and Celine Guéguen^{2,3*}

¹ Environmental and Life Sciences Graduate Program, Trent University, Peterborough, ON, Canada

² Chemistry Department, Trent University, Peterborough, ON, Canada

³ Water Quality Center, Trent University, Peterborough, ON, Canada

Edited by:

Veronique Schoemann, Royal Netherlands Institute for Sea Research, Netherlands

Reviewed by:

Rachel Narehood Austin, Bates College, USA

Sylvia McDevitt, Skidmore College, USA

Jeroen De Jong, Royal Netherlands Institute for Sea Research, Netherlands

*Correspondence:

Celine Guéguen, Department of Chemistry, Trent University, 1600 West Bank Drive, Peterborough, ON, Canada, K9J 7B8.
e-mail: celinegueguen@trentu.ca

Dissolved organic matter (DOM) is a universal part of all aquatic systems that largely originates with the decay of plant and animal tissue. Its polyelectrolytic and heterogeneous characters make it an effective metal-complexing agent with highly diverse characteristics. Microbes utilize DOM as a source of nutrients and energy and their enzymatic activity may change its composition, thereby altering the bioavailability and toxicity of metals. This study investigated the impacts of microbial inoculation upon the optical and copper-binding properties of freshly produced leaf-litter leachate over 168 h. Copper speciation was measured using voltammetry, and using fluorescence quenching analysis of independent fluorophores determined using parallel factor analysis (PARAFAC). Two protein/polyphenol-like and two fulvic/humic-like components were detected. Thirty-five percent of total protein/polyphenol-like fluorescence was removed after 168-h of exposure to riverine microbes. The microbial humic-like and tryptophan-like PARAFAC components retained significantly different log *K* values after 168 h of incubation ($p < 0.05$), while their complexing capacities were similar. Using voltammetry, a sixfold increase in copper-complexing capacity (CC, from 130 to 770 $\mu\text{mol Cu g C}^{-1}$) was observed over the exposure period, while the conditional binding constant (log *K*) decreased from 7.2 to 5.8. Overall binding parameters determined using voltammetry and fluorescence quenching were in agreement. However, the electrochemically based binding strength was significantly greater than that exhibited by any of the PARAFAC components, which may be due to the impact of non-fluorescent DOM, or differences in the concentration ranges of metals analyzed (i.e., different analytical windows). It was concluded that the microbial metabolism of maple leaf leachate has a significant impact upon DOM composition and its copper-binding characteristics.

Keywords: biodegradation, metal binding, dissolved organic matter, dissolved organic carbon, voltammetry, parallel factor analysis, fluorescence quenching, copper

INTRODUCTION

Dissolved organic matter (DOM) is a ubiquitous, complex, and polymorphous mixture of molecules that originates chiefly from the degradation of plant and animal matter. At the point of production, this molecular soup includes proteins, carbohydrates, polyphenols, and other vital compounds, many of which are quickly metabolized by microbes (Sutton and Sposito, 2005). Selective microbial metabolism of labile DOM components changes its overall chemical character (Fellman et al., 2008), which may affect its reactivity and environmental functioning. In particular, since DOM controls the mobility, speciation, and therefore toxicity of metals (Guéguen and Dominik, 2003; Nogueira et al., 2009), microbial processing may alter metal-binding properties, and thereby change the level of toxicity.

Leaf litter is a readily available source of DOM, has an important impact throughout freshwater systems, and serves as a key source of nutrients and energy for microorganisms (Tank et al., 2010). Given its abundance, importance, and the ease and reproducibility of leaching DOM from leaf litter, it is an excellent

candidate for studying microbially mediated changes in the metal-binding characteristics of DOM. Copper, an essential metal that can also be toxic at higher concentrations, has been widely employed as a representative for metal behavior with respect to DOM-binding properties (Ružic, 1982; Ryan and Weber, 1982; Perdue and Lytle, 1983; Tipping, 1998; Manceau and Matynia, 2010).

Anodic stripping voltammetry (ASV) is a very sensitive method for determining the key metal-binding parameters involved in copper-DOM speciation, such as the conditional equilibrium constant or binding strength (log *K*), and metal-complexing capacity (CC), which may be derived from the equilibrium relationship between bound and unbound sites:

$$K = \frac{[\text{ML}]}{[\text{M}] \cdot [\text{L}]} \quad (1)$$

where [M] and [L] are the concentrations of free copper and ligand, respectively, and [ML] is the concentration of bound ligand.

CC and K may be obtained from the linearized titration curve (Ružic, 1982; Durán and Nieto, 2011):

$$\frac{[M]}{[M]_{\text{Total}} - [M]} = \frac{M + \frac{1}{K}}{CC} \quad (2)$$

Fluorescence spectroscopy permits the three-dimensional mapping of the DOM complex into excitation–emission matrices (EEMs), revealing multiple fluorophore groups that are related to specific classes of molecules, and therefore potentially correspond to different binding sites (Ohno and Bro, 2006). Leaf leachate is highly fluorescent in regions related to proteins and polyphenols, and this fluorescence is quenched during the electrostatic interaction involved in metal binding (Ryan and Weber, 1982). Thus, the metal-binding characteristics determined using ASV and the single-site model (1:1 metal:DOM stoichiometry; Ružic, 1982) may also be determined for distinct fluorescent sites. Further, the proportion of fluorescence that is quenched by binding (% f) at each site may be determined, which may differ according to site properties. Parallel factor analysis (PARAFAC; Stedmon et al., 2003) of EEMs resolves fluorophore groups into statistically independent components, so that binding-site identification is more precise (Yamashita and Jaffé, 2008). Site-specific binding information also facilitates the incorporation of competition for metals among binding sites (Smith and Kramer, 1998), which is a likely occurrence in the complex mixture of molecules in leaf-litter leachate. Hence, fluorescence quenching using PARAFAC extracts site-specific metal-binding characteristics, and increases the information yield obtained by ASV.

In this study, fresh DOM was leached from leaf litter, inoculated with microbes, and analyzed for its optical and copper-binding properties over the course of 7 days of incubation using ASV and fluorescence quenching with PARAFAC. The unique combination of quenching with EEM–PARAFAC and ASV conducted under similar matrix conditions (i.e., pH and ionic strength) exploits the strength of both methods, permitting deeper insight into the metal-binding characteristics of DOM. This approach provides unprecedented information about the metal-binding properties of fluorescing DOM, as well as the bulk DOM leached directly from leaves.

MATERIALS AND METHODS

INITIAL SAMPLING/STORAGE

Leaf litter

Sugar maple (*Acer saccharum*) leaves were sampled from trees on the Trent University campus (Latitude 44.36°N, Longitude 78.29°W) in Peterborough, Ontario. Tree species identity was confirmed by a federally certified expert (Andrew McDonough, Trent University). Samples were taken on August 26th, 2011 by shaking the lower branches of two mature (~70'' height) trees and gathering freshly fallen litter, and by collecting litter dislodged by wind. Litter was air-dried, frozen, and prepared following the procedure used previously.

Microbial inocula

Naturally occurring microbes were collected from the Otonabee River (Peterborough, ON, Canada) using a pre-combusted,

acid-washed, 500-mL amber-glass bottle. The sample was immediately transported to the laboratory, filtered through a 5- μ m nitrocellulose filter (Millipore), and separated into 10.0-mL portions. Microbes used in experiment LL1 were stored overnight in the refrigerator ($\leq 5^{\circ}\text{C}$), while the inoculum for LL2 was frozen to minimize adaptive disruptions to community structure over the longer storage period ($\leq -5^{\circ}\text{C}$; Koponen et al., 2006) in 15-mL acid-washed polypropylene centrifuge tubes. The latter was moved to the refrigerator 7 days prior to use to allow a return to normal levels of respiration (Feng et al., 2007).

LEACHING, INOCULATION, SAMPLING, AND FLUORESCENCE

Leaching and organic carbon

Litter was leached by placing whole leaves in a 250-mL Pyrex beaker and filling with 200 mL milli-Q water (MQW, $\leq 18 \text{ M}\Omega \text{ cm}^{-1}$; Millipore). Two leaching experiments were conducted (LL1 and LL2), using 10 and 7 leaves (5.2 and 3.7 g wet weight, respectively). Leaf cleaning and leachate consistency were achieved by decanting the leachate and refreshing it with fresh MQW after 1 and 3 h of leaching, and using the complete volume from the 5-h leachates for the experiment. Five-hour leachates were consecutively filtered through Millipore pre-combusted glass-fiber (0.7 μ m) and nitrocellulose (0.22 μ m) filters that were pre-rinsed with MQW and leachate (respectively) to remove loose fibers and minimize the introduction of nitrogen. Prior to adding microbes directly to the leachate in a 250-mL Pyrex beaker, samples were adjusted to pH 7 using NaOH (Sigma).

Since leaching and initial biodegradation in Southern Ontario take place mainly in the late fall and early spring when temperatures oscillate between -5 and 10°C , the leaching, storage, and inoculation conditions were completed at 5°C to reflect natural spring and autumn conditions in southern Ontario. Similarly, freezing constitutes a normal stress upon the structure of the microbial community (Koponen et al., 2006).

Inoculation and sampling

Immediately after inoculation, a sample (B_0) was taken to evaluate the immediate effects of microbial addition. The inoculated leachate was then stored in the dark at 5°C . Samples (B_i) were taken from the active leachate at $i = 24, 48, 96$, and 168 h after inoculation. In experiment LL1, additional dissolved organic carbon (DOC) analyses were conducted after 2.5 and 4 h, and a control sample (i.e., non-inoculated leachate) was stored at 5°C in a pre-combusted, amber-glass vial for the duration of the experiment. Biological controls (i.e., NaN_3) were not added to the control, as they have been found to affect optical properties and cause undesirable reactions (Scully et al., 2004). The DOC concentration of all samples was measured using a TOC analyzer (Shimadzu TOC-VCPH). Samples were filtered (0.22- μ m nitrocellulose; Millipore) and stored at 5°C in pre-combusted amber-glass vials prior to EEM, quenching, and voltammetric analyses, all of which took place within 7 days.

Fluorescence and PARAFAC

Fluorescence was analyzed following manual injection into the stopped-flow cell of an on-line fluorescence detector (Agilent 1200-series model G1321A). MQW was used to clean the cell

between injections, ensured by monitoring continuous scanning channels at excitation/emission wavelengths (Ex/Em) of 270, 300, 355, 370/460 nm. Injections of 0.01 M NaCl (pH 6) were periodically analyzed between samples to convert fluorescence to Raman units (r.u.) using the area under the Raman water peak at Ex = 350 nm (r.u.; Lawaetz and Stedmon, 2009). Wavelengths of the on-line fluorescence detector were calibrated daily following the manufacturer-recommended procedure.

Excitation–emission matrices were captured in ratio (S/R) mode by scanning over an excitation (Ex) and emission range (Em) of 200–450 and 280–600 nm in 1 and 5 nm increments, respectively. Fluorescence EEMs were measured for three distinct subsamples of each leachate for each sample B_i from both LL1 and LL2, and once for each quenched sample (LL2 only). Four-fold dilution of all leachate samples ensured that absorbance was low enough to avoid inner filtering effects ($A_{254} < 0.01$ A.U. in a 1-cm cell, Lakowicz, 2006). Blank EEMs (0.01 M NaCl; pH = 6) were subtracted from each sample EEM to remove background fluorescence. PARAFAC analysis was conducted after Raman normalization, blank subtraction, and removal of Raman and Rayleigh scatter lines in MATLAB R2010a using an in-house modified EEM-Cut algorithm and the DOMFluor toolbox (Stedmon and Bro, 2008).

SPECIATION ANALYSES

Quenching

A 2.5-mM Cu^{2+} copper stock solution was made in 0.001 M NaCl solution (pH 6) using hydrated cupric nitrate (Baker), and was diluted to 0.5 mM Cu^{2+} on each day immediately prior to use. Samples were diluted fourfold with 0.001 M NaCl/0.1 M MES (pH = 6) prior to analysis to ensure that $A_{254} < 0.01$ AU. Copper was added to 14 individual samples for each B_i from experiment LL2 with final copper concentrations ranging from 2.4 to 320 μM (Figure A1 in Appendix). Quenched samples were stored overnight at 5°C in the dark to ensure equilibration of the complexation reaction.

Fluorescence quenching was described using the multi-site Ryan-Weber model following Smith and Kramer (1998, 2000). The Ryan-Weber model derives a non-linear regression equation from the equilibrium equation for the formation constant of the bound metal (Ryan and Weber, 1982), assuming a single binding site. The Smith and Kramer model accounts for multiple sites, incorporates competition among binding sites, and assumes that fluorescence is a linear function of metal concentration. A 95% CI was calculated for K and CC at each binding site and sampling time by fitting quenching curves with the maxima and minima of the 95% CI for each point, as determined from triplicate EEMs of each B_i (Statistica 8; StatSoft).

Voltammetry

A 0.5-mM Cu^{2+} stock solution was prepared by diluting copper reference standard solution (1000 ppm, >99.0%; Fisher) in 0.01 M NaNO_3 /0.1 M MES (SigmaUltra) adjusted to pH 6.0. Samples were diluted 10-fold to <5 ppm C with 0.01 M NaNO_3 /0.1 M MES (pH = 6) prior to analysis to minimize interferences caused by the adsorption of DOM on the electrode surface. Copper was added to 14 individual samples for each B_i from experiment LL2

with final concentrations ranging from 0.32 to 5.2 μM (Figure A2 in Appendix).

Square wave ASV analysis of copper speciation was conducted on samples from LL2 using a 663 VA polarographic stand (Metrohm) coupled to an Eco-Chemie AutoLab PGSTAT10 running in static mercury drop mode. The analytical procedure followed Durán and Nieto (2011), with the following instrument settings: accumulation potential, −1.1 V; accumulation time, 2 min.; equilibration time, 20 s; scan range, −1.1 to 0.2 V at 25 Hz, an amplitude of 25 mV and a 2-mV scan increment. The automatic stirrer was set to maximum during the purging and accumulation steps. The peak current at a potential of 0.056 V was measured for 14 metal additions along each voltammetric curve.

The conditional stability constant K and complexation capacity CC were determined for each sample B_i by fitting the linear portion of plots of free copper concentration against the ratio of free to bound copper, and assuming single-site Langmuirian adsorption with a 1:1 stoichiometry (Ružić, 1982; Durán and Nieto, 2011). The SD of the voltammetric procedure was determined using three distinct subsamples of B_{168} . The initial copper concentration of the leachate solution was found to be negligible (1.13 ± 0.04 ppb; \pm SD) following analysis by inductively coupled mass spectrophotometer (XSeries II, Thermo Fisher).

RESULTS

DISSOLVED ORGANIC CARBON

A twofold difference in DOC concentration was found in the 5-h leachates between the two experiments (2.3 mg C g^{-1} litter $^{-1}$ vs. 1.2 mg C g^{-1} litter $^{-1}$ for LL1 and LL2, respectively; Table 1). No significant change in DOC concentration was observed due to the introduction of microbes in LL2 ($p > 0.05$). Unfortunately, no DOC data were available for LL1 B_0 . Since the DOC concentration of the leachate was not significantly different from that of the pre-inoculated sample, it is referred to as initial.

Dissolved organic carbon losses over incubation were well-described using the recalcitrant-labile exponential decay model (Scully et al., 2004):

$$[\text{DOC}] = [\text{DOC}]_R + [\text{DOC}]_L \bullet e^{-b \bullet t} \quad (3)$$

where R and L denote the recalcitrant and labile compartments of DOC, respectively, and b is the rate of change in h^{-1} (Figure 1). DOC decreased very rapidly in both experiments, showing more than 95% of overall losses within the first 6 h. The modeled proportions of labile carbon and loss rates were 37%, 0.59 h^{-1} , and 13%, 2.6 h^{-1} for LL1 and LL2, respectively. Differences in the rates of DOC loss may have been caused by freezing the microbes prior to experiment LL2, or by differences in the concentrations of leachates. A 20% decrease in DOC concentration (from 65.4 to 52.4 mg L^{-1}) was observed in the control sample over 7 days of storage in experiment LL1.

FLUORESCENCE PROPERTIES

PARAFAC

The initial PARAFAC dataset included 189 EEMs, and one outlier was excluded during preliminary analysis (i.e., $B_{48} + 190 \mu\text{M Cu}$). Since the outlier constituted only 1 of 14 titration points at the tail

Table 1 | DOC concentrations (ppm) and PARAFAC loadings of leachate samples over 168 h of degradation by river microbes ($n=3$).

Trial	Initial DOC	DOC after 168 h	Component (peak)	Initial loading	Loading after 168 h	Control loading (168 h)	Initial % loading	% Loading after 168 h
LL1	65.4 (1.62)	38.9 (0.31)	C1 (B)	0.63 (0.014)	0.40 (0.006)	0.50 (0.004)	56	47
			C2 (M)	0.28 (0.008)	0.24 (0.007)	0.30 (0.007)	25	28
			C3 (T)	0.15 (0.005)	0.14 (0.002)	0.18 (0.001)	13	16
			C4 (C)	0.07 (0.001)	0.07 (0.002)	0.09 (0.003)	6	8
LL2	25.5 (1.73)	22.1 (0.88)	C1 (B)	0.48 (0.021)	0.33 (0.006)	n/a	55	49
			C2 (M)	0.19 (0.002)	0.20 (0.005)	n/a	22	30
			C3 (T)	0.15 (0.014)	0.11 (0.005)	n/a	17	16
			C4 (C)	0.05 (0.003)	0.03 (0.002)	n/a	6	4

SD is shown in parentheses, and significant changes are shown in bold type. Peak designations follow Coble (1996).

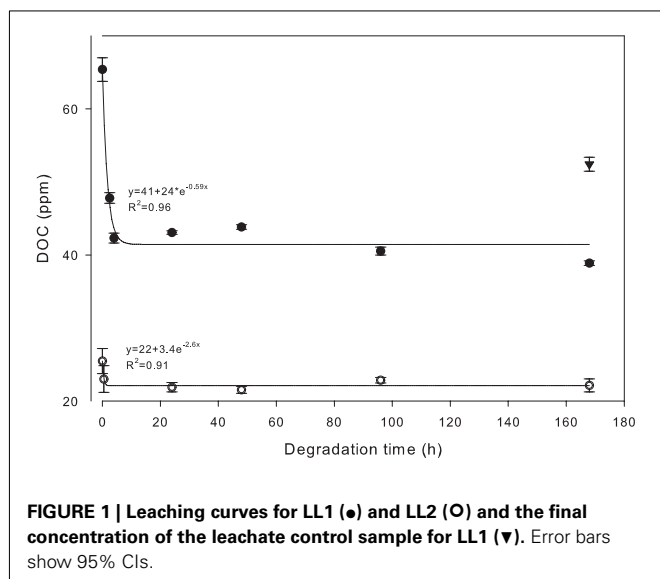


FIGURE 1 | Leaching curves for LL1 (●) and LL2 (○) and the final concentration of the leachate control sample for LL1 (▼). Error bars show 95% CIs.

of the quenching curve, it is unlikely that the results were seriously affected.

A six-component PARAFAC model was cross-validated, which identified four components (Figure 2) previously associated with DOM from fresh and marine waters (Coble, 1996; Stedmon and Markager, 2005), and with leaf leachates (Wickland et al., 2007; Wong and Williams, 2010). Component 1 (C1, Ex/Em = 220, 280/320 nm) resembled tyrosine/polyphenol-like peak B; component 2 (C2, 210, 315/430 nm) was similar to humic/carbohydrate-like peak M; C3 (225, 275/350 nm) was similar to tryptophan/polyphenol-like peak T; and C4 (235, 380/465 nm) resembled fulvic-like peak C. In all EEMs, the loading of C1 was dominant.

The two additional components had sharply defined excitation wavelengths and emission spectra that spanned all wavelengths (Ex/Em = 205/370 and 220/320 nm), and were associated with the nitrate added to the quenching samples (Stewart and Wetzel, 1980). Samples containing nitrate-related components (42%) were removed from the data set and a second PARAFAC analysis was completed. The second analysis was cross-validated for four components, which were identical to the non-anomalous

components from the first analysis in shape, loadings, and order of importance. Consequently, all EEMs were included in the PARAFAC model, and the components associated with nitrate were ignored.

Changes after inoculation

As with DOC losses over incubation (Figure 1), changes in PARAFAC loadings were best described using the recalcitrant-labile exponential decay model (Figure 3). In general, the loadings of all PARAFAC components either decreased or remained the same after 168 h in both experiments, with the exception of a slight increase in C2 in experiment LL2 (Table 1). However, as a proportion of overall loading only the changes to C1 and C2 were significant in LL2 ($p < 0.05$). The proportions of all components were quite similar in both experiments, both before and after inoculation. Despite high variability in DOC losses over the two experiments, the changes in total component loading were similar to those of DOC, with an average (\pm SD) loading reduction of $23.9 \pm 1.37\%$, and an average DOC loss of $26.9 \pm 19.2\%$.

To assess the reproducibility of the experiment in terms of biodegradable DOM, component loadings were partitioned into two groups (protein/polyphenol-like and humic/fulvic-like), which have been respectively associated with relatively labile and recalcitrant DOM (Stedmon and Markager, 2005; Fellman et al., 2008, 2009). The average protein/polyphenol-like loading (C1 + C3) was calculated for each sample, and fit with the recalcitrant-labile exponential model (Eq. 3; Figure 4A). The relatively recalcitrant fraction (i.e., that remaining after incubation; Eq. 3) of the protein/polyphenol-like fluorescence constituted 64 and 66% of total protein/polyphenol-like fluorescence for LL1 and LL2, respectively, so that the portion lost over the incubation period was considered to be more labile ($p < 0.0005$ for both experiments). To assess the corresponding impact on overall DOM quality, the combined protein/polyphenol-like (C1 + C3) and humic/fulvic-like (C2 + C4) loadings were converted to proportional loadings [e.g., $(C1 + C3)/\Sigma C_{1-4}$], and transformed to ensure normality of the distribution (arcsin-square root; Figure 4B). Statistically identical linear decreases in the proportion of protein-like components were found for LL1 and LL2 ($p > 0.05$). The corresponding loss rates (i.e., slopes) and original protein/polyphenol concentrations (i.e., intercepts) were 0.04%

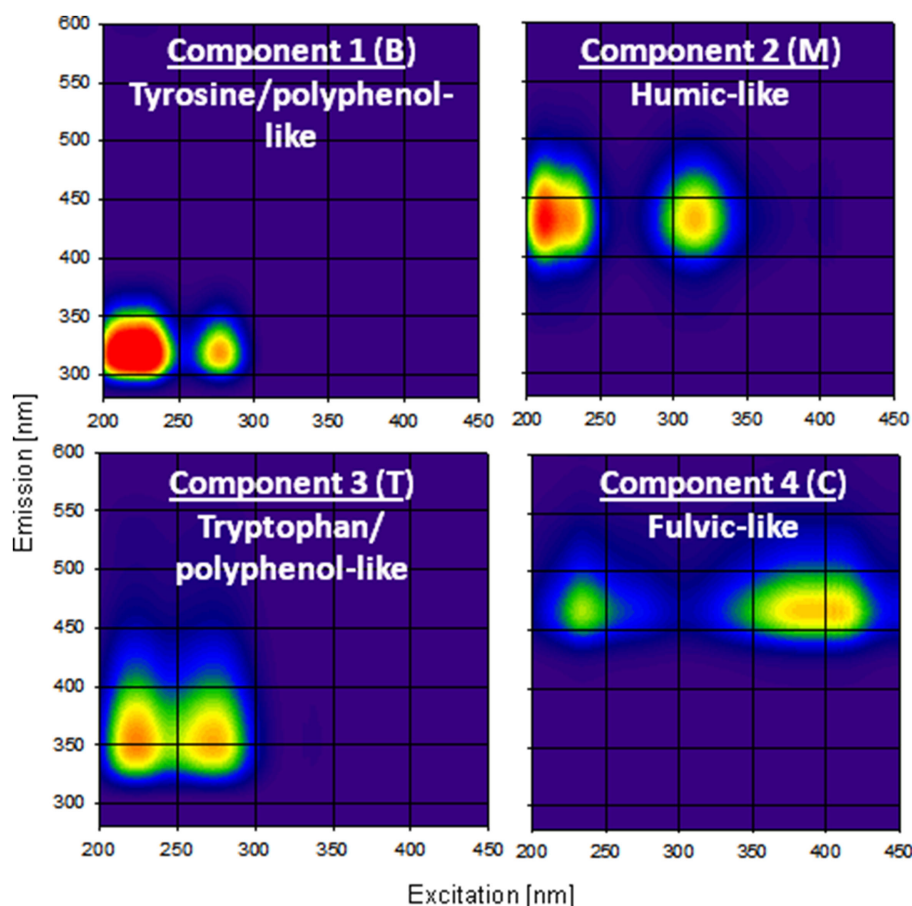


FIGURE 2 | PARAFAC components found in this study and their associated identities following Coble (1996).

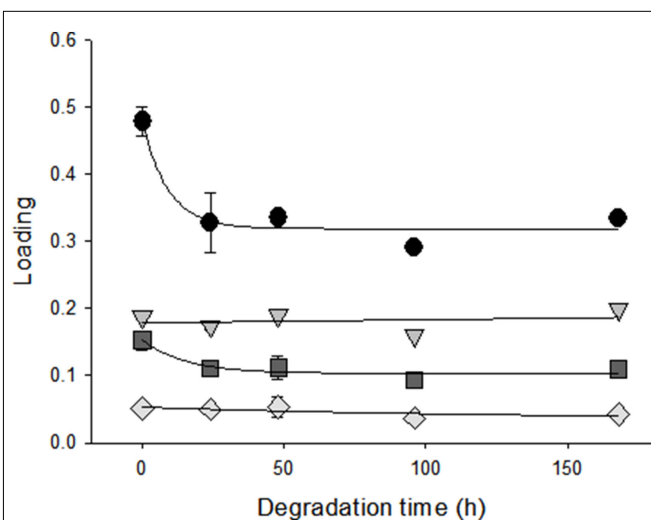


FIGURE 3 | Changes in average PARAFAC component loadings [C1 (●), C2 (▼), C3 (■), and C4 (◆)] over the microbial incubation period during experiment LL2. Error bars (\pm SD) that are not apparent are smaller than their respective symbols.

h^{-1} and 69.9%, and 0.03% h^{-1} and 69.0% of DOM for LL1 and LL2, respectively (Figure 4B).

Compared to B_0 , changes in the control sample mirrored those observed over the microbial exposure period, but were decidedly less severe. The DOC concentration and PARAFAC loadings for components C1–4 in the control sample were 52.4 mg L^{-1} , and 0.50 ± 0.004 , 0.30 ± 0.007 , 0.18 ± 0.001 , and 0.09 ± 0.003 , respectively. These changes correspond to percentage losses of 19.8% DOC and 12.6% total loading, respectively (Table 1).

QUENCHING

Quenching behaviors and binding characteristics differed by PARAFAC component and over the period of microbial exposure for all components, generally changing from significantly different ($p < 0.05$) to more similar (Figures 5A–C; Table 2). The log K and CC values of all components were significantly different from each other (by component) in B_0 , and both parameters were significantly different for each component in B_0 compared to B_{168} ($p < 0.05$; Table 2).

In the leachate, protein/polyphenol-like C1 visibly quenched more slowly than other components and had a significantly lower log K value (4.73 vs. 5.42–6.11). However, the differences in log K

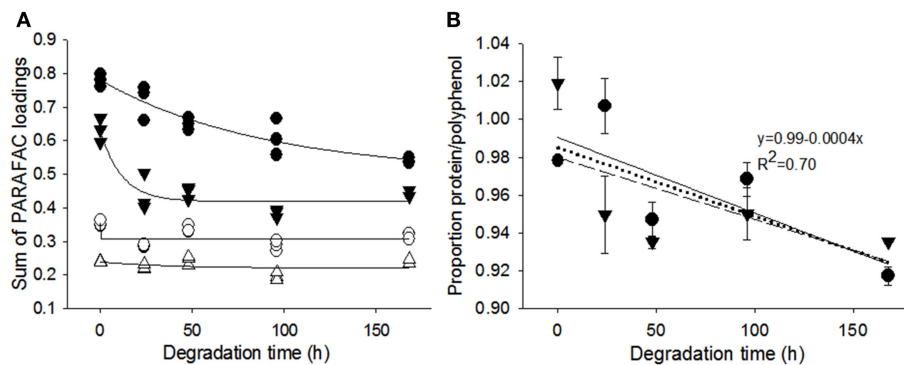


FIGURE 4 | Changes in (A) PARAFAC component loadings and (B) mean proportions (arcsin-square root transformed) of grouped protein/polyphenol- (filled) and humic/fulvic-like constituents (open) for experiments LL1 (●) and LL2 (▼) over the course of

degradation. The regression equation is for the overall mean proportion of protein/polyphenol-like loadings for both experiments (dotted line). Some error bars (\pm SD) are smaller than their respective symbols.

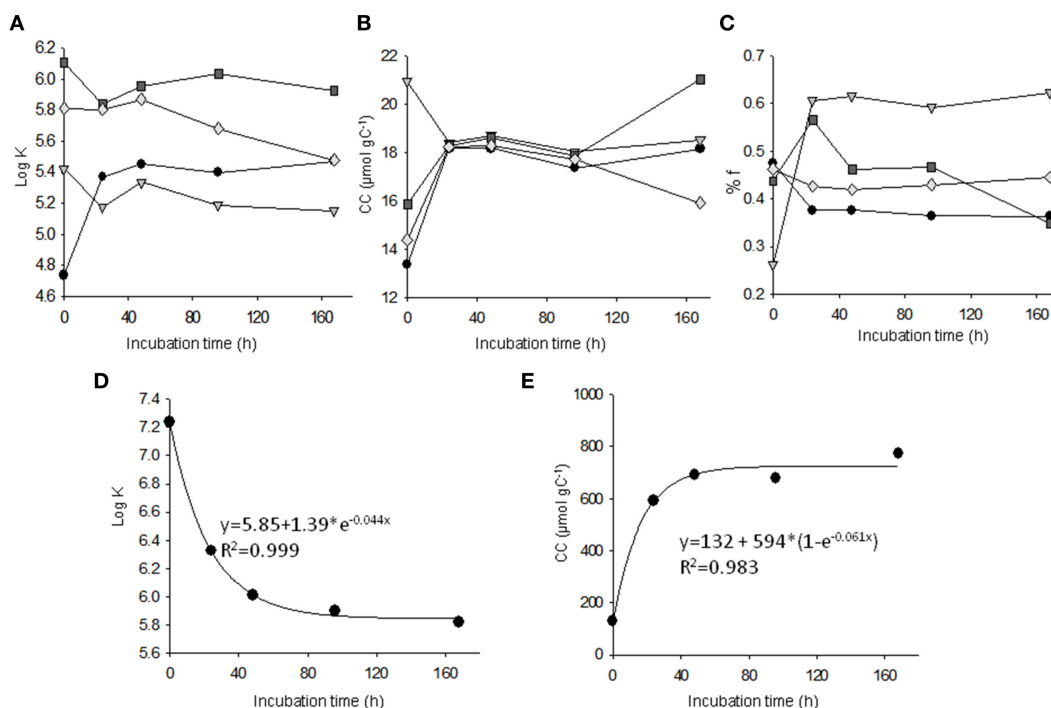


FIGURE 5 | Changes in binding parameters after incubation determined by fluorescence quenching for (A–C) PARAFAC components C1 (●), C2 (▼), C3 (■), and C4 (◆) and (D,E) voltammetry.

were significantly reduced after inoculation, corresponding with an increase in CC from 13.3 to $18.2 \mu\text{mol Cu g C}^{-1}$ (Figures 5A,B) and a decrease in the proportion of fluorescence quenched by binding (% f) from 47.5 to 31.6% (Figure 5C). For C2 the opposite trends were apparent, with decreases observed in log K and CC (from 5.42 to 5.15 and from 21.0 to $18.5 \mu\text{mol Cu g C}^{-1}$, respectively) and a 2.4-fold increase in % f (from 26.1 to 62.3%). The patterns of change for CC and % f in C1 and C2 closely resembled the exponential curves observed for DOC and fluorescence, while only the log K of C1 underwent exponential-type change

(Figures 2, 5A). The log K values of C3 and C4 were also significantly lower after 168 h of leaching, whereas their CC values were significantly higher ($p < 0.05$). Exponential patterns of change were observed for CC and % f . However, no significant differences in % f were observed between B_0 and B_{168} for C3 or C4 (Table 2).

VOLTAMMETRY

Binding parameters (log K and CC) determined by voltammetry exhibited significant, exponential change after inoculation (from

Table 2 | Confidence ranges (95%) for conditional binding constant (log *K*), complexing capacity (CC), and proportion of fluorescence quenched (% *f*) determined by the fluorescence quenching of leaf-litter leachate over 168 h of degradation by microbes.

Component (peak)	Initial Log <i>K</i>	Log <i>K</i> after 168 h	Initial CC (μmol Cu g C ⁻¹)	CC after 168 h (μmol Cu g C ⁻¹)	Initial <i>f</i> (%)	<i>f</i> after 168 h (%)
C1 (B)	4.73–4.74	5.44–5.54	13.3–13.7	18.1–21.1	45.2–49.7	26.8–36.3
C2 (M)	5.42–5.42	5.07–5.25	21.0–22.6	17.3–18.0	18.1–32.1	62.1–62.7
C3 (T)	6.11–6.11	5.83–6.01	15.9–17.7	18.0–22.3	35.4–48.6	30.8–44.0
C4 (C)	5.78–5.81	5.48–5.55	14.4–15.7	15.9–20.2	40.1–47.1	32.6–54.3

Confidence ranges were determined by modeling quenching curves in triplicate, using maxima and minima of 95% CI from triplicate fluorescence measurements of each sample prior to metal addition. Values that changed significantly over degradation are shown in bold type.

7.2 to 5.82 and from 130 to 770 μmol Cu g C⁻¹, respectively; $p < 0.005$), and the rates of change were very similar for both parameters (0.044 and 0.061, respectively; $p > 0.05$; **Figures 5D,E**).

DISCUSSION

BIODEGRADATION

Changes in the leaf-litter leachate occurred at an extremely rapid rate (exponential loss rates of 0.59 and 2.6 h⁻¹ for DOC in LL1 and LL2, respectively) and a significant difference was observed for all PARAFAC components between both experiments, before and after inoculation ($p < 0.05$). The multiple consistent sampling points observed along the tail of exponential curves imply that the early stages of decomposition have reached a relatively steady state. However, only protein/polyphenol-like component C1 decreased in its overall average proportion (from 56 to 47% of total loading). The proportional increase in C2 (from 22 to 30%; **Table 1**) was relatively high in LL2, suggesting that the net effect of microbial action may have been the production of C2 and consumption of C1. Although the loadings of components C3 and C4 decreased over incubation, their proportional contribution to fluorescent DOC did not change significantly in LL2 ($p > 0.05$; **Figure 3**; **Table 1**). These changes were different from those observed in experiment LL1, where the proportions of C3 and C4 increased significantly (**Table 1**; $p < 0.05$). Differences in DOC processing and component loadings observed between experiments LL1 and LL2 may have been caused by the freezing of the microbial community in LL1, and subsequent nutrient depletion over the 7-day recuperation period (Jansson et al., 2006). Despite this difference, the overall effect of rapid protein/polyphenol-like consumption (C1, C3) and carbohydrate/humic-like production (C2) was consistent across experiments, and is generally considered to reflect microbial processing (Parlanti et al., 2000; Scully et al., 2004; Wickland et al., 2007; Bowen et al., 2009; Fellman et al., 2009; Hur et al., 2009).

Similar changes were observed in the DOC concentration and component loadings of the control sample, suggesting some microbial processing may be due to ambient microbes, or the possibility that ambient and riverine populations effect similar changes in leaf leachate. However, the possibility of preferential decomposition of different DOM compartments by one microbial community, and concomitant transformation of waste products by other communities makes the intricacies of processing unclear (Covert and Moran, 2001; Docherty et al., 2006). Since absolutely abiotic conditions are practically impossible in leaf leachates,

ambient microbial populations may have contributed to some of the observed changes. The changes in the control sample were significantly lower than in the inoculated samples, suggesting that the observed changes in copper-binding properties were mainly due to the inoculum.

The observed rapidity of initial DOC decline has also been attributed to the adsorption of relatively large components to the surfaces of colloids and microbes introduced during inoculation (Maurice et al., 2004; Young et al., 2004). To explore this possibility, colloid formation was investigated by observing second-order fluorescence scattering at Ex/Em = 300/600 nm, following the procedure used by Guéguen et al. (2002). No substantial increases from the level of scattering in the leachate were evident immediately after inoculation, during the observed changes in optical properties, or in the control sample. The apparent absence of particles, similarities between the patterns of change in DOC and protein/polyphenol-like components, and recent reports of extremely rapid protein and carbohydrate consumption by microbes under natural and artificial conditions, together imply that much of these losses are due to the processing of labile constituents (Fellman et al., 2009; Huang et al., 2011).

CHANGES IN DOM COMPOSITION AND METAL-BINDING PROPERTIES

Exponential increases in the binding strength and ligand concentration of C1 were contrasted by an exponential decrease in ligand concentration and a linear decrease in binding strength in C2 (**Figures 5A,B**; **Table 2**). Further, % *f* decreased exponentially for C1, and increased exponentially for C2. Overall, exponential changes in metal-binding properties over incubation coincided with those of component loadings for C1 and C2, and for DOC (**Figures 2 and 5**). Components C3 and C4 also exhibited significantly lower log *K* and increased CC after inoculation ($p < 0.05$), but % *f* was not significantly different after 168 h of microbial exposure for these components ($p > 0.05$).

The binding strength and complexing capacities of PARAFAC components changed from being significantly different in leachates, to being more similar in biodegraded samples (**Figure 5**; **Table 2**). These changes may reflect the partial consumption or transformation of protein/polyphenol-like molecules (C1 and C3). The results of binding parameters based on fluorescence showed a marked increase in variability after incubation (i.e., width of 95% CI increased substantially; **Table 2**). Changes in copper-binding characteristics measured by voltammetric analysis were also exponential in nature, paralleling rates of change

for component loadings and DOC concentration (**Figures 2 and 5D,E**). Decreases in the binding strength of the overall leachate measured by voltammetry reflected those observed for components C2–4 in fluorescence quenching rather than the increase observed for C1. However, the complexing capacity determined using voltammetry increased in harmony with changes to C1, C3, and C4 (**Figures 5B,E**). Thus, voltammetric and fluorescence quenching measurements were found to be in general agreement about the effects of inoculation on the copper-binding parameters of leaf leachate. However, the cumulative copper-binding strength of the leachate determined by voltammetry was significantly greater than the binding strength exhibited by any of the PARAFAC components in the quenching experiments (7.2 vs. 4.73–6.11; **Figures 5A,D; Table 2**), which may be due to the impact of non-fluorescent DOM, or differences in the concentration ranges of metals analyzed (i.e., different analytical windows; Buffle, 1988). Nonetheless, fluorescence quenching analysis yields key information about how the effects of changes in the character of DOM upon binding properties, as it provides site-specific binding parameters for several PARAFAC components that have been related to known constituents of DOM.

Despite the similarities in fluorescence characteristics and chemical properties attributed to protein/polyphenol-like components C1 and C3, and to humic/fulvic-like C2 and C4, both the individual responses of components to incubation and their binding properties were distinct. These unique responses and properties underscore the complex nature of fluorescent DOM both in fresh leaf-litter leachate, and in leachates exposed to microbial action.

Meaningful comparison of specific results with the findings of other researchers is challenging, as studies of copper-binding characteristics that use fresh leaf-litter leachates are scarce and research groups tend to employ distinct methods of analysis, binding models, numbers of sites, litter conditioning, matrix characteristics, etc. Increases in copper-complexing capacity of the same magnitude as those observed using voltammetric analysis have been observed elsewhere for extracts of wheat straw and crimson clover following inoculation with soil microbes, which were also related to similar changes in fluorescence (0.11–6.28 to 0.29–32.1 mmol Cu g C⁻¹; Merritt and Erich, 2003). The log *K* values found in bulk and low-molecular-weight fractions of wheat straw and

crimson clover leachates also tended to become similar over 7 days of exposure to soil microbes, which was attributed to increased polymerization measured as increasing molecular weight. In general, the copper-binding strengths of fresh litter leachates (Merritt and Erich, 2003; Hur and Lee, 2011) are greater than those of microbially degraded litter leachates (Merritt and Erich, 2003) which agrees with the results of this study (**Table 2**). Thus, the overall changes and general ranges in binding characteristics measured using voltammetry are on the lower end of the general range observed by other researchers.

This study has shown that the copper-binding capability of leachates extracted from maple leaves increased rapidly after inoculation with riverine microbes. Fresh leachates were found to have a relatively low copper-binding capacity and a higher overall binding strength, while degraded material was capable of complexing more material, but with a lower binding strength. Generally, metal toxicity decreases when it is bound to organic matter (Nogueira et al., 2009; Sánchez-Marín et al., 2010), but this is not true for all metals, organisms, or aquatic chemistries (Meyer et al., 1999; Sánchez-Marín et al., 2007). Based on the results of this study, differences in toxicities may also be caused by differences in the degree of organic matter processing, with corresponding differences in the exposure of organisms to metals that are bound to DOM constituents with variable binding strengths. This result underscores the potential importance of the dynamic relationship between microbes, metals, and organic matter, where DOM serves both as a source of nutrition and as a regulator of metal speciation and its effectiveness in the latter role is partially controlled by microbial activities.

ACKNOWLEDGMENTS

The authors wish to thank the many people involved in making this project a success: B. Marcere for DOC analysis; W. Chen for assistance with the modeling of metal speciation; and A. McDonough for tree species identification. We would like to thank the Editor Veronique Schoemann and the three anonymous reviewers for improving this manuscript with their constructive comments. This work was funded in part by the Canada Research Chairs program, Natural Sciences and Engineering Research Council grants. Chad. W. Cuss gratefully acknowledges the financial support accorded by the Ontario Student Assistance Program Ontario Graduate Scholarship.

REFERENCES

- Bowen, S. R., Gregorich, E. G., and Hopkins, D. W. (2009). Biochemical properties and biodegradation of dissolved organic matter from soils. *Biol. Fertil. Soils* 45, 733–742.
- Buffle, J. (1988). *Complexation Reactions in Aquatic Systems: An Analytical Approach*. Chichester: Ellis Horwood Limited.
- Coble, P. G. (1996). Characterization of marine and terrestrial DOM in seawater using excitation-emission matrix spectroscopy. *Mar. Chem.* 51, 325–246.
- Covert, J. S., and Moran, M. A. (2001). Molecular characterization of estuarine bacterial communities that use high- and low-molecular weight fractions of dissolved organic carbon. *Aquat. Microb. Ecol.* 25, 127–139.
- Docherty, K. M., Young, K. C., Maurice, P. A., and Bridgman, S. D. (2006). Dissolved organic matter concentration and quality influences upon structure and function of freshwater microbial communities. *Microb. Ecol.* 52, 378–388.
- Durán, I., and Nieto, O. (2011). Electrochemical speciation of dissolved Cu, Pb and Zn in an estuarine ecosystem (Ría de Vigo, NW Spain): comparison between data treatment methods. *Talanta* 85, 1888–1896.
- Fellman, J. B., D'Amore, D. V., Hood, E., and Boone, R. D. (2008). Fluorescence characteristics and biodegradability of dissolved organic matter in forest and wetland soils from coastal temperate watersheds in southeast Alaska. *Biogeochemistry* 88, 169–184.
- Fellman, J. B., Hood, E., Edwards, R. T., and Jones, J. B. (2009). Uptake of allochthonous dissolved organic matter from soil and salmon in coastal temperate rainforest streams. *Ecosystems* 12, 747–759.
- Feng, X., Nielsen, L. L., and Simpson, M. J. (2007). Responses of soil organic matter and microorganisms to freeze-thaw cycles. *Soil Biol. Biochem.* 39, 2027–2037.
- Guéguen, C., Belin, C., and Dominik, J. (2002). Organic colloid separation in contrasting aquatic environments with tangential flow filtration. *Water Res.* 36, 1677–1684.

- Guéguen, C., and Dominik, J. (2003). Partitioning of trace metals between particulate, colloidal and truly dissolved fractions in a polluted river: the Upper Vistula River (Poland). *Appl. Geochem.* 18, 457–470.
- Huang, G., Meng, F., Zheng, X., Wang, Y., Wang, Z., Liu, H., and Jekel, M. (2011). Biodegradation behavior of natural organic matter (NOM) in a biological aerated filter (BAF) as a pretreatment for ultrafiltration (UF) of river water. *Appl. Microbiol. Biotechnol.* 90, 1795–1803.
- Hur, J., and Lee, B.-M. (2011). Characterization of binding site heterogeneity for copper within dissolved organic matter fractions using two-dimensional correlation fluorescence spectroscopy. *Chemosphere* 83, 1603–1611.
- Hur, J., Park, M.-H., and Schlautman, M. A. (2009). Microbial transformation of dissolved leaf litter organic matter and its effects on selected organic matter operational descriptors. *Environ. Sci. Technol.* 43, 2315–2321.
- Jansson, M., Bergström, A.-K., Lymer, D., Vrede, K., and Karlsson, J. (2006). Bacterioplankton growth and nutrient use efficiencies under variable organic carbon and inorganic phosphorous ratios. *Microb. Ecol.* 52, 358–364.
- Koponen, H. T., Jaakko, T., Keinänen-Toivola, M. M., Kaipainen, S., Tuomainen, J., Servomaa, K., and Martikainen, P.-J. (2006). Microbial communities, biomass, and activities in soils as affected by freeze thaw cycles. *Soil Biol. Biochem.* 38, 1861–1871.
- Lakowicz, J. R. (2006). *Principles of Fluorescence Spectroscopy*, 3rd Edn. New York: Springer, 54–57.
- Lawaetz, A. J., and Stedmon, C. A. (2009). Fluorescence intensity calibration using the Raman scatter peak of water. *Appl. Spectrosc.* 63, 936–940.
- Manceau, A., and Matynia, A. (2010). The nature of Cu bonding to natural organic matter. *Geochim. Cosmochim. Acta* 74, 2256–2580.
- Maurice, P. A., Manecki, M., Fein, J. B., and Schaefer, J. (2004). Fractionation of an aquatic fulvic acid upon adsorption to the bacterium, *Bacillus subtilis*. *Geomicrobiol. J.* 21, 69–78.
- Merritt, K. A., and Erich, M. S. (2003). Influence of organic matter decomposition on soluble carbon and its copper-binding capacity. *J. Environ. Qual.* 32, 2122–2131.
- Meyer, J. S., Santore, R. C., Bobbitt, J. P., Debrey, L. D., Boese, C. J., Paquin, P. R., Allen, H. E., Bergman, H. L., and Ditoro, D. M. (1999). Binding of nickel and copper to fish gills predicts toxicity when water hardness varies, but free-ion activity does not. *Environ. Sci. Technol.* 33, 913–916.
- Nogueira, P. F. M., Melão, M. G. G., Lombardi, A. T., and Nogueira, M. M. (2009). Natural DOM affects copper speciation and bioavailability to bacteria and ciliate. *Arch. Environ. Contam. Toxicol.* 57, 274–281.
- Ohno, T., and Bro, R. (2006). Dissolved organic matter characterization using multiway spectral decomposition of fluorescence landscapes. *Soil Sci. Soc. Am. J.* 70, 2028–2037.
- Parlanti, E., Wörz, K., Geoffroy, L., and Lamotte, M. (2000). Dissolved organic matter fluorescence spectroscopy as a tool to estimate biological activity in a coastal zone submitted to anthropogenic inputs. *Org. Geochem.* 31, 1765–1781.
- Perdue, E. M., and Lytle, C. R. (1983). Distribution model for binding of protons and metal ions by humic substances. *Environ. Sci. Technol.* 17, 654–660.
- Ruzic, I. (1982). Theoretical aspects of the direct titration of natural waters and its information yield for trace metal speciation. *Anal. Chim. Acta* 140, 99–113.
- Ryan, D. K., and Weber, J. H. (1982). Fluorescence quenching titration for determination of complexing capacities and stability constants of fulvic acid. *Anal. Chem.* 54, 986–990.
- Sánchez-Marín, P., Lorenzo, J. I., Blust, R., and Beiras, R. (2007). Humic acids increase dissolved lead bioavailability for marine invertebrates. *Environ. Sci. Technol.* 41, 5679–5684.
- Sánchez-Marín, P., Santos-Echeandía, J., Nieto-Cid, M., Álvarez-Salgado, X. A., and Beiras, R. (2010). Effect of dissolved organic matter (DOM) of contrasting origins on Cu and Pb speciation and toxicity to *Paracrotus lividus* larvae. *Aquat. Toxicol.* 96, 90–102.
- Scully, N. M., Maie, N., Dailey, S. K., Boyer, J. N., Jones, R. D., and Jaffé, R. (2004). Early diagenesis of plant-derived dissolved organic matter along a wetland, mangrove, estuary ecotone. *Limnol. Oceanogr.* 49, 1667–1678.
- Smith, D. S., and Kramer, J. R. (1998). Multi-site aluminum speciation with natural organic matter using multiresponse fluorescence data. *Anal. Chim. Acta* 363, 21–29.
- Smith, D. S., and Kramer, J. R. (2000). Multi-site metal binding to fulvic acid determined using multiresponse fluorescence. *Anal. Chim. Acta* 416, 211–220.
- Stedmon, C. A., and Bro, R. (2008). Characterizing dissolved organic matter fluorescence using parallel factor analysis: a tutorial. *Limnol. Oceanogr. Methods* 6, 572–579.
- Stedmon, C. A., and Markager, S. (2005). Resolving the variability in dissolved organic matter fluorescence in a temperate estuary and its catchment using PARAFAC analysis. *Limnol. Oceanogr.* 50, 686–697.
- Stedmon, C. A., Markager, S., and Bro, R. (2003). Tracing dissolved organic matter in aquatic environments using a new approach to fluorescence spectroscopy. *Mar. Chem.* 82, 239–254.
- Stewart, A. J., and Wetzel, R. G. (1980). Fluorescence:absorbance ratios—a molecular-weight tracer of dissolved organic matter. *Limnol. Oceanogr.* 25, 559–564.
- Sutton, R., and Sposito, G. (2005). Molecular structure in soil humic substances: the new view. *Environ. Sci. Technol.* 39, 9009–9015.
- Tank, J. L., Rosi-Marshall, E. J., Griffiths, N. A., Entrekin, S. A., and Stephen, M. L. (2010). A review of allochthonous organic matter dynamics and metabolism in streams. *J. North Am. Benthol. Soc.* 29, 118–146.
- Tipping, E. (1998). Humic ion-binding model VI: and improved description of the interactions of protons and metal ions with humic substances. *Aquat. Geochem.* 4, 3–48.
- Wickland, K. P., Neff, J. C., and Aiken, G. R. (2007). Dissolved organic carbon in Alaskan boreal forest: sources, chemical characteristics, and biodegradability. *Ecosystems* 10, 1323–1340.
- Wong, J. C. Y., and Williams, D. D. (2010). Sources and seasonal patterns of dissolved organic matter (DOM) in the hyporheic zone. *Hydrobiologia* 647, 99–111.
- Yamashita, Y., and Jaffé, R. (2008). Characterizing the interactions between trace metals and dissolved organic matter using excitation-emission matrix and parallel factor analysis. *Environ. Sci. Technol.* 42, 7374–7379.
- Young, K. C., Maurice, P. A., Docherty, K. M., and Bridgman, S. D. (2004). Bacterial degradation of dissolved organic matter from two northern Michigan streams. *Geomicrobiol. J.* 21, 521–528.

Conflict of Interest Statement: The authors declare that the research was conducted in the absence of any commercial or financial relationships that could be construed as a potential conflict of interest.

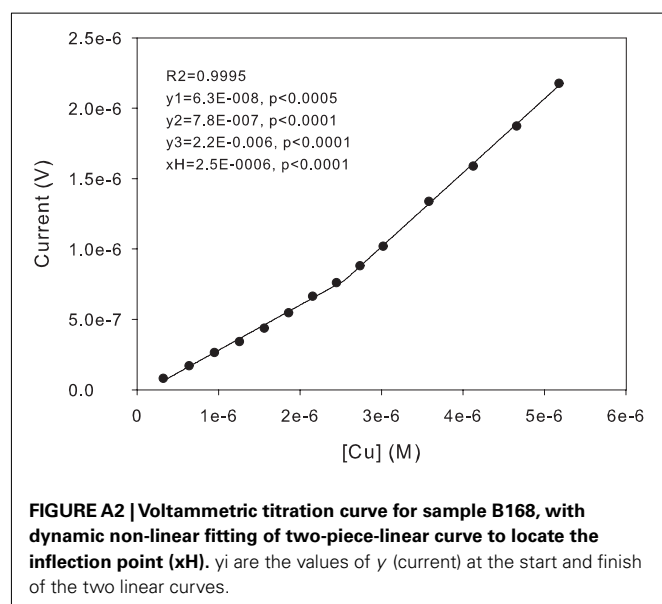
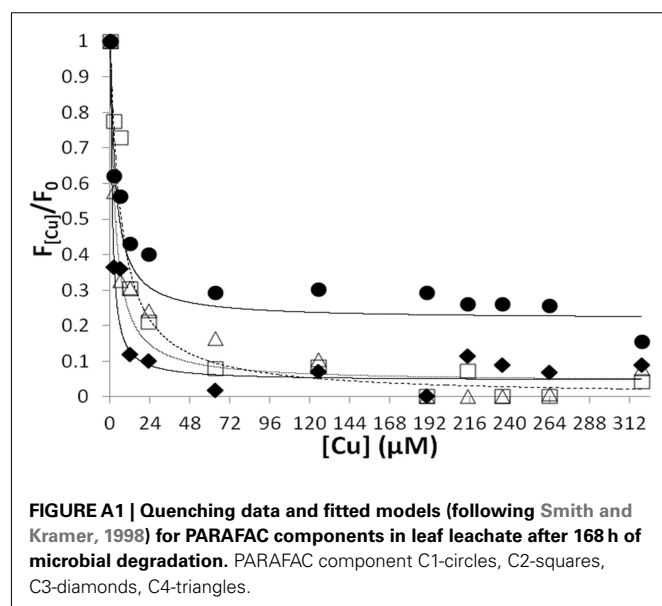
Received: 05 December 2011; accepted: 13 April 2012; published online: 07 May 2012.

Citation: Cuss CW and Guéguen C (2012) Impacts of microbial activity on the optical and copper-binding properties of leaf-litter leachate. *Front. Microbio.* 3:166. doi: 10.3389/fmicb.2012.00166

This article was submitted to *Frontiers in Microbiological Chemistry*, a specialty of *Frontiers in Microbiology*.

Copyright © 2012 Cuss and Guéguen. This is an open-access article distributed under the terms of the Creative Commons Attribution Non Commercial License, which permits non-commercial use, distribution, and reproduction in other forums, provided the original authors and source are credited.

APPENDIX





Iron utilization in marine cyanobacteria and eukaryotic algae

Joe Morrissey and Chris Bowler*

Ecole Normale Supérieure, Institut de Biologie de l'ENS, Paris, France
Inserm U1024, Paris, France
CNRS UMR 8197, Paris, France

Edited by:

Martha Gledhill, University of
Southampton, UK

Reviewed by:

Tom Bibby, University of
Southampton, UK
Adrian Marchetti, University of
North Carolina at Chapel Hill, USA

*Correspondence:

Chris Bowler, Institut de Biologie de
l'ENS, 46 Rue d'Ulm, 75005 Paris,
France.
e-mail: cbowler@biologie.ens.fr

Iron is essential for aerobic organisms. Additionally, photosynthetic organisms must maintain the iron-rich photosynthetic electron transport chain, which likely evolved in the iron-replete Proterozoic ocean. The subsequent rise in oxygen since those times has drastically decreased the levels of bioavailable iron, indicating that adaptations have been made to maintain sufficient cellular iron levels in the midst of scarcity. In combination with physiological studies, the recent sequencing of marine microorganism genomes and transcriptomes has begun to reveal the mechanisms of iron acquisition and utilization that allow marine microalgae to persist in iron limited environments.

Keywords: iron, cyanobacteria, diatoms, algae, phytoplankton, genomics, prasinophytes

INTRODUCTION

Iron is essential for all aerobic organisms, but is highly reactive and toxic via the Fenton reaction (Halliwell and Gutteridge, 1992). Consequently, organisms tightly control iron homeostasis and have highly coordinated responses to iron deficiency and iron overload. Photosynthetic organisms must also maintain the iron-rich photosynthetic electron transport chain, which likely evolved in the iron-replete reducing environments of the Proterozoic ocean (Falkowski, 2006). The levels of bioavailable iron have decreased drastically over time, concurrent with the rise in oxygen, indicating adaptations have been made to maintain sufficient iron levels in the midst of scarcity.

Still, limited iron availability impairs phytoplankton growth in as much as 40% of the ocean, notably in the Southern Ocean, equatorial Pacific Ocean, and north Pacific Ocean (Moore et al., 2001). As the levels of other nutrients are sufficient, these areas are categorized as high-nutrient, low-carbon (HNLC). This iron limitation has been evidenced by iron fertilization experiments of HNLC waters, which can produce rapidly growing algal blooms (Boyd et al., 2007; **Figure 1**), and ultimately, speculation that these blooms could be utilized to capture and sequester carbon from the atmosphere (Chisholm et al., 2001). At the same time, elevated atmospheric carbon will likely acidify the ocean, almost certainly altering iron bioavailability, and thus algal productivity (Shi et al., 2010). Consequently, much effort has been made to predict how climate change will affect iron availability and phytoplankton growth, and how altered phytoplankton growth will itself affect climate change.

Despite the large-scale experiments related to iron and the ocean, our current understanding of the underlying mechanisms of iron homeostasis in phytoplankton remains limited. Earlier work has shown that iron quotas are often optimized in marine phytoplankton, yet the mechanisms of iron uptake in these organisms remain obscure. The sequencing of

marine phytoplankton genomes and community metagenomes has revealed a plethora of genes of unknown function, many of which are species-specific (e.g., Rocap, 2003; Venter et al., 2004; Allen et al., 2008; Frias-Lopez et al., 2008; Maheswari et al., 2010). Thus it is proposed that phytoplankton survival in iron-starved waters could rely on novel adaptations encoded by these genes. Indeed, it was recently found that the newly cultured marine species *Chromera velia* appears to lack any of the currently characterized systems of iron uptake (Sutak et al., 2010); while the halophilic green alga *Dunaliella salina* was found to utilize a transferrin, an uptake system well-characterized in mammals, but otherwise unknown in plants (Paz et al., 2007). This review will focus on the recent advances in genomics in marine phytoplankton models that have begun to shed light on the adaptations that allow survival in environments where iron is vanishingly rare.

MARINE CYANOBACTERIA

Cyanobacteria, modern examples of the oldest oxygenic phototrophs, are proposed to have begun the great oxidation event – the initial oxygenation of the earth's atmosphere around 2.4 billion years ago (Kasting and Siefert, 2002). While metagenomic approaches have begun to reveal the diversity of bacteria in the oceans (e.g., Venter et al., 2004; Frias-Lopez et al., 2008; Zehr et al., 2008), the physiological characterization of iron homeostasis in free-living marine cyanobacteria has been primarily limited to the diazotrophs *Trichodesmium* and *Crocospaera watsonii*, and the non-diazotrophs *Synechococcus* and *Prochlorococcus*. The genome sequencing and expression analysis in these genera, combined with physiological characterization, suggest that several mechanisms to survive iron limitation exist across marine cyanobacteria species (**Table 1**):

1. Iron uptake is likely mediated by the FutA/IdiA-based ABC transporter system (**Figure 2**), genes for which have been

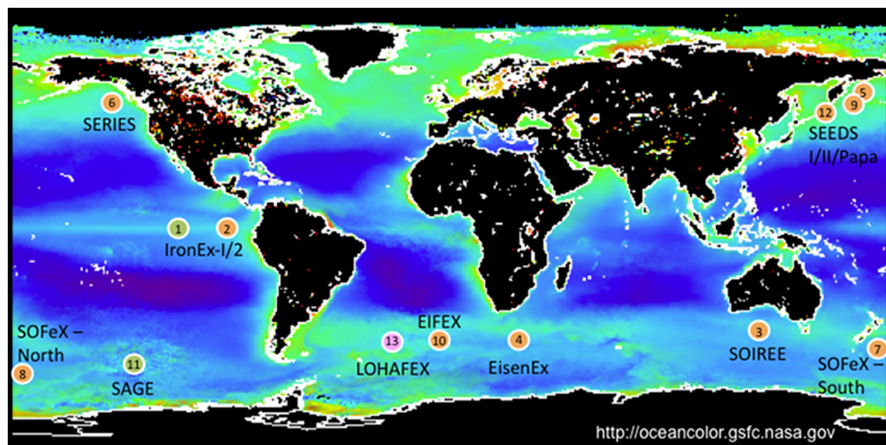


FIGURE 1 | Examples of iron limitation in the ocean as evidenced by rapid growth of diatoms and other plankton after iron fertilization experiments. Circle color indicates dominant plankton in resultant blooms: orange – diatoms; green – picophytoplankton; pink – zooplankton. 1 – IronEx-I,

1993; 2 – IronEx-II, 1995; 3 – SOIREE, 1999; 4 – EisenEx, 2000; 5 – SEEDS-I, 2001; 6 – SERIES, 2002; 7 – SOFeX North, 2002; 8 – SOFeX South, 2002; 9 – SEEDS-II, 2004; 10 – EIFEX, 2004; 11 – SAGE, 2004; 12 – PAPA-SEEDS, 2006; 13 – LOHAFEX, 2009. Adapted from Trick et al. (2010).

found in 28 unicellular cyanobacteria genomes of *Prochlorococcus*, *Synechococcus*, and *Synechocystis* (Rivers et al., 2009). *futA/idiA* is predicted to encode a periplasmic iron binding protein; *futB* likely encodes a Fe(III) permease; and *futC* an ATPase binding protein. Levels of FutA/IdiA protein increase under iron starvation in *Prochlorococcus* (Bibby et al., 2003; Thompson et al., 2011), *Trichodesmium* sp. IMS 101, *Crocosphaera* sp. WH8501, and *Synechococcus* spp. WH8103 and WH7803 (Webb et al., 2001). Work in freshwater cyanobacteria found that the *futA/idiA* ortholog *futA2* encodes a periplasmic iron concentrating protein essential for Fe(III) uptake (Katoh et al., 2001; Badarau et al., 2008). Additionally, freshwater cyanobacteria possess FutA1, which also functions in iron uptake (Katoh et al., 2001) but is found to localize to the thylakoid membrane and plays an unknown role in the protection of PSII (Michel et al., 1998; Exss-Sonne et al., 2000; Tölle et al., 2002). The role, if any, of FutA1 in marine cyanobacteria remains uninvestigated.

2. Iron limitation remodels the machinery of photosynthesis (Barber et al., 2006). Specifically, the number of photosynthetic complexes is reduced: iron-rich PSI (12 iron atoms) decreases, in favor of PSII (three iron atoms), and the number of phycobilisomes (which are synthesized by iron-containing proteins) decreases.
3. Finally, genome analysis of *Prochlorococcus*, *Synechococcus*, *Crocosphaera*, and *Trichodesmium* species suggests that nickel superoxide dismutase (SOD) is utilized in place of iron SOD to remove reactive oxygen species (ROS; Dufresne et al., 2003; Palenik et al., 2003; Rocap, 2003; Eitinger, 2004).

NON-DIAZOTROPHS

Prochlorococcus and *Synechococcus* are the two most prominent genera of picoplanktonic marine cyanobacteria (Partensky et al., 1999a). Although they overlap in some ecosystems and may have participated in lateral gene transfer (Beiko et al., 2005;

Zhaxybayeva et al., 2009), *Synechococcus* has a broader global distribution, especially in temperate latitudes and coastal regions, while *Prochlorococcus* is more abundant in tropical latitudes and oligotrophic environments (Zwirgmaier et al., 2008). *Synechococcus* and *Prochlorococcus* also differ in their light-harvesting apparatus: *Synechococcus* utilizes chlorophyll *a*, while *Prochlorococcus* utilizes divinyl chlorophylls *a* and *b* (Partensky et al., 1999b). The sequencing of these genomes is beginning to reveal the diverse genetic adaptations that allow survival in a range of nutrient environments.

Prochlorococcus

Prochlorococcus is a very small cyanobacteria (0.5–0.7 μm in diameter), ubiquitous within the latitudes 40°S to 40°N, and perhaps the most abundant photosynthetic organism on earth (Partensky et al., 1999b). Some natural populations have been shown to be somewhat iron-starved, as iron addition experiments have resulted in increased *Prochlorococcus* cell division, cell size, and chlorophyll levels (Cavender-Bares et al., 1999; Mann and Chisholm, 2000), and *Prochlorococcus* dominates *Synechococcus* in the iron limited equatorial Pacific (Campbell et al., 1997). *Prochlorococcus* populations, however, have been shown to be much less iron-starved than larger cells such as diatoms (Partensky et al., 1999b). The high surface-to-volume ratio of the small *Prochlorococcus* cell presumably aids nutrient uptake in these iron limited environments (Chisholm, 1992), although the MIT9313 ecotype was found to be more tolerant of iron limitation than the smaller-sized MED4 (Thompson et al., 2011). Presumably, this is because MIT9313 is from waters with 25-fold less total iron levels than MED4.

Prochlorococcus has a small genome of less than 2000 genes (Rocap et al., 2002), and the sequences of over a dozen strains have now been published. Several *Prochlorococcus* ecotypes possess iron homeostasis genes missing in some species of *Synechococcus* (Rocap, 2003), suggesting that they could be environmental adaptations. These include (Table 1):

Table 1 | Iron-related genes and proteins mentioned in the review (see text for reference).

ELECTRON TRANSPORT	
<i>isiA</i>	Novel chlorophyll-binding protein that forms chlorophyll-protein-antenna super-complexes during Fe-starvation
<i>isiB</i> (flavodoxin)	Fe-free electron transfer protein that can replace ferredoxin during Fe-starvation.
<i>petF</i> (ferredoxin)	Fe-S cluster based electron transfer protein used in a wide variety of reactions, including electron transfer to NADP ⁺ reductase during photosynthesis.
<i>petE</i> (plastocyanin)	Cu-based electron transfer protein that can replace cytochrome <i>c₆</i> during Fe-starvation; transfers electrons from cytochrome <i>b₆f</i> complex to PSI.
<i>petJ</i> (cytochrome <i>c₆</i>)	Cyanobacterial heme-based electron transport protein in thylakoid lumen downregulated during Fe-starvation; transfers electrons from cytochrome <i>b₆f</i> complex to PSI.
cytochrome <i>c_m</i>	Cyanobacterial heme-based electron transport protein downregulated during Fe-starvation; may function in PS and respiratory electron transport chains.
cytochrome <i>b₆f</i> complex	Fe-rich electron transfer and proton pumping complex in thylakoid membrane, down-regulated during Fe-starvation; mediates electron movement from PSII to PSI.
IRON TRANSPORT	
Bacterial Fe(III) transport system	
<i>idiA/futA/afuA</i>	Fe(III) binding protein
<i>idiB/futB</i>	Permease
<i>idiC/futC</i>	ATPase
Bacterial Fe(II) transport system	
<i>feoA</i>	Small soluble protein
<i>feoB</i>	Predicted Fe(II) permease
<i>feoC</i>	Predicted regulator
Divalent metal transporters	
<i>ZIP</i>	ZRT, IRT-like proteins – transports divalent transition metals into cytoplasm, e.g., Fe(II), Zn, Mn, Cu(II), Co, Ni, Cd
<i>NRAMP</i>	Natural resistance-associated macrophage proteins – transports divalent transition metals into cytoplasm, e.g., Fe(II), Zn, Mn, Cu(II), Co, Cd
Oxidase-permease based transport system	
<i>FRE</i>	Ferric chelate reductase – transfers electrons from NADH via heme to reduce Fe(III)
<i>FET3</i>	Multicopper ferroxidase that oxidizes Fe(II) from ferric reductases and passes Fe(III) to FTR
<i>FTR</i>	High affinity iron permease – transports Fe(III) across the plasma membrane, in complex with Fet3
OTHER	
<i>Fur</i>	Canonical bacterial transcriptional regulator that represses iron uptake genes
<i>FER</i>	Ferritin – sequesters and oxidizes Fe(II) in a multimer; found in the plastid and mitochondria of plants, and the cytosol and mitochondria of human; expression is induced by excess iron, thus mitigating oxidative stress.
<i>Ftn</i>	Bacterial ferritin.
<i>Dps</i>	DNA-binding proteins from starved cells – bacterial Fe-sequestering protein, that can also bind DNA.

- Flavodoxin (*isiB*), an iron-free electron transfer protein that can replace the functionally equivalent Fe-S protein ferredoxin (*petF*) under iron limitation (Erdner and Anderson, 1999).
- One to two ferritin genes (Figure 2). Ferritin is an iron storage protein associated with survival in low iron marine environments (Marchetti et al., 2009), and prevention of iron-induced oxidative stress in terrestrial organisms, e.g., *Arabidopsis* (Ravet et al., 2009) and humans (Corsi et al., 1998; Orino et al., 2001);
- Two to three *fur* genes, the canonical bacterial transcriptional regulator that represses iron uptake genes.
- Candidates for a high affinity iron scavenging system (Rocap et al., 2002).

The *Prochlorococcus* core genome lacks Fe-siderophore complex-related genes, but has components of a bacterial Fe(III) ABC transporter encoded by *idiA/futA/afuA*, *futB*, and *futC* (Rocap et al., 2003). However, it remains unclear what iron species

Prochlorococcus is able to transport. MIT9313 is more sensitive to copper than MED4 and possesses putative iron transport genes that are missing in MED4, suggesting variation exists in substrate specificity of iron uptake systems between the ecotypes (Thompson et al., 2011).

Examination of the transcriptional response to iron starvation using qPCR and microarrays found that flavodoxin (*isiB*) is upregulated and that ferredoxin (*petF*) is downregulated (Bibby et al., 2003; Thompson et al., 2011), while some genes associated with the iron-rich PSI and cytochrome *b₆f* complexes are downregulated, presumably allowing the reallocation of iron. To increase iron uptake, *idiA* is upregulated (although *futB* and *futC* are constitutively expressed under both iron-sufficiency and deficiency; Thompson et al., 2011). Finally, *hli* genes are upregulated, presumably to protect the photosystems from oxidative stress.

Comparisons of different *Prochlorococcus* “ecotypes” have found that there are differences in expression of iron-regulated

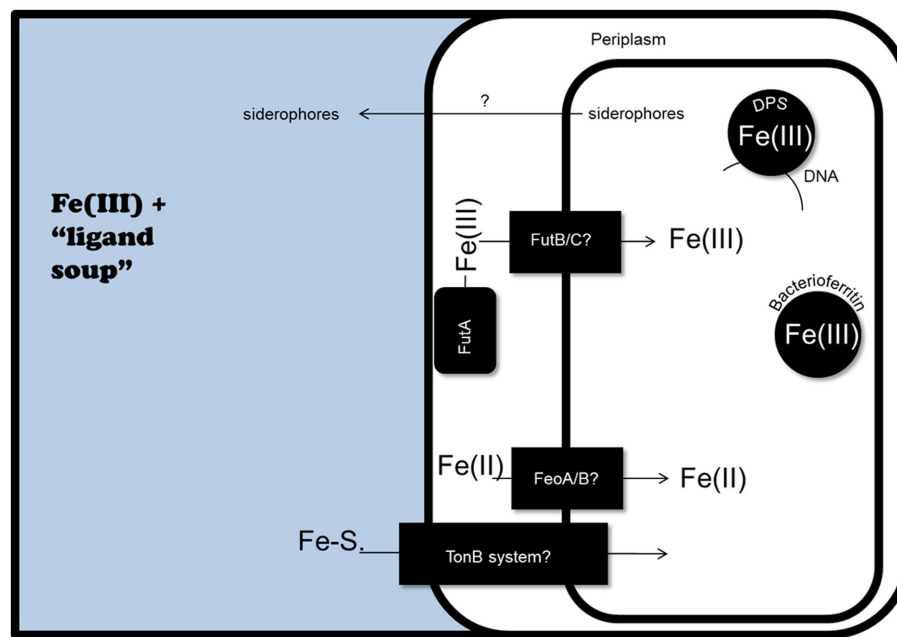


FIGURE 2 | Potential iron homeostasis systems in marine cyanobacteria, as predicted by genomic analyses. At least in part, iron uptake in cyanobacteria is likely facilitated by the concentration of Fe(III) in the periplasmic space by FutA, followed by transport into the cytoplasm by the FutB/FutC ABC transporter system. The presence of *FeoA/B* genes in

marine cyanobacteria genomes suggests Fe(II) uptake could also occur. Finally, the *Synechococcus* sp. PCC 7002 genome contains genes for siderophore biosynthesis, as well as Fe-siderophore (Fe-S.) uptake via a TonB dependent receptor system. Within the cell, iron could be sequestered by bacterioferritin and Dps.

genes, indicating there is natural variation in the iron deficiency response (Bibby et al., 2003; Thompson et al., 2011). An examination of MIT9313 and MED4 found that the iron-regulated transcriptome was enriched with genes from the genomic islands and genes outside the core genome (Thompson et al., 2011). It was previously shown that *Prochlorococcus* ecotypes use gene islands with nutrient transport and assimilation genes, perhaps gained by lateral gene transfer, to adapt to the phosphate and nitrogen availability of their environment (Martiny et al., 2006, 2009), so it is plausible that lateral gene transfer has also provided adaptations to iron limitation. Another potential adaptation strategy was identified in two ecotypes from low iron regions of the Eastern Equatorial Pacific upwelling and the tropical Indian Ocean through reconstruction of putative genomes of previously unidentified ecotypes from the 73 metagenomic samples of the Global Ocean Sampling expedition (Rusch et al., 2010). These two new genomes had the same assortment of iron uptake and stress genes as other ecotypes; however, six iron-containing proteins were absent. Assuming that the absence from these metagenomic data sets represents the absence from these actual genomes, this would indicate that the iron quotas are minimized via the loss of approximately 10% of the genes for iron-based proteins found in other *Prochlorococcus* ecotypes (Rusch et al., 2010). The missing iron-containing proteins include nitrate reductase, and several electron transfer proteins that are associated with the optimization of photosynthetic efficiency: two ferredoxins, plastoquinol oxidase (PTOX), and cytochrome c_m (Table 1). It was proposed that this reduces the maximum photosynthetic efficiency of these

ecotypes, but allows survival in a low iron environment. At the same time, this likely limits the ability of these ecotypes to respond and grow rapidly following the appearance of iron, as iron addition experiments in this part of the ocean show only a minimal response from *Prochlorococcus* (Rusch et al., 2010).

Synechococcus

Iron starvation of marine *Synechococcus* results in accumulation of glycogen granules, decreased chlorophyll *a* and thylakoid leaflets, and decreased protein levels of phycocyanin, allophycocyanin, and the PSII reaction center D1 peptide PsbA (Sherman and Sherman, 1983; Webb et al., 1994; Michel et al., 2003). The iron quota is likely minimized by the use of (Table 1):

- The copper-containing plastocyanin in place of the iron–protein cytochrome c_6 for electron transport from cytochrome b_6f complex to PSI.
- A cobalt-dependent ribonucleotide reductase.
- A putative nickel SOD (Rivers et al., 2009).

Flavodoxin (*isiB*) is present in all *Prochlorococcus* examined so far, but absent in nearly two-thirds of the marine *Synechococcus* genomes currently available. Finally, the gene *isiA* is present in the genomes of three out of the four marine *Synechococcus* species from environments that are perhaps iron limited (Bibby et al., 2009); thus it has been proposed to be an adaptation to low iron environments, although it is absent from the oligotrophic strain WH8102 (Dufresne et al., 2008). In the thermophilic freshwater

species *S. elongates*, *isiA* is upregulated in response to iron starvation (Park et al., 1999; Bibby et al., 2001a), resulting in the formation of giant PSI-IsiA-chlorophyll-protein-antenna super-complexes (Bibby et al., 2001a,b; Boekema et al., 2001). Disruption of *isiA* in the freshwater species results in increased photoinhibition and reduced growth under iron starvation (Michel et al., 1996; Park et al., 1999), suggesting it is an important component of the iron deficiency response. Again, the relationship of freshwater *IsiA* to that found in marine species has not yet been investigated.

How iron moves through the outer membrane is unknown, although the *Synechococcus* genome is heavily enriched with genes predicted to encode transporters (Palenik et al., 2003). Both a coastal (PCC 7002) and open ocean (CCMP 1334/WH7803) species of *Synechococcus* can utilize a variety of siderophores (Hutchins et al., 1999), although siderophore uptake genes have not been identified in the WH8102 genome (Palenik et al., 2003). However, it was observed that the freshwater cyanobacteria *Synechocystis* sp. PCC 6803 utilizes Fe(III)-siderophores through reduction, and then presumably transport of Fe(II) (Kranzler et al., 2011). Some coastal marine *Synechococcus* species produce siderophores (Wilhelm and Trick, 1994; Ito and Alison, 2005), and the genome of one of these, PCC 7002, contains genes related to siderophore biosynthesis and uptake via putative TonB dependent receptors (Hopkinson and Morel, 2009). However, siderophore secretion has not been found in oligotrophic *Synechococcus*, and siderophore synthesis and uptake genes have not been identified in WH8102 (Palenik et al., 2003), nor in genomes from other open ocean strains, including CCMP 1334/WH7803 (Hopkinson and Morel, 2009).

Further sequencing has revealed variation between genomes of coastal and open ocean *Synechococcus*, perhaps representing environment-specific adaptations for metal homeostasis. The open ocean is a more constant environment with lower nutrient levels, while wind-driven nutrient upwellings and inputs from land result in higher total iron concentrations in coastal environments (Ryther and Kramer, 1961). Appropriately, coastal species have higher iron quotas (Sunda et al., 1991), and the genome of the coastal species CC9311 was found to possess more genes for iron-containing proteins than the open ocean WH8102 (Palenik et al., 2006). Also unique to the coastal genome was *feoA/B*, predicted to encode putative Fe(II) transporters absent from WH8102 (Figure 2). This is of interest because it is proposed that bioavailable Fe(II) may be more abundant in the coastal ocean through photochemical reactions with organic matter (Kuma et al., 1992). In the CC9311 genome, *feoA/B* was located in islands of atypical trinucleotide composition, suggesting it was acquired through horizontal gene transfer (Palenik et al., 2006). Further examination of the genomes of several coastal *Synechococcus* species (WH5701, RS9917, and CC9311) again found *feoB*, while it is absent from *Prochlorococcus* genomes (Rivers et al., 2009).

The CC9311 genome also contains five copies of a bacterial ferritin, including one in an island suggestive of horizontal gene transfer (Palenik et al., 2006). Also present is *dpsA* (Palenik et al., 2006; Figure 2), a divergent member of the bacterioferritin super-family found in most marine *Synechococcus* genomes, and absent from most *Prochlorococcus* genomes (Rivers et al., 2009). In bacteria and Archaea, *dps* genes are often expressed during periods

of oxidative stress, long term nutrient deficiency, and stationary growth phase. In freshwater *S. elongates* species, disruption of *dpsA* results in death under iron starvation (Sen et al., 2000). Although its function remains unclear, *DpsA* from freshwater *Synechococcus* PCC 7942 contains heme and has weak catalase activity *in vitro* (Peña and Bullerjahn, 1995), is localized to the photosynthetic membranes (Durham and Bullerjahn, 2002), and can bind chromosomal DNA *in vitro* (Peña et al., 1995).

DIAZOTROPHS

Nitrogen fixation by diazotrophs allows growth in nitrogen starved waters; however this process is iron intensive, as the nitrogenase protein complex is composed of the iron-rich proteins NifH (four iron atoms per homodimer) and NifDK (15 iron atoms per homodimer; Rubio and Ludden, 2008). Biological nitrogen fixation in cyanobacteria is believed to have evolved in the anoxic ocean where Fe(II) was soluble and thus more bioavailable (Falkowski, 1997). Consequently, the scarcity of readily available iron in the modern ocean limits nitrogen fixation (Berman-Frank et al., 2001; Moore et al., 2009). At the same time, oxygenic photosynthesis and nitrogen fixation must be separated due to the extreme sensitivity of the nitrogenase Fe-S clusters to oxygen (Fay, 1992). Thus, diazotrophs must balance nitrogen and iron metabolism, both in terms of iron utilization, and the spatial and temporal arrangement of these incompatible reactions. Metagenomic analysis of oligotrophic seawater identified perhaps the most extreme adaptation to this dilemma in the ostensible absence of PSII genes from the genome of UCYN-A, an uncultured nitrogen-fixing cyanobacteria (Zehr et al., 2008; Tripp et al., 2010).

Trichodesmium

Trichodesmium is a nitrogen-fixing, filamentous, non-heterocystous cyanobacteria. Abundant in tropical and subtropical surface waters, *Trichodesmium* forms blooms thousands of kilometers wide and completes more marine nitrogen fixation than any other organism (Capone et al., 1997). However, the combination of iron-rich photosynthetic complexes and nitrogenase results in higher intracellular iron quotas for *Trichodesmium* than other phytoplankton (Kustka et al., 2003a). Iron limitation in *T. erythraeum* IMS101 results in decreased growth, filament length, and chlorophyll levels, in addition to decreased nitrogen fixation and photosynthetic efficiency (Shi et al., 2007; Küpper et al., 2008). Similar changes were seen in four other *Trichodesmium* species (Chappell and Webb, 2010). A unique adaptation to this high iron quota is found in puff colonies of *Trichodesmium* collected from the Red Sea (although not in laboratory cultures), which actively acquire desert dust and utilize the iron (Rubin et al., 2011). Striking movies show that dust particles quickly move along the cell surface of the trichome from the colony periphery to the core, where dust and oxides are actively dissolved by an unknown mechanism. As dust inputs are correlated with *Trichodesmium* abundance, the ability to directly and efficiently utilize wind-blown desert dust could fuel the giant blooms.

In the iron deficiency response, a “hierarchy of iron demand” is proposed to exist in *Trichodesmium*, with mRNA associated with nitrogen fixation being downregulated more quickly than

photosynthesis genes (Shi et al., 2007). In terms of upregulation, *idiA* and *isiA* expression were induced in response to iron starvation (Webb et al., 2001; Küpper et al., 2008), in addition to *isiB* (flavodoxin) and *feoB* (Chappell and Webb, 2010). The genomes of *Trichodesmium* species also contain multiple copies for the iron uptake regulator *fur*, and genes for bacterial ferritin and *dps* (Chappell and Webb, 2010). Additionally, the presence of TonB related genes suggests that *Trichodesmium* may have the ability to actively transport siderophores.

Crocospaera watsonii

The unicellular diazotroph *C. watsonii* is found in the tropical and subtropical open ocean. Intracellular iron levels change throughout the day, increasing at night with the expression of nitrogenase (Tuit et al., 2004). Analysis of the *C. watsonii* transcriptomes by qPCR revealed a temporal pattern to iron demand, correlating with increased expression of flavodoxin and the iron homeostasis genes *feoAB*, and *fur* in the evening (Shi et al., 2009). This suggests coordination with nitrogenase activity. Indeed, one *feoAB* operon is found within the *nif* cluster. A similar increase in evening expression of these iron-related genes is also seen in the unicellular diazotrophic cyanobacteria *Cyanothece* (Stockel et al., 2008).

Absolute quantitation of the protein levels (using selected reaction monitoring mass spectrometry with isotopically labeled peptide standards) across the diel cycle found that the synthesis of photosynthesis related proteins peaks in the day, and that the proteins are degraded as evening approaches. Conversely, the nitrogenase complex proteins are absent in the day and synthesized at night (Saito et al., 2011). At the same time, bacterioferritin protein levels cycle, with peaks matching both the maximum iron utilization points for photosynthesis and nitrogen fixation. This could suggest a role in handling the iron being transferred between the two systems. Thus, it is proposed that by shifting iron from photosynthesis in the day to nitrogen fixation at night, *C. watsonii* minimizes its iron quota and creates temporal separation of the two incompatible systems. Indeed, *C. watsonii* is predicted to have half the cellular iron concentration (relative to carbon) as *Trichodesmium*, which fixes nitrogen during the day (Kustka et al., 2003b; Saito et al., 2011).

EUKARYOTES

As described above for cyanobacteria, metagenomic approaches are uncovering a wealth of unknown marine eukaryotic phytoplankton species. In particular, alveolates and stramenopiles of great diversity and novelty are detected in almost all metagenome surveys (Massana and Pedrós-Alió, 2008). Community interactions may also be relevant to iron homeostasis. For example, a potential alga–bacteria mutualism in iron uptake between the dinoflagellate *Scrippsiella trochoidea* and *Marinobacter* could be representative of a more common iron uptake strategy among other phytoplankton (Amin et al., 2009). At the other end of the size spectrum, iron-rich whale feces also appears to serve as an important source of iron for phytoplankton in the Southern Ocean (Lavery et al., 2010). Additionally, the role of zooplankton grazing during iron fertilization experiments is of particular interest (Figure 1), as it may prevent the long term sequestration of carbon on the seafloor by diatoms (Bishop and Wood, 2009;

Mazzocchi et al., 2009). The haptophyte *Phaeocystis* also appears to play an important role in blooms from polar iron fertilization experiments (Pollard et al., 2009). However, relatively little is known about the physiologies of many of these organisms, and the genome sequences of most of them are not yet available.

Most progress to date has been made in understanding the genetic underpinnings of iron homeostasis in green algae and diatoms. Significantly, genome and transcriptome data, combined with the development of stable transformants to overexpress and knockdown genes in diatoms (Poulsen and Kröger, 2005; Saut et al., 2007; De Riso et al., 2009) and the green alga *Ostreococcus tauri* (Corellou et al., 2009) will likely accelerate our understanding of iron homeostasis in eukaryotic phytoplankton through functional genetics.

OSTREOCOCCUS

Ostreococcus are marine green algae belonging to the prasinophytes, and are described as the smallest free-living eukaryotes. *Ostreococcus* species possess very small, dense nuclear genomes of 12.5–13.0 Mbp. For comparison, the diatom *Phaeodactylum tricornutum* genome is 27.4 Mbp, and the *Chlamydomonas reinhardtii* genome is 120 Mbp. The two species of *Ostreococcus* that have been sequenced are from contrasting environments: *O. lucimarinus* from the open coastal waters of the Pacific Ocean (Worden et al., 2004); and *O. tauri* from a more nutrient-replete oyster production lagoon on the Mediterranean coast of France. TransportDB (www.membranetransport.org) predicts the presence of genes for divalent metal transporters ZIP and NRAMP (Ren et al., 2006; Table 1; Figure 3). Genes with similarity to prokaryotic siderophore uptake are present, and *O. lucimarinus* has genes that could represent a siderophore biosynthesis pathway (Palenik et al., 2007). Much like other marine phytoplankton, the iron quota is minimized: iron-free plastocyanin substitutes for cytochrome *c*₆; flavodoxin is present; and Ni–SOD, Cu/Zn–SOD, and Mn–SODs appear to replace Fe–SOD (Palenik et al., 2007). Transcript levels of ferritin and a ferredoxin family protein in *O. tauri* are clock regulated, both peaking at dusk (Monnier et al., 2010). It would thus be worthwhile to investigate the relationship between free iron and the recently identified *O. tauri* redox clock (O'Neill et al., 2011).

There are species-specific differences in the repertoire of iron homeostasis genes, although it is unclear how these relate to the different nutrient profiles of their respective environments. The *O. tauri* genome has genes that could encode a multi-copper oxidase and two putative ferric reductases lacking in *O. lucimarinus*, while *O. lucimarinus* has two copies of ferritin genes and *O. tauri* has only one (Palenik et al., 2007; Jancek et al., 2008).

MARINE DIATOMS

Diatoms, which carry out nearly 20% of photosynthesis on earth (Tréguer et al., 1995), are often found in the most iron limited regions of the ocean (Moore et al., 2001). Iron fertilization experiments often result in blooms dominated by diatoms, suggesting diatoms have adaptations that allow survival in iron limited waters and a subsequent rapid multiplication when iron becomes available. The recent metatranscriptomic analysis of iron fertilization bottle experiments found that diatoms possess a unique transcriptional response to the sudden appearance of iron (Marchetti et al.,

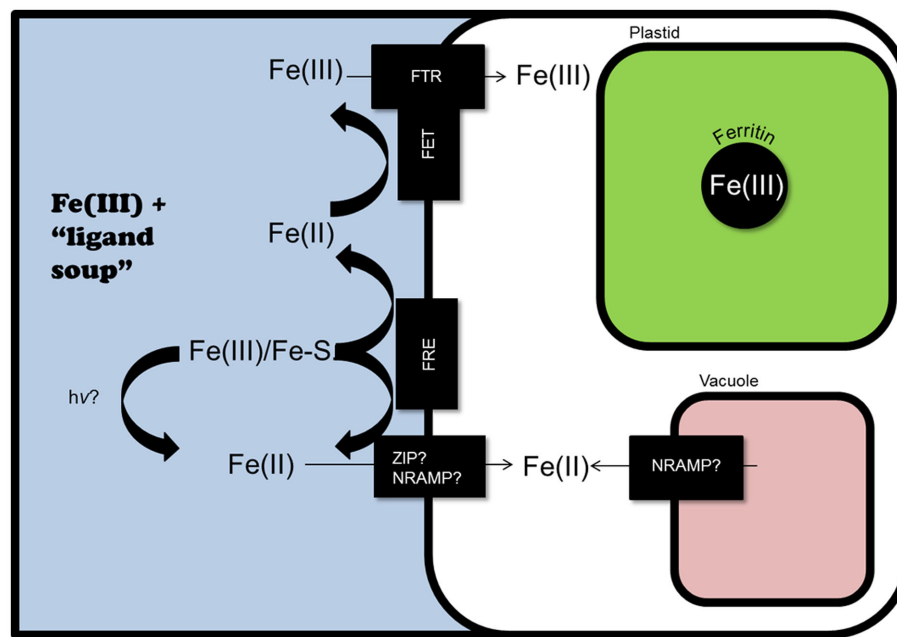


FIGURE 3 | Potential iron homeostasis systems in marine diatoms, as predicted by genomic analyses. Iron-regulated ferric reductase genes have been identified in *T. pseudonana* and *P. tricornutum*. These could reduce Fe(III) and Fe bound by siderophores (Fe-S), as could photoreduction ($h\nu$). Fe(II) could then enter the cytoplasm through iron-regulated transporters: ZIP in *P. tricornutum*, and NRAMP in *T. pseudonana* (although if TpnRAMP is localized to the tonoplast, it could

also serve to release iron from the vacuole during iron starvation). In *T. pseudonana*, extracellular Fe(II) could also be reoxidized and transported through a yeast-like Fe(III) uptake system, utilizing the iron-regulated multi-copper ferroxidase (*TpFET3*) and Fe(III) permeases (*TpFTR1* and *TpFTR2*). If ferritin is present (it is present in some pennate diatom genomes, but not in *T. pseudonana*), it can store iron, likely in the plastid.

2012). While other phytoplankton in the community increase gene expression for a broad array of iron-proteins like ferredoxin, cytochrome c_6 , and Fe-SOD, diatoms appear to prioritize expression of genes related to photosynthesis and nitrate uptake, reduction, and assimilation. Ostensibly, this strategy allows rapid diatom growth and bloom domination.

Representatives of the pennate and centric diatom lineages, *Thalassiosira pseudonana* and *P. tricornutum*, respectively, have been sequenced, and extensive molecular biology tools have been developed. Additionally, the publication of the polar pennate diatom *Fragilariopsis cylindrus* genome is imminent, and the bloom-forming pennate *Pseudo-nitzschia multiseries* is currently being sequenced. Despite these resources, predicting how diatom iron homeostasis systems function is complicated by the prevalence of unique genes of unknown function and by horizontal gene transfer. Currently, less than 50% of diatom genes have a putative function (Bowler et al., 2008; Maheswari et al., 2010), and the nuclear genome of *P. tricornutum* contains at least 587 genes predicted to be of bacterial origin (of which, around 60% are shared with *T. pseudonana*; Bowler et al., 2008).

Thalassiosira pseudonana

Thalassiosira pseudonana was the first eukaryotic marine phytoplankton sequenced. *T. pseudonana* has a small genome and has served as a model for marine centric diatom physiology experiments. *T. pseudonana* is often described as a marine coastal diatom, although recent phylogenetic analysis suggests *T. pseudonana* is

more closely related to the freshwater and marine diatom genus *Cyclotella* (Alverson et al., 2011). Consequently, it was postulated that *T. pseudonana* may be a freshwater diatom that is adapted to salinity, rather than a marine *Thalassiosira* species (Alverson et al., 2011).

Iron limitation of *T. pseudonana* results in:

- Decreased growth (Sunda and Huntsman, 1995) and photosynthetic efficiency (Bidle and Bender, 2007).
- Increased cell aggregation and silica deposition on the cell wall (Mock et al., 2008), with the relative proportion of iron in the cell wall increasing (Ellwood and Hunter, 2000).
- Increased oxidative stress and caspase activity, ultimately resulting in programmed cell death (Bidle and Bender, 2007; Thamatrakoln et al., 2011).

The sequencing of *T. pseudonana* revealed possible components of a yeast-like Fe(III) uptake system, including a multi-copper ferroxidase (*TpFET3*) and two iron permeases (*TpFTR1* and *TpFTR2*; Table 1; Figure 3; Armbrust et al., 2004). Additionally, there are at least two putative ferric reductases (*TpFRE1* and *TpFRE2*) and a putative divalent metal transporter (*TpNRAMP*), which could suggest a second, reduction-based uptake system, similar to those in *Arabidopsis* and humans. A similar combination of systems has been predicted to exist in *C. reinhardtii* (Merchant et al., 2006).

Transcript levels of *FRE1*, *FTR1*, *FTR2*, and *NRAMP* increase in response to iron limitation (Kustka et al., 2007), as does the

transcript for flavodoxin, and those of several genes associated with oxidative stress and programmed cell death (Thamatrakoln et al., 2011). The upregulation of the ferric reductases is of additional interest, as *T. pseudonana*, *T. weissflogii*, and *T. oceanica* can utilize iron–siderophores via reduction (Hutchins et al., 1999; Maldonado and Price, 2001; Shaked et al., 2005). Finally, microarray analysis found that more than a third of iron-regulated genes were genes of unknown function and hypothetical proteins (Thamatrakoln et al., 2011), suggesting the existence of novel adaptations to iron starvation. Of the genes upregulated in response to iron limitation, 84 were also upregulated under silicon limitation, providing further evidence that the iron and silicon starvation pathways are interconnected, particularly at the point of cell wall synthesis (Mock et al., 2008). It was thus proposed that iron is incorporated with silicon into the cell wall, or that iron–proteins could play a role in cell wall deposition (Mock et al., 2008). X-ray fluorescence tomography of the diatom *Cyclotella meneghiniana* revealed distinct iron bands girding the frustules, supporting the idea that iron has a specialized function in the cell wall (de Jonge et al., 2010). Unfortunately, it is difficult to draw conclusions for *T. pseudonana* from this interesting result, as the sample tested was a desiccated, freshwater diatom.

Thalassiosira oceanica

Relative to other *Thalassiosira* species, the open ocean species *T. oceanica* is more adapted to iron limitation, growing faster under these conditions than the coastal species *T. pseudonana* (Sunda et al., 1991; Maldonado and Price, 1996) and *T. weissflogii* (Strzepek and Harrison, 2004). Biochemical measurements found that a novel photosynthetic architecture minimizes the iron quota of *T. oceanica*, decreasing the concentrations of the iron-rich PSI (12 iron atoms) and cytochrome *b₆f* complexes (six iron atoms) by fivefold and sevenfold, respectively (Strzepek and Harrison, 2004). Additionally, the cytochrome *c₆* complex (one iron atom) is replaced by the copper-protein plastocyanin – a protein not found in *T. weissflogii* nor *T. pseudonana* (Peers and Price, 2006; Table 1). While photosynthetic efficiency of *T. oceanica* is not altered under normal light conditions, under high light it is more susceptible to photoinhibition and photosynthesis becomes nearly half as efficient as in *T. weissflogii*. The utilization of plastocyanin makes *T. oceanica* much more sensitive to copper limitation than *T. weissflogii* (Peers and Price, 2006). Thus, it is proposed that these adaptations to its low iron environment impair adjustment to rapid fluctuations in light intensity and copper limitation – environmental characteristics less common in the open ocean. Further adaptations to iron starvation likely exist in *T. oceanica*, because during iron limitation it is estimated that 100% of cellular iron is utilized by the electron transport carriers of photosynthesis, compared to only 50% in *T. weissflogii* (Strzepek and Harrison, 2004). The fate of the mitochondrial electron transport chain and other iron-containing proteins in iron-starved *T. oceanica* is worth investigating.

Finally, sequencing of the *T. oceanica* chloroplast genome revealed that the ferredoxin gene (*petF*) appears to have been transferred from the chloroplast genome to the nuclear genome (Lommer et al., 2010). Because the ferredoxin gene remains in the *T. pseudonana* and *T. weissflogii* chloroplast genomes, it is proposed that this change could alter regulation of ferredoxin

expression under iron limitation, presumably contributing to the observed tolerance to iron limitation (Lommer et al., 2010); although under iron limitation the ratio of ferredoxin to flavodoxin in *T. oceanica* is not significantly lower than in *T. weissflogii* (Strzepek and Harrison, 2004).

Phaeodactylum tricornutum

Phaeodactylum tricornutum can grow at iron levels 50 times lower than *T. pseudonana* (Kustka et al., 2007). *P. tricornutum* appears to use a fundamentally different iron uptake system than *T. pseudonana*, raising the possibility that it could be more effective at iron uptake under limiting conditions. The ferroxidase and iron permeases indicative of a yeast-like system in *T. pseudonana* have not been identified in the *P. tricornutum* genome (Kustka et al., 2007; Bowler et al., 2008). Examination of genes upregulated in response to iron starvation using expressed sequenced tags revealed two ferric reductases, *PtFRE1* and *PtFRE2* (Allen et al., 2008; Figure 3). The predicted *PtFRE2* protein appears highly similar to the root epidermal ferric reductase required for iron uptake in *Arabidopsis*, *AtFRO2* (Robinson et al., 1999; Bowler et al., 2008). Also highly upregulated is a putative ZIP family transporter that could serve to transport Fe(II) (Allen et al., 2008), as *AtIRT1* does in *Arabidopsis* (Palmer and Guerinot, 2009). Finally, the presence of *PtFBP*, a gene orthologous to the bacterial ferrichrome binding protein FhuD, raises the possibility of iron–siderophore utilization, perhaps through the scavenging of cyanobacteria siderophores. *FRE* and *FBP* may thus play a role in the ability of *P. tricornutum* to utilize iron–siderophore complexes, both through reduction (Figure 3) and the apparent uptake of intact complexes (Soria-Dengg and Horstmann, 1995).

At the same time, iron limitation results in a decrease in transcripts associated with iron intensive processes like photosynthesis, mitochondrial electron transport, and nitrate assimilation (Allen et al., 2008). At the protein level, the ratio of PSII to PSI increases, cytochrome *b₆f* and cytochrome *c₆* proteins decrease (Allen et al., 2008), and the activity of the iron-rich mitochondrial electron chain decreases (Kudo et al., 2000). The upregulation of transcript encoding the mitochondrial alternative oxidase (AOX) in response to iron limitation is proposed to mitigate the ROS presumably generated by iron-compromised electron transport chains (Allen et al., 2008). About 32% of genes regulated by iron in *P. tricornutum* have no ortholog in *T. pseudonana*, and iron starvation upregulates expression of several unique gene clusters in *P. tricornutum* (Allen et al., 2008). Of these genes, all but *FRE2* are present in *P. tricornutum* but not *T. pseudonana*, and many are of unknown function. Indeed, the most highly expressed transcript under iron limitation, *ISIP1*, encodes a predicted protein of unknown function found in metatranscriptomic samples from iron limited waters (Marchetti et al., 2012), and with no ortholog in *T. pseudonana* (Allen et al., 2008). And like *T. pseudonana*, there is a subset of silicon starvation regulated genes that are also regulated by iron (38 out of 223 Si-sensitive genes), although there is no apparent overlap between the *P. tricornutum* and *T. pseudonana* subsets (Sapriel et al., 2009).

***Pseudo-nitzschia* spp.**

Pseudo-nitzschia is a ubiquitous genus of pennate diatom, frequently dominating blooms in iron addition experiments (Hutchins and Bruland, 1998; de Baar, 2005; Trick et al., 2010).

Among *Pseudo-nitzschia* species, the oceanic *P. granii* is more tolerant of iron limitation than the coastal species *P. multiseriata* (Marchetti et al., 2009). *P. granii* is also more tolerant to iron starvation than *T. oceanica*, presumably because *P. granii* utilizes ferritin (Figure 3) to store iron during times of iron availability. Ferritin has not been detected in *T. oceanica* (Marchetti et al., 2009) and is absent from the *T. pseudonana* genome (Armbrust et al., 2004).

In addition to the utilization of ferritin, *Pseudo-nitzschia* is of interest because it is a eukaryotic marine phytoplankton which secretes the phytosiderophore-like compound domoic acid (DA), which is also a neurotoxin, and is causative of wildlife death and amnesic shellfish poisoning in humans. DA binds iron and copper (Rue and Bruland, 2001), and is structurally similar to the plant siderophore mugineic acid, which is secreted into soil by graminaceous plants. Because of its similarity to mugineic acid, it is proposed that DA could facilitate the extraction of iron from terrestrial sediments found in coastal waters (Rue and Bruland, 2001). The addition of exogenous DA to natural seawater samples increases iron uptake and growth of *Pseudo-nitzschia* (Maldonado et al., 2002; Wells et al., 2005), suggesting it is part of a *Pseudo-nitzschia* specific iron uptake system.

Domoic acid production has been observed to be induced by both metal availability and limitation: elevated copper (Rue and Bruland, 2001), copper limitation (Wells et al., 2005), iron limitation (Rue and Bruland, 2001), and iron fertilization (Silver et al., 2010; Trick et al., 2010). This suggests DA plays a role in both metal uptake during rapidly growing blooms and survival during limitation. DA binds iron with a low affinity, but the concentrations of DA in naturally occurring blooms are predicted to be sufficient to facilitate iron uptake (Rue and Bruland, 2001). The ability to monopolize iron availability via a species-specific phytosiderophore could thus explain the dominance of *Pseudo-nitzschia* in blooms.

CONCLUSION AND QUESTIONS FOR FUTURE RESEARCH

Other marine phytoplankton species have been sequenced (e.g., *Emiliania huxleyi*, *F. cylindrus*), and ever more will be. Presumably, transcriptome level analysis similar to those described above will be performed to determine which genes play a role in iron homeostasis. Additionally, metagenomic transcriptional analysis could be further applied to both classical bottle enrichment experiments (Marchetti et al., 2012), and large-scale iron fertilization experiments to elucidate the expression changes that underlie iron utilization during bloom formation.

REFERENCES

- Allen, A., LaRoche, J., Maheswari, U., Lommer, M., Schauer, N., Lopez, P., Finazzi, G., Fernie, A., and Bowler, C. (2008). Whole-cell response of the pennate diatom *Phaeodactylum tricornutum* to iron starvation. *Proc. Natl. Acad. Sci. U.S.A.* 105, 10438–10443.
- Alverson, A., Beszteri, B., Julius, M., and Theriot, E. (2011). The model marine diatom *Thalassiosira pseudonana* likely descended from a freshwater ancestor in the genus *Cyclotella*. *BMC Evol. Biol.* 11, 125. doi:10.1186/1471-2148-11-125
- Amin, S. A., Green, D. H., Hart, M. C., Küpper, F. C., Sunda, W. G., and Carrano, C. J. (2009). Photolysis of iron–siderophore chelates promotes bacterial–algal mutualism. *Proc. Natl. Acad. Sci. U.S.A.* 106, 17071–17076.
- Armbrust, E. V., Berges, J. A., Bowler, C., Green, B. R., Martinez, D., Putnam, N. H., Zhou, S., Allen, A. E., Apt, K. E., Bechner, M., Brzezinski, M. A., Chaal, B. K., Chiovitti, A., Davis, A. K., Demarest, M. S., Detter, J. C., Glavina, T., Goodstein, D., Hadi, M. Z., Hellsten, U., Hildebrand, M., Jenkins, B. D., Jurka, J., Kapitonov, V. V., Kröger, N., Lau, W. W. Y., Lane, T. W., Larimer, F. W., Lippmeier, J. C., Lucas, S., Medina, M., Montsant, A., Obornik, M., Parker, M. S., Palenik, B., Pazour, G. J., Richardson, P. M., Rynearson, T. A., Saito, M. A., Schwartz, D. C., Thamatrakoln, K., Valentin, K., Vardi, A., Wilkerson, F. P., and Rokhsar, D. S. (2004). The genome of the diatom *Thalassiosira pseudonana*: ecology, evolution, and metabolism. *Science* 306, 79–86.
- Badarau, A., Firkbank, S. J., Waldron, K. J., Yanagisawa, S., Robinson, N. J., Banfield, M. J., and Dennison, C. (2008). FutA2 is a ferric binding protein from *Synechocystis* PCC 6803. *J. Biol. Chem.* 283, 12520–12527.
- Barber, J., Nield, J., Duncan, J., and Bibby, T. S. (2006). “Accessory chlorophyll proteins in cyanobacterial photosystem I,” in *Photosystem I*, ed. J. H. Golbeck (Dordrecht: Springer), 99–117.

Genome level studies have offered hints about the genes responsible for iron acquisition. This has allowed the leveraging of the extensive research done in organisms like *Arabidopsis*, *Chlamydomonas*, yeast, and humans, to identify and predict the function of marine orthologs. Nevertheless, the mechanisms of iron uptake utilized by eukaryotic marine phytoplankton ultimately remain unclear. Predicting which genes comprise the marine iron uptake systems using the well-characterized terrestrial models is complicated by the unique nature of the ocean environment, both in terms of iron–ligand chemistry (Volker and Wolf-Gladrow, 1999; Morel, 2008; Hassler et al., 2011), and in terms of the convoluted evolutionary path of organisms like diatoms (Moustafa et al., 2009).

A more daunting gap in our understanding of iron homeostasis is the abundance of genes of unknown function. These are often species-specific, and found to comprise large portions of the ever growing number of genomic and metagenomic data sets. This is further complicated by the inability to cultivate and genetically transform many of the new species that metagenomic surveys are uncovering (e.g., UCYN-A, with its apparent lack of PSII genes; Zehr et al., 2008). Additionally, the absence of canonical genes does not necessarily prove the absence of a pathway, as was recently demonstrated in freshwater cyanobacteria. Since the late 1960s, cyanobacteria were believed to lack a complete TCA cycle, as the 2-oxoglutarate dehydrogenase protein was undetected and the gene was missing from freshwater and marine cyanobacteria genomes. However, the recent functional characterization of candidate genes from *Synechococcus* sp. PCC 7002 identified two enzymes that perform the same role as 2-oxoglutarate dehydrogenase, completing the TCA cycle (Zhang and Bryant, 2011). It also appears that further divergence is possible, as these two genes are present in all cyanobacteria genomes except those of marine *Synechococcus* and *Prochlorococcus*.

Thus, functional characterization of putative uptake genes in model organisms is required to establish even the most basic mechanisms for iron transport in marine phytoplankton, while genetic screening (e.g., mutagenesis, expression of gene libraries derived from marine microorganisms in heterologous systems, etc.) could be utilized to identify novel iron homeostasis systems that have evolved in iron limited ocean environments.

ACKNOWLEDGMENTS

We thank the reviewers for their helpful comments. Funding in the laboratory is supported by the Agence Nationale de la Recherche.

- Beiko, R. G., Harlow, T. J., and Ragan, M. A. (2005). Highways of gene sharing in prokaryotes. *Proc. Natl. Acad. Sci. U.S.A.* 102, 14332–14337.
- Berman-Frank, I., Cullen, J. T., Shaked, Y., Sherrell, R. M., and Falkowski, P. G. (2001). Iron availability, cellular iron quotas, and nitrogen fixation in *Trichodesmium*. *Limnol. Oceanogr.* 46, 1249–1260.
- Bibby, T., Nield, J., Partensky, F., and Barber, J. (2001a). Antenna ring around photosystem I. *Nature* 413, 590.
- Bibby, T. S., Nield, J., and Barber, J. (2001b). Iron deficiency induces the formation of an antenna ring around trimeric photosystem I in cyanobacteria. *Nature* 412, 743–745.
- Bibby, T. S., Mary, I., Nield, J., Partensky, F., and Barber, J. (2003). Low-light-adapted *Prochlorococcus* species possess specific antennae for each photosystem. *Nature* 424, 1051–1054.
- Bibby, T. S., Zhang, Y., and Chen, M. (2009). Biogeography of photosynthetic light-harvesting genes in marine phytoplankton. *PLoS ONE* 4, e4601. doi:10.1371/journal.pone.0004601
- Bidle, K. D., and Bender, S. J. (2007). Iron starvation and culture age activate metacaspases and programmed cell death in the marine diatom *Thalassiosira pseudonana*. *Eukaryot. Cell* 7, 223–236.
- Bishop, J. K. B., and Wood, T. J. (2009). Year-round observations of carbon biomass and flux variability in the Southern Ocean. *Global Biogeochem. Cycles* 23, GB2019.
- Boekema, E. J., Hifney, A., Yakushevskaya, A. E., Piotrowski, M., Keegstra, W., Berry, S., Michel, K. P., Pistorius, E. K., and Kruip, J. (2001). A giant chlorophyll-protein complex induced by iron deficiency in cyanobacteria. *Nature* 412, 745–748.
- Bowler, C., Allen, A., Badger, J., Grimwood, J., Jabbari, K., Kuo, A., Maheswari, U., Martens, C., Maumus, F., and Otilar, R. (2008). The *Phaeodactylum* genome reveals the evolutionary history of diatom genomes. *Nature* 456, 239–244.
- Boyd, P., Jickells, T., Law, C., Blain, S., Boyle, E., Buesseler, K., Coale, K., Cullen, J., de Baar, H., Follows, M., Harvey, M., Lancelot, C., Levasseur, M., Owens, N., Pollard, R., Rivkin, R., Sarmiento, J., Schoemann, V., Smetacek, V., Takeda, S., Tsuda, A., Turner, S., and Watson, A. (2007). Mesoscale iron enrichment experiments 1993–2005: synthesis and future directions. *Science* 315, 612–617.
- Campbell, L., Liu, H., Nolla, H. A., and Vault, D. (1997). Annual variability of phytoplankton and bacteria in the subtropical North Pacific Ocean at Station ALOHA during the 1991–1994 ENSO event. *Deep Sea Res. Part I Oceanogr. Res. Pap.* 44, 167–192.
- Capone, D. G., Zehr, J. P., Paerl, H. W., Bergman, B., and Carpenter, E. J. (1997). *Trichodesmium*, a globally significant marine cyanobacterium. *Science* 276, 1221–1229.
- Cavender-Bares, K. K., Mann, E. L., Chisholm, S. W., Ondrusek, M. E., and Bidigare, R. R. (1999). Differential response of equatorial Pacific phytoplankton to iron fertilization. *Limnol. Oceanogr.* 44, 237–246.
- Chappell, P. D., and Webb, E. A. (2010). A molecular assessment of the iron stress response in the two phylogenetic clades of *Trichodesmium*. *Environ. Microbiol.* 12, 13–27.
- Chisholm, S. W. (1992). "Phytoplankton size," in *Primary Productivity and Biogeochemical Cycles in the Sea*, eds P. G. Falkowski and A. D. Woodhead (New York, NY: Plenum Press), 213–237.
- Chisholm, S. W., Falkowski, P. G., and Cullen, J. J. (2001). Dis-crediting ocean fertilization. *Science* 294, 309–310.
- Corellou, F., Schwartz, C., Motta, J.-P., Djouani-Tahri, E. B., Sanchez, F., and Bouget, F.-Y. (2009). Clocks in the green lineage: comparative functional analysis of the circadian architecture of the picoeukaryote *Ostreococcus*. *Plant Cell* 21, 3436–3449.
- Corsi, B., Perrone, F., Bourgeois, M., Beaumont, C., Panzeri, M. C., Cozzi, A., Sangregorio, R., Santambrogio, P., Albertini, A., and Arosio, P. (1998). Transient overexpression of human H- and L-ferritin chains in COS cells. *Biochem. J.* 330, 315.
- de Baar, H. J. W. (2005). Synthesis of iron fertilization experiments: from the iron age in the age of enlightenment. *J. Geophys. Res.* 110, C09S16.
- de Jonge, M. D., Holzner, C., Baines, S. B., Twining, B. S., Ignatyev, K., Diaz, J., Howard, D. L., Legnini, D., Miceli, A., McNulty, I., Jacobsen, C. J., and Vogt, S. (2010). Quantitative 3D elemental microtomography of *Cyclotella meneghiniana* at 400-nm resolution. *Proc. Natl. Acad. Sci. U.S.A.* 107, 15676–15680.
- De Riso, V., Raniello, R., Maumus, F., Rogato, A., Bowler, C., and Falcitatore, A. (2009). Gene silencing in the marine diatom *Phaeodactylum tricornutum*. *Nucleic Acids Res.* 37, e96.
- Dufresne, A., Ostrowski, M., Scanlan, D., Garczarek, L., Mazard, S., Palenik, B., Paulsen, I., de Marsac, N., Wincker, P., Dossat, C., Ferreira, S., Johnson, J., Post, A., Hess, W., and Partensky, F. (2008). Unraveling the genomic mosaic of a ubiquitous genus of marine cyanobacteria. *Genome Biol.* 9, R90.
- Dufresne, A., Salanoubat, M., Partensky, F., Artiguenave, F., Axmann, I. M., Barbe, V., Duprat, S., Galperin, M. Y., Koonin, E. V., Le Gall, F., Makarova, K. S., Ostrowski, M., Oztas, S., Robert, C., Rogozin, I. B., Scanlan, D. J., de Marsac, N. T., Weissenbach, J., Wincker, P., Wolf, Y. I., and Hess, W. R. (2003). Genome sequence of the cyanobacterium *Prochlorococcus marinus* SS120, a nearly minimal oxyphototrophic genome. *Proc. Natl. Acad. Sci. U.S.A.* 100, 10020–10025.
- Durham, K. A., and Bullerjahn, G. S. (2002). Immunocytochemical localization of the stress-induced DpsA protein in the cyanobacterium *Synechococcus* sp. strain PCC 7942. *J. Basic Microb.* 42, 367–372.
- Eitinger, T. (2004). In vivo production of active nickel superoxide dismutase from *Prochlorococcus marinus* MIT9313 is dependent on its cognate peptidase. *J. Bacteriol.* 186, 7821.
- Ellwood, M. J., and Hunter, K. A. (2000). The incorporation of zinc and iron into the frustule of the marine diatom *Thalassiosira pseudonana*. *Limnol. Oceanogr.* 1517–1524.
- Erdner, D. L., and Anderson, D. M. (1999). Ferredoxin and flavodoxin as biochemical indicators of iron limitation during open-ocean iron enrichment. *Limnol. Oceanogr.* 44, 1609–1615.
- Exss-Sonne, P., Toelle, J., Bader, K., Pistorius, E., and Michel, K. P. (2000). The IdiA protein of *Synechococcus* sp. PCC 7942 functions in protecting the acceptor side of photosystem II under oxidative stress. *Photosynth. Res.* 63, 145–157.
- Falkowski, P. G. (1997). Evolution of the nitrogen cycle and its influence on the biological sequestration of CO₂ in the ocean. *Nature* 387, 272–275.
- Falkowski, P. G. (2006). Tracing oxygen's imprint on Earth's metabolic evolution. *Science* 311, 1724.
- Fay, P. (1992). Oxygen relations of nitrogen fixation in cyanobacteria. *Microbiol. Rev.* 56, 340–373.
- Frias-Lopez, J., Shi, Y., Tyson, G. W., Coleman, M. L., Schuster, S. C., Chisholm, S. W., and DeLong, E. F. (2008). Microbial community gene expression in ocean surface waters. *Proc. Natl. Acad. Sci. U.S.A.* 105, 3805–3810.
- Halliwel, B., and Gutteridge, J. (1992). Biologically relevant metal ion-dependent hydroxyl radical generation, an update. *FEBS Lett.* 307, 108–112.
- Hassler, C. S., Schoemann, V., Nichols, C. M., Butler, E. C. V., and Boyd, P. W. (2011). Saccharides enhance iron bioavailability to Southern Ocean phytoplankton. *Proc. Natl. Acad. Sci. U.S.A.* 108, 1076–1081.
- Hopkinson, B., and Morel, F. (2009). The role of siderophores in iron acquisition by photosynthetic marine microorganisms. *Biometals* 22, 659–669.
- Hutchins, D. A., and Bruland, K. W. (1998). Iron-limited diatom growth and Si:N uptake ratios in a coastal upwelling regime. *Nature* 393, 561–564.
- Hutchins, D. A., Witter, A. E., Butler, A., and Luther, G. W. (1999). Competition among marine phytoplankton for different chelated iron species. *Nature* 400, 858–861.
- Ito, Y., and Alison, B. (2005). Structure of synechobactins, new siderophores of the marine cyanobacterium *Synechococcus* sp. PCC 7002. *Limnol. Oceanogr.* 50, 1918–1923.
- Jancek, S., Gourbière, S., Moreau, H., and Piganeau, G. (2008). Clues about the genetic basis of adaptation emerge from comparing the proteomes of two *Ostreococcus* ecotypes (Chlorophyta, Prasinophyceae). *Mol. Biol. Evol.* 25, 2293–2300.
- Kasting, J. F., and Siefert, J. L. (2002). Life and the evolution of Earth's atmosphere. *Science* 296, 1066–1068.
- Katoh, H., Hagino, N., and Ogawa, T. (2001). Iron-binding activity of FutA1 subunit of an ABC-type iron transporter in the cyanobacterium *Synechocystis* sp. strain PCC 6803. *Plant Cell Physiol.* 42, 823.
- Kranzler, C., Lis, H., Shaked, Y., and Keren, N. (2011). The role of reduction in iron uptake processes in a unicellular, planktonic cyanobacterium. *Environ. Microbiol.* 13, 2990–2999.
- Kudo, I., Miyamoto, M., Noiri, Y., and Maita, Y. (2000). Combined effects of temperature and iron on the growth and physiology of the marine diatom *Phaeodactylum tricornutum* (Bacillariophyceae). *J. Phycol.* 36, 1096–1102.
- Kuma, K., Nakabayashi, S., Suzuki, Y., Kudo, I., and Matsunaga, K. (1992). Photo-reduction of Fe(III) by dissolved organic substances and existence of Fe(II) in seawater during spring blooms. *Mar. Chem.* 37, 15–27.

- Küpper, H., Šetlík, I., Seibert, S., Prášil, O., Šetlikova, E., Strittmatter, M., Levitan, O., Lohscheider, J., Adamska, I., and Berman-Frank, I. (2008). Iron limitation in the marine cyanobacterium *Trichodesmium* reveals new insights into regulation of photosynthesis and nitrogen fixation. *New Phytol.* 179, 784–798.
- Kustka, A., Allen, A., and Morel, F. (2007). Sequence analysis and transcriptional regulation of iron acquisition genes in two marine diatoms. *J. Phycol.* 43, 715–729.
- Kustka, A., Sainudo-Wilhelmy, S., Carpenter, E. J., Capone, D. G., and Raven, J. A. (2003a). A revised estimate of the iron use efficiency of nitrogen fixation, with special reference to the marine cyanobacterium *Trichodesmium* spp. (Cyanophyta). *J. Phycol.* 39, 12–25.
- Kustka, A. B., Sainudo-Wilhelmy, S. A., Carpenter, E. J., Capone, D., Burns, J., and Sunda, W. G. (2003b). Iron requirements for dinitrogen and ammonium-supported growth in cultures of *Trichodesmium* (IMS 101): comparison with nitrogen fixation rates and iron: carbon ratios of field populations. *Limnol. Oceanogr.* 48, 1869–1884.
- Lavery, T. J., Roudnew, B., Gill, P., Seymour, J., Seuront, L., Johnson, G., Mitchell, J. G., and Smetacek, V. (2010). Iron defecation by sperm whales stimulates carbon export in the Southern Ocean. *Proc. R. Soc. Lond. B Biol. Sci.* 277, 3527–3531.
- Lommer, M., Roy, A.-S., Schilabel, M., Schreiber, S., Rosenstiel, P., and LaRoche, J. (2010). Recent transfer of an iron-regulated gene from the plastid to the nuclear genome in an oceanic diatom adapted to chronic iron limitation. *BMC Genomics* 11, 718. doi:10.1186/1471-2164-11-718
- Maheswari, U., Jabbari, K., Petit, J.-L., Porcel, B., Allen, A., Cadoret, J.-P., De Martino, A., Heijde, M., Kaas, R., La Roche, J., Lopez, P., Martin-Jezequel, V., Meichenin, A., Mock, T., Schnitzler Parker, M., Vardi, A., Armbrust, E. V., Weisenbach, J., Katinka, M., and Bowler, C. (2010). Digital expression profiling of novel diatom transcripts provides insight into their biological functions. *Genome Biol.* 11, R85.
- Maldonado, M. T., Hughes, M. P., Rue, E. L., and Wells, M. L. (2002). The effect of Fe and Cu on growth and domoic acid production by *Pseudo-nitzschia multiseries* and *Pseudo-nitzschia australis*. *Limnol. Oceanogr.* 47, 515–526.
- Maldonado, M. T., and Price, N. M. (1996). Influence of N substrate on Fe requirements of marine centric diatoms. *Mar. Ecol. Prog. Ser.* 141, 161–172.
- Maldonado, M. T., and Price, N. M. (2001). Reduction and transport of organically bound iron by *Thalassiosira oceanica* (Bacillariophyceae). *J. Phycol.* 37, 298–310.
- Mann, E. L., and Chisholm, S. W. (2000). Iron limits the cell division rate of *Prochlorococcus* in the eastern equatorial Pacific. *Limnol. Oceanogr.* 45, 1067–1076.
- Marchetti, A., Parker, M. S., Moccia, L. P., Lin, E. O., Arrieta, A. L., Ribalet, F., Murphy, M. E. P., Maldonado, M. T., and Armbrust, E. V. (2009). Ferritin is used for iron storage in bloom-forming marine pennate diatoms. *Nature* 457, 467–470.
- Marchetti, A., Schruth, D. M., Durkin, C. A., Parker, M. S., Kodner, R. B., Berthiaume, C. T., Morales, R., Allen, A. E., and Armbrust, E. V. (2012). Comparative metatranscriptomics identifies molecular bases for the physiological responses of phytoplankton to varying iron availability. *Proc. Natl. Acad. Sci. U.S.A.* 109, E317–E325.
- Martiny, A. C., Coleman, M. L., and Chisholm, S. W. (2006). Phosphate acquisition genes in *Prochlorococcus* ecotypes: evidence for genome-wide adaptation. *Proc. Natl. Acad. Sci. U.S.A.* 103, 12552–12557.
- Martiny, A. C., Kathuria, S., and Berube, P. M. (2009). Widespread metabolic potential for nitrite and nitrate assimilation among *Prochlorococcus* ecotypes. *Proc. Natl. Acad. Sci. U.S.A.* 106, 10787–10792.
- Massana, R., and Pedrós-Alió, C. (2008). Unveiling new microbial eukaryotes in the surface ocean. *Curr. Opin. Microbiol.* 11, 213–218.
- Mazzocchi, M. G., González, H. E., Vandromme, P., Borrión, I., DeAlcala, M., Gauns, M., Assmy, P., Fuchs, B., Klaas, C., and Martin, P. (2009). A non-diatom plankton bloom controlled by copepod grazing and amphipod predation: preliminary results from the LOHAFEX iron-fertilisation experiment. *GLOBEC International Newsletter* 15, 3–6.
- Merchant, S. S., Allen, M. D., Kropat, J., Moseley, J. L., Long, J. C., Tottey, S., and Terauchi, A. M. (2006). Between a rock and a hard place: trace element nutrition in *Chlamydomonas*. *Biochim. Biophys. Acta* 1763, 578–594.
- Michel, K.-P., Berry, S., Hifney, A., Kruip, J., and Pistorius, E. (2003). Adaptation to iron deficiency: a comparison between the cyanobacterium *Synechococcus elongatus* PCC 7942 wild-type and a DpsA-free mutant. *Photosynth. Res.* 75, 71–84.
- Michel, K.-P., Exss-Sonne, P., Scholten-Beck, G., Kahmann, U., Ruppel, H. G., and Pistorius, E. K. (1998). Immunocytochemical localization of IdIA, a protein expressed under iron or manganese limitation in the mesophilic cyanobacterium *Synechococcus* PCC 6301 and the thermophilic cyanobacterium *Synechococcus elongatus*. *Planta* 205, 73–81.
- Michel, K.-P., Thole, H. H., and Pistorius, E. K. (1996). IdIA, a 34 kDa protein in the cyanobacteria *Synechococcus* sp. strains PCC 6301 and PCC 7942, is required for growth under iron and manganese limitations. *Microbiology* 142, 2635–2645.
- Mock, T., Samanta, M. P., Iverson, V., Berthiaume, C., Robison, M., Holtermann, K., Durkin, C., Bon-Durant, S. S., Richmond, K., Rodesch, M., Kallas, T., Huttlin, E. L., Cerrina, E., Sussman, M. R., and Armbrust, E. V. (2008). Whole-genome expression profiling of the marine diatom *Thalassiosira pseudonana* identifies genes involved in silicon bioprocesses. *Proc. Natl. Acad. Sci. U.S.A.* 105, 1579–1584.
- Monnier, A., Liverani, S., Bouvet, R., Jesson, B., Smith, J., Mosser, J., Corellou, F., and Bouget, F.-Y. (2010). Orchestrated transcription of biological processes in the marine picoeukaryote *Ostreococcus* exposed to light/dark cycles. *BMC Genomics* 11, 192. doi:10.1186/1471-2164-11-192
- Moore, C. M., Mills, M. M., Achterberg, E. P., Geider, R. J., LaRoche, J., Lucas, M. I., McDonagh, E. L., Pan, X., Poulton, A. J., Rijkenberg, M. J. A., Suggett, D. J., Ussher, S. J., and Woodward, E. M. S. (2009). Large-scale distribution of Atlantic nitrogen fixation controlled by iron availability. *Nat. Geosci.* 2, 867–871.
- Moore, J. K., Doney, S. C., Glover, D. M., and Fung, I. Y. (2001). Iron cycling and nutrient-limitation patterns in surface waters of the World Ocean. *Deep Sea Res. Part I Oceanogr. Res. Pap.* 49, 463–507.
- Morel, F. M. M. (2008). The co evolution of phytoplankton and trace element cycles in the oceans. *Geobiology* 6, 318–324.
- Moustafa, A., Beszteri, B., Maier, U. G., Bowler, C., Valentin, K., and Bhat-tacharya, D. (2009). Genomic footprints of a cryptic plastid endosymbiosis in diatoms. *Science* 324, 1724–1726.
- O'Neill, J. S., van Ooijen, G., Dixon, L. E., Troein, C., Corellou, F., Bouget, F.-Y., Reddy, A. B., and Millar, A. J. (2011). Circadian rhythms persist without transcription in a eukaryote. *Nature* 469, 554–558.
- Orino, K., Lehman, L., Tsuji, Y., Ayaki, H., Torti, S. V., and Torti, F. M. (2001). Ferritin and the response to oxidative stress. *Biochem. J.* 357, 241.
- Palenik, B., Brahamsha, B., Larimer, F. W., Land, M., Hauser, L., Chain, P., Lamerdin, J., Regala, W., Allen, E. E., McCarrren, J., Paulsen, I., Dufresne, A., Partensky, F., Webb, E. A., and Waterbury, J. (2003). The genome of a motile marine *Synechococcus*. *Nature* 424, 1037–1042.
- Palenik, B., Grimwood, J., Aerts, A., Rouze, P., Salamov, A., Putnam, N., Dupont, C., Jorgensen, R., Derelle, E., and Rombauts, S. (2007). The tiny eukaryote *Ostreococcus* provides genomic insights into the paradox of plankton speciation. *Proc. Natl. Acad. Sci. U.S.A.* 104, 7705–7710.
- Palenik, B., Ren, Q., Dupont, C. L., Myers, G. S., Heidelberg, J. F., Badger, J. H., Madupu, R., Nelson, W. C., Brinkac, L. M., Dodson, R. J., Durkin, A. S., Daugherty, S. C., Sullivan, S. A., Khouri, H., Mohamoud, Y., Halpin, R., and Paulsen, I. T. (2006). Genome sequence of *Synechococcus* CC9311: insights into adaptation to a coastal environment. *Proc. Natl. Acad. Sci. U.S.A.* 103, 13555–13559.
- Palmer, C. M., and Guerinet, M. L. (2009). Facing the challenges of Cu, Fe and Zn homeostasis in plants. *Nat. Chem. Biol.* 5, 333–340.
- Park, Y.-I., Sandström, S., Gustafsson, P., and Öquist, G. (1999). Expression of the isiA gene is essential for the survival of the cyanobacterium *Synechococcus* sp. PCC 7942 by protecting photosystem II from excess light under iron limitation. *Mol. Microbiol.* 32, 123–129.
- Partensky, F., Blanchot, J., and Vaulot, D. (1999a). Differential distribution and ecology of *Prochlorococcus* and *Synechococcus* in oceanic waters: a review. *Bull. Inst. Oceanogr. Monaco Numero Spec.* 19, 431–449.
- Partensky, F., Hess, W., and Vaulot, D. (1999b). *Prochlorococcus*, a marine photosynthetic prokaryote of global significance. *Microbiol. Mol. Biol. Rev.* 63, 106.
- Paz, Y., Katz, A., and Pick, U. (2007). A multicopper ferroxidase involved in iron binding to transferrins in *Dunaliella salina* plasma membranes. *J. Biol. Chem.* 282, 8658–8666.

- Peers, G., and Price, N. (2006). Copper-containing plastocyanin used for electron transport by an oceanic diatom. *Nature* 441, 341–344.
- Peña, M. M. O., and Bullerjahn, G. S. (1995). The DpsA protein of *Synechococcus* sp. strain PCC7942 is a DNA-binding hemoprotein. *J. Biol. Chem.* 270, 22478–22482.
- Peña, M. M. O., Burkhardt, W., and Bullerjahn, G. S. (1995). Purification and characterization of a *Synechococcus* sp. strain PCC 7942 polypeptide structurally similar to the stress-induced Dps/PexB protein of *Escherichia coli*. *Arch. Microbiol.* 163, 337–344.
- Pollard, R. T., Salter, I., Sanders, R. J., Lucas, M. I., Moore, C. M., Mills, R. A., Statham, P. J., Allen, J. T., Baker, A. R., Bakker, D. C. E., Charette, M. A., Fielding, S., Fones, G. R., French, M., Hickman, A. E., Holland, R. J., Hughes, J. A., Jickells, T. D., Lampitt, R. S., Morris, P. J., Nedelec, F. H., Nielsdottir, M., Planquette, H., Popova, E. E., Poulton, A. J., Read, J. F., Seeyave, S., Smith, T., Stinchcombe, M., Taylor, S., Thomalla, S., Venables, H. J., Williamson, R., and Zubkov, M. V. (2009). Southern Ocean deep-water carbon export enhanced by natural iron fertilization. *Nature* 457, 577–580.
- Poulsen, N., and Kröger, N. (2005). A new molecular tool for transgenic diatoms. *FEBS J.* 272, 3413–3423.
- Ravet, K., Touraine, B., Boucherez, J., Briat, J.-F., Gaymard, F., and Cellier, F. (2009). Ferritins control interaction between iron homeostasis and oxidative stress in *Arabidopsis*. *Plant J.* 57, 400–412.
- Ren, Q., Chen, K., and Paulsen, I. T. (2006). TransportDB: a comprehensive database resource for cytoplasmic membrane transport systems and outer membrane channels. *Nucleic Acids Res.* 35, D274.
- Rivers, A. R., Jakuba, R. W., and Webb, E. A. (2009). Iron stress genes in marine *Synechococcus* and the development of a flow cytometric iron stress assay. *Environ. Microbiol.* 11, 382–396.
- Robinson, N. J., Procter, C. M., Connolly, E. L., and Guerinot, M. L. (1999). A ferric-chelate reductase for iron uptake from soils. *Nature* 397, 694–697.
- Rocap, G. (2003). Genome divergence in two *Prochlorococcus* ecotypes reflects oceanic niche differentiation. *Nature* 424, 1042–1047.
- Rocap, G., Distel, D. L., Waterbury, J. B., and Chisholm, S. W. (2002). Resolution of *Prochlorococcus* and *Synechococcus* ecotypes by using 16S-23S rDNA internal transcribed spacer (ITS) sequences. *Appl. Environ. Microbiol.* 68, 1180–1191.
- Rocap, G., Larimer, F. W., Lamerding, J., Malfatti, S., Chain, P., Ahlgren, N. A., Arellano, A., Coleman, M., Hauser, L., Hess, W. R., Johnson, Z. I., Land, M., Lindell, D., Post, A. F., Regala, W., Shah, M., Shaw, S. L., Steglich, C., Sullivan, M. B., Ting, C. S., Tolonen, A., Webb, E. A., Zinser, E. R., and Chisholm, S. W. (2003). Genome divergence in two *Prochlorococcus* ecotypes reflects oceanic niche differentiation. *Nature* 424, 1042–1047.
- Rubin, M., Berman-Frank, I., and Shaked, Y. (2011). Dust- and mineral-iron utilization by the marine dinitrogen-fixer *Trichodesmium*. *Nat. Geosci.* 4, 529–534.
- Rubio, L. M., and Ludden, P. W. (2008). Biosynthesis of the iron-molybdenum cofactor of nitrogenase. *Annu. Rev. Microbiol.* 62, 93–111.
- Rue, E., and Bruland, K. (2001). Domoic acid binds iron and copper: a possible role for the toxin produced by the marine diatom *Pseudo-nitzschia*. *Mar. Chem.* 76, 127–134.
- Rusch, D. B., Martiny, A. C., Dupont, C. L., Halpern, A. L., and Venter, J. C. (2010). Characterization of *Prochlorococcus* clades from iron-depleted oceanic regions. *Proc. Natl. Acad. Sci. U.S.A.* 107, 16184–16189.
- Ryther, J. H., and Kramer, D. D. (1961). Relative iron requirement of some coastal and offshore plankton algae. *Ecology* 42, 444–446.
- Saito, M. A., Bertrand, E. M., Dutkiewicz, S., Bulygin, V. V., Moran, D. M., Monteiro, F. M., Follows, M. J., Valois, F. W., and Waterbury, J. B. (2011). Iron conservation by reduction of metalloenzyme inventories in the marine diazotroph *Crocosphaera watsonii*. *Proc. Natl. Acad. Sci. U.S.A.* 108, 2184–2189.
- Sapriel, G., Quinet, M., Heijde, M., Jourdain, L., Tanty, V., Luo, G., Le Crom, S., and Lopez, P. J. (2009). Genome-wide transcriptome analyses of silicon metabolism in *Phaeodactylum tricornutum* reveal the multilevel regulation of silicic acid transporters. *PLoS ONE* 4, e7458. doi:10.1371/journal.pone.0007458
- Sen, A., Dwivedi, K., Rice, K. A., and Bullerjahn, G. S. (2000). Growth phase and metal-dependent regulation of the *dpsA* gene in *Synechococcus* sp. strain sp. strain PCC 7942. *Arch. Microbiol.* 173, 352–357.
- Shaked, Y., Kustka, A. B., and Morel, F. M. M. (2005). A general kinetic model for iron acquisition by eukaryotic phytoplankton. *Limnol. Oceanogr.* 50, 872–882.
- Sherman, D., and Sherman, L. (1983). Effect of iron deficiency and iron restoration on ultrastructure of *Anacystis nidulans*. *J. Bacteriol.* 156, 393.
- Shi, D., Xu, Y., Hopkinson, B. M., and Morel, F. M. M. (2010). Effect of ocean acidification on iron availability to marine phytoplankton. *Science* 327, 676–679.
- Shi, T., Sun, Y., and Falkowski, P. G. (2007). Effects of iron limitation on the expression of metabolic genes in the marine cyanobacterium *Trichodesmium erythraeum* IMS101. *Environ. Microbiol.* 9, 2945–2956.
- Shi, Y., Tyson, G. W., and DeLong, E. F. (2009). Metatranscriptomics reveals unique microbial small RNAs in the ocean's water column. *Nature* 459, 266–272.
- Siaut, M., Heijde, M., Mangogna, M., Montsant, A., Coesel, S., Allen, A., Manfredonia, A., Falciorato, A., and Bowler, C. (2007). Molecular toolbox for studying diatom biology in *Phaeodactylum tricornutum*. *Gene* 406, 23–35.
- Silver, M. W., Bargu, S., Coale, S. L., Benitez-Nelson, C. R., Garcia, A. C., Roberts, K. J., Sekula-Wood, E., Bruland, K. W., and Coale, K. H. (2010). Toxic diatoms and domoic acid in natural and iron enriched waters of the oceanic Pacific. *Proc. Natl. Acad. Sci. U.S.A.* 107, 20762–20767.
- Soria-Dengg, S., and Horstmann, U. (1995). Ferrioxamines B and E as iron sources for the marine diatom *Phaeodactylum tricornutum*. *Mar. Ecol. Prog. Ser.* 127, 269–277.
- Stockel, J., Welsh, E. A., Liberton, M., Kunnavakkam, R., Aurora, R., and Pakrasi, H. B. (2008). Global transcriptomic analysis of *Cyanothece* 51142 reveals robust diurnal oscillation of central metabolic processes. *Proc. Natl. Acad. Sci. U.S.A.* 105, 6156–6161.
- Strzepek, R., and Harrison, P. (2004). Photosynthetic architecture differs in coastal and oceanic diatoms. *Nature* 431, 689–692.
- Sunda, W., and Huntsman, S. A. (1995). Iron uptake and growth limitation in oceanic and coastal phytoplankton. *Mar. Chem.* 50, 189–206.
- Sunda, W. G., Swift, D. G., and Huntsman, S. A. (1991). Low iron requirement for growth in oceanic phytoplankton. *Nature* 351, 55–57.
- Sutak, R., Šlapeta, J., San Roman, M., Camadro, J.-M., and Lesuisse, E. (2010). Nonreductive iron uptake mechanism in the marine alveolate *Chromera velia*. *Plant Physiol.* 154, 991–1000.
- Thamatrakoln, K., Korenovska, O., Niheu, A. K., and Bidle, K. D. (2011). Whole-genome expression analysis reveals a role for death-related genes in stress acclimation of the diatom *Thalassiosira pseudonana*. *Environ. Microbiol.* 14, 67–81.
- Thompson, A. W., Huang, K., Saito, M. A., and Chisholm, S. W. (2011). Transcriptome response of high- and low-light-adapted *Prochlorococcus* strains to changing iron availability. *ISME J.* 5, 1580–1594.
- Tölle, J., Michel, K.-P., Kruij, J., Kahmann, U., Preisfeld, A., and Pistorius, E. K. (2002). Localization and function of the IdIA homologue Slr1295 in the cyanobacterium *Synechocystis* sp. strain PCC 6803. *Microbiology* 148, 3293–3305.
- Tréguer, P., Nelson, D. M., Van Bennekom, A. J., DeMaster, D. J., Leynaert, A., and Quéguiner, B. (1995). The silica balance in the world ocean: a reestimate. *Science* 268, 375.
- Trick, C. G., Bill, B. D., Cochlan, W. P., Wells, M. L., Trainer, V. L., and Pickell, L. D. (2010). Iron enrichment stimulates toxic diatom production in high-nitrate, low-chlorophyll areas. *Proc. Natl. Acad. Sci. U.S.A.* 107, 5887–5892.
- Tripp, H. J., Bench, S. R., Turk, K. A., Foster, R. A., Desany, B. A., Niazi, F., Affourtit, J. P., and Zehr, J. P. (2010). Metabolic streamlining in an open-ocean nitrogen-fixing cyanobacterium. *Nature* 464, 90–94.
- Tuit, C., Waterbury, J., and Ravizza, G. (2004). Diel variation of molybdenum and iron in marine diazotrophic cyanobacteria. *Limnol. Oceanogr.* 49, 978–990.
- Venter, J. C., Remington, K., Heidelberg, J. F., Halpern, A. L., Rusch, D., Eisen, J. A., Wu, D., Paulsen, I., Nelson, K. E., Nelson, W., Fouts, D. E., Levy, S., Knap, A. H., Lomas, M. W., Nealson, K., White, O., Peterson, J., Hoffman, J., Parsons, R., Baden-Tillson, H., Pfannkuch, C., Rogers, Y.-H., and Smith, H. O. (2004). Environmental genome shotgun sequencing of the Sargasso sea. *Science* 304, 66–74.
- Volker, C., and Wolf-Gladrow, D. A. (1999). Physical limits on iron uptake mediated by siderophores or surface reductases. *Mar. Chem.* 65, 227–244.
- Webb, E. A., Moffett, J. W., and Waterbury, J. B. (2001). Iron stress

- in open-ocean cyanobacteria (*Synechococcus*, *Trichodesmium*, and *Crocosphaera* spp.): identification of the IdiA protein. *Appl. Environ. Microbiol.* 67, 5444–5452.
- Webb, R., Troyan, T., Sherman, D., and Sherman, L. A. (1994). MapA, an iron-regulated, cytoplasmic membrane protein in the cyanobacterium *Synechococcus* sp. strain PCC7942. *J. Bacteriol.* 176, 4906–4913.
- Wells, M. L., Trick, C. G., Cochlan, W. P., Hughes, M. P., and Trainer, V. L. (2005). Domoic acid: the synergy of iron, copper, and the toxicity of diatoms. *Limnol. Oceanogr.* 50, 1908–1917.
- Wilhelm, S. W., and Trick, C. G. (1994). Iron-limited growth of cyanobacteria: multiple siderophore production is a common response. *Limnol. Oceanogr.* 39, 1979–1984.
- Worden, A. Z., Nolan, J. K., and Palenik, B. (2004). Assessing the dynamics and ecology of marine picophytoplankton: the importance of the eukaryotic component. *Limnol. Oceanogr.* 49, 168–179.
- Zehr, J. P., Bench, S. R., Carter, B. J., Hewson, I., Niazi, F., Shi, T., Tripp, H. J., and Affourtit, J. P. (2008). Globally distributed uncultivated oceanic N₂-fixing cyanobacteria lack oxygenic photosystem II. *Science* 322, 1110–1112.
- Zhang, S., and Bryant, D. A. (2011). The tricarboxylic acid cycle in cyanobacteria. *Science* 334, 1551–1553.
- Zhaxybayeva, O., Doolittle, W. F., Papke, R. T., and Gogarten, J. P. (2009). Intertwined evolutionary histories of marine *Synechococcus* and *Prochlorococcus* *marinus*. *Genome Biol. Evol.* 1, 325–339.
- Zwirgmaier, K., Jardillier, L., Ostrowski, M., Mazard, S., Garczarek, L., and Vaulot, D. (2008). Global phylogeography of marine *Synechococcus* and *Prochlorococcus* reveals a distinct partitioning of lineages among oceanic biomes. *Environ. Microbiol.* 10, 147–161.

Conflict of Interest Statement: The authors declare that the research was conducted in the absence of any commercial or financial relationships that could be construed as a potential conflict of interest.

Received: 01 November 2011; paper pending published: 25 November 2011; accepted: 27 January 2012; published online: 07 March 2012.

Citation: Morrissey J and Bowler C (2012) Iron utilization in marine cyanobacteria and eukaryotic algae. *Front. Microbio.* 3:43. doi: 10.3389/fmicb.2012.00043

This article was submitted to *Frontiers in Microbiological Chemistry*, a specialty of *Frontiers in Microbiology*.

Copyright © 2012 Morrissey and Bowler. This is an open-access article distributed under the terms of the Creative Commons Attribution Non Commercial License, which permits non-commercial use, distribution, and reproduction in other forums, provided the original authors and source are credited.



Factors influencing the diversity of iron uptake systems in aquatic microorganisms

Dhwani K. Desai^{*†}, Falguni D. Desai[†] and Julie LaRoche

Biological Oceanography Division, Helmholtz-Zentrum für Ozeanforschung Kiel (GEOMAR), Kiel, Germany

Edited by:

Martha Gledhill, University of Southampton, UK

Reviewed by:

Amy M. Grunden, North Carolina State University, USA

Katherine Barbeau, University of California San Diego, USA
Sylvia McDevitt, Skidmore College, USA

*Correspondence:

Dhwani K. Desai, Biological Oceanography Division, Helmholtz-Zentrum für Ozeanforschung Kiel (GEOMAR), Düsternbrooker Weg 20, 24015 Kiel, Germany.

e-mail: dhwanidesai@gmail.com

[†]Dhwani K. Desai and Falguni D. Desai have contributed equally to this work.

Iron (Fe) is an essential micronutrient for many processes in all living cells. Dissolved Fe (dFe) concentrations in the ocean are of the order of a few nM, and Fe is often a factor limiting primary production. Bioavailability of Fe in aquatic environments is believed to be primarily controlled through chelation by Fe-binding ligands. Marine microbes have evolved different mechanisms to cope with the scarcity of bioavailable dFe. Gradients in dFe concentrations and diversity of the Fe-ligand pool from coastal to open ocean waters have presumably imposed selection pressures that should be reflected in the genomes of microbial communities inhabiting the pelagic realm. We applied a hidden Markov model (HMM)-based search for proteins related to cellular iron metabolism, and in particular those involved in Fe uptake mechanisms in 164 microbial genomes belonging to diverse taxa and occupying different aquatic niches. A multivariate statistical approach demonstrated that in phototrophic organisms, there is a clear influence of the ecological niche on the diversity of Fe uptake systems. Extending the analyses to the metagenome database from the Global Ocean Sampling expedition, we demonstrated that the Fe uptake and homeostasis mechanisms differed significantly across marine niches defined by temperatures and dFe concentrations, and that this difference was linked to the distribution of microbial taxa in these niches. Using the dN/dS ratios (which signify the rate of non-synonymous mutations) of the nucleotide sequences, we identified that genes encoding for TonB, Ferritin, Ferric reductase, IdiA, ZupT, and Fe²⁺ transport proteins FeoA and FeoB were evolving at a faster rate (positive selection pressure) while genes encoding ferrisiderophore, heme and Vitamin B12 uptake systems, siderophore biosynthesis, and IsiA and IsiB were under purifying selection pressure (evolving slowly).

Keywords: marine microbes, eukaryotic phytoplankton, Fe limitation, Fe-binding ligands, multivariate statistics, metagenomes, dN/dS ratio, aquatic niches

INTRODUCTION

Iron-containing metalloenzymes are essential for many life processes, including photosynthesis, respiration, and nitrogen fixation. Due to the tendency of Fe³⁺ to form ferric hydroxides and oxyhydroxide polymers in the presence of oxygen, the dFe concentration in surface seawater is <0.5 nM (Johnson et al., 1997). Aeolian dust deposition is the dominant external source of iron in the open ocean surface waters (Duce and Tindale, 1991; Jickells et al., 2005) of the North Atlantic and North-East Pacific accounting for 48 and 22% of total Fe deposition respectively (Gao et al., 2001). In around 40% of the world's oceans where surface waters are high in nutrient and low in chlorophyll (HNLC regions), low Fe supply limits the growth of resident eukaryotic phytoplankton and cyanobacteria responsible for primary production (Martin et al., 1994; Coale et al., 1996; Boyd et al., 2000; Gall et al., 2001; Tsuda et al., 2003; de Baar et al., 2005).

Diverse strategies have evolved to competitively acquire enough iron for survival in various oceanic habitats. This competition is intensified by the fact that >99.9% of dFe is complexed to Fe-binding ligands of diverse nature (Gledhill and van den Berg, 1994; Rue and Bruland, 1995; Gledhill and Buck, 2012). Thus,

microorganisms have developed systems to take up Fe from a wide range of Fe-binding ligands. Although ubiquitous in nature, Fe-binding ligands vary in their Fe-binding affinities and their distribution from surface to deep waters (Rue and Bruland, 1995; Hunter and Boyd, 2007) and from coastal to open ocean waters (Boye et al., 2003; Buck and Bruland, 2007).

The ability to produce siderophores in the open ocean is apparently, largely confined to heterotrophic bacteria (Reid et al., 1993; Martinez et al., 2000; Butler, 2005; Martinez and Butler, 2007; Homann et al., 2009a,b). While siderophore biosynthesis pathways have been found in some coastal (Ito and Butler, 2005) or fresh water (Ito et al., 2004) cyanobacteria, they appear to be absent in open ocean cyanobacteria. Coastal strains of *Synechococcus* that have been reported to produce siderophores (Ito and Butler, 2005) have high Fe-quotas compared to oceanic strains (Palenik et al., 2006). Even though only a few marine microorganisms can synthesize siderophores, the ability to take up siderophores may be more widespread, as evidenced by the abundance of TonB-dependent (TBD) siderophore uptake systems observed in terrestrial and freshwater microorganisms devoid of siderophore synthesis pathways (Plessner et al., 1993; Katoh et al., 2001; Poole

and McKay, 2003; Joshi et al., 2008). Additionally, various heme-acquisition systems have been identified in bacteria for the utilization of Fe bound to heme (Stojiljkovic and Hantke, 1994; Cope et al., 1995; Thompson et al., 1999; Ochsner et al., 2000; Hopkinson et al., 2008). Notably, siderophore biosynthesis and TBD siderophore/heme uptake receptors are absent from the genomes of *Prochlorococcus* and strains of *Synechococcus* that dominate the microbial communities of open ocean surface waters (Waterbury et al., 1979; Liu et al., 1997, 1999; Hopkinson and Morel, 2009). The reduction of cellular Fe requirements provides an alternate adaptive strategy for surviving Fe limitation in open ocean surface waters. This strategy has been observed in the *Prochlorococcus* ecotypes (Thompson et al., 2011) dominant in HNLC waters, which have decreased their Fe-quotas by eliminating several Fe-requiring proteins (Rusch et al., 2010).

The availability of a large number of marine prokaryotic and eukaryotic microbial genomes and the Global Ocean Sampling (GOS) metagenomes, have greatly enhanced our understanding of the Fe-acquisition strategies used by various groups of microorganisms. Recent studies by Hopkinson and Barbeau (2012) and Toulza et al. (2012) presented sequence-based approaches to analyze the differences in occurrence patterns of proteins involved in Fe-metabolism in marine prokaryotic genomes and metagenomes, respectively. Hopkinson and Barbeau (2012) reported a dominance of TBD uptake systems in *Gammaproteobacteria*, and identified a novel heme TBDT in *Prochlorococcus* which may have been acquired by horizontal gene transfer, providing niche specific adaptation in this organism. Their study further revealed the widespread occurrence of Fe³⁺ ABC transporters in all groups of marine bacteria except for Flavobacteria, and a lack of the specific Fe²⁺ uptake system (FeoAB) in picocyanobacteria and *Alphaproteobacteria*. They identified that the TBDTs were less common in the metagenomes than in the genomes, an observation that reflects the numerical dominance of *Pelagibacter* and *Prochlorococcus* (Rusch et al., 2007) in the current collection of GOS metagenomes. Both genera have small genomes and non-specialized iron uptake systems (Smith et al., 2010; Thompson et al., 2011). A more detailed analysis of the Fe-metabolism proteins in the GOS metagenomes revealed a distribution pattern influenced by dFe concentrations (Toulza et al., 2012). The frequencies of occurrence of Fe³⁺ transporters and of Fe²⁺ uptake systems were negatively correlated with each other, the former being more abundant in the open ocean environments and the latter in the coastal environments, respectively. The taxonomic diversity and Fe-pathway prevalence differed significantly with habitat or niche type (Open Ocean or Coastal). However the GOS samples are distributed along a wide range of latitudes possibly confounding the effect of temperature, which varies widely within both Open Ocean and Coastal niches. In addition, prior studies did not directly investigate the exact nature of the link between taxonomic diversity and Fe-pathway prevalence within the metagenomes.

Here, we build on the results presented in the studies of Hopkinson and Barbeau (2012) and Toulza et al. (2012), by extending the analyses to marine eukaryotic genomes of phytoplankton. We established a link between the Fe-metabolism profiles and taxonomic diversity prevalent in the metagenomes by comparing

the Fe-metabolism protein occurrence profiles (Table 1) from the genomes of various taxa and those obtained from various aquatic niches defined by environmental characterization of metagenomes. Marine prokaryotic and eukaryotic microorganisms were grouped according to their location of isolation (Open Ocean, Coastal, or Freshwater) to check for niche specific adaptations reflected in their genomes. The GOS metagenomes were subjected to a more complex grouping in order to account for differences in Fe-metabolism protein profiles of the microbial community, which could be attributed to temperature, dFe concentration, or a coastal versus Open Ocean sampling location. Thus, we defined three contrasting niche group pairs in the GOS metagenomes such that the groups of samples in a pair differed with respect to only one of the above environmental factors. A multivariate statistical approach was used to study the differential distribution of Fe-metabolism protein profiles in genomes and in the above GOS metagenomic groupings to establish whether the Fe-metabolism strategies were correlated with the taxonomic distribution in the GOS metagenomes. We found a set of proteins that were statistically discriminating between the aquatic niches. Calculations of the non-synonymous mutation rates (dN/dS) for this set of proteins indicated that they were under positive selection pressure and therefore were evolving rapidly.

MATERIALS AND METHODS

HIDDEN MARKOV MODEL-MODE PROFILES OF IRON METABOLISM GENES

The set of non-redundant (Uniref 100) protein sequences for the genes listed in Table 1 were downloaded from Uniprot and HMM-ModE profiles were created as described earlier (Srivastava et al., 2007). The HMM-ModE protocol allows the construction of HMM profiles with increased specificity by using negative training sequences.

The training sequences for each protein were first clustered using the Markov Clustering Algorithm (MCL) (Enright et al., 2002). For each subgroup of each protein, the training sequences were aligned with MUSCLE (Edgar, 2004) and HMMs were generated using *hmmbuild* from the HMMER2 package (Eddy, 1998). The discrimination threshold of each protein HMM was optimized by an *n*-fold cross-validation exercise. The training sequences for each were divided into *n* test sets such that each sequence is part of at least one test set. For each test set *t*, the remaining (*n*-1) sets were combined to form the train set and used to build an HMM. The sequences in *t* were scored using this HMM by *hmmsearch* program to get a True Positive (TP) score distribution. False positives (FP) were identified from the negative training set (in this case the entire UniProt database excluding the training sequences for the gene in question). The sensitivity, specificity, and Matthews Correlation Coefficient (MCC) distribution for each of *n* sets was calculated (Hannenhalli and Russell, 2000). The optimal discrimination threshold was identified as the mid-point of the MCC distribution averaged over the *n* sets. Further increase in specificity was obtained by modifying the emission probabilities of the gene HMM by using the FP alignment as described earlier (Srivastava et al., 2007).

These HMM-ModE profiles with their optimized threshold were used with the program *hmmsearch* to scan the protein

Table 1 | List of proteins involved in Fe-ligand (siderophore and heme) uptake, siderophore, and heme biosynthesis and Fe homeostasis in microorganisms.

System	Abbreviation	Genetic nomenclature	Reference
Heme direct uptake	Heme-Upt	PhuRSTUVW (<i>Pseudomonas aeruginosa</i>), HemRSTUV (<i>Yersinia enterocolitica</i>), HutABCD, HutR (<i>Vibrio cholerae</i>), BhuRSTUV (<i>Bordetella pertussis</i>), HmuRSTUV (<i>Y. pestis</i>)	Stojiljkovic and Hantke (1994), Thompson et al. (1999), Ochsner et al. (2000), Mey and Payne (2001), Vanderpool and Armstrong (2003)
Hemophore-mediated heme uptake		HasRADEF (<i>Pseudomonas aeruginosa</i>)	Lewis et al. (1997), Ochsner et al. (2000)
Heme uptake through bipartite receptors		HpuAB (<i>Neisseria</i> sp.)	Lewis et al. (1997)
Hydroxamate siderophore uptake	Hydrox	FhuABCD (ferrichrome), FhuE (rhodotorulic acid), IutA (aerobactin) and FoxA (ferrioxamine B) in <i>E. coli</i> K-12, FcuA (ferrichrome) in <i>Yersinia enterocolitica</i> , FegAB in <i>Bradyrhizobium japonicum</i> 61A152, RhtAX (rhizobactin) in <i>Sinorhizobium meliloti</i> , PupA and PupB pseudobactin receptors in <i>Pseudomonas putida</i>	Fecker and Braun (1983), Koebnik et al. (1993b), Koster et al. (1995), Lynch et al. (2001), Braun (2003), Benson et al. (2005)
Catecholate siderophore uptake	Catech	FepABCD for enterobactin, BtuBFCD for vitamin B12 and colicin receptor CirA in <i>E. coli</i> , pesticin receptor FyuA in <i>Yersinia enterocolitica</i> , PfeA for ferric-enterobactin in <i>Pseudomonas</i> , vibriobactin receptor ViuA and enterobactin receptor IrgA in <i>Vibrio cholera</i>	Worsham and Konisky (1985), Butterson et al. (1992), Rakin et al. (1994), Cadieux et al. (2002), Braun (2003), Cornelis and Bodilis (2009)
Citrate siderophore uptake	Citrate	FecABCD (citrate) in <i>Escherichia coli</i>	Braun (2003)
Ferric binding periplasmic protein dependent Fe ³⁺ transporters	Fe ³⁺	IdiA, HitABC, FbpA	Sanders et al. (1994), Adhikari et al. (1995), Ferreiros et al. (1999), Webb et al. (2001)
Fe ²⁺ uptake or uptake of divalent cations	Fe ²⁺	FeoAB, ZupT, MgtE, FTR1	Kammler et al. (1993), Guerinot (2000), Grass et al. (2005)
Energy coupling for TonB-dependent (TBD) ligand uptake	Ener Coup	TonB/ExbB/ExbD	Koebnik et al. (1993a)
Non-ribosomal peptide synthetase	NRPS	NRPS	Jeanjean et al. (2008)
NRPS independent siderophore synthesis	NIS	IucA, IucC – aerobactin; RhbB, RhbDF – rhizobactin; DesB, DesD – Desferrioxamine	Challis (2005)
Heme/chlorophyll biosynthesis	Hem-Syn	HemBCEF	Mochizuki et al. (2010)
Heme oxygenase	Hem-Oxy	HemO, HemS, HmuS, HO1, HmuO	Thompson et al. (1999)
Regulatory elements	Regul	Fur, DtxR, Rir	Wexler et al. (2003), Johnston et al. (2007)
Ferritin-like Fe storage	FeStor	Ferritin-dps, BfrAB	Andrews (1998)
Fe-stress induced homeostasis genes	IsiA	IsiA	Burnap et al. (1993)
Flavodoxin	IsiB	IsiB	LaRoche et al. (1996)
Ferric reductase	Fe-Red	Ferric reductase	Kosman (2003)

sequences from the marine microbial genomes as well as from the GOS metagenomes. All the above steps were performed using customized Perl scripts that are available for download from <https://sites.google.com/site/dhwanidesai/home/bioinformatics>.

OBTAINING THE COMPLETE GENOME SEQUENCES OF MARINE MICROBES

Complete genome sequences of marine microbes whose sequencing projects were commissioned by the Gordon and Betty Moore Foundation under their Marine Microbiology Initiative¹ were downloaded from NCBI in the form of protein FASTA

files. Complete genomes of six eukaryotic marine microorganisms including *diatoms* (*Thalassiosira pseudonana*, *T. oceanica*, and *Phaeodactylum tricornutum*), a pelagophyte (*Aureococcus anophagefferens*), green algae (*Ostreococcus lucimarinus* and *Ostreococcus tauri*), and a prymnesiophyte (*Emiliania huxleyi*) were also downloaded from NCBI as FASTA files of protein sequences. We also analyzed 12 Freshwater microbial genomes mentioned in (Hopkinson and Morel, 2009) making a total of 164 genomes.

OBTAINING THE METAGENOME SEQUENCES

The GOS metagenomic sequences and the corresponding meta-data were downloaded from the CAMERA portal (Seshadri et al., 2007). The nucleotide sequences were translated in all six frames

¹<http://www.moore.org/microgenome/>

and all translations with a length less than 25 amino acids were discarded. Since there was a large variation in the number of sequences in each sample, we used the Daisychopper² strategy to randomly select an equal number of sequences from all the samples. From the 44 GOS samples, we selected 30 samples that were obtained from a 0.1–0.8 μm filter and were classified as “Open Ocean” or “Coastal” (Table S2 in Supplementary Material). The sample GS07, from the Northern Gulf of Maine (43.63°N, 66.84°W), had the least number of sequences (50980). Hence, 50980 sequences were randomly selected from each of the other samples for the *hmmsearch*. The taxonomic profiles for these samples were downloaded from the MG-RAST server³.

STATISTICAL ANALYSIS

The results of the *hmmsearch* program were parsed and tabulated as $m \times n$ matrix (m genomes or metagenomes in rows \times n genes in columns). This matrix was used for making the non-parametric multidimensional scaling (NMDS) plots using the Primer-E v6 software (Clarke, 2006). Discarding gene columns which did not have any hits in any of the genomes, we obtained a 164×85 matrix. For the metagenomic samples, an environmental matrix was also created using the metadata provided in CAMERA for the GOS samples. Apart from the geographical coordinates of the samples, the environmental matrix contained “sample depth,” “water column depth,” “temperature,” and “dFe deposition” as variables. The dissolved iron concentration at the surface for the sample coordinates was obtained from the PELAGOS model simulation (Vichi et al., 2007a,b; data kindly provided by Dr. Marcello Vichi). We used the yearly mean concentration of dissolved iron, averaged over the entire period of simulation, i.e., from 1980 to 2002.

Analysis of Similarities (ANOSIM) test for statistically significant differences between prior groupings of the samples made according to taxonomy or location and the Similarity Percentages (SIMPER) analysis comparing relative abundances of genes in the said prior groupings to identify discriminating genes were carried out using Primer-E. Principal Components Analysis (PCA) of the GOS samples using the environmental matrix (Tables S1 and S2 in Supplementary Material) was also performed using Primer-E. Following is a brief description of the non-parametric statistical methods implemented in Primer-E (Clarke, 1993) that we have used here.

Data transformations

Whereas the abundance matrices were log-transformed, for the environmental matrix, the variables were individually transformed to reduce the collinearity as much as possible. So, Latitude and Longitude were square-root transformed, “Water column depth” was log-transformed and “dFe deposition” was exponential-transformed.

Bray–Curtis similarity

The first step in the analysis of multivariate data was the calculation of a similarity measure between the samples. The similarities between all pairs of samples (the similarity matrix) were then used

for a number of analyses. The Bray–Curtis similarity coefficient is the most common measure for comparing ecological samples with species abundance data. The Bray–Curtis measure is independent of scale of measurements (counts, biomass etc.) and joint absences of variables in a pair of samples have no effect on the similarity between them. For two samples j and k the Bray–Curtis similarity is described by

$$S_{jk} = 100 \frac{\sum_{i=1}^p 2 \min(y_{ij}, y_{ik})}{\sum_{i=1}^p (y_{ij} + y_{ik})} \quad (1)$$

where y_{ij} and y_{ik} are the abundance of the i th variable in the j th sample and k th sample respectively and p is the total number of variables. The Bray–Curtis dissimilarity is then simply represented as $100 - S_{jk}$.

Non-metric multidimensional scaling

Ordination plots visually display the similarity between ecological samples by mapping the high-dimensional community structure to two or three dimensions such that the physical distance between samples on the plot reflects the similarity between their communities.

In an NMDS ordination plot, the distances between the samples (in this case genomes or metagenomes) are first calculated using complete profiles of occurrence of the variables (in our case the iron metabolism genes). The sample objects are then placed randomly in a 2-d space and the Euclidean or physical distance between the objects in 2-d is calculated. This distance matrix is then non-parametrically regressed on to the original distance matrix to calculate a stress value (goodness-of-fit of the regression) that gives an indication of the best fit between the two matrices. The samples are then iteratively rearranged such that the stress value is minimized. The NMDS plot thus is a 2-d representation of the distances between the samples in a high-dimensional space. The distance between two genomes in such an ordination diagram gives an indication of the similarity of their gene profiles. A stress value less than 0.2 combined with an overlay of pre-defined group names provides reliable inferences about the clustering of the samples.

Analysis of similarities

The ANOSIM test is the non-parametric multivariate analog of the Analysis of Variance tests for univariate, normally distributed data. Instead of the group means as in the univariate case, here only the rank similarities between the samples in the underlying similarity matrix are considered. For n samples having replicates for two or more categories (in our case the taxonomic or ecological niche groups) a test statistic R is calculated as follows

$$R = \frac{\bar{r}_B - \bar{r}_W}{\frac{1}{2}M} \quad (2)$$

where \bar{r}_W is average of rank similarities in the replicates within a category, \bar{r}_B is the average of rank similarities among all pairs of replicates between the categories, $M = n(n - 1)/2$ and n is the total number of samples. The statistical significance of the observed R value is evaluated using the null hypothesis H_0 that there are no

²<http://www.genomics.ceh.ac.uk/GeneSwyatch/Tools.html>

³<http://metagenomics.anl.gov/>

differences between the groups of samples. This is accomplished by a permutation test where all the group labels are sequentially applied to all the samples and the R statistic recalculated for each permutation. The null hypothesis H_0 is rejected if the observed R value lies outside of the distribution of R values from the permutation test. For instance if t R values of the T total permutations are greater than or equal to the observed R value then we can reject H_0 at a significance level of $(t + 1)/(T + 1)$. This is what is referred to as the Global R test, i.e., between all the groupings of the samples. Pairs of the groups were also similarly compared to each other in terms of the R statistic and its significance value. Following convention, we tolerated a significance value of up to 5% (Type I error, i.e., rejecting the null hypothesis when it is true) as being small enough to rule out the possibility of H_0 being true.

Similarity percentages

This method disaggregates the Bray–Curtis similarity matrix in order to identify the species that contribute most to the differences (average dissimilarities) between the prior groupings of the samples. For two samples j and k SIMPER calculates the contribution for the i th species as follows:

$$\delta_{jk}(i) = 100|y_{ij} - y_{ik}| / \sum_{i=1}^p (y_{ij} + y_{ik}) \quad (3)$$

The terms y_{ij} and y_{ik} are defined as before for Eq. (1). The average contribution $\bar{\delta}_i$ of the i th species to the overall dissimilarity $\bar{\delta}$ is just the average $\delta_{jk}(i)$ for all pairs (j,k) such that j is from the first group and k is from the second group. If $\bar{\delta}_i$ is high and the standard deviation SD (δ_i) of the $\delta_{jk}(i)$ values is low, it implies that this species i has a significant contribution to the overall dissimilarity in a majority of pairwise comparisons between the two groups. A high $\bar{\delta}_i/\text{SD}(\delta_i)$ ratio therefore means that species i is a good discriminator.

Principal components analysis

Principal components analysis is an ordination where the high-dimensional data is represented in terms of two or three orthogonal axes (Principal Components). The procedure involves finding a linear combination of the original variables (first PC) such that the variance of the sample points projected perpendicularly on this new axis is maximized. The second PC is restricted to be perpendicular to the first PC and again chosen in the direction that maximizes the variance of the sample points and so on. The percentage of the variance explained by the first three PCs gives an idea about the loss of information resulting from reducing the dimensions. The variable vectors can be plotted on top of the PCA ordination to visualize the directions of the variable gradients.

PHYLOGENETIC AND POSITIVE SELECTION ANALYSIS

The 16S rRNA gene sequences for the genomes were retrieved from GenBank along with the *E. coli* 16S rRNA sequence. These were aligned using MUSCLE and imported into the ARB software (Ludwig et al., 2004). A Maximum Likelihood tree was calculated with the FastDNAML (Olsen et al., 1994) implementation in ARB using a filter for base 800 to base 1300 encompassing and extending on both sides, the v6 hypervariable region in *E. coli*. An in-house

script was used to calculate the average phylogenetic distance of a gene as follows:

$$P = \text{Avg}D_p(g) \quad (4)$$

where $D_p(g)$ is the set of pairwise phylogenetic distances between all pairs of genomes where gene g occurs.

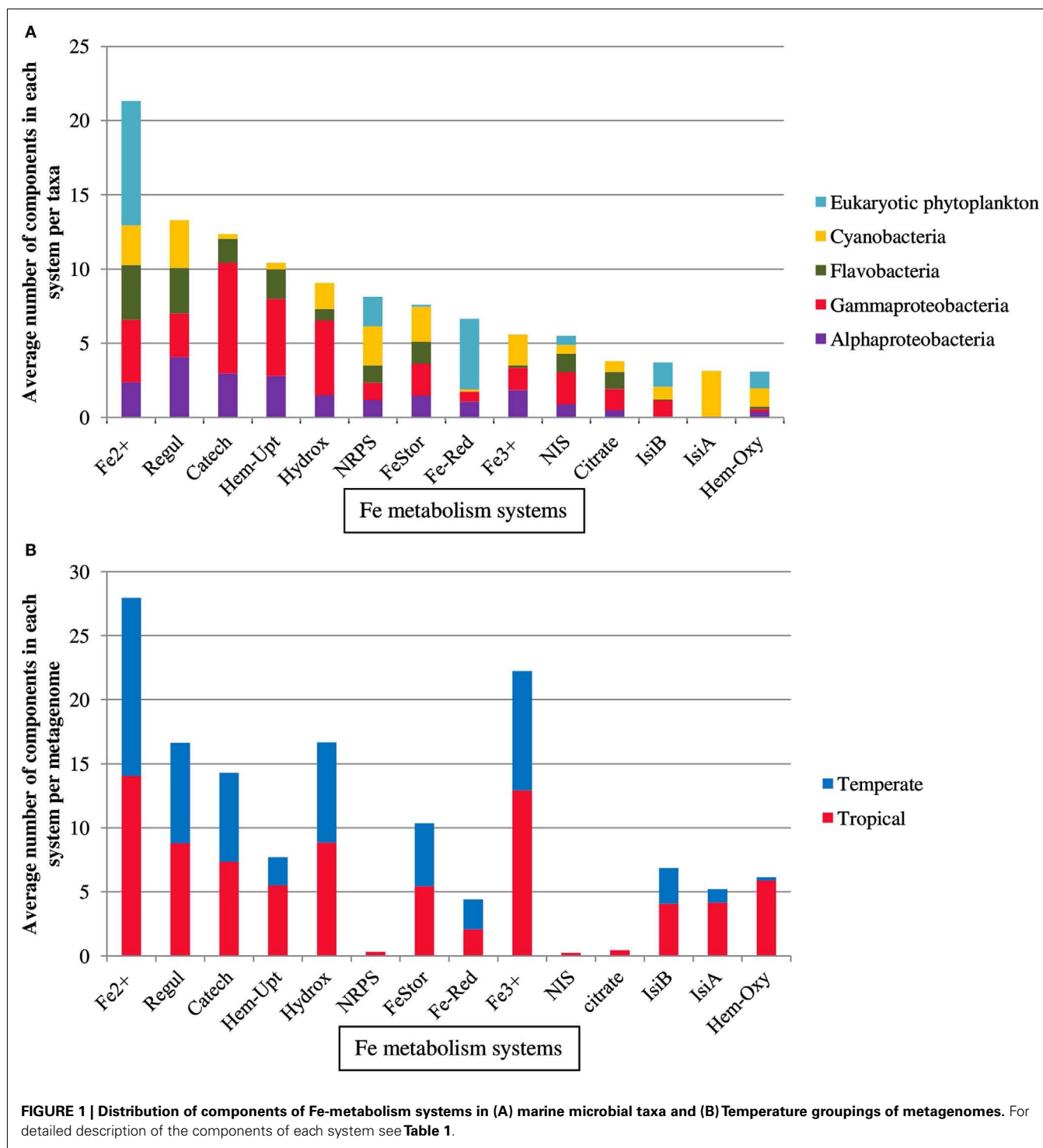
For the genes discriminating between taxa or locations, the nucleotide sequences were retrieved from GenBank and the Maximum Likelihood estimations of average pairwise non-synonymous by synonymous mutation (dN/dS) ratios were calculated using CodeML (runmode = -2) from the PAML package (Yang, 2007).

RESULTS

A set of proteins involved in iron metabolism (Table 1) was recovered from 164 marine microbial genomes belonging to *Cyanobacteria*, eukaryotic phytoplankton, *Alphaproteobacteria*, *Gammaproteobacteria*, and *Flavobacteria* (Figure 1A) using HMMs with optimized thresholds and modified emission probabilities as described earlier (Srivastava et al., 2007). The heme biosynthesis system, the TonB/ExbB/ExbD system, ferredoxin, and the iron-sulfur cluster assembly protein IscA1 (Table 1) were present in almost all prokaryotic genomes and therefore removed from further analysis. The observed abundances of TBD Fe-siderophore uptake systems, components of Fe^{2+} or divalent cation uptake and Fe^{3+} transporters were in agreement with previous reports (Hopkinson and Barbeau, 2012). The TBD uptake systems for catecholate, hydroxamate, and citrate siderophores were more widespread in *Gammaproteobacteria* (60, 55, and 37% of the genomes, respectively) as compared to *Alphaproteobacteria* (24, 16, and 13%, respectively), *Flavobacteria* (13, 8, and 30%, respectively), and *Cyanobacteria* (2, 19, and 19%, respectively). Fe^{2+} or divalent cation transporters were abundant in all the taxa but were most abundant in the eukaryotic phytoplankton genomes (39%). Ferric reductase was characteristic of the eukaryotic phytoplankton group (71%), but was also present in *Cyanobacteria* (2%), *Alphaproteobacteria* (16%), and *Gammaproteobacteria* (10%). Fe^{3+} transporters occurred in *Cyanobacteria* (37%), *Alphaproteobacteria* (33%), and *Gammaproteobacteria* (27%), but were uncommon in *Flavobacteria* (2%) and absent from eukaryotic phytoplankton. NRPS and NIS components involved in siderophore biosynthesis were present in *Alphaproteobacteria* (14 and 16%), *Gammaproteobacteria* (14 and 39%), *Flavobacteria* (14 and 22%), *Cyanobacteria* (32 and 11%), and also in eukaryotic phytoplankton (24 and 11% respectively).

SIDEROPHORE BIOSYNTHESIS COMPONENTS IN PHOTOTROPHIC GENOMES

Recent surveys involving searches of NIS components represented by PFAM domains AlcB (Acetyl transferase) and IucA_IucC (siderophore synthetase for Aerobactin) suggest that none of the eukaryotic phytoplankton and only around 4% of marine picocyanobacteria possess this system (Hopkinson and Morel, 2009; Hopkinson and Barbeau, 2012). Here our HMM search utilized a more extensive set of NIS proteins involved in the biosynthesis of aerobactin, desferrioxamine, and rhizobactin 1021 siderophores



(Challis, 2005; Table 1). NRPS was detected in picocyanobacteria *P. marinus* MIT9303 and NRPS along with the NIS component RhbB (a PLP dependent decarboxylase) were detected in *P. marinus* MIT 9303 and MIT 9313. It is possible that the high specificity of our HMM-ModE models led to a slight drop in sensitivity. To confirm whether the other components of this pathway were indeed present in the phototrophic genomes and were being missed due to

this lowered sensitivity of HMM-ModE, we used the Search Tool for Interacting Genes/Proteins (STRING) database (Szklarczyk et al., 2011). For a given query sequence, this database identifies a set of proteins that repeatedly co-occur with the query in the genomes of many different organisms. In addition to *P. marinus* MIT9303 and MIT9313, using the *S. meliloti* RhbB sequence as the query, the STRING database showed the co-occurrence

of RhbB and RhbA (diaminobutyrate aminotransferase involved in rhizobactin biosynthesis) in *P. marinus* CCMP1375, NATL1A, CCMP1986, MIT9211, MIT9515, MIT9215, MIT9312, NATL2A, AS9601, and MIT9301. A corresponding siderophore uptake gene was not detected in the *Prochlorococcus* genomes. Our profiles detected a putative gene for NRPS in eukaryotic phytoplankton *A. anophagefferens*, *E. huxleyi*, *O. tauri*, *P. tricornutum*, and *T. pseudonana*, and the NIS component RhbB in *E. huxleyi*, *F. cylindrus*, and *O. lucimarinus*. Using the STRING database we detected genes similar to rhizobactin biosynthesis components RhbA and RhbB in *O. tauri*, *O. lucimarinus*, *T. pseudonana*, and *P. tricornutum* along with RhtX, a special permease involved in the uptake of rhizobactin 1021. The sequences identified as RhbA, RhbB, and RhtX from these genomes shared 48.18, 35.48, and 30% identity at the protein level within each group, respectively. A neighbor-joining tree calculated from the multiple sequence alignments of these sequences showed a higher similarity of the Freshwater organisms with the *Sinorhizobium* genes while the eukaryotic sequences clustered with the *Prochlorococcus* sequences (Figure 2). We also detected the NRPS as well as NIS components in the metagenomes, though their abundances were low (Figure 1B).

ANALYSIS OF GENOMES IN TERMS OF THEIR TAXONOMIC AFFILIATION

We generated occurrence matrices showing the abundance of Fe-metabolism proteins (variables) in each genome or metagenome (samples) and used NMDS plots to visualize the clustering of the samples based on similarities of their gene occurrence profiles. The distance between the sample points on a NMDS plot is indicative of the extent to which samples share species (or proteins in this case). We grouped the individual genomes according to either their taxonomic class or to their ecological niches and applied a multivariate non-parametric test (ANOSIM) to check for differences in distribution of the Fe uptake systems across these groupings. For groups that showed a significant difference (a positive ANOSIM *R* value with significance <5%) in the type and frequencies of occurrence of Fe uptake systems, the SIMPER method was used to identify the proteins that contributed the most to this difference (see Materials and Methods for details). The taxonomic groups took into account the heterotrophic genomes, comprised of *Alphaproteobacteria*, *Gammaproteobacteria*, and *Flavobacteria*, and the phototrophic genomes consisting of picocyanobacteria (*Synechococcus* and *Prochlorococcus*), other-*Cyanobacteria* (*Cyanobacteria* excluding picocyanobacteria), and the eukaryotic phytoplankton. The genomes were grouped into niches based on only the isolation location of the source organism, e.g., Open Ocean, Coastal, or Freshwater (Table S1 in Supplementary Material).

The NMDS plot of 110 heterotrophic genomes showed three distinct clusters corresponding to the three taxa (Figure 3A). The differences in Fe-metabolism systems among the three groups were statistically significant (Table 2). The greatest diversity of TBD hydroxamate/catecholate siderophore and heme uptake components, and occurrence frequency of bacterioferritin and NIS biosynthesis component RhbB, as identified by SIMPER, was seen in *Gammaproteobacteria* (Table 3A). The *Alphaproteobacteria* genomes had the highest occurrence frequencies of Ferric reductase, the Zinc uptake protein ZupT (free Fe²⁺ and other divalent cations), and FbpA (Fe³⁺ transporter component) as well

as regulatory elements Fur and RirA. The ferric citrate uptake protein FecA, the FeoAB proteins (Fe²⁺ uptake), and Ferritin were amongst the most abundant in *Flavobacteria* and infrequent in the other two groups of heterotrophic bacteria. The regulatory element DtxR was only present in *Flavobacteria* and absent in *Alphaproteobacteria* and *Gammaproteobacteria*.

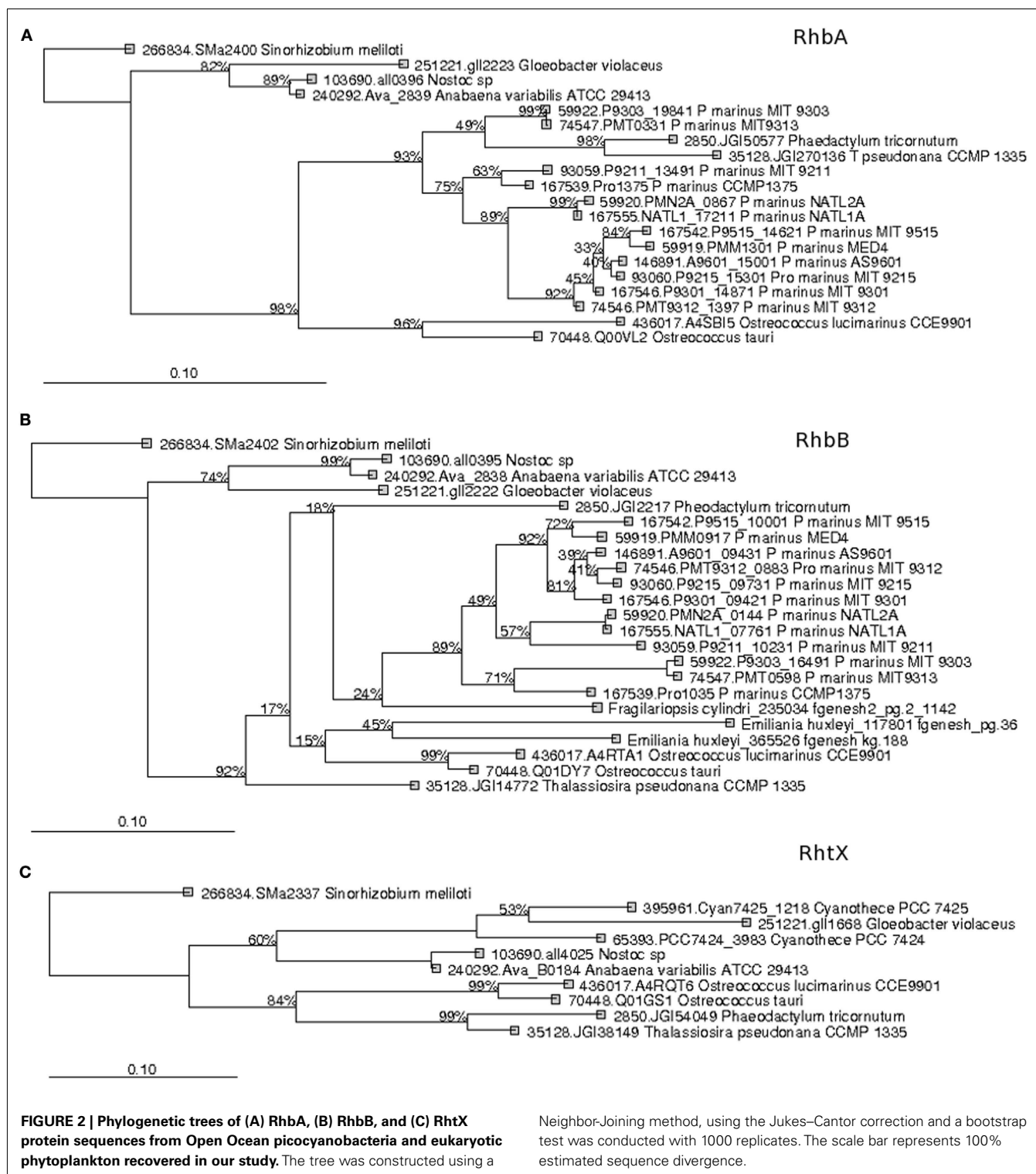
Figure 3B shows the NMDS plots labeled by taxonomy for the 54 phototrophic genomes. The *Cyanobacteria* and eukaryotic genomes formed separate clusters. Within the cyanobacterial cluster the picocyanobacteria, which had the highest number of representative genomes, and other-*Cyanobacteria* formed sub-clusters. The phototrophic genomes showed a statistically significant difference between the eukaryotic phytoplankton, picocyanobacteria, and other-*Cyanobacteria* groups (Table 2). The Fe uptake components which showed a marked difference in abundances across the phototrophic genome groups are given in Table 3. The picocyanobacteria were characterized by the periplasmic Fe³⁺ transport components IdiA and HitB which were infrequent in the other-*Cyanobacteria* and not detected at all in the available eukaryotic phytoplankton genomes (Table 3). On the other hand, GTP driven Fe²⁺ uptake components FeoAB, FTR1, and hydroxamate uptake components FhuA and RhtX were largely absent from picocyanobacteria and eukaryotic phytoplankton but were present in the other-*Cyanobacteria* group. Similarly, high occurrence frequencies of the Zinc transporter ZupT, Ferric reductase, IsiB, and NRPS were characteristic of the eukaryotic phytoplankton as compared to the *Cyanobacteria*.

ANALYSIS OF GENOMES IN TERMS OF THEIR ECOLOGICAL NICHES

The Open Ocean niche group of the phototrophic genomes (Figure 3C) was significantly different from the Coastal and Freshwater groups (Table 2). We observed that the TBD siderophore/heme uptake components as well as the Feo system for Fe²⁺ uptake were most widespread in the Freshwater niche, relatively less common in Coastal niche and rarely represented in the Open Ocean niche (Table 4). FTR1 (direct Fe²⁺ uptake), ferritin, HO1 (heme oxygenase), and NRPS were abundant in Freshwater niche. The Fe³⁺ transporter components (IdiA and HitB) were evenly present in all the three niches. The NIS biosynthesis protein RhbB was most abundant in the Coastal niche. The Open Ocean niche had a greater abundance of IsiA and IsiB than both other niches. The niche groups in the heterotrophic genomes were not distinguishable from each other in terms of the frequencies of iron uptake genes (Table 2).

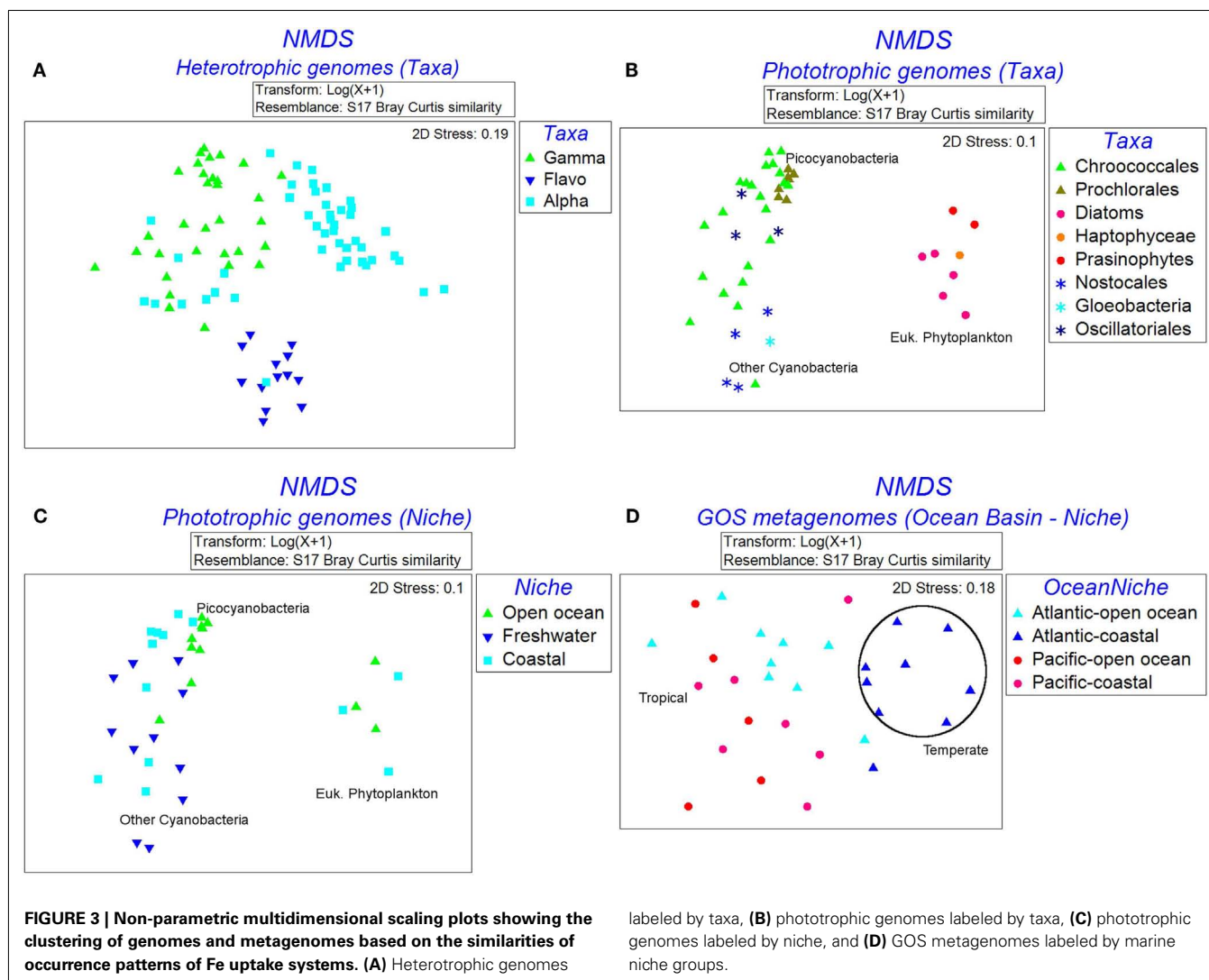
ENVIRONMENTAL CHARACTERIZATION OF THE GOS METAGENOMES

Figure 4 shows the GOS sample locations overlaid on the annual mean surface bioavailable dFe from the PELAGOS model (Vichi et al., 2007a,b). This model couples the biogeochemical fluxes with global ocean general circulation models. The iron dynamics in PELAGOS include fluxes for uptake of bioavailable Fe by phytoplankton, loss by turnover/cell lysis, and predation. The only external function that forces these fluxes is the monthly deposition of atmospheric Fe and a dissolution fraction of the Fe dust which is set at 1%. We used the surface dFe concentration predictions from the PELAGOS model to characterize the



aquatic niches. Since we were using model-derived dFe concentrations in place of actual observations, we compared the dFe concentrations used in this study with those used in Toulza et al. (2012). For the 22 GOS samples where dFe concentration predictions from both of these models were available, an

R^2 of 0.849 in a linear regression of the dFe values showed a good correlation between the outputs of the two models (Table S2 in Supplementary Material). There was a marked difference in the surface dFe concentration in samples collected from the Atlantic and the Pacific basins. However, apart from the dFe



differences in the niches (Open Ocean or Coastal) defined in Toulza et al. (2012), the spatial distribution of the samples across a wide range of latitudes also resulted in a separation along a temperature gradient (Temperate vs. Tropical) (Rusch et al., 2007).

The environmental matrix for the 30 GOS samples belonging to the Open Ocean and Coastal niche groups was subjected to a PCA (Figure 5). The Atlantic and Pacific samples were separated along the first PC, where the environmental parameters accounting for the separation were Longitude, Latitude, and Temperature. Within each ocean basin group (Atlantic or Pacific), along the second PC, the water column depth gradient separated the samples into Open Ocean and Coastal groups. The dFe gradient separated the Atlantic Open Ocean samples from the Pacific Open Ocean and Coastal samples (Figure 5). The first PC, which included the temperature gradient in addition to the dFe, also separated the samples into Temperate and Tropical groups (Figure 5).

To further understand the interaction between dFe and temperature and to define meaningful niche groups with contrasting parameters, we compared the median and range of

the dFe concentrations as well as the temperatures (suitably transformed as described in the methods) for different group of GOS samples (Figures 6A,B respectively). There was a significant difference in dFe concentrations in the Pacific and Atlantic samples (single factor ANOVA, p value = $6.31E-09$), and their median temperature difference was also significantly different (p value < 0.0005). The most noticeable difference of Fe concentrations was seen in the Atlantic Open Ocean samples and Pacific (Open Ocean and Coastal) samples (p value $1.3E-11$) whereas the corresponding temperature difference between these groups was not significant (p value 0.27 at $\alpha = 0.01$). Conversely, the Temperate, Coastal samples were primarily separated from the Tropical (Open Ocean and Coastal) samples by a temperature difference (p value $2.1E-07$) with no difference in the corresponding average Fe concentrations (p value 0.3 at $\alpha = 0.01$). Consequently, only these three pairs of groups (Atlantic Open Ocean vs. Pacific, Temperate vs. Tropical, and Open Ocean vs. Coastal) were further analyzed for the differences in their taxonomic profiles and their associated Fe-metabolism systems.

Table 2 | Statistical comparison (ANOSIM) of Fe-metabolism systems in various groupings of genomes and metagenomes.

Groups	<i>R</i> statistic	Significance level %
GENOME CATEGORIES		
Heterotrophs-taxa		
Gammaproteobacteria, Flavobacteria	0.862	0.1
Gammaproteobacteria, Alphaproteobacteria	0.455	0.1
Flavobacteria, Alphaproteobacteria	0.657	0.1
Phototrophs-taxa		
Picocyanobacteria, other-Cyanobacteria	0.406	0.1
Picocyanobacteria, Eukaryotic phytoplankton	0.942	0.1
Other-Cyanobacteria, Eukaryotic phytoplankton	0.964	0.1
Phototrophs-niche		
Open Ocean, fresh water	0.332	0.1
Open Ocean, coastal	0.125	3.1
Fresh water, coastal*	0.074	8.8
GOS Groups		
North Atlantic Open Ocean, South Pacific	0.142	3.7
Tropical, temperate	0.469	0.1
Coastal, Open Ocean	0.201	0.4

An *R* value with significance level more than 5% implies that the corresponding groups cannot be statistically differentiated from each other. The insignificant pair of groupings is marked with *.

TAXONOMIC DISTRIBUTION AND FE-METABOLISM COMPONENTS REPRESENTED IN THE GOS METAGENOME GROUPS

The taxonomic profiles (the occurrence of sequences from various taxonomic groups) of the aforementioned GOS metagenome groups were obtained from MG-RAST (Meyer et al., 2008) using an *E*-value cut-off of $1\text{E}-15$, minimum percent identity 50, and minimum alignment length 100. Using the set of sequences with a clear taxonomic identification we further processed the data to obtain the percentage contribution of each taxonomic group in the metagenomic groupings (Table 5). The Fe-metabolism protein frequency matrix was analyzed for differences in Fe-metabolism components across the GOS metagenomic groupings. The NMDS plots labeled by Ocean Basin – Niche categories as well as the Temperature – Niche groups are shown in Figure 3D. The ANOSIM tests for all these groups were significant (Table 2), suggesting that the distribution of Fe uptake system components was different. However, based on the environmental characterization (see the section above), we selected only the samples from Tropical vs. Temperate and Atlantic Open Ocean vs. Pacific for further analysis with SIMPER along with the previously defined Open Ocean vs. Coastal samples (Toulza et al., 2012). Differences in gene abundances between these groups are given in Table 3. The average abundance of the heme uptake machinery HmuTUV was higher in the Pacific, Tropical, and Coastal groups whereas the Fe^{3+} uptake (IdiA, HitB) and IsiA had a higher representation in the Atlantic Open Ocean (compared to the Pacific), Tropical (compared to Temperate), and Open Ocean (compared to Coastal) groups. The Fe^{2+} uptake components (FeoAB) and Ferric reductase were more abundant in Atlantic Open Ocean, Temperate, and Coastal groups. The Flavodoxin protein IsiB and heme oxygenase

HO1 had a higher average abundance in the Pacific, Tropical, and Open Ocean groups. While ZupT (zinc uptake protein) was more abundant in Pacific, Temperate, and Coastal groups, the storage protein ferritin had a higher abundance in Atlantic Open Ocean, Temperate, and Open Ocean groups.

PHYLOGENETIC SPREAD AND NON-SYNONYMOUS MUTATION RATE OF SELECTED GENES

The nucleotide sequences of some of the abundant genes, extracted from the genomes, were analyzed for the rate of non-synonymous mutations. Because non-synonymous mutations result in amino acid replacement, they are often eliminated by purifying selection, a form of natural selection that selectively removes deleterious mutations. Under certain selection pressures, non-synonymous mutations might be retained when they are advantageous (known as positive selection). The dN/dS ratio therefore provides a measure of the selection pressure operating on a gene. The dN/dS ratio for some of the genes was plotted (Figure 7) along with their average phylogenetic spread (the average phylogenetic distance among the genomes possessing the gene, calculated from a Maximum Likelihood tree of 16S rRNA gene sequences of the genomes). Ferric reductase, *feoA*, *feoB*, *idiA*, and the zinc uptake gene *zupT*, *tonB*, and ferritin genes all had a dN/dS value > 1 , indicating that non-synonymous mutations were possibly beneficial for these genes and that they were evolving rapidly under positive selection. With the exception of the *idiA* gene, all of these genes also had a wide phylogenetic spread indicating that they were present in a wide range of taxonomic groups (Figure 7). The remaining genes analyzed had a dN/dS ratio < 1 (28 out of 35), indicating that they were under purifying selection pressure. All proteins involved in siderophore biosynthesis or high-affinity uptake systems for hydroxamate or catecholate siderophore/heme or vitamin B12 were undergoing purifying selection. The regulatory element *fur*, *fbp*-family gene *fbpA*, *hitB*, *isiA*, *isiB*, and the Mg^{2+} transporter *mgtE* were also included in the category of purifying selection and, with the exception of *isiA*, retained a wide phylogenetic spread among the marine genomes.

DISCUSSION

MULTIVARIATE APPROACH USING FUNCTIONAL GENE SPECIFIC HMMs

Hidden Markov models of protein families or folds have been routinely used in genome wide studies of protein functions such as metal binding capabilities (Dupont et al., 2006, 2010) or Fe transport (Hopkinson and Barbeau, 2012). Some Fe uptake proteins have multiple domains, which could be shared among different functional classes. For example, the TonB-box is a conserved motif which is common to all TBD receptors binding to different substrates (hydroxamate, catecholate, heme, or citrate). The GTP-binding domain of FeoB which is conserved and involved in various other functions could also lead to increased FP, especially in the metagenomic sequences (Hopkinson and Barbeau, 2012). It has been shown earlier that the specificity of the identification of function at the substrate binding level can be increased by modifying the HMM using information from the negative training sequences (i.e., sequences of the same fold or family but having different substrate binding function) (Srivastava et al., 2007; Desai

Table 3 | Fe-metabolism protein components discriminating between the three major taxonomic groups of heterotrophs (A) and phototrophs (B) and groupings of the GOS metagenomes (C) identified using the Similarity Percentages (SIMPER) method.

Protein	(A) Heterotrophs			(B) Phototrophs			(C) GOS metagenomes					
	Gamma	Alpha	Flavo	Picocyano bacteria	Other Cyano bacteria	Eukaryotic Phyto plankton	Fe conc groups		Temperature groups		Niche groups	
							Atlantic Open Ocean	Pacific Ocean	Tropical	Temperate	Open Ocean	Coastal
HEMETBDT UPTAKE												
HasF	0.73	0.09										
PhuR	0.45	0.19	0.43									
HmuT	0.43	0.28	0.1				0.08	0.96	0.56	0	0.28	0.52
HmuU	0.81	0.67	0.25	0.13	0.48		0.15	0.83	0.55	0.31	0.43	0.53
HmuV	0.48	0.33	0.1				0.2	0.35	0.27	0.53	0.28	0.4
HemU	0.23	0.1	0.45			0						
HYDROXAMATE SIDEROPHORE UPTAKE												
FhuA	0.75	0.41	0.36	0.2	0.93	0						
IutA	0.46		0.05			0						
RhtX				0.13	0.43	0						
CATECHOLATE SIDEROPHORE UPTAKE												
BtuF	0.4	0.06										
BtuB	0.91	0.33	0.05									
CITRATE SIDEROPHORE UPTAKE												
FecA	0.38	0.07	0.52									
Fe3+ TRANSPORTERS												
IdiA				0.79	0.31	0	1.79	1.66	1.72	1.43	1.82	1.49
HitB	0.55	0.53	0.05	0.69	0.54	0	1.03	0.73	0.82	0	0.92	0.32
FbpA	0.43	0.59	0.05				0.46	0.61	0.52	0.26	0.54	0.37
FREE Fe2+ UPTAKE												
FeoA	0.45	0.09	0.69	0.31	0.61	0	0.63	0.36	0.51	1.38	0.89	1.29
FeoB	0.48	0.12	0.69	0.3	0.63	0	0.99	0.9	0.9	1.67	0.48	0.97
ZupT	0.27	0.49	0.38			1.52	0.12	1.29	1.19	1.25	1.15	1.25
FTR1				0.17	0.39							
MgtE						0.4	3.33	3.2				
REGULATORY ELEMENTS												
Fur	1.11	1.36	1.03			0			3.72	3.34	3.71	3.54
RirA	0.55	0.63										
DtxR	0	0	0.81				0.95	1.4	1.22	0.96	1.13	1.16
STORAGE												
BfrB	0.49	0.15										
Ferritin	0.67	0.49	0.87	1.02	1.56	0.09	1.82	1.41	1.51	1.69	1.6	1.53
NRPS INDEPENDENT SIDEROPHORE SYNTHESIS												
RhbB	0.62	0.42	0.52									
NRPS	0.46	0.59	0.49	0.36	1.67	0.95						
Ferric	0.44	0.65				1.48	1.29	1.27	1.34	2	1.2	1.79
reductase												
IsiA				1.27	1.27	0	1.72	1.34	1.49	0.17	1.82	0.55
IsiB	0.62	0.02		0.54	0.6	0.87	1.28	1.35	1.3	0.36	1.37	0.76

The numbers are average log abundances of components that were discriminating between groups with the highest abundance in a given category (A, B, or C) given in bold. An empty cell means that the component might be present in all the groups but is not discriminating between groups.

et al., 2011). We constructed profile HMMs of Fe-metabolism proteins covering most known Fe uptake systems (Table 1), using the HMM-ModE protocol (Srivastava et al., 2007) to increase the specificity at the substrate binding level. Our finding that TBD

Table 4 | Proteins discriminating between aquatic niche groups in phototrophic genomes identified using the Similarity Percentages (SIMPER) method.

Protein	Phototroph genomes (niche)		
	Open Ocean	Coastal	Freshwater
HEMETBDT UPTAKE			
HasF			
PhuR			
HmuT			
HmuU	0.12	0.19	0.36
HmuV			
HemU			
HYDROXAMATE SIDEROPHORE UPTAKE			
FhuA	0.12	0.24	0.87
IutA	0.04		0.32
FhuB	0		0.26
FhuC	0.06		0.23
RhtX	0.06	0.21	0.38
CITRATE SIDEROPHORE UPTAKE			
FecB	0.13	0.31	0.41
Fe³⁺ TRANSPORTERS			
IdiA	0.53	0.63	0.68
HitB	0.57	0.59	0.58
FbpA			
Fe²⁺ UPTAKE			
FeoA	0.19	0.3	0.74
FeoB	0.17	0.38	0.65
ZupT	0.28	0.28	0.17
FTR1	0.04	0.03	0.58
MgtE	0.64	0.67	0.71
REGULATORY ELEMENTS			
Fur	1.09	1.27	1.51
RirA			
DtxR			
STORAGE			
BfrB			
Ferritin	0.76	1.13	1.41
NRPS INDEPENDENT SIDEROPHORE SYNTHESIS			
RhbB	0.12	0.43	0.32
NRPS	0.49	0.67	1.3
Fe-Red	0.35	0.16	0.15
IsiA	1.51	0.89	1.05
IsiB	0.79	0.35	0.68

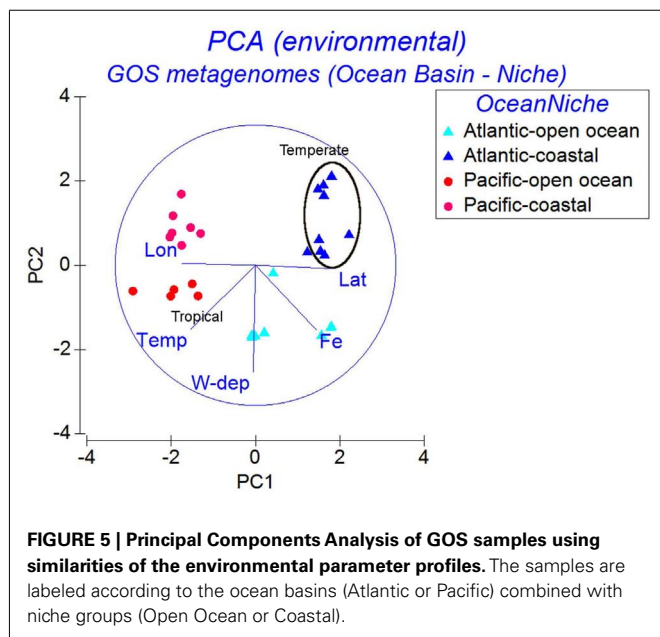
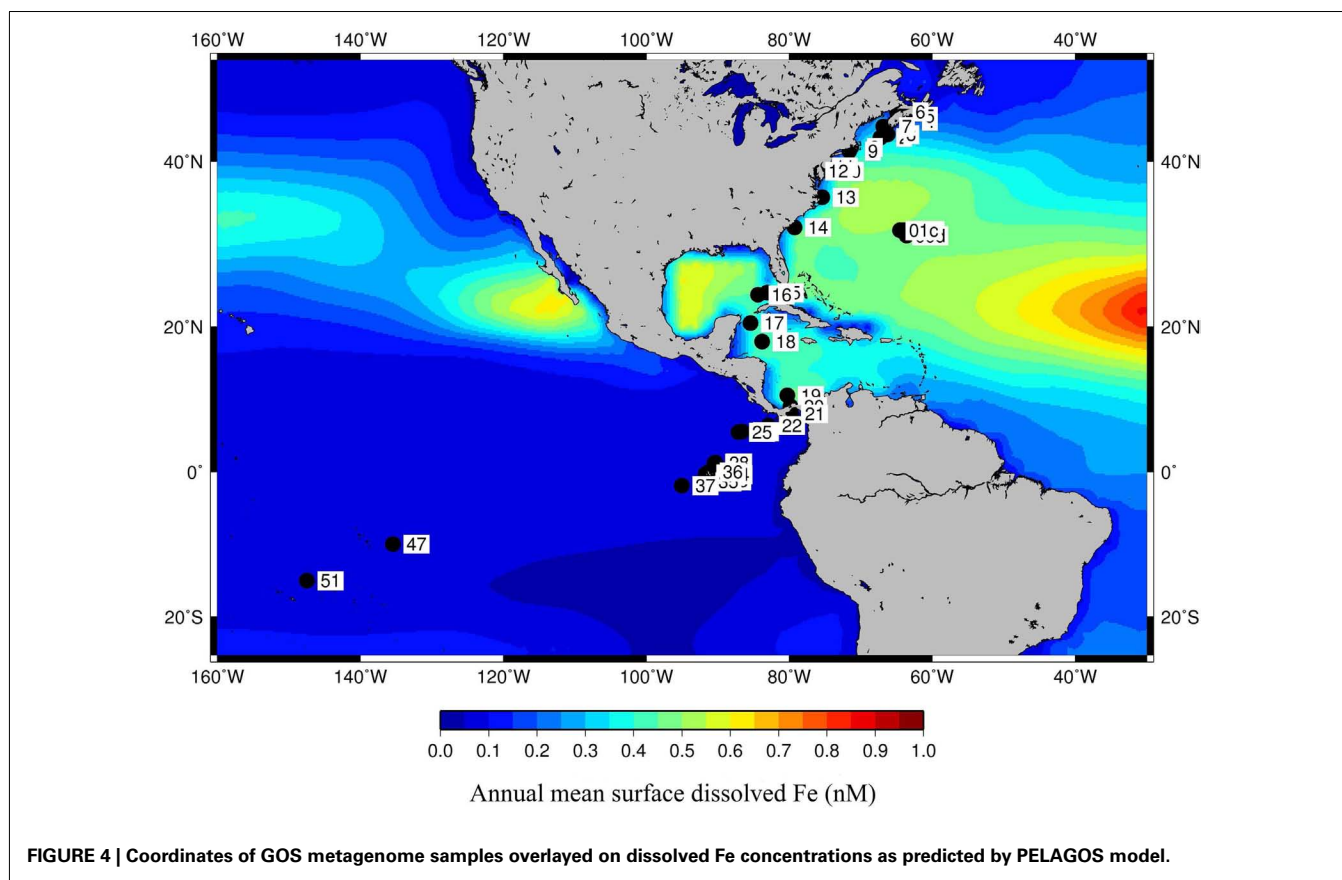
The numbers are average log abundances of components that were discriminating between groups. The abundances for the categories having the highest values for a given component are displayed in bold. An empty cell means that the component might be present in all the groups but is not discriminating between groups.

hydroxamate uptake components are relatively abundant in the metagenomes (Figure 1B) was in agreement with the fact that hydroxamate siderophores are abundant in seawater and constitute upto 5% of the dFe concentration in the Atlantic Ocean (Macrellis et al., 2001; Mawji et al., 2008; Velasquez et al., 2011; Gledhill and Buck, 2012).

Our method also provided a wider range of components to search for in the genomes and metagenomes as demonstrated by the hits obtained for the proteins RhbA (diaminobutyrate-2-oxoglutarate aminotransferase) and RhbB (L-2,4 diaminobutyrate decarboxylase) that suggest the presence of some of the components for rhizobactin siderophore biosynthesis in *Cyanobacteria* and eukaryotic phytoplankton genomes (Table S1 in Supplementary Material). However, the confirmation of siderophore biosynthesis pathways in these organisms will depend in part on the positive identification of the remaining genes for the many necessary components that could not be detected in these genomes using the HMMs and the STRING database as input for the search. Also, the homologs of RhtX detected in the eukaryotic genomes from the STRING database, were mostly annotated as Acetyl CoA transporters and had only a weak similarity with the *S. meliloti* RhtX protein (Tables S3–S5 in Supplementary Material), making their identification tenuous without supportive evidence. Siderophore biosynthesis has been reported in some *Synechococcus* species (Wilhelm and Trick, 1994; Ito and Butler, 2005; Hopkinson and Morel, 2009) and predicted to be present in the prasinophyte *O. lucimarinus* (Palenik et al., 2007) suggesting that they may be more widespread than originally thought. Recent reports have shown the production of Fe-binding ligands by microbial communities dominated by diatoms under Fe-depleted conditions with a distinct correlation between Fe-binding ligand concentration and diatom growth (Buck et al., 2010; King et al., 2012).

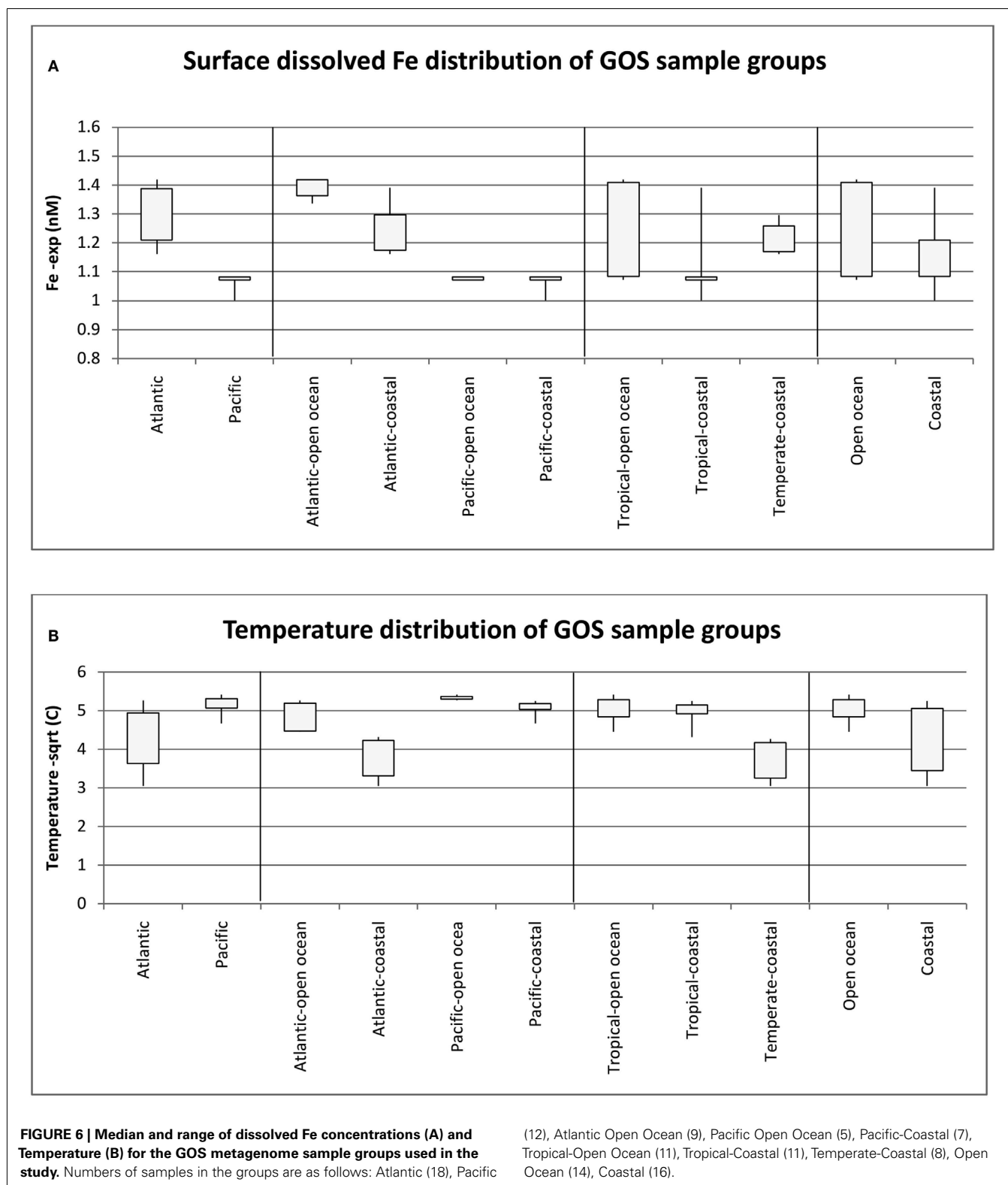
The increased specificity (and the related sensitivity drop) of the HMM search implies that we might miss identifying Fe-metabolism components in the genomes and metagenomes and our bottom-up approach (starting from known sequences) would prevent us from discovering novel or highly diverged forms of these Fe uptake systems. Also, for the metagenomes, since we sampled equal numbers of sequences, the reduced search space led to the under-representation of some Fe-metabolism systems. For example, even though the hydroxamate TBD uptake systems turned up as discriminating between the genome groups, they were not detected in sufficient numbers or discriminating between metagenome groupings (Table 3). To see if this under-representation was a result of the method and the reduced search space, we scanned all the sequences in the metagenomes with our profiles (Figure 1B). We did find components of hydroxamate, catecholate, and citrate siderophore uptake along with heme degrading oxygenases in all the groups of samples. However, since our aim was to compare samples from different locations, it was important to minimize the effect of sequencing effort (Gilbert et al., 2010), and so, all our comparisons were performed with the sampled metagenome sequence data.

Multivariate analysis is increasingly being applied in microbial ecology studies, for example, to trace the seasonal variation in bacterial communities (Gilbert et al., 2010), compare communities



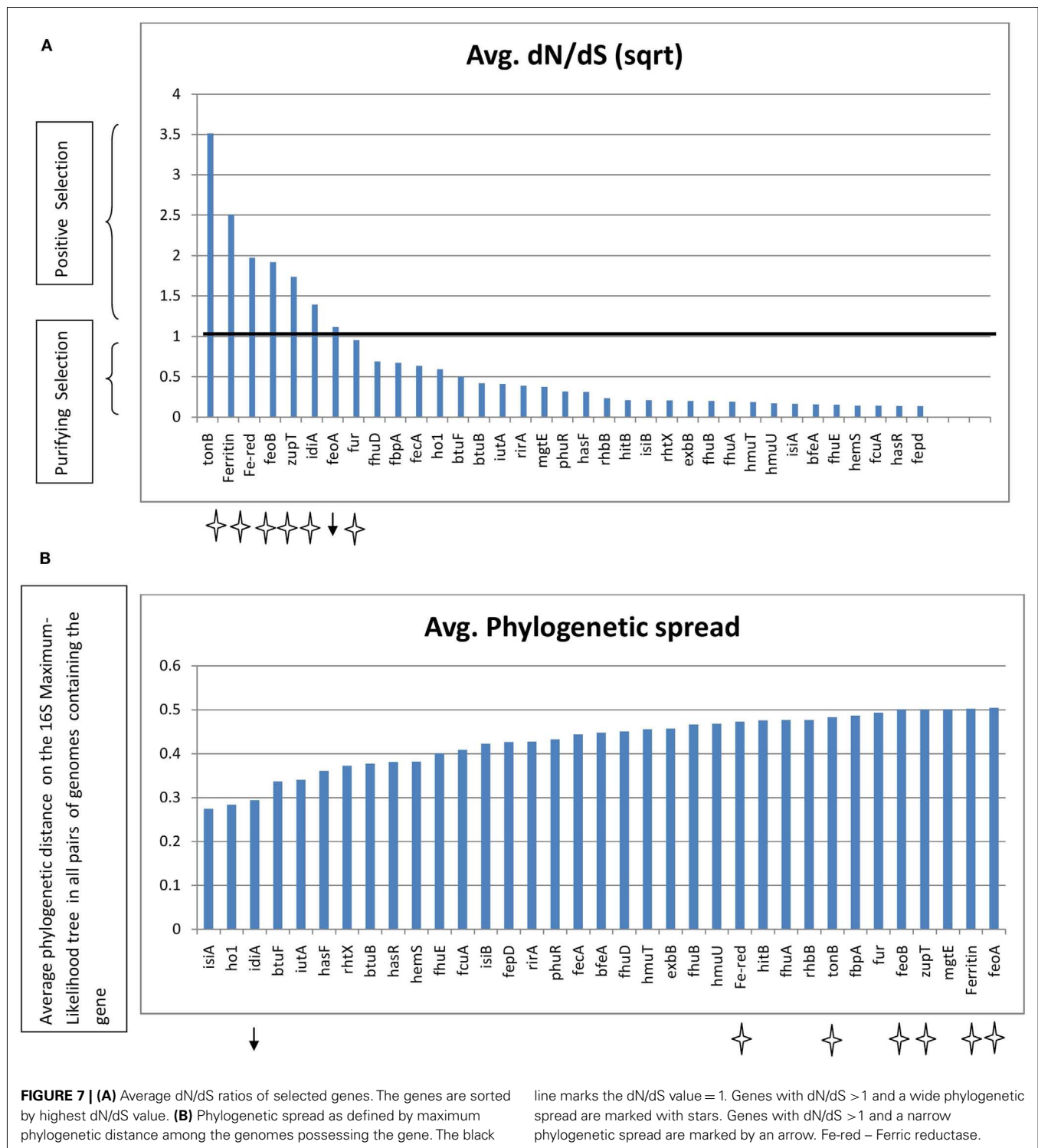
from different niches (Dinsdale et al., 2008) or investigate the correlation of environmental factors with the observed community structure and function in the GOS metagenomes (Gianoulis et al., 2009; Raes et al., 2011). The traditional concept of the

species as a fundamental unit of biological diversity does not apply to prokaryotes. A new bacterial equivalent of a species (an ecotype) arises when a bacterial lineage starts utilizing a different set of resources for occupying a new ecological niche or microhabitat (Cohan, 2002). The bacterial genome has the capability to re-organize itself according to environmental cues in a given niche by mechanisms such as horizontal gene transfer (Thompson et al., 2011; Hopkinson and Barbeau, 2012) and hence, could be viewed as an assemblage of genes. In our analysis, we therefore used the profiles of abundances of the Fe-metabolism components (as variables or species that are subject to change) in the genomes or metagenomes (the ecological equivalent of samples) to calculate the similarities between pairs of samples, and further, between *a priori* groupings of the samples. Our multivariate analysis detected distinct patterns of co-occurrence in the groups (both genomes and metagenomes) including the co-occurrence of multiple components of the same system. For example, in most of the comparisons of the groups that we performed, all components of the heme uptake machinery HmuTUV, Fe^{3+} transporters, or the FeoAB system were reported as significant. Concomitantly, the characteristic occurrence patterns for each genome group (Figure 1) were also captured accurately. The reliance of picocyanobacteria and *Alphaproteobacteria* on Fe^{3+} transporters and their absence from *Flavobacteria*, or the widespread use of FeoAB based Fe^{2+} uptake by *Flavobacteria* and its absence from picocyanobacteria and *Alphaproteobacteria* are facts borne out by recent studies



(Hopkinson and Barbeau, 2012) which were also apparent in our analysis. Thus, the multivariate analysis of uptake systems in genomes, using the genome as a unit of ecological treatment,

validated our approach and demonstrated that it could be used to determine similar differences between the niche groups of genomes and metagenomes.



ENVIRONMENTAL ENRICHMENT OF FE UPTAKE SYSTEM COMPONENTS CORRELATES WITH THE DISTRIBUTION OF DOMINANT TAXONOMIC GROUPS

The classification of a microbial genome as either Open Ocean or Coastal in our study was based on the location where they were isolated and does not preclude the possibility of it

being present in other niches. However, the abundance of a plethora of Fe uptake systems along with both NIS and NRPS siderophore biosynthesis components in Freshwater and Coastal phototrophs potentially reflected the diversity of Fe-binding ligands in these niches as compared to the oligotrophic Open Ocean organisms where only the homeostasis proteins IsiA,

Table 5 | Taxonomic profiles of GOS metagenome niche groupings.

Taxonomic groups	Fe concentration groups		Temperature groups		Niche groups	
	Atlantic Open Ocean	Pacific	Tropical	Temperate	Open Ocean	Coastal
Alphaproteobacteria	41.80	22.97	36.18	16.60	16.57	35.33
Gammaproteobacteria	26.97	24.21	19.99	39.20	35.16	20.18
Flavobacteria	6.26	22.68	6.22	12.47	2.64	7.51
Picocyanobacteria	13.61	1.01	11.55	0.28	5.37	8.86
Other-Cyanobacteria	0.20	0.55	0.23	0.08	0.53	0.11
Eukaryotic phytoplankton	0.05	0.94	0.04	0.49	0.04	0.16

The numbers indicate the percentage dominance of the taxa in the metagenome groups.

IsiB, and Ferric reductase were abundant (Table 3). The GOS metagenomes provided an opportunity for the same comparison at the community level and also afforded a correlation of these differences to temperature, dFe concentration, and a distinction between Open Ocean and Coastal niches which were set apart from each other by water column depth (Figure 5). The SIMPER analysis demonstrated that certain genes were enriched in a particular niche, i.e., they had a distinct environmental signature.

A detailed analysis of the occurrence patterns of major microbial taxa in the same GOS metagenomic groupings (Table 5) was instructive of how the distribution of Fe-metabolism systems was effected by the environmental parameters. The Tropical metagenomes were dominated by SAR11 cluster and other *Alphaproteobacteria* (36.18% of total identified taxa) and picocyanobacteria (11.55%). These taxa were notably under-represented in the Temperate metagenomes (16.6 and 0.28% respectively). On the other hand the Temperate metagenomes were mainly composed of *Flavobacteria* (12% as compared to 6% in Tropical) and *Gammaproteobacteria* (39%; Table 5). The major differences in the Fe uptake systems between these groups, i.e., more Fe^{3+} transporters, IsiA, and IsiB in Tropical vs. more Fe^{2+} uptake, ferritin and Ferric reductase in Temperate were in accordance with the differences between the picocyanobacteria and *Alphaproteobacteria* on one hand and the *Flavobacteria* on the other (Table 3). The HmuTUV system, though decidedly more widespread in *Gammaproteobacteria*, is nonetheless present in *Alphaproteobacteria* genomes (Table 3). The combined contribution of *Alphaproteobacteria* and *Gammaproteobacteria* sequences is roughly the same in both groups (58.17 and 55.80% of all Tropical and Temperate sequences respectively; Table 5). We also compared just the coastal samples from the Tropical and Temperate zones (Table S2 in Supplementary Material) to remove the effect of Open ocean and Coastal locations and the results were unchanged. The impact of temperature on the taxonomic and functional diversity of the GOS samples is well established (Rusch et al., 2007; Raes et al., 2011). Here, we showed that temperature, potentially, also has an impact on the Fe uptake system distribution.

In the metagenomic groups separated by dFe concentrations, picocyanobacteria were well represented in the Atlantic Open Ocean (Fe-replete) samples whereas *Alphaproteobacteria* clades dominated the Fe-depleted Pacific samples. Again

in this case, Fe uptake system distribution between the two groups (Table 3), i.e., more Fe^{3+} transporters, Fe^{2+} uptake, and IsiA in the Atlantic vs. more HmuTUV, FbpA, ZupT, and IsiB in the Pacific, was a reflection of the differences between corresponding dominant taxonomic groups (Table 5).

Niche specific adaptations and diversity in Fe uptake mechanisms among *Cyanobacteria* are well documented. For example, siderophore production and its associated receptor mediated uptake is more common in freshwater and coastal cyanobacteria but is not the preferred iron acquisition strategy in open ocean *Cyanobacteria* (Webb et al., 2001; Palenik et al., 2006; Hopkinson and Morel, 2009). Our results of the niche analysis of phototrophic genomes also showed this distinction (Table 4). Recent sequencing of various *Synechococcus* genomes points to the presence of Fe^{2+} uptake in coastal strains (Palenik et al., 2006) as an adaptation to the higher concentrations of bioavailable Fe^{2+} in coastal regions (Kuma et al., 1992). The upregulation of IdiA as a response to Fe limitation both in culture as well as in the Fe-limited open ocean is well known in *Cyanobacteria* (Rusch et al., 2010; Thompson et al., 2011). Additionally, presence of Fe^{3+} transporters, and lack of TBD Fe uptake systems in *Candidatus Pelagibacter ubique*, an open ocean alphaproteobacterium might also be a niche specific adaptation (Smith et al., 2010). In light of the above facts and because of possible differences in Fe-speciation (Boye et al., 2003; Buck and Bruland, 2007), niche specific adaptive differences in Fe-metabolism gene profiles were expected between the Open Ocean and Coastal groups. However since all the Temperate samples were also Coastal, some of the differences between Temperate and Tropical groups might, in essence, be reflected in the differences between the Coastal and Open Ocean niche groups. For example, the FeoAB system and Ferric reductase (over-represented in Temperate) were also more abundant in the Coastal group. Additionally, the Coastal group also had higher abundance of the HmuTUV. The Open Ocean group on the other hand had higher occurrence of Fe^{3+} transporters, IsiA, and IsiB (Table 3). Taxonomically, the Coastal group was again dominated by *Alphaproteobacteria* and *Gammaproteobacteria* together constituting around 55% of all identifiable sequences in the group. The Open Ocean group also had a similar proportion of the proteobacteria (roughly 52% of total). The *Flavobacteria* and picocyanobacteria were both over-represented in the Coastal group (Table 5). But within the picocyanobacteria

the pelagic *Prochlorococcus* was more abundant in Open Ocean while the Chroococcales (*Synechococcus* spp., *Synechocystis* spp. etc) were almost six times more abundant in the Coastal group than in Open Ocean (data not shown). The over-representation of Fe³⁺ transporters, IsiA, and IsiB in the Open Ocean could be explained by the abundance of *Prochlorococcus* while the FeoAB and Ferric reductase in the Coastal group could be due to the abundant Flavobacteria. In conclusion for each metagenomic group the Fe-metabolism component was representative of the taxonomic groups dominant in those metagenomic groups. The environmental niche defined the taxonomic dominance which in turn led to the enrichment of particular Fe uptake components in that particular niche.

DIFFERENTIAL SELECTION PRESSURES ON FE RESPONSIVE GENES

The genes for some of the proteins which were discriminatory between the niches also showed evidence of positive selection pressure at the sequence level (Figure 7). Most of these fast evolving genes perform generalized functions, which could involve interacting with multiple ligands. Both *idiA* and *fbpA* bind Fe³⁺, but only *idiA* was under positive selection pressure while *fbpA* was under purifying selection pressure. However the phylogenetic spread of FbpA was high and occurrence of *idiA* was more or less confined to the *Cyanobacteria*. It has been postulated that Fe³⁺ transporters such as *idiA* interact with Fe bound organic complexes rather than with free Fe³⁺ (Hopkinson and Barbeau, 2012). Hydroxamate siderophores have been detected throughout the Atlantic Ocean (Mawji et al., 2008), and it could be believed that by virtue of broadly specific Fe³⁺ transporter *idiA* or *fbpA* the Open Ocean cyanobacteria could make a variety of siderophores available to themselves. Similarly the non-specific nature of Ferric reductase mechanism (Schroder et al., 2003) might provide an edge to organisms by catering Fe bound to diverse ligands in an organically rich environment, as evident by our finding that Ferric reductase mechanism was relatively abundant in North Atlantic Open Ocean and Temperate (Coastal) groups of metagenomes. An exception is the abundance of TBD mechanisms in South Pacific group which is known to be oligotrophic. The components of the specialized TBD siderophore/heme uptake systems or the enzymes involved in siderophore biosynthesis, heme oxygenase etc were undergoing purifying selection and the phylogenetic spread was also low for many of them. This suggested that both, the design of the siderophore and the uptake machinery employed are species specific and not much variation at the amino acid sequence level is allowed in the proteins involved. In addition, because of the cost involved in the production of siderophore and the uptake machinery, when present they should confer a definite competitive advantage to the organism. The open ocean environment is highly diffusive and an organism in such a niche

cannot benefit from the possession of Fe uptake systems specific for a particular Fe-binding ligand or production of siderophores (Hopkinson and Morel, 2009). This could explain our observation that the specialized TBD uptake systems (e.g., HmuTUV) were more represented in the nutrient rich Coastal niche than in the Open Ocean. These dN/dS calculations were performed using only the genomic sequences. Thus there is a possibility that the results obtained were biased by the high specificity of the HMMs and that the actual rates of evolution in environmental sequences may differ. However, the HMM-ModE protocol has a sensitivity of ~90 and ~96% specificity for annotating complete gene sequences in bacterial genomes (Desai et al., 2011). A recent study of evolutionary rates of genes from environmental populations of coastal *Synechococcus* spp. reported that around 98% of the genes evolved under purifying selection (Tai et al., 2011). Also, the relationship between selection pressure and dN/dS ratio is only valid over long evolutionary time scales when comparing the sequences of divergent species (Kryazhimskiy and Plotkin, 2008).

In this time of rapid change in global oceanic conditions, the selection mechanisms operating on the evolution of genes conferring adaptation to a particular oceanic habitat are continuously shaping the genetic composition of microbial communities. We defined aquatic ecological niches for the GOS metagenomes in terms of dFe concentrations and temperature and investigated the differences in distribution of the taxonomic groups as well as the Fe-metabolism systems between these niches. The distribution of the Fe uptake proteins correlated with the taxonomic distribution of the organisms that possessed these systems, suggesting a role for temperature and Fe in shaping the microbial community in these niches. The biological availability of Fe is complicated by the presence of diverse organic ligands that bind to it. The high demand and low bioavailability of Fe mean that it is an abiotic stressor driving the evolution of microbial Fe-metabolism. We calculated rates of non-synonymous mutations for a set of genes that were discriminating between the above mentioned niches which were distinct with respect to temperature, dFe concentrations, or Coastal and Open Ocean location, and inferred that genes that exhibited higher rates of non-synonymous mutations were the ones involved in non-specific uptake of Fe bound to diverse ligands. This indicated that in the highly diffusive, oligotrophic open ocean marine environment possession of Fe uptake strategies with broad specificities provides a competitive edge to the microorganisms.

SUPPLEMENTARY MATERIAL

The Supplementary Material for this article can be found online at http://www.frontiersin.org/Microbiological_Chemistry/10.3389/fmicb.2012.00362/abstract

REFERENCES

- Adhikari, P., Kirby, S. D., Nowalk, A. J., Veraldi, K. L., Schryvers, A. B., and Mietzner, T. A. (1995). Biochemical characterization of a *Haemophilus influenzae* periplasmic iron transport operon. *J. Biol. Chem.* 270, 25142–25149.
- Andrews, S. C. (1998). Iron storage in bacteria. *Adv. Microb. Physiol.* 40, 281–351.
- Benson, H. P., Boncompagni, E., and Gueriot, M. L. (2005). An iron uptake operon required for proper nodule development in the *Bradyrhizobium japonicum*-soybean symbiosis. *Mol. Plant Microbe Interact.* 18, 950–959.
- Boyd, P. W., Watson, A. J., Law, C. S., Abraham, E. R., Trull, T., Murdoch, R., et al. (2000). A mesoscale phytoplankton bloom in the polar Southern Ocean stimulated by iron fertilization. *Nature* 407, 695–702.
- Boye, M., Aldrich, A. P., Van Den Berg, C. M. G., De Jong, J. T. M., Veldhuis, M., and De Baar, H. J. W. (2003). Horizontal gradient of the chemical speciation of iron in surface waters of the northeast Atlantic Ocean. *Mar. Chem.* 80, 129–143.

- Braun, V. (2003). Iron uptake by *Escherichia coli*. *Front. Biosci.* 8, S1409–S1421.
- Buck, K. N., and Bruland, K. W. (2007). The physicochemical speciation of dissolved iron in the Bering Sea, Alaska. *Limnol. Oceanogr.* 52, 1800–1808.
- Buck, K. N., Selp, K. E., and Barbeau, K. A. (2010). Iron-binding ligand production and copper speciation in an incubation experiment of Antarctic Peninsula shelf waters from the Bransfield Strait, Southern Ocean. *Mar. Chem.* 122, 148–159.
- Burnap, R. L., Troyan, T., and Sherman, L. A. (1993). The highly abundant chlorophyll-protein complex of iron-deficient *Synechococcus* sp. PCC7942 (CP43⁺) is encoded by the *isiA* gene. *Plant Physiol.* 103, 893–902.
- Butler, A. (2005). Marine siderophores and microbial iron mobilization. *Biometals* 18, 369–374.
- Butterton, J. R., Stoeber, J. A., Payne, S. M., and Calderwood, S. B. (1992). Cloning, sequencing, and transcriptional regulation of *viuA*, the gene encoding the ferric-vibriobactin receptor of *Vibrio cholerae*. *J. Bacteriol.* 174, 3729–3738.
- Cadioux, N., Bradbeer, C., Reeger-Schneider, E., Koster, W., Mohanty, A. K., Wiener, M. C., et al. (2002). Identification of the periplasmic cobalamin-binding protein BtuF of *Escherichia coli*. *J. Bacteriol.* 184, 706–717.
- Challis, G. L. (2005). A widely distributed bacterial pathway for siderophore biosynthesis independent of non-ribosomal peptide synthetases. *ChemBiochem* 6, 601–611.
- Clarke, K. (2006). *PRIMER v6: User Manual/Tutorial*, ed. R. Gorley (Plymouth: PRIMER-E).
- Clarke, K. R. (1993). Non-parametric multivariate analyses of changes in community structure. *Aust. J. Ecol.* 18, 117–143.
- Coale, K. H., Johnson, K. S., Fitzwater, S. E., Gordon, R. M., Tanner, S., Chavez, F. P., et al. (1996). A massive phytoplankton bloom induced by an ecosystem-scale iron fertilization experiment in the equatorial Pacific Ocean. *Nature* 383, 495–501.
- Cohan, F. M. (2002). What are bacterial species? *Annu. Rev. Microbiol.* 56, 457–487.
- Cope, L. D., Yoge, R., Muller-Eberhard, U., and Hansen, E. J. (1995). A gene cluster involved in the utilization of both free heme and heme:hemoexin by *Haemophilus influenzae* type b. *J. Bacteriol.* 177, 2644–2653.
- Cornelis, P., and Bodilis, J. (2009). A survey of TonB-dependent receptors in fluorescent pseudomonads. *Environ. Microbiol. Rep.* 1, 256–262.
- de Baar, H. J. W., Boyd, P. W., Coale, K. H., Landry, M. R., Tsuda, A., Assmy, P., et al. (2005). Synthesis of iron fertilization experiments: from the iron age in the age of enlightenment. *J. Geophys. Res. Oceans* 110, C09S16. doi:10.1029/2004JC002601
- Desai, D. K., Nandi, S., Srivastava, P. K., and Lynn, A. M. (2011). ModEnZA: accurate identification of metabolic enzymes using function specific profile HMMs with optimised discrimination threshold and modified emission probabilities. *Adv. Bioinformatics*. doi:10.1155/2011/743782
- Dinsdale, E. A., Edwards, R. A., Hall, D., Angly, F., Breitbart, M., Brulic, J. M., et al. (2008). Functional metagenomic profiling of nine biomes. *Nature* 452, U628–U629.
- Duce, R. A., and Tindale, N. W. (1991). Atmospheric transport of iron and its deposition in the ocean. *Limnol. Oceanogr.* 36, 1715–1726.
- Dupont, C. L., Butcher, A., Valas, R. E., Bourne, P. E., and Caetano-Anolles, G. (2010). History of biological metal utilization inferred through phylogenomic analysis of protein structures. *Proc. Natl. Acad. Sci. U.S.A.* 107, 10567–10572.
- Dupont, C. L., Yang, S., Palenik, B., and Bourne, P. E. (2006). Modern proteomes contain putative imprints of ancient shifts in trace metal geochemistry. *Proc. Natl. Acad. Sci. U.S.A.* 103, 17822–17827.
- Eddy, S. (1998). *HMMER: Biological Sequence Analysis Using Profile Hidden Markov Models*. Available at: <http://hmmer.org>
- Edgar, R. C. (2004). MUSCLE: a multiple sequence alignment method with reduced time and space complexity. *BMC Bioinformatics* 5, 113. doi:10.1186/1471-2105-5-113
- Enright, A. J., Van Dongen, S., and Ouzounis, C. A. (2002). An efficient algorithm for large-scale detection of protein families. *Nucleic Acids Res.* 30, 1575–1584.
- Fecker, L., and Braun, V. (1983). Cloning and expression of the *fhu* genes involved in the iron(III)-hydroxamate uptake by *Escherichia coli*. *J. Bacteriol.* 156, 1301–1314.
- Ferreiros, C., Criado, M. T., and Gomez, J. A. (1999). The neisserial 37 kDa ferric binding protein (FbpA). *Comp. Biochem. Physiol. B Biochem. Mol. Biol.* 123, 1–7.
- Gall, M. P., Boyd, P. W., Hall, J., Safi, K. A., and Chang, H. (2001). Phytoplankton processes. Part 1: community structure during the Southern Ocean Iron Release Experiment (SOIREE). *Deep Sea Res. Part II Top. Stud. Oceanogr.* 48, 2551–2570.
- Gao, Y., Kaufman, Y. J., Tanre, D., Kolber, D., and Falkowski, P. G. (2001). Seasonal distributions of aeolian iron fluxes to the global ocean. *Geophys. Res. Lett.* 28, 29–32.
- Gianoulis, T. A., Raes, J., Patel, P. V., Bjornson, R., Korb, J. O., Letunic, I., et al. (2009). Quantifying environmental adaptation of metabolic pathways in metagenomics. *Proc. Natl. Acad. Sci. U.S.A.* 106, 1374–1379.
- Gilbert, J. A., Field, D., Swift, P., Thomas, S., Cummings, D., Temperton, B., et al. (2010). The taxonomic and functional diversity of microbes at a temperate coastal site: a ‘multi-omic’ study of seasonal and diel temporal variation. *PLoS ONE* 5, e15545. doi:10.1371/journal.pone.0015545
- Gledhill, M., and Buck, K. N. (2012). The organic complexation of iron in the marine environment: a review. *Front. Microbiol.* 3:69. doi:10.3389/fmicb.2012.00069
- Gledhill, M., and van den Berg, C. M. G. (1994). Determination of complexation of iron(III) with natural organic complexing ligands in seawater using cathodic stripping voltammetry. *Mar. Chem.* 47, 41–54.
- Grass, G., Franke, S., Taudte, N., Nies, D. H., Kucharski, L. M., Maguire, M. E., et al. (2005). The metal permease ZupT from *Escherichia coli* is a transporter with a broad substrate spectrum. *J. Bacteriol.* 187, 1604–1611.
- Guerinot, M. L. (2000). The ZIP family of metal transporters. *Biochim. Biophys. Acta* 1465, 190–198.
- Hannenhalli, S. S., and Russell, R. B. (2000). Analysis and prediction of functional sub-types from protein sequence alignments. *J. Mol. Biol.* 303, 61–76.
- Homann, V. V., Edwards, K. J., Webb, E. A., and Butler, A. (2009a). Siderophores of *Marinobacter aquaeoli*: petrobactin and its sulfonated derivatives. *Biometals* 22, 565–571.
- Homann, V. V., Sandy, M., Tincu, J. A., Templeton, A. S., Tebo, B. M., and Butler, A. (2009b). Loihichelins A–F, a suite of amphiphilic siderophores produced by the marine bacterium *Halomonas* LOB-5. *J. Nat. Prod.* 72, 884–888.
- Hopkinson, B. M., and Barbeau, K. A. (2012). Iron transporters in marine prokaryotic genomes and metagenomes. *Environ. Microbiol.* 14, 114–128.
- Hopkinson, B. M., Roe, K. L., and Barbeau, K. A. (2008). Heme uptake by *Microscilla marina* and evidence for heme uptake systems in the genomes of diverse marine bacteria. *Appl. Environ. Microbiol.* 74, 6263–6270.
- Hunter, K. A., and Boyd, P. W. (2007). Iron-binding ligands and their role in the ocean biogeochemistry of iron. *Environ. Chem.* 4, 221–232.
- Ito, Y., and Butler, A. (2005). Structure of synechobactins, new siderophores of the marine cyanobacterium *Synechococcus* sp. PCC 7002. *Limnol. Oceanogr.* 50, 1918–1923.
- Ito, Y., Ishida, K., Okada, S., and Murakami, M. (2004). The absolute stereochemistry of anachelins, siderophores from the cyanobacterium *Anabaena cylindrica*. *Tetrahedron* 60, 9075–9080.
- Jeanjean, R., Talla, E., Latifi, A., Havaux, C. M., Janicki, A., and Zhang, C. C. (2008). A large gene cluster encoding peptide synthetases and polyketide synthetases is involved in production of siderophores and oxidative stress response in the cyanobacterium *Anabaena* sp. strain PCC 7120. *Environ. Microbiol.* 10, 2574–2585.
- Jickells, T. D., An, Z. S., Andersen, K. K., Baker, A. R., Bergametti, G., Brooks, N., et al. (2005). Global iron connections between desert dust, ocean biogeochemistry, and climate. *Science* 308, 67–71.
- Johnson, K. S., Gordon, R. M., and Coale, K. H. (1997). What controls dissolved iron concentrations in the world ocean? *Mar. Chem.* 57, 137–161.
- Johnston, A. W. B., Todd, J. D., Curson, A. R., Lei, S., Nikolaidou-Katsaridou, N., Gelfand, M. S., et al. (2007). Living without Fur: the subtlety and complexity of iron-responsive gene regulation in the symbiotic bacterium *Rhizobium* and other alpha-proteobacteria. *Biometals* 20, 501–511.
- Joshi, F. R., Kholiya, S. P., Archana, G., and Desai, A. J. (2008). Siderophore cross-utilization amongst nodule isolates of the cowpea miscellany group and its effect on plant growth in the presence of antagonistic organisms. *Microbiol. Res.* 163, 564–570.

- Kammler, M., Schön, C., and Hantke, K. (1993). Characterization of the ferrous iron uptake system of *Escherichia coli*. *J. Bacteriol.* 175, 6212–6219.
- Katoh, H., Hagino, N., Grossman, A. R., and Ogawa, T. (2001). Genes essential to iron transport in the cyanobacterium *Synechocystis* sp. strain PCC 6803. *J. Bacteriol.* 183, 2779–2784.
- King, A. L., Buck, K. N., and Barbeau, K. A. (2012). Quasi-Lagrangian drifting studies of iron speciation and cycling off point conception, California. *Mar. Chem.* 128, 1–12.
- Koebnik, R., Bäuml, A. J., Heesemann, J., Braun, V., and Hantke, K. (1993a). The TonB protein of *Yersinia enterocolitica* and its interactions with TonB-box proteins. *Mol. Gen. Genet.* 237, 152–160.
- Koebnik, R., Hantke, K., and Braun, V. (1993b). The TonB-dependent ferriochrome receptor FcuA of *Yersinia enterocolitica*: evidence against a strict co-evolution of receptor structure and substrate specificity. *Mol. Microbiol.* 7, 383–393.
- Kosman, D. J. (2003). Molecular mechanisms of iron uptake in fungi. *Mol. Microbiol.* 47, 1185–1197.
- Koster, M., Ova, W., Bitter, W., and Weisbeek, P. (1995). Multiple outer membrane receptors for uptake of ferric pseudobactins in *Pseudomonas putida* WCS358. *Mol. Gen. Genet.* 248, 735–743.
- Kryazhimskiy, S., and Plotkin, J. B. (2008). The population genetics of dN/dS. *PLoS Genet.* 4, e1000304. doi:10.1371/journal.pgen.1000304
- Kuma, K., Nakabayashi, S., Suzuki, Y., Kudo, I., and Matsunaga, K. (1992). Photo-reduction of Fe (III) by dissolved organic substances and existence of Fe(II) in seawater during spring blooms. *Mar. Chem.* 37, 15–27.
- LaRoche, J., Boyd, P. W., McKay, R. M. L., and Geider, R. J. (1996). Flavodoxin as an in situ marker for iron stress in phytoplankton. *Nature* 382, 802–805.
- Lewis, L. A., Gray, E., Wang, Y. P., Roe, B. A., and Dyer, D. W. (1997). Molecular characterization of hpuAB, the haemoglobin-haptoglobin-utilization operon of *Neisseria meningitidis*. *Mol. Microbiol.* 23, 737–749.
- Liu, H. B., Landry, M. R., Vault, D., and Campbell, L. (1999). *Prochlorococcus* growth rates in the central equatorial Pacific: an application of the fmax approach. *J. Geophys. Res. Oceans* 104, 3391–3399.
- Liu, H. B., Nolla, H. A., and Campbell, L. (1997). *Prochlorococcus* growth rate and contribution to primary production in the equatorial and subtropical North Pacific Ocean. *Aquat. Microb. Ecol.* 12, 39–47.
- Ludwig, W., Strunk, O., Westram, R., Richter, L., Meier, H., Yadukumar, et al. (2004). ARB: a software environment for sequence data. *Nucleic Acids Res.* 32, 1363–1371.
- Lynch, D., O'Brien, J., Welch, T., Clarke, P., Cuiv, P. O., Crosa, J. H., et al. (2001). Genetic organization of the region encoding regulation, biosynthesis, and transport of rhizobactin 1021, a siderophore produced by *Sinorhizobium meliloti*. *J. Bacteriol.* 183, 2576–2585.
- Macrellis, H. M., Trick, C. G., Rue, E. L., Smith, G., and Bruland, K. W. (2001). Collection and detection of natural iron-binding ligands from seawater. *Mar. Chem.* 76, 175–187.
- Martin, J. H., Coale, K. H., Johnson, K. S., Fitzwater, S. E., Gordon, R. M., Tanner, S. J., et al. (1994). Testing the iron hypothesis in ecosystems of the equatorial Pacific Ocean. *Nature* 371, 123–129.
- Martinez, J. S., and Butler, A. (2007). Marine amphiphilic siderophores: Marinobactin structure, uptake, and microbial partitioning. *J. Inorg. Biochem.* 101, 1692–1698.
- Martinez, J. S., Zhang, G. P., Holt, P. D., Jung, H. T., Carrano, C. J., Haygood, M. G., et al. (2000). Self-assembling amphiphilic siderophores from marine bacteria. *Science* 287, 1245–1247.
- Mawji, E., Gledhill, M., Milton, J. A., Tarran, G. A., Ussher, S., Thompson, A., et al. (2008). Hydroxamate siderophores: occurrence and importance in the Atlantic Ocean. *Environ. Sci. Technol.* 42, 8675–8680.
- Mey, A. R., and Payne, S. M. (2001). Haem utilization in *Vibrio cholerae* involves multiple TonB-dependent haem receptors. *Mol. Microbiol.* 42, 835–849.
- Meyer, F., Paarmann, D., D'souza, M., Olson, R., Glass, E. M., Kubal, M., et al. (2008). The metagenomics RAST server – a public resource for the automatic phylogenetic and functional analysis of metagenomes. *BMC Bioinformatics* 9, 386. doi:10.1186/1471-2105-9-386
- Mochizuki, N., Tanaka, R., Grimm, B., Masuda, T., Moulin, M., Smith, A. G., et al. (2010). The cell biology of tetrapyrroles: a life and death struggle. *Trends Plant Sci.* 15, 488–498.
- Ochsner, U. A., Johnson, Z., and Vasil, M. L. (2000). Genetics and regulation of two distinct haem-uptake systems, phu and has, in *Pseudomonas aeruginosa*. *Microbiology* 146, 185–198.
- Olsen, G. J., Matsuda, H., Hagstrom, R., and Overbeek, R. (1994). fastDNAml: a tool for construction of phylogenetic trees of DNA sequences using maximum likelihood. *Comput. Appl. Biosci.* 10, 41–48.
- Palenik, B., Grimwood, J., Aerts, A., Rouze, P., Salamov, A., Putnam, N., et al. (2007). The tiny eukaryote *Ostreococcus* provides genomic insights into the paradox of plankton speciation. *Proc. Natl. Acad. Sci. U.S.A.* 104, 7705–7710.
- Palenik, B., Ren, Q. H., Dupont, C. L., Myers, G. S., Heidelberg, J. F., Badger, J. H., et al. (2006). Genome sequence of *Synechococcus* CC9311: insights into adaptation to a coastal environment. *Proc. Natl. Acad. Sci. U.S.A.* 103, 13555–13559.
- Plessner, O., Klapatch, T., and Guerinet, M. L. (1993). Siderophore utilization by *Bradyrhizobium japonicum*. *Appl. Environ. Microbiol.* 59, 1688–1690.
- Poole, K., and McKay, G. A. (2003). Iron acquisition and its control in *Pseudomonas aeruginosa*: many roads lead to Rome. *Front. Biosci.* 8, D661–D686.
- Raes, J., Letunic, I., Yamada, T., Jensen, L. J., and Bork, P. (2011). Toward molecular trait-based ecology through integration of biogeochemical, geographical and metagenomic data. *Mol. Syst. Biol.* 7, 473.
- Rakin, A., Saken, E., Harmsen, D., and Heesemann, J. (1994). The pesticin receptor of *Yersinia enterocolitica*: a novel virulence factor with dual function. *Mol. Microbiol.* 13, 253–263.
- Reid, R. T., Live, D. H., Faulkner, D. J., and Butler, A. (1993). A siderophore from a marine bacterium with an exceptional ferric ion affinity constant. *Nature* 366, 455–458.
- Rue, E. L., and Bruland, K. W. (1995). Complexation of iron(III) by natural organic ligands in the Central North Pacific as determined by a new competitive ligand equilibration/adsorptive cathodic stripping voltammetric method. *Mar. Chem.* 50, 117–138.
- Rusch, D. B., Halpern, A. L., Sutton, G., Heidelberg, K. B., Williamson, S., Yooseph, S., et al. (2007). The sorcerer II global ocean sampling expedition: Northwest Atlantic through Eastern Tropical Pacific. *PLoS Biol.* 5, e77. doi:10.1371/journal.pbio.0050077
- Rusch, D. B., Martiny, A. C., Dupont, C. L., Halpern, A. L., and Venter, J. C. (2010). Characterization of *Prochlorococcus* clades from iron-depleted oceanic regions. *Proc. Natl. Acad. Sci. U.S.A.* 107, 16184–16189.
- Sanders, J. D., Cope, L. D., Muller-Eberhard, U., and Hansen, E. J. (1994). Identification of a locus involved in the utilization of iron by *Haemophilus influenzae*. *Infect. Immun.* 62, 4515–4525.
- Schroder, I., Johnson, E., and De Vries, S. (2003). Microbial ferric iron reductases. *FEMS Microbiol. Rev.* 27, 427–447.
- Seshadri, R., Kravitz, S. A., Smarr, L., Gilna, P., and Frazier, M. (2007). CAMERA: a community resource for metagenomics. *PLoS Biol.* 5, e75. doi:10.1371/journal.pbio.0050075
- Smith, D. P., Kitner, J. B., Norbeck, A. D., Clauss, T. R., Lipton, M. S., Schwalbach, M. S., et al. (2010). Transcriptional and translational regulatory responses to iron limitation in the globally distributed marine bacterium *Candidatus Pelagibacter ubique*. *PLoS ONE* 5, e10487. doi:10.1371/journal.pone.0010487
- Srivastava, P. K., Desai, D. K., Nandi, S., and Lynn, A. M. (2007). HMM-Mode – improved classification using profile hidden Markov models by optimising the discrimination threshold and modifying emission probabilities with negative training sequences. *BMC Bioinformatics* 8, 104. doi:10.1186/1471-2105-8-104
- Stojiljkovic, I., and Hantke, K. (1994). Transport of haemin across the cytoplasmic membrane through a haemin-specific periplasmic binding-protein-dependent transport system in *Yersinia enterocolitica*. *Mol. Microbiol.* 13, 719–732.
- Szklarczyk, D., Franceschini, A., Kuhn, M., Simonovic, M., Roth, A., Minguez, P., et al. (2011). The STRING database in 2011: functional interaction networks of proteins, globally integrated and scored. *Nucleic Acids Res.* 39, D561–D568.
- Tai, V., Poon, A. F. Y., Paulsen, I. T., and Palenik, B. (2011). Selection in coastal *Synechococcus* (Cyanobacteria) populations evaluated from environmental metagenomes. *PLoS ONE* 6, e24249. doi:10.1371/journal.pone.0024249
- Thompson, A. W., Huang, K., Saito, M. A., and Chisholm, S. W. (2011). Transcriptome response of high- and low-light-adapted *Prochlorococcus* strains to changing iron availability. *ISME J.* 5, 1580–1594.

- Thompson, J. M., Jones, H. A., and Perry, R. D. (1999). Molecular characterization of the hemin uptake locus (hmu) from *Yersinia pestis* and analysis of hmu mutants for hemin and hemoprotein utilization. *Infect. Immun.* 67, 3879–3892.
- Toulza, E., Tagliabue, A., Blain, S., and Piganeau, G. (2012). Analysis of the Global Ocean Sampling (GOS) Project for trends in iron uptake by surface ocean microbes. *PLoS ONE* 7, e30931. doi:10.1371/journal.pone.0030931
- Tsuda, A., Takeda, S., Saito, H., Nishioka, J., Nojiri, Y., Kudo, I., et al. (2003). A mesoscale iron enrichment in the Western Subarctic Pacific induces a large centric diatom bloom. *Science* 300, 958–961.
- Vanderpool, C. K., and Armstrong, S. K. (2003). Heme-responsive transcriptional activation of *Bordetella* bhu genes. *J. Bacteriol.* 185, 909–917.
- Velasquez, I., Nunn, B. L., Ibanmí, E., Goodlett, D. R., Hunter, K. A., and Sander, S. G. (2011). Detection of hydroxamate siderophores in coastal and Sub-Antarctic waters off the South Eastern Coast of New Zealand. *Mar. Chem.* 126, 97–107.
- Vichi, M., Masina, S., and Navarra, A. (2007a). A generalized model of pelagic biogeochemistry for the global ocean ecosystem. Part II: numerical simulations. *J. Mar. Syst.* 64, 110–134.
- Vichi, M., Pinardi, N., and Masina, S. (2007b). A generalized model of pelagic biogeochemistry for the global ocean ecosystem. Part I: theory. *J. Mar. Syst.* 64, 89–109.
- Waterbury, J. B., Watson, S. W., Guillard, R. R. L., and Brand, L. E. (1979). Widespread occurrence of a unicellular, marine, planktonic cyanobacterium. *Nature* 277, 293–294.
- Webb, E. A., Moffett, J. W., and Waterbury, J. B. (2001). Iron stress in open-ocean cyanobacteria (*Synechococcus*, *Trichodesmium*, and *Crocosphaera* spp.): identification of the IdiA protein. *Appl. Environ. Microbiol.* 67, 5444–5452.
- Wexler, M., Todd, J. D., Kolade, O., Bellini, D., Hemmings, A. M., Sawers, G., et al. (2003). Fur is not the global regulator of iron uptake genes in *Rhizobium leguminosarum*. *Microbiology* 149, 1357–1365.
- Wilhelm, S. W., and Trick, C. G. (1994). Iron-limited growth of cyanobacteria: multiple siderophore production is a common response. *Limnol. Oceanogr.* 39, 1979–1984.
- Worsham, P. L., and Konisky, J. (1985). Locus affecting regulation of the colicin I receptor by iron. *J. Bacteriol.* 161, 428–431.
- Yang, Z. (2007). PAML 4: phylogenetic analysis by maximum likelihood. *Mol. Biol. Evol.* 24, 1586–1591.
- conducted in the absence of any commercial or financial relationships that could be construed as a potential conflict of interest.

Received: 16 January 2012; accepted: 24 September 2012; published online: 18 October 2012.

Citation: Desai DK, Desai FD and LaRoche J (2012) Factors influencing the diversity of iron uptake systems in aquatic microorganisms. *Front. Microbio.* 3:362. doi: 10.3389/fmicb.2012.00362

This article was submitted to *Frontiers in Microbiological Chemistry*, a specialty of *Frontiers in Microbiology*.

Copyright © 2012 Desai, Desai and LaRoche. This is an open-access article distributed under the terms of the Creative Commons Attribution License, which permits use, distribution and reproduction in other forums, provided the original authors and source are credited and subject to any copyright notices concerning any third-party graphics etc.

Conflict of Interest Statement: The authors declare that the research was



Mining genomes of marine cyanobacteria for elements of zinc homeostasis

James P. Barnett¹, Andrew Millard², Amira Z. Ksibe¹, David J. Scanlan², Ralf Schmid³ and Claudia Andrea Blindauer^{1*}

¹ Department of Chemistry, University of Warwick, Coventry, UK

² School of Life Sciences, University of Warwick, Coventry, UK

³ Department of Biochemistry, Henry Wellcome Building, Leicester, UK

Edited by:

Martha Gledhill, University of Southampton, UK

Reviewed by:

Mak Saito, Woods Hole Oceanographic Institution, USA
Nigel John Robinson, Durham University, UK
Jennifer Cavet, University of Manchester, UK

*Correspondence:

Claudia Andrea Blindauer,
Department of Chemistry, University of Warwick, Coventry CV4 7AL, UK.
e-mail: c.blindauer@warwick.ac.uk

Zinc is a recognized essential element for the majority of organisms, and is indispensable for the correct function of hundreds of enzymes and thousands of regulatory proteins. In aquatic photoautotrophs including cyanobacteria, zinc is thought to be required for carbonic anhydrase and alkaline phosphatase, although there is evidence that at least some carbonic anhydrases can be cambialistic, i.e., are able to acquire *in vivo* and function with different metal cofactors such as Co^{2+} and Cd^{2+} . Given the global importance of marine phytoplankton, zinc availability in the oceans is likely to have an impact on both carbon and phosphorus cycles. Zinc concentrations in seawater vary over several orders of magnitude, and in the open oceans adopt a nutrient-like profile. Most studies on zinc handling by cyanobacteria have focused on freshwater strains and zinc toxicity; much less information is available on marine strains and zinc limitation. Several systems for zinc homeostasis have been characterized in the freshwater species *Synechococcus* sp. PCC 7942 and *Synechocystis* sp. PCC 6803, but little is known about zinc requirements or zinc handling by marine species. Comparative metallo-genomics has begun to explore not only the putative zinc proteome, but also specific protein families predicted to have an involvement in zinc homeostasis, including sensors for excess and limitation (SmtB and its homologs as well as Zur), uptake systems (ZnuABC), putative intracellular zinc chaperones (COG0523) and metallothioneins (BmtA), and efflux pumps (ZiaA and its homologs).

Keywords: zinc limitation, Zur, COG0523, SmtA, BmtA

INTRODUCTION

Zinc might be considered as one of the most inconspicuous trace elements. To some extent, this is due to its “boring” (Levi, 1984) chemistry – in its only biologically relevant oxidation state, Zn(II) , it is colorless and does not display any redox chemistry of its own. Because Zn^{2+} is not redox-active, many authors tend to consider it as less important than iron or copper in terms of both essentiality and toxicity, even though between 5 and 9% of the predicted proteomes of most organisms correspond to zinc-requiring proteins – in most cases more than either the predicted iron or copper sub-proteomes (Andreini et al., 2009).

This is even true for prokaryotes which once were thought to “avoid the hidden cost of zinc homeostasis” (Luisi, 1992). Several recent bioinformatic approaches aimed at predicting metalloproteomes (Andreini et al., 2006, 2008; Dupont et al., 2010) found that although overall zinc utilization in bacteria is undoubtedly lower than in eukaryotes, Zn-binding domains are yet highly abundant in predicted bacterial proteomes. For the case of currently existing prokaryotes, there is clear evidence for widespread zinc utilization, in particular in hydrolytic enzymes (Decaria et al., 2010). A major reason for lower zinc utilization by bacteria is likely the much lower abundance of zinc finger domains in their proteomes. Furthermore, at least in heterotrophs, the cellular quotas for zinc and iron tend to be similar (Outten and O’Halloran, 2001), although

it should be emphasized that metal quotas do not necessarily bear a direct relationship to metal requirements.

Virtually all organisms have elaborate mechanisms to control zinc levels and distribution (Hantke, 2005; Eide, 2006; Fukada and Kambe, 2011). Total cellular concentrations typically are in the high micromolar range; however, various lines of evidence have indicated that “free” cytosolic zinc concentrations are extremely low. Values given in the literature vary between nanomolar and femtomolar – with the true regulated value probably somewhere in the picomolar range (Krezel and Maret, 2006). The apparent need for the narrow range of tolerable zinc concentrations had initially puzzled some researchers, as there seems to be a widespread belief that zinc is not particularly toxic to cells. It could be argued that this is only true for cells that have efficient mechanisms to deal with zinc; otherwise free zinc concentrations as low as nanomolar can be toxic (Bozym et al., 2010). Deleterious effects of Zn^{2+} may, at least to some extent, be due to its high position in the Irving–Williams series (Irving and Williams, 1953), meaning that it outcompetes less competitive metal ions such as Fe^{2+} and Mn^{2+} for their protein binding sites, as demonstrated recently for the Mn-binding protein MncA (Tottey et al., 2008). This latter study illustrated why it is important to limit the amount of exchangeable zinc in the cytosol of cells, by the demonstration that the major periplasmic Mn-binding protein MncA

of *Synechocystis* sp. PCC 6803 (a freshwater cyanobacterium) can only incorporate the essential cofactor Mn^{2+} to a significant extent if this is present in 100000-fold molar excess over Zn^{2+} . Since MncA folds and is loaded with Mn^{2+} in the cytosol, this finding implies the need for a very low free cytosolic zinc concentration in *Synechocystis* sp. PCC 6803. Little information is available on zinc toxicity to marine cyanobacteria. A study on *Synechococcus* strains in the strait of Gibraltar noted that even micromolar concentrations of zinc had only a moderate effect on growth (Debelius et al., 2011), but zinc sensitivity may differ considerably depending on the natural habitat of a given cyanobacterium.

There are indications for an impact of zinc on major global biogeochemical cycles. A “zinc hypothesis” was put forward in 1994 in a study that demonstrated zinc and carbon co-limitation in marine phytoplankton (Morel et al., 1994). A link between zinc and carbon fixation is also reflected in the arctic ice-core record (Hong et al., 1996): during periods of glaciation, zinc levels were at least 10 times higher, whilst CO_2 levels were significantly lower than in the intervening periods. Changes in zinc levels due to increased deposition of dust into the oceans are thought to have had an effect on marine microbial community structure, and the decrease in CO_2 levels could be attributed to increased $CaCO_3$ production by coccolithophores and a resulting decrease in atmospheric CO_2 (Schulz et al., 2004). The amount of data on geochemical zinc fluxes is limited, and it is not clear whether dust deposition today does (Thurocz et al., 2010) or does not (Bruland et al., 1994) significantly contribute. In terms of a direct biochemical link between zinc and organic CO_2 fixation, there are of course the carbonic anhydrases, which operate in all marine phytoplankton, including cyanobacteria (Cannon et al., 2010), although substitution with either Co or Cd has been demonstrated for eukaryotic phytoplankton (Xu et al., 2008). There are also strong indications for links between Zn and phosphorus cycles (Jakuba et al., 2008), thought to be due to the requirement of Zn for alkaline phosphatase.

An absolute requirement for zinc has been clearly demonstrated for marine eukaryotic phytoplankton (Sunda and Huntsman, 1995, 2005), but the situation is less clear for marine cyanobacteria, as discussed below. With this review, we aim to make a case for intensifying studies into the relevance of zinc for marine cyanobacteria.

MARINE CYANOBACTERIA

Cyanobacteria are a group of phototrophic prokaryotes that all have the ability to perform oxygenic photosynthesis. In the marine environment a large diversity of both unicellular (e.g., *Synechococcus*, *Prochlorococcus*, *Cyanobium*, *Acaryochloris*, and *Crocospaera*) and filamentous (e.g., *Trichodesmium*, *Lyngbya*, *Oscillatoria*, *Nodularia*, and *Microcoleus*) genera exist, occupying habitats ranging from intertidal microbial mats through to oligotrophic open-ocean waters (see Whitton and Potts, 2000).

The numerically dominant cyanobacteria in open-ocean waters are the unicellular genera *Synechococcus* and *Prochlorococcus* which contribute significantly to marine CO_2 fixation (Li, 1994; Jardillier et al., 2010). *Synechococcus* are the more widely distributed, being found in waters covering a broad temperature range, from ca. 2–3°C to >30°C (Shapiro and Haugen, 1988; Waterbury et al., 1996; Fuller et al., 2006; Zwirgmaier et al., 2008), and including

open-ocean, coastal and estuarine environments (Partensky et al., 1999; Scanlan, 2003). *Prochlorococcus* appears to be more constrained in its distribution occupying waters roughly between 45°N and 40°S but within these latitudes it is extremely abundant, routinely reaching concentrations of 10^5 cells per ml or higher (Partensky et al., 1999; Partensky and Garczarek, 2010). *Prochlorococcus* can be distinguished from *Synechococcus* by its lack of a phycobilisome light-harvesting antenna complex. Instead, it possesses thylakoid membrane proteins binding unique divinyl derivatives of chlorophyll *a* and *b* (Goerick and Repeta, 1992; Partensky and Garczarek, 2003). In stratified tropical and subtropical waters *Prochlorococcus* cells undergo vertical partitioning between distinct high light- and low light-adapted ecotypes (Moore et al., 1998; West and Scanlan, 1999). Both *Synechococcus* and *Prochlorococcus* have relatively small genomes ranging in size between 1.64 and 2.7 Mb in *Prochlorococcus* and from 2.2 to 2.86 Mb in *Synechococcus* (Kettler et al., 2007; Dufresne et al., 2008; Scanlan et al., 2009). In the case of *Prochlorococcus*, significant genome reduction has occurred during evolution of the genus, likely an adaptation to the oligotrophic gyre systems they inhabit, providing significant economies in energy and nutrients (Dufresne et al., 2005).

As well as contributing to marine carbon cycling, some cyanobacteria are also capable of nitrogen fixation (Zehr, 2011). *Trichodesmium*, a filamentous non-heterocystous genus, is ubiquitous in tropical and subtropical environments (Capone et al., 1997) and until recently was thought to be the dominant marine nitrogen-fixer. However, it is now clear that the unicellular UCYN-A and UCYN-B lineages, the latter encompassing the genera *Crocospaera* and *Cyanothece*, also contribute significantly to this process (Zehr, 2011). Surprisingly, despite its global distribution in the Atlantic and Pacific Oceans *Crocospaera* appears to have limited genetic diversity with high identity and synteny of the cultured genome sequence to environmental metagenomic datasets for this genus (Zehr et al., 2007). Interestingly, metabolic insights from the genome of the UCYN-A lineage reveals a cyanobacterium lacking photosystem II, RuBisCO, and a tricarboxylic acid cycle (Tripp et al., 2010) suggesting it requires a symbiotic partner.

The high diversity of marine cyanobacteria is epitomized by *Acaryochloris marina*, a cyanobacterium that uniquely utilizes chlorophyll *d* as its main photosynthetic pigment (Kuhl et al., 2005) trapping the far-red light that penetrates beneath the didemnid ascidians (sea squirts) upon which these organisms are found (Ohkubo et al., 2006). Curiously, the *A. marina* genome is considerably larger than other sequenced unicellular strains (Swingley et al., 2008) comprising a circular chromosome of 6.5 Mb and nine distinct plasmids giving a total DNA content of 8.3 Mb. Over 10% of the protein families contain duplicated copies in *A. marina* and this information, together with its utilization of far-red light that is not absorbed by other aerobic photoautotrophs, suggests that *Acaryochloris* species fill a non-competitive niche where they are apparently free to specialize their metabolic library, and potentially explains their expansive genome size (Swingley et al., 2008).

BIOLOGICAL AND CHEMICAL CO-EVOLUTION, AND CYANOBACTERIAL METAL REQUIREMENTS

It has been hypothesized that metal ion bioavailability presented an evolutionary selection pressure on the “choice” of metals

within metalloenzymes (Williams and Da Silva, 2003). Conversely, biological evolution and the emergence of life has changed the chemical composition, or more precisely, the speciation of the atmosphere, the lithosphere, and of course the hydrosphere. Arguably, cyanobacteria might be deemed responsible for the greatest change of all by inventing oxygenic photosynthesis (Raymond and Blankenship, 2004). Consequently, they were amongst the first organisms that encountered, and had to cope with, the changes in the chemical composition of their environment that oxygenation brought about (Cavet et al., 2003; Saito et al., 2003). For metal ion speciation, both fundamental considerations (Williams and Da Silva, 2001) as well as detailed studies (Saito et al., 2003) agree that the presence of oxygen meant a drastic reduction in iron, cobalt, nickel, and manganese availability, and a significant increase in the concentrations of zinc, copper, and cadmium (Williams and Da Silva, 2001; Williams, 2011). It is reasonable to accept that these changes in chemistry and bioavailability directed biological evolution, including that of metal-binding biomolecules (Williams and Da Silva, 2000). Indeed, even though it has been suggested that microbial metalloproteomes are still largely uncharacterized (Cvetkovic et al., 2010), bioinformatic genome analyses of known metal-binding protein domains (Dupont et al., 2010) as well as elemental analysis experiments on marine phytoplankton (Bertilsson et al., 2003; Heldal et al., 2003; Ho et al., 2003; Quigg et al., 2003, 2011; Morel, 2008) give a picture that is consistent with this idea. Thus, the “co-evolution of biology and chemistry” is imprinted on both the metallome and the metalloproteome. The interested reader is directed to a recent debate regarding the evolution of zinc-binding domains (Mulkidjanian and Galperin, 2009; Dupont and Caetano-Anolles, 2010).

In the case of cyanobacteria, metal ion requirements and sensitivities, as far as they have been experimentally determined, agree with the notion that they evolved in an environment with metal ion concentrations typical of a sulfidic or a ferrous ocean (Saito et al., 2003): both marine *Synechococcus* (Sunda and Huntsman, 1995) and *Prochlorococcus* (Saito et al., 2002) strains have been shown to be cobalt-limited, whereas the requirements for zinc are so low (Saito et al., 2003) that only mild reductions in growth rates were observed at the lowest possible free zinc concentrations (Saito et al., 2002).

Our previous genome-mining approaches have identified strong candidate genes for potentially zinc-requiring carboxysomal carbonic anhydrases, ABC-type zinc uptake systems, as well as for proteins involved in the intracellular handling of zinc (Blindauer, 2008b). Several other enzymes in cyanobacteria are also predicted to require zinc for function, including for example DNA ligase and alkaline phosphatase (Palenik et al., 2003), the latter leading to the suggestion that cyanobacteria may be Zn–P co-limited. Indeed, in certain cyanobacterial strains, alkaline phosphatase activity is elicited by phosphorus limitation (Moore et al., 2005), and direct crosstalk between P and Zn, mediated by the regulatory protein PtrA, has been found in *Synechococcus* sp. WH8102 (Ostrowski et al., 2010). PtrA responds to phosphorus depletion and its expression up-regulates not only the expression of phosphatases, but also that of proteins predicted to be involved in zinc acquisition and distribution – including ZnuABC and a member of the COG0523 family (see below). However, it has to

be noted that the true metal requirements of each of these proteins has yet to be experimentally verified, and there is reason to be cautious, with some evidence for the *in vivo* replacement of zinc with cobalt (Sunda and Huntsman, 1995) and cadmium (Lee and Morel, 1995) in marine phytoplankton. Very recently though, utilization of an alternative calcium-requiring phosphatase (PhoX) has been shown for uncultured *Prochlorococcus* (Kathuria and Martiny, 2011), suggesting a further mechanism for reducing zinc requirements.

In conclusion, although cyanobacteria are at the root of what life and marine trace metal chemistry are like today, their metal requirements require further study; none of the predicted major destinations for zinc are experimentally confirmed, and information about if, and how, zinc requirements can be alleviated by either Co or Cd substitution, is limited.

ZINC SPECIATION IN SEA WATER

In order to understand how cyanobacteria might acquire zinc from the marine environment, we must first understand its chemical nature in seawater. The concentration of zinc in oceanic waters follows typical nutrient-like depth profiles (Bruland, 1980; Butler, 1998), with the lowest concentrations found in the euphotic zone with dissolved zinc rapidly removed to lower depths as a constituent of colloidal particles (Bruland, 1989; Wells et al., 1998). Total dissolved zinc concentrations in surface waters of the North Atlantic Ocean range from just 0.1 to 0.3 nM (Ellwood and van den Berg, 2000), similar to values obtained from measurements taken in the North Pacific Ocean (Bruland, 1980). The vast majority of this zinc (~98%) is found complexed to uncharacterized organic ligands (Bruland, 1989; Donat and Bruland, 1990; Ellwood and van den Berg, 2000) with conditional stability constants, $\log K'_{ZnL}$, of between 10.0 and 10.5 (Wells et al., 1998; Ellwood and van den Berg, 2000). This results in a concentration of free Zn^{2+} of 1–20 pM. The distribution of these metal complexing ligands suggests a surface source (Bruland, 1980) that may include phytoplankton including cyanobacteria. This contribution could be through the direct secretion of zinc-binding ligands into the ocean. There is already some evidence that cyanobacteria actively secrete ligands that complex other biologically important trace metals including copper, iron, and cobalt. The marine *Synechococcus* sp. strains WH8101 and WH7805 have both been found to produce siderophores (Wilhelm and Trick, 1994) for scavenging iron from nutrient-depleted environments, whilst Cu-complexing ligands are produced to mitigate the toxic effects of copper (Wiramanaden et al., 2008), with cyanobacteria particularly sensitive to this metal (Mann et al., 2002). Significant quantities of strong cobalt-binding ligands were produced by a *Synechococcus*-dominated microbial community in the Costa Rica upwelling dome (Saito et al., 2005).

Alternatively the Zn complexing ligands could be released from cyanobacterial cells indirectly, perhaps as a consequence of cell lysis by marine phages (Wells et al., 1998). Despite the fact that the vast majority of zinc in ocean waters is present in the form of organic metal complexes, there is evidence that free Zn^{2+} is the major form of this nutrient taken up by phytoplankton (Anderson et al., 1978; Sunda and Huntsman, 1992; Sunda et al., 2005). In the Pacific Ocean the concentration of free Zn^{2+} in surface waters

ranges from only 1 to 14 pM (Bruland, 1980; Donat and Bruland, 1990), and in the Atlantic Ocean ranges from 6.8 to 20 pM (Brand et al., 1983). The concentration of free Zn^{2+} in surface waters is thought to be sufficiently low to limit the growth of some marine phytoplankton (Brand et al., 1983; Sunda and Huntsman, 1992) although one study found that phytoplankton growth was not limited by low Zn^{2+} concentrations even after iron limitation was alleviated (Coale et al., 1996). Conversely, productivity in the subtropical Atlantic was further boosted by addition of Zn or Co to water that had also been enriched with Fe and P (Dixon, 2008), providing evidence for Zn/Fe/P co-limitation. Similarly, the iron-depleted waters of the Southern Ocean and the sub-arctic Pacific are also extremely zinc-depleted (Sunda and Huntsman, 2000) which appears to induce high levels of Cd uptake and high Cd:P ratios in phytoplankton. It is thus clear that interactions between the cycles of different metal ions exist, and that co-limitation needs to be studied (Saito et al., 2008). How important such crosstalk is in cyanobacteria is not yet well understood, and further work is required to determine if mechanisms exist for the active uptake of zinc, and if so, in what form zinc is acquired by cyanobacteria, and to determine the impact that cyanobacteria have on trace metal speciation in ocean waters (Leao et al., 2007).

SYSTEMS FOR ZINC HOMEOSTASIS

Zinc homeostasis in bacteria is largely achieved through a balance of active uptake and efflux by specific membrane transporters (Hantke, 2005), plus proteins mediating intracellular zinc handling (Figure 1). In the freshwater cyanobacterium *Synechocystis* sp. PCC 6803, a zinc-specific high affinity ABC transporter termed ZnuABC has been identified for the active uptake of zinc from the periplasm (Cavet et al., 2003). Putative ZnuABC systems have also been identified in most strains of marine cyanobacteria (Blindauer, 2008b; Scanlan et al., 2009). The putative *znuABC* gene cluster of many of the marine strains also contains a putative *zur* gene (Blindauer, 2008b). Zur proteins (for zinc uptake regulator) are low-zinc sensors; their zinc-loaded forms repress the expression of *znuABC* under zinc-replete conditions (Patzer and Hantke, 2000).

To date no specific mechanisms for the active uptake of zinc across the outer cell membrane of cyanobacteria has been identified. It is generally considered that metal ions are small enough to diffuse freely through porins in the outer-membrane of Gram-negative bacteria; however, as described above, the concentration of free Zn^{2+} in surface layers of the world's oceans is extremely low, with the vast majority of zinc complexed to as yet uncharacterized ligands of unknown structure and origin (Bruland, 1989). Whether at least some of these ligands are actively secreted to aid in zinc acquisition remains an open question; there is also the possibility that at least in coastal environments, ligands are synthesized in response to zinc excess and hence to avoid toxicity (Lohan et al., 2005; Leao et al., 2007).

In order to deal with excess zinc, *Synechocystis* sp. PCC 6803 has a zinc-specific efflux pump, ZiaA (Thelwell et al., 1998), similar to other P1-type ATPase metal ion transporters, that transports Zn^{2+} from the cytoplasm to the periplasmic space (Figure 1). Expression of this efflux system is induced by zinc and is regulated by ZiaR (Thelwell et al., 1998), a zinc-specific repressor protein.

With the exception of *Lyngbya* sp. and *Nodularia* sp., most marine strains of cyanobacteria appear to lack zinc-specific efflux pumps (Blindauer, 2008b; Scanlan et al., 2009) reflecting the nutrient poor environments they occupy, with free Zn^{2+} concentrations being in the picomolar range in ocean waters (Hunter and Boyd, 1999). Instead, at least some marine cyanobacteria seem to rely on a mechanism of zinc sequestration by bacterial metallothioneins (BmtAs; Blindauer, 2008b) to deal with any eventual excess. Metallothioneins are small cytosolic proteins rich in cysteine residues that bind and sequester metal ions and thereby prevent any deleterious interactions (Blindauer and Leszczyszyn, 2010). The metallothionein SmtA of the freshwater cyanobacterium *Synechococcus* sp. PCC 7942 is induced by several metal ions but most prominently by zinc (Huckle et al., 1993) and its expression is controlled by the zinc sensor SmtB (Osman and Cavet, 2010) that is highly similar to ZiaR. Several marine strains of cyanobacteria appear to lack an SmtB/ZiaR type regulator (Blindauer, 2008b) despite the presence of one or more genes for a BmtA (Table 1). Furthermore, many also appear to lack any established mechanism for dealing with zinc excess, with all *Prochlorococcus* and some *Synechococcus* strains apparently lacking both a ZiaA efflux pump and a metallothionein encoding gene (Blindauer, 2008b). Presumably these bacteria never encounter toxic levels of zinc in

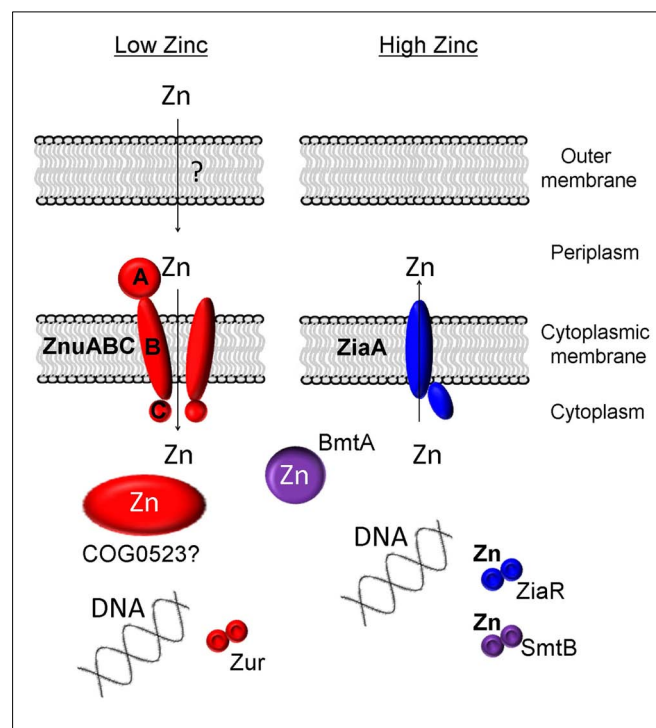


FIGURE 1 | Known and proposed elements of zinc homeostasis in cyanobacteria. A requirement for zinc is sensed by the transcriptional regulator Zur, leading to the upregulation of the components of the ZnuABC uptake system. Some members of the putative metallochaperone family COG0523 are also regulated by Zur, and have, in other bacteria, been shown to be expressed in response to zinc deficiency. In most freshwater cyanobacteria, excessive levels of zinc are sensed by SmtB and its homologs (ZiaR, AztR, BxmR), and these sensors regulate either the expression of efflux pumps (ZiaA) or metallothioneins (SmtA and homologs).

Table 1 | Presence of selected genes predicted to be involved in zinc homeostasis in marine cyanobacterial genomes.

Species/strain	Zur	Zinc-related COG0523? ^a	BmtA	SmtB	In gene cluster?
<i>Acaryochloris marina</i> MBIC11017	✓	✓✓	✓	✓	yes
<i>Crocospaera watsonii</i> WH 8501	✓	?	✓	?	
<i>Cyanobium</i> sp. PCC 7001 [D] ^b	✓	✓	✓	?	
<i>Lyngbya</i> sp. PCC 8106	✓	✓✓	✓	?	
<i>Microcoleus chthonoplastes</i> sp. PCC 7420 [D]	✓	✓	✓	✓	
<i>Nodularia spumigena</i> sp. CCY9414	✓	✓	✓	✓	
<i>Oscillatoria</i> sp. PCC 6506	✓	?	✓	✓	yes
<i>Synechococcus</i> sp. CC9311	✓	?	✓		
<i>Synechococcus</i> sp. CC9605	✓	?	✓		
<i>Synechococcus</i> sp. WH 7803	✓	?	✓		
<i>Synechococcus</i> sp. WH8102	✓	✓	✓		
<i>Synechococcus</i> sp. PCC 7002	✓	✓	✓	✓	yes
<i>Synechococcus</i> sp. WH 8109 [D]	✓	?	✓		
<i>Synechococcus</i> sp. WH5701	✓	?	✓		
<i>Synechococcus</i> sp. CC9902	✓	?			
<i>Synechococcus</i> sp. BL107 [D]	✓	?			
<i>Synechococcus</i> sp. PCC 7335 [D]	✓	?		✓	
<i>Synechococcus</i> sp. RCC307 [D]	✓	?			
<i>Synechococcus</i> sp. RS9916 [D]	✓	?			
<i>Synechococcus</i> sp. RS9917 [D]	✓	?			
<i>Synechococcus</i> sp. WH7805 [D]	✓	?			
<i>Trichodesmium erythraeum</i> IMS101	✓	✓			
<i>Prochlorococcus marinus</i> sp. AS9601	✓	✓			
<i>P. marinus</i> sp. MIT 9211	✓	✓			
<i>P. marinus</i> sp. MIT 9215	✓	✓			
<i>P. marinus</i> sp. MIT 9301	✓	✓			
<i>P. marinus</i> sp. MIT 9303	✓	✓			
<i>P. marinus</i> sp. MIT 9312	✓	✓			
<i>P. marinus</i> sp. MIT 9313	✓	?			
<i>P. marinus</i> sp. MIT 9515	✓	✓			
<i>P. marinus</i> sp. MIT9202 [D]	✓	✓			
<i>P. marinus</i> NATL1A	✓	✓			
<i>P. marinus</i> NATL2A	✓	✓			
<i>P. marinus marinus</i> CCMP1375 ^c	✓	✓			
<i>P. marinus pastoris</i> CCMP1986 ^c	✓	✓			

Empty cells indicate absence of a recognizable zinc-related homolog; “?” indicate presence of homologs with unclear metal specificity.

^aAccording to analysis of syntenic genome regions or presence of upstream Zur box.

^b[D] Draft genome.

^cCCMP1375 also known as SS120; CCMP1986 also known as MED4.

the environment, although it also remains possible that they may employ novel mechanisms for zinc homeostasis that have yet to be discovered.

SENSING A REQUIREMENT FOR ZINC: Zur TRANSCRIPTION FACTORS

In bacteria, the expression of proteins that deal with metal ion homeostasis is predominantly regulated at the transcriptional level (Finney and O’Halloran, 2003; Giedroc and Arunkumar, 2007; Waldron et al., 2009), and is mediated by sensor proteins for zinc excess (e.g., SmtB and its relatives; Giedroc and Arunkumar, 2007; Osman and Cavet, 2010) and zinc depletion (Zur and others). Seven major groups of bacterial metalloregulatory proteins have so far been defined: the Fur-family (for “ferric uptake regulator”) is one of them (COG0735; Bagge and Neilands, 1987), and also comprises paralogous sensors for zinc (Zur), nickel (Nur), manganese (Mur; Lee and Helmann, 2007), and hydrogen peroxide (PerR; Jacquamet et al., 2009).

Metal sensing in bacteria occurs overwhelmingly in the cytosol (Waldron and Robinson, 2009). Ultimately, the sensor proteins are the proteins that need to be the “most specific” – they should ideally either not bind any other metal ion, or if that is not possible, they should not respond to other metal ions in the same way as to their cognate metal. The key concepts of access and allostery, as well as the importance of relative affinities of different metalloproteins for different metal ions, have been highlighted by Waldron et al., 2009.

The dissociation constants of Zn^{2+} -Zur complexes are in the femtomolar range; similar data are also available for zinc excess sensors (Outten and O'Halloran, 2001; Giedroc and Arunkumar, 2007) – these data also support the idea that the free Zn^{2+} concentration in the cytosol is extremely low. Several crystal structures of representatives of the COG0735 family have been determined (Pohl et al., 2003; Lucarelli et al., 2007; Jacquamet et al., 2009; Sheikh and Taylor, 2009; Shin et al., 2011). All members studied adopt a “winged-helix” fold (**Figures 2A,C**) and all assemblies are homo-dimeric, as are many other proteins that specifically recognize DNA sequences.

All “urs” are thought to bind their cognate DNA in the presence of the entity to be sensed. Although no structures in the presence of DNA are available, it is thought that DNA-binding is mediated by the first ca. 80 residues, whilst dimerization, also a prerequisite of DNA-binding, is mediated by the C-terminal half, in particular by the formation of a six-stranded β -sheet formed by both monomers. The overall shape of the dimeric assembly can be described as an “arch” (**Figure 2C**), and the two DNA-binding domains are thought to “grip” the DNA using their DNA-recognition helices. It is likely that the interaction between protein and DNA requires a particular conformation that is stabilized by the presence of the sensed metal. The sensing appears to be mediated by two inter-domain hinges that are likely to be stabilized by metal-binding. In contrast to metal sensors of the SmtB family in which complete metal sites form *between* monomers, each metal site in Fur-family proteins is formed from residues from one monomer only. If the respective metal is absent, a different conformation may become more favorable, and DNA-binding no longer occurs, leading to the de-repression of gene transcription. Despite this general mechanistic idea, there is considerable ambiguity about the molecular detail of metal-binding, and how the binding of the “correct” metal mediates DNA-recognition. Despite the availability of X-ray structure for no less than seven Fur-family proteins, the identity of the residues involved in binding the metal ion to be sensed is unclear, in particular in those “urs” that contain three metal sites per monomer.

A structural zinc site formed by four conserved Cys residues is present in the majority of Fur-family members, independent of the sensed metal. One or two further sites participate in sensing. An inspection of various X-ray structures of Fur-family proteins suggested that sample preparation for such studies seems to be quite challenging; in particular, appropriate population with the correct complement of metal ions appears to be less than straightforward, and in several cases, workers appear to have resorted to populating all sites with Zn^{2+} . Whilst this is certainly appropriate for Zurs, in other cases this may lead to ambiguous conclusions, as the coordination preferences of Zn^{2+} are rather different to those of Fe^{2+} or Ni^{2+} . It has been demonstrated experimentally for SmtB/ArsR sensors that coordination geometry (Cavet et al., 2002) is an important discriminator in metal sensor proteins (via allostery). For *Pseudomonas aeruginosa* Fur, it has been shown *in vitro* that Zn^{2+} -loaded Fur interacted with a Fur-binding DNA sequence in a different manner to that observed with Fe^{2+} (Ochsner et al., 1995). It should also be noted that despite full conservation of the respective residues, the crystallographically observed metal-binding sites in the Fur proteins from *Pseudomonas aeruginosa*

on the one hand and *Vibrio cholerae* and *Helicobacter pylori* on the other (all structures contain only Zn^{2+} ions) are not identical (see **Figure 2B**), and that the domain orientations in the dimeric assemblies also differ significantly – likely as a consequence of the different coordination modes. It is conceivable that the binding mode for Fe^{2+} differs from both experimentally observed sites, with likely consequences for the structure that is competent to bind to Fur boxes.

Even in the case of the Zur sensors, metal population seems to be problematic, and as a consequence, there is some controversy over stoichiometry as well as the role of the various sites. For the Zurs from *Streptomyces coelicolor* (Shin et al., 2011) and *Bacillus subtilis* (Ma et al., 2011), there is agreement that site 2 (**Figure 2A**) is the major sensory site. Variations of site 2 are present in Fur, Nur, and PerR (**Figure 2B**), and in each case, this site has been identified as the sensory site. Site 3 was only partially occupied in the *M. tuberculosis* structure (Lucarelli et al., 2007), and the dimer displayed an open conformation, probably with reduced DNA-binding ability. In contrast, site 3 (site D) was fully occupied in the structure of *S. coelicolor* Zur, and the dimer showed a closed conformation, thought to be DNA-binding competent. This led to suggestions that site 3 fine-tunes the response to zinc (Shin et al., 2011). This assessment has been contested based on studies of mutants of *B. subtilis* Zur (Ma et al., 2011), which suggested that site 3 is not populated under physiological conditions at all, but that the two site 2s in the dimer have different affinities and show negative cooperativity. In either case, it was suggested that different metal affinities of the various sites allow the broadening of the operating range of the Zur proteins.

We believe that the preceding discussion demonstrates the challenges encountered in the study of metal-binding and -sensing proteins, but also highlights how important continued studies of metalloproteins are. Unfortunately, so far, no structure for any “ur” from a cyanobacterium has been elucidated, but in the following, we will explore what can be achieved using theoretical approaches.

BLAST searches in the genomes of marine cyanobacteria retrieved members of the COG0735 family as summarized in **Table 1**; **Figure 3** and **Figures S1** and **S2** in Supplementary Material. They cluster into four distinct groups. Although it should be recognized that sequence similarity and metal specificity of sensors (or indeed other metalloproteins) need not be congruent (Campbell et al., 2007), comparisons with other “urs” of known specificity, first and foremost *Synechocystis* Zur, suggest that the branch highlighted in light purple corresponds to Zurs. Furthermore, an analysis of the genome environments of the Zurs from the majority of *Prochlorococcus* strains supports this idea (**Figure 4**).

Intriguingly, sequence comparisons (**Figure 2B**) show that an equivalent of site 2 cannot be identified in the cyanobacterial Zur homologs, and neither are all residues of site 3 the same as in structurally characterized Zur proteins. We have constructed a homology model of the representative from *Prochlorococcus* sp. SS120 (CCMP1375) to test whether likely alternative binding sites might be predicted. The model obtained (**Figure 2C**) suggests that the cyanobacterial Zurs may contain a variation of site 3, comprising D80, H82, C98, and H118. Thus, the predicted zinc-sensing site is in a location corresponding to site 3, but has a ligand set that

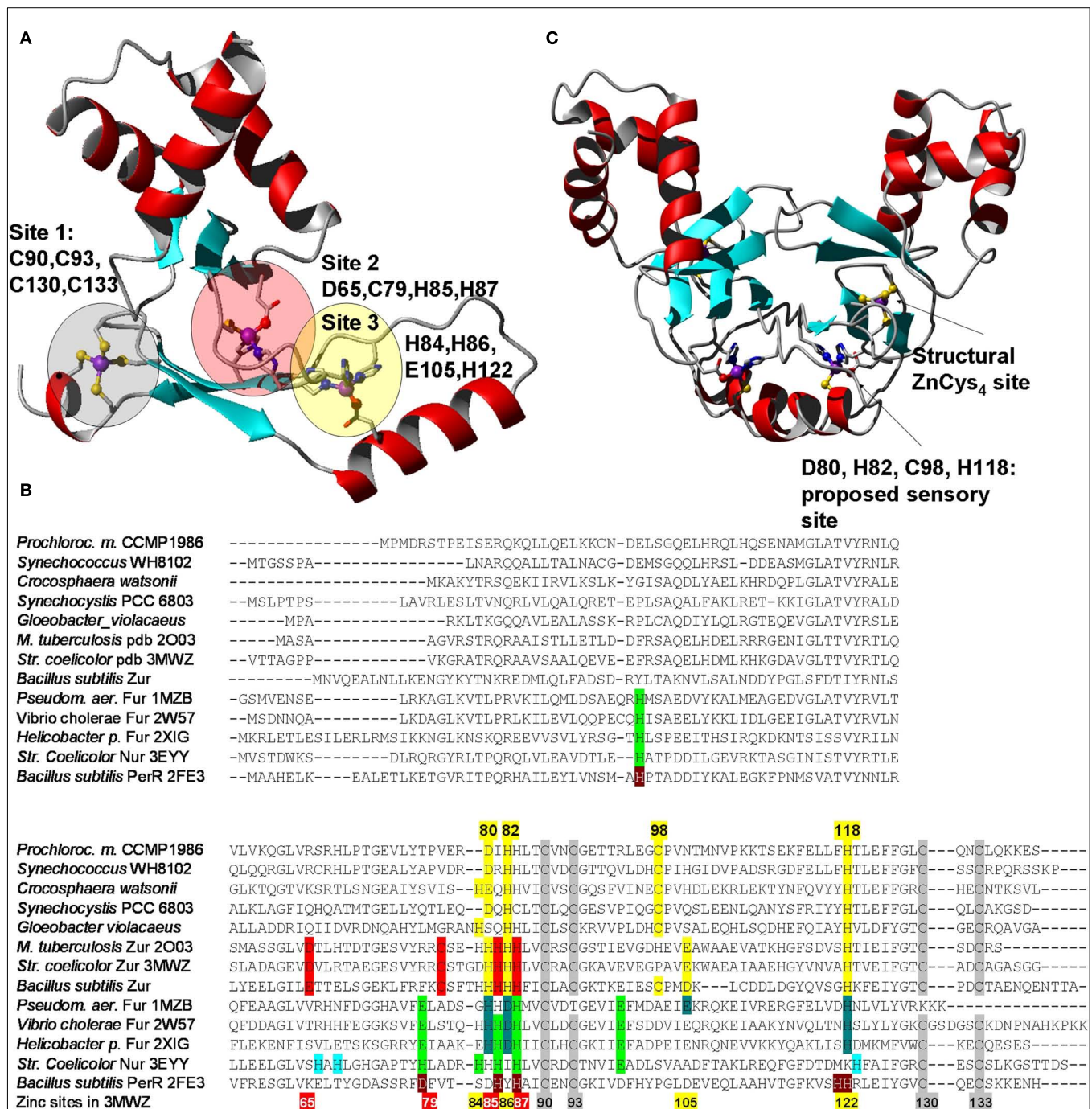


FIGURE 2 | Structural features of Zur proteins. (A) Crystal structure of Zur from *Streptomyces coelicolor* (Shin et al., 2011; pdb 3MWM). Only one monomer is shown. The three zinc-binding sites are highlighted in red (site 2 – major sensory site), yellow (site 3), and gray (site 1 – structural site). (B) Sequential alignment of structurally characterized Fur-family proteins from various bacteria together with selected sequences from cyanobacteria. The color-coding for the Zur proteins from *S. coelicolor* and *M. tuberculosis* corresponds to that shown in (A). The consensus sensory site 2 is clearly not present in cyanobacterial sequences, but a variation of site 3, highlighted in yellow, can be discerned. Corresponding sites in Fur/Nur/PerR proteins are highlighted in dark and light green, and gray for

the structural zinc site. (C) Homology model for Pro1502, a predicted Zur protein from *Prochlorococcus marinus* sp. CCPM1375. Inspection of initial metal-free models and conservation of potential ligands [see (B)] suggested that cyanobacterial Zurs contain only one sensory binding site that differs significantly from the sites in other Fur-family proteins including the two Zur proteins from *S. coelicolor* and *M. tuberculosis*, but the combination of donor atoms is the same as for site 2 (= N₂OS). Further variations within the cyanobacterial Zur proteins are possible, as indicated for the sequences from *Gloeobacter violaceus* (a genus forming the earliest branch of the cyanobacterial phylogenetic tree) and *Crocospheara watsonii*, which could form N₂S sites.

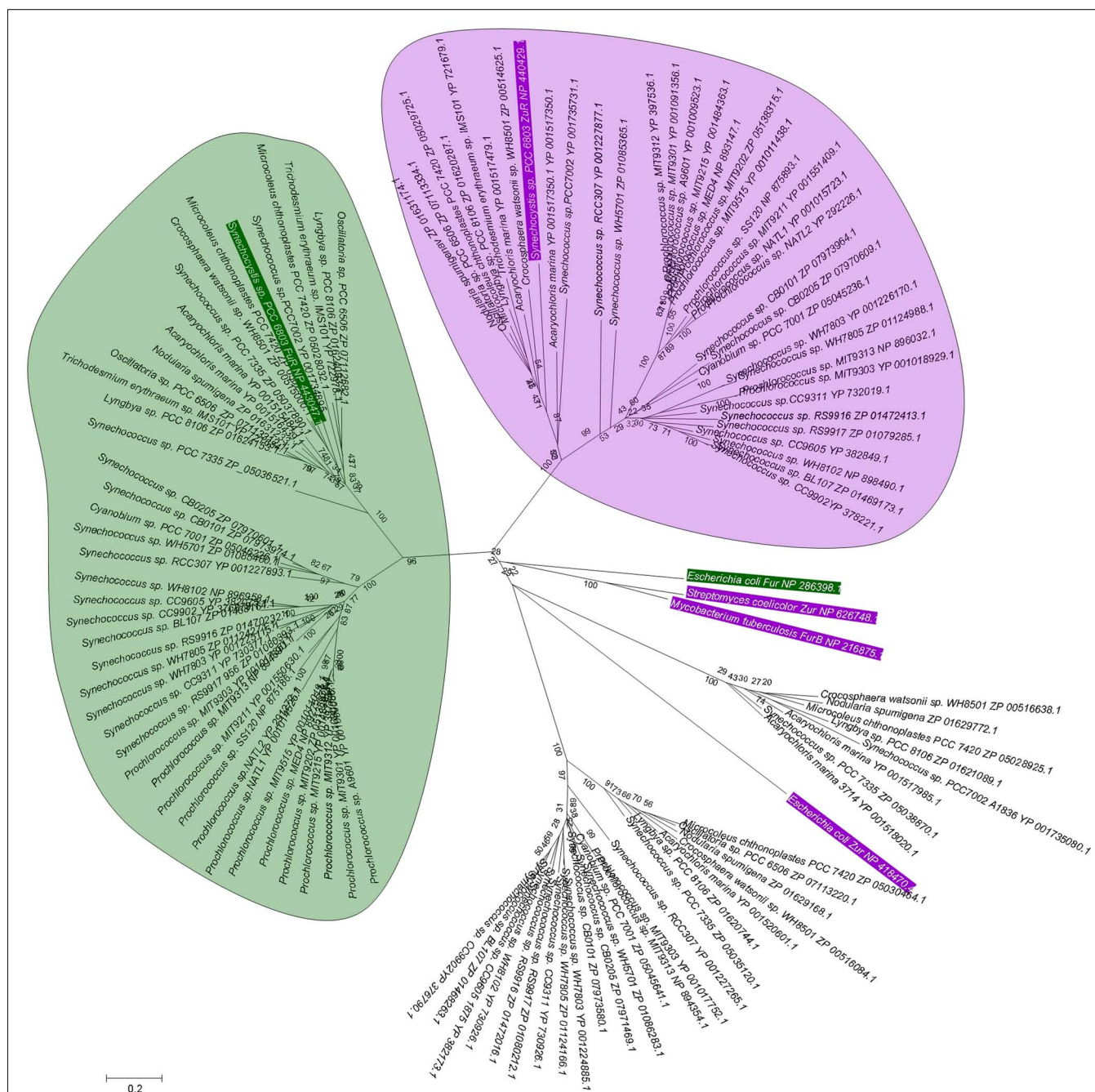


FIGURE 3 | Phylogenetic relationship among Fur-like proteins from marine cyanobacteria. Sequences are labeled with species and protein accession number; a rectangular tree including bootstrap statistics can be found in Figure S1 in Supplementary Material, and the actual sequences are documented in Figure S2 in Supplementary Material. Additional proteins for the experimentally verified Fur from *Escherichia coli* and *Synechocystis* sp. PCC 6803 are also included (green boxes), along with the Zur proteins from *Streptomyces coelicolor*, *Mycobacterium tuberculosis*, and *Synechocystis* sp. PCC 6803 (purple boxes). Amino acid sequences (see Figure S2 in Supplementary Material) were aligned using CLUSTALW (Larkin et al., 2007),

and manually edited prior to import into MEGA5 (Tamura et al., 2011). Phylogeny was inferred using the minimal evolution method. Bootstrap values are the result of 1000 replications. Evolutionary distance was estimated using the JTT model of substitution. There are four clear branches. Inclusion of *Synechocystis* Zur and Fur allows the suggestion that the branches containing these sequences correspond to zinc-responsive (light purple bubble) and iron-responsive (light green bubble) regulators. The Zur and Fur sequences from other bacteria do not cluster with any of the four branches, indicating that similarity between cyanobacterial sequences and those from other bacteria do not allow to infer metal specificity.

is similar to that of site 2, which may suggest that the zinc-binding affinity of this site is also closer to that of site 2. The four residues

identified are almost fully conserved in putative Zur proteins from all cyanobacteria (Figure S2 in Supplementary Material). A notable

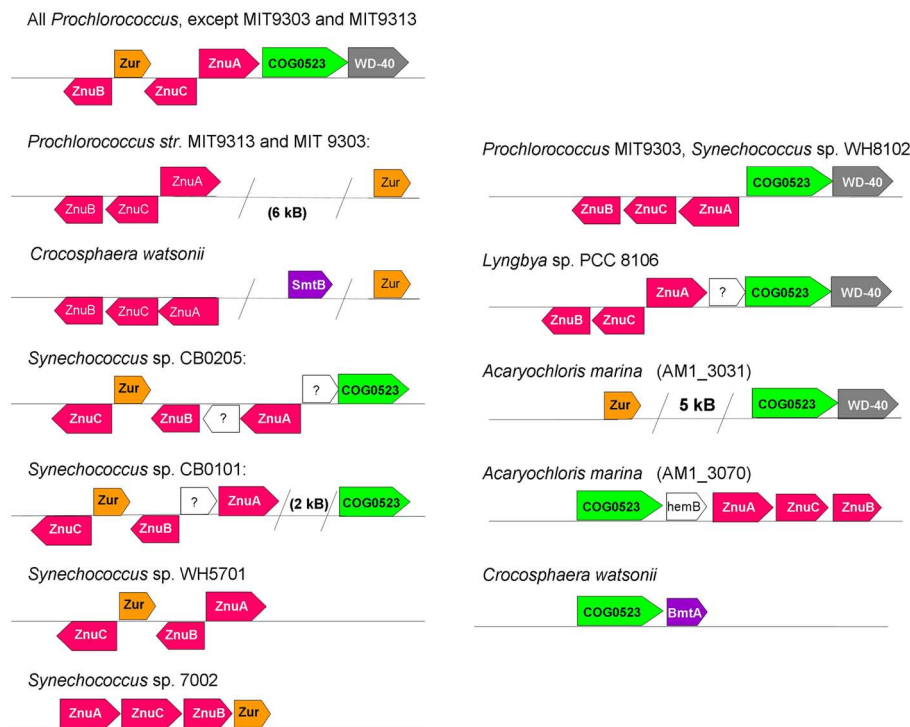


FIGURE 4 | Selected variations in genome neighborhoods of elements of zinc homeostasis in marine cyanobacteria, with a focus on putative Zur (left) and COG0523 (right) proteins. ZnuA is the periplasmic binding protein, ZnuB the permease, and ZnuC the ATPase component of the ZnuABC uptake transporter (also see **Figure 1**). In other strains and species (e.g., other *Synechococcus* strains, *Lyngbya* sp. PCC 8106, *Microcoleus chthonoplastes*), the gene for Zur is not co-localized with

recognizable elements of zinc homeostasis. Note that there appear to be two ZnuABC-type systems in *Prochlorococcus marinus* sp. MIT 9303. The *Acaryochloris marina* genome and plasmids harbor at least nine COG0523 family members; AM1_3070 (corresponding to UniProt entry B0CDJ7_ACAM1) and AM1_3031 (corresponding to UniProt entry B0CCJ8_ACAM1) are directly or indirectly associated with zinc homeostasis.

exception is the homolog from *Trichodesmium erythraeum*, in which H82 is replaced by a Tyr residue.

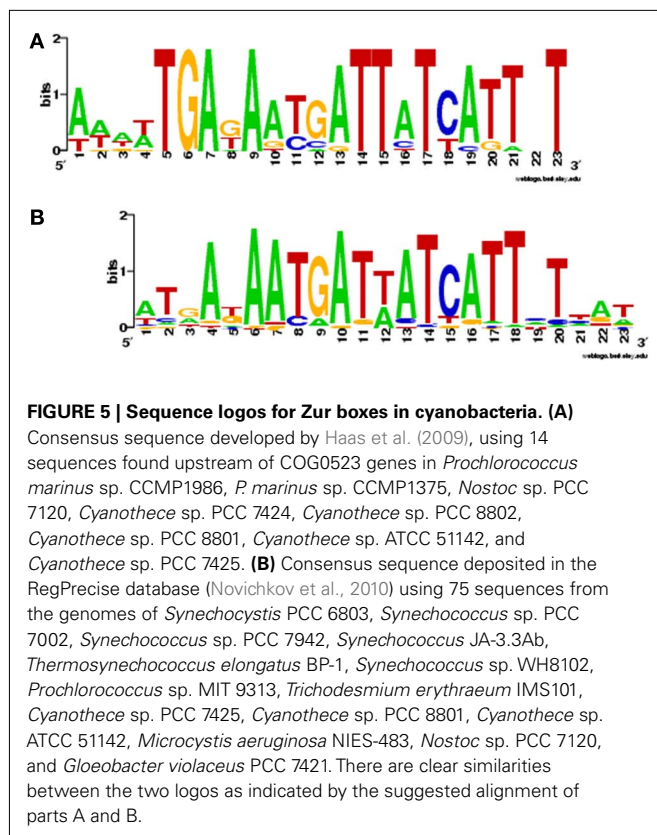
From this analysis, we would predict that the molecular mechanism for sensing in cyanobacterial Zurs differs to some extent from that of other bacterial Zurs with three metal sites, but the general idea of zinc stabilizing domain orientation still holds. Notably, the recognition motifs (Zur boxes) for cyanobacterial Zurs differ somewhat from those of other bacteria (Haas et al., 2009), which may require an adapted mode of operation of the protein.

Using the Zur box motif developed by Haas et al. (2009) we have interrogated the genomes of *Synechococcus* sp. CC9311, *Prochlorococcus* sp. CCMP1375, and *Prochlorococcus* sp. CCMP1986. We have also examined the entries for cyanobacterial Zur regulons in the RegPrecise database (Novichkov et al., 2010). The motifs developed by Haas and by RegPrecise differ (**Figure 5**), but common features can still be discerned, and it is likely that the consensus Zur box in cyanobacteria corresponds to an (imperfect) inverted repeat, analogous to Zur and Fur boxes from other bacteria (Gabriel et al., 2008).

In the *Prochlorococcus* strains examined, a putative Zur box was found in the intergenic region between a putative *znuA* and *znuC*. All three components of the ABC transporter are arranged into one gene cluster that also comprises the respective putative *zur* gene (**Figure 4**). All other strains inspected (*Trichodesmium*

erythraeum, *Synechococcus* sp. WH8102, *Synechococcus* sp. PCC 7002) also contain one or more Zur boxes in their *znuABC* gene cluster.

In the genome of *Prochlorococcus* sp. CCMP1986, Zur boxes were also identified upstream of several genes encoding ribosomal proteins (S7, S12, and S14p/S29e). This is of potential interest, because in other bacteria several ribosomal proteins, e.g., S14, L31, L33, and L36, occur in two versions, one requiring a zinc ion to stabilize a zinc-ribbon fold, and one version not requiring zinc (Makarova et al., 2001). The latter versions have been shown to be regulated by Zur in several bacterial species (Panina et al., 2003; Owen et al., 2007; Gabriel and Hermann, 2009). It has been suggested that the ribosome is, under zinc-replete conditions, a substantial store for cellular zinc, and that the “alternative” versions are expressed in response to zinc deprivation (Owen et al., 2007), operating as a backup for growth in Zn-poor environments, thus helping to reduce the overall requirement for zinc and the cellular zinc quota. The transcriptional response of *E. coli* to extreme zinc limitation (Graham et al., 2009) highlights that zinc limitation not only affects the transcription of genes encoding proteins involved in zinc homeostasis, and that are zinc-requiring, but also, importantly, zinc-independent proteins. Similarly, in other bacterial species it has been demonstrated that a variety of zinc-independent proteins including an alternative version of the global



transcription factor DksA in *Pseudomonas aeruginosa* (Blaby-Haas et al., 2011), are under the control of Zur, and genome analyses of Zur regulons suggest that this is a widespread phenomenon (Haas et al., 2009). However, neither of the two versions of S14 present in the genome of *Prochlorococcus* sp. MED4 displays any salient signatures for zinc-binding, and neither S7 nor S12 are known to bind zinc or occur in duplicate, so the significance of their vicinity to Zur boxes is in need of further investigation.

Another set of potential Zur boxes were found in a cluster that comprises FutC, ferritin, and a Rieske iron-sulfur protein. According to the manually curated database of bacterial regulons RegPrecise, the cognate sequences of Furs and Zurs differ significantly (Novichkov et al., 2010). Hence, the detection of potential Zur boxes within a cluster related to iron homeostasis suggests that there is some crosstalk between the homeostasis of these two metal ions; this has been observed in other bacteria, e.g., in *S. coelicolor*, where the gene cluster responsible for the production of the siderophore coelibactin is regulated by Zur (Kallifidas et al., 2010).

The only Zur box that we were able to identify in the genome of *Synechococcus* sp. CC9311 was upstream of a predicted ZIP transporter protein (Sync_2443). ZIP (for “zinc-iron permeases”) proteins are involved in zinc uptake in a variety of organisms including plants, animals, fungi, and bacteria. However, ZIP proteins have as yet not been reported for cyanobacteria, and no recognizable homologs of Sync_2443 were found in any other cyanobacterium; the closest match in a BLAST search was a zinc transporter from the γ -proteobacterium *Francisella novicida*. If Sync_2443 really is a zinc transporter, this coastal strain has an

even more remarkable repertoire for dealing with fluctuations in zinc concentrations than previously thought (Palenik et al., 2006). Two further notable RegPrecise entries were found for the genomes of *Trichodesmium erythraeum*, indicating Zur boxes upstream of a putative metallochaperone of the COG0523 family (Tery_4617), and *Synechococcus* sp. WH8102, which contains two Zur boxes upstream of a gene encoding a potential bacterial metallothionein (SYNW0359) – both groups of proteins are discussed below.

Very recently, Napolitano et al. (2012) studied the response of *Anabaena* sp. PCC7120 to zinc starvation. Aided by gel shift assays and a deletion mutant, the product of the *all2473* gene, previously designated FurB and thought to be involved in the response to oxidative stress (López-Gomollón et al., 2009), was identified as a true Zur. Several gene clusters that contain putative Zur boxes were shown to be regulated by changes in zinc levels in this organism. The expression of four categories of proteins was regulated by Zur: (i) zinc-free paralogs of zinc proteins, (ii) putative metallochaperones of the COG0523 family, (iii) ABC transporters including a predicted ZnuABC system, and (iv) outer-membrane proteins, particularly TonB-dependent receptors. A 7-1-7 palindromic DNA sequence to which Zur bound with high specificity was also determined, and agrees well with the Zur box consensus motifs shown in Figure 5. The protein sequence of the *all2473* product clusters with those predicted by us to be Zurs (Figure 3), and the four residues predicted to be involved in zinc-sensing are also conserved in the *all2473* protein.

MEMBERS OF THE COG0523 FAMILY AND ZINC

In our earlier work (Blindauer, 2008b), we noted that the genome neighborhood of putative *zur* and *znuABC* genes in numerous genomes from cyanobacteria harbored genes that were annotated as “Putative GTPase, G3E family”, “Cobalamin synthesis protein/P47K”, or “CobW”. The latter protein is a cobalt chaperone that is part of the machinery for Vitamin B12 synthesis, and at the time, this raised the question whether our putative zinc-related genes might actually be involved in the regulation and transport of cobalt. In the meantime however, Haas et al. (2009) have conducted a thorough analysis of the COG0523 family (Leipe et al., 2002) to which CobW belongs. All members of COG0523 have a P-loop GTPase domain, and are thus also related to nickel-chaperones of the G3E family with the same domain that are involved in the maturation and assembly of urease (UreG), and hydrogenase (HypB), as well as to the iron-chaperone Nha3 required for maturation of nitrile hydratase. G3E family proteins, and by inference, COG0523 proteins, function as either insertases – proteins that perform energy-requiring metal insertion into target proteins – or as cytosolic storage and transport devices for metals (=metallochaperones), or both.

The COG0523 members are composed of two domains, a well-conserved N-terminal GTPase domain, and a more variable C-terminal domain. They have been categorized as segmentally variable genes (Haas et al., 2009), and this points toward a role in adaptation to environmental stresses and/or variability, and indicates development of binding specificity for other proteins or small molecules. Haas et al. note that “the COG0523 family is a striking example of systematic homology-based misannotation” – a specific function (in this case a role in cobalamin

biosynthesis) being assigned even though the level of sequence similarity does not support this conclusion. We would add that such mis-annotation is certainly rife in the case of gene annotation for metal-binding proteins. The fact that many Zur proteins are annotated as Fur is another example of this problem, and issues surrounding the annotation of ABC-type transporters and metal-transporting ATPases have been discussed elsewhere (Blindauer, 2008b).

Importantly, the theoretical and experimental studies of Haas et al. as well as the work of other groups (Gabriel et al., 2008) strongly suggested that a subset of COG0523 proteins is involved in zinc homeostasis. The most prominent member of zinc-related COG0523 is probably *Bacillus subtilis* YciC (Gabriel et al., 2008); it has been established that its expression is under the control of Zur, leading to upregulation when zinc is scarce. It is suggested that the expression of zinc-related COG0523 proteins may provide advantages under conditions of poor zinc nutrition – obviously, these are conditions always present for open-ocean cyanobacteria. Unfortunately, no suitable studies at the protein level seem to be available for any COG0523 member, so although a link to zinc deprivation is solidly established at the transcriptional level, it is not known whether and which metal ion these proteins bind either *in vitro* or *in vivo*. Whilst the requirement of metallochaperones for copper, nickel, and cobalt can be easily understood, as the target proteins for whose assembly they are required are few and well identified, a similar scenario for zinc has been deemed unlikely, as it is thought that even in bacteria, there are too many destinations for zinc, so the tenet that there is one chaperone per metalloprotein is inconceivable. Hence, two hypotheses have been put forward regarding the role of the zinc-related COG0523 members (Haas et al., 2009): (i) they are up-regulated to function in the recruitment and supply of a metal ion that is not zinc to metalloproteins – the latter may be either normally zinc-requiring or a different paralog – (ii) these COG0523 proteins may be involved in the (re-)allocation of zinc when this becomes necessary.

Sequence analysis of cyanobacterial COG0523 proteins (Figure 7; Figures S3 and S4 in Supplementary Material) illustrates characteristic features, for example a well-conserved GCxCC motif which has been suggested as potential metal-binding site previously (Haas et al., 2009); however, its location in a β strand makes this less likely (see below and Figure 8). Another intriguing feature is the insertion of stretches with repetitive HHX, and HXH motifs of up to 70 amino acid residues in total. These His-rich stretches have been suggested to be hallmarks for metallochaperone activity of G3E GTPases. In the COG0523 subset we have analyzed 115 out of 150 proteins (77%) display such stretches. The phylogenetic tree for cyanobacterial COG0523 proteins (Figure 6) is roughly split into three major branches, each of which is divided into two sub-branches. Phylogenetic analysis, together with analyses of genome contexts (Figure 4), suggests that phylogeny and metal specificity are not congruent – in agreement with the findings of Haas et al. who defined 15 phylogenetic sub-groups for COG0523 members, with links to zinc homeostasis found in several sub-groups, and various sub-groups containing representatives with links to several different metal ions. A strong link to *znuABC*- and *zur*-containing gene clusters is present in one branch (1a) of the phylogenetic tree (Figure 6) for sequences from

Prochlorococcus and *Synechococcus* sp. WH8102. Analysis of the genome environment for these sequences reveals co-localization of COG0523 with a WD-40 repeat gene (Figure 4). This association is also strongly conserved for other members in this branch, although the functional significance of the WD-40 repeat protein is unclear. Interestingly, COG0523 sequences of branch 1a contain long inserts (ca. 150 aa), distinct from those described above, as they are not particularly rich in His residues (Figure 7). Secondary structure prediction for these inserts suggests the presence of four to six β -strands and one or two short α -helices. It is conceivable that this insert forms an additional domain in its own right, though no similarity to any known domains was found in an InterPro-scan search.

There is currently only one X-ray structure available for a COG0523 protein – the YjiA protein from *E. coli* (Khil et al., 2004). According to the analysis by Haas et al. (2009) YjiA belongs to their subgroup 9, for which no clear association with any particular metal ion was reported. The crystal structure (pdb 1NJI) also does not contain any metal ions, but considering that the structure is a product of a structural genomics effort, this may not be surprising. Analysis of potential metal sites in the structure using the CHED server (Levy et al., 2009) revealed the presence of two surface-exposed sites with potential for metal-binding; these are both in the GTPase domain and are composed of H23, E27, and H29, and D52, D79, and D82.

We were interested to see whether it would be possible to pinpoint distinguishing elements that would indicate metal-binding capacity, with the help of homology models for COG0523 proteins. We therefore chose B0CCJ8_ACAM1 from *Acaryochloris marina* that is present in branch 1 as a target for comparative modeling. The respective AM1_3031 gene is next to a WD-40 repeat gene and also in the neighborhood of a *zur* gene (Figure 4). In addition, we modeled B0CDJ7_ACAM1, since the gene for this protein (AM1_3070) is co-localized with a putative *znuABC* system (Figure 4). The sequence for this protein is located in branch 3b of the phylogenetic tree and is highlighted in Figure 6. Several other closely related sequences from the same organism (including some plasmid-encoded sequences) are present in all three branches, but none of these occurs in a zinc-related genomic context. The two models are shown in Figure 8. Beside a His-rich loop between the two domains that also contains two Asp and a Cys residue, there are no further recognizable metal sites in B0CDJ7_ACAM1. In contrast, B0CCJ8_ACAM1 has a much shorter loop comprising only two His and several Asp and Glu residues that might bind a metal. Other branch 1b members also contain this short loop, but so do some representatives from the other sub-branches. The model also displays two further potential metal sites composed of D132, H135, and H139, and E210, D212, and E300, as identified using the CHED server, but only D132 and H135 are conserved within the branch, questioning the significance of these sites. The quest for the true metal-binding sites and the mode of action of the zinc-related COG0523 proteins remains open.

INTRACELLULAR HANDLING: METALLOTHIONEINS (BmtAs)

Metallothioneins, small proteins with a high content of cysteine with the capability to bind multiple metal ions in metal–sulfur

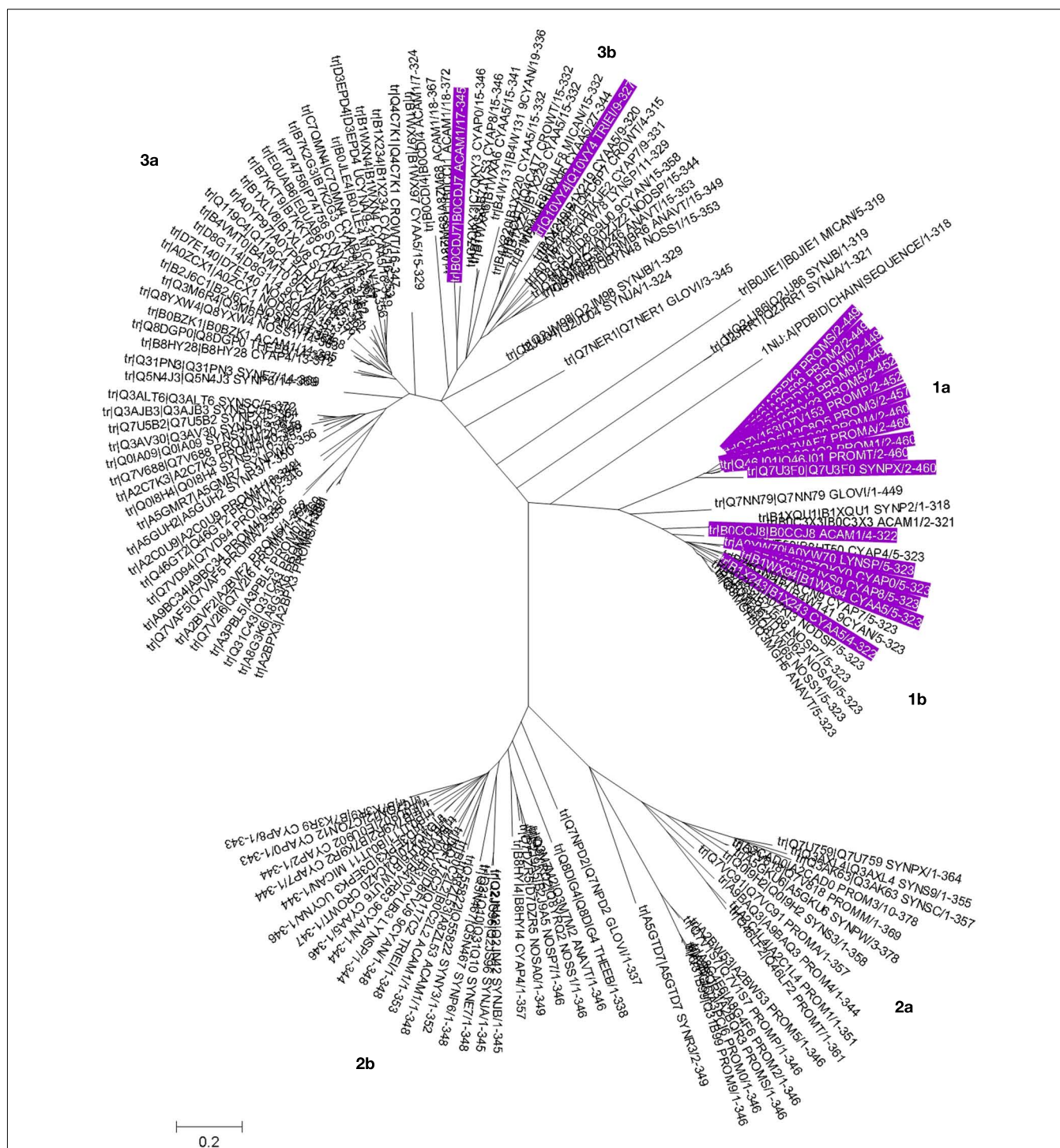


FIGURE 6 | Phylogenetic tree for COG0523 family members. The phylogenetic tree for cyanobacterial COG0523 family members was generated in MEGA5 using the maximum likelihood method with the JTT substitution model. Bootstrap values are the result of 1000 replications. Sequences are labeled with UniProt accession numbers; the actual sequences are documented Figure S3 in Supplementary Material, and a

rectangular tree including bootstrap statistics can be found Figure S4 in Supplementary Material. The sequence of *E. coli* YjiA, the only COG0523 member for which an experimentally determined structure is available, was also included in the tree. Entries with a genomic context linked to zinc homeostasis are highlighted in purple (also see **Table 1**). Sub-branches are labeled and discussed in the main text.

clusters, were initially reported as cadmium-binding proteins in the livers and kidneys of mammals (Kägi, 1991). In the five

decades since their discovery (Margoshes and Vallee, 1957), genes encoding metallothioneins have been identified in virtually all

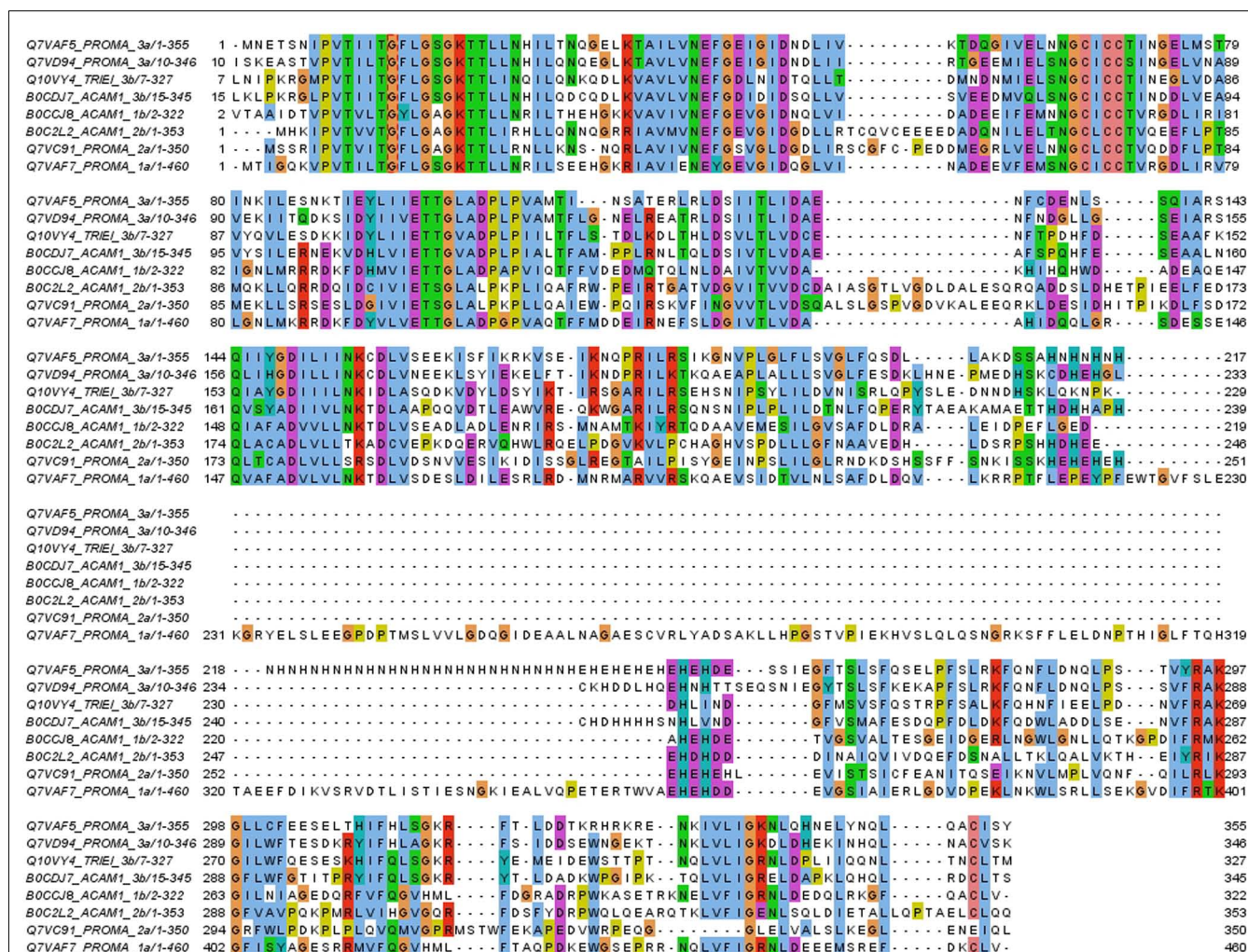


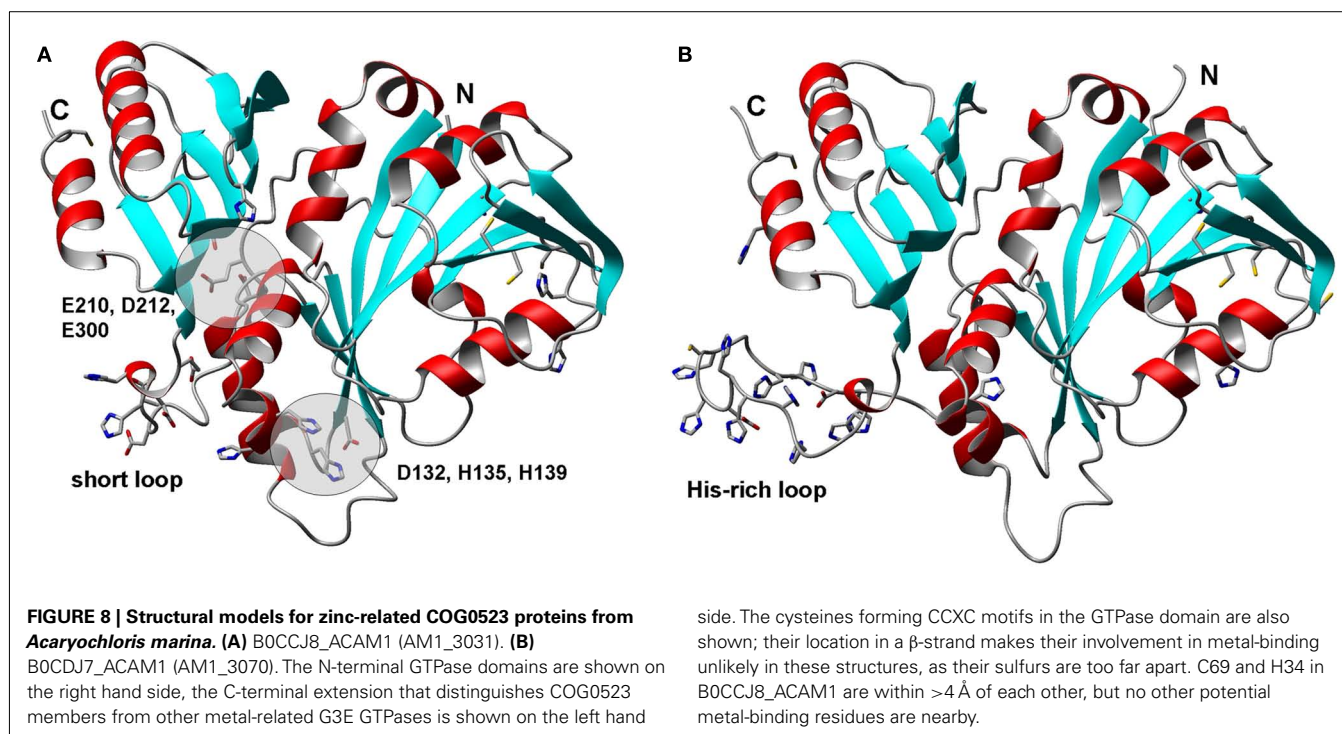
FIGURE 7 | Examples of the six sub-groups of COG0523 family members. All four homologs from *Prochlorococcus marinus* CCMP1375 are shown, as well as two sequences from *Acaryochloris marina*, structural models of which are shown in **Figure 8**. A further *A. marina* representative from branch 2b and the potentially Zur-regulated representative from *Trichodesmium erythraeum* (locus tag Tery_4617, see text) have also been added. The sequences are labeled with their

location in the phylogenetic tree (see **Figure 6**). The first three rows correspond to the GTPase domain. This is followed by a highly variable section. Group 1a is characterized by ca. 150 aa long inserts with no His residues. Inserts of medium length are found for some representatives of group 3. Very short linkers between the N-terminal GTPase domain and the C-terminal domain (which is relatively well-conserved again) are found in all three major groups.

phyla, and numerous studies regarding their biophysical properties (Blindauer and Leszczyszyn, 2010) and biological functions (Davis and Cousins, 2000; Cobbett and Goldsbrough, 2002; Klaassen et al., 2009) have been carried out. It has become clear that their main function is not restricted to cadmium detoxification nor to responses to other chemical and physical stresses. At least for vertebrates, it is now accepted that they also play a more general and essential role in zinc homeostasis (Maret, 2009; Colvin et al., 2010), and that they constitute an important link between cellular redox state and zinc signaling networks (Maret, 2011).

The presence of metallothionein-like proteins in bacteria (for recent reviews see (Blindauer, 2009, 2011)) was first indicated in 1979, namely in the marine cyanobacterium *Synechococcus*

RRIMP N1 (Olafson et al., 1979). So-called “pseudo-thioneins” were also discovered in cadmium-adapted *Pseudomonas putida* (Higham et al., 1984). The first gene for a bacterial metallothionein, *smtA*, was isolated from *Synechococcus* sp. PCC 7942 (Robinson et al., 1990), and was shown to be regulated by the zinc-sensing transcriptional repressor SmtB. Phenotypically, *smtA* knock-out mutants are hypersensitive to Zn^{2+} , and to a lesser extent to Cd^{2+} , with no effect on tolerance to other metal ions (Turner et al., 1993), even though *smtA* transcription is stimulated not only by Zn^{2+} (which is by far the strongest inducer) and Cd^{2+} , but also Hg^{2+} , Cu^{2+} , Co^{2+} , Cr^{3+} , and Ni^{2+} (Huckle et al., 1993). Moreover, SmtA expressed in *E. coli* was shown to bind not only zinc and cadmium, but also copper and mercury (Shi et al., 1992). Considering that SmtB is



clearly a Zn^{2+} -responsive metal sensor (Turner et al., 1996), the documented responses to other metal ions may be mediated indirectly, by displacement of Zn from proteins by these metal ions.

As soon as the protein sequence of what was later to be called SmtA was available, it was clear that apart from the high cysteine content, there was very little sequence similarity between previously characterized metallothioneins and their bacterial counterparts (Olafson et al., 1988). However, it should be made clear that this statement is essentially true for all MTs from different phyla (Blindauer and Leszczyszyn, 2010). For example, in the animal kingdom, the sequences from MTs from nematodes, snails, earthworms, and vertebrates are so divergent that it is not possible to demonstrate a clear evolutionary relationship. To some extent, this is due to their small size, their low level of complexity, and the absence of a defined protein fold. The latter feature is also reflected in the fact that the folding of MTs is dominated by the formation of the metal-sulfur clusters, and unless the “correct” complement of metal ions is bound, MTs do not adopt well-defined conformations.

In that sense, bacterial metallothioneins of the BmtA type are an exception – they contain a clearly identifiable zinc finger fold (Blindauer et al., 2001, 2002; Blindauer and Sadler, 2005; Figure 9A), and it has been demonstrated experimentally that the constituents of this fold (residues 7–38) form an ordered, folded structure, even if only one Zn^{2+} ion is bound to SmtA (Leszczyszyn et al., 2007a). Another “special feature” that is becoming less exceptional as more and more MTs from other phyla are being studied, is the presence of aromatic residues, including histidines, the latter often with a direct involvement in metal-binding (Blindauer et al., 2007; Leszczyszyn et al., 2007b; Blindauer, 2008a; Peroza et al., 2009; Zeitoun-Ghandour et al., 2010).

The high abundance of cysteine residues are the cause of the high thermodynamic stability of MT complexes with soft¹ metal ions such as Cu^+ and Cd^{2+} , and these tend to bind more strongly to MTs than Zn^{2+} , which is classified as a borderline metal ion. It should however be noted that thermodynamic stability is not necessarily a criterion to determine which metal ions are handled by a particular MT (or indeed a particular protein) *in vivo*. If the metal-lated protein has not been obtained in its natively metallated form from the natural source, it is important to take into account information on which metal ion(s) induce(s) MT gene transcription most strongly, whether the protein confers tolerance against a particular metal ion, and also on how well-folded the protein is in the presence of different metal ions. Bofill et al. (2009) have compiled large amounts of biophysical data on recombinantly expressed MTs from a variety of species, and have suggested that there are clear Cu-MTs and Zn/Cd-MTs, as well as MTs between these two extremes with less well-defined metal preferences.

SmtA is thought to be a prototypical Zn-MT. To some extent, this is indeed also reflected in the *in vitro* properties of the protein: the zinc finger site and fold require a four-coordinate metal ion – which excludes Cu^+ as it prefers trigonal or linear coordination modes with thiolate ligands. In addition, the two His-containing metal sites augment the relative affinity for Zn^{2+} compared to Cd^{2+} , although this is certainly not their sole purpose (Blindauer et al., 2007). Nevertheless, SmtA folds equally well in the presence of four Zn (Blindauer et al., 2001) or four Cd (Blindauer et al., 2008) ions, or any mixture thereof, a feature that greatly facilitated the determination of its 3D structure.

¹The terms “soft” and “borderline” refer to Pearson’s HSAB principle: Pearson (1990).

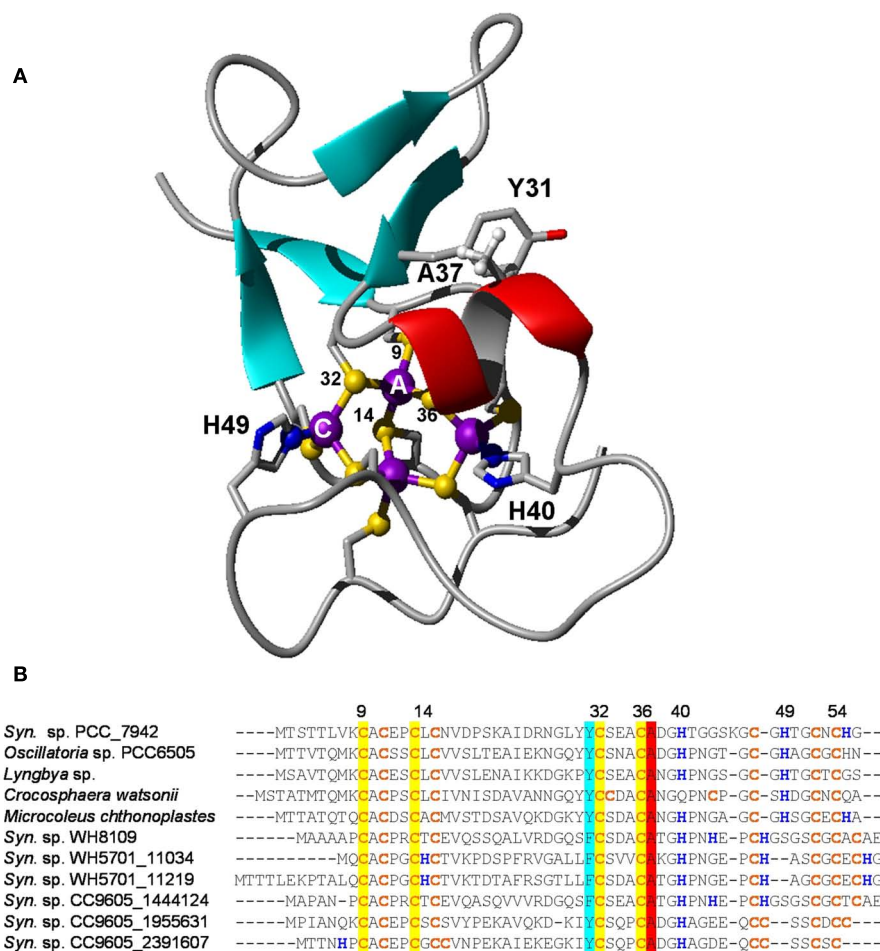


FIGURE 9 | Structural features of bacterial metallothioneins. (A) NMR solution structure of Zn_2SmtA . Residues important for the zinc finger fold and metal ligands are highlighted. **(B)** Selected primary sequences of BmtAs from marine cyanobacteria. The level of conservation is different for different metal sites. Site A, the zinc finger site, is fully conserved, as it is required for structural stability.

Conservation is also high for residues Y31 and A37; these mediate a CH- π interaction between β hairpin and α -helix. The least conserved site is site C, which is also the “business end” of BmtAs, i.e., the site that (in SmtA) releases zinc most readily (Leszczyszyn et al., 2007a). It is envisaged that the high variability of this site may allow to fine-tune the metal-binding and -release properties of different SmtAs.

Although no in-depth study of SmtA (or any other BmtA) loaded with copper ions has so far been carried out, recombinant expression of SmtA in the presence of added copper yielded samples with only ca. 1.5 copper ions bound, whereas contents of Cd^{2+} , Hg^{2+} , and Zn^{2+} varied between ca. 4 and 6 when the respective metal ion was added to the culture medium (Shi et al., 1992).

An analysis of the genomes of all marine cyanobacteria reveals that 14 out of 33 sequenced genomes contain one or more genes for a BmtA (Table 1; Figures 9B). The BmtA sequences were retrieved using a protein vs. DNA TBLASTN search with the *Synechococcus* sp. PCC 7942 sequence as query and the six-frame translations of the genomic nucleotide databases. This is necessary to ensure that all BmtAs are captured, as due to their small size, BmtA ORFs are easy to overlook. This is illustrated by the fact that *bmtA* genes are not annotated in the genomes of *Microcoleus*, *Cyanobium*, and *Crocospaera watsonii*, all of which are in their “Draft” stage, but

they have also been overlooked in the finished genome and plasmid sequences of *Acaryochloris marina*.

In a select few genomes (*Synechococcus* sp. PCC 7002, *Oscillatoria* sp. PCC 6506, and the genome as well as pREB2 and pREB6 plasmids of *Acaryochloris marina*) BmtAs occur in a cluster together with SmtB. On the latter two plasmids, a COG0523 homolog is also nearby. In the *Synechococcus* sp. WH5701 genome, both BmtAs are annotated, and WH5701_11219 (the latter number refers to the first base of the start codon) is located near a CsbD-like protein, thought to be involved in the general stress response, a Cd/Co/Hg/Pg/Zn-transporting ATPase, and the permease and ATPase components of an ABC transporter, but since no periplasmic component is present in the vicinity, the specificity for this transporter cannot be predicted.

Several of the benthic strains also have SmtB homologs, for example *Microcoleus chthonoplastes* and *Lyngbya* (in a cluster with ZiaA), and *Nodularia spumigena* (intriguingly in a gene cluster

with an ABC transporter), but even though several open-ocean and coastal marine *Synechococcus* (WH8102, WH8109, WH7803, CC9311, CC9605) have genes for BmtA, there are no identifiable SmtB or other known zinc excess sensors present. Therefore, it remains unclear how the expression of these metallothionein genes is regulated, although the discovery of two Zur boxes upstream of BmtA in *Synechococcus* sp. WH8102 gives rise to the suggestion that this strain might use its metallothionein in response to zinc limitation rather than excess.

We note that although the prototype *smtA* clearly responds most strongly to zinc, and the SmtA protein can be considered a “zinc-metallothionein,” this may not necessarily hold true for all homologs from marine strains. Since the concentrations of Cd²⁺ can be significant in various natural seawaters, the marine BmtAs may also help with dealing with this metal ion – potentially both for preventing toxicity as well as in preparation for utilization as a cofactor. Cd also has a nutrient-like profile in stratified marine waters, and there are several precedents where marine phytoplankton have been found to utilize Cd instead of Zn (Lane et al., 2005). If this was also common in marine cyanobacteria, BmtAs may be part of this utilization network. Furthermore, it can also be envisaged that some BmtAs may play a role in defense against oxidative stress, as shown for metallothioneins from other species (Zeitoun-Ghandour et al., 2011).

Finally, it should be highlighted that cyanobacteria are not the only marine microorganisms with metallothioneins. Several γ -proteobacteria of the genus *Nitrosococcus* also harbor *bmtA* genes in their genomes, and additional *bmtA* sequences can also be retrieved from marine metagenomes (Blindauer, 2008b), suggesting that many more marine bacterial species utilize these proteins.

CONCLUSION

At the time of writing this report (December 2011), there were 64 cyanobacterial genomes available, 35 of them from marine species. Genome annotation must, ultimately, be based on experimental evidence, and we have seen that there is a persistent shortfall of reliable information regarding function of predicted proteins. This is a general problem, witnessed by the large number of hypothetical proteins even in finished genomes, but even in the case of well-defined protein families, annotations regarding metal specificity have to be approached with caution. Our discussions emphasize that sequence similarity alone does not hold the key to determine metal specificity, but we believe that, amongst other approaches, the generation of more sound data at the protein level is central to refine our ideas about how metal homeostasis works.

With this caveat in mind, we are highlighting in the following some salient points from our analyses. The ubiquitous presence of bona-fide Zur and ZnuABC systems – both thought to be involved in responding to a lack of cellular zinc – in all strains we have studied suggests that these cyanobacteria are at the very least capable of utilizing zinc. The identification of putative Zur boxes in several genomes we and others have inspected also suggests that zinc levels are an integral part of the metabolic network of marine cyanobacteria. Nevertheless, an absolute requirement for zinc has not been demonstrated experimentally for any cyanobacterium – in the few instances where this has been studied, only

small reductions in growth rates were observed. This may indicate that marine cyanobacteria have either very low zinc requirements, or extremely efficient uptake mechanisms, or both, enabling them to thrive at extremely low free zinc concentrations. It would hence be interesting to study whether cyanobacteria that are growing at such extremely low zinc concentrations actually contain any zinc, and if so, what the ratio of bio-accumulation is.

Genes for zinc excess sensors appear to be absent from the genomes of open-ocean strains (Blindauer, 2008b), but other strains including *Microcoleus chthonoplastes*, *Synechococcus* sp. PCC 7002, and *Oscillatoria* sp. PCC 6506 have clear SmtB homologs. Although the coastal strain *Synechococcus* sp. CC9311 does not appear to have SmtB, it not only has four BmtA homologs, but also a putative CzrA efflux pump that is thought to be able to transport zinc (and cobalt). Together with at least one ZnuABC system and a putative ZIP transporter for uptake, as well as at least one zinc-related COG0523 protein, this strain is expected to cope well with both zinc excess and scarcity.

The suggestion that metallothioneins in marine *Synechococcus* (e.g., WH8102) may be under the control of Zur is exciting. Whilst this finding may at first seem counterintuitive, it suggests that, also in (some) bacteria, metallothioneins are not just devices to combat metal toxicity, but may play a more central role in essential zinc homeostasis. This hypothesis has been raised before (Robinson et al., 2001; Blindauer, 2009), and this newly identified association between Zur and BmtA provides support.

METHODS

Sequences of Fur-family proteins were retrieved from cyanobacterial genomes using BLAST (Altschul et al., 1997). Briefly, GenBank files were retrieved for each genome and all protein sequences were extracted using BioPerl (Stajich et al., 2002) and a custom BLAST database was created for each genome. Fur-like proteins were identified using the three Fur-like proteins previously identified in *Synechococcus* sp. CC9311 as queries (accessions YP_730377.1, YP_732019.1, and YP_730926.1) with an e value cutoff $<10^{-5}$. Any duplications were removed and amino acid sequences were aligned using CLUSTALW (Larkin et al., 2007). The Fur amino acid sequence from *Escherichia coli* and *Synechocystis* sp. PCC 6803, along with Zur from *Streptomyces coelicolor*, *Mycobacterium tuberculosis*, and *Synechocystis* sp. PCC 6803 were extracted from the Protein Data Bank². Phylogenetic analysis was carried out in MEGA version 5 (Tamura et al., 2011).

Sequences for COG0523 family proteins were collected by searching the fully sequenced and annotated cyanobacterial proteomes plus all sequences from *Oscillatoria* sp. PCC 6506, *Lyngbya* sp. PCC 8106, *Microcoleus chthonoplastes* sp. PCC 7420, *Nodularia spumigena* sp. CCY9414, *Crocospaera watsonii* WH 8501, and *Trichodesmium erythraeum* IMS101 from UniProt with the Pfam PF07683 Hidden Markov Model using HMMER4 with standard cutoffs. The collated sequences were filtered for fragments and aligned in JALVIEW and MUSCLE v.3.8 (Edgar, 2004), and were manually adjusted where necessary.

²<http://www.rcsb.org/>

Gene Ortholog Neighborhood analyses were performed using the respective resource on the Integrated Microbial Genome Server (Markowitz et al., 2010).

Comparative modeling was carried out using Modeller version 9.7 (Eswar et al., 2008). A dimeric assembly of *Streptomyces coelicolor* Zur was generated from the two B chains in the original pdb file (3MWM; Shin et al., 2011) using PISA³ (Krissinel and Henrick, 2007). This dimeric structure was used as a template for modeling the putative Zur from *Prochlorococcus marinus* CCMP1375 (locus tag Pro1502). Template and model sequences were aligned manually. Sidechains and improper dihedrals were optimized with SCWRL 3.0 (Wang et al., 2008). Inspection of initial models and sequence alignments suggested that Cys98 may be a zinc ligand; this residue is highly conserved in all putative Zur sequences from cyanobacteria (See Figure S2 in Supplementary Material). Hydrogens, Zn ions, and metal–ligand bonds were added in MOE v. 2004.03. Energy minimization of the final model was performed in MOE using a customized Amber94 force-field. Final structures were validated using the WHATIF server⁴. Structural images (Figures 2, 8, and 9) were generated with MOLMOL v.2K.2 (Koradi et al., 1996). A similar strategy was

applied for modeling two putatively zinc-binding representatives of the COG0523 family based on the *E. coli* protein as a template (pdb-entry 1NIJ). The target template sequence alignment made use of the HHPRED (Soding et al., 2005) fold recognition server.

ACKNOWLEDGMENTS

We wish to thank the Leverhulme Trust (F/00 215/AY) and the Natural Environment Research Council (grants NE/F004249/1 and NE/G017948/1) for their support of this work, and the Al-Baath University (Homs, Syria) for a scholarship to Amira Z. Ksibe.

SUPPLEMENTARY MATERIAL

The Supplementary Material for this article can be found online at http://www.frontiersin.org/Microbiological_Chemistry/10.3389/fmicb.2012.00142/abstract

Figure S1 | Phylogenetic tree for Fur/Zur-like proteins extracted from genomes of marine cyanobacteria.

Figure S2 | Sequence alignment of Fur/Zur-like proteins.

Figure S3 | Phylogenetic tree for COG0523 family members.

Figure S4 | Sequence alignment of members of the COG0523 protein family from the genomes of cyanobacteria.

REFERENCES

- Altschul, S. F., Madden, T. L., Schaffer, A. A., Zhang, J., Zhang, Z., Miller, W., and Lipman, D. J. (1997). Gapped BLAST and PSI-BLAST: a new generation of protein database search programs. *Nucleic Acids Res.* 25, 3389–3402.
- Anderson, M. A., Morel, F. M. M., and Guillard, R. R. L. (1978). Growth limitation of a coastal diatom by low zinc ion activity. *Nature* 276, 70–71.
- Andreini, C., Banci, L., Bertini, I., and Rosato, A. (2006). Zinc through the three domains of life. *J. Proteome Res.* 5, 3173–3178.
- Andreini, C., Bertini, I., Cavallaro, G., Holliday, G. L., and Thornton, J. M. (2008). Metal ions in biological catalysis: from enzyme databases to general principles. *J. Biol. Inorg. Chem.* 13, 1205–1218.
- Andreini, C., Bertini, I., and Rosato, A. (2009). Metalloproteomes: a bioinformatic approach. *Acc. Chem. Res.* 42, 1471–1479.
- Bagg, A., and Neilands, J. B. (1987). Ferric uptake regulation protein acts as a repressor, employing iron(II) as a cofactor to bind the operator of an iron transport operon in *Escherichia coli*. *Biochemistry* 26, 5471–5477.
- Bertilsson, S., Berglund, O., Karl, D. M., and Chisholm, S. W. (2003). Elemental composition of marine *Prochlorococcus* and *Synechococcus*: implications for the ecological stoichiometry of the sea. *Limnol. Oceanogr.* 48, 1721–1731.
- Blaby-Haas, C. E., Furman, R., Rodionov, D. A., Artsimovitch, I., and De Crecy-Lagard, V. (2011). Role of a Zn-independent DksA in Zn homeostasis and stringent response. *Mol. Microbiol.* 79, 700–715.
- Blindauer, C. A. (2008a). Metallothioneins with unusual residues: histidines as modulators of zinc affinity and reactivity. *J. Inorg. Biochem.* 102, 507–521.
- Blindauer, C. A. (2008b). Zinc handling in cyanobacteria – an update. *Chem. Biodivers.* 5, 1990–2013.
- Blindauer, C. A. (2009). “Bacterial metallothioneins,” in *Metallothioneins and Related Chelators*, eds A. Sigel, H. Sigel, and R. Sigel (Cambridge: The Royal Society of Chemistry), 51–81.
- Blindauer, C. A. (2011). Bacterial metallothioneins: past, present, and questions for the future. *J. Biol. Inorg. Chem.* 16, 1011–1024.
- Blindauer, C. A., Harrison, M. D., Parkinson, J. A., Robinson, A. K., Cavet, J. S., Robinson, N. J., and Sadler, P. J. (2001). A metallothionein containing a zinc finger within a four-metal cluster protects a bacterium from zinc toxicity. *Proc. Natl. Acad. Sci. U.S.A.* 98, 9593–9598.
- Blindauer, C. A., Harrison, M. D., Parkinson, J. A., Robinson, N. J., and Sadler, P. J. (2008). Isostructural replacement of zinc by cadmium in bacterial metallothionein. *Met. Ions Biol. Med.* 10, 167–173.
- Blindauer, C. A., Harrison, M. D., Robinson, A. K., Parkinson, J. A., Bowness, P. W., Sadler, P. J., and Robinson, N. J. (2002). Multiple bacteria encode metallothioneins and SmtA-like zinc fingers. *Mol. Microbiol.* 45, 1421–1432.
- Blindauer, C. A., and Leszczyszyn, O. I. (2010). Metallothioneins: unparalleled diversity in structures and functions for metal ion homeostasis and more. *Nat. Prod. Rep.* 27, 720–741.
- Blindauer, C. A., Razi, M. T., Campopiano, D. J., and Sadler, P. J. (2007). Histidine ligands in bacterial metallothionein enhance cluster stability. *J. Biol. Inorg. Chem.* 12, 393–405.
- Blindauer, C. A., and Sadler, P. J. (2005). How to hide zinc in a small protein. *Acc. Chem. Res.* 38, 62–69.
- Bofill, R., Capdevila, M., and Atrian, S. (2009). Independent metal-binding features of recombinant metallothioneins convergently draw a step gradation between Zn- and Cu-thioneins. *Metalomics* 1, 229–234.
- Bozym, R. A., Chimienti, F., Giblin, L. J., Gross, G. W., Korichneva, I., Li, Y. A., Libert, S., Maret, W., Parviz, M., Frederickson, C. J., and Thompson, R. B. (2010). Free zinc ions outside a narrow concentration range are toxic to a variety of cells *in vitro*. *Exp. Biol. Med.* 235, 741–750.
- Brand, L. E., Sunda, W. G., and Guillard, R. R. L. (1983). Limitation of marine phytoplankton reproductive rates by zinc, manganese, and iron. *Limnol. Oceanogr.* 28, 1182–1198.
- Bruland, K. W. (1980). Oceanographic distribution of cadmium, zinc, nickel, and copper in the North Pacific. *Earth Planet. Sci. Lett.* 47, 176–198.
- Bruland, K. W. (1989). Complexation of zinc by natural organic ligands in the central North Pacific. *Limnol. Oceanogr.* 34, 269–285.
- Bruland, K. W., Orians, K. J., and Cowen, J. P. (1994). Reactive trace metals in the stratified central North Pacific. *Geochim. Cosmochim. Acta* 58, 3171–3182.
- Butler, A. (1998). Acquisition and utilization of transition metal ions by marine organisms. *Science* 281, 207–210.
- Campbell, D. R., Chapman, K. E., Waldron, K. J., Tottey, S., Kendall, S., Cavallaro, G., Andreini, C., Hinds, J., Stoker, N. G., Robinson, N. J., and Cavet, J. S. (2007). Mycobacterial cells have dual nickel-cobalt sensors – sequence relationships and metal sites of metal-responsive repressors are not congruent. *J. Biol. Chem.* 282, 32298–32310.

- Cannon, G. C., Heinhorst, S., and Kerfeld, C. A. (2010). Carboxysomal carbonic anhydrases: structure and role in microbial CO₂ fixation. *Biochim. Biophys. Acta* 1804, 382–392.
- Capone, D. G., Zehr, J. P., Paerl, H. W., Bergman, B., and Carpenter, E. J. (1997). *Trichodesmium*, a globally significant marine cyanobacterium. *Science* 276, 1221–1229.
- Cavet, J. S., Borrelly, G. P. M., and Robinson, N. J. (2003). Zn, Cu and Co in cyanobacteria: selective control of metal availability. *FEMS Microbiol. Rev.* 27, 165–181.
- Cavet, J. S., Meng, W. M., Pennella, M. A., Applehoff, R. J., Giedroc, D. P., and Robinson, N. J. (2002). A nickel-cobalt-sensing ArsR-SmtB family repressor – contributions of cytosol and effector binding sites to metal selectivity. *J. Biol. Chem.* 277, 38441–38448.
- Coale, K. H., Johnson, K. S., Fitzwater, S. E., Gordon, R. M., Tanner, S., Chavez, F. P., Ferioli, L., Sakamoto, C., Rogers, P., Millero, F., Steinberg, P., Nightingale, P., Cooper, D., Cochlan, W. P., Landry, M. R., Constantinou, J., Rollwagen, G., Trassvina, A., and Kudela, R. (1996). A massive phytoplankton bloom induced by an ecosystem-scale iron fertilization experiment in the equatorial Pacific Ocean. *Nature* 383, 495–501.
- Cobbett, C., and Goldsbrough, P. (2002). Phytochelatins and metallothioneins: roles in heavy metal detoxification and homeostasis. *Annu. Rev. Plant Biol.* 53, 159–182.
- Colvin, R. A., Holmes, W. R., Fontaine, C. P., and Maret, W. (2010). Cytosolic zinc buffering and muffling: their role in intracellular zinc homeostasis. *Metallomics* 2, 306–317.
- Cvetkovic, A., Menon, A. L., Thorgersen, M. P., Scott, J. W., Poole, F. L., Jenney, F. E., Lancaster, W. A., Praissman, J. L., Shanmukh, S., Vaccaro, B. J., Trauger, S. A., Kalisiak, E., Apon, J. V., Siuzdak, G., Yannoni, S. M., Tainer, J. A., and Adams, M. W. W. (2010). Microbial metalloproteomes are largely uncharacterized. *Nature* 466, 779–782.
- Davis, S. R., and Cousins, R. J. (2000). Metallothionein expression in animals: a physiological perspective on function. *J. Nutr.* 130, 1085–1088.
- Debelius, B., Forja, J. M., and Lubian, L. M. (2011). Toxicity of copper, nickel and zinc to *synechococcus* populations from the strait of gibraltar. *J. Mar. Syst.* 88, 113–119.
- Decaria, L., Bertini, I., and Williams, R. J. P. (2010). Zinc proteomes, phylogenetics and evolution. *Metalomics* 2, 706–709.
- Dixon, J. L. (2008). Macro and micro nutrient limitation of microbial productivity in oligotrophic subtropical Atlantic waters. *Environ. Chem.* 5, 135–142.
- Donat, J. R., and Bruland, K. W. (1990). A comparison of 2 voltammetric techniques for determining zinc speciation in northeast Pacific-Ocean waters. *Mar. Chem.* 28, 301–323.
- Dufresne, A., Garczarek, L., and Partensky, F. (2005). Accelerated evolution associated with genome reduction in a free-living prokaryote. *Genome Biol.* 6, R14.
- Dufresne, A., Ostrowski, M., Scanlan, D. J., Garczarek, L., Mazard, S., Palenik, B. P., Paulsen, I. T., De Marsac, N. T., Wincker, P., Dossat, C., Ferreira, S., Johnson, J., Post, A. F., Hess, W. R., and Partensky, F. (2008). Unraveling the genomic mosaic of a ubiquitous genus of marine cyanobacteria. *Genome Biol.* 9, 16.
- Dupont, C. L., Butcher, A., Valas, R. E., Bourne, P. E., and Caetano-Anolles, G. (2010). History of biological metal utilization inferred through phylogenomic analysis of protein structures. *Proc. Natl. Acad. Sci. U.S.A.* 107, 10567–10572.
- Dupont, C. L., and Caetano-Anolles, G. (2010). Mulikidjanian and Galperin: Zn may have constrained evolution during the Proterozoic but not the Archean Reply. *Proc. Natl. Acad. Sci. U.S.A.* 107, E138.
- Edgar, R. C. (2004). MUSCLE: multiple sequence alignment with high accuracy and high throughput. *Nucleic Acids Res.* 32, 1792–1797.
- Eide, D. J. (2006). Zinc transporters and the cellular trafficking of zinc. *Biochim. Biophys. Acta* 1763, 711–722.
- Ellwood, M. J., and van den Berg, C. M. G. (2000). Zinc speciation in the Northeastern Atlantic Ocean. *Mar. Chem.* 68, 295–306.
- Eswar, N., Eramian, D., Webb, B., Shen, M.-Y., and Sali, A. (2008). “Protein structure modeling with MODELLER,” in *Methods in Molecular Biology*, eds B. Kobe, M. Guss, and T. Huber (Totowa, NJ: Humana Press Inc), 145–159.
- Finney, L. A., and O’Halloran, T. V. (2003). Transition metal speciation in the cell: insights from the chemistry of metal ion receptors. *Science* 300, 931–936.
- Fukada, T., and Kambe, T. (2011). Molecular and genetic features of zinc transporters in physiology and pathogenesis. *Metallomics* 3, 662–674.
- Fuller, N. J., Tarran, G. A., Yallop, M., Orcutt, K. M., and Scanlan, D. J. (2006). Molecular analysis of picocyanobacterial community structure along an Arabian Sea transect reveals distinct spatial separation of lineages. *Limnol. Oceanogr.* 51, 2515–2526.
- Gabriel, S. E., and Helmann, J. D. (2009). Contributions of Zur-controlled ribosomal proteins to growth under zinc starvation conditions. *J. Bacteriol.* 191, 6116–6122.
- Gabriel, S. E., Miyagi, F., Gaballa, A., and Helmann, J. D. (2008). Regulation of the *Bacillus subtilis* *yciC* gene and insights into the DNA-binding specificity of the zinc-sensing metalloregulator *zur*. *J. Bacteriol.* 190, 3482–3488.
- Giedroc, D. P., and Arunkumar, A. I. (2007). Metal sensor proteins: nature’s metalloregulated allosteric switches. *Dalton Trans.* 3107–3120.
- Goericke, R., and Repeta, D. J. (1992). The pigments of *Prochlorococcus marinus* – the presence of divinyl chlorophyll-*a* and chlorophyll-*b* in a marine prokaryote. *Limnol. Oceanogr.* 37, 425–433.
- Graham, A. I., Hunt, S., Stokes, S. L., Bramall, N., Bunch, J., Cox, A. G., Mcleod, C. W., and Poole, R. K. (2009). Severe zinc depletion of *Escherichia coli* roles for high affinity zinc binding by ZinT, zinc transport and zinc-independent proteins. *J. Biol. Chem.* 284, 18377–18389.
- Haas, C. E., Rodionov, D. A., Kropat, J., Malasarn, D., Merchant, S. S., and De Crecy-Lagard, V. (2009). A subset of the diverse COG0523 family of putative metal chaperones is linked to zinc homeostasis in all kingdoms of life. *BMC Genomics* 10, 470. doi:10.1186/1471-2164-10-470
- Hantke, K. (2005). Bacterial zinc uptake and regulators. *Curr. Opin. Microbiol.* 8, 196–202.
- Heldal, M., Scanlan, D. J., Norland, S., Thingstad, F., and Mann, N. H. (2003). Elemental composition of single cells of various strains of marine *Prochlorococcus* and *Synechococcus* using X-ray microanalysis. *Limnol. Oceanogr.* 48, 1732–1743.
- Higham, D. P., Sadler, P. J., and Scawen, M. D. (1984). Cadmium-resistant *Pseudomonas putida* synthesizes novel cadmium proteins. *Science* 225, 1043–1046.
- Ho, T. Y., Quigg, A., Finkel, Z. V., Milligan, A. J., Wyman, K., Falkowski, P. G., and Morel, F. M. M. (2003). The elemental composition of some marine phytoplankton. *J. Phycol.* 39, 1145–1159.
- Hong, S. M., Candelone, J. P., Turetta, C., and Bouter, C. F. (1996). Changes in natural lead, copper, zinc and cadmium concentrations in central Greenland ice from 8250 to 149,100 years ago: their association with climatic changes and resultant variations of dominant source contributions. *Earth Planet. Sci. Lett.* 143, 233–244.
- Huckle, J. W., Morby, A. P., Turner, J. S., and Robinson, N. J. (1993). Isolation of a prokaryotic metallothionein locus and analysis of transcriptional control by trace metal ions. *Mol. Microbiol.* 7, 177–187.
- Hunter, K. A., and Boyd, P. (1999). Biogeochemistry of trace metals in the ocean. *Mar. Freshw. Res.* 50, 739–753.
- Irving, H., and Williams, R. J. P. (1953). The stability of transition-metal complexes. *J. Chem. Soc.* 3192–3210.
- Jacquemet, L., Traore, D. A. K., Ferrer, J. L., Proux, O., Testemale, D., Hazemann, J. L., Nazarenko, E., El Ghazouani, A., Caux-Thang, C., Duarte, V., and Latour, J. M. (2009). Structural characterization of the active form of PerR: insights into the metal-induced activation of PerR and Fur proteins for DNA binding. *Mol. Microbiol.* 73, 20–31.
- Jakuba, R. W., Moffett, J. W., and Dyhrman, S. T. (2008). Evidence for the linked biogeochemical cycling of zinc, cobalt, and phosphorus in the western North Atlantic Ocean. *Global Biogeochem. Cycle* 22, 13.
- Jardillier, L., Zubkov, M. V., Pearman, J., and Scanlan, D. J. (2010). Significant CO₂ fixation by small prymnesiophytes in the subtropical and tropical northeast Atlantic Ocean. *ISME J.* 4, 1180–1192.
- Kägi, J. H. R. (1991). Overview of metallothionein. *Meth. Enzymol.* 205, 613–626.
- Kallifidas, D., Pascoe, B., Owen, G. A., Strain-Damerell, C. M., Hong, H. J., and Paget, M. S. B. (2010). The Zinc-responsive regulator Zur controls expression of the coelbactin gene cluster in *Streptomyces coelicolor*. *J. Bacteriol.* 192, 608–611.
- Kathuria, S., and Martiny, A. C. (2011). Prevalence of a calcium-based alkaline phosphatase associated with the marine cyanobacterium *Prochlorococcus* and other ocean bacteria. *Environ. Microbiol.* 13, 74–83.
- Kettler, G. C., Martiny, A. C., Huang, K., Zucker, J., Coleman, M. L., Rodrigue, S., Chen, F., Lapidus, A., Ferreira, S., Johnson, J., Steglich, C., Church, G. M., Richardson, P., and Chisholm,

- S. W. (2007). Patterns and implications of gene gain and loss in the evolution of *Prochlorococcus*. *PLoS Genet.* 3, e231. doi:10.1371/journal.pgen.0030231
- Khil, P. P., Obmolova, G., Teplyakov, A., Howard, A. J., Gilliland, G. L., and Camerini-Otero, R. D. (2004). Crystal structure of the *Escherichia coli* YjiA protein suggests a GTP-dependent regulatory function. *Proteins* 54, 371–374.
- Klaassen, C. D., Liu, J., and Diwan, B. A. (2009). Metallothionein protection of cadmium toxicity. *Toxicol. Appl. Pharmacol.* 238, 215–220.
- Koradi, R., Billeter, M., and Wuthrich, K. (1996). MOLMOL: a program for display and analysis of macromolecular structures. *J. Mol. Graph.* 14, 51–55.
- Krezel, A., and Maret, W. (2006). Zinc-buffering capacity of a eukaryotic cell at physiological pZn. *J. Biol. Inorg. Chem.* 11, 1049–1062.
- Krissinel, E., and Henrick, K. (2007). Inference of macromolecular assemblies from crystalline state. *J. Mol. Biol.* 372, 774–797.
- Kuhl, M., Chen, M., Ralph, P. J., Schreiber, U., and Larkum, A. W. D. (2005). A niche for cyanobacteria containing chlorophyll *d*. *Nature* 433, 820.
- Lane, T. W., Saito, M. A., George, G. N., Pickering, I. J., Prince, R. C., and Morel, F. M. M. (2005). A cadmium enzyme from a marine diatom. *Nature* 435, 42.
- Larkin, M. A., Blackshields, G., Brown, N. P., Chenna, R., McGettigan, P. A., McWilliam, H., Valentin, F., Wallace, I. M., Wilm, A., Lopez, R., Thompson, J. D., Gibson, T. J., and Higgins, D. G. (2007). Clustal W and Clustal X version 2.0. *Bioinformatics* 23, 2947–2948.
- Leao, P. N., Vasconcelos, M., and Vasconcelos, V. M. (2007). Role of marine cyanobacteria in trace metal bioavailability in seawater. *Microb. Ecol.* 53, 104–109.
- Lee, J. G., and Morel, F. M. M. (1995). Replacement of zinc by cadmium in marine phytoplankton. *Mar. Ecol. Prog. Ser.* 127, 305–309.
- Lee, J. W., and Helmann, J. D. (2007). Functional specialization within the Fur family of metalloregulators. *Bio-metals* 20, 485–499.
- Leipe, D. D., Wolf, Y. I., Koonin, E. V., and Aravind, L. (2002). Classification and evolution of P-loop GTPases and related ATPases. *J. Mol. Biol.* 317, 41–72.
- Leszczyszyn, O. I., Evans, C. D., Keiper, S. E., Warren, G. Z. L., and Blindauer, C. A. (2007a). Differential reactivity of individual zinc ions in clusters from bacterial metallothioneins. *Inorganica Chim. Acta* 360, 3–13.
- Leszczyszyn, O. I., Schmid, R., and Blindauer, C. A. (2007b). Toward a property/function relationship for metallothioneins: histidine coordination and unusual cluster composition in a zinc-metallothionein from plants. *Proteins* 68, 922–935.
- Levi, P. (1984). *The Periodic Table*. New York: Schocken Books.
- Levy, R., Edelman, M., and Sobolev, V. (2009). Prediction of 3D metal binding sites from translated gene sequences based on remote-homology templates. *Proteins* 76, 365–374.
- Li, W. K. W. (1994). Primary production of prochlorophytes, cyanobacteria, and eukaryotic ultraphytoplankton – measurements from flow cytometric sorting. *Limnol. Oceanogr.* 39, 169–175.
- Lohan, M. C., Crawford, D. W., Purdie, D. A., and Statham, P. J. (2005). Iron and zinc enrichments in the north-eastern subarctic Pacific: ligand production and zinc availability in response to phytoplankton growth. *Limnol. Oceanogr.* 50, 1427–1437.
- López-Gomollón, S., Sevilla, E., Bes, M. T., Peleato, M. L., and Fillat, M. F. (2009). New insights into the role of Fur proteins: FurB (All2473) from *Anabaena* protects DNA and increases cell survival under oxidative stress. *Biochem. J.* 418, 201–207.
- Lucarelli, D., Russo, S., Garman, E., Milano, A., Meyer-Klaucke, W., and Pohl, E. (2007). Crystal structure and function of the zinc uptake regulator FurB from *Mycobacterium tuberculosis*. *J. Biol. Chem.* 282, 9914–9922.
- Luisi, B. (1992). DNA transcription – zinc standard for economy. *Nature* 356, 379–380.
- Ma, Z., Gabriel, S. E., and Helmann, J. D. (2011). Sequential binding and sensing of Zn(II) by *Bacillus subtilis* Zur. *Nucleic Acids Res.* 39, 9130–9138.
- Makarova, K. S., Ponomarev, V. A., and Koonin, E. V. (2001). Two C or not two C: recurrent disruption of Zn-ribbons, gene duplication, lineage-specific gene loss, and horizontal gene transfer in evolution of bacterial ribosomal proteins. *Genome Biol.* 2, R33.
- Mann, E. L., Ahlgren, N., Moffett, J. W., and Chisholm, S. W. (2002). Copper toxicity and cyanobacteria ecology in the Sargasso Sea. *Limnol. Oceanogr.* 47, 976–988.
- Maret, W. (2009). Molecular aspects of human cellular zinc homeostasis: redox control of zinc potentials and zinc signals. *Bio-metals* 22, 149–157.
- Maret, W. (2011). Redox biochemistry of mammalian metallothioneins. *J. Biol. Inorg. Chem.* 16, 1079–1086.
- Margoshes, M., and Vallee, B. L. (1957). A cadmium protein from equine kidney cortex. *J. Am. Chem. Soc.* 79, 4813–4814.
- Markowitz, V. M., Chen, I. M. A., Palaniappan, K., Chu, K., Szeto, E., Grechkin, Y., Ratner, A., Anderson, I., Lykidis, A., Mavromatis, K., Ivanova, N. N., and Kyrpides, N. C. (2010). The integrated microbial genomes system: an expanding comparative analysis resource. *Nucleic Acids Res.* 38, D382–D390.
- Moore, L. R., Ostrowski, M., Scanlan, D. J., Feren, K., and Sweetsir, T. (2005). Ecotypic variation in phosphorus acquisition mechanisms within marine picocyanobacteria. *Aquat. Microb. Ecol.* 39, 257–269.
- Moore, L. R., Rocap, G., and Chisholm, S. W. (1998). Physiology and molecular phylogeny of coexisting *Prochlorococcus* ecotypes. *Nature* 393, 464–467.
- Morel, F. M. M. (2008). The co-evolution of phytoplankton and trace element cycles in the oceans. *Geobiology* 6, 318–324.
- Morel, F. M. M., Reinfelder, J. R., Roberts, S. B., Chamberlain, C. P., Lee, J. G., and Yee, D. (1994). Zinc and carbon co-limitation of marine phytoplankton. *Nature* 369, 740–742.
- Mulkidjanian, A. Y., and Galperin, M. Y. (2009). On the origin of life in the zinc world. 2. Validation of the hypothesis on the photosynthesizing zinc sulfide edifices as cradles of life on Earth. *Biol. Direct* 4, 37.
- Napolitano, M., Rubio, M. A., Santamaría-Gómez, J., Olmedo-Verd, E., Robinson, N. J., and Luque, I. (2012). Characterization of the response to zinc-deficiency in the cyanobacterium *Anabaena* sp. PCC 7120. *J. Bacteriol.* doi:10.1128/JB.00090–12.
- Novichkov, P. S., Laikova, O. N., Novichkova, E. S., Gelfand, M. S., Arkin, A. P., Dubchak, I., and Rodionov, D. A. (2010). RegPrecise: a database of curated genomic inferences of transcriptional regulatory interactions in prokaryotes. *Nucleic Acids Res.* 38, D111–D118.
- Ochsner, U. A., Vasil, A. I., and Vasil, M. L. (1995). Role of the ferric uptake regulator of *Pseudomonas aeruginosa* in the regulation of siderophores and exotoxin A expression: purification and activity on iron-regulated promoters. *J. Bacteriol.* 177, 7194–7201.
- Ohkubo, S., Miyashita, H., Murakami, A., Takeyama, H., Tsuchiya, T., and Mimuro, M. (2006). Molecular detection of epiphytic *Acaryochloris* spp. on marine macroalgae. *Appl. Environ. Microbiol.* 72, 7912–7915.
- Olafson, R. W., Abel, K., and Sim, R. G. (1979). Prokaryotic metallothionein – preliminary characterization of a blue green alga heavy metal-binding protein. *Biochem. Biophys. Res. Commun.* 89, 36–43.
- Olafson, R. W., McCubbin, W. D., and Kay, C. M. (1988). Primary- and secondary-structural analysis of a unique prokaryotic metallothionein from a *Synechococcus* sp. cyanobacterium. *Biochem. J.* 251, 691–699.
- Osman, D., and Cavet, J. S. (2010). Bacterial metal-sensing proteins exemplified by ArsR-SmtB family repressors. *Nat. Prod. Rep.* 27, 668–680.
- Ostrowski, M., Mazard, S., Tetu, S. G., Phillippy, K., Johnson, A., Palenik, B., Paulsen, I. T., and Scanlan, D. J. (2010). PtrA is required for coordinate regulation of gene expression during phosphate stress in a marine *Synechococcus*. *ISME J.* 4, 908–921.
- Outten, C. E., and O'Halloran, T. V. (2001). Femtomolar sensitivity of metalloregulatory proteins controlling zinc homeostasis. *Science* 292, 2488–2492.
- Owen, G. A., Pascoe, B., Kallifidas, D., and Paget, M. S. B. (2007). Zinc-responsive regulation of alternative ribosomal protein genes in *Streptomyces coelicolor* involves Zur and σ^R . *J. Bacteriol.* 189, 4078–4086.
- Palenik, B., Brahamsha, B., Larimer, F. W., Land, M., Hauser, L., Chain, P., Lamerdin, J., Regala, W., Allen, E. E., Mccarren, J., Paulsen, I., Dufresne, A., Partensky, F., Webb, E. A., and Waterbury, J. (2003). The genome of a motile marine *Synechococcus*. *Nature* 424, 1037–1042.
- Palenik, B., Ren, Q. H., Dupont, C. L., Myers, G. S., Heidelberg, J. F., Badger, J. H., Madupu, R., Nelson, W. C., Brinkac, L. M., Dodson, R. J., Durkin, A. S., Daugherty, S. C., Sullivan, S. A., Khouri, H., Mohamoud, Y., Halpin, R., and Paulsen, I. T. (2006). Genome sequence of *Synechococcus* CC9311: insights into adaptation to a coastal environment. *Proc. Natl. Acad. Sci. U.S.A.* 103, 13555–13559.
- Panina, E. M., Mironov, A. A., and Gelfand, M. S. (2003). Comparative genomics of bacterial zinc regulons: enhanced ion transport, pathogenesis, and rearrangement of ribosomal proteins. *Proc. Natl. Acad. Sci. U.S.A.* 100, 9912–9917.

- Partensky, C., and Garczarek, L. (2003). "The photosynthetic apparatus of chlorophyll *b*- and *d*-containing oxychlorobacteria," in *Photosynthesis in Algae*, Vol. 14, eds A. W. D. Larkum, S. E. Douglas, and J. A. Raven (Dordrecht: Kluwer Academic Publishers), 29–62.
- Partensky, F., and Garczarek, L. (2010). *Prochlorococcus*: advantages and limits of minimalism. *Ann. Rev. Mar. Sci.* 2, 305–331.
- Partensky, F., Hess, W. R., and Vault, D. (1999). *Prochlorococcus*, a marine photosynthetic prokaryote of global significance. *Microbiol. Mol. Biol. Rev.* 63, 106–127.
- Patzner, S. I., and Hantke, K. (2000). The zinc-responsive regulator Zur and its control of the *znu* gene cluster encoding the ZnuABC zinc uptake system in *Escherichia coli*. *J. Biol. Chem.* 275, 24321–24332.
- Pearson, R. G. (1990). Hard and soft acids and bases – the evolution of a chemical concept. *Coord. Chem. Rev.* 100, 403–425.
- Peroza, E. A., Schmucki, R., Guntert, P., Freisinger, E., and Zerbe, O. (2009). The β^E -domain of wheat E-c-1 metallothionein: a metal-binding domain with a distinctive structure. *J. Mol. Biol.* 387, 207–218.
- Pohl, E., Haller, J. C., Mijovilovich, A., Meyer-Klaucke, W., Garman, E., and Vasil, M. L. (2003). Architecture of a protein central to iron homeostasis: crystal structure and spectroscopic analysis of the ferric uptake regulator. *Mol. Microbiol.* 47, 903–915.
- Quigg, A., Finkel, Z. V., Irwin, A. J., Rosenthal, Y., Ho, T. Y., Reinfelder, J. R., Schofield, O., Morel, F. M. M., and Falkowski, P. G. (2003). The evolutionary inheritance of elemental stoichiometry in marine phytoplankton. *Nature* 425, 291–294.
- Quigg, A., Irwin, A. J., and Finkel, Z. V. (2011). Evolutionary inheritance of elemental stoichiometry in phytoplankton. *Proc. R. Soc. Lond. B Biol. Sci.* 278, 526–534.
- Raymond, J., and Blankenship, R. E. (2004). Biosynthetic pathways, gene replacement and the antiquity of life. *Geobiology* 2, 199–203.
- Robinson, N. J., Gupta, A., Fordham-Skelton, A. P., Croy, R. R. D., Whitton, B. A., and Huckle, J. W. (1990). Prokaryotic metallothionein gene characterization and expression: chromosome crawling by ligation-mediated PCR. *Proc. R. Soc. Lond. B Biol. Sci.* 242, 241–247.
- Robinson, N. J., Whitehall, S. K., and Cavet, J. S. (2001). Microbial metallothioneins. *Adv. Microb. Physiol.* 44, 183–213.
- Saito, M. A., Goepfert, T. J., and Ritt, J. T. (2008). Some thoughts on the concept of colimitation: three definitions and the importance of bioavailability. *Limnol. Oceanogr.* 53, 276–290.
- Saito, M. A., Moffett, J. W., Chisholm, S. W., and Waterbury, J. B. (2002). Cobalt limitation and uptake in *Prochlorococcus*. *Limnol. Oceanogr.* 47, 1629–1636.
- Saito, M. A., Rocap, G., and Moffett, J. W. (2005). Production of cobalt binding ligands in a *Synechococcus* feature at the Costa Rica upwelling dome. *Limnol. Oceanogr.* 50, 279–290.
- Saito, M. A., Sigman, D. M., and Morel, F. M. M. (2003). The bioinorganic chemistry of the ancient ocean: the co-evolution of cyanobacterial metal requirements and biogeochemical cycles at the Archean-Proterozoic boundary? *Inorganica Chim. Acta* 356, 308–318.
- Scanlan, D. J. (2003). Physiological diversity and niche adaptation in marine *Synechococcus*. *Adv. Microb. Physiol.* 47, 1–64.
- Scanlan, D. J., Ostrowski, M., Mazard, S., Dufresne, A., Garczarek, L., Hess, W. R., Post, A. F., Hagemann, M., Paulsen, I., and Partensky, F. (2009). Ecological genomics of marine picocyanobacteria. *Microbiol. Mol. Biol. Rev.* 73, 249–299.
- Schulz, K. G., Zondervan, I., Geringa, L. J. A., Timmermans, K. R., Veldhuis, M. J. W., and Riebesell, U. (2004). Effect of trace metal availability on coccolithophorid calcification. *Nature* 430, 673–676.
- Shapiro, L. P., and Haugen, E. M. (1988). Seasonal distribution and temperature tolerance of *Synechococcus* in Boothbay Harbor, Maine. *Estuar. Coast. Shelf Sci.* 26, 517–525.
- Sheikh, M. A., and Taylor, G. L. (2009). Crystal structure of the *Vibrio cholerae* ferric uptake regulator (Fur) reveals insights into metal co-ordination. *Mol. Microbiol.* 72, 1208–1220.
- Shi, J., Lindsay, W. P., Huckle, J. W., Morby, A. P., and Robinson, N. J. (1992). Cyanobacterial metallothionein gene expressed in *Escherichia coli*. Metal-binding properties of the expressed protein. *FEBS Lett.* 303, 159–163.
- Shin, J. H., Jung, H. J., An, Y. J., Cho, Y. B., Cha, S. S., and Roe, J. H. (2011). Graded expression of zinc-responsive genes through two regulatory zinc-binding sites in *Zur*. *Proc. Natl. Acad. Sci. U.S.A.* 108, 5045–5050.
- Soding, J., Biegert, A., and Lupas, A. N. (2005). The HHpred interactive server for protein homology detection and structure prediction. *Nucleic Acids Res.* 33, W244–W248.
- Stajich, J. E., Block, D., Boulez, K., Brenner, S. E., Chervitz, S. A., Dagdigan, C., Fuellen, G., Gilbert, J. G., Korf, I., Lapp, H., Lehvaslaiho, H., Matsalla, C., Mungall, C. J., Osborne, B. I., Pocock, M. R., Schattner, P., Senger, M., Stein, L. D., Stupka, E., Wilkinson, M. D., and Birney, E. (2002). The Bioperl toolkit: perl modules for the life sciences. *Genome Res.* 12, 1611–1618.
- Sunda, W. G., and Huntsman, S. A. (1992). Feedback Interactions between zinc and phytoplankton in seawater. *Limnol. Oceanogr.* 37, 25–40.
- Sunda, W. G., and Huntsman, S. A. (1995). Cobalt and zinc interreplacement in marine phytoplankton: biological and geochemical implications. *Limnol. Oceanogr.* 40, 1404–1417.
- Sunda, W. G., and Huntsman, S. A. (2000). Effect of Zn, Mn, and Fe on Cd accumulation in phytoplankton: implications for oceanic Cd cycling. *Limnol. Oceanogr.* 45, 1501–1516.
- Sunda, W. G., and Huntsman, S. A. (2005). Effect of CO₂ supply and demand on zinc uptake and growth limitation in a coastal diatom. *Limnol. Oceanogr.* 50, 1181–1192.
- Sunda, W. G., Price, N. M., and Morel, F. M. M. (2005). "Trace metal ion buffers and their use in culture studies," in *Algal Culturing Techniques*, ed. R. A. Andersen (Burlington, MA: Academic Press), 35–63.
- Swingle, W. D., Chen, M., Cheung, P. C., Conrad, A. L., Dejesa, L. C., Hao, J., Honchak, B. M., Karbach, L. E., Kurdoglu, A., Lahiri, S., Mastrian, S. D., Miyashita, H., Page, L., Ramakrishna, P., Satoh, S., Sattley, W. M., Shimada, Y., Taylor, H. L., Tomo, T., Tsuchiya, T., Wang, Z. T., Raymond, J., Mimuro, M., Blankenship, R. E., and Touchman, J. W. (2008). Niche adaptation and genome expansion in the chlorophyll *d*-producing cyanobacterium *Acaryochloris marina*. *Proc. Natl. Acad. Sci. U.S.A.* 105, 2005–2010.
- Tamura, K., Peterson, D., Peterson, N., Stecher, G., Nei, M., and Kumar, S. (2011). MEGA5: molecular evolutionary genetics analysis using maximum likelihood, evolutionary distance, and maximum parsimony methods. *Mol. Biol. Evol.* 28, 2731–2739.
- Thelwell, C., Robinson, N. J., and Turner-Cavet, J. S. (1998). An SmtB-like repressor from *Synechocystis* PCC 6803 regulates a zinc exporter. *Proc. Natl. Acad. Sci. U.S.A.* 95, 10728–10733.
- Thuroczy, C. E., Boye, M., and Losno, R. (2010). Dissolution of cobalt and zinc from natural and anthropogenic dusts in seawater. *Biogeochemistry* 7, 1927–1936.
- Tottey, S., Waldron, K. J., Firbank, S. J., Reale, B., Bessant, C., Sato, K., Cheek, T. R., Gray, J., Banfield, M. J., Dennison, C., and Robinson, N. J. (2008). Protein-folding location can regulate manganese binding versus copper- or zinc-binding. *Nature* 455, 1138–1142.
- Tripp, H. J., Bench, S. R., Turk, K. A., Foster, R. A., Desany, B. A., Niazi, F., Affourtit, J. P., and Zehr, J. P. (2010). Metabolic streamlining in an open-ocean nitrogen-fixing cyanobacterium. *Nature* 464, 90–94.
- Turner, J. S., Glands, P. D., Samson, A. C. R., and Robinson, N. J. (1996). Zn²⁺-sensing by the cyanobacterial metallothionein repressor SmtB: different motifs mediate metal-induced protein-DNA dissociation. *Nucleic Acids Res.* 24, 3714–3721.
- Turner, J. S., Morby, A. P., Whitton, B. A., Gupta, A., and Robinson, N. J. (1993). Construction of Zn²⁺/Cd²⁺ hypersensitive cyanobacterial mutants lacking a functional metallothionein locus. *J. Biol. Chem.* 268, 4494–4498.
- Waldron, K. J., and Robinson, N. J. (2009). How do bacterial cells ensure that metalloproteins get the correct metal? *Nat. Rev. Microbiol.* 7, 25–35.
- Waldron, K. J., Rutherford, J. C., Ford, D., and Robinson, N. J. (2009). Metalloproteins and metal sensing. *Nature* 460, 823–830.
- Wang, Q., Canutescu, A. A., and Dunbrack, R. L. (2008). SCWRL and MolIDE: computer programs for side-chain conformation prediction and homology modeling. *Nat. Protoc.* 3, 1832–1847.
- Waterbury, R. D., Byrne, R. H., Kelly, J., Leader, B., Mcelligott, S., and Russell, R. (1996). *Development of an Underwater In-Situ Spectrophotometric Sensor for Seawater pH*. Bellingham: Spie – Int Soc Optical Engineering.
- Wells, M. L., Kozelka, P. B., and Bruland, K. W. (1998). The complexation of 'dissolved' Cu, Zn, Cd and Pb by soluble and colloidal organic matter in Narragansett Bay, RI. *Mar. Chem.* 62, 203–217.

- West, N. J., and Scanlan, D. J. (1999). Niche-partitioning of *Prochlorococcus* populations in a stratified water column in the eastern North Atlantic Ocean. *Appl. Environ. Microbiol.* 65, 2585–2591.
- Whitton, B. A., and Potts, M. (2000). *The Ecology of Cyanobacteria: Their Diversity in Time and Space*. Dordrecht: Kluwer Academic Publishers.
- Wilhelm, S. W., and Trick, C. G. (1994). Iron-limited growth of cyanobacteria – multiple siderophore production is a common response. *Limnol. Oceanogr.* 39, 1979–1984.
- Williams, R. J. P. (2011). Chemical advances in evolution by and changes in use of space during time. *J. Theor. Biol.* 268, 146–159.
- Williams, R. J. P., and Da Silva, J. J. R. F. (2000). The distribution of elements in cells. *Coord. Chem. Rev.* 200, 247–348.
- Williams, R. J. P., and Da Silva, J. J. R. F. (2001). *The Biological Chemistry of the Elements: The Inorganic Chemistry of Life*. Oxford: Oxford University Press.
- Williams, R. J. P., and Da Silva, J. J. R. F. (2003). Evolution was chemically constrained. *J. Theor. Biol.* 220, 323–343.
- Wiramanaden, C. I. E., Cullen, J. T., Ross, A. R. S., and Orians, K. J. (2008). Cyanobacterial copper-binding ligands isolated from artificial seawater cultures. *Mar. Chem.* 110, 28–41.
- Xu, Y., Feng, L., Jeffrey, P. D., Shi, Y. G., and Morel, F. M. M. (2008). Structure and metal exchange in the cadmium carbonic anhydrase of marine diatoms. *Nature* 452, U56–U53.
- Zehr, J. P. (2011). Nitrogen fixation by marine cyanobacteria. *Trends Microbiol.* 19, 162–173.
- Zehr, J. P., Bench, S. R., Mondragon, E. A., McCarren, J., and Delong, E. F. (2007). Low genomic diversity in tropical oceanic N₂-fixing cyanobacteria. *Proc. Natl. Acad. Sci. U.S.A.* 104, 17807–17812.
- Zeitoun-Ghandour, S., Charnock, J., Hodson, M. E., Leszczyszyn, O. I., Blindauer, C. A., and Stürzenbaum, S. R. (2010). The two *Caenorhabditis elegans* metallothioneins (CeMT-1 and CeMT-2) discriminate between essential zinc and toxic cadmium. *FEBS J.* 277, 2531–2542.
- Zeitoun-Ghandour, S., Leszczyszyn, O. I., Blindauer, C. A., Geier, F. M., Bundy, J. G., and Stürzenbaum, S. R. (2011). *C. elegans* metallothioneins: response to and defence against ROS toxicity. *Mol. Biosyst.* 7, 2397–2406.
- Zwirgmaier, K., Jardillier, L., Ostrowski, M., Mazard, S., Garczarek, L., Vault, D., Not, F., Massana, R., Ulloa, O., and Scanlan, D. J. (2008). Global phylogeography of marine *Synechococcus* and *Prochlorococcus* reveals a distinct partitioning of lineages among oceanic biomes. *Environ. Microbiol.* 10, 147–161.
- Conflict of Interest Statement:** The authors declare that the research was conducted in the absence of any commercial or financial relationships that could be construed as a potential conflict of interest.

Received: 21 December 2011; accepted: 25 March 2012; published online: 11 April 2012.

Citation: Barnett JP, Millard A, Ksibe AZ, Scanlan DJ, Schmid R and Blindauer CA (2012) Mining genomes of marine cyanobacteria for elements of zinc homeostasis. *Front. Microbio.* 3:142. doi: 10.3389/fmicb.2012.00142

This article was submitted to *Frontiers in Microbiological Chemistry*, a specialty of *Frontiers in Microbiology*.

Copyright © 2012 Barnett, Millard, Ksibe, Scanlan, Schmid and Blindauer. This is an open-access article distributed under the terms of the Creative Commons Attribution Non Commercial License, which permits non-commercial use, distribution, and reproduction in other forums, provided the original authors and source are credited.



Trace metal requirements for microbial enzymes involved in the production and consumption of methane and nitrous oxide

Jennifer B. Glass* and Victoria J. Orphan

Division of Geological and Planetary Sciences, California Institute of Technology, Pasadena, CA, USA

Edited by:

Martha Gledhill, University of Southampton, UK

Reviewed by:

Aubrey L. Zerkle, Newcastle University, UK

Lisa Y. Stein, University of Alberta, Canada

*Correspondence:

Jennifer B. Glass, Division of Geological and Planetary Sciences, California Institute of Technology, 1200 E. California Blvd., MC 170-25, Pasadena, CA 91125, USA.
e-mail: jglass@caltech.edu

Fluxes of greenhouse gases to the atmosphere are heavily influenced by microbiological activity. Microbial enzymes involved in the production and consumption of greenhouse gases often contain metal cofactors. While extensive research has examined the influence of Fe bioavailability on microbial CO₂ cycling, fewer studies have explored metal requirements for microbial production and consumption of the second- and third-most abundant greenhouse gases, methane (CH₄), and nitrous oxide (N₂O). Here we review the current state of biochemical, physiological, and environmental research on transition metal requirements for microbial CH₄ and N₂O cycling. Methanogenic archaea require large amounts of Fe, Ni, and Co (and some Mo/W and Zn). Low bioavailability of Fe, Ni, and Co limits methanogenesis in pure and mixed cultures and environmental studies. Anaerobic methane oxidation by anaerobic methanotrophic archaea (ANME) likely occurs via reverse methanogenesis since ANME possess most of the enzymes in the methanogenic pathway. Aerobic CH₄ oxidation uses Cu or Fe for the first step depending on Cu availability, and additional Fe, Cu, and Mo for later steps. N₂O production via classical anaerobic denitrification is primarily Fe-based, whereas aerobic pathways (nitrifier denitrification and archaeal ammonia oxidation) require Cu in addition to, or possibly in place of, Fe. Genes encoding the Cu-containing N₂O reductase, the only known enzyme capable of microbial N₂O conversion to N₂, have only been found in classical denitrifiers. Accumulation of N₂O due to low Cu has been observed in pure cultures and a lake ecosystem, but not in marine systems. Future research is needed on metalloenzymes involved in the production of N₂O by enrichment cultures of ammonia oxidizing archaea, biological mechanisms for scavenging scarce metals, and possible links between metal bioavailability and greenhouse gas fluxes in anaerobic environments where metals may be limiting due to sulfide-metal scavenging.

Keywords: methane, nitrous oxide, microbes, metals, enzymes

INTRODUCTION

With increasing concern about the future impacts of global climate change, a detailed understanding of the sources and sinks of greenhouse gases is essential to mitigating their environmental impact. Although CO₂ is the most abundant greenhouse gas, many other climatically important gases exist (Montzka et al., 2011). The second- and third-most abundant naturally produced greenhouse gases are methane (currently ~1.8 ppm; Heimann, 2011) and nitrous oxide (currently ~322 ppb; Montzka et al., 2011) and are ~25× and 300× more efficient at absorbing infrared radiation than CO₂, respectively. Furthermore, CH₄ is oxidized to CO₂ in the atmosphere, contributing to rising CO₂ levels. N₂O has a very long residence time in the atmosphere (120 years) and reacts with atomic O to form nitric oxide (NO), which is involved in ozone destruction (Montzka et al., 2011).

Both humans and microbes play important, and often interwoven, roles in the production of CH₄ and N₂O. Humans have bred and expanded the habitats of ruminants that contain methanogenic archaea in their guts, cultivated rice paddies, and

built wastewater and sewage treatment plants where methanogens proliferate. Humans have also extensively applied inorganic N as fertilizer to agricultural soils, leading to increased microbial N₂O emissions in soils, wetlands, and coastal hypoxic zones (Schlesinger, 2009). Understanding the controls and regulation of microbial greenhouse gas emissions is therefore fundamental to quantifying and managing both natural and anthropogenic fluxes of these gases.

This review will focus on two potent greenhouse gases, CH₄ and N₂O, both of which are produced as natural by-products of microbial energy-generating metabolisms. CH₄ is the final product of the anaerobic degradation of organic matter, whereas N₂O formation results from incomplete conversion of nitrate or nitrite to N₂. At the heart of the pathways that generate these gases are enzymes that catalyze redox reactions. Many of these enzymes contain transition metals as cofactors for electron transport or as catalytic centers at active sites. Important transition metals in the pathway of CH₄ production (methanogenesis) and anaerobic methane oxidation include Fe, Ni, Co, Mo/W, and Zn, whereas

aerobic (and intra-aerobic) methanotrophy and N_2O production require Fe-, Cu-, and Mo-containing proteins. Only one protein, the Cu-rich nitrous oxidase reductase, is known to reduce N_2O to N_2 . Physiological studies of pure cultures have shown that optimal metal concentrations for microbial metabolism are orders of magnitude higher than *in situ* concentrations in most aquatic environments. These findings lead to the question: are some microbes perennially metal-limited in nature? If so, does metal availability exert influence on the flux of greenhouse gases? If not, what mechanisms do microbes use in natural environments to acquire trace metals?

Previous environmental studies of metal requirements for microbes have largely focused on those microbes directly involved in CO_2 cycling, principally phytoplankton that consume CO_2 during photosynthesis. Driving these studies was the “Fe hypothesis” by John Martin positing that CO_2 -consuming marine phytoplankton could be fertilized by Fe (Martin and Fitzwater, 1988). Far less attention has been aimed at metal requirements for microbes involved in the cycling of non- CO_2 greenhouse gases, although many of these organisms also live in ecosystems with very low metal bioavailability. A notable exception is the enormous wealth of literature generated by the wastewater scientific community about metal (particularly Fe, Ni, and Co) controls on methanogenesis in anaerobic digesters (see Demirel and Scherer, 2011).

The purpose of this article is to review the current state of literature on the metalloenzymes and trace metal physiology of organisms involved in CH_4 and N_2O processing. In each section, we discuss environmental studies if they exist and compare metal concentrations for optimal growth of pure cultures to measured values of trace metals in natural environments. In the final sections of the article, we compare the metal requirements of microbes involved in the CH_4 and N_2O cycles and discuss future research directions. Readers are referred to previous reviews (Rogers and Whitman, 1991; Conrad, 1996) for other aspects of microbial controls on greenhouse gas cycling.

METHANOGENESIS

Methanogenesis is the microbial process whereby CO_2 , acetate, or methyl-compounds are converted to methane in order to generate ATP through the build-up of a sodium ion or proton gradient. All methanogens are in the Euryarchaeota phylum (Whitman et al., 2006) and account for 75–80% of the annual global production of CH_4 (IPCC, 2007). Approximately two-thirds of biologically produced CH_4 is generated by acetoclastic methanogens that oxidize the carbonyl group of acetate to CO_2 and reduce the methyl group to CH_4 (Rogers and Whitman, 1991; Ferry, 2010b). The remaining one-third of biogenic methane is produced by reduction of CO_2 with electrons from H_2 or formate and the conversion of methyl groups from compounds such as methanol, methylamines, and dimethylsulfide. Therefore, methanogenesis is divided into three pathways: hydrogenotrophic (i.e., CO_2 reduction), acetoclastic (acetate disproportionation), and methylotrophic (C1 utilization). The three pathways differ in the enzymes used to generate methyl-tetrahydro(methano/sarcina)pterin ($\text{CH}_3\text{-H}_4(\text{M/S})\text{PT}$), the intermediate common to all pathways, but converge in the last two steps used to generate CH_4 (Ferry, 2010b).

In the first section we review the metal inventory of metalloenzymes in each of the three pathways. This is not intended as a definitive review as many of these enzymes are still understudied and more complete reviews of methanogenic enzymes are available (Thauer, 1998; Thauer et al., 2008, 2010). Instead, our goal is to estimate the transition metal stoichiometry of the three methanogenic pathways, illustrated in **Figure 1**. In the next section we discuss physiological studies of the metal requirements for methanogenesis and relate these findings back to the metal content of each pathway. Pure culture, anaerobic digester, and environmental studies are reviewed. Lastly, a summary of previous studies examining metal requirements for methanogenesis is provided, and topics warranting further research are discussed. This general format is also used in the sections on methanotrophy (see Methanotrophy) and nitrous oxide cycling (see Nitrous Oxide Production and Consumption).

METALLOENZYMES IN METHANOGENESIS

Methanogenesis is one of the most metal-rich enzymatic pathways in biology (Zerkle et al., 2005). Depending on the pathway, exact metal requirements may differ, but the general trends remain the same: Fe is the most abundant metal, followed by Ni and Co, and smaller amounts of Mo (and/or W) and Zn. Fe is primarily present as Fe-S clusters used for electron transport and/or catalysis. Ni is either bound to Fe-S clusters or in the center of a porphyrin unique to methanogens, cofactor F_{430} . Co(balt) is present in cobamides involved in methyl group transfer. Zn occurs as a single structural atom in several enzymes. Mo or W is bound to a pterin cofactor to form “molybdopterin” or “tungstopterin,” which catalyze two-electron redox reactions. Other alkali metals and metalloids, such as Na and Se, are essential for methanogenesis, but the discussion here is limited to the transition metals. So far, no Cu-dependent methanogenesis enzymes have been identified, which is striking given the huge importance of Cu in aerobic methanotrophy (see the Section “Aerobic Methanotrophy”). It is plausible that scarce Cu in anaerobic early-earth marine ecosystems selected for use of other metals (i.e., Fe, Ni, and Co) in primitive methanogens whereas Cu was more bioavailable to aerobic methanotrophs after the rise of atmospheric oxygen (Dupont et al., 2006, 2010; David and Alm, 2010).

Most methanogen orders – Class I (Methanobacteriales, Methanococcales, and Methanopyrales) and Class II (Methanomicrobiales) – obtain energy by reducing CO_2 to CH_4 using electrons from H_2 or in some cases formate (Anderson et al., 2009). These methanogens do not contain cytochrome proteins, in which Fe is bound to heme. Only one order of methanogens, the Methanosarcinales (Class III), contain cytochromes and are capable of metabolizing a wider range of substrates for methanogenesis, including methanol, methylamines, methyl sulfides, acetate, and/or CO_2 with H_2 . Members of the Methanosarcinales play a key ecological role because the acetoclastic pathway is estimated to account for two-thirds of biologically sourced methane (Rogers and Whitman, 1991).

The Fe requirement for methanogenesis is vast: almost every metalloenzyme involved in the pathway contains multiple Fe_2S_2 , Fe_3S_4 , or Fe_4S_4 clusters. The first enzyme in the CO_2 reduction pathway, formylmethanofuran dehydrogenase (abbreviated Fmd

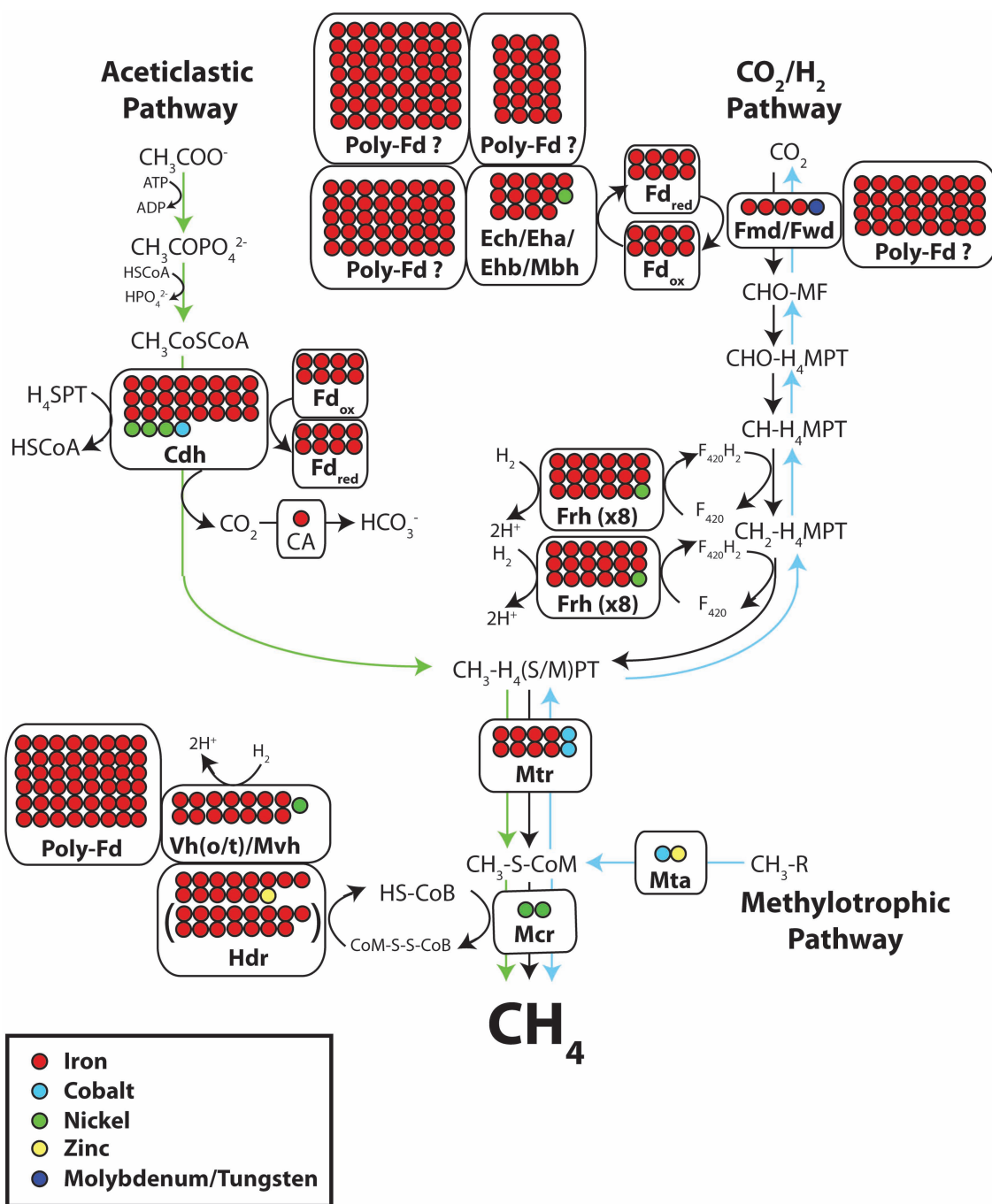


FIGURE 1 | Metal content of metalloenzymes in the three pathways of methanogenesis: H₂/CO₂ (black arrows), aceticlastic (green arrows), and methylotrophic (blue arrows). Each circle represents one metal atom. Parentheses show varying metal content of a given enzyme. Question marks mean that enzyme may not be present in all methanogens (6x[Fe₄S₄] and 10x[Fe₄S₄]polyferredoxins are encoded in the *eha* operon and a 14x[Fe₄S₄]polyferredoxin is encoded in the *ehb* operon). Abbreviations: CA, carbonic anhydrase; Cdh, carbon monoxide dehydrogenase/acetyl-CoA synthase; Ech/Eha/Ehb/Mbh,

energy-converting hydrogenase; Fd, ferredoxin; Fmd/Fwd, Mo/W formylmethanofuran dehydrogenase; Frh, F₄₂₀-reducing hydrogenase; Hdr, heterodisulfide reductase; Hmd, Ni-free Fe hydrogenase; Mcr, methyl coenzyme M reductase; Mta, methanol-coenzyme M methyltransferase; Mtr, CH₃-H₄(S)PT-coenzyme M methyltransferase; Vh(o/t)/Mvh, Ni-Fe hydrogenase. For simplicity, only metalloenzymes are labeled. See the Section "Metalloenzymes in Methanogenesis" for more details, abbreviations for intermediates and enzyme substitutions that occur in specific conditions and species.

for the Mo form and Fwd for the W form) can bind up to nine Fe₄S₄ clusters: one cluster in the Mo/W-pterin binding subunit and up

to eight additional clusters in polyferredoxin (Vorholt et al., 1996; **Figure 1**). It is likely that Fwd can bind additional Fe₄S₄ clusters

(Ferry, 1999). Ferredoxins that transfer electrons from H_2 to other methanogenesis enzymes require additional Fe in the form of two Fe_4S_4 clusters (Daas et al., 1994).

All hydrogenases involved in methanogenesis are Ni-Fe enzymes that oxidize H_2 and reduce ferredoxin, coenzyme F_{420} , and other electron carriers (Thauer et al., 2010). The four different types of Ni-Fe hydrogenases involved in methanogenesis all contain abundant Fe. The energy-converting membrane-associated hydrogenase [abbreviated Ech, Eha, Ehb, or Mbh depending on the class of methanogen (Anderson et al., 2009)] contains three Fe_4S_4 clusters and a Ni-Fe active site (Thauer et al., 2010), and can contain additional polyferredoxin subunits with 6, 10, or 14 Fe_4S_4 clusters (Tersteegen and Hedderich, 1999; **Figure 1**).

Another Ni-Fe hydrogenase is used to reduce coenzyme F_{420} . Coenzyme F_{420} , a flavin derivative that plays a critical role in two intermediate electron-transfer steps in methanogenesis, is reduced with H_2 by the cytoplasmic hydrogenase Frh (Alex et al., 1990). The Frh enzyme complex contains a Ni-Fe active site and four Fe_4S_4 clusters (**Figure 1**), and forms large aggregates, multiplying its metal requirements approximately eightfold (Fox et al., 1987). Under conditions of Ni limitation, some methanogens without cytochromes substitute Frh for a Ni-free Fe hydrogenase (Hmd) to decrease Ni requirements (Afting et al., 1998). The Ni-free Fe hydrogenase has a significantly lower Fe requirement, using only two Fe atoms per complex (Zirngibl et al., 1992; Shima et al., 2008; Thauer et al., 2010). When formate is used as an electron source instead of H_2 , Frh is replaced by formate dehydrogenase (Fdh), which contains one Mo/W-pterin cofactor, two Zn atoms and between 21 and 24 Fe atoms (Schauer and Ferry, 1986).

Co(balt)-containing methyltransferases are essential for methanogenesis. All methanogens utilize the energy-conserving $CH_3-H_4M(S)PT$ -coenzyme M methyltransferase (Mtr) to transfer the methyl group from $CH_3-H_4M(S)PT$ to HS-CoM. The Mtr enzyme complex contains two cobamide cofactors (with one Co each) and eight Fe atoms (Gartner et al., 1993). A wide range of other Co(balt)-containing methyltransferases are required for methyl coenzyme M formation in methylotrophic methanogens, some of which contain additional metals (Thauer, 1998). For instance, the methanol-coenzyme M methyltransferase enzyme (Mta) expressed by methanol-utilizing methanogens contains one Zn in addition to one cobalamin Co (Hagemeier et al., 2006).

Heterodisulfide reductase (Hdr) is an Fe-S and Zn-containing enzyme that catalyzes the reduction of heterodisulfide (CoM-S-S-CoB) to form HS-CoM and HS-CoB in the second-to-last step in methanogenesis. In methanogens without cytochromes, Hdr has three subunits (HdrABC) whereas methanogens with cytochromes have a two-subunit protein (HdrDE; Hedderich et al., 2005; Thauer et al., 2008). HdrABC contains seven Fe_4S_4 clusters and one structural Zn atom (Hamann et al., 2007) and forms a tight complex with the Ni-Fe hydrogenase Mvh, which contains one Ni-Fe active site, one Fe_2S_2 cluster, two Fe_4S_4 clusters, one Fe_3S_4 cluster, and polyferredoxin with 12 Fe_4S_4 clusters (Reeve et al., 1989; **Figure 1**). In *Methanosarcinales*, HdrDE is reduced by methanophenazine, a lipid-soluble electron, and proton carrier with very low redox potential. HdrDE contains three Fe_4S_4 clusters, one heme *b* cofactor, and one structural Zn atom (Heiden et al., 1994; Kunkel et al., 1997; Simianu et al., 1998).

Methanophenazine is in turn reduced by the Ni-Fe hydrogenase Vht/Vho, which contains one Ni-Fe center, two *b*-type hemes, one Fe_3S_4 cluster, and two Fe_4S_4 clusters (Deppenmeier et al., 1992; Thauer et al., 2010). In the marine strain *Methanosarcina acetivorans*, Vht/Vho is replaced by Rnf, which contains six Fe_4S_4 clusters and no Ni, and uses reduced ferredoxin instead of H_2 (Li et al., 2006; Ferry, 2010a).

Methyl coenzyme M reductase (Mcr), common to all methanogenic pathways, catalyzes the final step in methanogenesis: the reduction of $CH_3-S-CoM$ to CH_4 and the formation of CoM-CoB heterodisulfide with electrons derived from HS-CoB. The crystal structure of Mcr has been solved and contains two coenzyme F_{430} Ni tetrapyrroles (Ermler et al., 1997). Previous studies have shown that the F_{430} content of cells is dependent on cellular Ni content (Diekert et al., 1980, 1981; Lin et al., 1989). Methanogens actively transport Ni and Co using ATP-dependent uptake systems in order to fulfill enzymatic requirements (Jarrell and Sprott, 1982; Baudet et al., 1988; Rodionov et al., 2006; Zhang et al., 2009).

When grown on acetate, methanogens use two metalloenzymes for the conversion of the methyl group from acetate to CH_3-H_4SPT , which differ from those used in CO_2 reduction and methylotrophic pathways. The most metal-rich aceticlastic enzyme is CO dehydrogenase/acetyl-CoA synthase (Cdh), which cleaves the methyl group off of acetyl-CoA and transfers it to CH_3-H_4SPT . The Cdh complex contains one Fe_4S_4 cluster bridged to an Ni-Ni site (Funk et al., 2004), four Fe_4S_4 clusters and a $NiFe_4S_4$ cluster (Gong et al., 2008), and reduces a $2 \times [Fe_4S_4]$ ferredoxin (Terlesky and Ferry, 1988; Ferry, 2010b). The CO_2 by-product of Cdh is converted to bicarbonate by an Fe-containing carbonic anhydrase (CA) instead of the Zn-form, which is commonly in CAs from other species (Macauley et al., 2009). Overall, the metal content of enzymes involved in aceticlastic methanogenesis is similar to the H_2/CO_2 pathway (**Figure 1**). The Fe and Mo/W requirements are likely lower in the aceticlastic pathway because the Fe-rich polyferredoxins involved in the CO_2 reduction route are not present, nor is Fmd/Fwd.

PHYSIOLOGICAL STUDIES OF TRACE METAL REQUIREMENTS FOR METHANOGENESIS

Previous physiological studies of metals as micronutrients for methanogenesis have been compromised by significant metal contamination in growth vessels and sampling equipment. The requirements for gas-tight material to maintain anaerobic conditions has favored the use of glass culturing bottles with butyl rubber stoppers and stainless steel needles for sampling, both of which are notoriously dirty with respect to metals. In fact, Ni requirements for methanogens were overlooked in early studies due to the high Ni content ($\sim 10\%$) of stainless steel syringe needles. Dissolution of Ni in stainless steel needles by H_2S in the media supplied ample Ni for growth of methanogens on media not supplemented with Ni salts (S. Zinder, personal comm, 2011; Diekert et al., 1981; Whitman et al., 1982). The need for anaerobic conditions excludes the use of acid-washed plastics, which have extremely low metal contamination and are commonly used for trace metal limitation experiments with aerobes, but are permeable to O_2 diffusion. To address these concerns, researchers have

acid-washed glassware with sulfuric acid, treated butyl rubber stoppers, and polypropylene pipet tips with NaHCO₃/EDTA and covered cannula needles with Teflon tubing (Whitman et al., 1982; Sowers and Ferry, 1985). Such methods were used in some, though not all, of the studies reviewed in the Section “Pure Cultures.” To our knowledge, Teflon-lined glass bottles have not been used to minimize metal contamination in previous anaerobic studies, but may be a good option for future research.

The experiments discussed in Section “Mixed Cultures and Anaerobic Bioreactors” on mixed cultures and anaerobic bioreactors were conducted, for the most part, not in defined media but rather in sludge or wastewater treatment effluent. Studies of metal requirements for pure cultures and anaerobic digesters typically report only total added metal, although these reactors usually have higher background metal contents than pure cultures. However, the ubiquitous presence of sulfide, carbonate, and phosphate in methanogenic cultures leads to metal precipitation, so dissolved metal concentrations generally decline throughout experiments (Callander and Barford, 1983a,b). Indeed, precipitation–dissolution kinetics of metal sulfides may play a key role in bioavailability of metals in anaerobic digesters (Gonzalez-Gil et al., 1999; Jansen et al., 2007). However, increased rates of methanogenesis after addition of a particular metal are clear evidence of environmental (albeit human-contributed) metal limitation as compared to axenic cultures.

Pure cultures

Based on the metal content of the enzymes involved in methanogenesis, one would predict that methanogens require very high

concentrations of Fe, relatively high levels of Ni and Co, trace Zn and Mo/W, and negligible amounts of Cu and Mn. This prediction does not take into account complications if enzymes have differing K_m values for their respective substrates, which could result in shifts in enzyme ratios, nor does it consider metal requirements for metabolic pathways besides methanogenesis. Nevertheless, it roughly agrees with the cellular metal contents of 11 previously analyzed methanogens, which contained 700–2800 ppm Fe, 17–180 ppm Ni, 23–1810 ppm Zn, 10–120 ppm Co, 10–70 ppm Mo, <10–160 ppm Cu, and 2–27 ppm Mn, in terms of dry weight (Diekert et al., 1981; Whitman et al., 1982; Scherer et al., 1983). These data suggest that the metal requirements for methanogenesis have a strong influence on whole cell metal contents.

Early studies on *Methanobacterium thermoautotrophicum* (renamed *Methanothermobacter thermautotrophicus*) grown on H₂ and CO₂ showed that low concentrations of Fe, Ni, Co, and Mo in growth media could limit growth (Taylor and Pirt, 1977; Schönheit et al., 1979). For the formation of 1 g of biomass (dry weight), 10 μmol of Fe, 150 nmol of Ni, 20 nmol of Co, and 20 nmol of Mo were required, a stoichiometry of 500 Fe: 7.5 Ni: 1 Co: 1 Mo (Schönheit et al., 1979). Optimal growth was observed at 300–500 μM Fe (Patel et al., 1978) and 1 μM Ni, while addition of Cu, Zn, and Mn to the media did not stimulate growth (Schönheit et al., 1979; Table 1). Interestingly, optimal growth of another H₂/CO₂-utilizing methanogen, *Methanococcus voltae*, occurred at much lower Fe and Ni concentrations (10 and 0.2 μM, respectively), despite the more rigorous cleaning protocols used in this study (Whitman et al., 1982).

Table 1 | Optimal dissolved metal concentrations (calculated from total amounts of salt added) in defined growth media for pure methanogenic cultures grown on H₂/CO₂, formate, acetate, methanol, or trimethylamine.

Metal	Substrate	Concentration (μM)	Species	Reference
Fe	H ₂ /CO ₂	300–500	<i>Methanospirillum hungatei</i> , <i>Methanobacterium bryantii</i> strain MOH	Patel et al. (1978)
	H ₂ /CO ₂	>15	<i>Methanococcus voltae</i>	Whitman et al. (1982)
	Acetate	100	<i>Methanotherx soehngenii</i> VNB ¹	Fathepure (1987)
	Methanol	50	<i>Methanosarcina barkeri</i>	Lin et al. (1990)
	Trimethylamine	5	<i>Methanococcoides methylutens</i>	Sowers and Ferry (1985)
Ni	H ₂ /CO ₂	1	<i>Methanobacterium thermoautotrophicum</i> ²	Schönheit et al. (1979)
	H ₂ /CO ₂	0.2	<i>Methanococcus voltae</i>	Whitman et al. (1982)
	Acetate	2	<i>Methanotherx soehngenii</i> VNB ¹	Fathepure (1987)
	Methanol	0.1	<i>Methanosarcina barkeri</i>	Scherer and Sahm (1981)
	Trimethylamine	0.25	<i>Methanococcoides methylutens</i>	Sowers and Ferry (1985)
Co	Acetate	2	<i>Methanotherx soehngenii</i> VNB ¹	Fathepure (1987)
	Methanol	1	<i>Methanosarcina barkeri</i>	Scherer and Sahm (1981)
	Trimethylamine	0.1	<i>Methanococcoides methylutens</i>	Sowers and Ferry (1985)
Mo	Acetate	2	<i>Methanotherx soehngenii</i> VNB ¹	Fathepure (1987)
	Methanol (with NH ₄ ⁺)	0.5	<i>Methanosarcina barkeri</i>	Scherer and Sahm (1981), Scherer (1988)
	Methanol (N ₂ -fixing)	5	<i>Methanosarcina barkeri</i>	Scherer (1988)
W	H ₂ /CO ₂	1	<i>Methanocorpusculum parvum</i>	Zellner and Winter (1987)
	Formate	0.5	<i>Methanocorpusculum parvum</i>	Zellner and Winter (1987)

¹ Renamed *Methanosaeta concilii*; ² Renamed *Methanothermobacter thermautotrophicus*.

Adapted from Takashima and Speece (1990).

How do metal requirements change when methanogens are grown on substrates other than H_2/CO_2 ? Optimal growth of *Methanotherix soehngenii* VNBF (renamed *Methanosaeta concilii*) grown on acetate was observed at $100\text{ }\mu\text{M}$ Fe, $2\text{ }\mu\text{M}$ Ni, $2\text{ }\mu\text{M}$ Co, and $2\text{ }\mu\text{M}$ Mo (Fathepure, 1987; **Table 1**). Optimal growth of methanol-utilizing *Methanosarcina barkeri* was observed at lower concentrations: $50\text{ }\mu\text{M}$ Fe, $0.1\text{ }\mu\text{M}$ Ni, $1\text{ }\mu\text{M}$ Co and $0.5\text{ }\mu\text{M}$ Mo, and addition of Cu and Mn had no effect on growth (Scherer and Sahm, 1981; Lin et al., 1990). Optimal growth of trimethylamine-grown *Methanococcoides methylutens* was lower still: $5\text{ }\mu\text{M}$ Fe, $0.25\text{ }\mu\text{M}$ Ni, and $0.1\text{ }\mu\text{M}$ Co, with no stimulation by addition of Mo, Zn, Mn, W, and Cu (Sowers and Ferry, 1985). These studies suggest that metal requirements are higher on acetate than methyl-compounds, although the opposite – particularly for Co – has been found in mixed culture anaerobic digester studies (see the Section “Mixed Cultures and Anaerobic Bioreactors”).

In some methanogens, W-containing formylmethanofuran dehydrogenases (Fwd) and W-containing formate dehydrogenases (W-Fdh) are expressed in place of Mo-containing forms of the enzymes. W was first shown to stimulate growth of *Methanococcus vannielii* on formate (Jones and Stadtman, 1977). A subsequent study revealed that optimal growth on H_2/CO_2 required more W ($1\text{ }\mu\text{M}$) than growth on formate ($0.5\text{ }\mu\text{M}$) and that more W was incorporated into cells during growth on H_2/CO_2 than on formate (Zellner and Winter, 1987), suggesting that Fwd has a higher W requirement than W-Fdh.

In addition to metal cofactors in enzymes directly involved in methanogenesis, additional metals are required for other metabolic pathways in methanogens, such as nitrogen fixation. In a study of metal requirements for two strains of *M. barkeri*, Scherer (1988) found that optimal Mo media concentrations for diazotrophic growth were $10\times$ greater ($5\text{ }\mu\text{M}$ Mo) than NH_4 -based growth ($0.5\text{ }\mu\text{M}$ Mo). One of the two strains (strain 227) could grow just as well with vanadium (V) instead of Mo in the media, suggesting that it contained a V-nitrogenase (Scherer, 1988) as later confirmed by Chien et al. (2000). However, differing results have been published regarding the extent to which V stimulates nitrogen fixation in this strain (Lobo and Zinder, 1988). Other methanogens, such as *Methanococcus maripaludis*, lack the V-nitrogenase and have an absolute requirement for Mo for diazotrophy (Kessler et al., 1997).

Mixed cultures and anaerobic bioreactors

The potential of metals to increase the efficiency of methanogenesis in industrial settings has led to a steady stream of studies on metal requirements for optimal functioning of anaerobic waste (sewage, agricultural, and food-processing) treatment bioreactors since the late 1970s (Demirel and Scherer, 2011). The production of methane from small organic molecules such as acetate and methanol in waste treatment reactors is a beneficial by-product because it can be captured and used as a renewable fuel source.

Several studies suggest that the addition of Fe, Ni, and Co can increase the rate of aceticlastic methanogenesis in anaerobic digesters. An early study of aceticlastic methanogenesis in mixed cultures originally obtained from sewage sludge and maintained in a defined medium showed that the optimal soluble Fe concentrations for methanogenesis were $0.2\text{--}2\text{ mM}$ (lower than the total

$5\text{--}10\text{ mM}$ FeCl_2 added due to precipitation as ferrous carbonate), whereas background soluble Fe was $\sim 25\text{ }\mu\text{M}$ (Hoban and van den Berg, 1979). The authors suggested that mixed methanogenic cultures might have higher Fe requirements than pure cultures. Addition of Ni and Co stimulated aceticlastic methanogenesis and increased the thickness of biofilms in anaerobic food waste digesters (Murray and van den Berg, 1981), municipal sludge digesters (Speece et al., 1983), and synthetic wastewaters (Kida et al., 2001). Addition of Mo (50 nM) had a smaller effect (Murray and van den Berg, 1981). In another study, individual addition of Fe, Ni, Co, Mn, Zn, Mo, and Cu to a wastewater treatment sludge did not produce any significant increase in the conversion of acetate to methane (Florencio et al., 1993). It is possible that the sludge in the latter study contained sufficient metal carry-over that these metals were not limiting for aceticlastic methanogenesis. Metal speciation almost certainly influences bioavailability in these bioreactors, where up to 95% of dissolved Ni and Co is present in strongly bound forms (Jansen et al., 2005). It is currently unknown whether methanogens can directly take up soluble metal-sulfide complexes or metal-organic complexes (Jansen et al., 2007). Additionally, temperature may exert influence on the trace metal requirements; higher trace metal requirements have been found for thermophilic than mesophilic mixed reactors, despite smaller biomass yield (Takashima et al., 2011).

Limitation of methanogenesis by low Co(balt) bioavailability has been identified in numerous studies of anaerobic mixed cultures grown on methanol. A study of methylotrophic methanogens in wastewater treatment sludge showed a pronounced increase in methanogenic activity when Co was added, and a significant decline when it was absent from the media (Florencio et al., 1993). Follow-up studies have confirmed the high Co(balt) requirements for methanol-grown anaerobic bioreactors (Zandvoort et al., 2006). The same trend was observed for Ni, although to a lesser extent, but minimal effect was found for other metals (Fe, Zn, Mo, Cu, and Zn). Optimal Ni and Co concentrations for methanogenesis was $\sim 2\text{ }\mu\text{M}$ (Florencio et al., 1993, 1994; Zandvoort et al., 2002). The increased need for Co for methanol-based growth vs. other substrates is likely due to additional Co(balt)-containing methyltransferases required for growth on methyl-compounds. This concurs with previous findings that the highest amount of corrinoids are produced in methanogens grown on methanol compared to other substrates, with about $3\times$ as much corrinoids in methanol-grown cell vs. acetate-grown cells (Krzycki and Zeikus, 1980) and that cobalamin production increases with media Co concentration up to $\sim 50\text{ }\mu\text{M}$ (Lin et al., 1989).

Environmental studies

Very few studies have investigated the effects of metal additions on natural methanogenic ecosystems. To our knowledge, the only published experiment was performed in five North American peatlands (Basiliko and Yavitt, 2001). Ambient dissolved metal concentrations in mineral-poor peatlands were low ($2\text{--}20\text{ nM}$ Ni, 30 nM Co, and $<2\text{ }\mu\text{M}$ Fe) due to the high metal-binding capacity of peat. In mineral-rich peatlands, concentrations were $40\text{--}60\text{ nM}$ Ni, $2\text{--}5\text{ }\mu\text{M}$ Co, and $20\text{--}30\text{ }\mu\text{M}$ Fe. The authors found that combined addition of Fe ($12\text{ }\mu\text{M}$), Ni ($12\text{ }\mu\text{M}$), and Co ($6\text{ }\mu\text{M}$) to mineral-poor surface samples resulted in an enhancement of

CH₄ production, whereas no effect or inhibition was observed at mineral-rich peatlands. The effect of individual metals was not tested. No effect was observed for CO₂ production in mineral-poor peatlands, suggesting that heterotrophic microbes are not as metal-limited as methanogens. Addition of the chelator citrate, but not EDTA, led to increased CH₄ production in the peat with the lowest metal concentrations, suggesting either that methanogens can take up metal–citrate complexes or that they can compete with citrate for metal-binding.

Other anoxic ecosystems have similar trace metal concentrations to peat bogs, suggesting that metal limitation of methanogenesis may be widespread in natural environments. The concentration range of Ni, Co, and Mo in five representative anoxic waters was consistently below the optima for growth of pure cultures (Tables 1 and 2). Optimal methanogenic growth occurs at 0.2–2 μM Ni and in natural anoxic waters Ni ranges from 0.002 to 0.07 μM. Optimal media concentrations of Co are 0.1–2 μM and in natural environments Co is generally <0.02 μM. Optimal Mo concentrations are 0.5–5 μM; ambient Mo is 0.01–0.2 μM in anoxic environments. Zn is also generally very low (<0.04 μM) in anoxic waters, and may contribute to trace metal limitation of methanogenesis, although pure culture studies are not available to determine optimal Zn concentrations. The opposite is true for W: few data are available on *in situ* W concentrations, but in most ecosystems W is below the growth optima of 0.5–1 μM. Optimal Fe concentrations are present in anoxic sediment pore waters (such as the Santa Monica Basin) where Fe reaches 200 μM, but other anoxic waters have significantly lower Fe (Table 2). Therefore, it is quite reasonable to expect that bioavailability of trace metals may be important limiting growth factors in natural methanogenic environments.

SUMMARY AND AREAS FOR FUTURE RESEARCH

Based on the metal content of enzymes in methanogenesis, one would predict (1) roughly equal Fe, Ni, and Zn requirements for CO₂ reduction, aceticlastic, and methylotrophic pathways; (2) higher Mo/W requirements for CO₂ reduction and methylotrophic pathways than aceticlastic methanogenesis; and (3) higher Co(balt) requirement for the methylotrophic pathway than CO₂ reduction and aceticlastic pathways. Previous studies are difficult to compare because few of them simultaneously vary methanogenic pathways using the same experimental conditions

and/or organism. Every laboratory likely had different levels of trace metal contamination and metal-sulfide precipitation, and thus the given optimal metal concentrations are all estimates to varying degrees. Nonetheless, a few trends are clear: (1) Fe concentrations required for optimal growth in media are much higher than all other metals (in the 10^{−5} to 10^{−4} M range); (2) optimal Ni, Co, Mo, and W concentrations are in the 10^{−7} to 10^{−6} M range, and higher Mo concentrations (10^{−5} M) are needed for diazotrophic growth; (3) addition of Cu and Mn is not needed for growth. Few studies have investigated Zn requirements for methanogenesis, although Zn is present in at least two enzymes in the pathway.

Studies of anaerobic digesters and peatlands suggest that Fe, Ni, and Co – and possibly other metals – may limit methanogenesis in the natural ecosystems. The high Co(balt) requirement for methylotrophic methanogenesis in anaerobic digesters is of particular interest. To our knowledge, only one study has looked into the possibility of metal limitation of methanogenesis in a natural setting (Basiliko and Yavitt, 2001). More environmental studies are essential to better understand the nature of metal bioavailability and/or limitation in the ecosystems that contribute 75–80% of the world's annual CH₄ sources, but preliminary comparison of optimal concentrations for growth of pure cultures and *in situ* levels shows that trace metal (particularly Ni and Co) limitation of methanogenesis may be widespread in anoxic settings.

METHANOTROPHY

Methanotrophy is the microbial process whereby CH₄ is oxidized as an energy and carbon source. Aerobic methanotrophy is estimated to consume ~35% (0.6 Gt) of the total global CH₄ produced per year, whereas anaerobic methanotrophy is estimated to consume ~18% (0.3 Gt; Thauer, 2011). Aerobic methanotrophy is performed by certain bacteria that combine molecular oxygen with CH₄ to produce methanol (CH₃OH). Methanol is then oxidized to formaldehyde (CH₂O), which is incorporated into organic compounds using either the serine or ribulose monophosphate pathway (Semrau et al., 2010). Sulfate-dependent anaerobic methane oxidation (AOM) occurs primarily in anoxic marine sediments and is performed by archaea that have not been isolated in pure culture, but are most closely related to Methanosarcinales and Methanomicrobiales. These archaea are believed to oxidize methane anaerobically through a reverse methanogenesis pathway

Table 2 | Compiled dissolved trace metal concentrations in representative anoxic waters.

Sample site	Fe	Ni	Co	Cu	Zn	Mo	Reference
Peat bog waters	0.4–40	0.002–0.07	0.002–4	0.02–2			Basiliko and Yavitt (2001), Bragazza (2006)
Santa Monica basin sediment pore waters (>5 cm depth)	100–200	0.01	0.01–0.02	<0.005		0.2	Shaw et al. (1990)
Black Sea sulfidic water column (>200 m)	0.01–0.3	0.01	<0.004	<0.002	<0.004	<0.01	Haraldsson and Westerlund (1988), Emerson and Huested (1991)
Framvaren Fjord water column (>20 m)	0.03–2	<0.07	0.001–0.01	<0.001	0.002–0.01	<0.04	Haraldsson and Westerlund (1988), Emerson and Huested (1991)
Baltic Sea water column (>150 m)	0.1–2	0.01	<0.002	<0.007	0.01–0.04		Kremling (1983)

All concentrations are in units of micromolar (μM).

(Scheller et al., 2010; Thauer, 2011). Thus, phylogenetically unrelated aerobic and anaerobic methanotrophs accomplish the same task using very different enzymes (Chistoserdova et al., 2005) and are therefore predicted to have different metal requirements. Cu requirements for aerobic methanotrophy have been the subject of a great deal of research, whereas metal requirements for AOM are just beginning to be explored, but are expected to be similar to metal requirements for methanogenesis.

AEROBIC METHANOTROPHY

Aerobic methanotrophs (abbreviated “MOB” for “methane-oxidizing bacteria”) are commonly found at oxic/anoxic interfaces of environments where CH₄ is produced. Methanotroph genera, beginning with “*Methylo-*,” are found in the Gammaproteobacteria and Alphaproteobacteria (Hanson and Hanson, 1996; Semrau et al., 2010). Recently, MOB have also been discovered in the Verucomicrobia (Op den Camp et al., 2009). Furthermore, the newly discovered freshwater phylum NC10 bacterium *Methylomirabilis oxyfera* performs intra-aerobic methane oxidation using pMMO and internally produced O₂ from NO (Ettwig et al., 2010; Wu et al., 2011). In addition to being important in greenhouse gas processing, some MOB play important roles in pollutant degradation and bioremediation (Semrau, 2011).

Metalloenzymes in aerobic methanotrophy

Classical aerobic methanotrophy. The metal requirements for MOB are largely regulated by copper (Cu) availability. When Cu is abundant, MOB express a membrane-bound Cu (and possibly Fe and Zn)-containing enzyme (particulate methane monooxygenase, pMMO) that catalyzes the first step of CH₄ oxidation. When Cu is lacking, some MOB can synthesize a soluble protein for methane oxidation that contains Fe instead of Cu (soluble methane monooxygenase, sMMO). Subsequent enzymatic steps in aerobic methanotrophy rely primarily on Fe, with lesser amounts of Ca, Mo, and possibly Zn (Figure 2). Below is a general overview of the metal content of enzymes in methanotrophy. For a more extensive discussion of the biochemistry of aerobic methanotrophy, the reader is referred to other reviews (Hanson and Hanson, 1996; Hakemian and Rosenzweig, 2007; Trotsenko and Murrell, 2008; Semrau et al., 2010; Chistoserdova, 2011).

The first step of aerobic methanotrophy, the oxidation of CH₄ to CH₃OH, is catalyzed by methane monooxygenase (MMO). All aerobic methanotrophs (with the exception of facultative methanotrophic species in the genus *Methylocella*) are capable of expressing pMMO (Hanson and Hanson, 1996). The metal content of pMMO has been a matter of debate for many years, namely regarding whether the active site coordinates Fe or Cu for function (Bollinger, 2010). Crystal structures and experiments have provided strong evidence that the active site is a two Cu center in the pMMO-B subunit (Lieberman and Rosenzweig, 2005; Balasubramanian and Rosenzweig, 2007; Hakemian et al., 2008; Balasubramanian et al., 2010). An additional mono-nuclear Cu atom is present in one of crystal structures (from *Methylococcus capsulatus* Bath) but not in *Methylosinus trichosporium* OB3b and is not required for CH₄ oxidation (Balasubramanian et al., 2010). Crystal structures predict coordination of another metal ion (Zn in *M. capsulatus* Bath and Cu in *M. trichosporium* OB3b), positioned

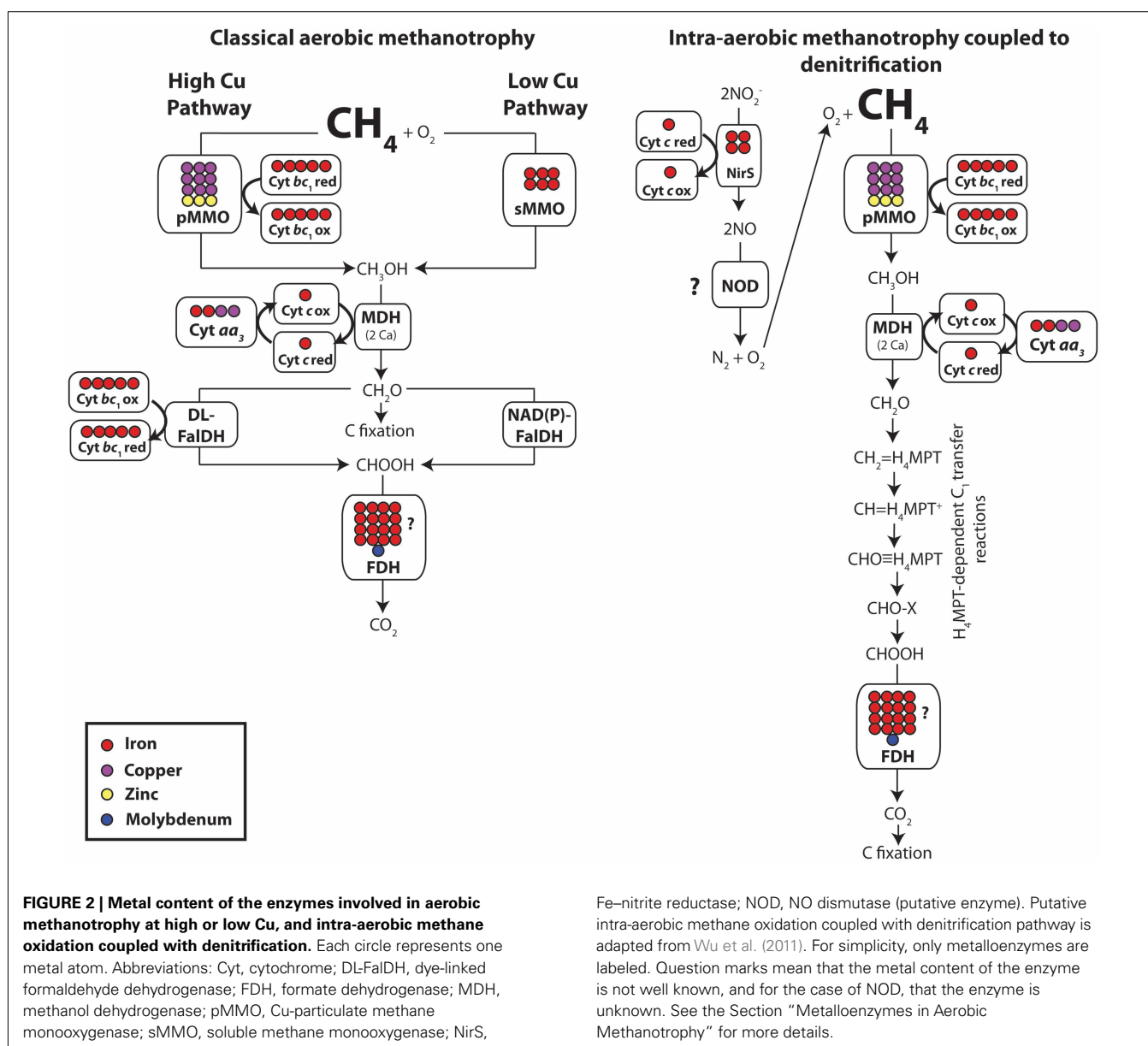
between the pMMO-B and pMMO-C subunits (Lieberman and Rosenzweig, 2005; Hakemian et al., 2008). Since pMMO is a heterotrimer, it therefore contains nine Cu atoms (and possibly three Zn atoms; Figure 2). Recent Mössbauer evidence suggests that Fe could also be present in pMMO, as supported by previous protein preparations that contained Fe (Martinho et al., 2007; Semrau et al., 2010). The electron donor to pMMO is a cytochrome *bc₁* complex, containing three heme groups and one Fe₂S₂ cluster (Zahn and DiSpirito, 1996).

Several strains of aerobic methanotrophs are also capable of expressing a cytoplasmic soluble MMO (sMMO), which contains a dimeric hydroxylase with two Fe ions in a di-Fe active site cluster and an additional Fe₂S₂ cluster in a reductase subunit (Lipscomb, 1994; Merckx et al., 2001). Expression of particulate vs. soluble MMO is regulated by Cu availability (Murrell et al., 2000). Work with pure cultures has shown that a “Cu switch” occurs at 0.85–1 µmol/g dry weight: at lower Cu:biomass ratios, sMMO is expressed, and at higher Cu:biomass ratios, pMMO is expressed (Stanley et al., 1983; Hanson and Hanson, 1996; Nielsen et al., 1997). In contrast to pMMO, the electron donor to sMMO is NADH (Lipscomb, 1994; Merckx et al., 2001).

After CH₄ is oxidized to CH₃OH by either pMMO or sMMO, the periplasmic pyrroloquinoline quinone-dependent enzyme methanol dehydrogenase (abbreviated MDH or Mxa) oxidizes CH₃OH to formaldehyde (CHOH) using two cytochrome *c* proteins (*c_L* and *c_H*) as electron acceptors (Hanson and Hanson, 1996). These cytochromes are then oxidized by cytochrome *aa₃*, containing two hemes and two Cu atoms (Figure 2). MDH/Mxa does not contain any transition metal cofactors, but does possess 2 mol of Ca per mole of tetramer. Approximately 50% of the CHOH produced by MDH/Mxa is assimilated into biomass, and the other half is further oxidized to formate (CHOOH) and then to CO₂ to generate reducing equivalents (Hanson and Hanson, 1996; Trotsenko and Murrell, 2008; Chistoserdova, 2011). This step is mediated by either a membrane-bound cytochrome-linked formaldehyde dehydrogenase (DL-FalDH) when cells are grown under high Cu conditions or a soluble NAD(P)⁺-linked enzyme (N-FalDH) when cells are grown under low Cu conditions (Zahn et al., 2001). Neither protein contains metal cofactors, but DL-FalDH does require cytochrome *bc₁* as an electron acceptor (Zahn et al., 2001). The final step in aerobic methane oxidation is formate oxidation to CO₂, catalyzed by NAD⁺-formate dehydrogenase (Fdh). The only characterized Fdh protein in MOB (from *M. trichosporium* OB3b) contains four Fe_xS_x clusters and one molybdopterin cofactor (Jollie and Lipscomb, 1991; Figure 2). Multiple Fdh enzymes are present in *M. capsulatus* Bath genome (Ward et al., 2004) and it is possible that one or more of them contains W in place of Mo, similar to Fdh proteins from methylophs (Laukel et al., 2003).

Intra-aerobic methane oxidation coupled to denitrification.

The genome of the denitrifying bacterium *M. oxyfera*, coupled to proteomic, transcriptomic, and stable isotope labeling experiments, have revealed that this organism also contains pMMO but uses a different pathway for methane oxidation than other MOB. Instead of obtaining O₂ from the environment, *M. oxyfera*



generates its own supply of O_2 internally from NO. Therefore, this metabolism has been called intra-aerobic methane oxidation coupled to denitrification (Ettwig et al., 2010; Wu et al., 2011). In the proposed pathway, an Fe-based cytochrome *cd*₁ nitrite reductase [*cd*₁NIR or NirS; see the Section “Nitrate/Nitrite Reduction to $\text{N}_2\text{O}/\text{N}_2$ Pathway (Denitrification)”], likely containing four Fe atoms (Fülöp et al., 1995), is used to reduce NO_2^- to NO (Ettwig et al., 2010; Wu et al., 2011). In contrast to classical denitrification, where NO is reduced to N_2O and then N_2 , *M. oxyfera* disproportionates two molecules of NO to O_2 and N_2 (Figure 2). The NO dismutase enzyme that performs this reaction is currently unknown. The O_2 generated by this uncharacterized NO dismutase is then used to oxidize CH_4 to CH_3OH using pMMO, followed by oxidation of CH_3OH to CH_2O by MDH/Mxa (see the Section “Classical

Aerobic Methanotrophy”; Ettwig et al., 2010; Wu et al., 2011). Instead of using FalDH for oxidation of CH_2O to CHOOH , *M. oxyfera* contains several genes encoding enzymes responsible for tetrahydromethanopterin (H_4MPT)-dependent C_1 transfer reactions (Ettwig et al., 2010; Wu et al., 2011). The enzymes involved in these reactions are not known to contain metals (Vorholt, 2002). In the last step, CHOOH is oxidized to CO_2 by formate dehydrogenase [Fdh; see the Section “Nitrate/Nitrite Reduction to $\text{N}_2\text{O}/\text{N}_2$ Pathway (Denitrification)”]. Carbon assimilation in *M. oxyfera* likely proceeds via CO_2 fixation with the Calvin–Benson–Bassham cycle instead of the serine and ribulose monophosphate (RuMP) pathways used by other MOB (Ettwig et al., 2010; Wu et al., 2011). This pathway remains to be confirmed biochemically, but likely requires abundant Cu for pMMO.

Physiological studies of metal requirements for aerobic methanotrophy

Pure cultures. Studies of the physiological importance of metals for MOB have focused largely on Cu. Addition of Cu to the growth media in strains encoding both the particulate and the soluble forms of MMO fundamentally changes methanotroph physiology by triggering the “Cu switch,” turning on the expression of pMMO (Stanley et al., 1983; Choi et al., 2003). Further increases in Cu concentration can lead to up to 55-fold higher pMMO expression, with optimal pMMO activity occurring at 60 μM Cu for *M. capsulatus* Bath (Choi et al., 2003; Semrau et al., 2010). Cellular Cu contents in laboratory cultures of aerobic methanotrophs amended with high Cu in the growth media can be extremely high, up to ~ 250 nmol Cu/mg protein (Choi et al., 2003).

In order to maintain Cu homeostasis and protect against the potentially toxic effects of high levels of Cu, some aerobic methanotrophs express the Cu-chelating “chalkophore” molecule methanobactin (Kim et al., 2004; Balasubramanian and Rosenzweig, 2008). Methanobactin is a 1217-Da molecule that binds one atom of Cu(I) with high affinity (Kim et al., 2004; Choi et al., 2006) and accumulates in the growth media when Cu is <0.7 μM (DiSpirito et al., 1998). Cu-loaded methanobactin is actively transported into methanotrophic cells when Cu concentrations rise between 0.7 and 1 μM (Semrau et al., 2010; Balasubramanian et al., 2011). Furthermore, it has recently been shown that *M. capsulatus* Bath contains numerous proteins on its surface that respond to changing Cu concentrations in growth medium, including abundant Fe-containing cytochrome *c* peroxidases and multi-heme *c*-type cytochromes (Karlsen et al., 2011). It is perhaps interesting to note that abundant extracellular iron is evident on other methanotrophs in the genera *Crenothrix* and *Clonothrix* (Kolk, 1938; Vigliotta et al., 2007), although separate pathways and functional roles may be at play in these cases.

Environmental studies. Environmental studies on Cu availability to MOB are lacking, which is striking considering that Cu has been known to be involved in methanotrophy for many years. Knapp et al. (2007) suggest that the reason that correlations between environmental dissolved Cu (which in oxic settings is <1 μM ; Table 3) and methanotrophic activity have not been noted is because some MOB can access mineral- and organic-bound Cu using small Cu-binding peptides, most notably methanobactin. In the absence of dissolved Cu, *M. trichosporium* OB3b acquired sufficient Cu from Cu-containing minerals to express pMMO, but only when methanobactin was present (Knapp et al., 2007). CH_4 oxidation rates were highest at ~ 100 ppm mineral Cu (Kulczycki et al., 2011).

Low Cu minerals were dissolved more quickly by methanobactin than high Cu minerals (Kulczycki et al., 2007). Similarly, increasing concentrations of surface sites on minerals lead to decreased Cu bioavailability to *M. trichosporium* OB3b in common soil minerals (Morton et al., 2000). Therefore, particulate Cu content and sediment or soil mineral geochemistry may display a more robust correlation with methanotrophic activity than dissolved Cu levels in aquatic systems or pore waters (Knapp et al., 2007; Fru, 2011), although this remains to be tested in natural systems.

ANAEROBIC METHANOTROPHY

The process of anaerobic methane oxidation (AOM) has been known for over 30 years based on geochemical data (Martens and Berner, 1977), but the identity of the microorganisms carrying out this metabolism remained elusive until the early 2000s due to the extreme difficulty of culturing AOM microbes. Combined molecular and stable isotope studies revealed that archaeal groups (anaerobic methanotrophic archaea, abbreviated “ANME”) were responsible for AOM activity in CH_4 seep sediments through syntrophic associations with sulfate-reducing bacteria (Hinrichs et al., 1999; Boetius et al., 2000; Orphan et al., 2001, 2002). Described ANME lineages currently belong to three distinct phylogenetic groups, with members of the ANME-1 forming a novel clade between the Methanomicrobiales and Methanosarcinales orders, and groups ANME-2 and ANME-3 belonging to the Methanosarcinales. Together, these methanotrophic lineages are believed to be responsible for the oxidation of $\sim 80\%$ of the methane naturally seeping upward from marine sediments, or ~ 7 – 25% of total global methane (Reeburgh, 2007). Although ANME have not been cultured, metagenomic, and environmental proteomic studies have provided insight into their metabolic strategies for AOM (Hallam et al., 2003, 2004; Krüger et al., 2003; Meyerdiercks et al., 2005; Pernthaler et al., 2008).

Metalloenzymes in anaerobic methanotrophy

Evidence is accumulating that ANME anaerobically oxidize methane by running the methanogenesis pathway in reverse (Scheller et al., 2010), as was predicted based on the close phylogenetic relationship of ANME to methanogens in the orders Methanomicrobiales and Methanosarcinales (Knittel and Boetius, 2009). The discovery of gene homologs to *mcrA* in ANME provided the first clues that these microbes were using reverse methanogenesis to oxidize CH_4 (Hallam et al., 2003). High concentrations of the Ni-containing cofactor F_{430} and a slightly modified variant of F_{430} (Mayr et al., 2008) were found in microbial mats performing AOM in the Black Sea (Krüger et al., 2003), adding further support

Table 3 | Compiled dissolved trace metal concentrations in representative oxic waters.

Sample site	Fe	Ni	Co	Cu	Zn	Mo	Reference
Seawater	<0.001	0.002–0.01	<0.001	<0.001 –0.005	<0.001 –0.009	0.1	Bruland (1980), Collier (1985), Johnson et al. (1997)
Soil pore water	1–20			0.1–0.5	0.1–2		Kinniburgh and Miles (1983)
Oxic lake water	0.01–10		<0.001 –0.03	0.01–0.8	0.02–0.6	0.004–0.3	Wetzel (2001)

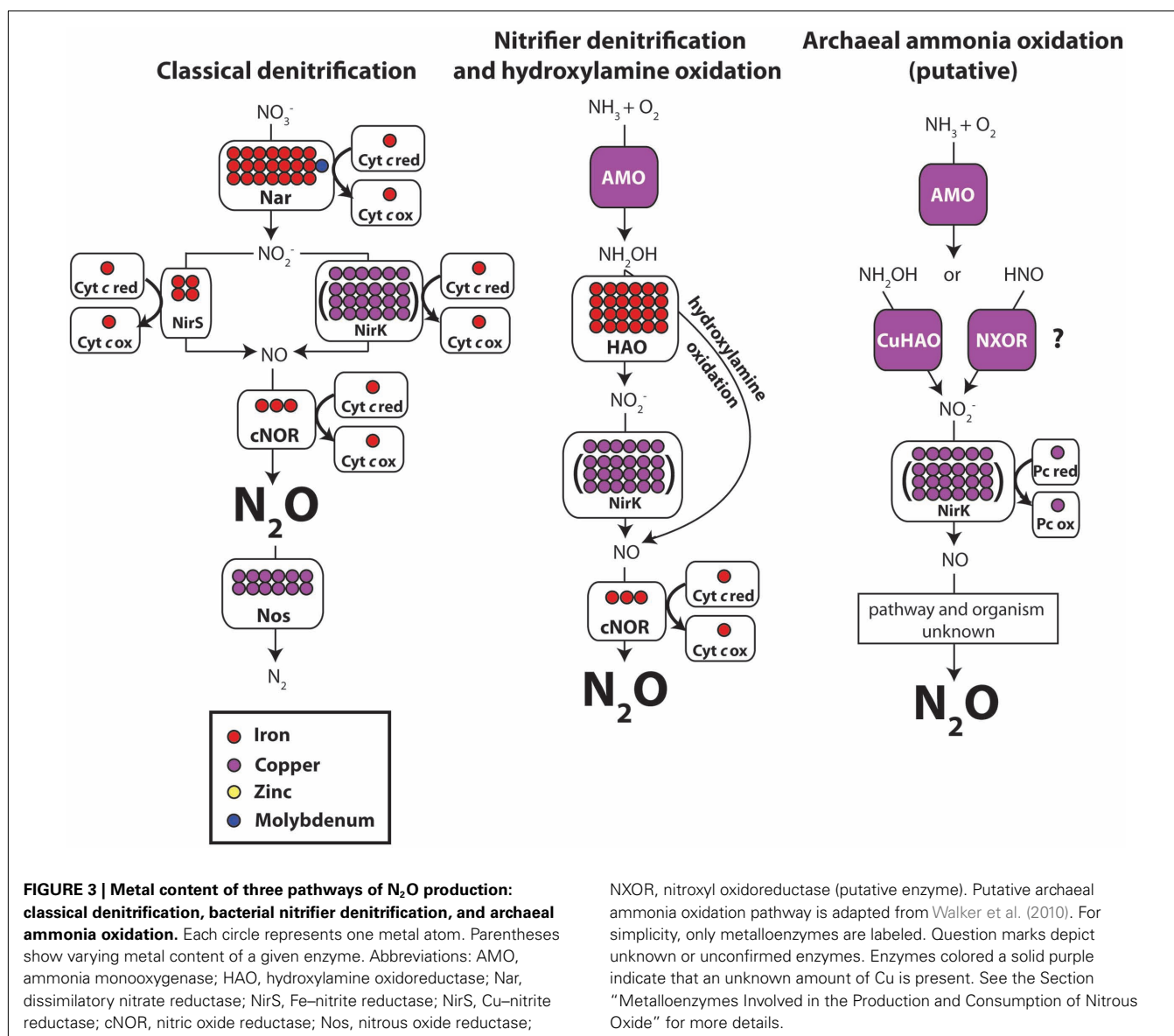
All concentrations are in units of micromolar (μM).

for the model. Immunolocalization and biochemical studies have provided clear evidence that Mcr catalyzes the first step of AOM in ANME (Heller et al., 2008; Scheller et al., 2010) and metagenomic studies of ANME communities identified the presence of genes encoding almost all of the other methanogenic enzymes with the exception of the Ni-Fe hydrogenases Eha/Ehb and two of the three subunits of the Ni-Fe hydrogenase Mvh (Hallam et al., 2004; Meyerdiercks et al., 2005; Thauer, 2011). Therefore, it is reasonable to predict that metal requirements for the enzymes involved in AOM are similar to those used for methanogenesis, involving high levels of Fe, Ni, Co, and additional Mo/W and Zn (see the Section “Metalloenzymes in Methanogenesis”), but possibly with slightly lower Fe and Ni requirements due to the absence of two of the Ni-Fe hydrogenases involved in methanogenesis. The finding that ANME can also fix N_2 (Dekas et al., 2009) suggests that they may have additional Fe and Mo/V requirements. ANME occur in anoxic and sulfidic environments where Ni, Co, Mo, and possibly Fe likely

occur at levels lower than their growth optima (Table 2), assuming that their metal requirements are similar to those of methanogens. For a full review of the biochemistry of AOM, readers are referred to Thauer and Shima (2008).

SUMMARY

Extensive research has been focused on the importance of Cu for particulate methane monooxygenase, resulting in a detailed understanding of physiological and biochemical aspects of Cu in pure cultures of MOB. However, few studies have attempted to relate Cu bioavailability, particularly in mineral form, to rates of aerobic CH_4 oxidation in the environment. Furthermore, few studies have investigated additional metal requirements, particularly Fe, but also small amounts of Mo and Zn, for aerobic and intra-aerobic methanotrophy, although clearly Fe in particular is important for these metabolisms (Figure 2) and cell surface Cu acquisition mechanisms (Karlsen et al., 2011). In contrast to



aerobic methanotrophy, essentially nothing is known about the metal requirements for AOM besides the need for large amounts of Ni in cofactor F₄₃₀ (Krüger et al., 2003). Presumably, metal requirements for reverse methanogenesis by ANME are similar to those of the canonical seven-step methanogenic pathway, but this hypothesis remains to be tested.

NITROUS OXIDE PRODUCTION AND CONSUMPTION

A diverse range of organisms using several different pathways are known to produce N₂O. Whereas CH₄ production is only known to occur within the archaea, N₂O production is more widespread. Pathways for biological N₂O production include dissimilatory nitrate/nitrite reduction (e.g., denitrification), nitrifier denitrification (Wrage et al., 2001), hydroxylamine oxidation, and NO_x detoxification (also known as the “nitrosative stress” pathway; Stein, 2011). N₂O is also produced by MOB (Sutka et al., 2006; Campbell et al., 2011) and enrichment cultures of ammonia oxidizing archaea (AOA; Jung et al., 2011; Santoro et al., 2011). Bacterial denitrification and nitrifier denitrification together account for ~70% of the global N₂O flux (IPCC, 2007), although recent data suggest that AOA may also be an important source of N₂O in marine and terrestrial systems (Jung et al., 2011; Santoro et al., 2011). For an in-depth review of the methods used to identify N₂O-producing bacteria by their key enzymes, readers are referred to Stein (2011).

Metalloenzymes involved in N₂O production primarily contain Fe and/or Cu, with additional Mo needed for the dissimilatory nitrate reduction pathway to N₂O and/or N₂ and possibly additional Zn in nitrifier denitrification. A schematic of the metal content of proteins involved in N₂O production and consumption is shown in **Figure 3**. Below we review biochemical and physiological studies of the metal requirements for N₂O production through the standard and nitrifier denitrification pathways, and touch on new discoveries of metalloenzymes putatively involved in archaeal ammonia oxidation. Metalloenzymes involved in the nitrosative stress pathway are mentioned briefly, but are outside the scope of this review.

METALLOENZYMES INVOLVED IN THE PRODUCTION AND CONSUMPTION OF NITROUS OXIDE

Nitrate/nitrite reduction to N₂O/N₂ pathway (denitrification)

Nitrous oxide is a gaseous intermediate in the process of denitrification, the anaerobic microbial respiratory process whereby NO₃[−] is reduced to N₂ in the sequence: NO₃[−] → NO₂[−] → NO → N₂O → N₂. The process is leaky and therefore N₂O is almost always found in trace abundances in environments where denitrification occurs (Rogers and Whitman, 1991). Since NO₃[−] is typically present at higher abundances than NO₂[−] in natural environments, denitrification typically starts with dissimilatory nitrate reduction. The most well-studied dissimilatory nitrate reductase is the membrane-bound NarGHI complex, which contains two *b*-type cytochromes (each binding one Fe atom), one Fe₃S₄ cluster, four Fe₄S₄ clusters, and a molybdopterin (Mo) active site (Bertero et al., 2003; Jormakka et al., 2004; **Figure 3**). It is possible for dissimilatory nitrate reduction to occur with Fe or V in place of Mo,

although such alternative nitrate reductases have so far only been found in metal-reducing bacteria (Antipov et al., 1998, 2005).

The next step in denitrification, nitrite reduction to nitric oxide (NO), is catalyzed by either a cytochrome *cd*₁ (four Fe)-containing nitrite reductase (abbreviated *cd*₁NIR or NirS; Fülöp et al., 1995) or a Cu-containing nitrite reductase (abbreviated CuNIR or NirK) that possesses either 6 or 24 Cu atoms depending on its subunit content (Godden et al., 1991; Nojiri et al., 2007; **Figure 3**).

NO reduction to N₂O occurs almost instantaneously after its formation due to the toxicity of NO. In denitrifying bacteria, NO reductases (NORs) are members of the heme/copper cytochrome oxidase enzyme superfamily that substitute Fe in place of Cu at their active site (Hendriks et al., 2000). Other enzymes in this family cannot efficiently reduce NO, suggesting that the replacement of Cu with Fe is important for the enzyme mechanism. The most common type of NOR in denitrifying bacteria is NorBC (or cNOR), a cytochrome *bc* complex that contains Fe in the form of two hemes and one non-heme Fe and uses cytochrome *c* as an electron donor (Hendriks et al., 2000; Zumft, 2005; **Figure 3**). The nitrosative stress pathway uses a different NO reductase called qNOR, which contains only the NorB subunit and accepts electrons from quinols (Hendriks et al., 2000; Zumft, 2005). Two additional Fe-containing NOR enzymes, the flavohemoglobin Hmp and the flavorubredoxin NorVW, are important for relieving nitrosative stress under anoxic conditions by NO reduction to N₂O (Poole and Hughes, 2000; Gardner et al., 2003). Fungal NORs are members of the cytochrome P-460 family and also contain only Fe (Hendriks et al., 2000).

After its production, N₂O can either escape to the atmosphere or be further reduced to N₂ by nitrous oxide reductase (Nos). Nos is a Cu-rich enzyme, binding 12 atoms of Cu per homodimer (Brown et al., 2000; **Figure 3**). Low pH and/or trace amounts of O₂ tend to increase the ratio of N₂O:N₂ released because Nos is inhibited at low pH and is more sensitive to O₂ than other reductases in denitrification (Knowles, 1982).

Bacterial ammonia oxidation to N₂O (nitrifier denitrification and hydroxylamine oxidation)

Autotrophic ammonia oxidizing Bacteria (AOB; Shaw et al., 2006) and MOB (Yoshinari, 1985; Ren et al., 2000) are capable of aerobic production of N₂O during the process of ammonia oxidation (NH₃ → NH₂OH → NO₂[−] → NO₃[−]). N₂O is produced from two offshoots of the nitrification pathway: nitrifier denitrification (Ritchie and Nicholas, 1972; Poth and Focht, 1985; Wrage et al., 2001; Shaw et al., 2006) and hydroxylamine oxidation (Cantera and Stein, 2007b; Stein, 2011). In nitrifier denitrification, NO₂[−] is reduced to NO, and then N₂O or N₂, instead of being oxidized to NO₃[−]. In hydroxylamine oxidation, NH₂OH is oxidized to NO, which is then reduced to N₂O. Little is known about the controls on N₂O:N₂ ratios for both of these processes.

In the first step of nitrifier denitrification and hydroxylamine oxidation, ammonia (NH₃) is oxidized to hydroxylamine (NH₂OH), catalyzed by the enzyme ammonia monooxygenase (AMO). Although the crystal structure of AMO has not been solved, AMO shares high similarity to pMMO of aerobic methanotrophs (Holmes et al., 1995; Arp and Stein, 2003 and references therein), suggesting that it also contains three Cu atoms per

monomer and possibly additional Zn and Fe (see the Section “Metalloenzymes in Aerobic Methanotrophy”; **Figure 3**). A Cu requirement for AMO is supported by experiments showing that Cu addition activates AMO (Ensign et al., 1993).

The next step of nitrifier denitrification, NH_2OH oxidation to NO_2^- , is catalyzed by the enzyme hydroxylamine oxidoreductase (HAO), which contains 24 Fe atoms in c -type cytochromes (Igarashi et al., 1997; **Figure 3**). Orthologs of the copper-containing NirK enzymes are typically used for the reduction of NO_2^- to NO (Casciotti and Ward, 2001; Cantera and Stein, 2007a,b). NO, a toxic intermediate, is then reduced to N_2O by an unknown enzyme, likely either NorBC (Beaumont et al., 2004; Casciotti and Ward, 2005), the tetraheme cytochrome c_{554} (Upadhyay et al., 2006), or NorS (Stein, 2011). In hydroxylamine oxidation, NH_2OH is oxidized by HAO to NO instead of NO_2^- (**Figure 3**). Reduction of NO to N_2O is then catalyzed by cytochrome c_{554} or NorS as with nitrifier denitrification (Stein, 2011).

Although N_2 has been shown to be produced by the nitrifier denitrification pathway (Poth, 1986), *nos* genes have not been found in the genomes of bacterial nitrifiers (Stein et al., 2007) so it is unclear how N_2 is formed during nitrifier denitrification.

Archaeal ammonia oxidation

Archaeal nitrification was first reported in 2005 (Könneke et al., 2005) and archaeal enrichment cultures have recently been shown to produce N_2O (Jung et al., 2011; Santoro et al., 2011). For a review of AOA, see Hatzepichler (in preparation). The genomes of AOA *Cenarchaeum symbiosum* and *Nitrosopumilus maritimus* suggest that AOA have higher Cu requirements than AOB (Hallam et al., 2006; Walker et al., 2010). *C. symbiosum* and *N. maritimus* contain *amo* genes with conserved motifs that bind the metal centers in *M. capsulatus* Bath, suggesting that archaeal AMO also contains abundant Cu (Hallam et al., 2006; Walker et al., 2010). Both AOA genomes lack genes to encode a bacterial-type HAO complex. AOA may use a Cu-based electron-transfer system instead of the Fe-based system used by AOB, as implied by the abundance of genes encoding copper-containing proteins, including numerous multi-copper oxidases and small Cu-binding plastocyanin-like domains (Hallam et al., 2006; Walker et al., 2010). The *N. maritimus* genome contains *nirK* genes (Walker et al., 2010) and AOA *nirK* homologs have been found to be widespread in environmental samples (Bartossek et al., 2010). Walker et al. (2010) propose a model for the AOA nitrification pathway whereby the products of AMO (either NH_2OH , or alternatively the highly reactive intermediate nitroxyl, HNO) are oxidized to nitrous acid (HNO_2) by a Cu-containing protein, either a Cu-HAO or a multi-copper oxidase acting as a nitroxyl oxidoreductase (NXOR; **Figure 3**). Following these reactions, NO_2^- is reduced to NO by NirK, with plastocyanin acting as an electron donor. Future studies are needed to test whether pure cultures of AOA can produce N_2O or whether an N intermediate such as NO is produced by AOA and reduced to N_2O by bacterial partners. If AOA can indeed produce N_2O as supported by isotopic studies (Santoro et al., 2011), future biochemical studies are required to determine what pathway is used, and whether they can consume it.

PHYSIOLOGICAL STUDIES

As reviewed in the Section “Metalloenzymes Involved in the Production and Consumption of Nitrous Oxide,” the metal content of enzymes involved in N_2O production and consumption is composed primarily of Fe and Cu (**Figure 3**). The influence of Cu on N_2O processing by denitrifying bacteria has been the subject of a number of pure culture and environmental investigations. The influence of Fe availability on growth of AOB and denitrifiers is less studied, and very little is known about the importance of Fe for N_2O processing in these microbes. Research is also lacking on the influence of Fe and Cu availability on N_2O processing during nitrifier denitrification and in AOA enrichment cultures. These pathways are of particular interest due to the likelihood of high Cu requirements for their first step (AMO), whereas N_2O can be produced (but not consumed) without Cu by denitrifiers.

Pure cultures

The importance of Cu for the consumption of N_2O by denitrifying bacteria has been clearly demonstrated by laboratory studies (Iwasaki and Terai, 1982; Matsubara et al., 1982; Granger and Ward, 2003; Twining et al., 2007). These studies showed that N_2O accumulates when denitrifying bacteria are grown without added Cu, whereas complete denitrification to N_2 occurs when Cu is present above a certain threshold. In early studies with *Pseudomonas perfectomarinus* and two *Alcaligenes* strains, background Cu contamination in growth medium was not quantified and high levels of Cu were added in the replete condition (1–6 μM ; Iwasaki and Terai, 1982; Matsubara et al., 1982). In follow-up studies with *Paracoccus denitrificans* and *Pseudomonas denitrificans*, trace metal-clean growth protocols were utilized and total dissolved Cu background contamination was measured to be 0.3–0.5 nM (Granger and Ward, 2003; Twining et al., 2007). At less than 1 nM total dissolved Cu, N_2O accumulated; above 1 nM, it was consumed (Granger and Ward, 2003; Twining et al., 2007). Enzyme activity of nitrous oxide reductase (Nos) was below the detection limit in denitrifiers grown at 0.3 nM total dissolved Cu, suggesting that the reason for build-up of N_2O was Cu limitation of Nos (Granger and Ward, 2003). Supplementation of 10 nM Cu to Cu-limited cultures caused increased growth rate and complete consumption of N_2O (Granger and Ward, 2003). These laboratory studies led to the hypothesis that low Cu concentrations in natural aquatic ecosystems may promote N_2O accumulation (see the Section “Environmental Studies”).

Metal requirements for AOB have not been studied as extensively as those for denitrifiers, but preliminary studies support a high importance of Fe for nitrification. An early study of nitrifying bacterial cultures showed that addition of Fe alone produced a 56% increase in NO_2^- production whereas addition of Cu alone produced a 17% increase (Lees and Meiklejohn, 1948). The few subsequent studies of metal requirements for AOB have focused on Fe requirements (Meiklejohn, 1953; Wei et al., 2006). Both AMO and HAO activity were reduced in *Nitrosomonas europaea* cultures grown at 0.2 vs. 10 μM Fe (Wei et al., 2006). Lowered HAO activity is expected due to the high heme content of HAO in AOB cells (Whittaker et al., 2000). AMO activity dependence on Fe suggests that Fe is a component of AMO or that Fe is present in the electron donor to AMO. The Fe content of AMO is difficult

to assess due to the lack of *in vitro* protein preparations. It is also possible that AOB scavenge/co-opt Fe-loaded siderophores produced by other bacteria; if supplied with exogenous siderophores, *N. europaea* expresses genes for siderophore transporters and ferric transporters when Fe is limiting (Wei et al., 2006; Stein et al., 2007). Lastly, the fact that AOB cells are bright red in color further supports the major requirement for Fe in their metabolism.

Environmental studies

Several recent field studies have suggested that Cu limitation prohibits N₂O consumption. Cu addition stimulated N₂O consumption in Linsley Pond, a temperate lake ecosystem with 3 nM Cu (Twining et al., 2007). Similarly, the ratio of N₂O/N₂ decreased as water-extractable Cu concentration increased in freshwater sediments (Jacinthe and Tedesco, 2009). While scarce Cu can limit denitrification, excess Cu (above 100 mg kg⁻¹ sediment) in polluted ecosystems can inhibit the pathway (Sakadevan et al., 1999; Magalhães et al., 2011). On the other hand, denitrification in three major marine oxygen minimum zones does not appear to be Cu-limited: addition of Cu had minimal effect on denitrification rates in seawater incubations with background Cu concentrations of 1–3 nM (Ward et al., 2008). Therefore, it is likely that marine denitrifiers have evolved mechanisms to satisfy their Cu requirements by taking up Cu that is strongly bound to natural ligands, which can bind 99% of the total Cu in temperate lakes (Twining et al., 2007) and in the ocean (Moffett and Dupont, 2007).

Metal bioavailability varies considerably between freshwater and seawater oxic environments. In general, dissolved Fe and Cu are present at much lower concentrations in seawater than in lakes and soil pore waters (Table 3). Therefore, N₂O production by marine ammonia oxidizers may be Fe or Cu-limited and/or they may have evolved strategies to scavenge these metals.

SUMMARY

In contrast to CH₄, N₂O can be produced by diverse microorganisms via numerous pathways containing varying amounts of Fe and Cu, small amounts of Mo and possibly Zn. To date, only one enzyme has been found to convert N₂O to N₂: the Cu-containing Nos enzyme found in denitrifiers. The absence of *nos* genes from the genomes of AOA and AOB (Hallam et al., 2006; Stein et al., 2007; Walker et al., 2010) suggests either that N₂O is their final gaseous product or that they have alternative nitrous oxide reductases. The ability of some AOB to produce N₂ (Poth, 1986) lends support to the presence of alternative reductases. A search for such alternative enzymes deserves attention, as ammonia oxidizers are important players in the global N₂O budget. Research on the biochemistry of N₂O production in AOA enrichment cultures is essential to understand the exciting findings of recent studies suggesting that large amounts of Cu may be involved in AOA metabolism.

COMPARISONS, CONCLUSION, AND FUTURE RESEARCH

Trace metals present in microbial enzymes involved in CH₄ and N₂O cycling include Fe, Co, Ni, Cu, Zn, Mo, and W. While Fe-containing enzymes are present in almost all pathways we reviewed (with the possible exception of archaeal ammonia oxidation), other metals differ by metabolism. For instance, Ni, Co, and W are

present in methanogenic enzymes, but not in enzymes involved in aerobic methanotrophy and N₂O cycling. In contrast, Cu is not used in methanogenesis, but is very important for aerobic methanotrophy and N₂O cycling. Small amounts of Mo and Zn are common in most pathways. If ongoing biochemical studies confirm that anaerobic methanotrophs use the reverse methanogenesis pathway to oxidize methane, they likely require the same suite of metals as methanogens: Fe, Co, Ni, Zn, and Mo/W.

How do metal requirements for CH₄ and N₂O cycling compare with other ecologically important microbes? The metal stoichiometry of 15 marine eukaryotic phytoplankton showed an average trace metal stoichiometry of Fe₁Mn_{0.53}Zn_{0.08}Cu_{0.05}Co_{0.03}Mo_{0.005} (Ho et al., 2003; Barton et al., 2007). High Mn requirements are likely reflective of the oxygen-generating Mn-containing photosystem II complex. The elemental stoichiometry of CH₄ and N₂O processing microbes is not nearly as well-constrained as that of eukaryotic phytoplankton, but preliminary studies of methanogens suggest that, after Fe, Ni is an extremely important metal for methanogenesis and anaerobic methanotrophy. Very little is known about the metal stoichiometry of aerobic and intra-aerobic methanotrophs and N₂O-producing microbes, although it is predicted that their Cu content is much higher than both methanogens and phytoplankton, especially in the case of archaeal ammonia oxidizers. Metallomics – the comprehensive analysis of the entirety of metal-containing species within a cell (Szpunar, 2005) – may reveal still more unexpected metals or natural products excreted by microbes to alter metal bioavailability. For example, a recent metallomics study of the hyperthermophilic sulfur-reducing Archeon, *Pyrococcus furiosus*, revealed 158 unassigned metalloprotein peaks, 75 of which contained metals that the organism was not known to assimilate, such as Pb and U (Cvetkovic et al., 2010). Furthermore, it is likely that the metal requirements for each of the pathways reviewed here are amplified by additional metalloenzymes involved in complex metal cofactor biosynthesis, such is the case for hydrogenases and nitrogenases (Rubio and Ludden, 2008; Shepard et al., 2011).

More studies are needed to address gaps in our knowledge of microbial trace metal physiology. Ideally these studies will make use of well-defined media and trace metal-clean conditions, such as Teflon-lined glass bottles for anaerobic studies. Understudied topics include Zn requirements for methanogenesis, trace metal content of ANME enzymes (other than the well-studied Mcr), the influence of Cu on N₂O production by archaeal enrichment cultures, the biochemistry of Cu-enzymes in archaeal ammonia oxidizers, and strategies for metal-binding ligand production (i.e., methanobactin) in greenhouse gas cycling microbes. The search for alternative N₂O-consuming enzymes in ammonia oxidizers deserves particular attention, as suggested by the ability of some bacterial nitrifiers lacking the Cu-containing nitrous oxide reductase enzyme to convert N₂O to N₂.

In order to better connect the findings from biochemical and physiological studies of pure cultures with the larger picture of global greenhouse gas cycling and environmental metal bioavailability, more *in situ* studies are necessary. Preliminary studies suggest that rates of methanogenesis in peatlands may be controlled by Fe, Ni, and Co availability, since addition of all three metals stimulated methanogenesis in mineral-poor peats. It is

currently unknown whether one metal was the primary limiting growth element or whether multiple metals were co-limiting (Saito et al., 2008). If co-limitation was occurring, the addition of all three elements would result in higher rates of methanogenesis than any metal added solely. On the other hand, other systems and pathways may be dominantly regulated by the bioavailability of only one scarce metal; this seems to be the case for Co(balt) limitation of methylotrophic methanogenesis in anaerobic digesters, Cu limitation of N₂O consumption by freshwater denitrifying bacteria and possibly Cu limitation of ammonia oxidizing archaea as suggested by numerous genes encoding Cu-containing proteins in AOA genomes.

Lastly, relationships between metal bioavailability and fluxes of greenhouse gases remain largely unexplored, particularly in anaerobic ecosystems. High sulfide environments likely pose particular challenges for microbial metal acquisition due to abiotic sulfide scavenging and precipitation of metal sulfides. Of the bioessential metals involved in greenhouse gas cycling, Mo, Fe, and Cu are most susceptible to sulfide scavenging, followed by Co, Ni, and Zn (Morse and Luther, 1999). Microbial metal limitation due to sulfide drawdown may have driven major evolutionary episodes and geochemical transitions in Earth history (Anbar and

Knoll, 2002; Scott et al., 2008; Dupont et al., 2010). Several such scenarios have been proposed for metal limitation of microbial greenhouse gas cycling: a decline in seawater Ni due to cooling of the Earth's mantle in the late Archean may have limited methanogenesis and contributed to the Great Oxidation Event 2.4 billion years ago (Konhauser et al., 2009) while low Cu due to sulfide scavenging in the Proterozoic ocean could have led to global warming through the build-up of N₂O (Buick, 2007). The question of how metal bioavailability influences greenhouse gas cycling in ancient and modern ecosystems is just beginning to be investigated.

ACKNOWLEDGMENTS

The authors acknowledge funding from the National Aeronautics and Space Administration (NASA) Astrobiology Postdoctoral Fellowship (to Jennifer B. Glass), the NASA Astrobiology Institute (NNA04CC06A), and the U.S. Department of Energy's Office of Biological and Environmental Research Early Career Award (to Victoria J. Orphan). Thanks to Roland Hatzepichler, Patricia Tavormina, Shawn McGlynn, Anne Dekas, Joshua Steele, Hiroyuki Imachi, Lisa Stein and Aubrey Zerkle for helpful comments on drafts of this manuscript.

REFERENCES

- Afting, C., Hochheimer, A., and Thauer, R. (1998). Function of H₂-forming methylenetetrahydromethanopterin dehydrogenase from *Methanobacterium thermoautotrophicum* in coenzyme F₄₂₀ reduction with H₂. *Arch. Microbiol.* 169, 206–210.
- Alex, L. A., Reeve, J. N., Orme-Johnson, W. H., and Walsh, C. T. (1990). Cloning, sequence determination, and expression of the genes encoding the subunits of the nickel-containing 8-hydroxy-5-deazaflavin reducing hydrogenase from *Methanobacterium thermoautotrophicum* delta H. *Biochemistry* 29, 7237–7244.
- Anbar, A. D., and Knoll, A. H. (2002). Proterozoic ocean chemistry and evolution: a bioinorganic bridge? *Science* 297, 1137–1142.
- Anderson, I., Ulrich, L. E., Lupa, B., Susanti, D., Porat, I., Hooper, S. D., Lykidis, A., Sieprawka-Lupa, M., Dharmarajan, L., Goltsman, E., Lapidus, A., Saunders, E., Han, C., Land, M., Lucas, S., Mukhopadhyay, B., Whitman, W. B., Woese, C., Bristow, J., and Kyrpides, N. (2009). Genomic characterization of Methanomicrobiales reveals three classes of methanogens. *PLoS ONE* 4, e5797. doi:10.1371/journal.pone.0005797
- Antipov, A. N., Lyalikova, N. N., Khijniak, T. V., and Lvov, N. P. (1998). Molybdenum-free nitrate reductases from vanadate-reducing bacteria. *FEBS Lett.* 441, 257–260.
- Antipov, A. N., Morozkina, E. V., Sorokin, D. Y., Golubeva, L. I., Zvyagil'skaya, R. A., and Lvov, N. P. (2005). Characterization of molybdenum-free nitrate reductase from haloalkalophilic bacterium *Halomonas* sp strain AGJ 1-3. *Biochemistry* 70, 799–803.
- Arp, D. J., and Stein, L. Y. (2003). Metabolism of inorganic N compounds by ammonia-oxidizing bacteria. *Crit. Rev. Biochem. Mol. Biol.* 38, 471–495.
- Balasubramanian, R., Kenney, G. E., and Rosenzweig, A. C. (2011). Dual pathways for copper uptake by methanotrophic bacteria. *J. Biol. Chem.* 286, 37313–37319.
- Balasubramanian, R., and Rosenzweig, A. C. (2007). Structural and mechanistic insights into methane oxidation by particulate methane monooxygenase. *Acc. Chem. Res.* 40, 573–580.
- Balasubramanian, R., and Rosenzweig, A. C. (2008). Copper methanobactin: a molecule whose time has come. *Curr. Opin. Chem. Biol.* 12, 245–249.
- Balasubramanian, R., Smith, S. M., Rawat, S., Yatsunyk, L. A., Stemmler, T. L., and Rosenzweig, A. C. (2010). Oxidation of methane by a biological dicopper centre. *Nature* 465, 115–119.
- Barton, L. L., Goulhen, F., Bruschi, M., Woodards, N. A., Plunkett, R. M., and Rietmeijer, F. J. M. (2007). The bacterial metallome: composition and stability with specific reference to the anaerobic bacterium *Desulfovibrio desulfuricans*. *Biomaterials* 20, 291–302.
- Bartossek, R., Nicol, G. W., Lanzen, A., Klenk, H. P., and Schleper, C. (2010). Homologues of nitrite reductases in ammonia-oxidizing archaea: diversity and genomic context. *Environ. Microbiol.* 12, 1075–1088.
- Basiliko, N., and Yavitt, J. B. (2001). Influence of Ni, Co, Fe, and Na additions on methane production in *Sphagnum*-dominated Northern American peatlands. *Biogeochemistry* 52, 133–153.
- Baudet, C., Sprott, G. D., and Patel, G. B. (1988). Adsorption and uptake of nickel in *Methanotrix concilii*. *Arch. Microbiol.* 150, 338–342.
- Beaumont, H. J. E., Van Schooten, B., Lens, S. I., Westerhoff, H. V., and Van Spanning, R. J. M. (2004). *Nitrosomonas europaea* expresses a nitric oxide reductase during nitrification. *J. Bacteriol.* 186, 4417–4421.
- Bertero, M. G., Rothery, R. A., Palak, M., Hou, C., Lim, D., Blasco, F., Weiner, J. H., and Strynadka, N. C. J. (2003). Insights into the respiratory electron transfer pathway from the structure of nitrate reductase A. *Nat. Struct. Biol.* 10, 681–687.
- Boetius, A., Ravensschlag, K., Schubert, C. J., Rickert, D., Widdel, F., Gieseke, A., Amann, R., Jørgensen, B. B., Witte, U., and Pfannkuche, O. (2000). A marine microbial consortium apparently mediating anaerobic oxidation of methane. *Nature* 407, 623–626.
- Bollinger, J. M. (2010). Biochemistry: getting the metal right. *Nature* 465, 40–41.
- Bragazza, L. (2006). Heavy metals in bog waters: an alternative way to assess atmospheric precipitation quality? *Glob. Planet. Change* 53, 290–298.
- Brown, K., Tegoni, M., Prudencio, M., Pereira, A. S., Besson, S., Moura, J. J., Moura, I., and Cambillau, C. (2000). A novel type of catalytic copper cluster in nitrous oxide reductase. *Nat. Struct. Biol.* 7, 191–195.
- Brunland, K. W. (1980). Oceanographic distributions of cadmium, zinc, nickel, and copper in the North Pacific. *Earth Planet. Sci. Lett.* 47, 176–198.
- Buick, R. (2007). Did the Proterozoic Canfield Ocean cause a laughing gas greenhouse? *Geobiology* 5, 97–100.
- Callander, I., and Barford, J. (1983a). Precipitation, chelation, and the availability of metals as nutrients in anaerobic digestion. I. Methodology. *Biotechnol. Bioeng.* 25, 1947–1957.
- Callander, I., and Barford, J. (1983b). Precipitation, chelation, and the availability of metals as nutrients in anaerobic digestion. II. Applications. *Biotechnol. Bioeng.* 25, 1959–1972.
- Campbell, M. A., Nyerges, G., Kozłowski, J. A., Poret-Peterson, A. T., Stein, L. Y., and Klotz, M. G. (2011). Model of the molecular basis for hydroxylamine oxidation and nitrous oxide production in methanotrophic bacteria. *FEMS Microbiol. Lett.* 322, 82–89.

- Cantera, J. J. L., and Stein, L. Y. (2007a). Molecular diversity of nitrite reductase genes (nirK) in nitrifying bacteria. *Environ. Microbiol.* 9, 765–776.
- Cantera, J. J. L., and Stein, L. Y. (2007b). Role of nitrite reductase in the ammonia-oxidizing pathway of *Nitrosomonas europaea*. *Arch. Microbiol.* 188, 349–354.
- Casciotti, K. L., and Ward, B. B. (2001). Dissimilatory nitrite reductase genes from autotrophic ammonia-oxidizing bacteria. *Appl. Environ. Microbiol.* 67, 2213–2221.
- Casciotti, K. L., and Ward, B. B. (2005). Phylogenetic analysis of nitric oxide reductase gene homologues from aerobic ammonia oxidizing bacteria. *FEMS Microbiol. Ecol.* 52, 197–205.
- Chien, Y. T., Auerbuch, V., Brabban, A. D., and Zinder, S. H. (2000). Analysis of genes encoding an alternative nitrogenase in the archaeon *Methanosarcina barkeri* 227. *J. Bacteriol.* 182, 3247–3253.
- Chistoserdova, L. (2011). Modularity of methylotrophy, revisited. *Environ. Microbiol.* 13, 2603–2622.
- Chistoserdova, L., Vorholt, J. A., and Lidstrom, M. E. (2005). A genomic view of methane oxidation by aerobic bacteria and anaerobic archaea. *Genome Biol.* 6, 208–213.
- Choi, D. W., Corbin, J., Do, Y. S., Semrau, J. D., Antholine, W. E., Hargrove, M. S., Pohl, N. L., Boyd, E. S., Geesey, G., Hartsel, S. C., Shafe, P. H., McEllistrem, M. T., Kisting, C. J., Campbell, D., Rao, V., de la Mora, A. M., and DiSpirito, A. A. (2006). Spectral, kinetic, and thermodynamic properties of Cu(I) and Cu(II) binding by methanobactin from *Methylosinus trichosporium* OB3b. *Biochemistry* 45, 1442–1453.
- Choi, D.-W., Kunz, R. C., Boyd, E. S., Semrau, J. D., Antholine, W. E., Han, J.-I., Zahn, J. A., Boyd, J. M., De La Mora, A. M., and DiSpirito, A. A. (2003). The membrane-associated methane monooxygenase (pMMO) and pMMO-NADH: quinone oxidoreductase complex from *Methylococcus capsulatus* Bath. *J. Bacteriol.* 185, 5755–5764.
- Collier, R. W. (1985). Molybdenum in the northeast Pacific Ocean. *Limnol. Oceanogr.* 30, 1351–1354.
- Conrad, R. (1996). Soil microorganisms as controllers of atmospheric trace gases (H₂, CO, CH₄, OCS, N₂O, and NO). *Microbiol. Mol. Biol. Rev.* 60, 609–640.
- Cvetkovic, A., Menon, A. L., Thorgersen, M. P., Scott, J. W., Poole II, F. L., Jenney, F. E. Jr., Lancaster, W. A., Praissman, J. L., Shanmukh, S., Vaccaro, B. J., Trauger, S. A., Kalisiak, E., Apon, J. V., Siuzdak, G., Yannone, S. M., Tainer, J. A., and Adams, M. W. W. (2010). Microbial metalloproteomes are largely uncharacterized. *Nature* 466, 779–782.
- Daas, P. J. H., Hagen, W. R., Keltjens, J. T., and Vogels, G. D. (1994). Characterization and determination of the redox properties of the [2[4Fe-4S] ferredoxin from *Methanosarcina barkeri* strain MS. *FEBS Lett.* 356, 342–344.
- David, L. A., and Alm, E. J. (2010). Rapid evolutionary innovation during an Archaean genetic expansion. *Nature* 469, 93–96.
- Dekas, A., Poretsky, R. S., and Orphan, V. J. (2009). Deep-sea archaea fix and share nitrogen in methane-consuming microbial consortia. *Science* 326, 422–426.
- Demirel, B., and Scherer, P. (2011). Trace element requirements of agricultural biogas digesters during biological conversion of renewable biomass to methane. *Biomass Bioenergy* 35, 992–998.
- Deppenmeier, U., Blaut, M., Schmidt, B., and Gottschalk, G. (1992). Purification and properties of a F₄₂₀-nonreactive, membrane-bound hydrogenase from *Methanosarcina* strain Gö1. *Arch. Microbiol.* 157, 505–511.
- Diekert, G., Konheiser, U., Piechulla, K., and Thauer, R. K. (1981). Nickel requirement and factor F₄₃₀ content of methanogenic bacteria. *J. Bacteriol.* 148, 459–464.
- Diekert, G., Weber, B., and Thauer, R. K. (1980). Nickel dependence of factor F₄₃₀ content in *Methanobacterium thermoautotrophicum*. *Arch. Microbiol.* 127, 273–277.
- DiSpirito, A. A., Zahn, J. A., Graham, D. W., Kim, H. J., Larive, C. K., Derrick, T. S., Cox, C. D., and Taylor, A. (1998). Copper-binding compounds from *Methylosinus trichosporium* OB3b. *J. Bacteriol.* 180, 3606–3613.
- Dupont, C. L., Butcher, A., Ruben, R. E., Bourne, P. E., and Caetano-Anollés, G. (2010). History of biological metal utilization inferred through phylogenomic analysis of protein structures. *Proc. Natl. Acad. Sci. U.S.A.* 107, 10567–10572.
- Dupont, C. L., Yang, S., Palenik, B., and Bourne, P. E. (2006). Modern proteomes contain putative imprints of ancient shifts in trace metal geochemistry. *Proc. Natl. Acad. Sci. U.S.A.* 103, 17822.
- Emerson, S. R., and Huested, S. S. (1991). Ocean anoxia and the concentrations of molybdenum and vanadium in seawater. *Mar. Chem.* 34, 177–196.
- Ensign, S. A., Hyman, M. R., and Arp, D. J. (1993). In vitro activation of ammonia monooxygenase from *Nitrosomonas europaea* by copper. *J. Bacteriol.* 175, 1971–1980.
- Ermiler, U., Grabarse, W., Shima, S., Goubeaud, M., and Thauer, R. K. (1997). Crystal structure of methyl-coenzyme M reductase: the key enzyme of biological methane formation. *Science* 278, 1457–1462.
- Ettwig, K. F., Butler, M. K., Le Paslier, D., Pelletier, E., Mangenot, S., Kuypers, M. M. M., Schreiber, F., Dutilh, B. E., Zedelius, J., De Beer, D., Gloerich, J., Wessels, H. J., van Alen, T., Luesken, E., Wu, M. L., van de Pas-Schoonen, K. T., Op den Camp, H. J., Janssen-Megens, E. M., Francoijs, K. J., Stunnenberg, H., Weissenbach, J., Jetten, M. S., and Strous, M. (2010). Nitrite-driven anaerobic methane oxidation by oxygenic bacteria. *Nature* 464, 543–548.
- Fatthepure, B. Z. (1987). Factors affecting the methanogenic activity of *Methanoxanthus soehngenii* VNB. *Appl. Environ. Microbiol.* 53, 2978–2982.
- Ferry, J. G. (1999). Enzymology of one carbon metabolism in methanogenic pathways. *FEMS Microbiol. Rev.* 23, 13–38.
- Ferry, J. G. (2010a). The chemical biology of methanogenesis. *Planet. Space Sci.* 58, 1775–1783.
- Ferry, J. G. (2010b). How to make a living by exhaling methane. *Annu. Rev. Microbiol.* 64, 453–473.
- Florencio, L., Field, J. A., and Lettinga, G. (1994). Importance of cobalt for individual trophic groups in an anaerobic methanol-degrading consortium. *Appl. Environ. Microbiol.* 60, 227–234.
- Florencio, L., Jenicek, P., Field, J. A., and Lettinga, G. (1993). Effect of cobalt on the anaerobic degradation of methanol. *J. Ferment. Bioeng.* 75, 368–374.
- Fox, J. A., Livingston, D. J., Orme-Johnson, W. H., and Walsh, C. T. (1987). 8-Hydroxy-5-deazaflavin-reducing hydrogenase from *Methanobacterium thermoautotrophicum*: 1. Purification and characterization. *Biochemistry* 26, 4219–4227.
- Fru, E. C. (2011). Copper biogeochemistry: a cornerstone in aerobic methanotrophic bacterial ecology and activity? *Geomicrobiol. J.* 28, 601–614.
- Fülöp, V., Moir, J. W. B., Ferguson, S. J., and Hajdu, J. (1995). The anatomy of a bifunctional enzyme: structural basis for reduction of oxygen to water and synthesis of nitric oxide by cytochrome *cd₁*. *Cell* 81, 369–377.
- Funk, T., Gu, W., Friedrich, S., Wang, H., Gencic, S., Grahame, D. A., and Cramer, S. P. (2004). Chemically distinct Ni sites in the A-cluster in subunit of the acetyl-CoA decarbonylase/synthase complex from *Methanosarcina thermophila*: Ni L-edge absorption and X-ray magnetic circular dichroism analyses. *J. Am. Chem. Soc.* 126, 88–95.
- Gardner, A. M., Gessner, C. R., and Gardner, P. R. (2003). Regulation of the nitric oxide reduction operon (norRVW) in *Escherichia coli*. *J. Biol. Chem.* 278, 10081–10086.
- Gartner, P., Ecker, A., Fischer, R., Linder, D., Fuchs, G., and Thauer, R. K. (1993). Purification and properties of N₅ methyltetrahydromethanopterin: coenzyme M methyltransferase from *Methanobacterium thermoautotrophicum*. *Eur. J. Biochem.* 213, 537–545.
- Godden, J. W., Turley, S., Teller, D. C., Adman, E. T., Liu, M. Y., Payne, W. J., and Legall, J. (1991). The 2.3 angstrom X-ray structure of nitrite reductase from *Achromobacter cycloclastes*. *Science* 253, 438–442.
- Gong, W., Hao, B., Wei, Z., Ferguson, D. J., Tallant, T., Krzycki, J. A., and Chan, M. K. (2008). Structure of the 2 Ni-dependent CO dehydrogenase component of the *Methanosarcina barkeri* acetyl-CoA decarbonylase/synthase complex. *Proc. Natl. Acad. Sci. U.S.A.* 105, 9558–9563.
- Gonzalez-Gil, G., Kleerebezem, R., and Lettinga, G. (1999). Effects of nickel and cobalt on kinetics of methanol conversion by methanogenic sludge as assessed by on-line CH₄ monitoring. *Appl. Environ. Microbiol.* 65, 1789–1793.
- Granger, J., and Ward, B. B. (2003). Accumulation of nitrogen oxides in copper-limited cultures of denitrifying bacteria. *Limnol. Oceanogr.* 48, 313–318.
- Hagemier, C. H., Krueger, M., Thauer, R. K., Warkentin, E., and Ermiler, U. (2006). Insight into the mechanism of biological methanol activation based on the crystal structure of the methanol-cobalamin methyltransferase complex. *Proc. Natl. Acad. Sci. U.S.A.* 103, 18917–18922.
- Hakemian, A. S., Kondapalli, K. C., Telser, J., Hoffman, B. M., Stemmler, T. L., and Rosenzweig, A. C. (2008). The metal centers of particulate methane monooxygenase from *Methylosinus trichosporium* OB3b. *Biochemistry* 47, 6793–6801.

- Hakemian, A. S., and Rosenzweig, A. C. (2007). The biochemistry of methane oxidation. *Annu. Rev. Biochem.* 76, 243–241.
- Hallam, S. J., Girguis, P. R., Preston, C. M., Richardson, P. M., and DeLong, E. F. (2003). Identification of methyl coenzyme M reductase A (mcrA) genes associated with methane-oxidizing archaea. *Appl. Environ. Microbiol.* 69, 5483–5491.
- Hallam, S. J., Mincer, T. J., Schleper, C., Preston, C. M., Roberts, K., Richardson, P. M., and DeLong, E. F. (2006). Pathways of carbon assimilation and ammonia oxidation suggested by environmental genomic analyses of marine Crenarchaeota. *PLoS Biol.* 4, e95. doi:10.1371/journal.pbio.0040095
- Hallam, S. J., Putman, N., Preston, C. M., Detter, J. C., Rokhsar, D., Richardson, P. M., and DeLong, E. F. (2004). Reverse methanogenesis: testing the hypothesis with environmental genomics. *Science* 305, 1457–1462.
- Hamann, N., Mander, G. J., Shokes, J. E., Scott, R. A., Bennati, M., and Hedderich, R. (2007). A cysteine-rich CCG domain contains a novel [4Fe-4S] cluster binding motif as deduced from studies with subunit B of heterodisulfide reductase from *Methanothermobacter marburgensis*. *Biochemistry* 46, 12875–12885.
- Hanson, R. S., and Hanson, T. E. (1996). Methanotrophic bacteria. *Microbiol. Rev.* 60, 439–471.
- Haraldsson, C., and Westerlund, S. (1988). Trace metals in the water columns of the Black Sea and Framvaren Fjord. *Mar. Chem.* 23, 417–424.
- Hedderich, R., Hamann, N., and Bennati, M. (2005). Heterodisulfide reductase from methanogenic archaea: a new catalytic role for an iron-sulfur cluster. *Biol. Chem.* 386, 961–970.
- Heiden, S., Hedderich, R., Setzke, E., and Thauer, R. K. (1994). Purification of a two subunit cytochrome b containing heterodisulfide reductase from methanol grown *Methanosarcina barkeri*. *Eur. J. Biochem.* 221, 855–861.
- Heimann, M. (2011). Atmospheric science: enigma of the recent methane budget. *Nature* 476, 157–158.
- Heller, C., Hoppert, M., and Reitner, J. (2008). Immunological localization of coenzyme M reductase in anaerobic methane-oxidizing archaea of ANME 1 and ANME 2 type. *Geomicrobiol. J.* 25, 149–156.
- Hendriks, J., Oubrie, A., Castresana, J., Urbani, A., Gemeinhardt, S., and Saraste, M. (2000). Nitric oxide reductases in bacteria. *Biochim. Biophys. Acta* 1459, 266–273.
- Hinrichs, K.-U., Hayes, J. M., Sylva, S. P., Brewer, P. G., and DeLong, E. F. (1999). Methane-consuming archaeobacteria in marine sediments. *Nature* 398, 802–805.
- Ho, T. Y., Quigg, A., Finkel, Z. V., Milligan, A. J., Wyman, K., Falkowski, P. G., and Morel, F. M. M. (2003). The elemental composition of some marine phytoplankton. *J. Phycol.* 39, 1145–1159.
- Hoban, D., and van den Berg, L. (1979). Effect of iron on conversion of acetic acid to methane during methanogenic fermentations. *J. Appl. Microbiol.* 47, 153–159.
- Holmes, A. J., Costello, A., Lidstrom, M. E., and Murrell, J. C. (1995). Evidence that participate methane monooxygenase and ammonia monooxygenase may be evolutionarily related. *FEMS Microbiol. Lett.* 132, 203–208.
- Igarashi, N., Moriyama, H., Fujiwara, T., Fukumori, Y., and Tanaka, N. (1997). The 2.8 Å structure of hydroxylamine oxidoreductase from a nitrifying chemoautotrophic bacterium, *Nitrosomonas europaea*. *Nat. Struct. Biol.* 4, 276–284.
- IPCC. (2007). *The Physical Science Basis: Contribution of Working Group I to the Fourth Assessment Report of the Intergovernmental Panel on Climate Change*. New York: Cambridge University Press.
- Iwasaki, H., and Terai, H. (1982). N₂ and N₂O produced during growth of denitrifying bacteria in copper-depleted and -supplemented media. *J. Gen. Appl. Microbiol.* 28, 189–193.
- Jacinto, P. A., and Tedesco, L. P. (2009). Impact of elevated copper on the rate and gaseous products of denitrification in freshwater sediments. *J. Environ. Qual.* 38, 1183–1192.
- Jansen, S., Gonzalez-Gil, G., and van Leeuwen, H. P. (2007). The impact of Co and Ni speciation on methanogenesis in sulfidic media – biouptake versus metal dissolution. *Enzyme Microb. Technol.* 40, 823–830.
- Jansen, S., Steffen, F., Threels, W. F., and van Leeuwen, H. P. (2005). Speciation of Co (II) and Ni (II) in anaerobic bioreactors measured by competitive ligand exchange-adsorptive stripping voltammetry. *Environ. Sci. Technol.* 39, 9493–9499.
- Jarrell, K., and Sprott, G. (1982). Nickel transport in *Methanobacterium bryantii*. *J. Bacteriol.* 151, 1195–1203.
- Johnson, K. S., Gordon, R. M., and Coale, K. H. (1997). What controls dissolved iron concentrations in the world ocean? *Mar. Chem.* 57, 137–161.
- Jollie, D., and Lipscomb, J. D. (1991). Formate dehydrogenase from *Methylosinus trichosporium* OB3b. Purification and spectroscopic characterization of the cofactors. *J. Biol. Chem.* 266, 21853–21863.
- Jones, J., and Stadtman, T. C. (1977). *Methanococcus vannielii*: culture and effects of selenium and tungsten on growth. *J. Bacteriol.* 130, 1404–1406.
- Jormakka, M., Richardson, D., Byrne, B., and Iwata, S. (2004). Architecture of NarGH reveals a structural classification of Mo-bisMGD enzymes. *Structure* 12, 95–104.
- Jung, M.-Y., Park, S.-J., Min, D., Kim, J.-S., Rijpsma, W. I. C., Sinninghe Damsté, J. S., Kim, G.-J., Madsen, E. L., and Rhee, S.-K. (2011). Enrichment and characterization of an autotrophic ammonia-oxidizing archaeon of mesophilic crenarchaeal group I. 1a from an agricultural soil. *Appl. Environ. Microbiol.* 77, 8635–8647.
- Karlsen, O. A., Larsen, O., and Jensen, H. B. (2011). The copper responding surfaceome of *Methylococcus capsulatus* Bath. *FEMS Microbiol. Lett.* 323, 97–104.
- Kessler, P. S., McLarnan, J., and Leigh, J. A. (1997). Nitrogenase phylogeny and the molybdenum dependence of nitrogen fixation in *Methanococcus maripaludis*. *J. Bacteriol.* 179, 541–543.
- Kida, K., Shigematsu, T., Kijima, J., Numaguchi, M., Mochinaga, Y., Abe, N., and Morimura, S. (2001). Influence of Ni²⁺ and Co²⁺ on methanogenic activity and the amounts of coenzymes involved in methanogenesis. *J. Biosci. Bioeng.* 91, 590–595.
- Kim, H. J., Graham, D. W., DiSpirito, A. A., Alterman, M. A., Galeva, N., Larive, C. K., Asunskis, D., and Sherwood, P. M. A. (2004). Methanobactin, a copper-acquisition compound from methane-oxidizing bacteria. *Science* 305, 1612–1615.
- Kinniburgh, D. G., and Miles, D. L. (1983). Extraction and chemical analysis of interstitial water from soils and rocks. *Environ. Sci. Technol.* 17, 362–368.
- Knapp, C. W., Fowle, D. A., Kulczycki, E., Roberts, J. A., and Graham, D. W. (2007). Methane monooxygenase gene expression mediated by methanobactin in the presence of mineral copper sources. *Proc. Natl. Acad. Sci. U.S.A.* 104, 12040–12045.
- Knittel, K., and Boetius, A. (2009). Anaerobic oxidation of methane: progress with an unknown process. *Annu. Rev. Microbiol.* 63, 311–334.
- Knowles, R. (1982). Denitrification. *Microbiol. Mol. Biol. Rev.* 46, 43–70.
- Kolk, L. A. (1938). A comparison of the filamentous iron organisms, *Clonothrix fusca* Roze and *Crenothrix polyspora* Cohn. *Am. J. Bot.* 25, 11–17.
- Konhauser, K. O., Pecoits, E., Lalonde, S. V., Papineau, D., Nisbet, E. G., Barley, M. E., Arndt, N. T., Zahnle, K., and Kamber, B. S. (2009). Oceanic nickel depletion and a methanogen famine before the Great Oxidation Event. *Nature* 458, 750–753.
- Könneke, M., Bernhard, A. E., De La Torre, J. R., Walker, C. B., Waterbury, J. B., and Stahl, D. A. (2005). Isolation of an autotrophic ammonia-oxidizing marine archaeon. *Nature* 437, 543–546.
- Kremling, K. (1983). The behavior of Zn, Cd, Cu, Ni, Co, Fe, and Mn in anoxic Baltic waters. *Mar. Chem.* 13, 87–108.
- Krüger, M., Meyerdieck, A., Glöckner, F. O., Amann, R., Widdel, F., Kube, M., Reinhardt, R., Kahnt, R., Böcher, R., Thauer, R. K., and Shima, S. (2003). A conspicuous nickel protein in microbial mats that oxidize methane anaerobically. *Nature* 426, 878–881.
- Krzycki, J., and Zeikus, J. (1980). Quantification of corrinoids in methanogenic bacteria. *Curr. Microbiol.* 3, 243–245.
- Kulczycki, E., Fowle, D. A., Kenward, P. A., Leslie, K., Graham, D. W., and Roberts, J. A. (2011). Stimulation of methanotroph activity by Cu-substituted borosilicate glass. *Geomicrobiol. J.* 28, 1–10.
- Kulczycki, E., Fowle, D. A., Knapp, C., Graham, D. W., and Roberts, J. A. (2007). Methanobactin-promoted dissolution of Cu-substituted borosilicate glass. *Geobiology* 5, 251–263.
- Kunkel, A., Vaupel, M., Heim, S., Thauer, R. K., and Hedderich, R. (1997). Heterodisulfide reductase from methanol grown cells of *Methanosarcina barkeri* is not a flavoenzyme. *Eur. J. Biochem.* 244, 226–234.
- Laukel, M., Chistoserdova, L., Lidstrom, M. E., and Vorholt, J. A. (2003). The tungsten-containing formate dehydrogenase from *Methylobacterium extorquens* AM1: purification and properties. *Eur. J. Biochem.* 270, 325–333.
- Lees, H., and Meiklejohn, J. (1948). Trace elements and nitrification. *Nature* 161, 398–399.

- Li, Q., Li, L., Rejtar, T., Lessner, D. J., Karger, B. L., and Ferry, J. G. (2006). Electron transport in the pathway of acetate conversion to methane in the marine archaeon *Methanosarcina acetivorans*. *J. Bacteriol.* 188, 702–710.
- Lieberman, R. L., and Rosenzweig, A. C. (2005). Crystal structure of a membrane-bound metalloenzyme that catalyses the biological oxidation of methane. *Nature* 434, 177–182.
- Lin, D., Kakizono, T., Nishio, N., and Nagai, S. (1990). Enhanced cytochrome formation and stimulated methanogenesis rate by the increased ferrous concentrations in *Methanosarcina barkeri* culture. *FEMS Microbiol. Lett.* 68, 89–92.
- Lin, D. G., Nishio, N., Mazumder, T. K., and Nagai, S. (1989). Influence of Co^{2+} , Ni^{2+} and Fe^{2+} on the production of tetrapyrroles by *Methanosarcina barkeri*. *Appl. Microbiol. Biotechnol.* 30, 196–200.
- Lipscomb, J. D. (1994). Biochemistry of the soluble methane monooxygenase. *Annu. Rev. Microbiol.* 48, 371–399.
- Lobo, A. L., and Zinder, S. H. (1988). Diazotrophy and nitrogenase activity in the archaeobacterium *Methanosarcina barkeri* 227. *Appl. Environ. Microbiol.* 54, 1656–1661.
- Macauley, S. R., Zimmerman, S. A., Apolinario, E. E., Evilia, C., Hou, Y.-M., Ferry, J. G., and Sowers, K. R. (2009). The archetype gamma-class carbonic anhydrase (Cam) contains iron when synthesized in vivo. *Biochemistry* 48, 817–819.
- Magalhães, C. M., Machado, A., Matos, P., and Bordalo, A. A. (2011). Impact of copper on the diversity, abundance and transcription of nitrite and nitrous oxide reductase genes in an urban European estuary. *FEMS Microbiol. Ecol.* 77, 274–284.
- Martens, C. S., and Berner, R. A. (1977). Interstitial water chemistry of anoxic Long Island Sound sediments. 1. Dissolved gases. *Limnol. Oceanogr.* 22, 10–25.
- Martin, J. H., and Fitzwater, S. E. (1988). Iron deficiency limits phytoplankton growth in the north-east Pacific subarctic. *Nature* 331, 341–343.
- Martinho, M., Choi, D. W., DiSpirito, A. A., Antholine, W. E., Semrau, J. D., and Münck, E. (2007). Mössbauer studies of the membrane-associated methane monooxygenase from *Methylococcus capsulatus* Bath: evidence for a diiron center. *J. Am. Chem. Soc.* 129, 15783–15785.
- Matsubara, T., Frunzke, K., and Zumft, W. (1982). Modulation by copper of the products of nitrite respiration in *Pseudomonas perfectomarinus*. *J. Bacteriol.* 149, 816–823.
- Mayr, S., Latkoczy, C., Krüger, M., Günther, D., Shima, S., Thauer, R. K., Widdel, F., and Jaun, B. (2008). Structure of an F₄₃₀ variant from archaea associated with anaerobic oxidation of methane. *J. Am. Chem. Soc.* 130, 10758–10767.
- Meiklejohn, J. (1953). Iron and the nitrifying bacteria. *J. Gen. Microbiol.* 8, 58–65.
- Merkx, M., Kopp, D. A., Sazinsky, M. H., Blazyk, J. L., Müller, J., and Lippard, S. J. (2001). Dioxygen activation and methane hydroxylation by soluble methane monooxygenase: a tale of two irons and three proteins. *Angew. Chem. Int. Ed. Engl.* 40, 2782–2807.
- Meyerdiercks, A., Kube, M., Lombardot, T., Knittel, K., Bauer, M., Glöckner, F. O., Reinhardt, R., and Amann, R. (2005). Insights into the genomes of archaea mediating the anaerobic oxidation of methane. *Environ. Microbiol.* 7, 1937–1951.
- Moffett, J. W., and Dupont, C. (2007). Cu complexation by organic ligands in the sub-arctic NW Pacific and Bering Sea. *Deep Sea Res. Part I Oceanogr. Res. Pap.* 54, 586–595.
- Montzka, S., Dlugokencky, E., and Butler, J. (2011). Non-CO₂ greenhouse gases and climate change. *Nature* 476, 43–50.
- Morse, J. W., and Luther, G. W. (1999). Chemical influences on trace metal-sulfide interactions in anoxic sediments. *Geochim. Cosmochim. Acta* 63, 3373–3378.
- Morton, J. D., Hayes, K. F., and Semrau, J. D. (2000). Bioavailability of chelated and soil-adsorbed copper to *Methylosinus trichosporium* OB3b. *Environ. Sci. Technol.* 34, 4917–4922.
- Murray, W. D., and van den Berg, L. (1981). Effects of nickel, cobalt, and molybdenum on performance of methanogenic fixed-film reactors. *Appl. Environ. Microbiol.* 42, 502–505.
- Murrell, J. C., McDonald, I. R., and Gilbert, B. (2000). Regulation of expression of methane monooxygenases by copper ions. *Trends Microbiol.* 8, 221–225.
- Nielsen, A. K., Gerdes, K., and Murrell, J. C. (1997). Copper-dependent reciprocal transcriptional regulation of methane monooxygenase genes in *Methylococcus capsulatus* and *Methylosinus trichosporium*. *Mol. Microbiol.* 25, 399–409.
- Nojiri, M., Xie, Y., Inoue, T., Matsumura, H., Kataoka, K., Deligeer, Yamaguchi, K., Kai, Y., and Suzuki, S. (2007). Structure and function of a hexameric copper-containing nitrite reductase. *Proc. Natl. Acad. Sci. U.S.A.* 104, 4315–4320.
- Op den Camp, H. J. M., Islam, T., Stott, M. B., Harhangi, H. R., Hynes, A., Schouten, S., Jetten, M. S. M., Birkeland, N.-K., Pol, A., and Dunfield, P. F. (2009). Environmental, genomic and taxonomic perspectives on methanotrophic Verrucomicrobia. *Environ. Microbiol. Rep.* 1, 293–306.
- Orphan, V. J., House, C. H., Hinrichs, K.-U., McKeegan, K. D., and DeLong, E. F. (2001). Methane-consuming archaea revealed by directly coupled isotopic and phylogenetic analysis. *Science* 293, 484–487.
- Orphan, V. J., House, C. H., Hinrichs, K.-U., McKeegan, K. D., and DeLong, E. F. (2002). Multiple archaeal groups mediate methane oxidation in anoxic cold seep sediments. *Proc. Natl. Acad. Sci. U.S.A.* 99, 7663–7668.
- Patel, G., Khan, A., and Roth, L. (1978). Optimum levels of sulphate and iron for the cultivation of pure cultures of methanogens in synthetic media. *J. Appl. Microbiol.* 45, 347–356.
- Pernthaler, A., Dekas, A. E., Brown, C. T., Goffredi, S. K., Embaye, T., and Orphan, V. J. (2008). Diverse syntrophic partnerships from deep-sea methane vents revealed by direct cell capture and metagenomics. *Proc. Natl. Acad. Sci. U.S.A.* 105, 7052–7057.
- Poole, R. K., and Hughes, M. N. (2000). New functions for the ancient globin family: bacterial responses to nitric oxide and nitrosative stress. *Mol. Microbiol.* 36, 775–783.
- Poth, M. (1986). Dinitrogen production from nitrite by a *Nitrosomonas* isolate. *Appl. Environ. Microbiol.* 52, 957–959.
- Poth, M., and Focht, D. D. (1985). ¹⁵N kinetic analysis of N₂O production by *Nitrosomonas europaea*: an examination of nitrifier denitrification. *Appl. Environ. Microbiol.* 49, 1134–1141.
- Reeburgh, W. S. (2007). Oceanic methane biogeochemistry. *Chem. Rev.* 107, 486–513.
- Reeve, J. N., Beckler, G. S., Cram, D. S., Hamilton, P. T., Brown, J. W., Krzycki, J. A., Kolodziej, A. F., Alex, L., Orme-Johnson, W. H., and Walsh, C. T. (1989). A hydrogenase-linked gene in *Methanobacterium thermoautotrophicum* strain delta H encodes a polyferredoxin. *Proc. Natl. Acad. Sci. U.S.A.* 86, 3031–3035.
- Ren, T., Roy, R., and Knowles, R. (2000). Production and consumption of nitric oxide by three methanotrophic bacteria. *Appl. Environ. Microbiol.* 66, 3891–3897.
- Ritchie, G. A., and Nicholas, D. J. (1972). Identification of the sources of nitrous oxide produced by oxidative and reductive processes in *Nitrosomonas europaea*. *Biochem. J.* 126, 1181–1191.
- Rodionov, D. A., Hebbeln, P., Gelfand, M. S., and Eitinger, T. (2006). Comparative and functional genomic analysis of prokaryotic nickel and cobalt uptake transporters: evidence for a novel group of ATP-binding cassette transporters. *J. Bacteriol.* 188, 317–327.
- Rogers, J. E., and Whitman, W. B. (1991). *Microbial Production and Consumption of Greenhouse Gases: Methane, Nitrogen Oxides, and Halomethanes*. Washington: American Society for Microbiology.
- Rubio, L. M., and Ludden, P. W. (2008). Biosynthesis of the iron-molybdenum cofactor of nitrogenase. *Annu. Rev. Microbiol.* 62, 93–111.
- Saito, M. A., Goepfert, T. J., and Ritt, J. T. (2008). Some thoughts on the concept of colimitation: three definitions and the importance of bioavailability. *Limnol. Oceanogr.* 53, 276–290.
- Sakadevan, K., Zheng, H., and Bavor, H. J. (1999). Impact of heavy metals on denitrification in surface wetland sediments receiving wastewater. *Water Sci. Technol.* 40, 349–355.
- Santorio, A. E., Buchwald, C., McIlvin, M. R., and Casciotti, K. L. (2011). Isotopic signature of N₂O produced by marine ammonia-oxidizing archaea. *Science* 333, 1282–1285.
- Schauer, N. L., and Ferry, J. G. (1986). Composition of the coenzyme F₄₂₀-dependent formate dehydrogenase from *Methanobacterium formicicum*. *J. Bacteriol.* 165, 405–411.
- Scheller, S., Goenrich, M., Boecher, R., Thauer, R. K., and Jaun, B. (2010). The key nickel enzyme of methanogenesis catalyses the anaerobic oxidation of methane. *Nature* 465, 606–608.
- Scherer, P. (1988). Vanadium and molybdenum requirement for the fixation of molecular nitrogen by two *Methanosarcina* strains. *Arch. Microbiol.* 151, 44–48.
- Scherer, P., Lippert, H., and Wolff, G. (1983). Composition of the major elements and trace elements of 10 methanogenic bacteria determined by inductively coupled plasma emission spectrometry. *Biol. Trace Elem. Res.* 5, 149–163.

- Scherer, P., and Sahm, H. (1981). Effect of trace elements and vitamins on the growth of *Methanosarcina barkeri*. *Acta Biotechnol.* 1, 57–65.
- Schlesinger, W. H. (2009). On the fate of anthropogenic nitrogen. *Proc. Natl. Acad. Sci. U.S.A.* 106, 203–208.
- Schönheit, P., Moll, J., and Thauer, R. K. (1979). Nickel, cobalt, and molybdenum requirement for growth of *Methanobacterium thermoautotrophicum*. *Arch. Microbiol.* 123, 105–107.
- Scott, C., Lyons, T. W., Bekker, A., Shen, Y., Poulton, S. W., Chu, X., and Anbar, A. D. (2008). Tracing the stepwise oxygenation of the Proterozoic ocean. *Nature* 452, 456–459.
- Semrau, J. D. (2011). Bioremediation via methanotrophy: overview of recent findings and suggestions for future research. *Front. Microbiol.* 2:209. doi:10.3389/fmicb.2011.00209
- Semrau, J. D., DiSpirito, A. A., and Yoon, S. (2010). Methanotrophs and copper. *FEMS Microbiol. Rev.* 34, 496–531.
- Shaw, L. J., Nicol, G. W., Smith, Z., Fear, J., Prosser, J. I., and Baggs, E. M. (2006). *Nitrosospira* spp. can produce nitrous oxide via a nitrifier denitrification pathway. *Environ. Microbiol.* 8, 214–222.
- Shaw, T. J., Gieskes, J. M., and Jahnke, R. A. (1990). Early diagenesis in differing depositional environments: the response of transition metals in pore water. *Geochim. Cosmochim. Acta* 54, 1233–1246.
- Shepard, E. M., Boyd, E. S., Broderick, J. B., and Peters, J. W. (2011). Biosynthesis of complex iron-sulfur enzymes. *Curr. Opin. Chem. Biol.* 15, 319–327.
- Shima, S., Pilak, O., Vogt, S., Schick, M., Stagni, M. S., Meyer-Klaucke, W., Warkentin, E., Thauer, R. K., and Ermler, U. (2008). The crystal structure of [Fe]-hydrogenase reveals the geometry of the active site. *Science* 321, 572–575.
- Simianu, M., Murakami, E., Brewer, J. M., and Ragsdale, S. W. (1998). Purification and properties of the heme- and iron-sulfur-containing heterodisulfide reductase from *Methanosarcina thermophila*. *Biochemistry* 37, 10027–10039.
- Sowers, K. R., and Ferry, J. G. (1985). Trace metal and vitamin requirements of *Methanococcoides methylutens* grown with trimethylamine. *Arch. Microbiol.* 142, 148–151.
- Speece, R. E., Parkin, G. F., and Gallagher, D. (1983). Nickel stimulation of anaerobic digestion. *Water Res.* 17, 677–683.
- Stanley, S. H., Prior, S. D., Leak, D., and Dalton, H. (1983). Copper stress underlies the fundamental change in intracellular location of methane mono-oxygenase in methane-oxidizing organisms: studies in batch and continuous cultures. *Biotechnol. Lett.* 5, 487–492.
- Stein, L. Y. (2011). Surveying N₂O-producing pathways in bacteria. *Meth. Enzymol.* 486, 131–152.
- Stein, L. Y., Arp, D. J., Berube, P. M., Chain, P. S., Hauser, L., Jetten, M. S., Klotz, M. G., Larimer, F. W., Norton, J. M., Op den Camp, H. J. M., Shin, M., and Wei, X. (2007). Whole genome analysis of the ammonia oxidizing bacterium, *Nitrosomonas eutropha* C91: implications for niche adaptation. *Environ. Microbiol.* 9, 2993–3007.
- Sutka, R. L., Ostrom, N. E., Ostrom, P. H., Breznak, J. A., Gandhi, H., Pitt, A. J., and Li, F. (2006). Distinguishing nitrous oxide production from nitrification and denitrification on the basis of isotopomer abundances. *Appl. Environ. Microbiol.* 72, 638–644.
- Szpunar, J. (2005). Advances in analytical methodology for bio-inorganic speciation analysis: metallomics, metalloproteomics and heteroatom-tagged proteomics and metabolomics. *Analyst* 130, 442–465.
- Takashima, M., Shimada, K., and Speece, R. E. (2011). Minimum requirements for trace metals (iron, nickel, cobalt, and zinc) in thermophilic and mesophilic methane fermentation from glucose. *Water Environ. Res.* 83, 339–346.
- Takashima, M., and Speece, R. E. (1990). Mineral requirements for methane fermentation. *Crit. Rev. Environ. Control* 19, 465–479.
- Taylor, G. T., and Pirt, S. J. (1977). Nutrition and factors limiting the growth of a methanogenic bacterium (*Methanobacterium thermoautotrophicum*). *Arch. Microbiol.* 113, 17–22.
- Terlesky, K., and Ferry, J. (1988). Purification and characterization of a ferredoxin from acetate-grown *Methanosarcina thermophila*. *J. Biol. Chem.* 263, 4080–4082.
- Tersteegen, A., and Hedderich, R. (1999). *Methanobacterium thermoautotrophicum* encodes two multisubunit membrane-bound [NiFe] hydrogenases. *Eur. J. Biochem.* 264, 930–943.
- Thauer, R. K. (1998). Biochemistry of methanogenesis: a tribute to Marjory Stephenson. *Microbiology* 144, 2377–2406.
- Thauer, R. K. (2011). Anaerobic oxidation of methane with sulfate: on the reversibility of the reactions that are catalyzed by enzymes also involved in methanogenesis from CO₂. *Curr. Opin. Microbiol.* 14, 292–299.
- Thauer, R. K., Kaster, A.-K., Goenrich, M., Schick, M., Hiromoto, T., and Shima, S. (2010). Hydrogenases from methanogenic archaea, nickel, a novel cofactor, and H₂ storage. *Annu. Rev. Biochem.* 79, 507–536.
- Thauer, R. K., Kaster, A.-K., Seedorf, H., Buckel, W., and Hedderich, R. (2008). Methanogenic archaea: ecologically relevant differences in energy conservation. *Nat. Rev. Microbiol.* 6, 579–591.
- Thauer, R. K., and Shima, S. (2008). Methane as fuel for anaerobic microorganisms. *Ann. N. Y. Acad. Sci.* 1125, 158–170.
- Trotenko, Y. A., and Murrell, J. C. (2008). Metabolic aspects of aerobic obligate methanotrophy. *Adv. Appl. Microbiol.* 63, 183–229.
- Twining, B. S., Mylon, S. E., and Benoit, G. (2007). Potential role of copper availability in nitrous oxide accumulation in a temperate lake. *Limnol. Oceanogr.* 52, 1354–1366.
- Upadhyay, A. K., Hooper, A. B., and Hendrich, M. P. (2006). NO reductase activity of the tetraheme cytochrome c₅₅₄ of *Nitrosomonas europaea*. *J. Am. Chem. Soc.* 128, 4330–4337.
- Vigliotta, G., Nutricati, E., Carata, E., Tredici, S. M., De Stefano, M., Pontieri, P., Massardo, D. R., Prati, M. V., De Bellis, L., and Alifano, P. (2007). *Clonothrix fusca* 1896, a filamentous, sheathed, methanotrophic gamma-proteobacterium. *Appl. Environ. Microbiol.* 73, 3556–3565.
- Vorholt, J. A. (2002). Cofactor-dependent pathways of formaldehyde oxidation in methylotrophic bacteria. *Arch. Microbiol.* 178, 239–249.
- Vorholt, J. A., Vaupel, M., and Thauer, R. K. (1996). A polyferredoxin with eight [4Fe-4S] clusters as a subunit of molybdenum formyl-methanofuran dehydrogenase from *Methanosarcina barkeri*. *Eur. J. Biochem.* 236, 309–317.
- Walker, C., De La Torre, J., Klotz, M., Urakawa, H., Pinel, N., Arp, D., Brochier-Armanet, C., Chain, P., Chan, P., Gollabgir, A., Hemp, J., Hügler, M., Karr, E. A., Könneke, M., Shin, M., Lawton, T. J., Lowe, T., Martens-Habbena, W., Sayavedra-Soto, L. A., Lang, D., Sievert, S. M., Rosenzweig, A. C., Manning, G., and Stahl, D. A. (2010). *Nitrosopumilus maritimus* genome reveals unique mechanisms for nitrification and autotrophy in globally distributed marine crenarchaea. *Proc. Natl. Acad. Sci. U.S.A.* 107, 8818–8823.
- Ward, B. B., Tuit, C. B., Jayakumar, A., Rich, J. J., Moffett, J., and Naqvi, S. W. A. (2008). Organic carbon, and not copper, controls denitrification in oxygen minimum zones of the ocean. *Deep Sea Res. Part I Oceanogr. Res. Pap.* 55, 1672–1683.
- Ward, N., Larsen, Ø., Sakwa, J., Bruseth, L., Khouri, H., Durkin, A. S., Dimitrov, G., Jiang, L., Scanlan, D., Kang, K. H., Lewis, M., Nelson, K. E., Methé, B., Wu, M., Heidelberg, J. F., Paulsen, I. T., Fouts, D., Ravel, J., Tettelin, H., Ren, Q., Read, T., DeBoy, R. T., Seshadri, R., Salzberg, S. L., Jensen, H. B., Birkeland, N. K., Nelson, W. C., Dodson, R. J., Grindhaug, S. H., Holt, I., Eidhammer, I., Jonassen, I., Vanaken, S., Utterback, T., Feldblyum, T. V., Fraser, C. M., Lillehaug, J. R., and Eisen, J. A. (2004). Genomic insights into methanotrophy: the complete genome sequence of *Methylococcus capsulatus* (Bath). *PLoS Biol.* 2, e303. doi:10.1371/journal.pbio.0020303
- Wei, X., Vajjala, N., Hauser, L., Sayavedra-Soto, L. A., and Arp, D. J. (2006). Iron nutrition and physiological responses to iron stress in *Nitrosomonas europaea*. *Arch. Microbiol.* 186, 107–118.
- Wetzel, R. G. (2001). *Limnology: Lake and River Ecosystems*, 3rd Edn. San Diego: Academic Press.
- Whitman, W. B., Ankwarda, E., and Wolfe, R. S. (1982). Nutrition and carbon metabolism of *Methanococcus voltae*. *J. Bacteriol.* 149, 852–863.
- Whitman, W. B., Bowen, T. L., and Boone, D. R. (2006). The methanogenic bacteria. *Prokaryotes* 3, 165–207.
- Whittaker, M., Bergmann, D., Arciero, D., and Hooper, A. B. (2000). Electron transfer during the oxidation of ammonia by the chemolithotrophic bacterium *Nitrosomonas europaea*. *Biochim. Biophys. Acta* 1459, 346–355.
- Wrage, N., Velthof, G. L., van Beusichem, M. L., and Oenema, O. (2001). Role of nitrifier denitrification in the production of nitrous oxide. *Soil Biol. Biochem.* 33, 1723–1732.

- Wu, M. L., Ettwig, K. F., Jetten, M. S., Strous, M., Keltjens, J. T., and van Niftrik, L. (2011). A new intra-aerobic metabolism in the nitrite-dependent anaerobic methane-oxidizing bacterium *Candidatus 'Methyloirabilis oxyfera.'* *Biochem. Soc. Trans.* 39, 243–248.
- Yoshinari, T. (1985). Nitrite and nitrous oxide production by *Methylosinus trichosporium*. *Can. J. Microbiol.* 31, 139–144.
- Zahn, J. A., Bergmann, D. J., Boyd, J. M., Kunz, R. C., and DiSpirito, A. A. (2001). Membrane-associated quinoprotein formaldehyde dehydrogenase from *Methylococcus capsulatus* Bath. *J. Bacteriol.* 183, 6832–6840.
- Zahn, J. A., and DiSpirito, A. A. (1996). Membrane-associated methane monooxygenase from *Methylococcus capsulatus* (Bath). *J. Bacteriol.* 178, 1018–1029.
- Zandvoort, M. H., Osuna, M. B., Geerts, R., Lettinga, G., and Lens, P. N. (2002). Effect of nickel deprivation on methanol degradation in a methanogenic granular sludge bioreactor. *J. Ind. Microbiol. Biotechnol.* 29, 268–274.
- Zandvoort, M. H., van Hullebusch, E. D., Gieteling, J., and Lens, P. N. L. (2006). Granular sludge in full-scale anaerobic bioreactors: trace element content and deficiencies. *Enzyme Microb. Technol.* 39, 337–346.
- Zellner, G., and Winter, J. (1987). Growth promoting effect of tungsten on methanogens and incorporation of tungsten-185 into cells. *FEMS Microbiol. Ecol.* 40, 81–87.
- Zerkle, A. L., House, C. H., and Brantley, S. L. (2005). Biogeochemical signatures through time as inferred from whole microbial genomes. *Am. J. Sci.* 305, 467–502.
- Zhang, Y., Rodionov, D. A., Gelfand, M. S., and Gladyshev, V. N. (2009). Comparative genomic analyses of nickel, cobalt and vitamin B12 utilization. *BMC Genomics* 10, 1–26. doi:10.1186/1471-2164-10-78
- Zirngibl, C., van Dongen, W., Schwörer, B., Büнау, R., Richter, M., Klein, A., and Thauer, R. K. (1992). H₂-forming methylenetetrahydromethanopterin dehydrogenase, a novel type of hydrogenase without iron-sulfur clusters in methanogenic archaea. *Eur. J. Biochem.* 208, 511–520.
- Zumft, W. G. (2005). Nitric oxide reductases of prokaryotes with emphasis on the respiratory, heme-copper oxidase type. *J. Inorg. Biochem.* 99, 194–215.
- that could be construed as a potential conflict of interest.

Received: 05 December 2011; paper pending published: 21 December 2011; accepted: 05 February 2012; published online: 21 February 2012.

Citation: Glass JB and Orphan VJ (2012) Trace metal requirements for microbial enzymes involved in the production and consumption of methane and nitrous oxide. *Front. Microbio.* 3:61. doi: 10.3389/fmicb.2012.00061

This article was submitted to *Frontiers in Microbiological Chemistry*, a specialty of *Frontiers in Microbiology*.

Copyright © 2012 Glass and Orphan. This is an open-access article distributed under the terms of the Creative Commons Attribution Non Commercial License, which permits non-commercial use, distribution, and reproduction in other forums, provided the original authors and source are credited.



The unique biogeochemical signature of the marine diazotroph *Trichodesmium*

Jochen Nuester^{1*}, Stefan Vogt², Matthew Newville³, Adam B. Kustka⁴ and Benjamin S. Twining¹

¹ Bigelow Laboratory for Ocean Sciences, East Boothbay, ME, USA

² X-ray Science Division, Advanced Photon Source, Argonne National Laboratory, Argonne, IL, USA

³ Center for Advanced Radiation Sources, The University of Chicago, Argonne, IL, USA

⁴ Department of Earth and Environmental Sciences, Rutgers University, Newark, NJ, USA

Edited by:

Martha Gledhill, University of Southampton, UK

Reviewed by:

Mark Moore, University of Southampton, UK

William Landing, Florida State University, USA

*Correspondence:

Jochen Nuester, Bigelow Laboratory for Ocean Sciences, 60 Bigelow Drive, P.O. Box 380, East Boothbay, ME 04544, USA.
e-mail: jnuester@bigelow.org

The elemental composition of phytoplankton can depart from canonical Redfield values under conditions of nutrient limitation or production (e.g., N fixation). Similarly, the trace metal metallome of phytoplankton may be expected to vary as a function of both ambient nutrient concentrations and the biochemical processes of the cell. Diazotrophs such as the colonial cyanobacteria *Trichodesmium* are likely to have unique metal signatures due to their cell physiology. We present metal (Fe, V, Zn, Ni, Mo, Mn, Cu, Cd) quotas for *Trichodesmium* collected from the Sargasso Sea which highlight the unique metallome of this organism. The element concentrations of bulk colonies and trichomes sections were analyzed by ICP-MS and synchrotron x-ray fluorescence, respectively. The cells were characterized by low P contents but enrichment in V, Fe, Mo, Ni, and Zn in comparison to other phytoplankton. Vanadium was the most abundant metal in *Trichodesmium*, and the V quota was up to fourfold higher than the corresponding Fe quota. The stoichiometry of 600C:101N:1P (mol mol⁻¹) reflects P-limiting conditions. Iron and V were enriched in contiguous cells of 10 and 50% of *Trichodesmium* trichomes, respectively. The distribution of Ni differed from other elements, with the highest concentration in the transverse walls between attached cells. We hypothesize that the enrichments of V, Fe, Mo, and Ni are linked to the biochemical requirements for N fixation either directly through enrichment in the N-fixing enzyme nitrogenase or indirectly by the expression of enzymes responsible for the removal of reactive oxygen species. Unintentional uptake of V via P pathways may also be occurring. Overall, the cellular content of trace metals and macronutrients differs significantly from the (extended) Redfield ratio. The *Trichodesmium* metallome is an example of how physiology and environmental conditions can cause significant deviations from the idealized stoichiometry.

Keywords: extended redfield ratio, metallome, nitrogen fixation, vanadium, iron, nickel, zinc

INTRODUCTION

The biogeochemical cycling of many trace metals is controlled, to a large degree, by their incorporation into plankton biomass in surface waters and remineralization from degrading plankton at depth. This linkage was proposed for macronutrients by Redfield (Redfield, 1934, 1958; Redfield et al., 1963), and more recent studies have expanded the concept to metals (Morel and Hudson, 1985; Bruland et al., 1991; Ho et al., 2003). Indeed, the molar stoichiometry of particulate C:N:P in surface waters has been observed to be strikingly similar to stoichiometries of dissolved CO₂:nitrate:phosphate in deep ocean seawater (Sverdrup et al., 1942; Takahashi et al., 1985; Körtzinger et al., 2001). Similar relationships can be observed for trace metals, although the comparisons break down for metals with significant lithogenic inputs, redox transformations, or scavenging behavior (Morel, 2008). Despite the relative constancy of average C:N:P in the ocean, macronutrient ratios in specific ocean regions and specific phytoplankton groups depart significantly from the Redfield ratio (Sverdrup et al., 1942; Geider and La Roche, 2002; Arrigo, 2005).

Similarly, although bulk plankton communities are often characterized by a fairly consistent metal stoichiometry (Bruland et al., 1991; Ho, 2006), individual species and taxonomic groups can vary significantly in their metal stoichiometries (or quotas), even when grown under the same conditions (Ho et al., 2003; Twining et al., 2004, 2011).

The elemental composition of phytoplankton can depart from canonical Redfield values under conditions of nutrient limitation or production (e.g., N fixation). The diazotrophic cyanobacterium *Trichodesmium* has significantly elevated N contents, relative to P, when fixing N (White et al., 2006), and blooms of *Trichodesmium* can significantly alter the major nutrient stoichiometry of particulate matter in surface waters of the ocean (Karl et al., 1992). Phytoplankton also vary their major nutrient stoichiometry under P-limiting conditions (Sterner and Elser, 2002; Ji and Sherrell, 2008), which may be encountered by *Trichodesmium* in the ocean (Sañudo-Wilhelmy et al., 2001). Macronutrient limitation can also result in altered trace metal stoichiometries as cells adjust their biochemical machinery to deal with changing nutrient supplies. For

example, cells require more Fe, Ni, and Zn to grow on nitrate, urea, and organic P, respectively, because of the biochemical composition of the metalloenzymes nitrate reductase, urease, and alkaline phosphatase (Price and Morel, 1991; Maldonado and Price, 1996; Ji and Sherrell, 2008). Additionally, taxonomic groups can vary in their metal response to identical macronutrient stresses (Ji and Sherrell, 2008).

Similarly, diazotrophs such as *Trichodesmium* are likely to have unique metal signatures due to their cell physiology. The metalloenzyme nitrogenase contains at least 38 atoms of Fe per holozyyme (Whittaker et al., 2011). Kustka et al. (2003b) estimated that 19–53% of cellular Fe in *Trichodesmium* is bound in nitrogenase. Such presence of Fe-rich enzymes leads consequently to elevated Fe quotas in comparison to other phytoplankton (Berman-Frank et al., 2001). Cellular Mo enrichment relative to non-diazotrophic phytoplankton also likely results from the presence of a Mo and Fe (MoFe) cofactor of nitrogenase (Dominic et al., 2000; Tuit et al., 2004). Furthermore, the concomitant fixation of N and C in *Trichodesmium* requires an additional biochemical defense mechanism against reactive oxygen species, which deactivate the nitrogenase enzyme. The removal of hydrogen peroxide or superoxide by enzymes such haloperoxidase and superoxide dismutase is thus essential for the process of N fixation (Dupont et al., 2008b; Johnson et al., 2011). These enzymes have metal co-factors of their own which may be elevated in *Trichodesmium*, thus imparting to the organism a unique trace metal stoichiometry.

In this study we present data on the metal contents, or metallome (Williams, 2001; Haraguchi, 2004), of *Trichodesmium* collected from the Sargasso Sea in the western sub-tropical North Atlantic Ocean. Metal stoichiometries of whole colonies were determined using inductively coupled plasma mass spectrometry (ICP-MS), and trichome sections were assayed using synchrotron x-ray fluorescence (SXRF). In addition to providing independent assessment of the elemental content of the organisms, the micro-analytical analyses allow us to study the spatial allocation of these elements and probe their sources. Information about the metallome is then linked to the biology of *Trichodesmium* and several hypotheses are presented regarding the potential biochemical associations of these trace metals in this organism.

MATERIALS AND METHODS

SAMPLE COLLECTION

Trichodesmium samples were collected from the Sargasso Sea in August 2010 during a cruise to the region aboard the R/V Atlantic Explorer (Bermuda Atlantic Time-Series Study cruise 261). Samples were collected at six different stations at different times of the day. All stations were within a 13 km radius and were located within the same mesoscale water mass as indicated by sea surface height anomaly (Figure 1). Thus the stations are interpreted to represent one geographical location. *Trichodesmium* colonies were collected at a depth of ca. 5 m using a 100- μ m plankton net with a PVC frame. Immediately after collection, 15–20 colonies were transferred using acid-washed polystyrene inoculation loops from the cod end to Teflon vials filled with Milli-Q water (> 18 M Ω) for subsequent digestion and ICP-MS analysis. In order to normalize metal quotas to C and N, as well as to P (which is

obtained via ICP-MS), 20–30 colonies were concurrently picked at each station for CHN analysis and placed into Teflon vials filled with filtered seawater. Subsequently, colonies for CHN analysis were filtered onto pre-combusted GF/F filters, wrapped in aluminum foil, and frozen until samples could be dried overnight at 60°C. Additional samples were transferred from the cod end to two 50-mL centrifuge tubes and amended immediately with cleaned glutaraldehyde to a final concentration of 0.5% for preparation of SXRF samples.

All shipboard handling was carried out using trace metal clean materials and tools under a laminar flow hood. The elemental composition of whole colonies was determined using ICP-MS and CHN analysis (Table 1). Element distributions and concentrations in individual trichome sections were assessed with SXRF. Specific efforts to disaggregate colonies during SXRF sample preparation were not made, but individual free (i.e., non-overlapping) trichomes were chosen for analysis to enable interpretation of the resulting 2D element maps. No effort was made to identify or remove any attached bacteria, eukaryotes, or mineral material associated with colonies prior to analysis.

BULK ELEMENT ANALYSIS

Trichodesmium colonies were digested in Teflon vials prior to ICP-MS analysis. Vials were first cleaned via an overnight soak in 2 M HCl followed by boiling in aqua regia for 4 h. Vials were then rinsed five times with Milli-Q and dried in a class-100 laminar flow hood. *Trichodesmium* samples were digested in 6 M Optima HNO₃ at 150°C for 4 h. This was repeated twice with dry-down in between. Following digestion, each sample was taken up in 0.6 M HCl (Optima Grade) and In-115 was added as internal standard. Elemental contents of samples were more than 40-fold above those of blank digest vials that were filled with Milli-Q water in the field and treated exactly as samples. Digest blank values were subtracted from samples.

Samples were analyzed by high-resolution inductively coupled mass spectrometry (HR-ICP-MS, FinniganMAT, Element 2) using an Apex PFA desolvator/nebulizer (Elemental Scientific, Omaha, NE). A freshwater plankton standard (BCR-414, Commission of the European Communities) was analyzed to check analyte recoveries. The elements Al, Mn, Fe, Cu, and Zn had recoveries of $100 \pm 5\%$, while recoveries of Cd (110%), Mo (132%), and Ni (150%) were higher. *Trichodesmium* C and N quotas were determined using a Perkin-Elmer 2400 CHN analyzer. Element signals were 23- to 41-fold above those in blank ashed GF/F filters; blank values were subtracted from samples.

SXRF SAMPLE ANALYSIS

Samples for single-trichome SXRF analysis were prepared either with or without an oxalate-EDTA treatment to remove adsorbed Fe (Tovar-Sanchez et al., 2003). For the non-oxalate-treated samples, glutaraldehyde-fixed *Trichodesmium* colonies or single trichomes were removed from the centrifuge tube and pipetted in 10- μ L drops onto LUX film-coated Cu TEM grids (Ted Pella, Redding, CA). In order to avoid the formation of salt crystals, seawater was delicately wicked from the grids using the corner of a Kimwipe. A 10- μ L droplet of Milli-Q was then pipetted onto the grid and immediately removed from the grid using a Kimwipe.

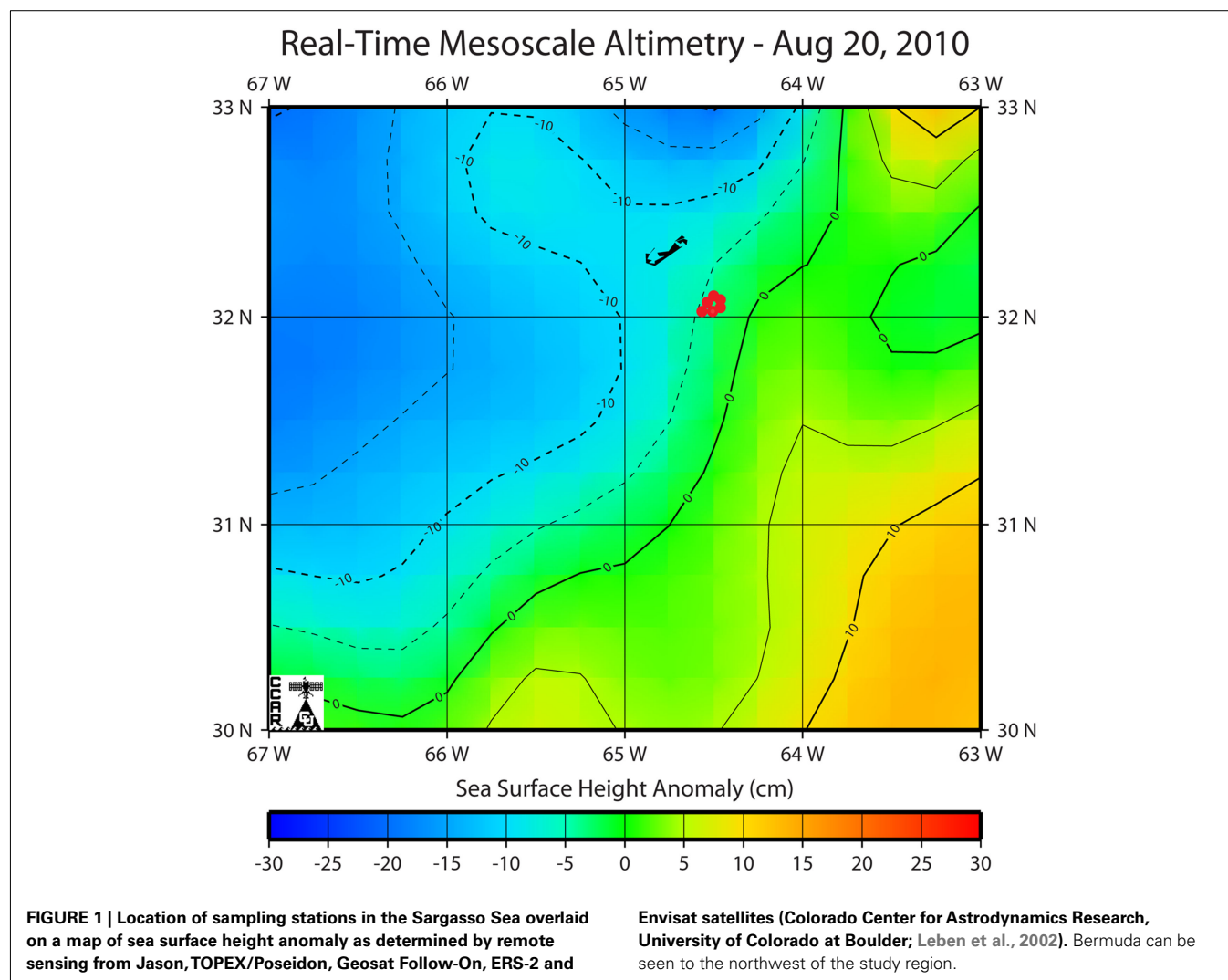


Table 1 | Summary of locations, sampling times, ambient temperature and salinity, and analyses performed.

Station	Latitude	Longitude	Local date	Local time	Temperature	Salinity	ICP-MS/CHN	SXRF (GSECARS)	SXRF (2ID-E)
1	32° 10'N	64° 30'W	8/19/10	14:30	n.d.	n.d.	4	n.d.	n.d.
2	31° 58'N	64° 17'W	8/19/10	23:00	28.9	36.7	3	n.d.	n.d.
3	31° 66'N	64° 17'W	8/20/10	8:00	28.5	36.7	4	9	n.d.
4	31° 66'N	64° 17'W	8/20/10	19:30	28.7	36.7	4	2	n.d.
5	31° 70'N	64° 16'W	8/21/10	15:00	28.7	36.7	4	11	n.d.
7	31° 67'N	64° 17'W	8/22/10	12:00	28.8	36.7	n.d.	7	14

The number of replicate samples analyzed is listed for each technique. For inductively coupled plasma mass spectrometry (ICP-MS) and CHN analysis the number of replicate bulk colony assemblages analyzed is shown. For synchrotron x-ray fluorescence (SXRF) the number of trichome sections analyzed is shown. GSECARS and 2ID-E indicate the beamlines used to conduct SXRF analyses at the Advanced Photon Source.

The samples were then allowed to air dry in a laminar flow hood. For the oxalate-treated samples, a second batch of glutaraldehyde-fixed colonies were filtered onto 25-mm diameter 1- μ m pore polycarbonate filter membranes under low vacuum pressure (< 50 mm Hg) and soaked for 15 min in trace-metal clean oxalate-EDTA reagent (Tovar-Sanchez et al., 2003). Soaked cells were

subsequently rinsed three times with 0.8 mol L⁻¹ ammonium formate solution isotonic to seawater. *Trichodesmium* colonies were then resuspended in fresh ammonium formate solution and individual colonies or trichomes were pipetted onto LUXfilm grids and allowed to air dry. Dried grids were stored in the dark until SXRF analysis.

Element concentrations and distributions within sections of trichomes were analyzed at the Advanced Photon Source (Argonne National Laboratory, Argonne, IL, USA) using hard x-ray microprobe beamlines 2ID-E and GSECARS 13ID-C. The 2ID-E beamline allows for high-resolution imaging (ca. 0.4 μm FWHM) via a 10 keV x-ray beam focused with a Fresnel zone plate with a 320 micron diameter and 100 nm outermost zonewidth (X-radia, Inc, Pleasanton, CA). The 13ID-C beamline uses Kirkpatrick-Baez mirrors to focus a larger beam (ca. 2 μm FWHM) useful for efficient scanning of larger areas. The lower resolution at GSECARS 13ID-C enables scanning of larger sections of trichomes at the expense of higher spatial resolution. Samples were analyzed at both beamlines inside a He-filled sample chamber to reduce background Ar fluorescence and maximize efficiency of detection of x-ray fluorescence originating from low-Z elements. At GSECARS samples were analyzed using a monochromatic 7.3 keV x-ray beam in order to improve sensitivity for elements of lower energy such as P and S.

Element quantification of spatial regions of interest (ROI; e.g., trichome section, background) within each trichome section was performed as described by Twining et al. (2011). Briefly, spectra of pixels belong to each ROI were averaged and fit using the software package MAPS (Vogt, 2003). A multi-element exponentially modified Gaussian peak model was used to convert peak areas to areal element concentrations using NBS-certified thin-film standards (SRM 1832 and SRM 1833). The conversion factor for the elements P and S which are not present in either SRM was obtained interpolating the conversion factor of other elements as a function of their theoretical fluorescence yield (Núñez-Milland et al., 2010). The areal element concentration of each trichome ROI was calculated after subtraction of a background ROI recorded in close proximity to the trichome ROI.

STATISTICAL TREATMENT

Phosphorous-normalized element stoichiometries for samples taken at different time points and measured using ICP-MS were compared using a non-parametric Kruskal–Wallis test (JMP 9,

SAS Institute, Cary, NC, USA). As a subsample of SXRF samples was treated with an oxalate solution, a two-way ANOVA was used to test the significance of sampling time and oxalate treatment effects. As the oxalate and non-oxalate samples showed no significant difference ($p > 0.05$) for metal and S quotas, these data were subsequently grouped together, and temporal variability of S-normalized metal stoichiometries was tested using a non-parametric Kruskal–Wallis test.

RESULTS

ELEMENTAL CONTENT OF *TRICHODESMIUM* COLONIES

The bulk elemental content of *Trichodesmium* colonies was assessed by analyses of picked colonies (Table 2). The measurement of C and N on concurrent samples for each station allowed normalizing ICP-MS element signatures to these additional biomass proxies. Mean (\pm SD) C:N ($6.03 \pm 1.05 \text{ mol mol}^{-1}$) was slightly below the canonical Redfield ratio (6.7 mol mol^{-1}). However mean N:P ranged from 93 to 148 mol mol^{-1} at each station, and mean C:P was four- to seven-fold above the Redfield ratio of 106 mol mol^{-1} (Table 2), suggesting that cells were severely P-limited under the oligotrophic late-summer conditions present in the surface waters of the Sargasso Sea. Vanadium was the most abundant metal in the colonies ($66\text{--}100 \mu\text{mol mol}^{-1} \text{ C}$), followed by Fe ($21\text{--}40 \mu\text{mol mol}^{-1} \text{ C}$), Zn ($6\text{--}29 \mu\text{mol mol}^{-1} \text{ C}$), Ni and Mo ($9\text{--}17 \mu\text{mol mol}^{-1} \text{ C}$), and Mn and Cu ($4\text{--}9 \mu\text{mol mol}^{-1} \text{ C}$; Table 2). Cadmium was approximately two orders of magnitude less abundant in *Trichodesmium* ($0.01\text{--}0.12 \mu\text{mol mol}^{-1} \text{ C}$).

P- AND S-NORMALIZED METAL STOICHIOMETRIES

While C provides the most direct proxy for cell biomass, C was not measured on the exact same samples as trace metals due to the different analytical techniques required. Phosphorus, however, was measured on the same sample digests as the metals, so P-normalized metal stoichiometries are used to more precisely normalize metal contents to variations in colony biomass between the picked samples. Mean P content per colony

Table 2 | Mean element quotas measured by CHN and ICP-MS for *Trichodesmium* colonies collected from the Sargasso Sea.

Station	C	N	P	V	Mn	Fe	Ni	Cu	Zn	Mo	Cd	C:N	C:P	V:C	Mn:C	Fe:C	Ni:C	Cu:C	Zn:C	Mo:C	Cd:C
Blank	12.9 <i>6.58</i>	3.85 <i>1.72</i>	n.d. <i>n.d.</i>	0.03 <i>0.01</i>	0.02 <i>0.01</i>	0.38 <i>0.15</i>	0.01 <i>0.01</i>	n.d. <i>n.d.</i>	n.d. <i>n.d.</i>	n.d. <i>n.d.</i>	n.d. <i>n.d.</i>										
1	582 <i>129</i>	99.4 <i>24.6</i>	0.98 <i>0.28</i>	58.1 <i>n.d.</i>	5.09 <i>1.25</i>	17.3 <i>3.99</i>	6.34 <i>1.65</i>	3.9 <i>0.93</i>	6.31 <i>5.1</i>	8.39 <i>5.39</i>	58.1 <i>15.8</i>	5.9 <i>0.2</i>	596 <i>216</i>	100 <i>22</i>	8.7 <i>2.9</i>	30 <i>9.5</i>	11 <i>3.7</i>	6.7 <i>2.2</i>	11 <i>9.1</i>	14 <i>9.8</i>	0.10 <i>0.035</i>
2	545 <i>45.3</i>	92.3 <i>6.75</i>	0.76 <i>0.32</i>	36.1 <i>176</i>	3.86 <i>1.59</i>	11.7 <i>2.61</i>	4.74 <i>1.84</i>	2.76 <i>1.61</i>	3.02 <i>0.94</i>	9.22 <i>4.87</i>	39.7 <i>37</i>	5.9 <i>0.2</i>	716 <i>282</i>	66 <i>33</i>	7.1 <i>3.0</i>	21 <i>5.1</i>	8.7 <i>3.4</i>	5.1 <i>3.0</i>	5.5 <i>1.8</i>	17 <i>9.0</i>	0.07 <i>0.068</i>
3	633 <i>194</i>	97 <i>35.1</i>	1.34 <i>0.25</i>	57.4 <i>29</i>	5.83 <i>0.77</i>	22.2 <i>8.51</i>	9.58 <i>3.1</i>	3.56 <i>0.72</i>	13.31 <i>8.55</i>	6.43 <i>2.32</i>	72.9 <i>34.2</i>	6.8 <i>2.1</i>	474 <i>170</i>	91 <i>54</i>	9.2 <i>3.1</i>	35 <i>17</i>	15 <i>6.7</i>	5.6 <i>2.1</i>	21 <i>15</i>	10 <i>4.8</i>	0.12 <i>0.065</i>
4	518 <i>97.7</i>	86.9 <i>12.6</i>	0.74 <i>0.12</i>	45.2 <i>7.7</i>	3.91 <i>0.52</i>	11.4 <i>2.86</i>	5.57 <i>1.11</i>	2.19 <i>0.28</i>	9.8 <i>8.2</i>	5.2 <i>1.05</i>	27.7 <i>9.39</i>	5.9 <i>0.3</i>	702 <i>173</i>	87 <i>22</i>	7.5 <i>1.7</i>	22 <i>6.9</i>	11 <i>3.0</i>	4.2 <i>1.0</i>	19 <i>16</i>	10 <i>2.8</i>	0.05 <i>0.021</i>
5	379 <i>47.5</i>	67.9 <i>5.9</i>	0.74 <i>0.16</i>	32.9 <i>5.3</i>	3.43 <i>0.55</i>	15 <i>12.7</i>	5.94 <i>1.08</i>	2.3 <i>0.59</i>	11.08 <i>12.19</i>	6.08 <i>1.53</i>	31.8 <i>14</i>	5.6 <i>0.9</i>	514 <i>127</i>	87 <i>18</i>	9.1 <i>1.8</i>	40 <i>33.7</i>	16 <i>3.5</i>	6.1 <i>1.7</i>	29 <i>32</i>	16 <i>4.5</i>	0.08 <i>0.038</i>

C, N, and P are in units of nmol-colony^{-1} ; Fe, Zn, Mn, Cu, Ni, Mo, and V are in units of pmol-colony^{-1} , and Cd data are in units of fmol-colony^{-1} . C:N and C:P data are in units of mol mol^{-1} ; Fe:C, Zn:C, Mn:C, Cu:C, Ni:C, Mo:C, Cd:C, and V:C in $\mu\text{mol mol}^{-1}$. Blanks were calculated by dividing the mean elemental content of blank digestion vials by the typical number of colonies per sample vial ($n = 20$). SD for C-normalized ratios were calculated by propagation of error. The number of replicate samples analyzed for each element is shown in Table 1. Mean, bold; SD, italics; n.d., below detection limit.

varied 1.8-fold between stations (**Table 2**), but the P-normalized metal stoichiometries measured by ICP-MS follow the trends observed in the C-normalized stoichiometries (V:P > Fe:P > Zn:P ≈ Ni:P ≈ Mo:P > Mn:P ≫ Cd:P; **Table 3**).

Stoichiometries of several metals (Fe, Mn, V) were measured with both ICP-MS and SXRF in *Trichodesmium* collected from the same station, enabling direct comparisons between the techniques (**Figure 2**). Fe:P stoichiometries were generally comparable (10–25 mmol mol⁻¹), while Mn:P showed a systematic offset, with approximately threefold higher Mn:P measured in picked colonies with ICP-MS (4.4–5.3 mmol mol⁻¹) than measured in sections of trichomes with SXRF (1.1–1.7 mmol mol⁻¹). V:P stoichiometries were fairly constant in communities of picked *Trichodesmium* (41–63 mmol mol⁻¹) but were highly variable in subsections of the trichomes analyzed with SXRF, ranging more than 500-fold in trichomes collected from the same station. This complicates

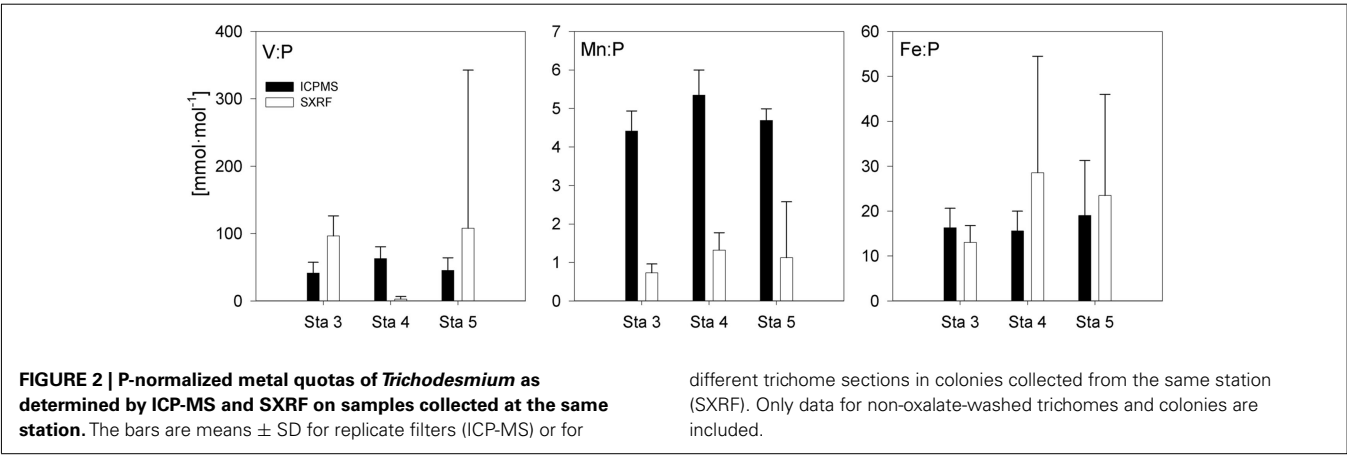
comparison between techniques. However, SXRF V:P stoichiometries were consistently higher than ICP-MS V:P stoichiometries at one station, consistently lower at another station, and spanned the ICP-MS stoichiometries at a third station, indicating that there was not a systematic offset in results between the techniques and that SXRF stoichiometries are a strong function of which trichome section is analyzed.

Sections of two *Trichodesmium* colonies were further analyzed at two different beamlines to examine variability on different spatial scales. The compatibility of the data from the two beamlines was assessed by comparing areal concentrations measured on the same trichome section. The overlapping regions of analysis are indicated for trichomes C and D in **Figures 3** and **4**, respectively. The areal concentrations for V, Mn, and Fe measured at GSECARS were consistently two- to five-fold below those measured in overlapping trichome sections at 2ID-E (**Figure 5**; **Table 4**). However

Table 3 | P-normalized mean metal stoichiometries of *Trichodesmium* measured by ICP-MS or SXRF.

Station	Technique	Time	V:P	Mn:P	Fe:P	Ni:P	Zn:P	Mo:P	Cd:P
1	ICP-MS	14:30	50.4	5.4	20.0	6.5	8.0	8.7	64.9
				<i>1.4</i>	<i>11.7</i>	<i>0.6</i>	<i>8.6</i>	<i>4.5</i>	<i>30.9</i>
2	ICP-MS	23:00	47.0	5.1	16.9	6.5	4.4	11.9	47.9
				<i>0.6</i>	<i>5.9</i>	<i>1.5</i>	<i>1.2</i>	<i>3.1</i>	<i>37.0</i>
3	ICP-MS	8:00	41.5	4.4	16.3	7.6	9.6	5.1	52.6
				<i>0.5</i>	<i>4.3</i>	<i>5.3</i>	<i>0.2</i>	<i>2.5</i>	<i>17.2</i>
3	SXRF	8:00	96	1	13				
				<i>0.2</i>	<i>3.7</i>				
4	ICP-MS	19:30	63.1	5.3	15.6	7.7	13.7	7.0	37.6
				<i>0.7</i>	<i>4.4</i>	<i>1.9</i>	<i>12.7</i>	<i>0.7</i>	<i>12.6</i>
4	SXRF	19:30	2.8	1.3	28.6				
				<i>0.5</i>	<i>25.9</i>				
5	ICP-MS	15:00	45.3	4.7	19.0	8.1	13.5	8.6	41.5
				<i>0.3</i>	<i>12.2</i>	<i>1.1</i>	<i>12.5</i>	<i>2.8</i>	<i>10.6</i>
5	SXRF	15:00	108	1	24				
				<i>1</i>	<i>22</i>				
7	SXRF	12:00	70	3	63		68		
				<i>2</i>	<i>32</i>		<i>54</i>		

Cd:P stoichiometry is presented as $\mu\text{mol mol}^{-1}$ and Mo:P, V:P, Mn:P, Fe:P, Ni:P, and Zn:P data are presented as mmol mol^{-1} . Mean, bold; SD, italics. Only data for non-oxalate-washed trichomes or colonies are included.



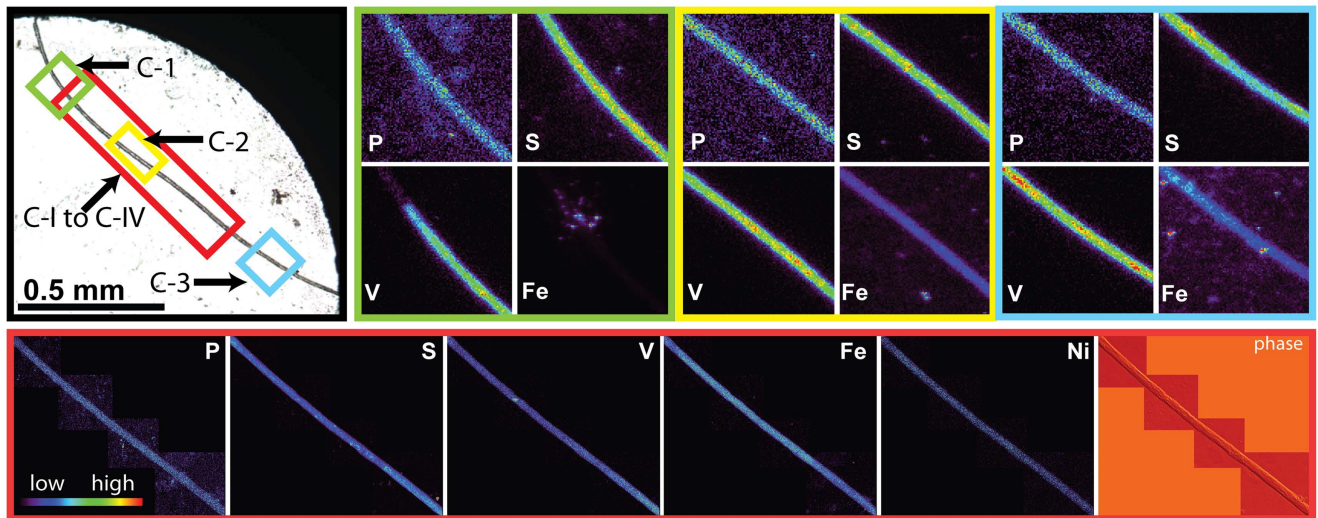


FIGURE 3 | Light micrographs, false-color element (P, S, V, Fe and Ni) maps, and differential phase contrast images (phase) (Hornberger et al., 2008) of *Trichodesmium* trichome C. The color scale for element maps is shown, with warmer colors indicating higher element concentrations. The color scheme of the differential phase

contrast image does not follow the color scale for the element maps. The location of each trichome section is indicated on the light micrograph with a unique outline color. Maps C-1 (green), C-2 (yellow), and C-3 (blue) were recorded at the GSECARS beamline, while maps C-I to C-IV (red) were recorded at 2ID-E.

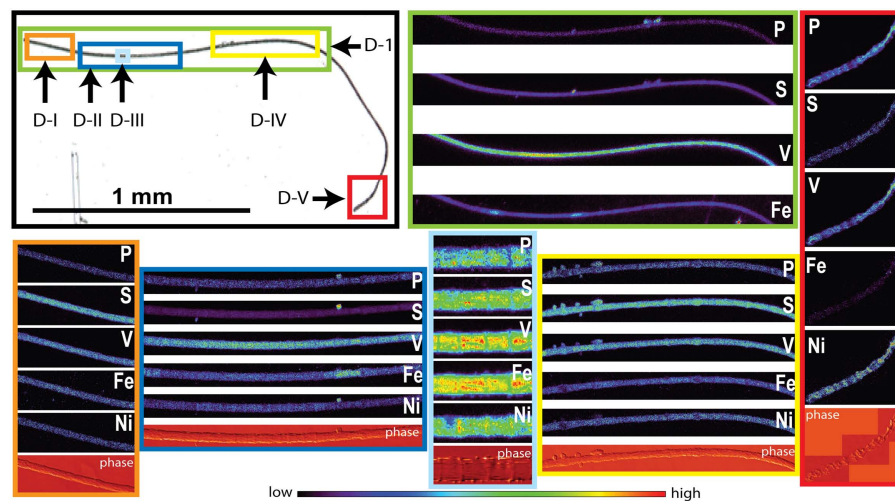


FIGURE 4 | Light micrographs, false-color element (P, S, V, Fe and Ni) maps, and differential phase contrast images (phase) (Hornberger et al., 2008) of *Trichodesmium* trichome D. The color scale for element maps is shown, with warmer colors indicating higher element concentrations. The color scheme of the differential phase contrast image

does not follow the color scale for the element maps. The location of each trichome section is indicated on the light micrograph with a unique outline color. MAP D-1 (green) was recorded at the GSECARS beamline, while maps D-I (orange), D-II (dark blue), D-III (light blue), D-IV (yellow), and D-V (red) were recorded at 2ID-E.

metal concentrations normalized to biomass proxies P or S were generally comparable between beamlines (Figure 5).

A subset of the *Trichodesmium* colonies analyzed with SXRF was treated with an oxalate-EDTA solution to remove externally bound Fe, enabling comparisons between treated and untreated trichomes. Areal concentrations (nmol cm^{-2}) of S, Fe, Mn, and V were not significantly different in oxalate-treated trichome sections compared to non-oxalate-treated trichome sections (two-way ANOVA, $p > 0.267$), however least-square mean

P concentrations were 47% lower in treated trichomes ($p = 0.012$; Figure 6). Due to the sparse *Trichodesmium* population encountered during the sampling campaign, the effect of an oxalate-EDTA treatment was only assessed for SXRF samples and not for ICP-MS and CHN samples.

Trichodesmium samples were collected at different times of day over the course of the cruise, and temporal differences were examined separately in the ICP-MS and SXRF datasets. Bulk ICP-MS P-normalized stoichiometries for non-oxalate-rinsed colonies

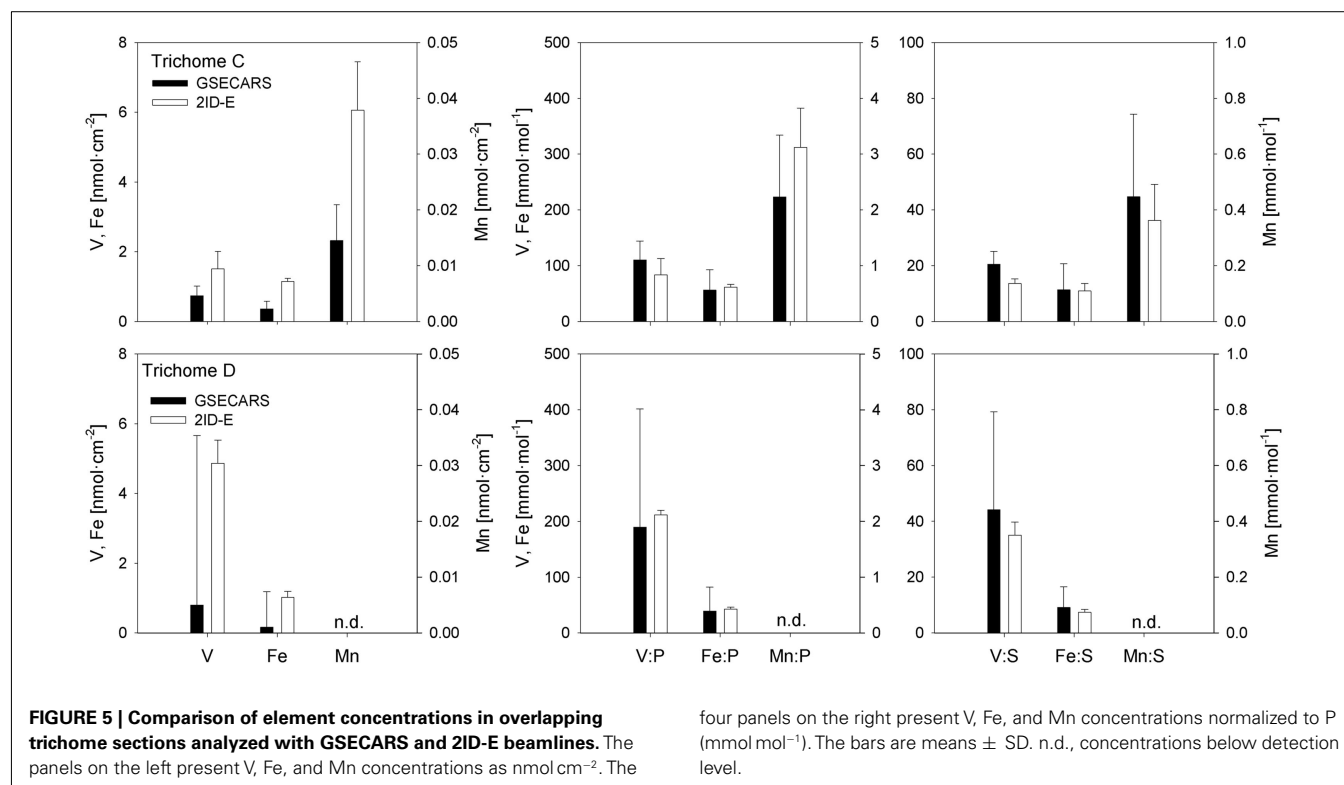


Table 4 | Comparison of areal element concentrations and P- and S-normalized stoichiometries for V, Mn, and Fe measured at GSECARS and at 2ID-E.

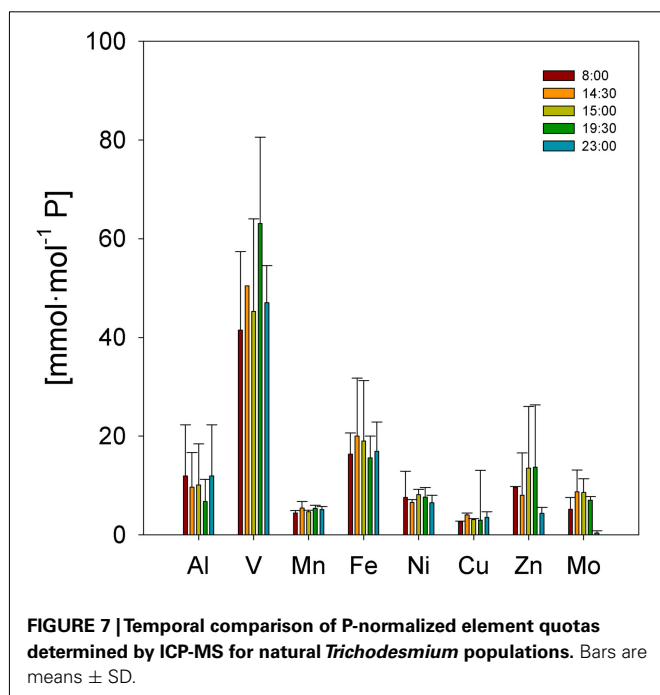
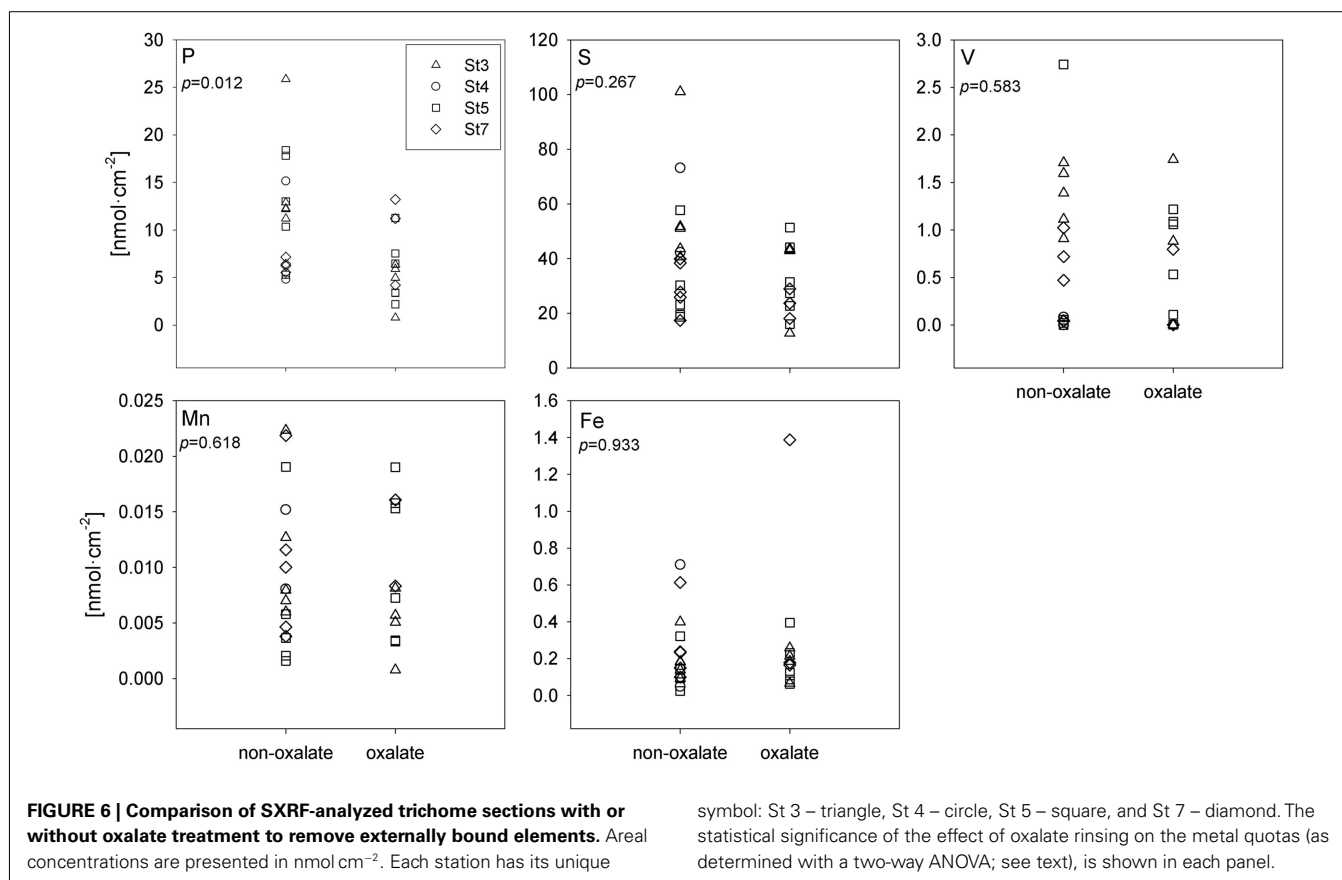
GSECARS										2ID-E									
Trichome	V	Mn	Fe	V:P	Mn:P	Fe:P	V:S	Mn:S	Fe:S	Trichome	V	Mn	Fe	V:P	Mn:P	Fe:P	V:S	Mn:S	Fe:S
C-1	1.02	0.01	0.24	143	1.62	33.3	25.7	0.29	5.97	C-I	2.08	0.03	1.06	116	2.85	56.3	15.5	0.23	7.86
C-2	0.47	0.02	0.61	75.5	3.51	98.4	17.0	0.79	22.12	C-II	1.27	0.05	1.17	74.4	3.92	67.0	13.1	0.49	12.1
C-3	0.72	0.01	0.23	112	1.56	36.5	18.8	0.26	6.10	C-III	1.16	0.03	1.22	59.8	2.59	60.8	12.1	0.36	12.8
D-1	0.80	n.d.	0.16	190	n.d.	39.3	44.2	n.d.	9.15	D-I	4.10	n.d.	0.88	209	n.d.	43.2	29.9	n.d.	6.41
										D-II	5.20	n.d.	1.21	205	n.d.	45.8	36.5	n.d.	8.45
										D-III	5.29	n.d.	0.97	221	n.d.	39.1	38.8	n.d.	7.14
										D-IV	3.49	n.d.	0.90	171	n.d.	42.4	26.3	n.d.	6.77

Areal concentrations are presented in nmol cm^{-2} , while P- and S-normalized data are presented in mmol mol^{-1} .

varied significantly with time only for Cu:P (Kruskal–Wallis test, $p = 0.042$), as variations in bulk V:P, Fe:P, Mn:P, Ni:P, Mo:P, Al:P, and Zn:P were not significant (Figure 7). Temporal variations in SXRF-analyzed trichomes were assessed with S-normalized stoichiometries due to the lack of an effect of oxalate on S; this allowed us to use all SXRF data in the comparison, increasing statistical power. Only Fe:S varied significantly with time (Kruskal–Wallis test, $p = 0.010$), with the highest Fe concentrations measured at noon (Figure 8). Bulk ICP-MS analyses could not be performed for the noon sampling station due to a lack of sufficient *Trichodesmium* biomass (Table 1), and this difference in the composition of the datasets likely explains the contrasting statistical results for the ICP-MS and SXRF data (as the highest Fe:P was observed at noon).

SPATIAL ELEMENT DISTRIBUTION WITHIN *TRICHODESMIUM* TRICHOMES

The spatial distribution of elements within *Trichodesmium* was studied using SXRF mapping at two different beamlines with different spatial resolution. The step size was 1.5 and 0.4 μm for GSECARS and 2ID-E, respectively. Element maps for P, S, V, Fe, and Ni were compared to each other and to light micrographs of the same trichome (Figures 3–4, 9–11). The outline of the *Trichodesmium* trichomes is evident in both the light micrographs and the element maps. Phosphorus and S were generally more evenly distributed along trichomes than V and Fe (e.g., Figures 3–4, 9–11). Where regions of Fe and V enrichment were observed, they typically did not overlap with each other. For example, in trichome section D-1 two zones of Fe enrichment are separated by a region of



elevated V in contiguous cells; this was confirmed at two separate beamlines (Figure 4). Other sections of the same trichome have very homogenous elemental distributions. While Fe enrichments zones were found in approximately 10% of trichomes, V was

less uniformly distributed and zones of enrichment were observed in ca. 50% of trichomes (e.g., Figure 3, Map C-1, C-2). The high spatial variability of V and Fe seen in trichome D is shown quantitatively in a 1-D line plot presenting per-pixel concentrations along the main axis of trichome section D-1 (Figure 12). The high variability within a trichome is further illustrated by a comparison of the areal concentrations of P- and S-normalized metal stoichiometries calculated for different regions of interest within trichomes C and D using data from either GSECARS or 2ID-E (Table 4). Both V and Fe varied two- to three-fold between sections of the same trichome.

The higher incident x-ray energy used at 2ID-E also allowed us to map the Ni distribution within trichome sections. In contrast to V or Fe, Ni did not show notable enrichment in contiguous cells of a trichome. However the sub-cellular Ni distribution within a trichome differed from the distribution of other elements such as P, S, V, Mn, and Fe. While the concentrations of the latter elements were highest within each cell, Ni was most abundant in the membranes connecting the cells (Figure 4, Maps D-III and D-V). Such Ni distribution was not observed in trichome C (Figure 3).

DISCUSSION

It is widely acknowledged that diazotrophs such as *Trichodesmium* have high Fe quotas as a result of the biochemical demands of the nitrogenase enzyme (Raven, 1988; Berman-Frank et al., 2001; Kustka et al., 2003a), however elevated quotas of other metals in *Trichodesmium* that may result from their unique physiology have received less attention. This study documents elevated V,

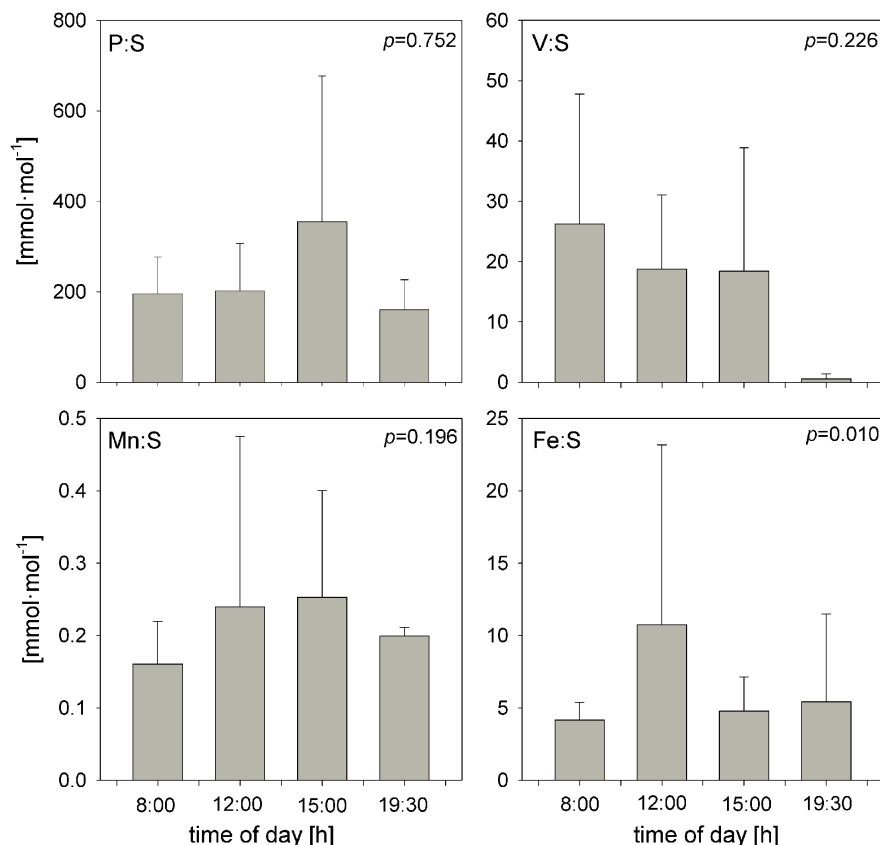


FIGURE 8 | Temporal comparison of S-normalized element stoichiometries determined with SXRF (combined oxalate and non-oxalate data from both beamlines) on individual trichome sections.

Bars are means ± SD. The statistical significance of the effect of sampling time on the element stoichiometries (as determined with a non-parametric Kruskal-Wallis test; see text), is shown in each panel.

Ni, and Mo in *Trichodesmium* collected from the Sargasso Sea, utilizing both bulk and single-cell elemental analyses, and attempts to understand the causes of this unique elemental signature.

Studies of metal quotas in plankton typically present metal contents normalized to cell biomass. The major elemental constituents C and P are often used as somewhat interchangeable proxies of biomass (e.g., Bruland et al., 1991), however the *Trichodesmium* samples analyzed in this study were significantly depleted in P relative to C and N, and thus comparisons between these results and other studies will depend on the choice of biomass proxy. Previous studies have documented similar enrichments in cellular C and N, relative to P, in *Trichodesmium* from the Sargasso Sea and grown in culture under P-limited conditions (White et al., 2006; Orchard et al., 2010b), and Sañudo-Wilhelmy et al. (2001) argue that *Trichodesmium* in the North Atlantic can be limited by P availability. Phosphorus limitation of *Trichodesmium* is further indicated by the *Trichodesmium* N:P ratios, which were elevated above 50; this has been suggested as an indicator of P limitation (Geider and La Roche, 2002). In contrast, *Trichodesmium* collected from more P-replete waters near Western Australia presented a mean C:N:P ratio of 154:25:1 (Berman-Frank et al., 2001).

Comparisons to cellular S measured with SXRF also indicate that the *Trichodesmium* were depleted in P. Sulfur is incorporated

into cells primarily via cysteine and methionine and has been used as an additional biomass proxy in previous SXRF studies (Twining et al., 2004, 2011; King et al., 2011). Phosphorus:sulfur ratios in P-replete cells experiencing elementally balanced growth are typically close to 1 (Payne and Price, 1999; Ho et al., 2003; Twining et al., 2011), but P:S reported here for *Trichodesmium* are approximately three- to six-fold below this (Table 5). *Trichodesmium* is able to substitute non-P sulfolipids for phospholipids under P limitation (Van Mooy et al., 2009), and this may also contribute to the reduced P:S stoichiometries.

Irregardless of the choice of biomass proxy, comparisons to published data clearly indicate that the *Trichodesmium* in this study have elevated V, Mo, and Ni contents. In most non-diazotrophic taxa Fe is generally the most abundant metal, followed by Zn, Mn, Ni, Cd, and Mo (Bruland et al., 1991; Sunda and Huntsman, 1995, 2000; Ho et al., 2003; Twining et al., 2011). In contrast, V was found to be the most abundant metal in *Trichodesmium*, with the mean V quota exceeding the mean Fe quota by threefold. While less abundant than Fe (and V), C-normalized Mo, and Ni quotas were approximately 50- and 3-fold higher in *Trichodesmium* than in previously studied non-diazotrophs (Ho et al., 2003; Twining et al., 2011). Indeed, Mo and Ni were present at levels similar to that of Zn, which is usually at least three times more abundant than these metals in phytoplankton (Bruland et al., 1991;

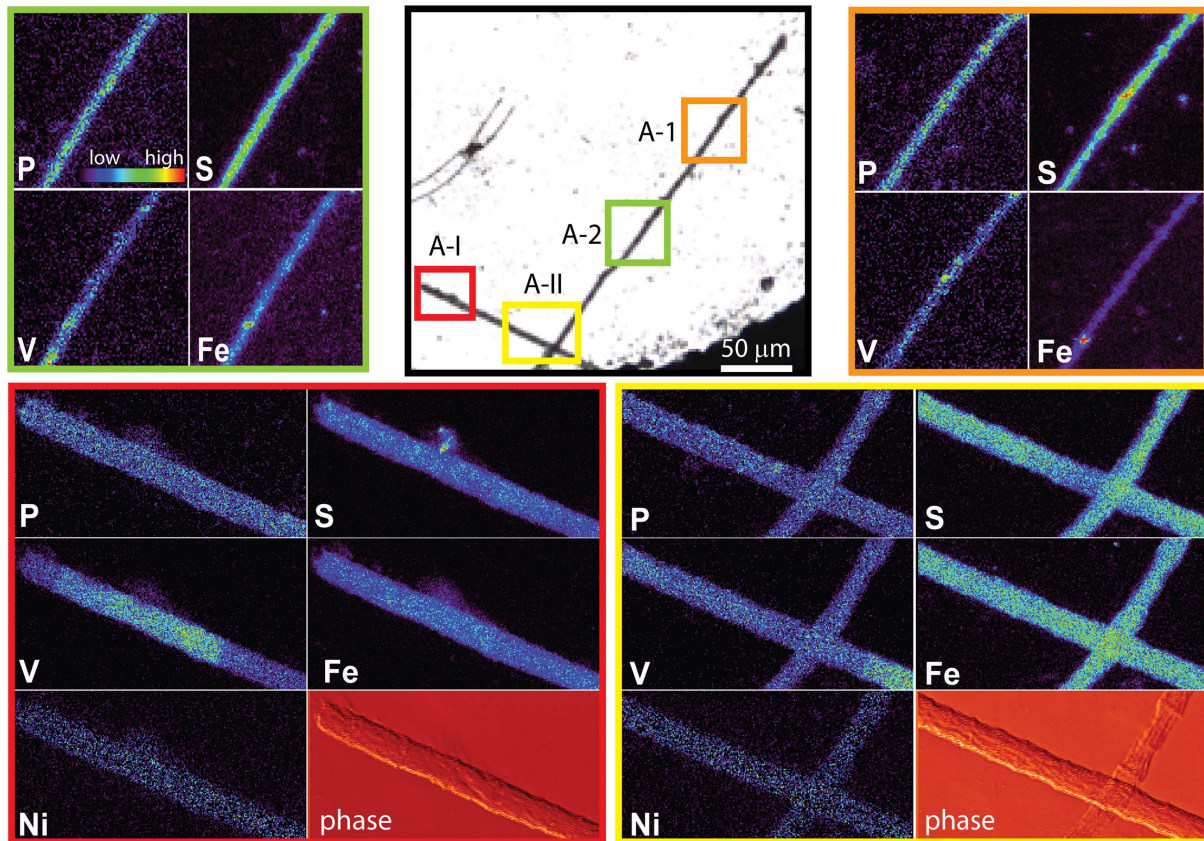


FIGURE 9 | Light micrographs, false-color element (P, S, V, Fe and Ni) maps, and differential phase contrast images (phase) (Hornberger et al., 2008) of a *Trichodesmium* trichome. The color scale for element maps is shown, with warmer colors indicating higher element concentrations. The color scheme of the differential phase

contrast image does not follow the color scale for the element maps. The location of each analyzed trichome section is indicated on the light micrograph. MAP A-1 (orange) and map A-2 (green) were recorded at the GSECARS beamline, while maps A-I (red) and A-II (yellow) were recorded at 2ID-E.

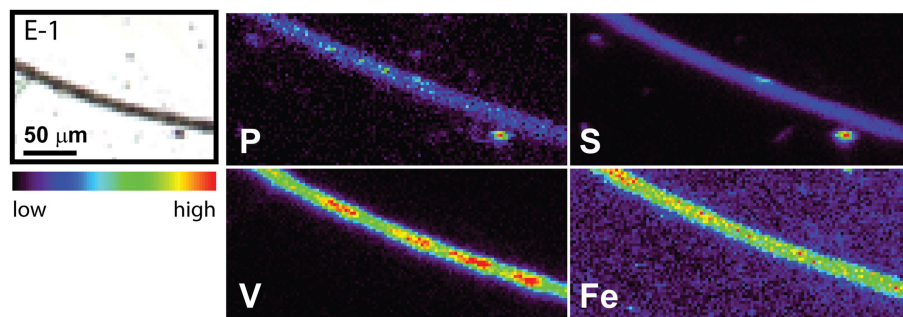
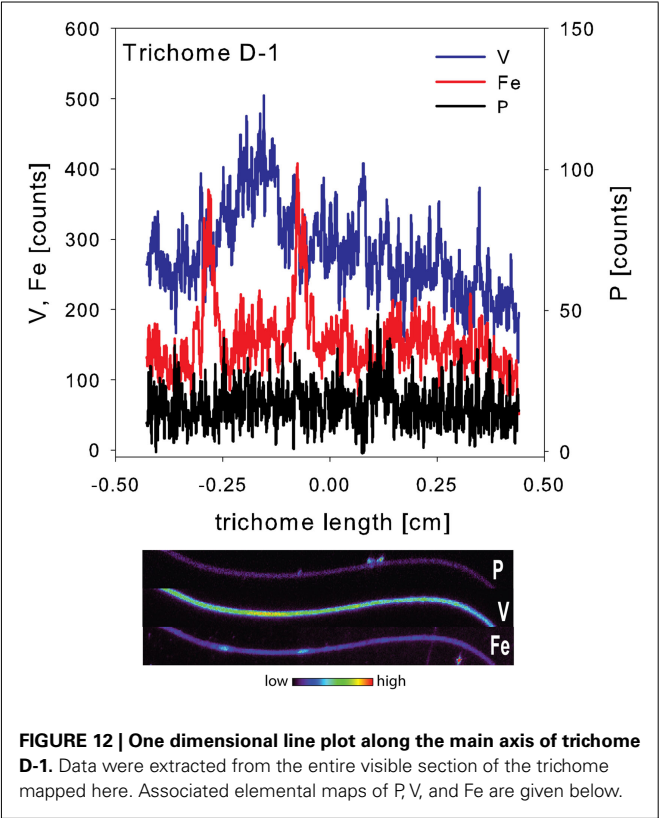
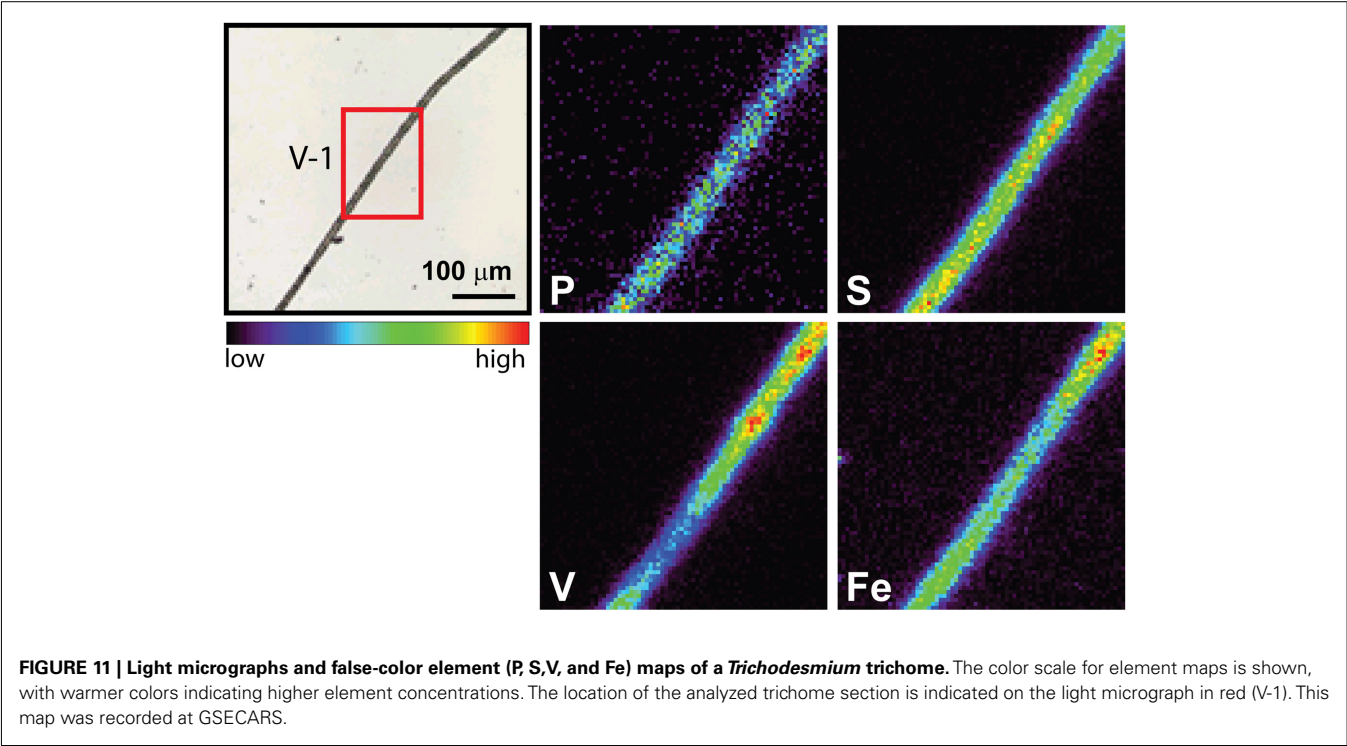


FIGURE 10 | Light micrographs and false-color element (P, S, V, and Fe) maps of a *Trichodesmium* trichome. The color scale for element maps is shown, with warmer colors indicating higher element concentrations. The trichome section E-1 shown in the light micrograph was analyzed at GSECARS.

Twining et al., 2011). Given the depressed P contents of the trichomes, P-normalized quotas of V, Fe, Zn, Mn, Ni, and Mo are also higher than has been observed in other groups of phytoplankton (Bruland et al., 1991; Ho et al., 2003; Twining et al., 2011). The present results are in agreement with previous studies on field populations of *Trichodesmium* collected from the western

sub-tropical North Atlantic (Tovar-Sanchez et al., 2006; Tovar-Sanchez and Sañudo-Wilhelmy, 2011), which also showed high cellular V, Mo, and Ni quotas. However, V stoichiometries reported here are at least 10-fold higher than measured in *Trichodesmium* from the other regions (Tovar-Sanchez et al., 2006; Tovar-Sanchez and Sañudo-Wilhelmy, 2011).



This unique elemental signature of *Trichodesmium* does not appear to result from external non-cellular material attached to the cells. As the Sargasso Sea receives atmospheric deposition of

Table 5 | Comparison of S-normalized stoichiometries for P, V, Mn, and Fe measured at GSECARS and at 2ID-E.

Time	P:S	V:S	Mn:S	Fe:S
8:00	196 <i>81.0</i>	26.2 <i>21.5</i>	0.16 <i>0.06</i>	4.15 <i>1.22</i>
12:00	203 <i>108</i>	18.8 <i>12.6</i>	0.24 <i>0.24</i>	11.0 <i>12.7</i>
15:00	355 <i>323</i>	18.4 <i>20.5</i>	0.25 <i>0.15</i>	4.78 <i>2.36</i>
19:30	160 <i>65.9</i>	0.57 <i>0.80</i>	0.20 <i>0.01</i>	5.43 <i>6.05</i>

Data are presented in mmol mol⁻¹. Mean, bold; SD: italics.

aerosols of anthropogenic origin due to fossil fuel combustion in North America, adsorbed dust particles are a possible cause of apparent increased quotas. Such combustion-derived aerosols are enriched in V and Ni in comparison to soil-derived dust particles (Sholkovitz et al., 2009). However only a few of the non-oxalate rinsed trichome sections analyzed by SXRF had localized V hotspots which do not correspond to the structure of contiguous cells within a trichome (Figure 3 C-I to C-IV). Similar Fe hotspots were also detected in a few trichomes (Figure 3 Map C-1 and C-3), but these hotspots do not drive the higher V and Fe quotas of the trichomes. Removing the pixels containing these potential external particles reduces the V and Fe quotas by less than 5%. Further, because V, Fe, and Ni do not co-localize in these hotspots, an anthropogenic origin for these particles is unlikely. Rather, it is likely that the particles are lithogenic. Recent work by Rubin et al. (2011) indicates that *Trichodesmium* may process

particulate Fe associated with colonies to obtain Fe. However, given that Fe:P ratios were comparable in analyzed colonies and individual trichomes, and that the Fe hotspots observed on the trichomes did not contribute significantly to their Fe content, it does not appear that external particles associated with colonies were a significant contributor to *Trichodesmium* elemental composition in this study. Although significant populations of metazoa, protozoa, algae, and bacteria may be associated with *Trichodesmium* colonies (Sheridan et al., 2002; Hewson et al., 2009), efforts were made to avoid these through manual isolation of individual colonies. The comparable Fe results for colonies and individual trichomes again suggest that such organisms, if present, also did not contribute significantly to the elemental content of the *Trichodesmium*.

Results from the oxalate rinse also indicate that the elevated metal quotas are not due to extracellular material. A comparison of the areal concentrations (nmol cm^{-2}) for oxalate and non-oxalate-treated cells from each station reveals that neither Fe and V, nor Mn and S, varied significantly between rinse treatments. To what extent this oxalate rinse can remove other elements such as V, Mn, or S has not been studied in detail. Although the oxalate treatment was developed to remove externally adsorbed Fe (Tovar-Sanchez et al., 2003), we observed P removal of up to 47% from oxalate-treated trichome sections; this matches previous reports of oxalate usage with *Trichodesmium* (Sañudo-Wilhelmy et al., 2004). The SXRF samples were fixed with glutaraldehyde prior to rinsing, and this could have impacted the lability of internal P as well (Tang and Morel, 2006), but other studies with unfixed *Trichodesmium* have reported even higher P removal with oxalate (Tovar-Sanchez and Sañudo-Wilhelmy, 2011). Overall the oxalate treatment did not affect the areal metal concentrations of *Trichodesmium* significantly, and we conclude that the influence of adsorbed lithogenic material on the quotas is insignificant.

While increased cell quotas do not necessarily indicate increased biological requirements, the elevated quotas of V, Fe, and Mo may result from *Trichodesmium*'s biochemical machinery, including metalloenzymes related to the demands of N fixation. Nitrogen fixation is enabled by the expression of the metalloenzyme nitrogenase. There are three known metallotypes of nitrogenase, containing either Mo and Fe (MoFe), V and Fe (FeV), or Fe only (FeFe; Bothe et al., 2010). Each type of nitrogenase requires a specific nitrogenase reductase (i.e., nifH, vnfH, and anfH, respectively) which is properly redox-tuned to the corresponding nitrogenase, as well as a suite of other proteins for proper enzyme assembly. While it is tempting to explain the V contents of *Trichodesmium* through expression of FeV nitrogenase, the *Trichodesmium erythraeum* genome lacks the δ subunit encoded by vnfG which is thought to be required for V-dependent N fixation (Eady, 2003; and references therein). Furthermore, in *Azotobacter vinelandii*, a model bacterium containing all three metallotypes of nitrogenase, nifDK (encoding for the MoFe protein) is universally expressed in the presence of MoFe whereas vnfDGK (encoding for FeV protein) is expressed only under low Mo conditions or under cooler temperatures. Neither condition applies to the Sargasso Sea, suggesting little if any selective pressure toward a V-dependent N fixation pathway in *Trichodesmium*. Given the high and nearly conservative concentrations of Mo in seawater (ca. 100 nM), the high intracellular Mo quotas measured here, and the lack of spatial or temporal correlations of V and Fe in cells, it appears that the

nitrogenase enzyme is likely responsible for the elevated Fe and Mo contents – but not the elevated V contents – of *Trichodesmium*.

The high V content of *Trichodesmium* may instead result from the presence of other V-dependent metalloenzymes. Vanadium can also serve as a cofactor in haloperoxidases, and vanadium haloperoxidases (VHPO) have been structurally characterized for marine red (*Corallina officinalis*) and brown (*Ascomyces nodosum*) algae, as well as in the fungi *Curvularia inaequalis* (reviews in Crans et al., 2004; Winter and Moore, 2009). If expressed, such VHPOs may act as an antioxidant and help neutralize reactive oxygen species such as hydrogen peroxide (Drábková et al., 2006, 2007). Hydrogen peroxide is a by-product of photosynthesis (Bienert et al., 2006) and is especially damaging to the nitrogenase enzyme (Fay, 1992). An antioxidant role of VHPOs in *Trichodesmium* would be especially beneficial because *Trichodesmium* fixes N during daylight, and neutralizing reactive oxygen species by VHPOs might help facilitate simultaneously fixation of C and N. Johnson et al. (2011) recently described a 68 kDa VHPO encoded in the genome of the coastal cyanobacterium *Synechococcus* CC9311 and demonstrated the protein's capacity for bromoperoxidase activity. As homologs were only present in one other sequenced *Synechococcus* genome, they suggested this may be the result of a recent horizontal gene transfer event into *Synechococcus*. The *T. erythraeum* genome contains a putative acid phosphatase/vanadium-dependent haloperoxidase related protein (Accession number ABG53180). However the putative *Trichodesmium* protein, predicted to be 151 amino acids long (16.6 kDa), is much smaller than the well-characterized 609 amino acid (67.5 kDa) VHPO from *Curvularia inaequalis* (Accession CAA59686.1; Simons et al., 1995), and the *T. erythraeum* protein does not align with the region of the *C. inaequalis* protein that contains the amino acids required for activity (Hemrika et al., 1999). At this point, genomic evidence for either a V-dependent nitrogenase or a V-dependent HPO (with amino acids known to coordinate V in other VHPOs) is lacking. However, there are numerous metalloproteins in prokaryotes, including those that incorporate V, that have yet to be identified (Cvetkovic et al., 2010).

Vanadium could also be accumulated unintentionally by *Trichodesmium* via phosphate uptake mechanisms. If not complexed by siderophore-like compounds (Bellenger et al., 2007, 2011), V is expected to be present primarily as HVO_4^{2-} at pH 8 under oxic conditions (Crans et al., 2004). Vanadate and phosphate are similar in structure and electronic properties, but phosphate is more inert and not involved in redox transformations (Crans et al., 2004). Given that *Trichodesmium* populations are sometimes P-limited in the North Atlantic (Sañudo-Wilhelmy et al., 2001; Mills et al., 2004) it is intriguing to speculate that vanadate acquisition may occur under vanishingly low phosphate concentrations. Arsenate is taken up by phytoplankton via phosphate transporters (Oremland and Stolz, 2003), and As reduction (which follows uptake) is correlated with chlorophyll concentrations in the western North Atlantic (Cutter et al., 2001). While a P dependence of arsenate uptake has not been confirmed at the ultra-low phosphate concentrations characteristic of the Sargasso Sea (Foster et al., 2008), it is quite plausible that V may be taken up through this mechanism. It is interesting to note that the spatial distributions of V and P in the trichomes are not identical (Figures 3–4, 9–11). The difference in cellular allocation may reflect redox reactions or other intracellular sequestration of V following uptake.

In order to allow for N fixation in the non-heterocystous cyanobacterium *Trichodesmium* spatial and temporal separation strategies are thought to separate the oxygen sensitive nitrogenase enzyme from the photosynthesis machinery (Berman-Frank, 2001; Berman-Frank et al., 2007; Finzi-Hart et al., 2009). Some trichomes collected at noon in this study showed the presence of contiguous cells enriched in Fe. In some samples these regions of elevated Fe were not evenly distributed over the whole trichome but were localized to zones separated by regions enriched in V (Figures 4, 11–12). Such zones of Fe enrichment appear similar to the diazocytes identified in *Trichodesmium* (El-Shehawey, 2003; Sandh et al., 2011) and may represent zones of N fixation. In addition, such Fe enrichment zones in *Trichodesmium* were only observed for trichomes collected at noon. Interestingly, the mean Fe:P ratio for *Trichodesmium* samples collected at noon was significant higher than at any other sampling time. This is in agreement with the hypothesis that the onset of N fixation follows C fixation at midday (Finzi-Hart et al., 2009) and the highest expression of *nifH* (El-Shehawey, 2003).

The enrichment of Ni in *Trichodesmium* biomass likely also follows from biochemical usage. Nickel shows a distinctive spatial distribution with the highest concentration in the transverse wall membrane of *Trichodesmium* trichomes. Such distribution is in agreement with Ni containing membrane-bound enzymes such as urease (Collier et al., 1999), NiFe uptake hydrogenase (Tamagnini et al., 2002), and Ni-superoxide dismutase (Ni-SOD; Dupont et al., 2008b). SOD provides an important defense tool against the toxicity of superoxide by converting superoxide to molecular oxygen and hydrogen peroxide (McCord and Fridovich, 1969; Fridovich, 1989). Hydrogen peroxide is then further converted to water by peroxidases such as the previously described VHPOs (Crans et al., 2004). All aerobic organisms contain at least one isoform of SOD (containing either Fe, Mn, Cu/Zn, or Ni) with *Trichodesmium* containing the gene coding for Ni-SOD and Mn-SOD (Dupont et al., 2008a). Such mechanism is beneficial for *Trichodesmium* as the 4Fe-4S cluster in the nitrogenase complex is highly susceptible to the inactivation of superoxide. As H₂ is a side product of N fixation, all diazotrophic organisms contain NiFe hydrogenases (Tamagnini et al., 2002). In general these are divided into four groups, of which cyanobacteria have an uptake hydrogenase clustering together with cytoplasmic H₂ sensors and a bidirectional hydrogenase. While the bidirectional hydrogenase enzyme probably plays a role in fermentation or in electron transfer processes during photosynthesis, the uptake NiFe hydrogenase rapidly catalyzes H₂ produced during N fixation (Tamagnini et al., 2007). Only genes belonging to the uptake hydrogenase have been confirmed in *Trichodesmium* (Tamagnini et al., 2007). In addition to SOD and NiFe hydrogenases, the genome of *Trichodesmium* revealed the presence of a urease subunit alpha, subunit beta, and subunit gamma (Dupont et al., 2008a). *Trichodesmium* is able to grow on urea and as well on nitrate and ammonia (LaRoche and Breitbarth, 2005; Post et al., 2012), however urea is unlikely to be a significant source of N to *Trichodesmium* in the Sargasso Sea in the late summer (Orcutt et al., 2001). Thus it is unlikely that urease is driving the elevated Ni quotas of *Trichodesmium*. Rather, Ni is likely primarily incorporated into membrane enzymes such as Ni-SOD and NiFe hydrogenase.

Zinc contents of *Trichodesmium* may also be explained by usage in metalloenzymes. It has been suggested that cyanobacteria evolved under sulfidic conditions of low Zn availability that has resulted in lower Zn contents of modern cyanobacteria (Saito et al., 2003). In contrast, the elevated Zn quotas of *Trichodesmium* reported here may reflect the P-limiting condition of the Sargasso Sea and the subsequent expression of the Zn metalloenzyme alkaline phosphatase in *Trichodesmium*, as would be expected in cells growing on organic P substrates (Orchard et al., 2010a,b). Similarly, *Synechococcus* in the Sargasso Sea increases its Zn quota substantially in anticyclonic eddies characterized by reduced phosphate delivery (Twining et al., 2010).

The Redfield ratio, and the proposed extension of this concept to include bioactive metals, is based on consistency of the average elemental composition of plankton. Indeed there is remarkable agreement in the bulk C:N:P ratios of plankton when data are aggregated (Geider and La Roche, 2002, and references therein), and compilations of selected bulk particulate metal studies have produced relative agreement (Bruland et al., 1991; Ho, 2006). However it has also been demonstrated that there is real and important spatial and taxonomic variability in the macronutrient and trace metal stoichiometries of plankton which underlie the average ratios (e.g., Geider and La Roche, 2002; Twining et al., 2004, 2011). Hence, a unified element stoichiometry should always be treated as a “statistical composition” (Redfield, 1958; Geider and La Roche, 2002). There is much to be learned about cell physiology, ecology and biogeochemistry from comparisons of plankton representing individual taxa and regions to the average elemental composition. The natural *Trichodesmium* populations described in this paper provide an example of how the physiology of an individual group, as well as the environmental conditions, can cause significant deviations from the averaged, idealized stoichiometric composition. The extent to which the unique elemental composition of *Trichodesmium* will impact nutrient and metal cycling in the surrounding waters will depend on the fate of the accumulated cell biomass. Future studies which combine elemental analyses of plankton with “-omics” approaches that constrain the genetic and biochemical composition of the same communities and populations will do much to advance our understanding of biogeochemistry in the ocean.

ACKNOWLEDGMENTS

We are grateful to the captain and crew of the R/V Atlantic Explorer and the staff of the Bermuda Atlantic Time-Series at Bermuda Institute of Ocean Sciences for enabling sample collection during cruise B-261. ICP-MS analyses were assisted by Mike Handley at the Orono campus of the University of Maine. CHN analyses were performed by Kathleen Thornton at the Darling Marine Center of the University of Maine. Conor Maginn and Sara Rauschenberg helped with SXRF analyses of *Trichodesmium* samples at the Advanced Photon Source. This work was supported by grants from the National Science Foundation to BST (OCE 0913080, OCE 0928289, and OCE 1061545). Use of the Advanced Photon Source, an Office of Science User Facility operated for the U.S. Department of Energy (DOE) Office of Science by Argonne National Laboratory, was supported by the U.S. DOE under Contract No. DE-AC02-06CH11357.

REFERENCES

- Arrigo, K. R. (2005). Marine microorganisms and global nutrient cycles. *Nature* 437, 349–355.
- Bellenger, J. P., Arnaud-Neu, F., Asfari, Z., Myneni, S. C. B., Stiefel, E. I., and Kraepiel, A. M. L. (2007). Complexation of oxoanions and cationic metals by the biscatecholate siderophore azotochelin. *J. Biol. Inorg. Chem.* 12, 367–376.
- Bellenger, J. P., Wichard, T., Xu, Y., and Kraepiel, A. M. L. (2011). Essential metals for nitrogen fixation in a free-living N₂-fixing bacterium: Chelation, homeostasis and high use efficiency. *Environ. Microbiol.* 13, 1395–1411.
- Berman-Frank, I. (2001). Segregation of nitrogen fixation and oxygenic photosynthesis in the marine cyanobacterium *Trichodesmium*. *Science* 294, 1534–1537.
- Berman-Frank, I., Cullen, J. T., Shaked, Y., Sherrell, R. M., and Falkowski, P. G. (2001). Iron availability, cellular iron quotas, and nitrogen fixation in *Trichodesmium*. *Limnol. Oceanogr.* 46, 1249–1260.
- Berman-Frank, I., Quigg, A., Finkel, Z. V., Irwin, A. J., and Haramaty, L. (2007). Nitrogen-fixation strategies and Fe requirements in cyanobacteria. *Limnol. Oceanogr.* 52, 2260–2269.
- Bienert, G. P., Schjoerring, J. K., and Jahn, T. P. (2006). Membrane transport of hydrogen peroxide. *Biochim. Biophys. Acta* 1758, 994–1003.
- Bothe, H., Schmitz, O., Yates, M. G., and Newton, W. E. (2010). Nitrogen fixation and hydrogen metabolism in cyanobacteria. *Microbiol. Mol. Biol. Rev.* 74, 529–551.
- Bruland, K. W., Donat, J. R., and Hutchins, D. A. (1991). Interactive influences of bioactive trace metals on biological production in oceanic waters. *Limnol. Oceanogr.* 36, 1555–1577.
- Collier, J. L., Brahamsha, B., and Palenik, B. (1999). The marine cyanobacterium *Synechococcus* sp. WH7805 requires urease (urea amidohydrolase, EC 3.5.1.5) to utilize urea as a nitrogen source: molecular-genetic and biochemical analysis of the enzyme. *Microbiology* 145, 447–459.
- Crans, D. C., Smee, J. J., Gaidamauskas, E., and Yang, L. (2004). The chemistry and biochemistry of vanadium and the biological activities exerted by vanadium compounds. *Chem. Rev.* 104, 849–902.
- Cutter, G. A., Cutter, L. S., Featherstone, A. M., and Lohrenz, S. E. (2001). Antimony and arsenic biogeochemistry in the western Atlantic Ocean. *Deep Sea Res. Part II Top. Stud. Oceanogr.* 48, 2895–2915.
- Cvetkovic, A., Menon, A. L., Thorgersen, M. P., Scott, J. W., Poole II, F. L., Jenney, F. E. Jr., Lancaster, W. A., Praissman, J. L., Shanmukh, S., Vaccaro, B. J., Trauger, S. A., Kalisiak, E., Apon, J. V., Siuzdak, G., Yannone, S. M., Tainer, J. A., and Adams, M. W. W. (2010). Microbial metalloproteomes are largely uncharacterized. *Nature* 466, 779–782.
- Dominic, B., Zani, S., Chen, Y.-B., Mellon, M. T., and Zehr, J. P. (2000). Organization of the *nif* genes of the nonheterocystous cyanobacterium *Trichodesmium* Sp. IMS101. *J. Phycol.* 36, 693–701.
- Drábková, M., Admiraal, W., and Maršálek, B. (2006). Combined exposure to hydrogen peroxide and light – selective effects on cyanobacteria, green algae, and diatoms. *Environ. Sci. Technol.* 41, 309–314.
- Drábková, M., Matthijs, H., Admiraal, W., and Maršálek, B. (2007). Selective effects of H₂O₂ on cyanobacterial photosynthesis. *Photosynthetica* 45, 363–369.
- Dupont, C. L., Barbeau, K., and Palenik, B. (2008a). Ni uptake and limitation in marine *Synechococcus* strains. *Appl. Environ. Microbiol.* 74, 23–31.
- Dupont, C. L., Neupane, K., Shearer, J., and Palenik, B. (2008b). Diversity, function and evolution of genes coding for putative Ni-containing superoxide dismutases. *Environ. Microbiol.* 10, 1831–1843.
- Eady, R. R. (2003). Current status of structure function relationships of vanadium nitrogenase. *Coord. Chem. Rev.* 237, 23–30.
- El-Shehaw, R. (2003). Diurnal expression of *hetR* and diazocyte development in the filamentous non-heterocystous cyanobacterium *Trichodesmium erythraeum*. *Microbiology* 149, 1139–1146.
- Fay, P. (1992). Oxygen relations of nitrogen fixation in cyanobacteria. *Microbiol. Rev.* 56, 340–373.
- Finzi-Hart, J. A., Pett-Ridge, J., Weber, P. K., Popa, R., Fallon, S. J., Gunderson, T., Hutcheon, I. D., Nealson, K. H., and Capone, D. G. (2009). Fixation and fate of C and N in the cyanobacterium *Trichodesmium* using nanometer-scale secondary ion mass spectrometry. *Proc. Natl. Acad. Sci. U.S.A.* 106, 6345–6350.
- Foster, S., Thomson, D., and Maher, W. (2008). Uptake and metabolism of arsenate by anoxic cultures of the microalgae *Dunaliella tertiolecta* and *Phaeodactylum tricornutum*. *Mar. Chem.* 108, 172–183.
- Fridovich, I. (1989). Superoxide dismutases. An adaptation to a paramagnetic gas. *J. Biol. Chem.* 264, 7761–7764.
- Geider, R. J., and La Roche, J. (2002). Redfield revisited: Variability of C:N:P in marine microalgae and its biochemical basis. *Eur. J. Phycol.* 37, 1–17.
- Haraguchi, H. (2004). Metallomics as integrated biometal science. *J. Anal. At. Spectrom.* 19, 5.
- Hemrika, W., Renirie, R., Macedo-Ribeiro, S., Messerschmidt, A., and Wever, R. (1999). Heterologous expression of the vanadium-containing chloroperoxidase from *Curvularia inaequalis* in *Saccharomyces cerevisiae* and site-directed mutagenesis of the active site residues His496, Lys353, Arg360, and Arg490. *J. Biol. Chem.* 274, 23820–23827.
- Hewson, I., Poretsky, R. S., Dyhrman, S. T., Zielinski, B., White, A. E., Tripp, H. J., Montoya, J. P., and Zehr, J. P. (2009). Microbial community gene expression within colonies of the diazotroph, *Trichodesmium*, from the Southwest Pacific Ocean. *ISME J.* 3, 1286–1300.
- Ho, T. Y. (2006). “The trace metal composition of marine microalgae in cultures and natural assemblages,” in *Algal Cultures, Analogues of blooms and Applications*, ed. D. V. Subba Rao. (Enfield, NH: Science Publishers).
- Ho, T. Y., Quigg, A., Finkel, Z. V., Milligan, A. J., Wyman, K., Falkowski, P. G., and Morel, F. M. M. (2003). The elemental composition of some marine phytoplankton. *J. Phycol.* 39, 1145–1159.
- Hornberger, B., De Jonge, M. D., Feser, M., Holl, P., Holzner, C., Jacobsen, C., Legnini, D., Paterson, D., Rehak, P., Struder, L., and Vogt, S. (2008). Differential phase contrast with a segmented detector in a scanning X-ray microprobe. *J. Synchrotron Radiat.* 15, 355–362.
- Ji, Y., and Sherrell, R. M. (2008). Differential effects of phosphorus limitation on cellular metals in *Chlorella* and *Microcystis*. *Limnol. Oceanogr.* 53, 1790–1804.
- Johnson, T. L., Palenik, B., and Brahamsha, B. (2011). Characterization of a functional vanadium-dependent bromoperoxidase in the marine cyanobacterium *Synechococcus* Sp. CC9311. *J. Phycol.* 47, 792–801.
- Karl, D., Letelier, R. M., Hebel, D. V., Bird, D. F., and Winn, C. D. (1992). “*Trichodesmium* blooms and new nitrogen in the North Pacific gyre,” in *Marine Pelagic Cyanobacteria: Trichodesmium and Other Diazotrophs*, 362nd Edn, eds E. J. Carpenter, D. G. Capone, and J. G. Rueter (Boston, MA: Kluwer Academic), 219–237.
- King, A., Sañudo-Wilhelmy, S. A., Boyd, P. W., Twining, B. S., Wilhelm, S. W., Breene, C., Ellwood, M. J., and Hutchins, D. A. (2011). A comparison of biogenic iron quotas during a diatom spring bloom using multiple approaches. *Biogeosci. Discuss.* 8, 9381–9430.
- Körtzinger, A., Hedges, J. I., and Quay, P. D. (2001). Redfield ratios revisited: removing the biasing effect of anthropogenic CO₂. *Limnol. Oceanogr.* 46, 964–970.
- Kustka, A., San Udo-Wilhelmy, S., Carpenter, E. J., Capone, D. G., and Raven, J. A. (2003a). A revised estimate of the iron use efficiency of nitrogen fixation, with special reference to the marine cyanobacterium *Trichodesmium* spp. (*Cyanophyta*). *J. Phycol.* 39, 12–25.
- Kustka, A. B., Sañudo-Wilhelmy, S. A., Carpenter, E. J., Capone, D. G., Burns, J., and Sunda, W. G. (2003b). Iron requirements for dinitrogen- and ammonium-supported growth in cultures of *Trichodesmium* (IMS 101): Comparison with nitrogen fixation rates and iron: Carbon ratios of field populations. *Limnol. Oceanogr.* 48, 1869–1884.
- LaRoche, J., and Breitbarth, E. (2005). Importance of the diazotrophs as a source of new nitrogen in the ocean. *J. Sea Res.* 53, 67–91.
- Leben, R. R., Born, G. H., and Engbreth, B. R. (2002). Operational altimeter data processing for mesoscale monitoring. *Marine Geodesy* 25, 3–18.
- Maldonado, M. T., and Price, N. M. (1996). Influence of N substrate on Fe requirements of marine centric diatoms. *Mar. Ecol. Prog. Ser.* 141, 161–172.
- McCord, J. M., and Fridovich, I. (1969). Superoxide dismutase. *J. Biol. Chem.* 244, 6049–6055.
- Mills, M. M., Ridame, C., Davey, M., La Roche, J., and Geider, R. J. (2004). Iron and phosphorus co-limit nitrogen fixation in the eastern tropical North Atlantic. *Nature* 429, 292–294.
- Morel, F. M. M. (2008). The co-evolution of phytoplankton and trace element cycles in the oceans. *Geobiology* 6, 318–324.
- Morel, F. M. M., and Hudson, R. J. M. (1985). “The geobiological cycle of trace elements in aquatic systems: Redfield revisited,” in *Chemical Processes in Lakes*, ed. W. Stumm (New York: John Wiley), 251–281.

- Núñez-Milland, D. R., Baines, S. B., Vogt, S., and Twining, B. S. (2010). Quantification of phosphorus in single cells using synchrotron X-ray fluorescence. *J. Synchrotron. Radiat.* 17, 560–566.
- Orchard, E. D., Ammerman, J. W., Lomas, M. W., and Dyhrman, S. T. (2010a). Dissolved inorganic and organic phosphorus uptake in *Trichodesmium* and the microbial community: the importance of phosphorus ester in the Sargasso Sea. *Limnol. Oceanogr.* 55, 1390–1399.
- Orchard, E. D., Benitez-Nelson, C. R., Pellechia, P. J., Lomas, M. W., and Dyhrman, S. T. (2010b). Polyphosphate in *Trichodesmium* from the low-phosphorus Sargasso Sea. *Limnol. Oceanogr.* 55, 2161–2169.
- Orcutt, K. M., Lipschultz, F., Gunderesen, K., Arimoto, R., Michaels, A. F., Knap, A. H., and Gallon, J. R. (2001). A seasonal study of the significance of N₂ fixation by *Trichodesmium* spp. at the Bermuda Atlantic Time-series Study (BATS) site. *Deep Sea Res. Part II Top. Stud. Oceanogr.* 48, 1583–1608.
- Oremland, R. S., and Stolz, J. F. (2003). The ecology of arsenic. *Science* 300, 939–944.
- Payne, C. D., and Price, N. M. (1999). Effect of Cadmium toxicity on growth and elemental composition of marine phytoplankton. *J. Phycol.* 35, 293–302.
- Post, A. F., Rihtman, B., and Wang, Q. (2012). Decoupling of ammonium regulation and ntcA transcription in the diazotrophic marine cyanobacterium *Trichodesmium* sp. IMS101. *ISME J.* 6, 629–637.
- Price, N. M., and Morel, F. M. M. (1991). Colimitation of phytoplankton growth by nickel and nitrogen. *Limnol. Oceanogr.* 36, 1071–1077.
- Raven, J. A. (1988). The iron and molybdenum use efficiencies of plant growth with different energy, carbon and nitrogen sources. *New Phytol.* 109, 279–287.
- Redfield, A. C. (1934). “On the proportions of organic derivatives in sea water and their relation to the composition of plankton,” in *James Johnstone Memorial Volume*, ed. R. J. Daniel. (Liverpool: Liverpool University Press), 176–192.
- Redfield, A. C. (1958). The biological control of chemical factors in the environment. *Am. Sci.* 46, 205–221.
- Redfield, A. C., Ketchum, B. H., and Richards, F. A. (1963). “The influence of organisms on the composition of seawater,” in *The Sea*, ed. M. N. Hill (New York: John Wiley), 26–77.
- Rubin, M., Berman-Frank, I., and Shaked, Y. (2011). Dust- and mineral-iron utilization by the marine dinitrogen-fixer *Trichodesmium*. *Nat. Geosci.* 4, 529–534.
- Saito, M. A., Sigman, D. M., and Morel, F. M. M. (2003). The bioinorganic chemistry of the ancient ocean: the co-evolution of cyanobacterial metal requirements and biogeochemical cycles at the Archean–Proterozoic boundary? *Inorganica Chim. Acta* 356, 308–318.
- Sandh, G., Xu, L., and Bergman, B. (2011). Diazocycle development in the marine diazotrophic cyanobacterium *Trichodesmium*. *Microbiol. doi: 10.1099/mic.0.051268-0*. [Epub ahead of print].
- Sañudo-Wilhelmy, S. A., Kustka, A. B., Gobler, C. J., Hutchins, D. A., Yang, M., Lwiza, K., Burns, J., Capone, D. G., Raven, J. A., and Carpenter, E. J. (2001). Phosphorus limitation of nitrogen fixation by *Trichodesmium* in the central Atlantic Ocean. *Nature* 411, 66–69.
- Sañudo-Wilhelmy, S. A., Tovar-Sanchez, A., Fu, F. X., Capone, D. G., Carpenter, E. J., and Hutchins, D. A. (2004). The impact of surface-adsorbed phosphorus on phytoplankton Redfield stoichiometry. *Nature* 432, 897–901.
- Sheridan, C. C., Steinberg, D. K., and Kling, G. W. (2002). The microbial and metazoan community associated with colonies of *Trichodesmium* spp.: a quantitative survey. *J. Plankton Res.* 24, 913–922.
- Sholkovitz, E. R., Sedwick, P. N., and Church, T. M. (2009). Influence of anthropogenic combustion emissions on the deposition of soluble aerosol iron to the ocean: empirical estimates for island sites in the North Atlantic. *Geochim. Cosmochim. Acta* 73, 3981–4003.
- Simons, B. H., Barnett, P., Vollenbroek, E. G. M., Dekker, H. L., Muijsers, A. O., Messerschmidt, A., and Wever, R. (1995). Primary structure and characterization of the vanadium chloroperoxidase from the fungus *Carvularia inaequalis*. *Eur. J. Biochem.* 229, 566–574.
- Sterner, R. W., and Elser, J. J. (2002). *Ecological Stoichiometry: The Biology of Elements from Molecules to the Biosphere*. Princeton, NJ: Princeton University Press.
- Sunda, W. G., and Huntsman, S. A. (1995). Iron uptake and growth limitation in oceanic and coastal phytoplankton. *Mar. Chem.* 50, 189–206.
- Sunda, W. G., and Huntsman, S. A. (2000). Effect of Zn, Mn, and Fe on Cd accumulation in phytoplankton: implications for oceanic Cd cycling. *Limnol. Oceanogr.* 45, 1501–1516.
- Sverdrup, H. U., Johnson, M. W., and Fleming, R. H. (1942). *The Oceans, Their Physics, Chemistry, and General Biology*. New York: Prentice-Hall.
- Takahashi, T., Broecker, W. S., and Langer, S. (1985). Redfield ratio based on chemical data from isopycnal surfaces. *J. Geophys. Res.* 90, 6907–6924.
- Tamagnini, P., Axelsson, R., Lindberg, P., Oxelfelt, F., Wünschiers, R., and Lindblad, P. (2002). Hydrogenases and hydrogen metabolism of cyanobacteria. *Microbiol. Mol. Biol. Rev.* 66, 1–20.
- Tamagnini, P., Leitão, E., Oliveira, P., Ferreira, D., Pinto, F., Harris, D. J., Heidorn, T., and Lindblad, P. (2007). Cyanobacterial hydrogenases: diversity, regulation and applications. *FEMS Microbiol. Rev.* 31, 692–720.
- Tang, D., and Morel, F. (2006). Distinguishing between cellular and Fe-oxide-associated trace elements in phytoplankton. *Mar. Chem.* 98, 18–30.
- Tovar-Sanchez, A., and Sañudo-Wilhelmy, S. A. (2011). Influence of the Amazon River on dissolved and intra-cellular metal concentrations in *Trichodesmium* colonies along the western boundary of the sub-tropical North Atlantic Ocean. *Biogeosciences* 8, 217–225.
- Tovar-Sanchez, A., Sañudo-Wilhelmy, S. A., Garcia-Vargas, M., Weaver, R. S., Popels, L. C., and Hutchins, D. A. (2003). A trace metal clean reagent to remove surface-bound iron from marine phytoplankton. *Mar. Chem.* 82, 91–99.
- Tovar-Sanchez, A., Sañudo-Wilhelmy, S. A., Kustka, A. B., Agustí, S., Dachs, J., Hutchins, D. A., Capone, D. G., and Duarte, C. M. (2006). Effects of dust deposition and river discharges on trace metal composition of *Trichodesmium* spp. in the tropical and subtropical North Atlantic Ocean. *Limnol. Oceanogr.* 51, 1755–1761.
- Tuit, C., Waterbury, J., and Ravizza, G. (2004). Diel variation of molybdenum and iron in marine diazotrophic cyanobacteria. *Limnol. Oceanogr.* 49, 978–990.
- Twining, B., Baines, S., Fisher, N., and Landry, M. (2004). Cellular iron contents of plankton during the Southern Ocean Iron Experiment (SOFEX). *Deep Sea Res. Part I Oceanogr. Res. Pap.* 51, 1827–1850.
- Twining, B. S., Baines, S. B., Bozard, J. B., Vogt, S., Walker, E. A., and Nelson, D. M. (2011). Metal quotas of plankton in the equatorial Pacific Ocean. *Deep Sea Res. Part II Top. Stud. Oceanogr.* 58, 325–341.
- Twining, B. S., Núñez-Milland, D., Vogt, S., Johnson, R. S., and Sedwick, P. N. (2010). Variations in *Synechococcus* cell quotas of phosphorus, sulfur, manganese, iron, nickel, and zinc within mesoscale eddies in the Sargasso Sea. *Limnol. Oceanogr.* 55, 492–506.
- Van Mooy, B. a. S., Fredricks, H. F., Pedler, B. E., Dyhrman, S. T., Karl, D. M., Koblížek, M., Lomas, M. W., Mincer, T. J., Moore, L. R., Moutin, T., Rappé, M. S., and Webb, E. A. (2009). Phytoplankton in the ocean use non-phosphorus lipids in response to phosphorus scarcity. *Nature* 458, 69–72.
- Vogt, S. (2003). MAPS: A set of software tools for analysis and visualization of 3D X-ray fluorescence data sets. *Journal De Physique IV* 104, 635–638.
- White, A. E., Spitz, Y. H., Karl, D. M., and Letelier, R. M. (2006). Flexible elemental stoichiometry in *Trichodesmium* spp. and its ecological implications. *Limnol. Oceanogr.* 51, 1777–1790.
- Whittaker, S., Bidle, K. D., Kustka, A. B., and Falkowski, P. G. (2011). Quantification of nitrogenase in *Trichodesmium* IMS 101: implications for iron limitation of nitrogen fixation in the ocean. *Environ. Microbiol. Rep.* 3, 54–58.
- Williams, R. J. P. (2001). Chemical selection of elements by cells. *Coord. Chem. Rev.* 216–217, 583–595.
- Winter, J. M., and Moore, B. S. (2009). Exploring the chemistry and biology of vanadium-dependent haloperoxidases. *J. Biol. Chem.* 284, 18577–18581.

Conflict of Interest Statement: The authors declare that the research was conducted in the absence of any commercial or financial relationships that could be construed as a potential conflict of interest.

Received: 13 January 2012; accepted: 30 March 2012; published online: 26 April 2012.

Citation: Nuester J, Vogt S, Newville M, Kustka AB and Twining BS (2012) The unique biogeochemical signature of the marine diazotroph *Trichodesmium*. *Front. Microbio.* 3:150. doi: 10.3389/fmicb.2012.00150

This article was submitted to *Frontiers in Microbiological Chemistry, a specialty of Frontiers in Microbiology*.

Copyright © 2012 Nuester, Vogt, Newville, Kustka and Twining. This is an open-access article distributed under the terms of the Creative Commons Attribution Non Commercial License, which permits non-commercial use, distribution, and reproduction in other forums, provided the original authors and source are credited.



Characterization of lead–phytochelatin complexes by nano-electrospray ionization mass spectrometry

Christian Scheidegger^{1,2}, Marc J.-F. Suter^{1,2*}, Renata Behra¹ and Laura Sigg^{1,2}

¹ Department of Environmental Toxicology, Eawag, Swiss Federal Institute of Aquatic Science and Technology, Dübendorf, Switzerland

² Department of Environmental Systems Science, ETH Zürich, Institute of Biogeochemistry and Pollutant Dynamics, Zürich, Switzerland

Edited by:

Martha Gledhill, University of Southampton, UK

Reviewed by:

Jeffrey M. Dick, Curtin University of Technology, Australia

Claude Fortin, Institut National de la Recherche Scientifique, Canada

*Correspondence:

Marc J.-F. Suter, Department of Environmental Toxicology, Eawag, Swiss Federal Institute of Aquatic Science and Technology, PO Box 611, CH-8600 Dübendorf, Switzerland.
e-mail: marc.suter@eawag.ch

The role of phytochelatins (PC_n, metal-binding oligopeptides with the general structure (γ-Glu-Cys)_n-Gly (*n* = 2–11) in metal detoxification is assumed to be based on immobilization of metals, which prevents binding of metals to important biomolecules. Although induction of phytochelatin synthesis has often been observed in algae upon exposure to metals, direct evidence for binding of the inducing metal to phytochelatins is scarce. In this study, a nano-electrospray ionization mass spectrometry (nano-ESI-MS) method is developed for identification and characterization of Pb(II)–PC_n and Zn(II)–PC_n complexes. Complexes of Pb(II) with standard PC_n (*n* = 2–4; 0.25 mM Pb(II) and 0.5 mM PC_n) were examined by nano-ESI-MS with respect to their stoichiometry. Pb–PC_n mass spectra indicated the presence of the [M + H]⁺ peak of PC_n and complexes with various stoichiometries. Analysis of Pb–PC₂ allowed the identification of four different complexes observed at *m/z* 746.10, 952.06, 1285.24, and 1491.20, corresponding to [Pb–PC₂]⁺, [Pb₂–PC₂]⁺, [Pb–(PC₂)₂]⁺, and [Pb₂–(PC₂)₂]⁺. Their *m/z* indicated coordination of Pb(II) by PC₂ through the thiol groups of PC cysteine and possibly carboxylic groups. For each of the standard PC₃ and PC₄, two different complexes were observed, corresponding to Pb–PC₃, Pb₂–PC₃, Pb–PC₄, and Pb₂–PC₄. The measured isotopic patterns were for all complexes identical to the theoretical isotopic patterns. Addition of Zn(II) (0.125–5 mM) to previously formed Pb–PC₂ complexes showed the appearance of the [Zn–PC₂]⁺ complexes at *m/z* 602.05 and the decrease of the [Pb–PC₂]⁺ peak. These findings corroborate the postulated Pb–PC complexes from a previous study using size exclusion chromatography of PC extracted from algae, as well as the concurrent formation of Pb–, Zn–, and Cu–PC complexes in algae.

Keywords: phytochelatin, mass spectrometry, nano-ESI-MS, lead, thiol

INTRODUCTION

Phytochelatins (PCs) are known to be induced in response to exposure to various metals in plants (Rauser, 1995; Zenk, 1996) and algae (Gekeler et al., 1988; Ahner et al., 1995; Le Faucheur et al., 2005; Scheidegger et al., 2011a). These metal-binding oligopeptides with the general structure (γ-Glu-Cys)_n-Gly (*n* = 2–11) are assumed to bind metals through thiolate coordination and are involved in metal homeostasis and detoxification. The role of PCs in metal detoxification likely results from immobilization of metals, preventing non-specific binding to important biomolecules, followed by the transport of the Me–PC complexes into the vacuole of the algal cell, or its excretion. In our previous studies, induction of phytochelatins by exposure of *Chlamydomonas reinhardtii* to Pb(II) has been observed (Scheidegger et al., 2011a). Binding of Pb(II) to phytochelatins has been postulated based on separation of metal complexes from *C. reinhardtii* by size exclusion chromatography (SEC; Scheidegger et al., 2011b). However, direct evidence for binding of the inducing metal to phytochelatins is scarce. It is therefore of interest to attempt to directly characterize metal–phytochelatin complexes.

Several analytical methods such as chromatographic separation (gel filtration or HPLC) coupled with UV detection, flame atomic

absorption spectrometry (AAS), radio-active labeling, differential pulse polarography, and inductively coupled plasma mass spectrometry (ICP-MS) have been used to analyze PC_n and metal–phytochelatin complexes (Me–PC; Grill et al., 1985; Maitani et al., 1996; Leopold and Günther, 1997; Leopold et al., 1999; Vacchina et al., 1999, 2000; Schmoger et al., 2000; Scarano and Morelli, 2002; Cruz et al., 2005; Kobayashi and Yoshimura, 2006). These methods, however, do not provide exact molecular weight, stoichiometry, or composition of Me–PC_n complexes. In most *in vivo* studies focusing on Me–PC complex characterization, Me–PC complexes were isolated by gel filtration and the resulting eluate fractions were further analyzed for PC and metal content. PC detection often involves acidification and derivatization, which lead to dissociation of the Me–PC complexes, followed by HPLC analysis. Based on the detected molecular weight range obtained from gel filtration and the PC oligomers detected by HPLC, assumptions on stoichiometry and composition of the Me–PC complexes can be made; however, unambiguous characterization of Me–PC complexes regarding stoichiometry and composition is not possible with these methods.

A technique to precisely detect and characterize the Me–PC_n complexes is thus required. Several studies reported identification

of Cd-PC, Zn-PC, and As(III)-PC complexes using electrospray ionization mass spectrometry (ESI-MS; Yen et al., 1999; Raab et al., 2005; Navaza et al., 2006; Chekmeneva et al., 2007; Chen et al., 2007; Bluemlein et al., 2008, 2009), but analysis of Me-PC complexes formed with lead has not been reported.

In our previous study, induction of PC₂-PC₄ synthesis by Pb(II) was observed in the green alga *C. reinhardtii* (Scheidegger et al., 2011a). Furthermore, formation of PC_n complexes with Cu, Zn, and Pb, and possible stoichiometric compositions of Pb-PC complexes were postulated based on the molecular weight obtained from SEC (Scheidegger et al., 2011b). Therefore, the aim of the present study is to develop an ESI-MS method to identify and characterize Me-PC_n complexes formed with Pb and to examine the competition with Cu and Zn. Sample composition and ESI-MS conditions to analyze Pb complexes with standard phytochelatin ($n = 2-4$) are optimized. The stoichiometry of the Pb-PC₂₋₄ complexes is derived.

MATERIALS AND METHODS

CHEMICALS

Pb(NO₃)₂, CuSO₄, and ZnSO₄ salts, ammonium acetate (NH₄CH₃COO), ammonium carbonate ((NH₄)₂CO₃; pH 7), polylysine, and 3-morpholinopropanesulfonic acid (MOPS) used in this study were analytical grade and obtained from Sigma-Aldrich (St. Louis, MO, USA). Phytochelatin standards (PC₂, PC₃, and PC₄) were obtained from Invitrogen (San Diego, CA, USA). Formic acid was a suprapure chemical obtained from Merck (Darmstadt, Germany). Ultrafree-MC centrifugal filters (0.45 μm cut-off) were ordered from Millipore AG (Zug, Switzerland).

SAMPLE PREPARATION

In preliminary experiments the solvent mixture for the analysis of Pb-PC complexes was optimized. The following sample composition resulted in the highest signal intensities in nano-electrospray ionization mass spectrometry (nano-ESI-MS) analysis. The ratio of PC_n to Pb was in the range observed in algal cells (Scheidegger et al., 2011a,b). PC_n and Pb were mixed, resulting in final concentrations of 0.5 mM PC_n and 0.25 mM Pb(NO₃)₂ in 100 mM NH₄CH₃COO and 50 mM (NH₄)₂CO₃. Complex formation was allowed for 15 min at room temperature. Prior to sample analysis 0.1% formic acid was added (pH 6), followed by sample filtration using an Ultrafree-MC centrifugal filter device with a 0.45-μm cut-off.

For competition experiments between Cu or Zn and Pb, standard Pb-PC₂ complexes were prepared as described and complex formation was allowed, followed by the addition of the Cu or Zn solution. Cu and Zn concentrations added to the Pb-PC₂ complexes were 0.125, 0.25, 0.5, and 5 mM. Acidification was done by addition of 0.1% formic acid. The ratios of Cu and Zn to Pb in the competition experiments were in the range Cu (or Zn): Pb = 0.5–20, and would thus simulate a similar or higher concentration of Cu and Zn than Pb, which may be representative for algal cells.

Mass spectra were acquired and analyzed using the software Xcalibur V2.0.7 (Thermo Fisher Scientific, San Jose, CA, USA). The isotopic distributions for the positively charged molecular ions of Me-PC complexes were generated with the spectrum simulation software integrated in Xcalibur.

NANO-ELECTROSPRAY IONIZATION MASS SPECTROMETRY ANALYSIS OF ME-PC COMPLEXES

Solvent mixture optimization for nano-ESI-MS analysis of Pb-PC_n ($n = 2-4$) were carried out on a API4000 triple quadrupole mass spectrometer (Applied Biosystems, Rotkreuz, Switzerland) with attached nanospray source (Sciex, NanoSpray® III Source, Zug, Switzerland).

Final analysis of Pb-PC_n complexes was carried out on a LTQ Orbitrap XL mass spectrometer (Thermo Fisher Scientific, San Jose, CA, USA). Capillaries for nano-ESI were prepared from coated fused silica tubing (TSP-FS; o.d. 375 μm; i.d. 100 μm; BGB, USA) using a needle puller (Model P-2000, Sutter Instruments Co., Novato, CA, USA). The samples were then analyzed by direct infusion. Between each measurement the syringe was cleaned with MeOH and H₂O.

Prior to analysis of Pb-PC_n complexes, the instrument performance and calibration was checked with polylysine. The flow rate for standard Pb-PC_n complex analysis was 1–3 μL/min. The optimal settings of the mass spectrometer operated in positive electrospray ionization mode were: needle voltage, 1.5 kV; capillary temperature, 200°C; capillary voltage, 11 V; tube lens, 130 V; resolution, 30,000; max. injection time, 100,000 ms; automatic gain control FT, 1×10^6 . The spectra were acquired from m/z 300 to 1,600 for Pb-PC₂ and from m/z 300 to 2,000 for Pb-PC₃ and Pb-PC₄. Mass accuracy of the measurement was better than 2 ppm for lower mass ions (<1,000 Da) of signal intensities >10%.

RESULTS

ANALYSIS OF STANDARD Pb-PC_n COMPLEXES

The full-scan mass spectrum of the Pb-PC₂ complexes (Figure 1) was dominated by the singly charged $[M + H]^+$ ion of PC₂ at m/z 540.1427, which matches the elemental composition of protonated PC₂ (C₁₈H₃₀N₅O₁₀S₂) of 540.1429 with an error <0.2 ppm and shows the expected isotopic distribution with a mass assignment <0.5 ppm for signals higher than 10% relative abundance (data not shown). In addition to the protonated molecular ion peaks at m/z 536.3 and 538.4 were also present (data not shown), probably corresponding to oxidized PC₂. A singly charged PC₂ dimer and its oxidation products could be seen at m/z 1079.2783, 1077.2632, and 1075.2474. The four peaks observed at m/z 746.1034, 952.0641, 1285.2379, and 1491.1964 correspond to the molecular weight of singly charged $[Pb-PC_2]^+$, $[Pb_2-PC_2]^+$, $[Pb-(PC_2)_2]^+$, and $[Pb_2-(PC_2)_2]^+$ complexes (Figure 1). Pb-PC₂ and Pb₂-PC₂ were present in sufficient intensity to detect the Pb-specific isotopic pattern of both complexes. The measured isotopic pattern of $[Pb-PC_2]^+$ in the m/z range 740–752 is shown in Figure 2 (front). The relative intensity of the peaks at m/z 742.11, 744.10, 745.10, and 746.10 was observed in a ratio, which reflects the distribution of Pb isotopes (naturally occurring ratio: ²⁰⁴Pb 1.5; ²⁰⁶Pb 23.6; ²⁰⁷Pb 22.6; ²⁰⁸Pb 52.3%). The measured isotopic pattern matched the theoretical pattern (Figure 2, back), with a mass error of 0.7 ppm or better for signals higher than 10%. Similarly, the isotopic pattern observed for $[Pb_2-PC_2]^+$ at m/z 944–958, including the isotopic pattern of two Pb ions, matched the simulated spectra (Figure 3), with a mass error of 1.1 ppm or less. The signal intensities of the complexes involving one or two Pb ions and two PC₂ molecules $[Pb_{1-2}-(PC_2)_2]$ were too low for isotope pattern detection.

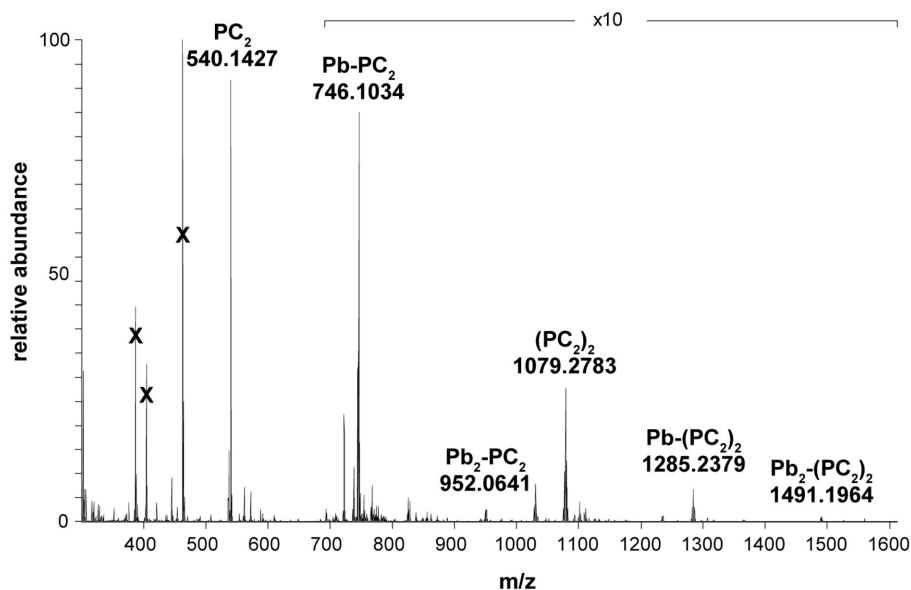


FIGURE 1 | Nano-ESI-MS full-scan spectrum (m/z 300–1,600) of 0.5 mM PC_2 ($C_{18}H_{29}N_5O_{10}S_2$) and 0.25 mM $Pb(NO_3)_2$ in 100 mM NH_4CH_3COO , 50 mM $(NH_4)_2CO_3$, and 0.1% $HCOOH$ (pH 6). X = matrix ions.

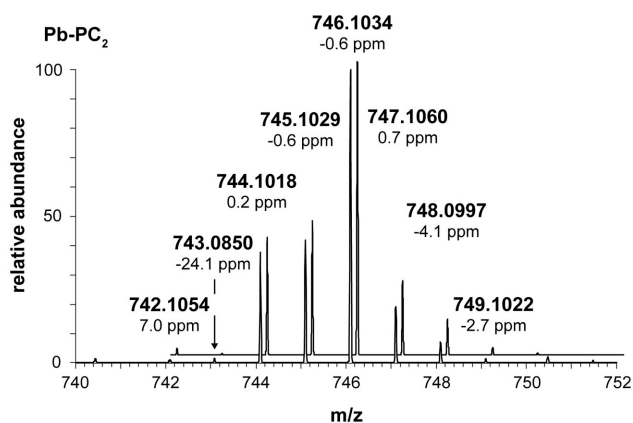


FIGURE 2 | Measured (front) and simulated spectrum (back) of the isotopic pattern of the $[Pb-PC_2]^+$ complex m/z 740–752. Isotopic distribution of Pb is identified in the peak distribution at m/z 742.11 (^{204}Pb , 1.5%), 744.10 (^{206}Pb , 23.6%), 745.10 (^{207}Pb , 22.6%), and 746.10 (^{208}Pb , 52.3%).

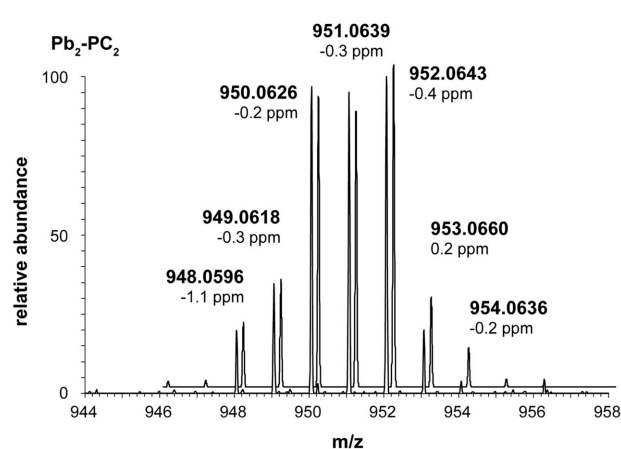


FIGURE 3 | Measured (front) and simulated spectrum (back) of the isotopic pattern of the $[Pb_2-PC_2]^+$ complex m/z 944–958. Isotopic distribution of two Pb (^{204}Pb 1.5%; ^{206}Pb 23.6%; ^{207}Pb 22.6%; ^{208}Pb 52.3%) is identified in the peak distribution of the m/z 948.06–952.06.

Analysis of $Pb-PC_3$ samples showed the $[M+H]^+$ peak for PC_3 at m/z 772.1946 matching the corresponding sum formula ($C_{26}H_{43}N_7O_{14}S_3$; data not shown). Similar to PC_2 , a peak at $[M+H-2]^+$ (m/z 770.1790), not present in the theoretical spectra, was present at high signal intensity. Two peaks at m/z 978.1559 and 1184.1151 corresponding to the molecular weight of singly charged $[Pb-PC_3]^+$ (mass error 0.3 ppm) and $[Pb_2-PC_3]^+$ (mass error 1.2 ppm) were detected. The measured isotopic pattern and the theoretical spectra were almost identical for both detected complexes (Figures 4 and 5).

Analysis of the $Pb-PC_4$ spectra showed the $[M+H]^+$ peak for PC_4 at m/z 1004.2406, corresponding to $C_{34}H_{55}N_9O_{18}S_4$. Comparison of the $[M+H]^+$ peak at 1004.2406 for PC_4 to the theoretical spectra shows an excellent match of the isotopic patterns except for the presence of the $[M+H-2]^+$ peak (m/z 1002.2238) as observed for PC_2 and PC_3 and the $[M+H-4]^+$ peak (m/z 1000.2084). Two peaks corresponding to the molecular weight of the PC_4 complexes, $[Pb-PC_4]^+$ and $[Pb_2-PC_4]^+$, were detected at m/z 1210.1986 (mass error 7.3 ppm) and 1416.1556 (mass error 8.8 ppm). The measured and theoretical isotopic patterns

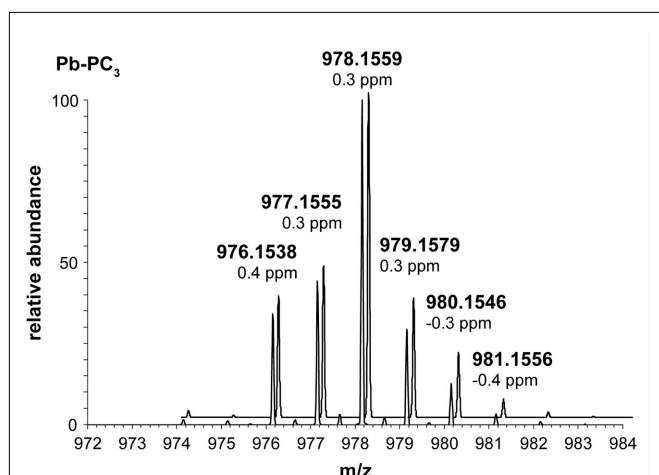


FIGURE 4 | Measured (front) and simulated spectrum (back) of the isotopic pattern of the $[\text{Pb-PC}_3]^+$ complex m/z 972–984. Isotopic distribution of Pb (^{204}Pb 1.5; ^{206}Pb 23.6; ^{207}Pb 22.6; ^{208}Pb 52.3%) is identified in the peak distribution at m/z 974.15, 976.15, 977.15, and 978.16.

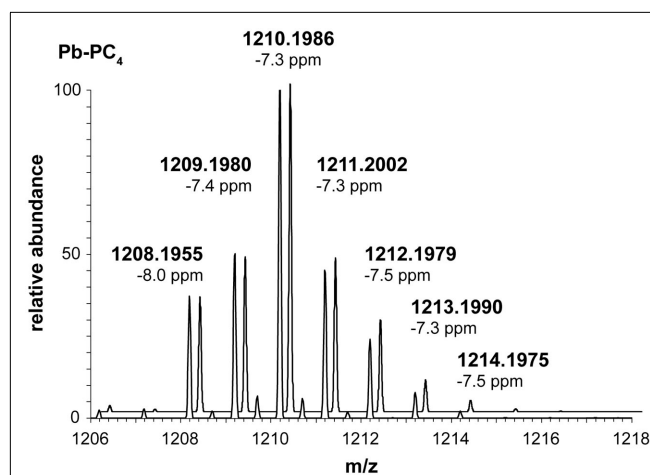


FIGURE 6 | Measured (front) and simulated spectrum (back) of the isotopic pattern of the $[\text{Pb-PC}_4]^+$ complex m/z 1,206–1,218. Isotopic distribution of Pb (^{204}Pb 1.5; ^{206}Pb 23.6; ^{207}Pb 22.6; ^{208}Pb 52.3%) is identified in the peak distribution at m/z 1208.20, 1209.20, and 1210.20.

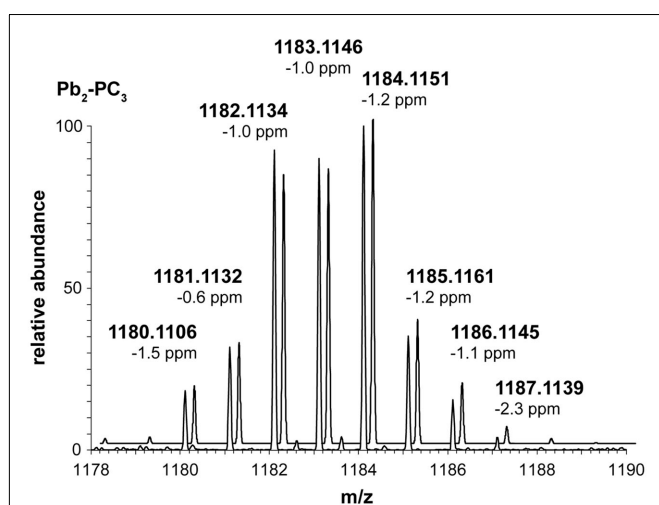


FIGURE 5 | Measured (front) and simulated spectrum (back) of the isotopic pattern of the $[\text{Pb}_2\text{-PC}_3]^+$ complex m/z 1,178–1,190. Isotopic distribution of two Pb (^{204}Pb 1.5; ^{206}Pb 23.6; ^{207}Pb 22.6; ^{208}Pb 52.3%) is identified in the peak distribution of the m/z 1180.11–1184.12.

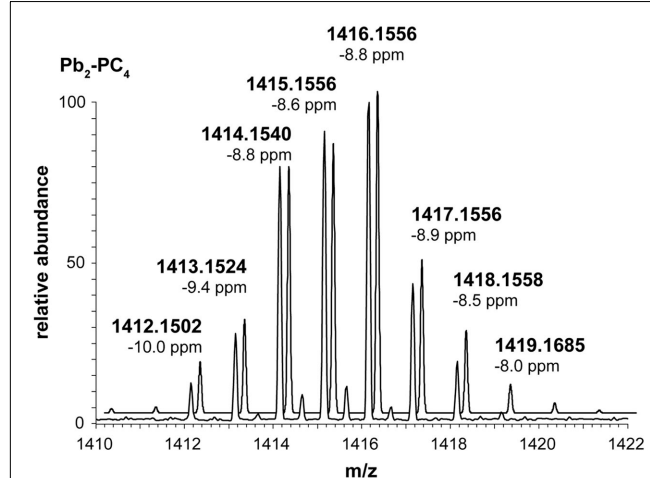


FIGURE 7 | Measured (front) and simulated spectrum (back) of the isotopic pattern of the $[\text{Pb}_2\text{-PC}_4]^+$ complex m/z 1,410–1,422. Isotopic distribution of two Pb (^{204}Pb 1.5; ^{206}Pb 23.6; ^{207}Pb 22.6; ^{208}Pb 52.3%) is identified in the peak distribution of the m/z 1412.15–1416.16.

are shown in **Figures 6 and 7**. In addition, a peak at m/z 605.6035 was observed, matching the isotopic pattern of $[\text{Pb-PC}_4]^{2+}$ (data not shown).

COMPETITION BETWEEN Cu OR Zn AND Pb FOR PC₂ BINDING

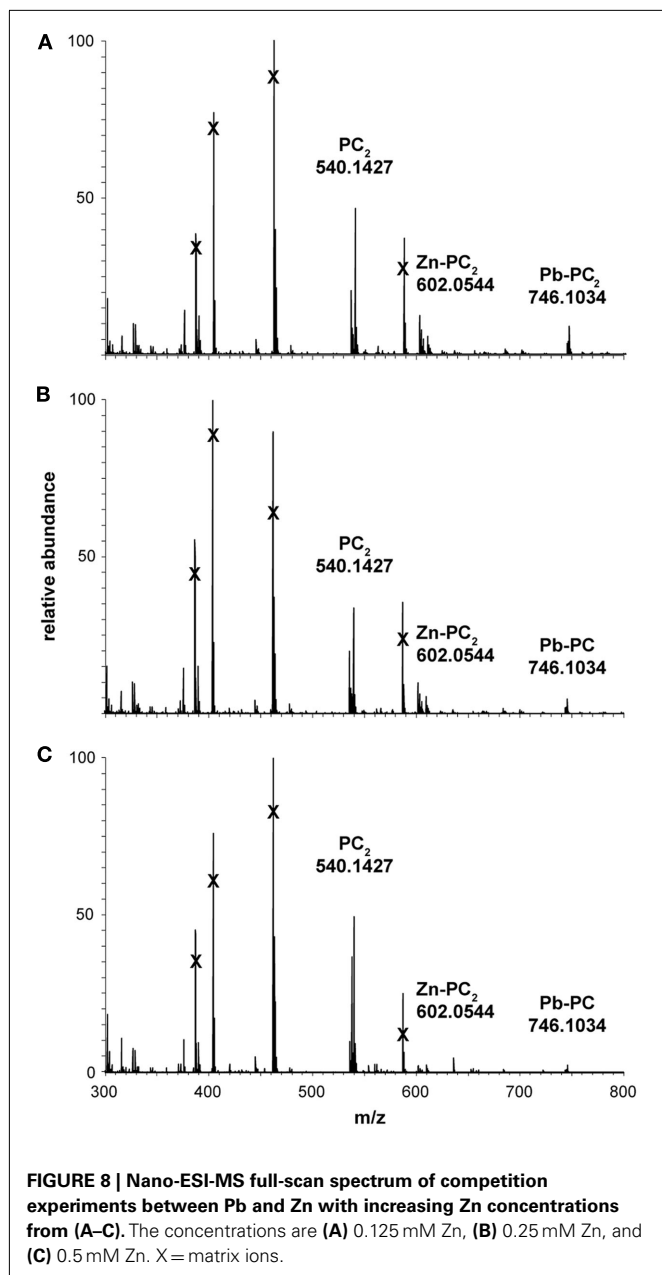
Addition of Zn to Pb-PC_2 complexes resulted in the appearance of the $[\text{Zn-PC}_2]^+$ peak at m/z 602.0544 already at the lowest Zn concentration (**Figure 8A**). In addition, the Pb-PC_2 peak was observed to decrease with increasing Zn concentration (**Figure 8**). Increasing metal concentration leads to a decrease of all PC signals and to an increase of the ratio between the $[\text{M} + \text{H}]^+$ peak for PC_2 at m/z 540.14 and the $[\text{M} + \text{H} - 2]^+$ peak at m/z 538.14. The isotopic

pattern of $[\text{Zn-PC}_2]^+$ matched with the theoretical distribution of Zn (naturally occurring ratio: ^{64}Zn 48.6; ^{66}Zn 27.9; ^{67}Zn 4.1; ^{68}Zn 18.8; ^{70}Zn 0.6%; **Figure 9**).

At the highest Zn concentration (5 mM) and at all Cu concentrations no Zn-PC or Cu-PC complexes were detected (data not shown).

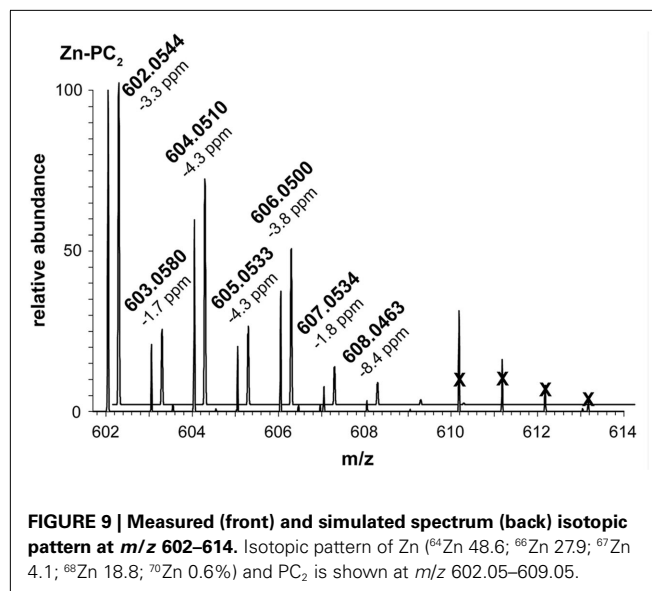
DISCUSSION

To test the applicability of nano-ESI-MS for the analysis of Me-PC complexes, complexes of Pb with standard PC_n ($n = 2\text{--}4$) were analyzed. A method for nano-ESI-MS was developed to characterize *in vitro* formed Me-PC complexes which might also be used for characterization of *in vivo* Me- PC_n complexes.



Considering that the mass spectra of the Pb-PC_n complexes were dominated by the [M + H]⁺ peak of the corresponding PC_n indicates that either not all PC was involved in complex formation, dissociation of Pb-PC complexes occurs during sample analysis, or that the complexes formed were neutral and therefore not visible in the nano-ESI-MS spectra. Furthermore, the relatively low pH 6, needed for optimal ionization, may lead to some complex dissociation.

The PC_n seem to occur mainly in charge state 1+ with the conditions used, as no signal was detected that corresponds to the doubly charged ion. The isotopic pattern of analyzed PC_n was completely resolved. For all PC_n the isotopic distribution matched the theoretical spectra of the corresponding elemental composition



and mass accuracy was high (<2 ppm for ions <1,000 Da and with relative intensities higher than 10%). The [M + H-2]⁺ peaks observed for PC₂–PC₄ as well as the [M + H-4]⁺ peak observed for PC₄, indicate the formation of one or two intramolecular disulfide bonds between cysteine thiol groups within the PC. The formation of a disulfide bond results in a loss of two hydrogens and therefore a shift from [M + H]⁺ to [M + H-2]⁺, which was also observed in other studies (Yen et al., 1999; Navaza et al., 2006).

Analysis of Pb-PC complexes revealed the *in vitro* formation of Pb-PC_n complexes with various stoichiometries and compositions. The m/z detected for the [Pb-PC₂]⁺ complex allows two different covalent complexes, assuming Pb coordination through thiol groups of PC cysteine. Either Pb is coordinated by one thiol group whereas the other is present as reduced thiol group, or the Pb ion is coordinated by both thiol groups present in PC₂. In the second case, additional protonation of the complex must occur to result in a singly charged complex detectable by nano-ESI-MS. For the [Pb₂-PC₂]⁺ complex the detected m/z corresponds to [PC₂ + 2Pb-3]⁺, indicating a loss of three H⁺. This observation suggests that in addition to the two protons from the SH-groups, one proton is lost from a carboxylic group. Further studies would be required to examine whether the complex formation between one Pb and PC₂ involves only thiol groups or Pb is coordinated by one thiol and one carboxylic group. Similarly, another study observed the loss of 2H⁺ and 4H⁺ for the binding of two Cd ions to standard PC₅. Binding of a third Cd ion to PC₅ was not accompanied by the loss of H⁺. The authors suggested the formation of complexes that involve two thiol coordinated cadmium ions and a Cd ion which is bound electrostatically to the Cd₂-PC₅ complex (Yen et al., 1999). To investigate whether the coordination of metals by PC is dependent on the metal and/or the chain length of PC needs to be further investigated.

From mass considerations four Pb-PC₂, two Pb-PC₃, and two Pb-PC₄ complexes were identified. To prove that both Pb and PC_n are contributing to the detected signals, the measured isotopic pattern was compared to the theoretical isotopic pattern.

The isotopic patterns of the Pb-PC complexes are complex owing to the isotopic pattern of one or more Pb ions coupled to the PCs (naturally occurring ratio: ^{204}Pb 1.5; ^{206}Pb 23.6; ^{207}Pb 22.6; ^{208}Pb 52.3%). This very pronounced lead signature is indicative for the presence of Pb in the $[\text{Pb-PC}_2]^+$ complex at m/z 740–752. The isotopic pattern of $[\text{Pb}_2\text{-PC}_2]^+$ is even more complex, since two Pb ions are present in the complex, but comparison of measured and theoretical isotopic pattern proves the presence of the two Pb ions (**Figure 3**). Formation of $[\text{Pb-PC}_2]$ and $[\text{Pb}_2\text{-PC}_2]$ complexes was also observed using differential pulse polarography (Alberich et al., 2007). Similar observations were made for Pb-PC₃ and Pb-PC₄ complexes, showing a good match between measured and theoretical patterns and a loss of 2H^+ for each additionally bound Pb ion. Surprisingly no complexes including three and four Pb ions were observed for PC₃ and PC₄. These results are also in agreement with the complexes observed using voltammetric methods (Alberich et al., 2008). In addition, accurate mass measurements confirmed the proposed elemental compositions.

The appearance of the $[\text{Zn-PC}_2]^+$ peak in the presence of Zn is indicative of complex formation between PC and Zn, which was confirmed by the isotopic pattern for Zn clearly visible in the zoom spectrum (**Figure 9**). This competition between Pb and Zn may be expected if their complex stability with PC₂ is similar to the stability of their complexes with glutathione, for which somewhat higher stability constants for Pb than for Zn are reported (Martell and Smith, 1989). Binding of Zn by PC₃ has been shown in a voltammetric study with multivariate curve resolution, and by PC₄ using voltammetry and ESI-MS (Cruz et al., 2005; Chekmeneva et al., 2007). The expected increase of the $[\text{Zn-PC}_2]^+$ peak with increasing Zn concentration was not observed, maybe due to an increase of oxidized PC₂, indicated by the increase of the ratio between m/z 538.14 and 540.14, leading to a loss of potential metal-binding sites. This could also explain the signal loss observed with increasing Zn concentration. In presence of Cu(II), phytochelatin oxidation may also explain why no Cu-PC complexes were detected. Similar observations were done in a study with Cd where a signal loss was observed at concentrations higher than 0.3 mM Cd (Yen et al., 1999).

In a previous study using SEC, the presence of PC complexes with Cu, Zn, and Pb was postulated upon analysis of PC from *C. reinhardtii* exposed to Pb (Scheidegger et al., 2011b). After

extraction of the algal cells under native conditions to preserve the metal complexes, PC₂ and PC₃ complexes were detected in a molecular weight range between 700 and 5,300 Da. PC₂ was mainly observed between 1,000 and 1,600 Da and complexes with $\text{Me}_{1-2}\text{-}(\text{PC}_2)_2$ were suggested, with $[\text{Pb-(PC}_2)_2]^+$ and $[\text{Pb}_2\text{-(PC}_2)_2]^+$ as the probable most abundant Pb species. The results obtained here are in qualitative agreement with this study, as the formation of $[\text{Pb-PC}_2]^+$, $[\text{Pb}_2\text{-PC}_2]^+$, $[\text{Pb-(PC}_2)_2]^+$, and $[\text{Pb}_2\text{-(PC}_2)_2]^+$ is shown. $[\text{Pb-PC}_2]^+$ and $[\text{Pb}_2\text{-PC}_2]^+$ would appear in the SEC fraction 700–1,050 Da, where PC₂ and Pb were also detected. The abundance distribution of these complexes obtained by ESI-MS appears to differ somewhat from the SEC results, but it must be taken into account that the ratio of PC-SH to Pb, as well as the pH were different in these two studies. Furthermore, it must be considered that nano-ESI-MS, albeit a soft ionization technique, may result in dissociation of complexes. The formation of the $[\text{Zn-PC}_2]^+$ complex after Zn addition also corroborates the results from SEC, which showed the presence of Zn and Cu, as well as Pb, in the PC containing fractions. These results also clearly indicate a possible competition of Zn and Pb for binding to phytochelatins. These findings support the hypothesis that upon induction of PC_n by Pb in algae, the PC_n may also be bound to other metals.

The application of nano-ESI-MS to examine Me-PC complexes in algae is challenged by practical issues related to the low intracellular concentration of the Me-PC complexes. Therefore, further research is needed to improve the sensitivity for Me-PC complexes by nano-ESI-MS, or respectively to improve sample preparation to obtain a sufficient amount of PC_n from the algae. For example, considering the measured concentration of 30 attomol/cell PC₂ in *C. reinhardtii* cells (Scheidegger et al., 2011a), about 1 L of algal suspension (with a cell density of 8.4×10^5 cell/mL) should be preconcentrated into a small volume (<1 mL) to obtain a sufficiently high PC₂ concentration for ESI-MS measurements. In addition, differences between *in vivo* and *in vitro* formed Me-PC complexes should be further examined to investigate which factors are determining the distribution among the various complexes.

ACKNOWLEDGMENTS

We thank René Schönenberger for help in the laboratory work and the Swiss National Science Foundation for funding this project.

REFERENCES

- Ahner, B. A., Kong, S., and Morel, F. M. M. (1995). Phytochelatin production in marine algae. 1. An interspecies comparison. *Limnol. Oceanogr.* 40, 649–657.
- Alberich, A., Arino, C., Diaz-Cruz, J. M., and Esteban, M. (2007). Soft modelling for the resolution of highly overlapped voltammetric peaks: application to some Pb-phytochelatin systems. *Talanta* 71, 344–352.
- Alberich, A., Diaz-Cruz, J. M., Arino, C., and Esteban, M. (2008). Combined use of the potential shift correction and the simultaneous treatment of spectroscopic and electrochemical data by multivariate curve resolution: analysis of a Pb(II)-phytochelatin system. *Analyst* 133, 470–477.
- Bluemlein, K., Raab, A., and Feldmann, J. (2009). Stability of arsenic peptides in plant extracts: off-line versus on-line parallel elemental and molecular mass spectrometric detection for liquid chromatographic separation. *Anal. Bioanal. Chem.* 393, 357–366.
- Bluemlein, K., Raab, A., Meharg, A., Charnock, J., and Feldmann, J. (2008). Can we trust mass spectrometry for determination of arsenic peptides in plants: comparison of LC-ICP-MS and LC-ES-MS/ICP-MS with XANES/EXAFS in analysis of *Thunbergia alata*. *Anal. Bioanal. Chem.* 390, 1739–1751.
- Chekmeneva, E., Diaz-Cruz, J. M., Arino, C., and Esteban, M. (2007). Binding of Cd^{2+} and Zn^{2+} with the phytochelatin $(\gamma\text{-Glu-Cys})(4)\text{-Gly}$: a voltammetric study assisted by multivariate curve resolution and electrospray ionization mass spectrometry. *Electroanalysis* 19, 310–317.
- Chen, L., Guo, Y., Yang, L., and Wang, Q. (2007). SEC-ICP-MS and ESI-MS/MS for analyzing *in vitro* and *in vivo* Cd-phytochelatin complexes in a Cd-hyperaccumulator *Brassica chinensis*. *J. Anal. At. Spectrom.* 22, 1403–1408.
- Cruz, B. H., Diaz-Cruz, J. M., Arino, C., and Esteban, M. (2005). Complexation of heavy metals by phytochelatins: voltammetric study of the binding of Cd^{2+} and Zn^{2+} ions by the phytochelatin $(\gamma\text{-Glu-Cys})_3\text{Gly}$ assisted by multivariate curve resolution. *Environ. Sci. Technol.* 39, 778–786.

- Gekeler, W., Grill, E., Winnacker, E.-L., and Zenk, M. H. (1988). Algae sequester heavy metals via synthesis of phytochelatin complexes. *Arch. Microbiol.* 150, 197–202.
- Grill, E., Winnacker, E. L., and Zenk, M. H. (1985). Phytochelatin: the principal heavy-metal complexing peptides of higher plants. *Science* 230, 674–676.
- Kobayashi, R., and Yoshimura, E. (2006). Differences in the binding modes of phytochelatin to Cadmium(II) and Zinc(II) ions. *Biol. Trace Elem. Res.* 114, 313–318.
- Le Faucheur, S., Behra, R., and Sigg, L. (2005). Phytochelatin induction, cadmium accumulation and algal sensitivity to free cadmium ions in *Scenedesmus vacuolatus*. *Environ. Toxicol. Chem.* 24, 1731–1737.
- Leopold, I., and Günther, D. (1997). Investigation of the binding properties of heavy-metal-peptide complexes in plant cell cultures using HPLC-ICP-MS. *Fresenius J. Anal. Chem.* 359, 364–370.
- Leopold, I., Günther, D., Schmidt, J., and Neumann, D. (1999). Phytochelatin and heavy metal tolerance. *Phytochemistry* 50, 1323–1328.
- Maitani, T., Kubota, H., Sato, K., and Yamada, T. (1996). The composition of metals bound to class III metallothionein (phytochelatin and its desglycyl peptide) induced by various metals in root cultures of *Rubia tinctorum*. *Plant Physiol.* 110, 1145–1150.
- Martell, A. E., and Smith, R. M. (1989). *Critical Stability Constants*. New York: Plenum Press.
- Navaza, A., Montes-Bayón, M., Leduc, D. L., Terry, N., and Sanz-Medel, A. (2006). Study of phytochelatin and other related thiols as complexing biomolecules of As and Cd in wild type and genetically modified *Brassica juncea* plants. *J. Mass Spectrom.* 41, 323–331.
- Raab, A., Schat, H., Meharg, A. A., and Feldmann, J. (2005). Uptake, translocation and transformation of arsenate and arsenite in sunflower *Helianthus annuus*: formation of arsenic-phytochelatin complexes during exposure to high arsenic concentrations. *New Phytol.* 168, 551–558.
- Rausser, W. E. (1995). Phytochelatin and related peptides – structure, biosynthesis, and function. *Plant Physiol.* 109, 1141–1149.
- Scarano, G., and Morelli, E. (2002). Characterization of cadmium- and lead-phytochelatin complexes formed in a marine microalga in response to metal exposure. *Biometals* 15, 145–151.
- Scheidegger, C., Behra, R., and Sigg, L. (2011a). Phytochelatin formation kinetics and toxic effects in the freshwater alga *C. reinhardtii* upon short- and long-term exposure to lead (II). *Aquat. Toxicol.* 101, 423–429.
- Scheidegger, C., Sigg, L., and Behra, R. (2011b). Characterization of lead induced metal-phytochelatin complexes in *Chlamydomonas reinhardtii*. *Environ. Toxicol. Chem.* 30, 2546–2552.
- Schmoger, M. E. V., Oven, M., and Grill, E. (2000). Detoxification of arsenic by phytochelatin in plants. *Plant Physiol.* 122, 793–802.
- Vacchina, V., Chassaigne, H., Oven, M., Zenk, M. H., and Lobinski, R. (1999). Characterisation and determination of phytochelatin in plant extracts by electrospray tandem mass spectrometry. *Analyst* 124, 1425–1430.
- Vacchina, V., Lobinski, R., Oven, M., and Zenk, M. H. (2000). Signal identification in size-exclusion HPLC-ICP-MS chromatograms of plant extracts by electrospray tandem mass spectrometry (ES MS/MS). *J. Anal. At. Spectrom.* 15, 529–534.
- Yen, T.-Y., Villa, J. A., and Dewitt, J. G. (1999). Analysis of phytochelatin-cadmium complexes from plant tissue culture using nano-electrospray ionization tandem mass spectrometry and capillary liquid chromatography/electrospray ionization tandem mass spectrometry. *J. Mass Spectrom.* 34, 930–941.
- Zenk, M. H. (1996). Heavy metal detoxification in higher plants – a review. *Gene* 179, 21–30.

Conflict of Interest Statement: The authors declare that the research was conducted in the absence of any commercial or financial relationships that could be construed as a potential conflict of interest.

Received: 05 December 2011; accepted: 26 January 2012; published online: 13 February 2012.

Citation: Scheidegger C, Suter MJ-F, Behra R and Sigg L (2012) Characterization of lead-phytochelatin complexes by nano-electrospray ionization mass spectrometry. *Front. Microbio.* 3:41. doi: 10.3389/fmicb.2012.00041

This article was submitted to *Frontiers in Microbiological Chemistry*, a specialty of *Frontiers in Microbiology*.

Copyright © 2012 Scheidegger, Suter, Behra and Sigg. This is an open-access article distributed under the terms of the Creative Commons Attribution Non Commercial License, which permits non-commercial use, distribution, and reproduction in other forums, provided the original authors and source are credited.



Modeling the habitat range of phototrophs in Yellowstone National Park: toward the development of a comprehensive fitness landscape

Eric S. Boyd^{1*}, Kristopher M. Fecteau², Jeff R. Havig³, Everett L. Shock^{2,3} and John W. Peters¹

¹ Department of Chemistry and Biochemistry, Astrobiology Biogeocatalysis Research Center, Montana State University, Bozeman, MT, USA

² Department of Chemistry and Biochemistry, Arizona State University, Tempe, AZ, USA

³ School of Earth and Space Exploration, Arizona State University, Tempe, AZ, USA

Edited by:

Martha Gledhill, University of Southampton, UK

Reviewed by:

Alan Angelo DiSpirito, Iowa State University, USA

James F. Holden, University of Massachusetts Amherst, USA

*Correspondence:

Eric S. Boyd, Department of Chemistry and Biochemistry, Astrobiology Biogeocatalysis Research Center, Montana State University, 103 Chemistry Research Building, Bozeman, MT 59717, USA.
e-mail: eboyd@montana.edu

The extent to which geochemical variation shapes the distribution of phototrophic metabolisms was modeled based on 439 observations in geothermal springs in Yellowstone National Park (YNP), Wyoming. Generalized additive models (GAMs) were developed to predict the distribution of phototrophic metabolism as a function of spring temperature, pH, and total sulfide. GAMs comprised of temperature explained 38.8% of the variation in the distribution of phototrophic metabolism, whereas GAMs comprised of sulfide and pH explained 19.6 and 11.2% of the variation, respectively. These results suggest that of the measured variables, temperature is the primary constraint on the distribution of phototrophs in YNP. GAMs comprised of multiple variables explained a larger percentage of the variation in the distribution of phototrophic metabolism, indicating additive interactions among variables. A GAM that combined temperature and sulfide explained the greatest variation in the dataset (53.4%) while minimizing the introduction of degrees of freedom. In an effort to verify the extent to which phototroph distribution reflects constraints on activity, we examined the influence of sulfide and temperature on dissolved inorganic carbon (DIC) uptake rates under both light and dark conditions. Light-driven DIC uptake decreased systematically with increasing concentrations of sulfide in acidic, algal-dominated systems, but was unaffected in alkaline, cyanobacterial-dominated systems. In both alkaline and acidic systems, light-driven DIC uptake was suppressed in cultures incubated at temperatures 10°C greater than their *in situ* temperature. Collectively, these quantitative results indicate that apart from light availability, the habitat range of phototrophs in YNP springs is defined largely by constraints imposed firstly by temperature and secondly by sulfide on the activity of these populations that inhabit the edges of the habitat range. These findings are consistent with the predictions from GAMs and provide a quantitative framework from which to translate distributional patterns into fitness landscapes for use in interpreting the environmental constraints that have shaped the evolution of this process through Earth history.

Keywords: photosynthesis, sulfide, temperature, fitness landscape, CO₂ uptake and fixation, habitat range, landscape ecology, distribution

INTRODUCTION

The distribution of organisms and the functions that they catalyze on Earth today is rooted, at least in part, to the numerous adaptations that enable life to radiate into new ecological niches that have played out over evolutionary time. Such responses are recorded in extant organismal distribution patterns (e.g., habitat range), as well as in the genetic record of organisms. This is a consequence of the predisposition for microorganisms to acquire their ecological traits through vertical inheritance, a phenomenon that manifests in a positive relationship between the ecological relatedness of organisms and their evolutionary relatedness (niche conservatism; Wiens, 2004; Wiens and Graham, 2005). Thus, extant patterns in the distribution of species or metabolic function offer “a window into the past” and can be used to infer

historical constraints on the evolution of a particular metabolic function as imposed by the environment (Wiens and Graham, 2005; Westoby, 2006; Boyd et al., 2010; Hamilton et al., 2011a,b). Such observations can in turn be used to predict the response of populations or metabolic guilds to changing environmental conditions (Keddy, 1992; Lavorel and Garnier, 2002; Guisan and Thuiller, 2005).

The extreme variation in the geochemical composition of present day environments is likely to encompass those that were present on early Earth (Shock and Holland, 2007), when key metabolic processes such as photosynthesis are thought to have evolved. Yellowstone National Park (YNP), Wyoming harbors >12,000 geothermal features that vary widely in temperature and geochemical composition, both spatially and temporally (Nordstrom et al.,

2005; Shock et al., 2010). Such environments provide a field laboratory for examining the tendency for guilds of organisms to inhabit particular ecological niches and to define the range of geochemical conditions tolerated by that functional guild (i.e., habitat range or zone of habitability; Hoehler, 2007; Shock and Holland, 2007). We assume that since it is unlikely that a metabolic process emerged under environmental conditions that no longer support that function, such information can help quantify the habitat range for a metabolic process, and can provide insight into the characteristics of an environment that enabled the adaptation of that process into new habitats.

Phototrophy is the utilization of solar energy by plants, algae, and certain bacteria to generate energy for the synthesis of complex organic molecules (Blankenship, 1992; Chew and Bryant, 2007). A number of recent studies have documented non-random pattern in the distribution of phototrophic assemblages along geochemical gradients in YNP, Wyoming (Boyd et al., 2010; Cox et al., 2011; Hamilton et al., 2011b). These studies qualitatively identified three ecological axes (temperature, pH, and total sulfide) that appear to constrain the habitat range of phototrophs in the geothermal features of YNP. However, the extent to which each environmental parameter, or combinations therein, shape the distribution of phototrophic metabolism in YNP is unclear. Moreover, it is unclear if the qualitative trends in the distribution of phototrophic metabolism in YNP noted previously are the result of the negative effects that temperature, pH, and sulfide have on the activity of phototrophic populations, which in turn would be expected to decrease fitness and limit their distribution.

Here, in an effort to better define the basis for the observed habitat range of phototrophs in YNP, we compiled environmental metadata and presence/absence distributional data from several-independent examinations of phototrophic metabolisms across the YNP geothermal complex (Boyd et al., 2010; Cox et al., 2011; Hamilton et al., 2011b). This binary dataset comprising 439-independent observations was used to construct generalized additive models (GAMs) for use in quantifying and ranking the role of temperature, pH, and total sulfide in shaping the habitat range of phototrophs. Using this approach, it was determined that temperature was the primary predictor of the distribution of phototrophs in YNP springs, followed by dissolved sulfide concentration and pH. We evaluated these predictions using short incubation (<1 h) microcosm studies in several select geothermal springs. Collectively, the GAMs and microcosm studies support a model whereby a temperature of 73°C sets the upper temperature limit for phototrophic metabolism in circum neutral to alkaline springs due to constraints imposed by these parameters on the fitness of the constituent populations. The upper temperature limit for the distribution of phototrophic metabolism decreases with decreasing pH due to the sulfide-dependent suppression of phototrophic activity in algae, the predominant phototrophs in springs with pH <5.0. These results establish the ecological constraints on the activity and presumably the fitness of phototrophs at the edge of their habitat range in YNP and provide insight into the environmental parameters that have shaped the evolution of this key metabolic process over evolutionary time.

MATERIALS AND METHODS

PREDICTIVE MODELING

The binary distribution (presence/absence) of genes involved in chlorophyll biosynthesis and/or phototrophic pigments in a number of geothermal springs sampled from across YNP (**Figure 1**) and the associated total sulfide, pH, and temperature of the spring water was extracted from three previous studies (Boyd et al., 2010; Cox et al., 2011; Hamilton et al., 2011b). The dataset extracted from Cox et al. (2011) was based on the visual distribution of pigments in geothermal springs, whereas the datasets extracted from Boyd et al. (2010) and Hamilton et al. (2011b) was based on the presence/absence of the protochlorophyllide reductase subunit L gene (*chlL/bchL*) required to synthesize chlorophyll in both anoxygenic and oxygenic phototrophs (Chew and Bryant, 2007) in biomass sampled from geothermal springs in YNP. While the data extracted from each of the aforementioned studies were from observations made in different springs from different regions during different years, plots of the overall phototroph distribution trends with respect to pH, temperature, and sulfide as presented in all three manuscripts (Boyd et al., 2010; Cox et al., 2011; Hamilton et al., 2011b) and in **Figures 2A,B** revealed the same trends, with an upper temperature limit for photosynthesis of ~73°C and a pH-dependent suppression of the upper temperature limit below pH ~6. Moreover, the distribution of phototrophic metabolism was constrained to environments with sulfide at a concentration of <5 µM (Cox et al., 2011; Hamilton et al., 2011b). Together, these observations indicate that both methods, as described above, were suitable for mapping the habitat range of phototrophic metabolism along ecological gradients in YNP. By combining the datasets, we were able to sample a much greater portion of the YNP geothermal complex that comprised more than 439 observations, than any one dataset provided alone.

Binomial GAMs describing the distribution of phototrophic pigments and genes involved in their synthesis as proxies for phototrophs were generated using the mgcv package (Wood, 2011) within the base package R (ver. 2.10.1), using default settings. GAMs are flexible models for fitting smooth curves to data, while maintaining parsimony. In essence, GAMs function to blend the properties of generalized linear models with the features of additive models. These approaches are commonly utilized in describing the distribution of plant species as a function of ecological parameters (Yee and Mitchell, 1991; Guisan et al., 2002). Here, a dependent variable (e.g., distribution of phototrophs) is plotted as a function of an independent variable(s) (e.g., temperature, pH, and sulfide) followed by the calculation of a smooth curve that goes through the data. The GAM approach is considered to be superior to linear-based regression methods (e.g., Pearson correlation analysis) since it does not require the problematic steps of *a priori* estimation of response curve shape or a specific parametric response function (Hastie and Tibshirini, 1986; Wood, 2004, 2011), but rather allows the data to determine the shape of the response curve in order to maximize the expected log likelihood, or fit of the model to the data. In the present study, GAMs were generated to describe the dependence of the distribution of phototrophic metabolism on environment, specifically spring temperature, pH, and dissolved sulfide concentration. We evaluated the fit of each GAM to the

data using a number of approaches including the Akaike Information Criterion (AIC), a maximum likelihood-based approach.

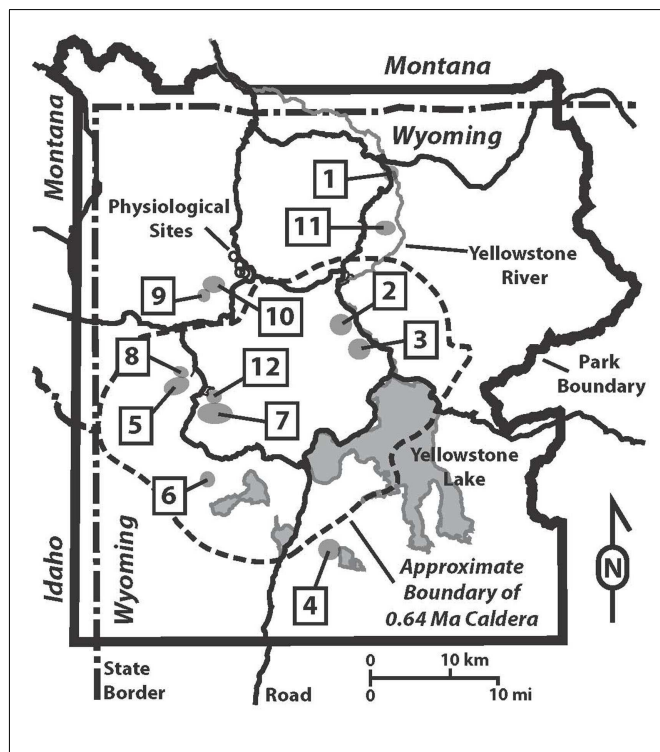


FIGURE 1 | Map of Yellowstone National Park showing hydrothermal areas sampled and locations of physiological sites. Hydrothermal areas are numbered alphabetically: 1, Calcite Springs; 2, Crater Hills; 3, Obsidian Pool Area; 4, Heart Lake; 5, Imperial Geyser Basin; 6, Lone Star; 7, Rabbit Creek; 8, Sentinel Meadows; 9, South of Sylvan Springs; 10, Sylvan Springs; 11, Washburn; 12, White Creek. Physiological samples, represented with open circles, in order from Northwest to Southeast are Bijah Spring, Nymph Creek, Dragon Spring, and Perpetual Spouter.

We considered the model with the lowest AIC value to be the best and evaluated the relative plausibility of each other model by examining differences between the AIC value for the best model and values for every other model (ΔAIC ; Johnson and Omland, 2004). The degrees of freedom (Df) for each model was used as a proxy to estimate the complexity of the model, with more complex models comprised of more Df. Models that achieve minimal AIC and residual deviance on the fewest Df (introduction of few smooth parameters during data fitting) are more likely to replicate in subsequent validation studies, when compared to those with greater Df (introduction of the additional smooth parameters during data fitting). Thus models with low AIC and low Df are lower complexity and are more parsimonious with the data.

GEOCHEMICAL ANALYSES

pH and temperature were measured with a WTW 330i meter and probe (WTW Inc., College Station, TX, USA) or a model 59002-00 Cole-Parmer temperature-compensated pH meter (Vernon Hills, IL, USA). Conductivity was measured with a model YSI30 or YSI EcoSense EC300 conductivity meter (YSI, Yellow Springs, OH, USA). Total dissolved sulfide was determined using the methylene blue method and a Hach DR/2000 spectrophotometer (Hach Company, Loveland, CO, USA). Aliquots used for analysis of dissolved inorganic carbon (DIC) were collected in 40 mL amber borosilicate vials with black butyl septa. All sample vials were filled to minimize head space and sealed to minimize degassing and atmospheric contamination. DIC concentrations were measured with an OI Analytical Model 1010 Wet Oxidation TOC Analyzer. DIC determinations for Perpetual Spouter and Dragon Spring, both of which were performed in August of 2011, were determined using an ON-LINE TOC-VCSHTOC/TIC and TN analyzer (Shimadzu Scientific Instruments, Columbia, MD, USA). Biofilms/sediments were dried in an oven for 3 days at $\sim 90^\circ\text{C}$, and ground with an agate mortar and pestle until uniformly powdered.

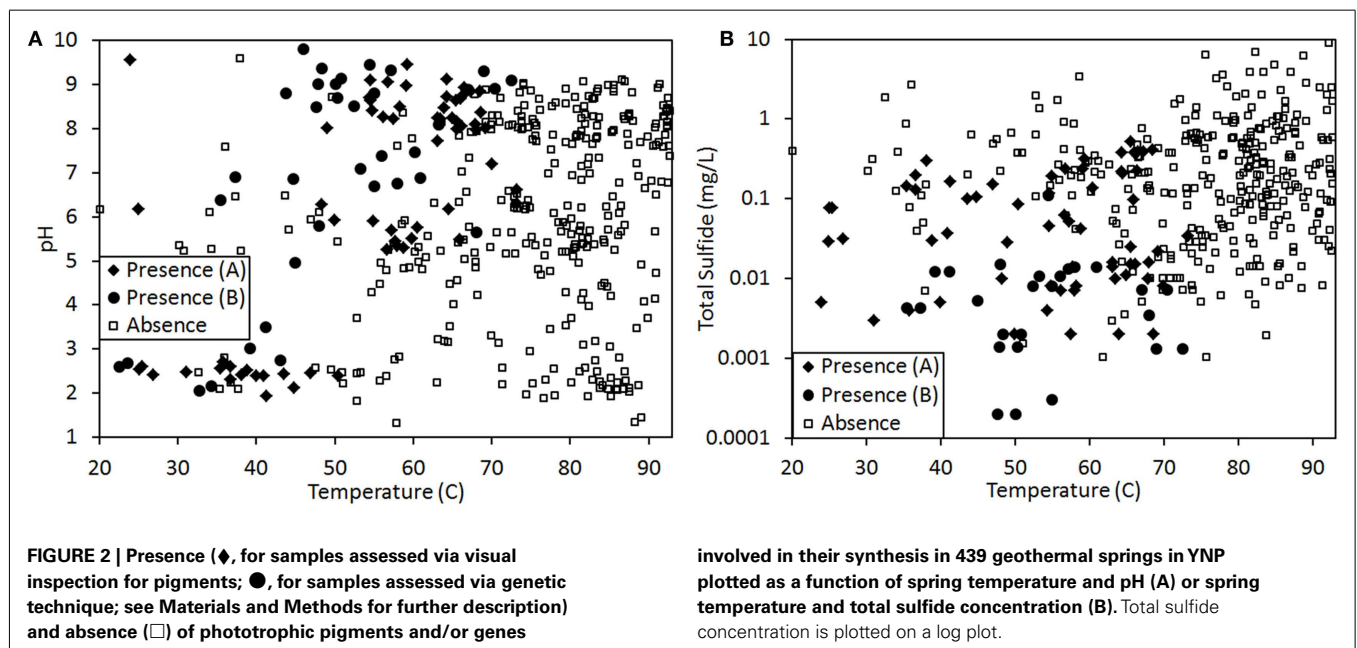


FIGURE 2 | Presence (◆, for samples assessed via visual inspection for pigments; ●, for samples assessed via genetic technique; see Materials and Methods for further description) and absence (□) of phototrophic pigments and/or genes

involved in their synthesis in 439 geothermal springs in YNP plotted as a function of spring temperature and pH (A) or spring temperature and total sulfide concentration (B). Total sulfide concentration is plotted on a log plot.

Samples were weighed and placed into tin cups, sealed, and analyzed via Costech Model ECS 4010 Elemental Analyzer (Costech Analytical Technologies Inc., Valencia, CA, USA) attached to a Thermo Delta^{plus} Advantage Isotope Ratio Mass Spectrometer (EA-IR-MS; Thermo Fisher Scientific Inc., Waltham, MA, USA). Data were standardized using the organic standards described above, and linearity was checked using NIST SRM 2710 (Montana Soil).

INORGANIC CARBON UPTAKE IN CHEMOTROPHIC AND PHOTOTROPHIC COMMUNITIES

Total DIC uptake was assessed using slight modifications to methods described previously (Boyd et al., 2009b). Briefly, chemotrophic and phototrophic mats were collected from points that were approximately 1 cm up gradient (chemotrophic mat) and 1 cm down gradient (chlorophototrophic mat) from the photosynthetic fringe at Bijah Spring (Norris-Mammoth Corridor; Easting: 521287, Northing: 4956460), Nymph Creek (Norris Geyser Basin; Easting: 521690, Northing: 4955601), and Dragon Spring (Norris Geyser Basin; Easting: 522889, Northing: 4953218; **Figure 1**) during March of 2010 (**Table 1**). The sampling locations in each spring were perpendicular to the photosynthetic fringe. Samples were collected aseptically using a syringe and were placed in a 15 mL sterile polypropylene tube, with the exception of the chemotrophic community at Bijah Spring (see below). The tube and the contents were shaken vigorously to uniformly resuspend the contents and create a slurry. From this slurry, 500 μ L aliquots of re-suspended solids were injected into pre-sterilized and anaerobic (N_2 headspace) 20 mL serum bottles sealed with a butyl stopper. Alternatively, in the case of chemotrophic communities from Bijah Spring, \sim 500 mg of sediment was placed in 20 mL serum bottles using a sterile scoop. Bottles containing Bijah Spring chemotrophic sediments were then capped, sealed, and purged with N_2 gas. In all experiments, 10 mL of spring water sampled directly at the photosynthetic fringe was injected into each vial such that the spring water and gas composition was the same. Killed controls were prepared by addition of glutaraldehyde to a final concentration of 2.0%, v/v. To assess the potential for dark DIC uptake, vials were wrapped completely in aluminum

foil. All assays (biological and killed controls, light and dark incubations) were performed in triplicate. The reaction was initiated by addition of $NaH_{14}CO_3$ (MP Biomedicals, 422 MBq/mmol) to a final concentration of 2.13×10^6 Bq/L. Serum bottles were placed in a clear polypropylene bag (secondary containment) and were incubated in the spring at the photosynthetic fringe for approximately 60 min. Following incubation, vials were placed directly on dry ice to stop the reaction. The vials remained frozen until further processed at the lab. Vials were thawed and acidified to pH <2.0 using concentrated HCl. Serum bottles and their contents were degassed with N_2 (\sim 5 min.) and the biomass was filtered onto 0.2 μ m pore size, 25 mm diameter white Nucleo-pore polycarbonate membranes (Whatman Inc., Florham Park, NJ, USA). Filtered biomass was washed with \sim 10 mL of sterile denionized water, placed in scintillation vials, and dried at 80°C overnight. In the case of samples from Bijah Spring, the vials containing sediment were then weighed and subtracted from empty vials such that all measurements could be normalized to grams of organic nitrogen present in the inoculum. The total solid content in each slurry used to inoculate the reactions (with the exception of Bijah chemotrophic communities) was determined by drying triplicate 1 mL aliquots at 80°C for 48 h.

Dried biomass and filters were overlain with 10 mL Cytoscint and were subjected to liquid scintillation counting as previously described (Boyd et al., 2009b). Total uptake was determined using previously described methods (Lizotte et al., 1996) using DIC numbers determined for each spring. For the purpose of comparing total DIC uptake between chemotrophic and phototrophic communities, rates of uptake were first normalized to dry weight of biomass per reaction and then to grams of organic nitrogen. All reported values reflect the difference in uptake between biological controls and glutaraldehyde-killed controls.

INFLUENCE OF SULFIDE AND TEMPERATURE ON DIC UPTAKE IN PHOTOTROPHIC COMMUNITIES

The influence of sulfide on DIC uptake in phototrophic communities was determined using the same approach as described above. Experiments were performed at Nymph Creek (May 2010),

Table 1 | Physical and chemical measurements made at sampling sites.

Source	Sampling date	Biofilm type ^a	Temperature (°C)	pH	DIC (ppm C)	DOC (ppm C)	wt% C ^b	wt% N ^b
Dragon Spring	3/13/2010	Chemo	58.0	3.13	5.9	0.91	1.08	0.13
	3/13/2010	Photo	46.5	2.95	0.6	0.90	0.95	0.44
Nymph Creek	3/14/2010	Chemo	56.8	2.99	10.5	0.60	11.71	2.85
	3/14/2010	Photo	53.0	3.00	26.4	0.53	11.45	2.01
Bijah Spring	3/14/2010	Chemo	72.5	7.52	57.8	0.78	0.19	0.02
	3/14/2010	Photo	68.8	7.65	60.2	0.68	0.70	0.09
Perpetual Spouter	8/18/2011	Photo	68.6	7.12	4.4	NA	2.91	0.46
Dragon Spring	8/18/2011	Photo	46.2	2.60	14.4	NA	7.67	1.36

DIC, dissolved inorganic carbon; ppm C, parts per million carbon; DOC, dissolved organic carbon; wt% C, weight percent organic carbon; wt% N, weight percent organic N; NA, not available.

^aThe type of biofilm as classified as either chemotrophic (Chemo) or phototrophic (Photo).

^bWeight percent organic carbon and organic nitrogen of bulk biofilms.

Dragon Spring (August 2011), and Perpetual Spouter (August 2011; **Table 1**). Perpetual Spouter (Norris Geyser Basin; Easting: 523034, Northing: 4952620) was chosen to replace Bijah Spring, due to difficulties in accessing the latter during periods of heavy visitor traffic. Prior to the initiation of the reaction with $\text{NaH}_2^{14}\text{CO}_3$, microcosms were amended with varying concentrations of an anaerobic and sterile sodium sulfide solution. Na_2S was added to microcosms from Nymph Creek at a concentration of 5 and $20\ \mu\text{M}$, whereas Na_2S amendments of only $5\ \mu\text{M}$ were made in microcosms from Perpetual Spouter and Dragon Spring. The concentration of sulfide to amend each microcosm with was determined empirically, such that the final concentration was $\sim 5\ \mu\text{M}$ greater than that present naturally at the photosynthetic fringe. Light-independent and killed controls were prepared as described above. All assays (biological and killed controls, light and dark incubations) were performed in triplicate. Reactions were initiated by addition of $\text{NaH}_2^{14}\text{CO}_3$ (MP Biomedicals, 422 MBq/mmol) to a final concentration of $1.66 \times 10^7\ \text{Bq/L}$. Serum bottles were incubated and processed as described above. The influence of elevated temperature on DIC uptake was examined in phototrophic communities sampled from Perpetual Spouter and Dragon Spring in August of 2011. Microcosms were set up as described above using biomass and spring water sampled from phototrophic mats near the fringe of each respective spring. Light-independent and killed controls were prepared as described above. All assays (biological and killed controls, light and dark incubations) were performed in triplicate. Reactions were initiated by addition of $\text{NaH}_2^{14}\text{CO}_3$ (MP Biomedicals, 422 MBq/mmol) to a final concentration of $1.66 \times 10^7\ \text{Bq/L}$. Serum bottles were incubated and processed as described above.

RESULTS

The presence or absence of phototrophic pigments and/or genes involved in their synthesis were used as proxies for examining the distribution of this metabolism along gradients in temperature, pH, and total sulfide in 439 samples (**Figure 2**) from a variety of geothermal springs throughout YNP (**Figure 1**) using GAM approaches. GAMs identified spring temperature as the top individual variable for predicting the distribution of phototrophic metabolisms ($\Delta\text{AIC} = 92.4$, $\text{Df} = 6.2$), followed by total sulfide concentration ($\Delta\text{AIC} = 192.1$, $\text{Df} = 3.9$) and spring pH ($\Delta\text{AIC} = 244.2$, $\text{Df} = 8.6$; **Table 2**). GAMs that comprised temperature explained 38.8% of the variance in the distribution of phototrophic metabolisms, whereas GAMs that comprised total sulfide or pH explained 19.6 and 11.2% of the variance in the dataset, respectively. GAMs that incorporated more than one environmental variable generally fit the data better and explained a greater amount of the variance than GAMs comprised of individual environmental variables, indicating additive interactions among variables. Importantly, the variation in temperature, pH, and sulfide in YNP springs were not correlated (Pearson $R^2 < 0.06$ for all pairwise regressions), indicating that these variables behave independently in the YNP springs analyzed in this study. A GAM that comprised spring temperature, pH, and total sulfide was the top ranking model ($\Delta\text{AIC} = 0.0$) and explained 66.6% of the variance in the dataset, the most of any GAM, although this

Table 2 | Statistics for GAMs whereby a binary dataset of the distribution of phototrophy in 439 springs in YNP served as the response variable.

GAM	ΔAIC	Df	adj R^2
Temp + pH + sulfide	0.0	14.7	0.666
Temp + sulfide	39.3	8.2	0.534
Temp + pH	51.3	11.1	0.529
Temp	92.4	6.2	0.388
pH + sulfide	151.6	9.7	0.289
Sulfide	192.1	3.9	0.196
pH	244.2	8.6	0.112

GAM, generalized additive model; Df, degrees of freedom; adj R^2 , sample size adjusted R^2 or the fraction percent of variance explained.

model required the introduction of 14.7 Df. GAMs that comprised temperature and sulfide ($\Delta\text{AIC} = 39.3$) and temperature and pH ($\Delta\text{AIC} = 51.3$) explained lower fractions of the variance in the dataset (53.4 and 52.9%, respectively), but required the introduction of fewer Df (8.2 and 11.1, respectively). Collectively, the GAM that comprised temperature and sulfide explained the greatest amount of the variation in the dataset while minimizing the introduction of Df.

Prior to examining the influence of physical and chemical constraints on the activity of phototrophs in YNP, it was necessary to determine if the photosynthetic fringe (**Figure 3**) was the result of competition between phototrophs and chemotrophs for this niche, as this was previously suggested (Boyd et al., 2009b). Competition experiments were performed at the photosynthetic fringe in Nymph Creek (pH 2.99, 52.7°C), Dragon Spring (pH 2.95, 46.5°C), and Bijah Spring (pH 7.40, 70.0°C) in March of 2010. The phototrophic assemblages near the photosynthetic fringe at both Nymph Creek and Dragon Spring are both comprised of algae related to *Cyanidioschyzon* sp. (Ferris et al., 2005; Lehr et al., 2007; Boyd et al., 2009a), whereas the phototrophic assemblages near the photosynthetic fringe at Bijah Spring are dominated by *Synechococcus* sp. and *Roseiflexus* sp. (King et al., 2006). Populations comprising the chemosynthetic assemblages near the fringe in both Nymph Creek and Dragon Spring are thought to be comprised primarily of organisms affiliated with *Hydrogenobacter* sp., *Desulfurella* sp., and *Acidimicrobium* sp. (Jackson et al., 2001; Ferris et al., 2003), whereas populations associated with chemotrophic assemblages in Bijah Spring are most closely related to *Thermotoga* sp. (King et al., 2006).

When incubated in the light, DIC uptake rates in chemotrophic assemblages sampled $\sim 1\ \text{cm}$ from the photosynthetic fringe at Nymph Creek, Dragon Spring, and Bijah Spring (**Figure 3**) were not significantly different ($P = 0.32, 0.62, 0.47$, respectively), from rates when incubated in the dark (**Figure 4**), which indicates that the mats were unlikely to be using light to drive DIC uptake. In contrast, rates of DIC uptake in photosynthetic assemblages sampled $\sim 1\ \text{cm}$ from the photosynthetic fringe at Nymph Creek, Dragon Spring, and Bijah Spring were significantly different ($P = 0.01, 0.04, 0.01$, respectively), when incubated in the light versus when incubated in the dark, indicating that these assemblages were using

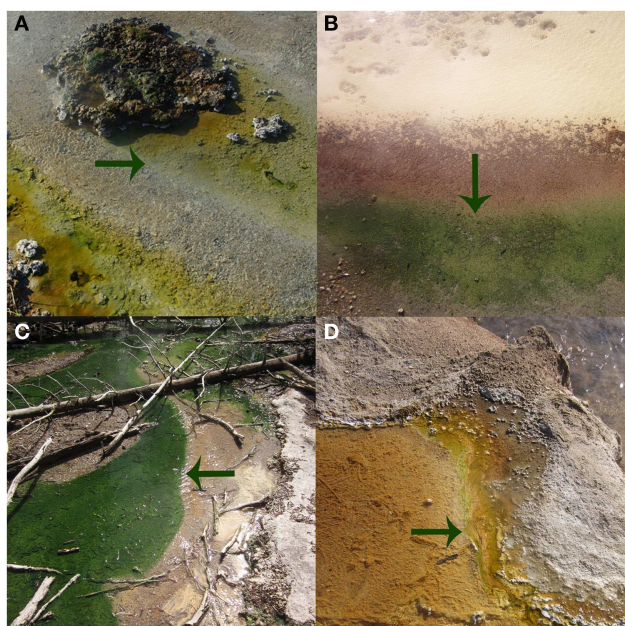


FIGURE 3 | The photosynthetic fringe, or the transition from chemosynthetic to photosynthetic metabolism, as denoted by arrows, for Bijah Spring in March 2010 (A), Dragon Spring in March 2010 (B), Nymph Creek in March 2010 (C), and Perpetual Spouter in August of 2011 (D).

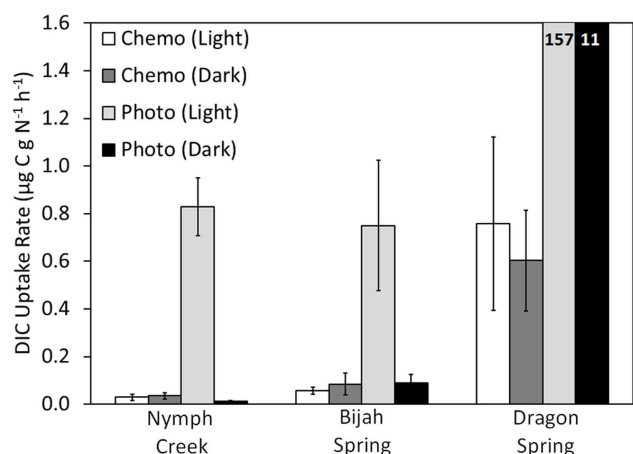


FIGURE 4 | Rate of DIC uptake for chemotrophic and phototrophic assemblages sampled from adjacent sides of the photosynthetic fringe in Nymph Creek (fringe pH = 2.99, Temp. = 52.7°C), Bijah Spring (fringe pH = 7.40, Temp. = 70.0°C), and Dragon Spring (fringe pH = 2.95, Temp. = 46.5°C). Microcosms were incubated both in the light and the dark and rates reflect the difference between triplicate killed controls and triplicate biological controls, for each treatment. For comparative purposes, DIC uptake rates were normalized to grams organic nitrogen present in the chemotrophic or phototrophic biomass used as inoculum (Table 1). All spring water used in the microcosms was sampled from the photosynthetic fringe and all microcosms were incubated in situ at the photosynthetic fringe temperature. Rates of DIC uptake for the phototrophic assemblages sampled from Dragon Spring are indicated as insets on the histogram.

light to drive a portion of DIC uptake. Rates of DIC uptake in phototrophic assemblages sampled ~1 cm from the photosynthetic fringe at Nymph Creek, Dragon Spring, and Bijah Spring, when incubated in the light, were significantly greater ($P < 0.05$ for all comparisons) than rates of DIC uptake in chemosynthetic mats from those springs, regardless of whether the chemosynthetic mats were incubated in the light or the dark. Importantly, rates of DIC uptake in chemotrophic and phototrophic assemblages sampled ~1 cm on either side of the photosynthetic fringe at Nymph Creek, Dragon Spring, and Bijah Spring, when incubated in the dark, were not significantly different ($P = 0.15, 0.93, 0.08$, respectively), suggesting that normalizing overall rates of uptake to organic N is unlikely to be responsible for the differences in the rates observed in chemotrophic and phototrophic assemblages. Collectively, these results suggest that competition for DIC between phototrophs and chemotrophs is unlikely to be the basis of the photosynthetic fringe observed in acidic (e.g., Nymph Creek and Dragon Spring) and alkaline (e.g., Bijah Spring) ecosystems.

The influence of sulfide on DIC uptake by phototrophic assemblages sampled near the photosynthetic fringe at Nymph Creek (fringe pH = 2.89, Temp. = 52.1°C, total sulfide ≤ 150 nM), Dragon Spring (fringe pH = 2.60, Temp. = 46.2°C, total sulfide ~ 1 μ M), and Perpetual Spouter (fringe pH = 7.12, Temp. = 68.6°C, total sulfide ≤ 150 nM) was examined in both light and dark incubations in March of 2010 (Nymph Creek) and August of 2011 (Dragon Spring and Perpetual Spouter; Figure 3). An amount of sodium sulfide was added to microcosms in order

to generate a final concentration that was ~ 5 μ M greater than that present in spring water flowing over the photosynthetic fringe in each spring. When compared to unamended controls, the addition of sulfide to a final concentration of 5 μ M in microcosms containing photosynthetic mat sampled from near the photosynthetic fringe at Nymph Creek resulted in a significant ($P = 0.04$) decrease ($\sim 56\%$ of unamended control rate) in the rate of DIC uptake (Figure 5A). The addition of sulfide to a final concentration of 20 μ M in microcosms containing photosynthetic mat sampled from near the photosynthetic fringe at Nymph Creek resulted in a significant ($P < 0.01$) decrease (31% of unamended control rate) when compared to the unamended control DIC uptake rate (Figure 5A). The DIC uptake rates in unamended controls were not significantly different from the sulfide amended controls (5 and 20 μ M) in microcosms containing photosynthetic mat from Nymph Creek when incubated in the dark, suggesting that sulfide did not significantly influence chemosynthetic DIC uptake in the microcosm incubations.

The rate of light-driven DIC uptake was also significantly ($P = 0.04$) suppressed ($\sim 55\%$ of unamended control rate) by the addition of sulfide to a final concentration of 5 μ M in microcosms containing microbial mat sampled near the photosynthetic fringe at Dragon Spring, whereas the rate of dark DIC were not significantly affected ($P = 0.33$) by the addition of sulfide (Figure 5B). Interestingly, the rate of light-driven DIC uptake was not significantly ($P = 0.08$) affected by the addition of sulfide when added to a final concentration of 5 μ M in microcosms

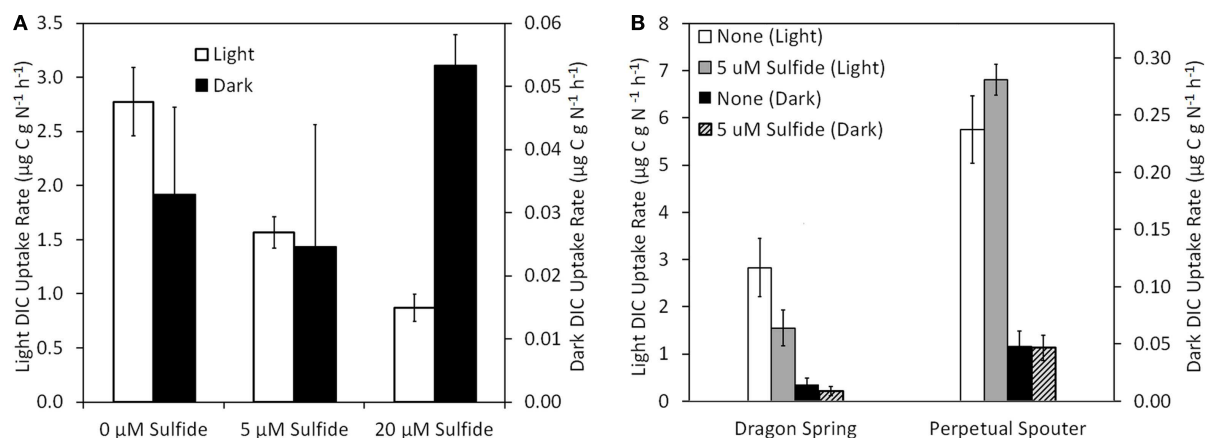


FIGURE 5 | Rate of DIC uptake in phototrophic assemblages sampled from near (<1 cm) the photosynthetic fringe at Nymph Creek (fringe pH = 2.89, Temp. = 52.1°C, total sulfide ≤ 150 nM) as a function of increasing amendment of sodium sulfide to final concentrations of 5 and 20 μM when incubated under light and dark conditions (A). Rate of DIC uptake in phototrophic assemblages sampled from near (<1 cm) the photosynthetic fringe at Dragon Spring (fringe pH = 2.60,

Temp. = 46.2°C, total sulfide = ~1 μM) and Perpetual Spouter (fringe pH = 7.12, Temp. = 68.6°C, total sulfide ≤ 150 nM) as a function of amendment of sodium sulfide to final concentrations of 5 μM when incubated under light and dark conditions (B). All spring water used in inoculums was sampled from the photosynthetic fringe and rates of DIC uptake were normalized to grams of organic nitrogen present in the biomass used as inoculum (Table 1).

containing photosynthetic mat sampled near the photosynthetic fringe at Perpetual Spouter. Likewise, the rate of dark DIC uptake was not significantly ($P = 0.93$) affected by the addition of sulfide when added to a final concentration of 5 μM in microcosms containing photosynthetic mat sampled near the photosynthetic fringe at Perpetual Spouter (Figure 5B). Thus, the addition of sulfide suppresses light-driven DIC uptake in the algal-dominated photosynthetic mats present in Nymph Creek and Dragon Spring, but has no significant influence on rates of DIC uptake in Perpetual Spouter, which is dominated by bacterial phototrophs most closely affiliated with *Synechococcus* sp. and *Roseiflexus* sp. (Hamilton et al., 2011b). The rate of DIC uptake when incubated in the dark was unaffected by the addition of sulfide, regardless of the sampling location.

The influence of temperature on DIC uptake was examined in phototrophic mats sampled from near the photosynthetic fringe at Dragon Spring (fringe pH = 2.60, Temp. = 46.2°C, total sulfide = ~1 μM) and Perpetual Spouter (fringe pH = 7.12, Temp. = 68.6°C, total sulfide ≤ 150 nM) in August of 2011. All components of the reaction (inoculum, spring water) were identical in the reactions, with the exception of where in the thermal transect the microcosms were incubated. Incubation of phototrophic mats at a thermal transect 10°C greater than that at the photosynthetic fringe resulted in a statistically significant ($P < 0.01$ for both Dragon Spring and Perpetual Spouter) decrease in light-driven DIC uptake rates when compared with rates of light-driven DIC uptake in microcosms incubated at the fringe temperature in both Dragon Spring and Perpetual Spouter (Figure 6). The rates of light-driven DIC uptake in microcosms incubated at the higher temperature locations (56 and 78°C for Dragon Spring and Perpetual Spring, respectively), were 3.9 and 2.2% of the rate of light-driven DIC uptake in microcosms at the fringe temperature of 46°C in Dragon Spring and 68°C in Perpetual Spouter, respectively (Figure 6). Interestingly, the rate

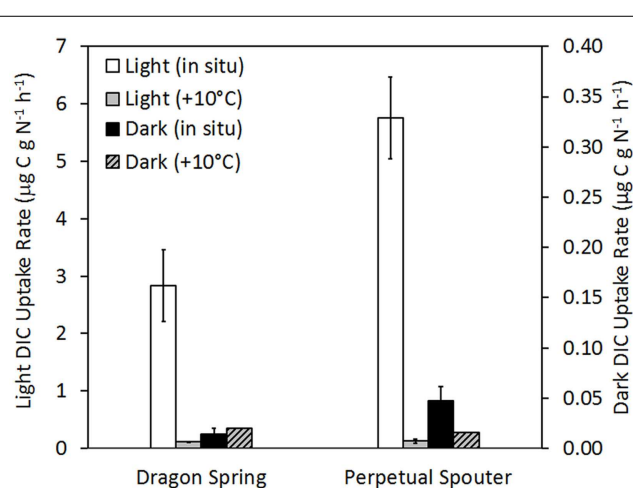


FIGURE 6 | Rate of DIC uptake in phototrophic assemblages sampled from near the photosynthetic fringe at Dragon Spring (fringe pH = 2.60, Temp. = 46.2°C, total sulfide = ~1 μM) and Perpetual Spouter (fringe pH = 7.12, Temp. = 68.6°C, total sulfide ≤ 150 nM) when incubated at the fringe temperature as well as at a temperature ~10°C greater than at the fringe temperature (58.0 and 78.4°C, respectively), under both light and dark conditions. All spring water used in microcosms was sampled from near the photosynthetic fringe and rates of DIC uptake were normalized to grams organic nitrogen in biomass that served as inoculum (Table 1).

of DIC uptake in microcosms incubated in the dark at the fringe in Dragon Spring was not significantly different ($P = 0.17$) from that measured in microcosms incubated in the dark at the higher temperature locations. In contrast, the rate of DIC uptake in microcosms incubated in the dark at the fringe in Perpetual Spouter was significantly lower ($P = 0.04$) from that measured in microcosms incubated in the dark at the higher temperature locations.

The rates of DIC uptake in microcosms incubated in the dark at the higher temperature locations in Dragon Spring and Perpetual Spouter were 139 and 32% of those measured in microcosms incubated at the fringe, respectively. Thus, DIC uptake in algal populations that comprise the phototrophic assemblage at Dragon Spring and the cyanobacterial populations that comprise the phototrophic assemblage at Perpetual Spouter are apparently more sensitive to temperature stress than the chemotrophic populations in these assemblages.

DISCUSSION

The innovation of photosynthesis, specifically the photosynthetic apparatus capable of splitting water into O_2 , protons, and electrons, was a pivotal point in the evolution of Earth's biogeochemical cycles (Blankenship, 1992; Anbar, 2008; Falkowski and Isozaki, 2008) and the emergence of complex life (Raymond and Segrè, 2006; Boyd et al., 2011; Wang et al., 2011a). While studies continue to refine our understanding of when these events are likely to have occurred (Anbar et al., 2007; Buick, 2008; Sessions et al., 2009), far fewer studies have focused on understanding the ecological interactions that are likely to have influenced the evolution of photosynthesis. The extreme variation in geochemical composition present in YNP's >12,000 geothermal features (Nordstrom et al., 2005; Shock et al., 2010) offer a multitude of spatial gradients that directly select for organisms with enhanced performance or fitness under a given set of conditions (Brock, 1967; Allewalt et al., 2006; Miller et al., 2009). In the present study, the distribution of photosynthesis along spatial gradients of temperature, sulfide, and pH from 439 geothermal springs was quantitatively mapped using GAMs in order to identify the constraints on the habitat range of phototrophic metabolisms in the YNP geothermal complex. Microcosm studies served to determine whether the edges of the habitat range were due to constraints on the activity of the constituent populations, in an attempt to begin to translate the habitat range to a fitness landscape.

Aside from light availability, GAMs indicated that the primary variable influencing the distribution of photosynthesis was temperature, with sulfide as the second most significant predictor of the distribution of photosynthetic metabolism. These quantitative rankings are consistent with previous qualitative distribution patterns noted across YNP (Cox et al., 2011; Hamilton et al., 2011b) as well as with physiological data obtained from cultivated algae and cyanobacteria. Photosystem II (PSII), the water splitting complex present in cyanobacteria, algae, and plants (Blankenship, 1992, 2010) is sensitive to sulfide in some, but not all, oxygenic phototrophs (Castenholz, 1977; Oren et al., 1979; Miller and Bebout, 2004). To examine whether the sulfide-dependent pattern in the distribution of phototrophs is due to suppression of photosynthetic activity (presumably through the toxicity to PSII) DIC uptake rates in the presence and absence of sulfide were compared. DIC uptake in alkaline phototrophic assemblages likely to be dominated by cyanobacteria was unaffected by the addition of $5\ \mu\text{M}$ sulfide, whereas DIC uptake in acidic phototrophic assemblages likely to be dominated by algae was suppressed by sulfide at a concentration of $5\ \mu\text{M}$. The predominant form of sulfide at acidic pH (pH <6–7) is $H_2S(aq)$

(Amend and Shock, 2001), which is also the form thought to be responsible for PSII toxicity since it easily diffuses across the cell membrane (Howsley and Pearson, 1979). Thus, the physiological sensitivity to sulfide at concentrations as low as $5\ \mu\text{M}$ observed in photosynthetic assemblages inhabiting acidic springs is consistent with the presence of algal phototrophs in acidic environments (pH <5.0) only when the total sulfide concentration was less than $\sim 5\ \mu\text{M}$ (Figure 2). Thus, the physiological constraints imposed by sulfide impairs activity, which in turn likely renders algal populations unfit to successfully replicate in these environments. This decrease in fitness would in turn likely limit the distribution of algae to YNP habitats with sulfide concentrations of < $5\ \mu\text{M}$.

Existing data indicate that the photosynthetic populations inhabiting the edge of the phototrophic habitat range in acidic environments (pH <5.0) are comprised primarily of algae related to *Cyanidioschyzon* sp. (Ferris et al., 2005; Lehr et al., 2007; Boyd et al., 2009a). The habitat range for *Cyanidioschyzon* sp. appears to vary depending on the spring being examined. For example, *Cyanidioschyzon* sp. mats are commonly observed in acidic springs in Norris Geyser Basin and other locales in YNP at temperatures approaching $\sim 57^\circ\text{C}$ (Lehr et al., 2007), yet in other acidic springs in YNP and global-distributed hydrothermal fields such as those in Japan, their distribution is constrained to lower temperatures (~ 40 – 50°C ; Cox et al., 2011; Hamilton et al., 2011b). This suggests that minor variations in the composition of the fluid in individual acidic springs might be limiting the activity of algal populations and impacting their reproductive fitness and distributional pattern. This hypothesis is consistent with the “patchy” distribution of phototrophic metabolism in environments with pH <5 and temperatures lower than 56°C (Figure 2A). Previous studies have noted rapid decreases in sulfide as a function of increasing distances from the source in acidic springs either through degassing or oxidation via biological or abiological mechanisms (Langner et al., 2001; D'Imperio et al., 2008; Cox et al., 2011). This observation, together with the variability in total sulfide concentrations in the source waters of acidic features (Shock et al., 2010), is likely to result in differences among points in the thermal transects where total sulfide concentrations drop below $5\ \mu\text{M}$, the apparent upper limit tolerated by *Cyanidioschyzon*-like populations in YNP (Figure 2B). In turn, such variation would likely impact the temperature at the point in the thermal transect where algal photosynthesis is possible.

The influence of temperature on DIC uptake rates was also examined in alkaline and acidic springs, since a previous study indicated that a strain of *Synechococcus* isolated from YNP was photosynthetically active at a temperature of 75°C (Allewalt et al., 2006), 2°C warmer than has been observed in YNP (Figure 2A). Although light-driven DIC uptake was observed in algal- and cyanobacterial-dominated phototrophic assemblages incubated at temperature locations that were 10°C higher (56 and 78°C , respectively), than the *in situ* temperature where the mats were sampled (46 and 68°C , respectively), it only represented 3 and 2%, respectively, of the activities observed at the *in situ* temperature. This finding is consistent with previous results indicating that photosynthesis in natural communities and isolates

is most efficient at temperatures that correspond to those of the environment where the phototrophic assemblages were sampled, apparently due to evolutionary optimization to inhabit that particular ecological niche (Brock, 1967; Miller and Castenholz, 2000; Allewalt et al., 2006). To the extent that DIC uptake reflects the overall physiological state of the photosynthetic assemblages, these results indicate that temperature constrains the distribution of photosynthesis due to its effects on the physiology of the organisms comprising the community, thereby decreasing their overall fitness. As summarized by Cox et al. (2011) numerous hypotheses have been put forth regarding the mechanisms through which temperature may limit phototrophy, including arguments regarding protein stability (Kempner, 1963) and the functionality of the CO₂-assimilating mechanism under thermal stress (Meeks and Castenholz, 1978). Biochemical experimentation that is beyond the scope of this study will be required to elucidate the molecules that are most sensitive to temperature stress and which are likely to restrict the diversification of phototrophs to environments with temperatures >73°C.

Although evidence is presented here to indicate that photosynthesis is possible at temperatures as high as 78°C, it is unlikely that this activity is sufficient for reproductive success considering that photosynthesis has never been observed in nature above a temperature of ~73°C (Brock, 1967). In acidic environments (pH <4–5), the upper temperature limit for the distribution of photosynthetic metabolism is limited to locations with temperatures of less than ~57°C (Lehr et al., 2007; Boyd et al., 2009b, 2010; Cox et al., 2011; Hamilton et al., 2011b). This is likely due to the transition from cyanobacterial-dominated phototrophic ecosystems to algal-dominated photosynthetic ecosystems over this pH interval (Brock, 1973; Hamilton et al., 2011b) coupled with the suppression of phototrophic activity in algae by hydrogen sulfide. As a result of degassing and oxidation (Langner et al., 2001; Cox et al., 2011), the elevated sulfide concentrations that are common in source fluids dissipate, ultimately reaching the concentrations of less than ~5 µM that enable algal phototrophs to grow and reproduce. Considering that numerous microorganisms have evolved to thrive at temperatures of >73°C (Brock, 1985) and a number of cyanobacteria have evolved to tolerate up to mM concentrations of sulfide (Oren et al., 1979; Miller and Bebout, 2004), it is unclear why phototrophs have not radiated and expanded their habitat boundaries in YNP. Perhaps the edges of the habitat range reflect intrinsic limits of the photosynthetic apparatus itself. Such a scenario corresponds to a deep valley on a fitness landscape, whereby the sole mechanism to adapt to a higher temperature (high physiological stress) is through significant and rapid adaptation (Keymer et al., 2006). However, if trade-offs or costs associated with adaptation to higher temperatures result in a loss of fitness at the expense of the adaptive advantage for a thermotolerant photosynthetic apparatus, the organism will not persist and diversification will collapse back to the ancestral state. Additional physiological studies, employing an evolutionary framework such as that used by Miller and colleagues (Miller and Castenholz, 2000; Miller, 2003), will be required to elucidate the physiological parameter(s) underlying the upper temperature limit for photosynthesis.

Generalized additive models that comprise multiple explanatory variables were significant predictors of the distribution of phototrophic metabolisms in YNP, indicating additive interactions among variables that constrain their habitat range. However, it is not known if the additive interactions that lead to distributional patterns reflect additive constraints on the fitness of populations that comprise the habitat edge communities. Additional studies using ecologically representative isolates will facilitate the examination of the effect of co-variation among target parameters under controlled conditions on the activities and fitness of phototrophic populations. Importantly, a GAM that comprised variation in temperature, sulfide, and pH was only capable of explaining 67% of the variation in the distribution of photosynthetic metabolisms, indicating that 33% of the variation is due to other unaccounted for variables. Elevated concentrations of metals are common in YNP geothermal environments including copper, mercury, and zinc (McCleskey et al., 2005; King et al., 2006; Boyd et al., 2009a; Wang et al., 2011b). Such metals have been shown to inhibit the activity of photosynthetic organisms, primarily through their disruption of the light harvesting apparatus (Clijsters and van Assche, 1985; Küpper et al., 2002). The speciation and bioavailability of many metals, including mercury (Barkay et al., 2010; Wang et al., 2011b), vary with the composition and pH of the environment. Thus, the influence of pH on defining the habitat range of photosynthetic metabolism as identified by GAMs may relate to the bioavailability and speciation of the numerous metals that co-vary with pH and result in a decrease in the fitness of phototrophic organisms in YNP. It has also been suggested that the availability of DIC, which tends to be lower at high temperature (Weyl, 1959) and which tends to speciate toward carbonic acid at low pH (Amend and Shock, 2001), may place additional constraints on the activity and fitness of phototrophs (Hamilton et al., 2011b). Without sufficient inorganic carbon to serve as the oxidizing agent, photoautotrophs can become severely photoinhibited, leading to oxidative stress (Murata et al., 2007) which would decrease fitness and would presumably place an additional constraint on their distribution. Indeed, the availability of DIC was inversely correlated with pH in the sites examined in the present study. A future goal of this work is to integrate measurements of phototroph *in situ* activity, phototroph abundance data, phylogenetic data, and more detailed geochemical data (e.g., DIC, trace metals, etc.) such that a comprehensive fitness landscape can be developed for photosynthesis in YNP in order to effectively predict the constraints on the evolution of this key metabolic process in this early Earth analog environment.

ACKNOWLEDGMENTS

This work was supported by National Science Foundation grants 1123689 to Eric S. Boyd, 1123649 to Everett L. Shock, and PIRE-0968421 to Eric S. Boyd and John W. Peters. Eric S. Boyd also acknowledges support from the NASA Astrobiology Institute (NAI) postdoctoral fellowship program for a portion of this work. The Astrobiology Biogeochemistry Research Center at Montana State University was supported by a grant from the NAI (NNA08CN85A) to Eric S. Boyd and John W. Peters. Eric S. Boyd would like to thank Tom “Elmo” Werner for logistical support during the completion of this project.

REFERENCES

- Allewalt, J. P., Bateson, M. M., Revsbech, N. P., Slack, K., and Ward, D. M. (2006). Effect of temperature and light on growth of and photosynthesis by *Synechococcus* isolates typical of those predominating in the Octopus Spring microbial mat community of Yellowstone National Park. *Appl. Environ. Microbiol.* 72, 544–550.
- Amend, J. P., and Shock, E. L. (2001). Energetics of overall metabolic reactions of thermophilic and hyperthermophilic archaea and bacteria. *FEMS Microbiol. Rev.* 25, 175–243.
- Anbar, A. D. (2008). Elements and evolution. *Science* 322, 1481–1483.
- Anbar, A. D., Duan, Y., Lyons, T. W., Arnold, G. L., Kendall, B., Creaser, R. A., Kaufman, A. J., Gordon, G. W., Scott, C., Garvin, J., and Buick, R. (2007). A whiff of oxygen before the great oxidation event? *Science* 317, 1903–1906.
- Barkay, T., Kritee, K., Boyd, E., and Geesey, G. (2010). A thermophilic bacterial origin and subsequent constraints by redox, light and salinity on the evolution of the microbial mercuric reductase. *Environ. Microbiol.* 12, 2904–2917.
- Blankenship, R. E. (1992). Origin and early evolution of photosynthesis. *Photosyn. Res.* 33, 91–111.
- Blankenship, R. E. (2010). Early evolution of photosynthesis. *Plant Physiol.* 154, 434–438.
- Boyd, E. S., Anbar, A. D., Miller, S., Hamilton, T. L., Lavin, M., and Peters, J. W. (2011). A late methanogen origin for molybdenum-dependent nitrogenase. *Geobiology* 9, 221–232.
- Boyd, E. S., Hamilton, T. L., Spear, J. R., Lavin, M., and Peters, J. W. (2010). [FeFe]-hydrogenase in Yellowstone National Park: evidence for dispersal limitation and phylogenetic niche conservatism. *ISME J.* 4, 1485–1495.
- Boyd, E. S., King, S., Tomberlin, J. K., Nordstrom, D. K., Krabbenhoft, D. P., Barkay, T., and Geesey, G. G. (2009a). Methylmercury enters an aquatic food web through acidophilic microbial mats in Yellowstone National Park, Wyoming. *Environ. Microbiol.* 11, 950–959.
- Boyd, E. S., Leavitt, W. D., and Geesey, G. G. (2009b). CO₂ uptake and fixation by a thermoacidophilic microbial community attached to precipitated sulfur in a geothermal spring. *Appl. Environ. Microbiol.* 75, 4289–4296.
- Brock, T. D. (1967). Micro-organisms adapted to high temperatures. *Nature* 214, 882–885.
- Brock, T. D. (1973). Lower pH limit for the existence of blue-green algae: evolutionary and ecological implications. *Science* 179, 480–483.
- Brock, T. D. (1985). Life at high temperatures. *Science* 230, 132–138.
- Buick, R. (2008). When did oxygenic photosynthesis evolve? *Philos. Trans. R. Soc. Lond. B Biol. Sci.* 363, 2731–2743.
- Castenholz, R. W. (1977). The effect of sulfide on the blue-green algae of hot springs II. Yellowstone National Park. *Microb. Ecol.* 3, 79–105.
- Chew, A. G. M., and Bryant, D. A. (2007). Chlorophyll biosynthesis in bacteria: the origins of structural and functional diversity. *Annu. Rev. Microbiol.* 61, 113–129.
- Clijsters, H., and van Assche, F. (1985). Inhibition of photosynthesis by heavy metals. *Photosyn. Res.* 7, 31–40.
- Cox, A., Shock, E. L., and Havig, J. R. (2011). The transition to microbial photosynthesis in hot spring ecosystems. *Chem. Geol.* 280, 344–351.
- D'Imperio, S., Lehr, C. R., Odoro, H., Druschel, G., Kühl, M., and McDermott, T. R. (2008). Relative importance of H₂ and H₂S as energy sources for primary production in geothermal springs. *Appl. Environ. Microbiol.* 74, 5802–5808.
- Falkowski, P. G., and Isozaki, Y. (2008). The story of O₂. *Science* 322, 540–542.
- Ferris, M. J., Magnuson, T. S., Fagg, J. A., Thar, R., Kühl, M., Sheehan, K. B., and Henson, J. M. (2003). Microbially mediated sulphide production in a thermal, acidic algal mat community in Yellowstone National Park. *Environ. Microbiol.* 5, 954–960.
- Ferris, M. J., Sheehan, K. B., Kühl, M., Cooksey, K., Wigglesworth-Cooksey, B., Harvey, R., and Henson, J. M. (2005). Algal species and light microenvironment in a low-pH, geothermal microbial mat community. *Appl. Environ. Microbiol.* 71, 7164–7171.
- Guisan, A., Edwards, T. C. Jr., and Hastie, T. (2002). Generalized linear and generalized additive models in studies of species distributions: setting the scene. *Ecol. Model.* 157, 89–100.
- Guisan, A., and Thuiller, W. (2005). Predicting species distribution: offering more than simple habitat models. *Ecol. Lett.* 8, 993–1009.
- Hamilton, T. L., Boyd, E. S., and Peters, J. W. (2011a). Environmental constraints underpin the distribution and phylogenetic diversity of nifH in the Yellowstone geothermal complex. *Microb. Ecol.* 61, 860–870.
- Hamilton, T. L., Vogl, K., Bryant, D. A., Boyd, E. S., and Peters, J. W. (2011b). Environmental constraints defining the distribution, composition, and evolution of chlorophyllotrophs in thermal features of Yellowstone National Park. *Geobiology* 10, 236–249.
- Hastie, R., and Tibshirani, R. (1986). Generalized additive models. *Stat. Sci.* 1, 297–318.
- Hoehler, T. M. (2007). An energy balance concept for habitability. *Astrobiology* 7, 824–838.
- Howesley, R., and Pearson, H. W. (1979). pH dependent sulfide toxicity to oxygenic photosynthesis in cyanobacteria. *FEMS Microbiol. Rev.* 6, 287–292.
- Jackson, C. R., Langner, H. W., Donahoe-Christiansen, J., Inskeep, W. P., and McDermott, T. R. (2001). Molecular analysis of microbial community structure in an arsenite-oxidizing acidic thermal spring. *Environ. Microbiol.* 3, 532–542.
- Johnson, J. B., and Omland, K. S. (2004). Model selection in ecology and evolution. *Trends Ecol. Evol.* 19, 101–108.
- Keddy, P. A. (1992). Assembly and response rules: two goals for predictive community ecology. *J. Veg. Sci.* 3, 157–164.
- Kempner, E. S. (1963). Upper temperature limit of life. *Science* 142, 1318–1319.
- Keymer, J. E., Galajda, P., Muldoon, C., Park, S., and Austin, R. H. (2006). Bacterial metapopulations in nanofabricated landscapes. *Proc. Natl. Acad. Sci.* 103, 17290–17295.
- King, S. A., Behnke, S., Slack, K., Krabbenhoft, D. P., Nordstrom, D. K., Burr, M. D., and Striegl, R. G. (2006). Mercury in water and biomass of microbial communities in hot springs of Yellowstone National Park, USA. *Appl. Geochem.* 21, 1868–1879.
- Küpper, H., Šetlík, I., Spiller, M., Küpper, F. C., and Prášil, O. J. (2002). Heavy metal-induced inhibition of photosynthesis: targets of *in vivo* heavy metal chlorophyll formation. *J. Phycol.* 38, 429–441.
- Langner, H. W., Jackson, C. R., McDermott, T. R., and Inskeep, W. P. (2001). Rapid oxidation of arsenite in a hot spring ecosystem, Yellowstone National Park. *Environ. Sci. Technol.* 35, 3302–3309.
- Lavorel, S., and Garnier, E. (2002). Predicting changes in community composition and ecosystem functioning from plant traits: revisiting the Holy Grail. *Funct. Ecol.* 16, 545–556.
- Lehr, C. R., Frank, S. D., Norris, T. B., D'Imperio, S., Kalinin, A. V., Toplin, J. A., Castenholz, R. W., and McDermott, T. R. (2007). Cyanidia (Cyanidiales) population diversity and dynamics in an acid-sulfate-chloride spring in Yellowstone National Park. *J. Phycol.* 43, 3–14.
- Lizotte, M. P., Sharp, T. R., and Priscu, J. C. (1996). Phytoplankton dynamics in the stratified water column of Lake Bonney, Antarctica: I. Biomass and productivity during the winter-spring transition. *Polar Biol.* 16, 155–162.
- McCleskey, R. B., Ball, J. W., Nordstrom, D. K., Holloway, J. M., and Taylor, H. E. (2005). *Water-Chemistry Data for Selected Hot Springs, Geysers, and Streams in Yellowstone National Park, Wyoming, 2001–2002*. Boulder, CO: U.S. Geological Survey.
- Meeks, J. C., and Castenholz, R. W. (1978). Photosynthetic properties of the extreme thermophile *Synechococcus lividus*. II. Stoichiometry between oxygen evolution and CO₂ assimilation. *J. Therm. Biol.* 3, 19–24.
- Miller, S. R. (2003). Evidence for the adaptive evolution of the carbon fixation gene *rbcL* during diversification in temperature tolerance of a clade of hot spring cyanobacteria. *Mol. Ecol.* 12, 1237–1246.
- Miller, S. R., and Bebout, B. M. (2004). Variation in sulfide tolerance of photosystem II in phylogenetically diverse cyanobacteria from sulfidic habitats. *Appl. Environ. Microbiol.* 70, 736–744.
- Miller, S. R., and Castenholz, R. W. (2000). Evolution of thermotolerance in hot spring cyanobacteria of the genus *Synechococcus*. *Appl. Environ. Microbiol.* 66, 4222–4229.
- Miller, S. R., Williams, C., Strong, A. L., and Carvey, D. (2009). Ecological specialization in a spatially structured population of the thermophilic cyanobacterium *Mastigocladus laminosus*. *Appl. Environ. Microbiol.* 75, 729–734.
- Murata, N., Takahashi, S., Nishiyama, Y., and Allakhverdiev, S. I. (2007). Photoinhibition of photosystem II under environmental stress. *Biochim. Biophys. Acta* 1767, 414–421.
- Nordstrom, D. K., Ball, J. W., and McCleskey, R. B. (2005). “Ground water to surface water: chemistry of thermal outflows in Yellowstone National Park,” in *Geothermal Biology and Geochemistry in Yellowstone National Park*, eds W. P. Inskeep and T. R. McDermott (Bozeman: Montana State University), 143–162.

- Oren, A., Padan, D., and Malkin, S. (1979). Sulfide inhibition of photosystem II in cyanobacteria (blue-green algae) and tobacco chloroplasts. *Biochim. Biophys. Acta* 546, 270–279.
- Raymond, J., and Segrè, D. (2006). The effect of oxygen on biochemical networks and the evolution of complex life. *Science* 311, 1764–1767.
- Sessions, A. L., Doughty, D. M., Welander, P. V., Summons, R. E., and Newman, D. K. (2009). The continuing puzzle of the Great Oxidation Event. *Curr. Biol.* 19, R567–R574.
- Shock, E. L., Holland, M., Meyer-Dombard, D., Amend, J. P., Osburn, G. R., and Fischer, T. P. (2010). Quantifying inorganic sources of geochemical energy in hydrothermal ecosystems, Yellowstone National Park, USA. *Geochim. Cosmochim. Acta* 74, 4005–4043.
- Shock, E. L., and Holland, M. E. (2007). Quantitative habitability. *Astrobiology* 7, 839–851.
- Wang, M., Jiang, Y.-Y., Kim, K. M., Qu, G., Ji, H.-F., Mittenthal, J. E., Zhang, H.-Y., and Caetano-Anollés, G. (2011a). A universal molecular clock of protein folds and its power in tracing the early history of aerobic metabolism and planet oxygenation. *Mol. Biol. Evol.* 28, 567–582.
- Wang, Y., Boyd, E., Crane, S., Lu-Irving, P., Krabbenhoft, D., King, S., Dighton, J., Geesey, G., and Barkay, T. (2011b). Environmental conditions constrain the distribution and diversity of archaeal merA in Yellowstone National Park, Wyoming, U.S.A. *Microb. Ecol.* 62, 739–752.
- Westoby, M. (2006). Phylogenetic ecology at world scale, a new fusion between ecology and evolution. *Ecology* 87, S163–S165.
- Weyl, P. K. (1959). The change in solubility of calcium carbonate with temperature and carbon dioxide content. *Geochim. Cosmochim. Acta* 17, 214–225.
- Wiens, J. J. (2004). Speciation and ecology revisited: phylogenetic niche conservatism and the origin of species. *Evolution* 58, 193–197.
- Wiens, J. J., and Graham, C. H. (2005). Niche conservatism: integrating evolution, ecology, and conservation biology. *Annu. Rev. Ecol. Syst.* 36, 519–539.
- Wood, S. N. (2004). Stable and efficient multiple smoothing parameter estimation for generalized additive models. *J. Am. Stat. Assoc.* 99, 673–686.
- Wood, S. N. (2011). Fast stable restricted maximum likelihood and marginal likelihood estimation of semiparametric generalized linear models. *J. R. Stat. Soc. B* 73, 3–36.
- Yee, T. W., and Mitchell, N. D. (1991). Generalized additive models in plant ecology. *J. Veg. Sci.* 2, 587–602.
- Conflict of Interest Statement:** The authors declare that the research was conducted in the absence of any commercial or financial relationships that could be construed as a potential conflict of interest.

Received: 05 December 2011; accepted: 30 May 2012; published online: 18 June 2012.

Citation: Boyd ES, Fecteau KM, Havig JR, Shock EL and Peters JW (2012) Modeling the habitat range of phototrophs in Yellowstone National Park: toward the development of a comprehensive fitness landscape. *Front. Microbio.* 3:221. doi: 10.3389/fmicb.2012.00221

This article was submitted to *Frontiers in Microbiological Chemistry*, a specialty of *Frontiers in Microbiology*.

Copyright © 2012 Boyd, Fecteau, Havig, Shock and Peters. This is an open-access article distributed under the terms of the Creative Commons Attribution Non Commercial License, which permits non-commercial use, distribution, and reproduction in other forums, provided the original authors and source are credited.



Effect of metals on the lytic cycle of the Coccolithovirus, EhV86

Martha Gledhill^{1*}, Aurélie Devez^{1†}, Andrea Highfield², Chloe Singleton², Eric P. Achterberg¹ and Declan Schroeder^{2*}

¹ School of Ocean and Earth Science, University of Southampton, National Oceanography Centre, Southampton, UK

² Marine Biological Association of the UK, Citadel Hill, Plymouth, UK

Edited by:

Christel Hassler, University of Technology Sydney, Australia

Reviewed by:

Rachel Narehood Austin, Bates College, USA

Peter Croot, National University of Ireland – Galway, Ireland

*Correspondence:

Martha Gledhill, Ocean and Earth Science, National Oceanography Centre – Southampton, University of Southampton, Southampton, SO14 3ZH, UK.

e-mail: martha@soton.ac.uk;

Declan Schroeder, Marine Biological Association of the UK, Citadel Hill, Plymouth, PL1 2PB, UK.

e-mail: dsch@mba.ac.uk

†Present address:

Aurélie Devez, IFREMER, Centre de Brest, Department ODE/DYNECO/PELAGOS, Pointe du Diable, BP 70, 29280 Plouzané, France

In this study we show that metals, and in particular copper (Cu), can disrupt the lytic cycle in the *Emiliania huxleyi* – EhV86 host–virus system. *E. huxleyi* lysis rates were reduced at high total Cu concentrations (> approximately 500 nM) in the presence and absence of EDTA (ethylenediaminetetraacetic acid) in acute short term exposure experiments. Zinc (Zn), cadmium (Cd), and cobalt (Co) were not observed to affect the lysis rate of EhV86 in these experiments. The cellular glutathione (GSH) content increased in virus infected cells, but not as a result of metal exposure. In contrast, the cellular content of phytochelatins (PCs) increased only in response to metal exposure. The increase in glutathione content is consistent with increases in the production of reactive oxygen species (ROS) on viral lysis, while increases in PC content are likely linked to metal homeostasis and indicate that metal toxicity to the host was not affected by viral infection. We propose that Cu prevents lytic production of EhV86 by interfering with virus DNA (deoxyribonucleic acid) synthesis through a transcriptional block, which ultimately suppresses the formation of ROS.

Keywords: copper, *Emiliania huxleyi*, phytoplankton, virus, cadmium, phytochelatins, thiols, glutathione

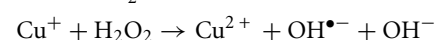
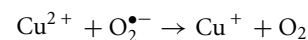
INTRODUCTION

Viruses have been shown to be the most ubiquitous biological entities detected in the ocean to date (Bergh et al., 1989; Sandaa, 2008), with over a quarter of organic carbon in the sea passing through the “viral shunt” (Wilhelm and Suttle, 1999). Viruses not only directly affect the abundance and diversity of the organisms they infect (e.g., Sorensen et al., 2009), but viral lyses results in the release of nutrients and organic carbon and thus influences the biogeochemical cycles of key elements such as carbon, nitrogen, and iron (Fe; Gobler et al., 1997; Mioni et al., 2005; Weinbauer et al., 2009). Therefore viruses are important players in global ecosystems (Suttle, 2007). The relationship between virus and host in the marine environment is thought to be complex, however the *Emiliania huxleyi* – EhV host–virus system has emerged as one of the best model systems to investigate algal host–virus interactions (Bidle and Vardi, 2011).

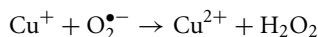
EhV86, a Coccolithovirus, is responsible for the termination of naturally occurring blooms of the coccolithophore *E. huxleyi* (Schroeder et al., 2002; Wilson et al., 2002). More recently, studies into the mechanisms of EhV86 infection have revealed an animal-like infection strategy (Mackinder et al., 2009), exploiting pathways previously thought to be restricted to higher multicellular organisms. These pathways include the synthesis of ceramide (Wilson et al., 2005; Han et al., 2006) inducing programmed cell death

(PCD) in the unicellular coccolithophore (Bidle and Falkowski, 2004; Pagarete et al., 2009; Vardi et al., 2009). Notably, viral lysis of *E. huxleyi* by EhV86 also triggers the production of reactive oxygen species (ROS; Evans et al., 2006), which in turn induces caspase activity and consequently PCD (Bidle et al., 2007).

Cellular processes in micro-organisms are also strongly influenced by the chemistry of trace metals, which in turn influence the primary production and community structure in the ocean (Sunda, 1988; Morel and Price, 2003). Copper (Cu) and cadmium (Cd) are two trace metals that can be found at elevated levels in coastal environments (e.g., Braungardt et al., 2007). Copper is an essential cofactor of enzymes involved in a variety of physiological processes including respiration, photosynthesis, oxygen transport, and antioxidant defense. Therefore, Cu is required for growth by marine phytoplankton, but is toxic at elevated concentrations (Morel et al., 1978; Brand et al., 1986; Gledhill et al., 1997). Copper predominantly occurs as Cu(II) but biological systems utilize the ability of Cu to undergo a redox cycle. It is this property that gives Cu its toxic potential. Copper catalyzes the reaction between superoxide and hydrogen peroxide, producing the highly reactive hydroxyl radical via the following cycle:



The reaction with hydrogen peroxide will compete with the faster reaction between Cu^+ and $\text{O}_2^{\bullet-}$ (Voelker et al., 2000; Heller and Croot, 2010, 2011):



so that the production of the hydroxide radical will be influenced by the ambient redox environment (which is reducing within cells; Schafer and Buettner, 2001) and the relative concentrations of Cu and superoxide.

Hydroxyl radicals can cause oxidative damage to cellular components such as deoxyribonucleic acid (DNA), proteins, and lipids. For example, Cu causes damage to DNA by binding near guanine bases, where it is reduced to Cu(I) and then reoxidized to Cu(II) by reaction with hydrogen peroxide producing hydroxyl radicals. The radicals then mediate DNA strand breakage in close proximity to the bound Cu (Sagripanti and Kraemer, 1989; Aruoma et al., 1991). The redox properties of Cu also allow the metal to bind to several types of amino acid residues and therefore Cu could be inappropriately incorporated into proteins and enzymes that normally bind other metal ions. This results in a loss of function through inactivation or changes in conformational fold. In humans for example, Cu may contribute to the development of Alzheimer's disease, along with Fe and zinc (Zn), as it has been found to induce aggregation of the β -amyloid (A β) protein and has been found in high quantities (0.44 mM) in Alzheimer plaques (Lovell et al., 1998; Curtain et al., 2001). Moreover, these high Cu levels are linked to an increase in oxidative stress which plays a central role in neurodegenerative disorders (Permyakov, 2009).

Copper has long been known to possess antimicrobial and antiviral properties, and in the last decade studies have suggested that Cu surfaces could be reintroduced into hospitals to reduce the transmission of microbes such as methicillin resistant *Staphylococcus aureus* (Noyce et al., 2006a), *Escherichia coli* O157 (Noyce et al., 2006b), and influenza A virus (Noyce et al., 2007). The mechanisms of Cu disruption of virus infection may vary depending on the virus and have yet to be fully understood (Karlstrom and Levine, 1991a,b; Sagripanti et al., 1997; Horie et al., 2008), however there is some evidence to suggest that inactivation of viruses can proceed via Cu mediated DNA damage as described above (Levinson et al., 1973; Sagripanti et al., 1997).

Cadmium (Cd) had been considered a non-essential metal, but more recently a unique biological role for Cd has been identified in marine diatoms. It has been shown that Cd can replace Zn as a metal of the Zn carbonic anhydrase (Price and Morel, 1990), and that Cd carbonic anhydrases can play a role in the acquisition of inorganic carbon for photosynthesis in the oceans (Lane et al., 2005). High levels of anthropogenic Cd in the coastal environment has also led to toxicological effects in exposed marine organisms. For example, Cd is reported to reduce reproduction rates in phytoplankton (Brand et al., 1986). The mechanism of Cd toxicity is known in animal systems where Cd complexes glutathione (GSH) and protein-bound sulfhydryl groups, resulting in enhanced production of ROS such as superoxide ion, hydroxyl radicals, and hydrogen peroxide (Stohs et al., 2001). Cadmium has been shown to inhibit the enzymatic activity of the Cu/Zn-superoxide dismutase (Cu/Zn-SOD) from rat liver (Hussain et al., 1987) and human

Cu/Zn-SOD (Huang et al., 2006). This occurs through replacement of the normally bound Zn(II) ion with a Cd(II) ion at the active site.

Elevated Cu and Cd concentrations in many marine eukaryotic phytoplankton are tolerated through the induction of phytochelatins, thiols of the general formula $(\gamma\text{-Glu-Cys})_n\text{-Gly}$, where n commonly ranges between 2 and 4 (Ahner and Morel, 1995; Ahner et al., 1995; Kawakami et al., 2006b,c; Devez et al., 2009). Phytochelatins and other thiols may also be released into the surrounding media, reducing free metal concentrations, and potentially affecting metal bioavailability (Lee et al., 1996; Leal et al., 1999; Vasconcelos and Leal, 2001; Vasconcelos et al., 2002). Phytochelatins are synthesized from GSH, which is also known to respond to oxidative stress. However, while the intracellular abundance of PCs is thought to be linked to metal concentrations in the surrounding water (e.g., Ahner and Morel, 1995; Ahner et al., 1995; Morelli and Scarano, 2001; Dupont and Ahner, 2005; Le Faucheur et al., 2005; Kawakami et al., 2006b; Pawlik-Skowronska et al., 2007; Morelli and Fantozzi, 2008; Devez et al., 2009), cellular GSH abundance, and metal concentrations are not necessarily directly related (Kawakami et al., 2006c; Scheidegger et al., 2011). Glutathione has many metabolic roles (Mendoza-Cozatl et al., 2005), however, exogenous GSH is known to affect replication of *Herpes simplex* virus type 1 (HSV-1) by interfering with the very late stages of the virus life cycle, without otherwise affecting host cellular metabolism (Palamara et al., 1995).

Metals thus have the potential to impact host-virus interactions. However, to our knowledge, the effects of metals have not yet been assessed for any marine host-virus system. The aim of this study was therefore to undertake a preliminary investigation into interactions between trace metals and the *E. huxleyi* – EhV86 system. We subsequently examined (1) the impact of elevated Cu and Cd concentrations on the EhV86 lytic cycle and (2) the cellular mechanism involved in these interactions.

MATERIALS AND METHODS

Sterile trace metal clean techniques were used for culturing. Glassware and polycarbonate bottles (Nalgene) were acid washed (1 M HCl) for at least 24 h prior to use, 4 L polycarbonate culture vessels (Nalgene) were double bagged (Nalgene autoclavable plastic bags) prior to autoclaving at 120°C for 30 min.

CULTURE CONDITIONS

Emiliania huxleyi (strain CCMP 1516) was obtained from the Provasoli-Guillard Center for Culture of Marine Phytoplankton (CCMP). Experiments reported here focused on acute short term (4 days) effects. *E. huxleyi* was batch cultured in f/2 minus Si medium prepared using 0.2 μm filtered seawater collected from the North Atlantic Gyre in the Canary Basin (between 24.1 and 29.5°N and 23.4 and 27.6°W). The culture medium ($\text{pH} = 7.8 \pm 0.1$) was allowed to equilibrate overnight and then filtered sterilized (0.2 μm , Sartorius) prior to seeding with *E. huxleyi*. Although it was possible that viruses already present in the seawater would have passed through the 0.2- μm filter, in practice we did not observe any evidence of lysis of *E. huxleyi* in our control cultures, indicating that this was not a problem in these experiments. Concentrations of the nutrients nitrate (NaNO_3) and phosphate

(NaH_2PO_4) added to the seawater were 3×10^{-4} and 1×10^{-5} M, respectively. Concentrations of trace metals added to the seawater were 10 nM Cu, 100 nM molybdenum, 4 nM Zn, 2.5 nM cobalt (Co), 23 nM manganese, 450 nM Fe, and 10 nM selenium. Media used for initial experiments with 2.5 μM added Cd, Co, Cu, and Zn were carried out in the presence of 5 μM ethylenediaminetetraacetic acid (EDTA). Experiments with different Cu concentrations were carried out in the presence and absence of 5 μM EDTA, and experiments investigating thiol production and RNA expression were carried out in the absence of EDTA. Cultures were maintained at $15 \pm 1^\circ\text{C}$ under a light/dark cycle of 12:12 h and at an illumination of $150 \mu\text{mol photons m}^{-2} \text{s}^{-1}$ in a growth cabinet (MLR-350, Sanyo).

VIRUS CULTURE MAINTENANCE

The Coccolithovirus EhV86 was propagated by using acclimated and synchronized batch cultures of *E. huxleyi* 1516 grown in f/2 medium without EDTA and Si (Schroeder et al., 2002). The occurrence of lysis was generally indicated by a change in the culture appearance, from a green to a chalky white color. The new virus stock solution was obtained from an *E. huxleyi* culture grown to a cell density of approximately 1×10^6 cells mL^{-1} at a multiplicity of infection of approximately 10. The new virus stock solution was labeled and stored in the dark at 4°C until required.

METAL AND VIRUS ADDITION

The virus and the single studied metal (Cd, Co, Cu, Zn) were added simultaneously. The addition of EhV86 virus, in excess for infection, was done to exponentially growing *E. huxleyi* host cultures approximately 4 days after subculturing. In initial experiments investigating effects of Cd, Co, Cu, and Zn, metals were added at a concentration of 2.5 μM in excess of concentrations already present in the media. A second experiment investigated a range of Cu concentrations between 125 nM and 1 μM . For the final experiment investigating the mechanism of the Cu virus interaction, Cu was added at a total concentration of 1.25 μM and Cd at 5.0 μM . Non-infected cultures with and without metal were used as a control in parallel for each virus/metal treatment.

Growth of the cultures was monitored daily by enumerating cells (Multisizer™ II coulter counter). Cell numbers were used to guide subsequent sampling frequency for PCs and viral ribonucleic acid (RNA). Cultures were sampled daily for virus counts and on alternate days for thiol content. RNA expression was sampled on days 5, 7, and 10 post infection for Cu and daily up to day 8 post infection for Cd. All analyses were carried out in duplicate. For virus counts, 1 mL was sampled and fixed using 50 μL of polyoxymethylene (paraformaldehyde, Sigma Aldrich, 1% final concentration) and subsequently stored at -80°C for later analysis by flow cytometry. For thiol analysis, 500 mL of culture solution was filtered (0.45 μm pore size nitrocellulose membrane filters, Whatman) under gentle vacuum pressure and stored at -80°C . For isolation of RNA, *E. huxleyi* cells were harvested via centrifugation and RNA was extracted from the pellets using the RNeasy Mini Kit (Qiagen) according to the manufacturer's instructions. Total RNA was DNase treated (Promega) to remove any DNA contamination and then quantified using the NanoDrop 1000 spectrophotometer (Thermo Scientific).

Cell counts from the coulter counter were used to calculate the average growth (μ) rates for *E. huxleyi* over the period of viral infection from the slope of a graph of $\ln(\text{cells})$ against time. The viral lysis rate is then calculated from

$$\mu_{+\text{virus}} = \mu - \gamma_{\text{lysis}}$$

where γ_{lysis} is the *E. huxleyi* lysis rate, μ is the growth rate of *E. huxleyi* in control cultures or treatments containing the added metal, and $\mu_{+\text{virus}}$ is the growth rate of *E. huxleyi* in infected cultures or infected cultures containing the added metal.

FLOW CYTOMETRY

Determination of the abundance of viral particles and *E. huxleyi* cells was performed simultaneously (FACSort, Becton Dickinson Biosciences). EhV86 were discriminated based on their green fluorescence and side scatter. *E. huxleyi* cells were counted based on their red and orange fluorescence signatures upon staining with SYBR Green I DNA dye (Schroeder et al., 2002; Wilson et al., 2002).

Comparison of fresh (coulter counter) and fixed (Flow Cytometry) *E. huxleyi* cell counts showed that a good agreement was observed between these two counting approaches (t test, $p > 0.05$, $n = 48$).

DETERMINATION OF PARTICULATE THIOLS

The total concentrations of glutathione (GSH) and phytochelators (PCs) in metal and virus exposed *E. huxleyi* cultures were determined according to the method reported by Kawakami et al. (2006a). Intracellular thiol measurements were performed in duplicate by reverse-phase high performance liquid chromatography (HPLC) with fluorescence detection.

Thiols were extracted on ice (5 min), following addition of 1.2 mL solution of 0.1 M HCl containing 5 mM diethylenetriamine pentaacetic acid (DTPA, Fluka Biochemica) to a 2-mL microcentrifuge tube (Fisher) containing the filter with *E. huxleyi* biomass. The extract was centrifuged (13000 g/20 min at 4°C) and syringe filtered (0.2 μm pore size cellulose membrane, Minisart RC4, Sartorius) prior to reduction (25 μL of a 20-mM 2-carboxyethylphosphine hydrochloride, 5 min, TCEP, Sigma). Further oxidation was minimized (5 mM DTPA) and the extract was buffered at pH 8.2 (200 mM N-2-hydroxyethylpiperazine-N'-2-ethanesulphonic acid, HEPES). After a further 5 min, 10 μL of a 100-mM of a sulfur-specific fluorescent tag monobromobimane was added (MBrB in acetonitrile, Fisher) followed by 465 μL of the HEPES/DTPA pH 8.2 solution. The derivatization procedure was carried out in a dark room under dim red light conditions. After 15 min, the reaction was stabilized and the derivatization of thiols by MBrB, stopped by addition of 100 μL of 1 M methanesulfonic acid (99%, Sigma). Vials were stored in the dark at 4°C until HPLC analysis.

Thiols were analyzed by reverse-phase HPLC with fluorescence detection (Kawakami et al., 2006a). The HPLC comprised a system controller (Shimadzu SCL-10A) and two pumps (Shimadzu LC-10ADvp), an autosampler (Shimadzu SIL-10ADVP) and a fluorescence detector (Shimadzu RF-10A XL) operating at 380 nm (excitation) and 470 nm (emission) wavelengths. Separation of the thiols was carried out using a 150 mm \times 2.1 mm C-18 HPLC column (Ascentis, Supelco) with a 3- μm particle size and a gradient program of 0–5 min, 10% B; 5–18 min, 10–22% B; 18–40 min,

22–35% B; 40–50 min, 35–100%; 50–55 min, isocratic 100% B; 55–58 min, 100–10% B; 58–60 min 10% B, where A was 0.1% trifluoroacetic acid (TFA, Fluka) and B was acetonitrile. The flow rate was 0.2 mL min⁻¹.

Phytochelatin concentrations were standardized with GSH (reduced form, purity 99%, Sigma) assuming that the fluorescence response was directly proportional to the number of thiol groups (Kawakami et al., 2006a). We used PCs directly produced by *Phaeodactylum tricornutum* under metal stress for identification of retention times for PC₂, PC₃, and PC₄. GSH eluted at 11.4 min and PC₂, 3, and 4 at 18.8, 21.7, and 24.2 min, respectively. Cellular GSH and PC concentrations were normalized to the number of cells and are thus expressed in amol SH cell⁻¹. The limit of detection, calculated from three times SD of a 5-pmol GSH standard, was 0.1 pmol with a 100-μL injection volume. Analytical variability within standards and samples was less than 10%. The recovery of GSH added to samples prior to derivatization was determined to be 86 ± 29% (*n* = 11).

ONE-STEP REVERSE TRANSCRIPTION-PCR

RT-PCR detection of virus-related gene expression was undertaken using primers designed to amplify four viral genes, DNA polymerase (DNA pol), Helicase, proliferating cell nuclear antigen (PCNA) protein, and major capsid protein (MCP; **Table 1**). One-step RT-PCR was used to amplify 10 ng RNA in 25 μL reactions containing 1 × One-step sensimix QPCR mix (with SYBR green), 7.5 pmol forward primer, 7.5 pmol reverse primer, and 5 units RNase inhibitor. Reactions were carried out in a Rotor-gene 6000 QPCR machine (Corbett Research) using the following conditions: reverse transcription at 49°C for 10 min, polymerase activation at 95°C for 10 min, followed by 40 cycles of 95°C for 15 s, 54°C for 15 s (60°C for MCP), and 72°C for 15 s. Fluorescence was acquired at the end of each extension step on the green channel. RT-PCR reactions were subjected to melt curve analysis to ensure a single product had been generated by gradual melting from 72 to 95°C and fluorescence acquisition at each 1°C increment. RT-PCR products were verified by gel electrophoresis on a 2% (w/v) agarose gel in 1 × TAE buffer and viewed on a UV transilluminator (Syngene).

STATISTICAL ANALYSIS

As analysis was only performed in duplicate, estimates of errors in growth, and lysis rates were calculated from the square root of the sum of squares of the SEs of the slopes of ln(cells) against

time. The lack of experimental replication meant that the statistical significance of our results could not be tested and comparisons between treatments are thus qualitative.

RESULTS

E. HUXLEYI – EhV86 INFECTION DYNAMICS IN THE PRESENCE OF VARIOUS METAL IONS

Preliminary experiments, carried out with a range of metals (Cu, Zn, Co, and Cd) on the *E. huxleyi* – EhV86 host–virus system indicated that viral lysis of *E. huxleyi* cells was disrupted in the presence of Cu, but was similar to controls for the metals Cd, Co, and Zn (**Figure 1A**). In this study we have interpreted our data qualitatively as lack of sufficient replicates in our experimental design precludes more quantitative estimates of the statistical significance of our results. However, Cu was consistently observed to disrupt viral lysis of *E. huxleyi* in all the experiments undertaken as part of this study. Furthermore varying the concentration of Cu in the absence and presence of EDTA indicated that viral lysis rates decreased with increasing Cu concentration and were lowest in the absence of EDTA (**Figure 1D**). Copper is known to be toxic to marine algae at high concentrations (e.g., Sunda and Guillard, 1976; Brand et al., 1986; Gledhill et al., 1997; Levy et al., 2007, 2008; Debelius et al., 2009), and indeed the growth rate of *E. huxleyi* was reduced at the highest Cu concentration when compared to control cultures (**Figures 1A,C**). However the cumulative effect of metal plus virus on host growth was only observed in Cu treatments and thus appeared to be a specific effect of Cu. Further short term exposure experiments aimed at understanding the interaction between Cu and the *E. huxleyi* virus–host system focused on Cd and Cu as these two metals are both known to be toxic and they exhibited contrasting behaviors in our preliminary experiments. Furthermore EDTA was omitted in order to maximize the effect of trace metals on both host and virus.

PRODUCTION OF GLUTATHIONE AND PHYTOCHELATINS BY *E. HUXLEYI*

The intracellular content of GSH and PCs in infected and non-infected *E. huxleyi* cells were determined in order to investigate oxidative stress and trace metal homeostasis during the course of the experiments. Post virus and metal addition growth curves for *E. huxleyi* in the thiol expression experiments are presented in **Figure 2**. Initial cell numbers were different for each experiment when virus and metals were added ($4.0 \pm 0.6 \times 10^5$ cells mL⁻¹ for the Cu experiment and $1.4 \pm 0.2 \times 10^5$ cells mL⁻¹ for the Cd experiment), however, calculated growth rates were similar for

Table 1 | Primers used in this study.

Primer name	Target (CDS)	Sequence (5'–3')	Amplicon size (bp)	Reference
EhVpol_F	DNA polymerase (ehv030)	TATAATGCACGCCAACTTGC	98	This study
EhVpol_R		GCAATTGCACCAAGTGATA		
EhVpcna_F	PCNA (ehv440)	GGGCATTTCATTGCCATAC	157	This study
EhVpcna_R		ATTCTCCGTCGACAATACGC		
EhVhel_F	Helicase (ehv104)	GCCAACTGGTACAGGGAAAA	184	This study
EhVhel_R		CATCCATGCATGTGTGACAA		
MCP_F2	MCP (ehv085)	GACCTTTAGGCCAGGGAG	134	Schroeder et al. (2002)
MCP_R2		GTTCGCGCTCGAGTCGAT		

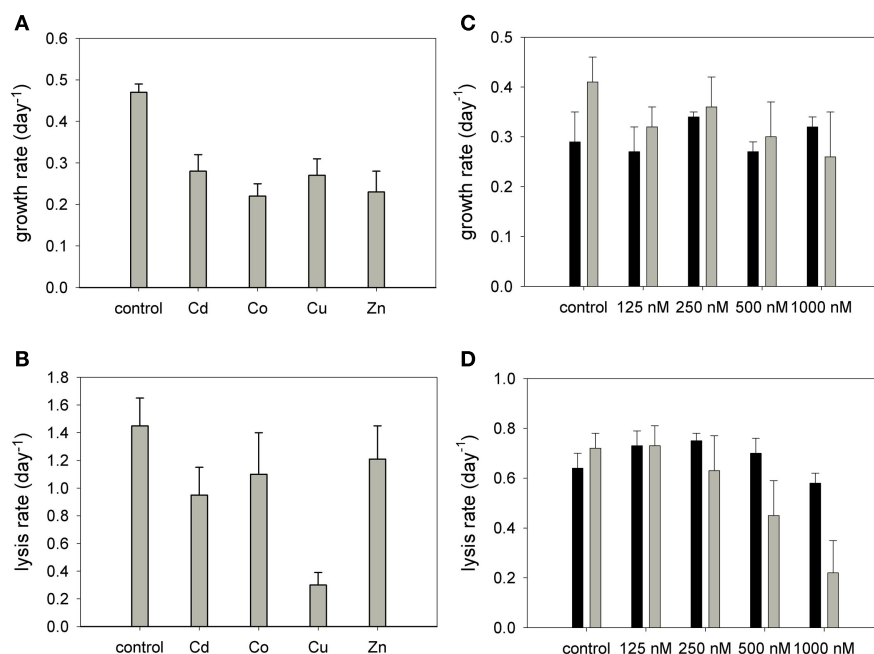


FIGURE 1 | Growth rates (A,C) and viral lysis rates (B,D) for the EhV86 Coccolithovirus in the presence of (A,B) Cd, Co, Cu, and Zn and (C,D) at Cu concentrations between 125 and 1000 nM in the presence (black bars) and absence (gray bars) of 5 μ M EDTA.

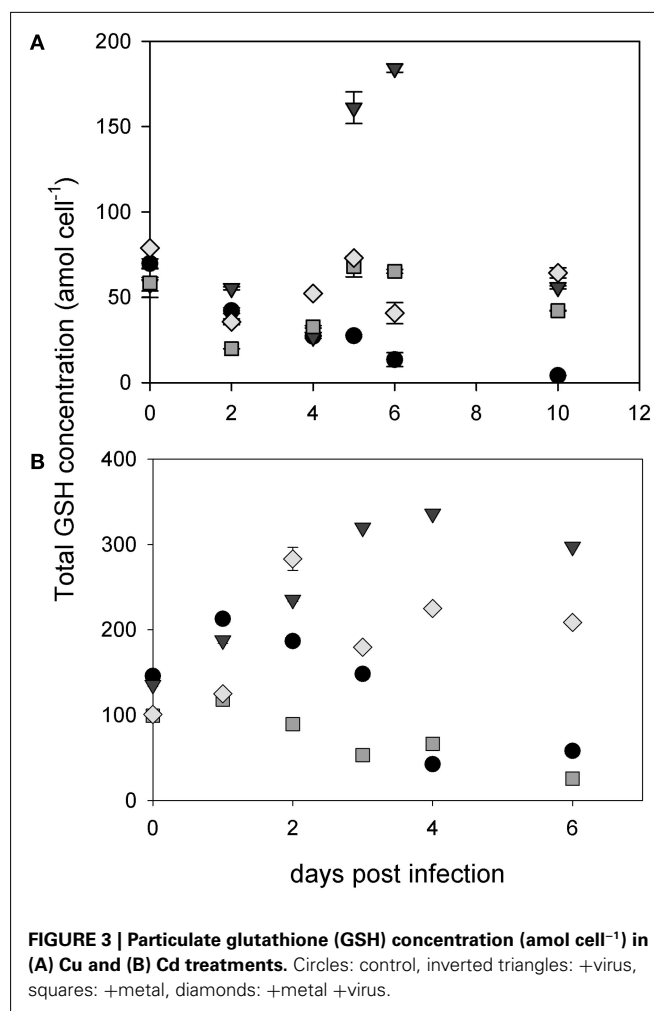
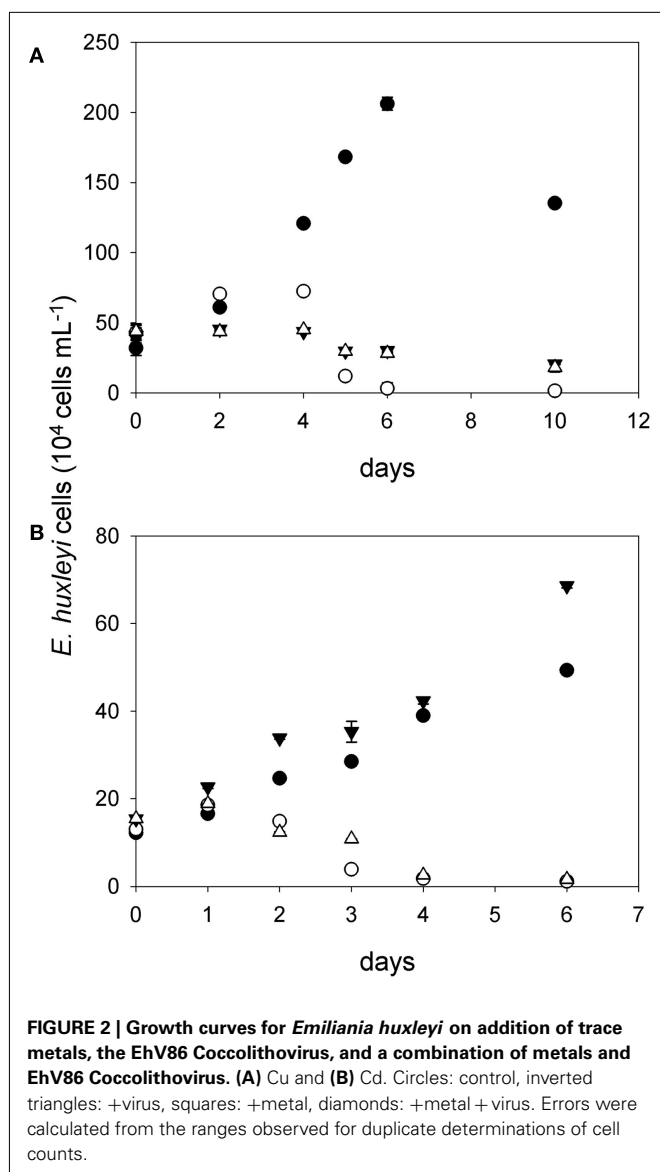
Errors were calculated from the square root of the sum of squares of the errors in the slopes obtained from linear regression of $\ln(\text{cells})$ against time for the period over which lysis occurred in the +virus treatment.

the controls in each experiment for the post infection period and reflected results observed in preliminary experiments (Figure 1). Cellular GSH concentrations (Figure 3) were $66 \pm 10 \text{ amol cell}^{-1}$ on day 0 for the Cu experiment and $120 \pm 20 \text{ amol cell}^{-1}$ for the Cd experiment and are similar to those reported previously for *E. huxleyi* and marine phytoplankton (Ahner et al., 1995; Kawakami et al., 2006c). Cellular GSH content increased in the infected treatments (Figure 3). For the Cu experiment, GSH remained similar in both Cu and +Cu + Virus treatments, while in the Cd experiment, cellular GSH levels in the Cd treatment were similar to the control, while levels increased in the +Cd + Virus treatment (Figure 3). A previous study on infected *E. huxleyi* cells indicated an increased intracellular occurrence of ROS and oxidative stress (Evans et al., 2006). The increase in GSH in virus infected cells in this study is consistent with a response to increased oxidative stress on viral infection. Glutathione content in the +Cd + Virus treatment increased to an average of $216 \pm 11 \text{ amol cell}^{-1}$ between days 4 and 6 after infection and was closer to that of the virus treatment ($316 \pm 27 \text{ amol cell}^{-1}$) than the Cd treatment ($46 \pm 29 \text{ amol cell}^{-1}$) and control ($50 \pm 11 \text{ amol cell}^{-1}$). In contrast the cellular GSH content of the +Cu + Virus treatment was $55 \pm 16 \text{ amol cell}^{-1}$, similar to that of the Cu treatment ($55 \pm 19 \text{ amol cell}^{-1}$), but less than GSH in the virus treatment ($124 \pm 85 \text{ amol cell}^{-1}$), although there was a marked increase in GSH variability in this treatment and the difference between the virus treatment and the control was not as marked as for the Cd experiment (Figure 3). These results indicate that the ROS event associated with viral infection is reduced by Cu.

Phytochelatin concentrations increased after addition of both Cu and Cd (Figure 4). Virus treatments showed only a slight increase in PC concentrations, although the small *E. huxleyi* bio-volume in these treatments resulted in very low absolute PC concentrations and the calculated errors are likely underestimated. Cellular phytochelatin concentrations were higher in the Cd and +Cd + Virus treatments than in the Cu or +Cu + Virus treatments. Thus in contrast to the cellular GSH content, PC concentrations were observed to vary with metal treatment and not with infection of *E. huxleyi* by EhV86.

EXPRESSION OF VIRUS-RELATED RNA

In order to confirm the presence of EhV86 within Cu and Cd exposed *E. huxleyi* cells and to determine whether EhV86 was transcriptionally active when exposed to elevated levels of Cu and Cd, RT-PCR on four EhV86 encoded genes – DNA dependent DNA pol – ehv030, PCNA protein – ehv440, Helicase – ehv104 and MCP – ehv085 – was carried out in duplicate before and after treatment (Tables 2 and 3). Particulate material from Cu and Cd experiments in the absence of virus were also analyzed and viral RNA was not detected in any treatment not infected with the virus (Tables 2 and 3). Genomic studies have previously revealed that all four genes are required for successful infection (Wilson et al., 2005; Allen et al., 2006). DNA pol and helicase are required for DNA synthesis and therefore virus replication. The MCP is required for virion assembly and PCNA is known to be involved in several metabolic pathways, including Okazaki fragment processing, DNA repair, translesion DNA synthesis, DNA methylation, chromatin remodeling, and cell cycle regulation. PCNA in mammalian cells



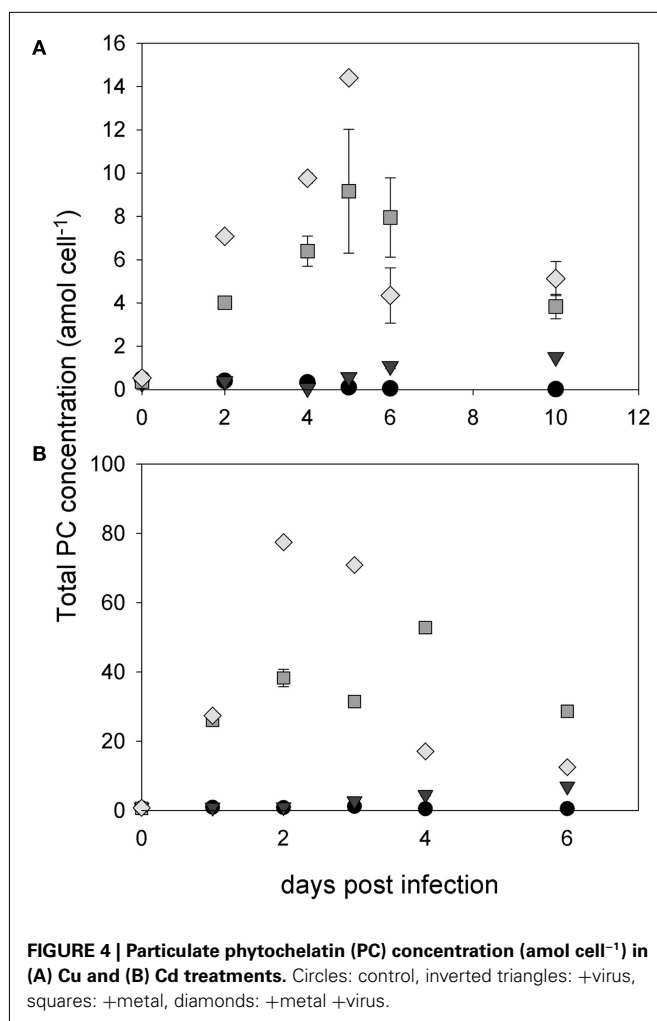
appears to play a key role in controlling several reactions through the coordination and organization of different partner proteins (Maga and Hubscher, 2003). DNA pol, helicase, and PCNA genes have been found to be expressed at around 2 h post infection, while MCP was only first detected 4 h post infection (Allen et al., 2006). We found that Cd had no observable effect on the transcription of all four genes (Table 3), consistent with observations of virus synthesis and culture lysis (Figures 3 and 4). However, in the presence of Cu, only PCNA, and MCP genes were expressed. These results show that Cu did not therefore prevent virus entry into *E. huxleyi* cells. However, viral replication within *E. huxleyi* appears to have been reduced by Cu via an unknown mechanism of transcriptional control.

DISCUSSION

Our experiments indicated that metals have a direct effect on virus production and consequently infection success in the *E.*

huxleyi – EhV86 system. Furthermore it appears that the effect is stronger for Cu than for Cd, Zn, and Co so that Cu caused a reduction in lytic infection in short term exposure experiments at high concentrations of total Cu (> approximately 500 nM). Although these concentrations are higher than commonly observed in the marine environment, such high concentrations have been recorded in contaminated estuarine systems (Braungardt et al., 2007). Furthermore, these experiments represented an acute exposure to high concentrations of metal. Further investigations are thus required in order to assess effects of long-term metal exposure.

The mechanism of the interaction between Cu and the *E. huxleyi* – EhV86 system is currently unknown. Our observations are summarized in Figure 5. Our data show that EhV86 did not have an impact on the production of PCs in *E. huxleyi* and thus was unlikely to have affected the toxicity of Cu to the host. The primary effect of Cu on the lytic cycle of EhV86 thus appears to result from greater sensitivity of the virus to Cu toxicity relative to the host. Viruses require metals for the functioning of their DNA and RNA replication enzymes, so it has been previously suggested that viral inactivation by Cu involves cleavage or damage of viral DNA or RNA (Sagripanti et al., 1997). Recent studies have linked

**Table 2 | RT-PCR results for Cu exposure experiments.**

	EhV86 genes			
	DNA pol	Helicase	PCNA	MCP
Control day 5	—	—	—	—
Control day 7	—	—	—	—
Cu day 5	—	—	—	—
Cu day 7	—	—	—	—
EhV86 day 7 (v2*)	+	+	+	+
EhV86 day 10 (v5*)	+	+	+	+
Cu + EhV86 day 5 (v0*)	—	—	—	—
Cu + EhV86 day 7 (v2*)	—	—	+	+
NTC [^]	—	—	—	—

*Days post EhV86 addition; [^]no template control.

Cu exposure to a complete decline in virus particles confirming antiviral properties of Cu-based agents and surfaces against major opportunistic pathogens (Noyce et al., 2006a,b, 2007; Huang et al., 2008; Weaver et al., 2008). However, in our study, virus particles were not observed to decline completely in the presence of Cu,

Table 3 | RT-PCR results for Cd exposure experiments.

	EhV86 genes			
	DNA pol	Helicase	PCNA	MCP
EhV86 day 4 (v0*)	—	—	—	—
EhV86 day 5 (v1*)	+	+	+	+
EhV86 day 6 (v2*)	+	+	+	+
EhV86 day 7 (v3*)	+	+	+	+
EhV86 day 8 (v4*)	+	+	+	+
Cd day 4	—	—	—	—
Cd day 5	—	—	—	—
Cd day 6	—	—	—	—
Cd day 7	—	—	—	—
Cd day 8	—	—	—	—
Cd + EhV86 day 4 (v0*)	—	—	—	—
Cd + EhV86 day 5 (v1*)	+	+	+	+
Cd + EhV86 day 6 (v2*)	+	+	+	+
Cd + EhV86 day 7 (v3*)	+	+	+	+
Cd + EhV86 day 8 (v4*)	+	+	+	+
NTC [^]	—	—	—	—

*Days post EhV86 addition; [^]no template control.

and furthermore, RNA transcripts for both PCNA and MCP were detected. The lack of DNA pol and helicase transcripts indicates that a specific mechanism of Cu inhibition was at play. DNA pol and helicase are both associated with DNA synthesis and replication, hence it appears that Cu disrupted virus replication within the host cell, although further work is needed to identify whether this is a result of exposure of the virus to elevated free Cu within the host cell or in the media prior to entry into the host. However since neither MCP or PCNA are affected, we hypothesize that virion assembly, DNA repair, and other cellular functions associated with PCNA were not regulated at the transcriptional level by Cu. Thus, despite being involved in DNA replication and repair, viral PCNA was not regulated in the same way as dedicated DNA replicative enzymes, DNA pol, and helicase. It is interesting to note that both DNA pol and helicase encode for magnesium containing proteins, while PCNA and MCP do not, although whether this factor might influence the inhibition of transcription of the associated RNA is unclear. Intracellular free Cu concentrations in eukaryotes and prokaryotes are generally thought to be tightly controlled, with Cu being buffered within the cell by thiols and chaperoned into Cu containing enzymes (Robinson and Winge, 2010; Rae et al., 1999). The intravirion behavior of metals however is less well known, but our studies indicate that EhV86 may be less able to regulate Cu. Previous studies on the effects of Cu on the transcriptional control of genes have indicated regulation of Cu is achieved by modulating the transcription of genes encoding proteins directly involved in Cu binding. Transcription of the *Ctr1/3* and *Fre1* genes are regulated by the DNA-binding protein Mac1 (Yamaguchi-Iwai et al., 1997). During Cu starvation, Mac1 binds to DNA initiating transcription. However, in Cu replete conditions, Jensen and Winge (1998) demonstrated that Cu ions bind to the protein, initiating a conformational change which inhibits transcription. Transcriptional regulation of these Cu uptake genes

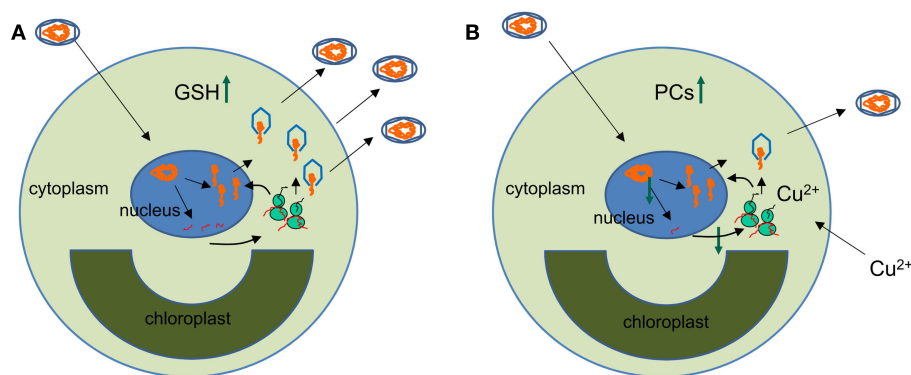


FIGURE 5 | Schematic of the interactive effect of Cu on the infection cycle of EhV86. (A) Simplified schematic of the normal infection cycle of EhV86 (after Mackinder et al., 2009). The virion particle (blue hexagon) enters the cell and targets the nucleus where it releases the viral genome. Viral genes are transcribed (red) first by host RNA polymerase in the nucleus and then by viral RNA polymerase in the cytoplasm. Virus DNA replication (orange) also takes place in the nucleus, while the capsid is assembled in the cytoplasm and released via a budding mechanism.

Cellular glutathione (GSH) increases (green arrow) as a result of reactive oxygen species generation, which occurs during capsid assembly. **(B)** Copper down-regulates (green arrow) the infection cycle prior to capsid assembly via transcriptional control of specific viral RNA. Cellular phytochelatin concentrations (PCs) increase in response to elevated copper concentrations, but GSH concentrations are similar to those in uninfected cells as capsid assembly is highly reduced. The ultimate result is a reduction in virus production.

has therefore been linked directly to cellular Cu concentrations (Graden and Winge, 1997).

The second observed effect of Cu in our study was on particulate GSH concentrations, which were similar to controls in infected *E. huxleyi* cells in the presence of Cu, but increased in *E. huxleyi* cells undergoing lysis, even when the concentrations of phytochelatin were higher (Figure 3). These results indicate that GSH, known to mitigate against ROS, is produced by the host when the virus replicates probably as a result of the viral induction of the hosts ceramide and apoptosis pathways (Schwarz, 1996; Stohs et al., 2001; Wilson et al., 2005; Bidle et al., 2007; Vardi et al., 2009). Moreover, GSH can also directly interfere with virus replication, mainly at the late stages of virion assembly (Palamara et al., 1995). Therefore, in our Cu exposed virus treatments, GSH production decreased when compared to virus treatments because the virus was unable to complete its replication and infection cycle and GSH was thus not induced to the same extent in the host.

To the authors knowledge, this is the first report of an interaction occurring between metals, virus, and host in a marine system. We have identified a specific interaction between Cu, *E. huxleyi* and its virus EhV86, however, further work is necessary

in order to understand the mechanism involved in this interaction. Concentrations of Cu required to initiate the inhibitory effect on virus replication and virion synthesis were found to be comparable to those observed in highly Cu contaminated estuaries (Braungardt et al., 2007). However the study focused on short term acute exposure to Cu. It is currently unknown if any effects would be observed on long-term exposure to lower concentrations. However, the increased use of Cu-based antifouling paints in marine systems (Schiff et al., 2004; Singh and Turner, 2009a,b) and the importance of phytoplankton communities in underpinning global climate control (Richardson and Schoeman, 2004; Bouvy et al., 2011) highlights the need to understand such mechanisms. The immediate medical benefit that can be had by fully characterizing the Cu inhibitory effort on the *E. huxleyi* – EhV86 model system for developing antiviral drugs and protocols against animal virus infections should also be considered.

ACKNOWLEDGMENTS

Gledhill was supported by UK – NERC Advanced Fellowship (NE/E013546/1) and Devez was supported by a Marie Curie Intra-European Fellowship (FP6-023215-QWSTRESS).

REFERENCES

- Ahner, B. A., Kong, S., and Morel, F. M. M. (1995). Phytochelatin production in marine algae. 1. An interspecies comparison. *Limnol. Oceanogr.* 40, 649–657.
- Ahner, B. A., and Morel, F. M. M. (1995). Phytochelatin production in marine algae 2. Induction by various metals. *Limnol. Oceanogr.* 40, 658–665.
- Allen, M. J., Forster, T., Schroeder, D. C., Hall, M., Roy, D., Ghazal, P., and Wilson, W. H. (2006). Locus-specific gene expression pattern suggests a unique propagation strategy for a giant algal virus. *J. Virol.* 80, 7699–7705.
- Aruoma, O. I., Halliwell, B., Gajewski, E., and Dizdaroglu, M. (1991). Copper ion dependent damage to the bases in DNA in the presence of hydrogen peroxide. *Biochem. J.* 273, 601–604.
- Bergh, O., Borsheim, K. Y., Bratbak, G., and Heldal, M. (1989). High abundance of viruses found in aquatic environments. *Nature* 340, 467–468.
- Bidle, K. D., and Falkowski, P. G. (2004). Cell death in planktonic, photo-synthetic microorganisms. *Nat. Rev. Microbiol.* 2, 643–655.
- Bidle, K. D., Haramaty, L., Barcelos, E., Ramos, J., and Falkowski, P. (2007). Viral activation and recruitment of metacaspases in the unicellular coccolithophore, *Emiliania huxleyi*. *Proc. Natl. Acad. Sci. U.S.A.* 104, 6049–6054.
- Bidle, K. D., and Vardi, A. (2011). A chemical arms race at sea mediates algal host-virus interactions. *Curr. Opin. Microbiol.* 14, 449–457.
- Bouvy, M., Bettarel, Y., Bouvier, C., Domaizon, I., Jacquet, S., Le Floch, E., Montanie, H., Mostajir, B., Sime-Ngando, T., Torretton, J. P., Vidussi, E., and Bouvier, T. (2011). Trophic interactions between viruses, bacteria and nanoflagellates under various nutrient conditions and simulated climate change. *Environ. Microbiol.* 13, 1842–1857.
- Brand, L. E., Sunda, W. G., and Guillard, R. L. L. (1986). Reduction of marine phytoplankton reproduction rates by copper and cadmium. *J. Exp. Mar. Biol. Ecol.* 96, 225–250.

- Braungardt, C. B., Achterberg, E. P., Gledhill, M., Nimmo, M., Elbaz-Poulichet, F., Cruzado, A., and Velasquez, Z. (2007). Chemical speciation of dissolved Cu, Ni, and Co in a contaminated estuary in southwest Spain and its influence on plankton communities. *Environ. Sci. Technol.* 41, 4214–4220.
- Curtain, C. C., Ali, F., Volitakis, I., Cherny, R. A., Norton, R. S., Beyreuther, K., Barrow, C. J., Masters, C. L., Bush, A. I., and Barnham, K. J. (2001). Alzheimer's disease amyloid-beta binds copper and zinc to generate an allosterically ordered membrane-penetrating structure containing superoxide dismutase-like subunits. *J. Biol. Chem.* 276, 20466–20473.
- Debelius, B., Forja, J. M., Delvalls, A., and Lubian, L. M. (2009). Toxicity and bioaccumulation of copper and lead in five marine microalgae. *Ecotoxicol. Environ. Saf.* 72, 1503–1513.
- Devez, A., Achterberg, E. P., and Gledhill, M. (2009). "Metal ion-binding properties of phytochelatin and related ligands," in *Metal Ions in Life Sciences*, eds A. Sigel, H. Sigel, and K. O. Sigel (Cambridge: Royal Society of Chemistry), 441–481.
- Dupont, C. L., and Ahner, B. A. (2005). Effects of copper, cadmium, and zinc on the production and exudation of thiols by *Emiliania huxleyi*. *Limnol. Oceanogr.* 50, 508–515.
- Evans, C., Malin, G., Mills, G. P., and Wilson, W. H. (2006). Viral infection of *Emiliania huxleyi* (Prymnesiophyceae) leads to elevated production of reactive oxygen species. *J. Phycol.* 42, 1040–1047.
- Gledhill, M., Nimmo, M., Hill, S. J., and Brown, M. T. (1997). The toxicity of copper(II) species to marine algae, with particular reference to macroalgae. *J. Phycol.* 33, 2–11.
- Gobler, C. J., Hutchins, D. A., Fisher, N. S., Cosper, E. M., and Sanudo-Wilhelmy, S. (1997). Release and bioavailability of C, N, P, Se and Fe following viral lysis of a marine chrysophyte. *Limnol. Oceanogr.* 42, 1492–1504.
- Graden, J. A., and Winge, D. R. (1997). Copper-mediated repression of the activation domain in the yeast Mac1p transcription factor. *Proc. Natl. Acad. Sci. U.S.A.* 94, 5550–5555.
- Han, G., Gable, K., Yan, L., Allen, M. J., Wilson, W. H., Moitra, P., Harmon, J. M., and Dunn, T. M. (2006). Expression of a novel marine viral single-chain serine palmitoyltransferase and construction of yeast and mammalian single-chain chimera. *J. Biol. Chem.* 281, 39935–39942.
- Heller, M. I., and Croot, P. L. (2010). Superoxide decay kinetics in the Southern Ocean. *Environ. Sci. Technol.* 44, 191–196.
- Heller, M. I., and Croot, P. L. (2011). Superoxide decay as a probe for speciation changes during dust dissolution in Tropical Atlantic surface waters near Cape Verde. *Mar. Chem.* 126, 37–55.
- Horie, M., Ogawa, H., Yoshida, Y., Yamada, K., Hara, A., Ozawa, K., Matsuda, S., Mizota, C., Tani, M., Yamamoto, Y., Yamada, M., Nakamura, K., and Imai, K. (2008). Inactivation and morphological changes of avian influenza virus by copper ions. *Arch. Virol.* 153, 1467–1472.
- Huang, H.-I., Shih, H.-Y., Lee, C.-M., Yang, T. C., Lay, J.-J., and Lin, Y. E. (2008). *In vitro* efficacy of copper and silver ions in eradicating *Pseudomonas aeruginosa*, *Stenotrophomonas maltophilia* and *Acinetobacter baumannii*: implications for on-site disinfection for hospital infection control. *Water Res.* 42, 73–80.
- Huang, Y. H., Shih, C. M., Huang, C. J., Lin, C. M., Chou, C. M., Tsai, M. L., Liu, T. P., Chiu, J. F., and Chen, C. T. (2006). Effects of cadmium on structure and enzymatic activity of Cu, Zn-SOD and oxidative status in neural cells. *J. Cell. Biochem.* 98, 577–589.
- Hussain, T., Shukla, G. S., and Chandra, S. V. (1987). Effects of cadmium on superoxide-dismutase and lipid peroxidation in liver and kidney of growing rats – *in vivo* and *in vitro* studies. *Pharmacol. Toxicol.* 60, 355–358.
- Jensen, L. T., and Winge, D. R. (1998). Identification of a copper-induced intramolecular interaction in the transcription factor Mac1 from *Saccharomyces cerevisiae*. *EMBO J.* 17, 5400–5408.
- Karlstrom, A. R., and Levine, R. L. (1991a). Copper inhibits the HIV-1 protease by both oxygen-dependent and oxygen independent mechanisms. *FASEB J.* 5, A452–A452.
- Karlstrom, A. R., and Levine, R. L. (1991b). Copper inhibits the protease from human immunodeficiency virus-1 by both cysteine-dependent and cysteine independent mechanisms. *Proc. Natl. Acad. Sci. U.S.A.* 88, 5552–5556.
- Kawakami, S. K., Gledhill, M., and Achterberg, E. P. (2006a). Determination of phytochelatin and glutathione in phytoplankton from natural waters using HPLC with fluorescence detection. *Trends Anal. Chem.* 25, 133–142.
- Kawakami, S. K., Gledhill, M., and Achterberg, E. P. (2006b). Effects of metal combinations on the production of phytochelatin and glutathione by the marine diatom *Phaeodactylum tricornutum*. *Bio-metals* 19, 51–60.
- Kawakami, S. K., Gledhill, M., and Achterberg, E. P. (2006c). Production of phytochelatin and glutathione by marine phytoplankton in response to metal stress. *J. Phycol.* 42, 975–989.
- Lane, T. W., Saito, M. A., George, G. N., Pickering, I. J., Prince, R. C., and Morel, F. M. M. (2005). A cadmium enzyme from a marine diatom. *Nature* 435, 42–42.
- Le Faucheur, S. V., Behra, R., and Sigg, L. (2005). Thiol and metal contents in periphyton exposed to elevated copper and zinc concentrations: a field and microcosm study. *Environ. Sci. Technol.* 39, 8099–8107.
- Leal, M. F. C., Vasconcelos, M. T. S. D., and van den Berg, C. M. G. (1999). Copper-induced release of complexing ligands similar to thiols by *Emiliania huxleyi* in seawater cultures. *Limnol. Oceanogr.* 44, 1750–1762.
- Lee, J., Ahner, B. A., and Morel, F. M. M. (1996). Export of cadmium and phytochelatin by the marine diatom *Thalassiosira weissflogii*. *Environ. Sci. Technol.* 30, 1814–1821.
- Levinson, W., Faras, A., Woodson, B., Jackson, J., and Bishop, J. M. (1973). Inhibition of RNA-dependent DNA polymerase of *Rous sarcoma* virus by thiosemicarbazones and several cations. *Proc. Natl. Acad. Sci. U.S.A.* 70, 164–168.
- Levy, J. L., Angel, B. M., Stauber, J. L., Poon, W. L., Simpson, S. L., Cheng, S. H., and Jolley, D. F. (2008). Uptake and internalisation of copper by three marine microalgae: comparison of copper-sensitive and copper-tolerant species. *Aquat. Toxicol.* 89, 82–93.
- Levy, J. L., Stauber, J. L., and Jolley, D. F. (2007). Sensitivity of marine microalgae to copper: the effect of biotic factors on copper adsorption and toxicity. *Sci. Total Environ.* 387, 141–154.
- Lovell, M. A., Robertson, J. D., Teesdale, W. J., Campbell, J. L., and Markesbery, W. R. (1998). Copper, iron and zinc in Alzheimer's disease senile plaques. *J. Neurol. Sci.* 158, 47–52.
- Mackinder, L. C. M., Worthy, C. A., Biggi, G., Hall, M., Ryan, K. P., Varsani, A., Harper, G. M., Wilson, W. H., Brownlee, C., and Schroeder, D. C. (2009). A unicellular algal virus, *Emiliania huxleyi* virus 86, exploits an animal-like infection strategy. *J. Gen. Virol.* 90, 2306–2316.
- Maga, G., and Hubscher, U. (2003). Proliferating cell nuclear antigen (PCNA): a dancer with many partners. *J. Cell. Sci.* 116, 3051–3060.
- Mendoza-Cozatl, D., Loza-Tavera, H., Hernandez-Navarro, A., and Moreno-Sanchez, R. (2005). Sulfur assimilation and glutathione metabolism under cadmium stress in yeast, protists and plants. *FEMS Microbiol. Rev.* 29, 653–671.
- Mioni, C., Poorvin, L., and Wilhelm, S. W. (2005). Virus and siderophore-mediated transfer of available Fe between heterotrophic bacteria: characterisation using an iron specific reporter. *Aquat. Microb. Ecol.* 41, 233–245.
- Morel, F. M. M., and Price, N. M. (2003). The biogeochemical cycles of trace metals in the oceans. *Science* 300, 944–947.
- Morel, N. M. L., Rueter, J. G., and Morel, F. M. M. (1978). Copper toxicity to *Skeletonema costatum* (Bacillariophyceae). *J. Phycol.* 14, 43–48.
- Morelli, E., and Fantozzi, L. (2008). Phytochelatin in the diatom *Phaeodactylum tricornutum* Bohlin: an evaluation of their use as biomarkers of metal exposure in marine waters. *Bull. Environ. Contam. Toxicol.* 81, 236–241.
- Morelli, E., and Scarano, G. (2001). Synthesis and stability of phytochelatin induced by cadmium and lead in the marine diatom *Phaeodactylum tricornutum*. *Mar. Environ. Res.* 52, 383–395.
- Noyce, J. O., Michels, H., and Keevil, C. W. (2006a). Potential use of copper surfaces to reduce survival of epidemic methicillin-resistant *Staphylococcus aureus* in the healthcare environment. *J. Hosp. Infect.* 63, 289–297.
- Noyce, J. O., Michels, H., and Keevil, C. W. (2006b). Use of copper cast alloys to control *Escherichia coli* O157 cross-contamination during food processing. *Appl. Environ. Microbiol.* 72, 4239–4244.
- Noyce, J. O., Michels, H., and Keevil, C. W. (2007). Inactivation of influenza A virus on copper versus stainless steel surfaces. *Appl. Environ. Microbiol.* 73, 2748–2750.
- Pagarete, A., Allen, M. J., Wilson, W. H., Kimmance, S. A., and De Vargas, C. (2009). Host-virus shift of the sphingolipid pathway along an *Emiliania huxleyi* bloom: survival of the fittest. *Environ. Microbiol.* 11, 2840–2848.

- Palamara, A. T., Perno, C. F., Ciriolo, M. R., Dini, L., Balestra, E., Dagostini, C., Difrancesco, P., Favalli, C., Rotilio, G., and Garaci, E. (1995). Evidence for antiviral activity of glutathione – *in vitro* inhibition of *Herpes simplex* virus type-1 replication. *Antiviral Res.* 27, 237–253.
- Pawlik-Skowronska, B., Pirszel, J., and Brown, M. T. (2007). Concentrations of phytochelatin and glutathione found in natural assemblages of seaweeds depend on species and metal concentrations of the habitat. *Aquat. Toxicol.* 83, 190–199.
- Permyakov, E. (2009). *Metalloproteomics*. Hoboken, NJ: John Wiley.
- Price, N. M., and Morel, F. M. M. (1990). Cadmium and cobalt substitution for zinc in a marine diatom. *Nature* 344, 658–660.
- Rae, T. D., Schmidt, P. J., Pufahl, R. A., Culotta, V. C., and O'Halloran, T. V. (1999). Undetectable intracellular free copper: the requirement of a copper chaperone for superoxide dismutase. *Science* 284, 805–808.
- Richardson, A. J., and Schoeman, D. S. (2004). Climate impact on plankton ecosystems in the Northeast Atlantic. *Science* 305, 1609–1612.
- Robinson, N. J., and Winge, D. R. (2010). "Copper metallochaperones," in *Annual Review of Biochemistry*, Vol. 79, eds R. D. Kornberg, C. R. H. Raetz, J. E. Rothman, and J. W. Thorner (Palo Alto: Annual Reviews), 537–562.
- Sagripanti, J. L., and Kraemer, K. H. (1989). Site specific oxidative DNA damage at polyguanosines produced by copper plus hydrogen peroxide. *J. Biol. Chem.* 264, 1729–1734.
- Sagripanti, J. L., Routson, L. B., Bonifacino, A. C., and Lytle, C. D. (1997). Mechanism of copper-mediated inactivation of *Herpes simplex* virus. *Antimicrob. Agents Chemother.* 41, 812–817.
- Sandaa, R. A. (2008). Burden or benefit? Virus-host interactions in the marine environment. *Res. Microbiol.* 159, 374–381.
- Schafer, F. Q., and Buettner, G. R. (2001). Redox environment of the cell as viewed through the redox state of the glutathione disulfide/glutathione couple. *Free Radic. Biol. Med.* 30, 1191–1212.
- Scheidegger, C., Behra, R., and Sigg, L. (2011). Phytochelatin formation kinetics and toxic effects in the freshwater alga *Chlamydomonas reinhardtii* upon short- and long-term exposure to lead(II). *Aquat. Toxicol.* 101, 423–429.
- Schiff, K., Diehl, D., and Valkirs, A. (2004). Copper emissions from antifouling paint on recreational vessels. *Mar. Pollut. Bull.* 48, 371–377.
- Schroeder, D. C., Oke, J., Malin, G., and Wilson, W. H. (2002). *Coccolithovirus* (Phycodnaviridae): characterisation of a new large dsDNA algal virus that infects *Emiliania huxleyi*. *Arch. Virol.* 147, 1685–1698.
- Schwarz, K. B. (1996). Oxidative stress during viral infection: a review. *Free Radic. Biol. Med.* 21, 641–649.
- Singh, N., and Turner, A. (2009a). Leaching of copper and zinc from spent antifouling paint particles. *Environ. Pollut.* 157, 371–376.
- Singh, N., and Turner, A. (2009b). Trace metals in antifouling paint particles and their heterogeneous contamination of coastal sediments. *Mar. Pollut. Bull.* 58, 559–564.
- Sorensen, G., Baker, A. C., Hall, M. J., Munn, C. B., and Schroeder, D. C. (2009). Novel virus dynamics in an *Emiliania huxleyi* bloom. *J. Plankton Res.* 31, 787–791.
- Stohs, S. J., Bagchi, D., Hassoun, E., and Bagchi, M. (2001). Oxidative mechanisms in the toxicity of chromium and cadmium ions. *J. Environ. Pathol. Toxicol. Oncol.* 20, 77–88.
- Sunda, W. G. (1988). Trace metal interactions with marine phytoplankton. *Biol. Oceanogr.* 6, 411–442.
- Sunda, W. G., and Guillard, R. R. L. (1976). The relationship between cupric ion activity and toxicity of copper to phytoplankton. *J. Mar. Res.* 34, 511–529.
- Suttle, C. A. (2007). Marine viruses – major players in the global ecosystem. *Nat. Rev. Microbiol.* 5, 801–812.
- Vardi, A., Van Mooy, B. A. S., Fredricks, H. F., Popendorf, K. J., Ossolinski, J. E., Haramaty, L., and Bidle, K. D. (2009). Viral glycosphingolipids induce lytic infection and cell death in marine phytoplankton. *Science* 326, 861–865.
- Vasconcelos, M., and Leal, M. F. C. (2001). Adsorption and uptake of Cu by *Emiliania huxleyi* in natural seawater. *Environ. Sci. Technol.* 35, 508–515.
- Vasconcelos, M., Leal, M. F. C., and van den Berg, C. M. G. (2002). Influence of the nature of the exudates released by different marine algae on the growth, trace metal uptake, and exudation of *Emiliania huxleyi* in natural seawater. *Mar. Chem.* 77, 187–210.
- Voelker, B. M., Sedlak, D. L., and Zafriou, O. C. (2000). Chemistry of superoxide radical in seawater: reactions with organic Cu complexes. *Environ. Sci. Technol.* 34, 1036–1042.
- Weaver, L., Michels, H. T., and Keevil, C. W. (2008). Survival of *Clostridium difficile* on copper and steel: futuristic options for hospital hygiene. *J. Hosp. Infect.* 68, 145–151.
- Weinbauer, M. G., Arrieta, J. M., Griebler, C., and Herndl, G. J. (2009). Enhanced viral production and infection of bacterioplankton during an iron-induced phytoplankton bloom in the Southern Ocean. *Limnol. Oceanogr.* 54, 774–784.
- Wilhelm, S. W., and Suttle, C. A. (1999). Viruses and nutrient cycles in the sea – viruses play critical roles in the structure and function of aquatic food webs. *Bioscience* 49, 781–788.
- Wilson, W. H., Schroeder, D. C., Allen, M. J., Holden, M. T. G., Parkhill, J., Barrell, B. G., Churcher, C., Harnlin, N., Mungall, K., Norbertczak, H., Quail, M. A., Price, C., Rabbnowitsch, E., Walker, D., Craigon, M., Roy, D., and Ghazal, P. (2005). Complete genome sequence and lytic phase transcription profile of a *Coccolithovirus*. *Science* 309, 1090–1092.
- Wilson, W. H., Tarran, G. A., Schroeder, D., Cox, M., Oke, J., and Malin, G. (2002). Isolation of viruses responsible for the demise of an *Emiliania huxleyi* bloom in the English channel. *J. Mar. Biolog. Assoc. U.K.* 82, 369–377.
- Yamaguchi-Iwai, Y., Serpe, M., Haile, D., Yang, W. M., Kosman, D. J., Klausner, R. D., and Dancis, A. (1997). Homeostatic regulation of copper uptake in yeast via direct binding of MAC1 protein to upstream regulatory sequences of FRE1 and CTR1. *J. Biol. Chem.* 272, 17711–17718.

Conflict of Interest Statement: The authors declare that the research was conducted in the absence of any commercial or financial relationships that could be construed as a potential conflict of interest.

Received: 08 December 2011; paper pending published: 01 February 2012; accepted: 04 April 2012; published online: 23 April 2012.

Citation: Gledhill M, Devez A, Highfield A, Singleton C, Achterberg EP and Schroeder D (2012) Effect of metals on the lytic cycle of the *Coccolithovirus*, EhV86. *Front. Microbio.* 3:155. doi: 10.3389/fmicb.2012.00155

This article was submitted to *Frontiers in Microbiological Chemistry*, a specialty of *Frontiers in Microbiology*.

Copyright © 2012 Gledhill, Devez, Highfield, Singleton, Achterberg and Schroeder. This is an open-access article distributed under the terms of the Creative Commons Attribution Non Commercial License, which permits non-commercial use, distribution, and reproduction in other forums, provided the original authors and source are credited.